Etude de la toxicité idiosyncratique de médicaments sur cellules HepaRG et levure : influence du stress inflammatoire et de la biotransformation

Houssein Al-Attrache

ANNÉE 2016

THESE EN COTUTELLE

Pour obtenir le grade de Docteur délivré par

L'Université Libanaise

Ecole Doctorale des Sciences et Technologie

et

L'Université de Rennes I

Ecole Doctorale Vie-Agro-Santé

Spécialité : Biologie et Sciences de la Santé

Présentée et soutenue publiquement par

AL-ATTRACHE Houssein

Préparée à l'unité de recherche INSERM UMR 991
Foie, Métabolismes et Cancer

Etude de la toxicité idiosyncratique de médicaments sur cellules HepaRG et levure : influence du stress inflammatoire et de la biotransformation

Thèse soutenue à Beyrouth le 22/09/2016

devant le jury composé de :

Mme El-Hajj Hiba
AUB-Assistant professor/ *rapporteur*

Mme Aggerbeck Martine
INSERM UMR-S 1124 Chargée de Recherches-HDR/ *rapporteur*

Mme Greije Hélène
Univ. Libanaise-Sciences 2-Professeur/ *examinateur*

Mr. Attieh Zouheir
AUST-Assistant professor/ *examinateur*

Mme Sergent Odile
Univ. De Rennes 1-Professeur/ *examinateur*

Mme Morel Isabelle
Univ. De Rennes 1-Professeur/ *directeur de thèse*

Mr. Abdel-Razzak Ziad
Univ. Libanaise-Sciences 2-Professeur- HDR/ *directeur de thèse*

Mr. Guillouzo André
Univ. De Rennes 1-Professeur/ *invité*

"Le succès n'est pas la clé du Bonheur. Le bonheur est la clé du succès. Si vous aimez ce que vous faites, vous réussirez »

ALBERT SCHWEITZER

Remerciement

Je vais remercier en premier lieu mes directeurs de thèse Pr André Guillouzo, Pr Ziad Abdel-Razzak et Pr Isabelle Morel. Je vous remercie pour chaque instant que vous avez passé avec moi pour me conseiller que ce soit pratiquement ou théoriquement. Je vous remercie pour le temps que vous avez dépensé pour corriger ce travail qui était impossible à réaliser sans votre aide. Merci de m'avoir accepté dans vos équipes qui étaient sans doute une deuxième famille pour moi. Merci pour tous vos conseils qui m'ont formé scientifiquement pour arriver à ce niveau d'apprentissage. Vous avez cultivé chez moi l'amour de la recherche pour servir le plus possible notre humanité. Ces quelques mots ne sont pas suffisants pour vous dire merci.

Un grand merci aux membres du jury : Mme El-Hajj Hiba, Mme Aggerbeck Martine, Mme Greije Hélène, Mr. Attieh Zouheir, Mme Sergent Odile. J'ai l'honneur d'avoir des gens comme vous pour juger ce travail.

Je veux remercier tous les membres de l'U991 « Foie, métabolisme et cancer » et particulièrement Bernard Fromenty, Marie –Anne Robin, Tatiana victoni, Nicolas Quesnot, Vincent Lagente, Elisabette Boichot, Karima Begriche, Patricia André, Sophie Martinais, Sacha Robert, Matthew Burbank, Dounia Le Guilloux, Simon Bucher, Thomas Gicquel.

Un remerciement particulier pour Eva Klimcakova et Audrey Burban.

Merci beaucoup à vous madame Christiane Guillouzo. Merci pour vos conseils.

Un grand merci à une personne qui n'est pas seulement un membre de mon équipe mais plutôt un frère à moi qui était toujours à côté de moi et qui m'a donné toujours une sensation que je ne suis pas seul même lorsque j'étais loin de mes parents. Merci beaucoup Ahmad Charanek.

Un grand merci au directeur du centre AZM pour la recherche à Tripoli « Pr Mohamad Khalil », aux directeurs des équipes de biotechnologies et de Microbiologie les Pr Samir Taha et Monzer Hamzé ainsi que tous mes collègues au centre.

Merci à mon père, ma mère, à mon frère et mes sœurs ainsi que toute ma famille. Vous étiez et vous restez les yeux que je vois à travers eux, vous êtes l'espoir, l'ambition et toutes les belles

choses qui m'ont poussé à chaque fois pour continuer et être le meilleur. Vous êtes la force et le cadeau que Dieu m'a donné dans cette vie.

Merci toujours et toujours à mon Dieu qui m'a donné tout ça pour être dans cette situation et réaliser mon rêve. Merci mon Dieu car vous avez mis toutes ces personnes dans mon chemin.

Abstract

In human, many drugs are toxic for only rare patients. Genetic and various other factors (daily doses, inflammatory stress, immune reaction, liver diseases) are thought to favor such idiosyncratic toxicity that is not predictable in animals. Its prediction and mechanisms involved are very challenging. In this work, we have investigated *in vitro* the influence of an inflammatory stress on cytotoxic, cholestatic and steatotic effects of 3 drugs which are known to cause idiosyncratic hepatotoxicity, i.e. diclofenac (DCF), trovafloxacin (TVX) and amiodarone (AMD), using as experimental models, metabolically competent differentiated HepaRG cells, and for comparison, undifferentiated HepaRG cells, HepG2 cells, primary human hepatocytes as well as a non hepatic eukaryotic cell, the yeast *Saccharomyces cerevisiae*. Our results show that differentiated HepaRG cells were less sensitive than their undifferentiated counterparts and that toxicity involved intrinsic apoptosis., associated with ROS (reactive oxygen species) generation and endoplasmic reticulum stress and was aggravated with TNF-α via extrinsic apoptosis.. DCF toxicity was augmented by co-treatment with TVX and further by co-addition of TNF-α. By contrast, this cytokine did not potentiate cholestatic effects of either drug, typified by dilatation of bile canaliculi and inhibition of some bile acids transporters (BSEP, NTCP). An inflammatory stress induced by the bacterial lipopolysaccharide aggravated cytotoxicity and steatosis induced by AMD, via ROS generation, fatty acid oxidation and triglycerides accumulation leading to a steatohepatitis-like state. Moreover, DCF toxicity was also augmented in *S. cerevisiae* containing mutations of transporters of phase III, such as *Pdr5,* and especially after co-treatment with N-acetyl-cysteine, via a pathway that is probably dependent on alterations of di-sulfure bounds in critical proteins (transporters, signaling proteins, transcription factors). Together, all the results suggest that environmental factors, such as inflammatory stress or genetic factors can modulate the toxic response to drugs by inducing oxidative and endoplasmic reticulum stress as well as by modifying metabolism, drug-drug interactions and key signaling pathways.

Résumé

Chez l'homme, de nombreux médicaments ne sont toxiques que chez un petit nombre de patients traités. Divers facteurs de susceptibilité, génétiques et autres (doses quotidiennes, stress inflammatoire, réaction immune, maladie hépatique,…), favoriseraient la survenue de ces toxicités de type idiosyncratique, non prévisibles par des études chez l'animal. Leur prédiction et la caractérisation des mécanismes impliqués représentent donc un challenge majeur. Dans ce travail, nous avons étudié *in vitro* l'influence d'un stress inflammatoire sur le potentiel cytotoxique, cholestatique et stéatosique de trois médicaments connus par leurs effets de type idiosyncratique au niveau du foie, le diclofenac (DCF), la trovafloxacine (TVX) et l'amiodarone (AMD) en utilisant comme modèles expérimentaux les cellules humaines HepaRG différenciées, métaboliquement compétentes, et pour comparaison les cellules HepaRG non différenciées, les cellules HepG2, les hépatocytes humains primaires ainsi qu'un autre modèle cellulaire eucaryote la levure *Saccharomyces cerevisiae*. Nos résultats montrent que les cellules HepaRG différenciées sont moins sensibles au DCF que les cellules métaboliquement non compétentes et que cette toxicité implique la voie intrinsèque de l'apoptose, associée à la génération de ROS (espèces réactives de l'oxygène) et d'un stress du réticulum endoplasmique. Elle est aggravée par le TNF-α via la voie apoptotique extrinsèque. La toxicité de DCF est aussi augmentée lors d'un co-traitement avec TVX et encore plus en présence de TNF-α. En revanche, cette cytokine ne potentialise pas les effets cholestatiques des 2 molécules, caractérisés notamment par une dilatation des canalicules biliaires et une inhibition de l'activité de certains transporteurs d'acides biliaires (BSEP, NTCP). Un stress inflammatoire induit par le lipopolysaccharide bactérien aggrave aussi les effets cytotoxiques et stéatosiques de l'AMD via une production de ROS, une inhibition de l'oxydation des acides gras et une accumulation des triglycérides, aboutissant à un contexte de stéatohépatite. De plus, une aggravation de la toxicité de DCF a également été observée dans *Saccharomyces cerevisiae* portant une mutation au niveau de certains transporteurs de la phase III, tel que *Pdr5*, et surtout après co-traitement avec la N-acétyl-cystéine via une voie qui pourrait être dépendante des perturbations des ponts di-sulfure au niveau de certaines protéines clés (transporteurs, protéines de signalisation ou facteurs de transcription, ...). Au total, tous ces résultats suggèrent que des facteurs environnementaux tels qu'un stress inflammatoire, et génétiques peuvent moduler la réponse toxique à des médicaments non seulement en induisant des stress oxydants et du réticulum endoplasmique mais aussi en modifiant leur métabolisme et donc les interactions entre médicaments, et certaines voies de signalisation essentielles.

Tableau des matières

Liste des figures

Liste des tableaux

Dans l'introduction

Liste des abrévaiations

ABC: transporteurs à ATP Binding Cassette

ABT: 1-aminobenzotriazole

ACACA: acetyl-coenzyme A carboxylase a

Ac-DEVD-AMC: N-acétyl-Asp-Glu-Val-Asp-7-amido-4-méthylcoumarine

AC-IETD-AMC: Ac-Ile-Glu-Thr-Asp-7-amino-4-méthylcoumarine

AC-LEHD-AMC: Ac-Leu-Glu-His-Asp-7-Amino-4-méthylcoumarine

ACLY: ATP-citrate synthase

ADFP: Adipose differentiation-related protein

ADME : Absorption, distribution, métabolisme, excrétion

ADN: acide désoxyrubonucléique

ADNc: ADN complémentaire

ADP : adénosine diphosphate

AG : acylglucuronides

AhR: Aryl hydrocarbon receptor

AIC: cholestase intra-hépatique aiguë

AINS : anti-inflammatoires non stéroïdiens

ALAT : alanine transaminase

Alb: Albumine

ALDB: Aldolase B

ALP : Alkaline phosphatase

ALT : Alanine transaminase

AMD : amiodarone

AP-1: Activating protein-1

APAF1 : Apoptotic protease activating factor 1

APAP: acétaminophène

ARN: Acide Ribonucléique

Asbt: Apical Sodium Dependent Bile Acid Transporter

ASML3A: Acid sphingomyelinase-like phosphodiesterase 3a

ATF4: Activating Transcription Factor 4

ATF6: Activating Transcription Factor 6

ATP : adénosine triphosphate

BC : canalicules biliaires

BclXL : B-cell lymphoma-extra large

BCRP: Breast Cancer Resistance Protein

Bid : BH3 interacting-domain death agonist

Bim: Bcl-2-like protein 11

Bpt1 : Bile Pigment Transporter

BRCA: Breast Cancer

BSEP: bile salt export pump

Ca2+ : calcium

CAR: Constitutive androstane receptor

CAR: Constitutively Active Androstane Receptor

Cas3: caspase 3

CCL18: Chemokine ligand 18

CCL2: Chemokine ligand 2

CD : cluster of differentiation

CD36: CD36 antigen

CDF: 5 (and 6)-carboxy-20,70-dichlorofluorescein

c-FLIP : FADD-like interleukin-1β–converting enzyme (FLICE)-inhibitory

CHC: cancer hépatocellulaire

CHOL : cholestérol

CHOP: C/EBP homologous protein

cm: centimètre

CPT1: Carnitine O-palmitoyltransférase 1

CPT1A: Carnitine O-palmitoyltransférase 1

CPZ: chlorpromazine

CRP: C-reactive protein

CXCL16 : Chemokine (C-X-C motif) ligand 16

CYP3A4: cytochromes P450 3A4

CYP450: cytochromes P450

Da : Dalton

DCF : diclofénac

DEA : mono-N-deséthylamiodarone

DMSO: diméthylsulfoxyde

DO : densité optique

DPP-IV : dipeptidyl peptidase IV

DTT: dithiothreitol

EC50: half maximal effective concentration

EH: époxydes hydrolases

eIF2α: Eukaryotic Initiation Factor 2

ELISA : enzyme-linked immunosorbent assay

ER stress : stress du réticulum endoplasmique

FAO: fatty acid oxidation

FASN: Fatty acid synthase

FXR : Farnesoid X-Activated Receptor

G: gramme

GDPD3: Glycerophosphodiester phosphodiesterase domain containing 3

GGT: Gamma-Glutamyl Transferase

GRP78: 78 kDa glucose-regulated protein

GST: Gluthation s transférase

H : heure

H2-DCFDA: dichlorodihydrofluorescein

H_2O: eau

H_2O_2 : peroxyde d'hydrogène

HFBS: Hyclone® fetal bovine serum

HH: hépatocytes humains

HNF: Hepatocyte Nuclear Factor

HO1: hème oxygénase 1

HSC70: Heat shock 70 kDa

IC50 : concentration inhibitrice à 50%

IDR: réactions médicamenteuses idiosyncrasiques

IFN : interféron

IL : interleukine

JNK: Jun N terminale kinase

KC: cellules de küpffer

kDa: kilodalton

Keap1: Kelch-like ECH-associated protein 1

Kg : kilogramme

Ki : constante d'inhibition

LB : Lymphocyte B

LC : L-cystéine

LC-HR-MS: Liquid Chromatography – High Resolution – Mass Spectrometer

LI: L-isoleucine

LL : L-Lysine

LPIN1: Lipin-1

LPL: Lipoprotein lipase

LPS: lipopolysaccharide

LSS: lanosterol synthase

LT : Lymphocyte T

LVX: lévofloxacine

MAPK : Mitogen-Activated Protein Kinase

MCP1 : Monocyte Chemoattractant Protein-1

MD2 : Lymphocyte antigen 96

MDR1: multidrug resistance protein 1

Mg2+ : magnésium

min: minute

ml : millilitre

MLC2 : Myosin light chain

mM : millimolaire

MM: masse moléculaire

MnSOD: manganèse superoxide dismutase

mol : molaire

MP : pores mitochondriaux

MRP2: Multidrug resistance protein 2

MRP3: Multidrug resistance protein 3

MRP4: Multidrug resistance protein 4

MRP6: Multidrug resistance protein 6

MTT: méthylthiazoltétrazolium

NAC : N-acetylcysteine

NADPH: Nicotinamide Adenine Dinucleotide Phosphate Hydrogen

NAFLD: Non-alcoholic fatty liver disease

NAT: N-acétyltransférases

ND : non déterminée

NFκB: Facteur nucléaire κB

ng : nanogramme

NK : natural killer

nm: nanomètre

NO : oxyde nitrique

NOS : oxyde nitrique synthase

Nrf2: Nuclear factor (erythroid-derived 2)-like 2

NTCP: sodium-taurocholate cotransporting polypeptide

OAT2: organic anion transporter 2

OATP: organic anion transporting polypeptide

OCT1: human organic cation transporter 1

OH : groupe hydroxy

Ost: Organic solute transporter

PA: phosphatases alcalines

PAI1 : inhibiteur 1 de l'activation du plasminogène

PANX1 : Pannexine 1

PBS: phosphate buffered saline

Pdr : Pleiotropic Drug Resistance

Pg: picogramme

PGC-1α: transcriptional coactivator peroxisome proliferator-activated receptor-γ coactivator-1α

P-gp: P-glycoprotéine

Pka: acid dissociation constant

PKC : protein kinase C

PKLR: liver pyruvate kinase

PLIN4: Perilipin-4

PMN : polynucléaires neutrophiles

PPAR : peroxisome proliferator activated-receptor

PUMA : Polyurethane Methyl Acrylate

PXR: Pregnane X receptor

Rap1 : Repressor/Activator site binding Protein

RAR: Retinoic Acid Receptor

ROS: espèces réactives d'oxygène

RT-qPCR: real-time quantitative polymerase chain reaction

RXRα : Retinoid X Receptor, Alpha

SCD: Acyl-CoA désaturase

SEM : standard error of the mean

SLC27A4: Long-chain fatty acid transport protein 4

SOAT1: Stérol O-acyltransférase 1

SOD: superoxide dismutase

SREBP1: Sterol regulatory element-binding protein 1

SULT: sulfotransférases

TA: acide taurocholique

TG : triglycérides

TGF-β: tumor growth factor β

THRSP: Thyroid hormone-inducible hepatic protein

TLR : Toll like receptor

TNF: facteur de nécrose tumorale

TNF-R: récepteur de TNF-α

TRIB3: Tribble 3

TVX : trovafloxacine

U: unité

UGT: UDP-glucuronosyltransférases

VBDS : vanishing bile duct syndrome

Vmr1: Vacuolar Multidrug Resistance 1

Yap1 : Yes associated protein 1

Yor1 : Yeast Oligomycin Resistance

YPD : Yeast Peptone Dextrose

z-LEHD-fmk: Z-Leu-Glu(OMe)-His-Asp(OMe)-fluorométhylkétone

γGT : gamma glutamyltransférase

ΔΨm : potentiel membranaire mitochondrial

µl: microlitre

µM : micromolaire

Introduction générale

Beaucoup des médicaments causent des lésions hépatiques qui peuvent être prévisibles dose-dépendantes (intrinsèques) ou non prévisibles, non dose-dépendantes (idiosyncratiques). Divers facteurs peuvent influencer la survenue de cette toxicité idiosyncratique. On peut citer le polymorphisme génétique, notamment celui des enzymes de métabolisme des xénobiotiques, le stress inflammatoire… Plusieurs travaux ont montré que ce dernier peut avoir une influence majeure sur la réponse toxique comme l'ont montré des co-traitements avec le lipopolysaccharide (LPS) et des médicaments responsables d'IADRs (réactions idiosyncratiques indésirables) chez le rat. C'est le cas de la ranitidine, la chlorpromazine, le diclofenac, et la trovafloxacine..

Afin d'étudier les effets d'un stress inflammatoire induit par le LPS ou des cytokines pro-inflammatoires sur la toxicité hépatique des médicaments, nous avons choisi de traiter des cellules humaines HepaRG qui expriment la majorité des fonctions hépatiques à des niveaux proches de ceux retrouvés dans des hépatocytes humains matures, avec le diclofénac, la trovafloxacine et l'amiodarone, trois médicaments connus pour induire des toxicités hépatiques idiosyncratiques et être sensibles aux effets d'un stress inflammatoire chez l'animal. Ces molécules, outre leurs effets cytotoxiques, peuvent induire des cholestases (diclofénac, trovafloxacine) ou des stéatoses (amiodarone).

Notre étude montre une influence possible du stress inflammatoire sur les différents types de toxicité observés. Ils montrent aussi que des interactions entre deux médicaments peuvent être potentialisées par un stress inflammatoire. Ces résultats peuvent être différents selon le modèle hépatique utilisé. Nous montrons également que la levure *Saccharomyces cerevisiae* est sensible au diclofénac et qu'en présence de N-acétylcysteine la toxicité de ce médicament est aggravée (alors que cet anti-oxydant réduit la toxicité dans les cellules HepaRG). Les effets opposés dans la levure pourraient être dus à une perturbation des liaisons disulfures dans des protéines jouant un rôle clé dans le fonctionnement de cette cellule eucaryote, particulièrement celles impliquées dans la résistance de cette cellule au stress chimique, comme les transporteurs ABC.

Introduction

I. Foie – Structure et fonctions

Le foie fait partie du système digestif; il assure trois fonctions vitales principales: celles de synthèse, de stockage et d'épuration. Il représente 2 % du poids corporel soit environ 1.5 kg chez l'homme adulte. Il comprend deux lobes principaux appelés lobe gauche et lobe droit et séparés par le ligament falciforme (Figure 1).

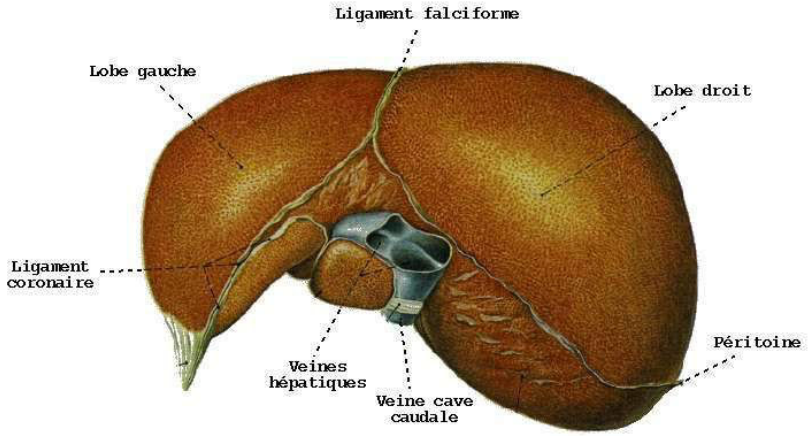

Figure 1: Structure générale du foie (Brooker, 2001) comportant pricipalement deux lobes (gauche et droite) séparés par le ligament falciforme.

C'est un organe très vascularisé qui reçoit un sang riche en oxygène par l'artère hépatique et un sang riche en nutriments d'origine intestinale via la veine porte. Le retour veineux est assuré par les veines sus-hépatiques.

Il est formé de plusieurs types cellulaires dont des hépatocytes pour 80 %, mais il contient aussi des cellules biliaires entourant les canaux biliaires, des cellules endothéliales, des cellules étoilées, des cellules immunitaires comme les cellules de Küpffer…). Les cellules hépatiques sont distribuées en lobules hépatiques ayant en leur centre une veine centrolobulaire et à leur périphérie des espaces-porte. Chaque espace-porte interlobulaire comprend une branche de l'artère hépatique, une branche de la veine porte et un canal biliaire. Le lobule hépatique constitue l'unité structurale du foie. Dans les lobules de forme polygonale les hépatocytes s'organisent en travées unicellulaires séparées par des sinusoïdes (Figure 2) (Brooker, 2001).

Par contre, les unités fonctionnelles sont représentées par des acini (Rappaport et al., 1954). Un acinus, bien que difficile à définir histologiquement, correspond à une unité de parenchyme hépatique centrée sur un espace porte et situé entre au moins deux veines centrolobulaires. L'acinus se divise en zones 1, 2 et 3 avec des hépatocytes à fonctions métaboliques différentes dans chaque zone (Wheater PR, 2001).

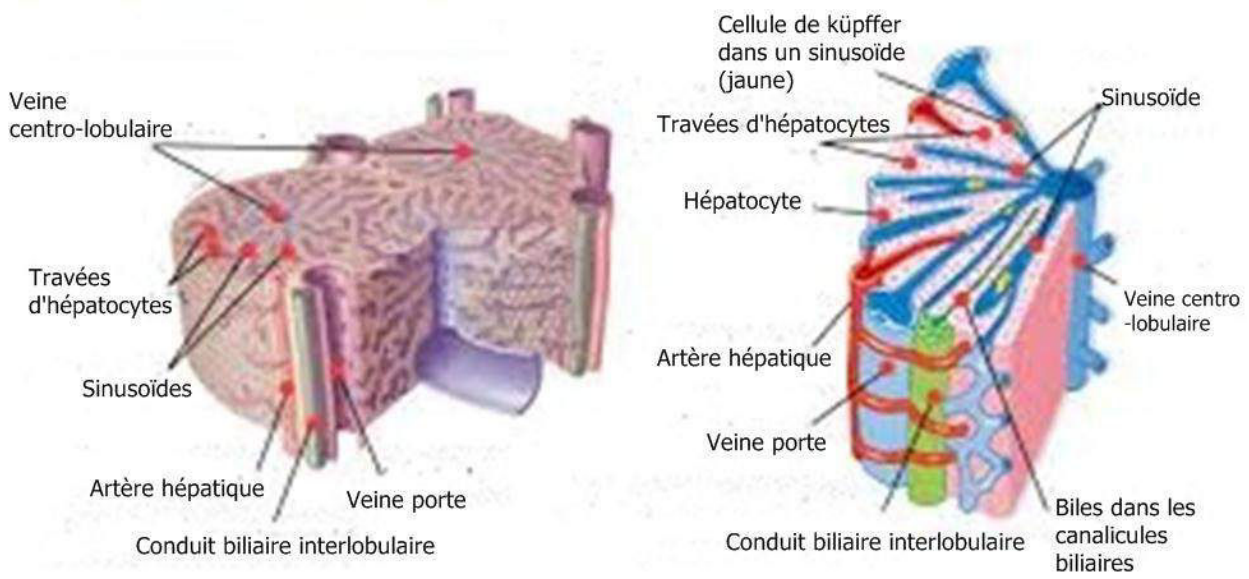

Figure 2: Représentation schématique d'un lobule hépatique (Moore, 2001).

Les hépatocytes assurent la majorité des fonctions du foie (Blouin et al., 1977). Ce sont des cellules polarisées présentant trois domaines membranaires différents et spécialisés : les domaines basolatéral (sinusoïdal), canaliculaire et latéral.

- Le domaine basolatéral ou sinusoïdal : chaque hépatocyte est en contact par au moins deux de ses faces avec le sang des sinusoïdes, tout en étant séparé par l'espace de Disse. La membrane sinusoïdale des hépatocytes constitue 70% de la surface totale membranaire. Les échanges hépatocyte-sang se font majoritairement par des phénomènes d'endocytose et d'exocytose via ce domaine membranaire. Les échanges qui ont lieu au niveau de ce pôle basolatéral sont bidirectionnels; certaines substances transportées par le sang sont absorbées par l'hépatocyte alors que des protéines néo-synthétisées, comme l'albumine, le fibrinogène, la prothrombine et certains facteurs de coagulation, sont secrétées dans le sang (Kierszenbaum, 2002).

- Le domaine canaliculaire ou apical : le domaine canaliculaire de la membrane plasmique hépatocytaire représente 15% de la surface cellulaire. Ce pôle est également appelé pôle biliaire de l'hépatocyte. Il forme le canalicule biliaire qui correspond à l'espace situé entre les faces opposées des deux hépatocytes adjacents. Un réseau de microfilaments contractiles situé dans la région cytoplasmique sous-jacente au canalicule commande l'ouverture des canalicules et ainsi, le flux biliaire. Toutefois, le diamètre du canalicule biliaire varie selon la place qu'il occupe dans l'acinus et de plus il s'ouvre et se ferme périodiquement.

- Le pôle latéral : ce pôle se situe entre les domaines sinusoïdal et biliaire de l'hépatocyte et constitue 15% de la surface cellulaire. Il renferme trois types de jonctions : les desmosomes, les jonctions serrées et les jonctions communicantes (Ramadori G, 2010).

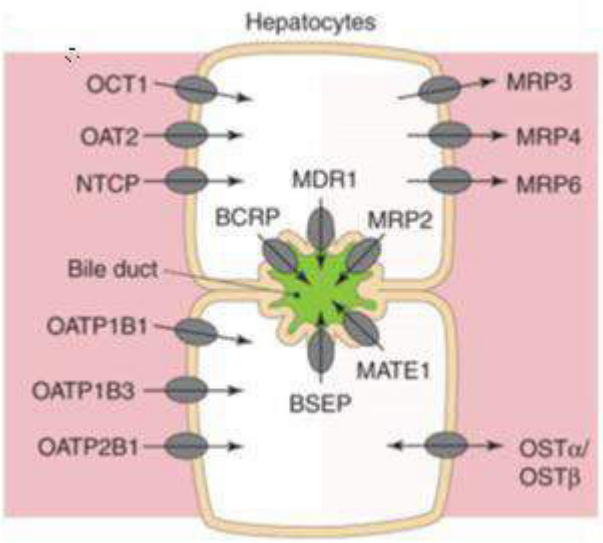

Figure 3: Schéma montrant les différents transporteurs hépatiques ainsi que les échanges intra- et extra-hépatiques (Moore, 2001) (modifiée). Les flèches marquent le mouvement d'efflux et d'influx.

Les échanges extra- ou intra-hépatiques des hépatocytes se font majoritairement par des transporteurs spécifiques dépendant ou non de la nature du substrat. C'est le cas par exemple des transporteurs latéraux comme notamment le MRP3, le MRP4, le MRP6, l'OCT1, l'OAT2 et le NTCP, des transporteurs canaliculaires comme le BCRP, le MDR1, le MRP2 et le BSEP (Figure 3).

I.1. Les fonctions du foie

Le foie exerce plusieurs fonctions majeures, parmi lesquelles des fonctions métaboliques et des fonctions de détoxification:

I.1.1. Des fonctions métaboliques

Le foie joue un rôle très important dans le métabolisme de différents constituants nutritionnels :

- Glucides : dégradation de l'insuline et d'autres hormones, glycogénolyse, glycogénogenèse, néoglucogénogenèse. Le foie a un rôle important dans la régulation de la glycémie puisqu'il est capable de stocker le glucose sous forme de glycogène grâce au phénomène de néoglucogenèse ; il est donc hypoglycémiant dans ce cas mais il est aussi hyperglycémiant en libérant dans le sang du glucose à partir du glycogène stocké surtout lors de périodes de jeûne, par glycogénolyse.

- Lipides : synthèse de cholestérol, production de triglycérides, synthèse de lipoprotéines, synthèse des acides biliaires à partir du cholestérol.

- Protéines : synthèse des protéines sériques (albumine, facteurs de coagulation, …), protéines de la phase aiguë (protéine C-réactive …) à l'exception des immunoglobulines.

I.1.2. Des fonctions de détoxification

Le foie joue un rôle majeur dans l'élimination des substances étrangères et notamment les médicaments. Il est également capable de détruire les hématies et les leucocytes vieux et de conjuguer la bilirubine libre en bilirubine conjuguée pour la rendre non toxique. Seuls seront détaillés ici le métabolisme des xénobiotiques et le rôle essentiel d'une superfamille d'enzymes de biotransformation : les cytochromes P450 (CYP).

L'organisme humain s'est doté de trois systèmes spécialisés et complémentaires permettant l'élimination des composés étrangers et participant ainsi à la détoxification cellulaire (Figure 4). Les enzymes dites de phase I (ou phase de fonctionnalisation) qui comprennent principalement les cytochromes P450 (CYPs), les enzymes de conjugaison ou transférases (Phase II), telles que les glucuro- ou glutathion-S-transférases, et les protéines de transport (influx et efflux), telles que la P-glycoprotéine (P-gp) (Phase III). Elles ont des localisations diverses, surtout au niveau du réticulum endoplasmique mais aussi les mitochondries voire la membrane plasmique et pour certaines enzymes de Phase II, le cytosol) et peuvent agir en synergie pour une plus grande

efficacité de détoxication du foie. Le CYP3A4 et la P-gp se caractérisent par une reconnaissance moléculaire multispécifique vis-à-vis d'une grande diversité de structures chimiques et partagent de nombreux substrats en commun. Du fait de leur hydrophobicité, ces substrats communs sont reconnus par ces protéines au sein même de la membrane.

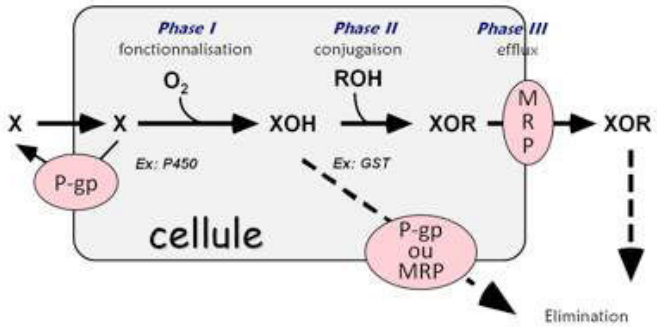

Figure 4: Métabolisme des xénobiotiques (Matouskova et al., 2016). Les 3 phases sont représentées. X : xénobiotique ; XOH : xénobiotique sous forme hydroxylée ; XOR : xénobiotique conjugué ; P-gp : P-glycoprotéine ; MRP : multidrug resistance protéine

- Phase I : Les réactions de phase I entrainent des modifications des fonctions chimiques des composés permettant généralement de diminuer leur toxicité en les rendant plus polaires. Cependant, il arrive que ces réactions conduisent à des métabolites plus toxiques que les molécules mères. La phase I consiste majoritairement en des réactions de type oxydation (hydroxylations, époxydations, déshydrogénations), réduction et hydrolyse (Iyanagi, 2007) (David Josephy et al., 2005) qui sont catalysées surtout par les cytochromes P450 (Evans and Relling, 1999).

Les réactions de phase I sont généralement suivies de réactions de phase II car les métabolites de phase I ne sont pas suffisamment polaires pour être éliminés tels quels.

- Phase II : Les réactions de phases II assurent la conjugaison des métabolites de phase I à des ligands endogènes (acide glucuronique, sulfate activé, glutathion,..) en vue d'augmenter leur hydrosolubilité et de favoriser leur élimination (Testa , 2008). Parmi les enzymes catalysant ces réactions on trouve les UDP-glucuronosyltransférases (UGT), les glutathion-transférases (GST), les sulfotransférases (SULT), les N-acétyltransférases (NAT) et les époxydes hydrolases (EH). Certains composés peuvent être directement conjugués.

- Phase III : Après avoir subi les modifications nécessaires par les enzymes des phases I et II, les composés conjugués sont pris en charge par des protéines de transport (phase III) pour être excrétés sans subir de modifications chimiques (David Josephy et al., 2005).

Les niveaux d'activité des enzymes de phase I ou phase II peuvent fortement varier d'un individu à l'autre. Des facteurs génétiques, physiologiques, pathologiques et environnementaux peuvent les moduler, en agissant au niveau transcriptionnel, post-transcriptionnel ou post-traductionnel. Ainsi, de nombreux composés peuvent inhiber ou induire l'activité de ces enzymes (Brooker, 2001).

Il est établi que les 2/3 des médicaments sont métabolisés par des CYPs et 1/3 par les UGTs et d'autres enzymes. La contribution totale des CYPs et des UGTs au métabolisme des médicaments est estimée à 80%.

Le foie est également responsable de la dégradation de plusieurs hormones comme les hormones thyroïdiennes, les glucocorticoïdes, l'insuline, le glucagon, les estrogènes et bien d'autres. Les produits de dégradation de ces hormones sont ensuite excrétés par la bile (Brooker, 2001).

I.1.2.1. Le rôle essentiel des cytochromes P450

Ce sont des complexes moléculaires ou des hémoprotéines (apoprotéines de 45 à 60 kDa ayant un groupe hème) qui dérivent tous du même gène ancestral (1,5 milliard d'années). Les études ont montré que la réduction de l'hème fournit à ces enzymes la capacité de se lier au monoxyde de carbone pour donner un pic d'absorption à une longueur d'onde de 450 nm (Omura and Sato, 1964). La fonction d'oxydation et le rôle de ces enzymes dans le métabolisme des xénobiotiques ont été étudiés dès les années 1960 (Klingenberg, 1958; Omura and Sato, 1962).

Les CYP450 catalysent plusieurs réactions mais la plus importante est une activité de monooxygénase où un atome d'hydrogène est inséré sur une position aliphatique d'un substrat organique et un atome d'oxygène est réduit en H_2O selon la réaction suivante :

$$RH + O_2 + NADPH + H^+ \rightarrow ROH + H_2O + NADP^+$$

Mais d'autres réactions peuvent être catalysées par les CYP450 telles que des réactions d'hydroxylation (RCH → RCOH), des réactions de N-oxydation (R1-NH-R2 →R1-NOH-R2), des réactions de S-oxydation (R1-S-R2 →R1-SO-R2) et des réactions de N- et O-déalkylation. Les CYP450 catalysent aussi des réactions réservées à des substances endogènes. C'est le cas du métabolisme des acides biliaires, la vitamine D3, la biosynthèse et le catabolisme des hormones stéroïdes.

Les CYP450 humains sont classés en au moins en 18 familles (CYP1, CYP2, CYP3 et CYP4) (Wang and Chou, 2010), 42 sous familles (CYP2B, CYP3A…), et isoenzymes (CYP3A4, CYP2C9…). Au total, le génome humain code 57 protéines CYP450 qui peuvent être classées selon leur type de substrat dans le tableau ci-dessous (Tableau 1).

Tableau 1: Classification des CYP450 humains selon le type de substrat (modifié) (Guengerich, 2006)

Stérols	***Xénobiotiques***	***Acides gras***	***Eicosanoides***	***Vitamines***	***Inconnu***
1B1	1A1	2J2	4F2	2R1	2A7
7A1	1A2	4A11	4F3	24A1	2S1
7B1	2A6	4B1	4F8	26A1	2U1
8B1	2A13	4F12	5A1	26B1	2W1
11A1	2B6		8A1	26C1	3A43
11B1	2C8			27B1	4A22
11B2	2C9				4F11
17A1	2C18				4F22
19A1	2C19				4V2
21A2	2D6				4X1
27A1	2E1				4Z1
39A1	2F1				20A1
46A1	3A4				27C1
51A1	3A5				
	3A7				

La nomenclature des CYP450 commencent par CYP désignant la super famille des cytochromes P450 suivie par la famille exprimée par un chiffre arabe (1, 2, 3…), la sous famille désignée par une lettre (A, B, C…), et les isoformes par un nombre arabe (1, 2, 3…). Cette classification repose sur l'homologie de la séquence en acides aminés : par exemple les éléments d'une même famille ont plus que 40% d'homologie, d'une sous famille plus de 55% … La plupart des références indique une classification des CYP450 en 4 familles (1, 2, 3, 4) car ces 4 familles sont les seules impliquées dans le métabolisme des xénobiotiques. Du point de vue du métabolisme des médicaments quelques CYP450 sont très impliqués ; le CYP majeur étant le CYP3A4. Les CYP450 les plus impliquées dans le métabolisme hépatique des médicaments sont : CYP1A2-18% ; CYP2E1-9% ; CYP2A6-6% ; CYP2D6-6% ; CYP2B6-1% ; CYP3A4-39%; les CYP2C-25% (Guengerich, 2006) comme indiqué dans la figure suivante :

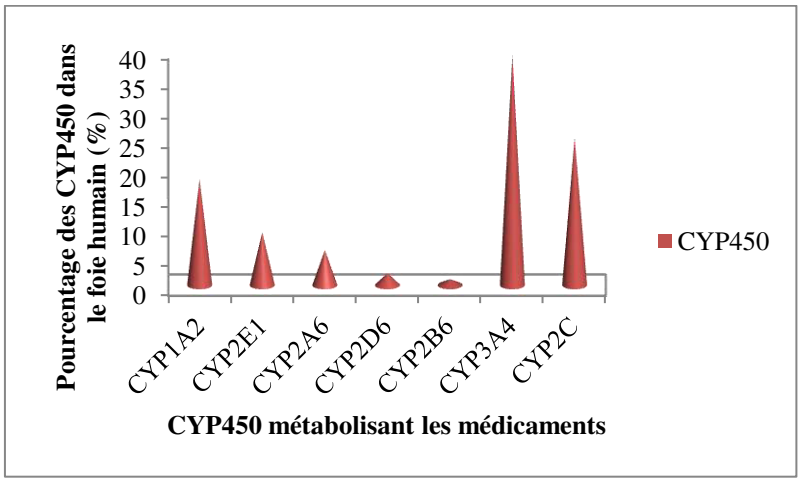

Figure 5: Répartition des CYP450 dans le foie humain (Guengerich, 2006) (modifiée). Le CYP3A4 constitue le CYP450 majeur métabolisant les médicaments.

Le foie est l'organe contenant la quantité la plus élevée et la plus grande diversité de CYPs mais ceux-ci sont aussi présents dans la plupart des autres tissus, notamment l'intestin, les reins, les poumons,….(Krishna and Klotz, 1994). De nombreux facteurs peuvent moduler leur niveau d'expression/activité.

I.2. Foie et Pathologies

Le foie peut être le siège de pathologies variées d'origine diverse (génétique, métabolique, virus, parasites, métaux, composés chimiques dont les médicaments,…). Ces maladies peuvent être aiguës ou chroniques, et résulter de réactions inflammatoires et de mort cellulaire (nécrose, apoptose), de surcharge (stéatose, phospholipidose,..) d'altérations de la sécrétion biliaire (cholestase intra- et extra-hépatiques). Les lésions chroniques (inflammatoires, cytolytiques)

peuvent conduire à des fibroses, des cirrhoses et aboutir à des cancers du foie. Tous les types de lésions et pathologies hépatiques peuvent être obtenues avec des médicaments.

- **La cytolyse :** elle se traduit par la mort des hépatocytes par apoptose ou nécrose. Elle peut être induite par de nombreux médicaments (paracétamol,…) et autres produits chimiques (Lee, 2003). Elle peut concerner préférentiellement certains hépatocytes, en particulier les hépatocytes centrolobulaires lorsque la cytolyse est associée à la production de métabolites réactifs (ces hépatocytes exprimant l'essentiel des CYPs impliqués dans le métabolisme des xénobiotiques. Une cytolyse hépatique se traduit au niveau sérique par une augmentation des transaminases d'un facteur>5.

- **La cholestase**: le terme « CHOLESTASE » a été introduit en 1970 par Popper et Schaffner pour décrire des pathologies résultant d'une inhibition de la sécrétion des acides biliaires et de leur accumulation intra-hépatique dans les hépatocytes ou les canalicules/ canaux biliaires intra-hépatiques (cholestase intra-hépatique) (Popper and Schaffner, 1970). Morphologiquement, la cholestase est caractérisée par la stagnation de bile sous la forme de bouchons biliaires dans les canalicules et des pigments biliaires dans les hépatocytes, ainsi que dans les cellules de Küpffer dans la région centro-lobulaire. Les médicaments induisant une cholestase intrahépatique sont classés en deux catégories : la cholestase pure et la cholestase associée à une hépatite cytolytique fréquemment observée dans les tests cliniques (Erlinger, 1997). Une cholestase seule serait observée dans 20-40% des cas et une cholestase mixte chez 12-20% des patients. Au niveau sérique les phosphatases alcalines (PA) sont augmentées. Le rapport PA/ transaminases est <2 dans le premier cas et entre 2 et 5 dans le second.

La cholestase intra-hépatique aiguë (AIC) est une caractéristique commune de lésion hépatique induite par les médicaments. Dans le cas des AIC, un ictère persiste généralement pendant quelques semaines puis disparait en moins de 3 mois (Sherlock, 1998). En général, le pronostic de l'AIC semble assez bon, mais, dans certains cas, l'AIC induite par le médicament peut être suivie d'une cholestase prolongée malgré l'arrêt des médicaments en cause. La cholestase prolongée induite par des médicaments a été définie par Larrey et Erlinger comme la persistance d'une jaunisse pendant plus que 6 mois ou la persistance des changements biochimiques pour la cholestase anictérique pendant plus d'un an (Larrey and Erlinger, 1988). Histologiquement, le syndrome de fuite biliaire « vanishing bile duct syndrome » (VBDS) a été rapporté comme étant

une caractéristique importante de la cholestase intrahépatique prolongée (Degott et al., 1992; Desmet, 1997).

Les hypothèses concernant les mécanismes de cholestase intrahépatique induite par les médicaments sont basées sur la biologie cellulaire de la sécrétion biliaire. On observe généralement un dysfonctionnement de la mobilité des canalicules biliaires (Watanabe and Phillips, 1984) (Watanabe et al., 1991) et des anomalies des transporteurs des acides biliaires (Trauner et al., 1998b) (Trauner et al., 1999b). Des études sur animaux (Trauner, 1997) et sur foie humain ont démontré une inhibition de la pompe d'export des sels biliaires (BSEP) et de la multidrug resistance protein 2 (MRP2) (Trauner et al., 1997) (Zollner et al., 2001). D'autres facteurs peuvent aussi être impliqués dans la cholestase; c'est le cas des espèces réactives de l'oxygène qui induisent un stress oxydant et peuvent être considérées comme un facteur aggravant l'effet cholestatique comme cela a été montré pour la chlorpromazine (CPZ) (Antherieu et al., 2013).

- **La stéatose** : elle peut se présenter sous forme macrovésiculaire ou microvésiculaire. La forme macrovésiculaire se présente comme une simple accumulation de graisses (triglycérides) principalement dans une large vésicule intracytoplasmique. Il s'agit d'une affection bénigne également connue sous le nom de stéatose simple qui peut être réversible car les graisses s'accumulent habituellement sans causer de dommage aux cellules hépatiques. Cependant, cette stéatose peut évoluer vers une forme plus sévère connue sous le nom de stéatohépatite. La stéatohépatite non alcoolique est une affection plus grave, car l'inflammation et la nécrose des cellules hépatiques peuvent mener à des dommages irréversibles puis une fibrose et une cirrhose, voire même au carcinome hépatocellulaire (Farrell and Larter, 2006) (Reddy and Rao, 2006). La stéatose microvésiculaire qui se traduit par la présence de plusieurs vésicules intracytoplasmiques par cellule, entraine une diminution du nombre de mitochondries ; elle est potentiellement grave et peut être associée à une hypoglycémie majeure. Les 2 types de stéatose peuvnt co-exister.

- **La phospholipidose :** caractérisée par une accumulation intracellulaire excessive de phospholipides sous forme des corps lamellaires. Elle ne constitue pas en soi une toxicité (Xu et al., 2004) mais elle est prédictive de l'accumulation d'un médicament ou de métabolites dans plusieurs tissus cibles, et en tant que telle peut être associée à une toxicité. En effet, les phospholipides accumulés peuvent interférer avec les fonctions cellulaires. Plus de 50

médicaments amphiphiles cationiques, notamment des agents anti-cholestérolémiants, peuvent induire une phospholipidose (Halliwell, 1997). Certains de ces médicaments (tels que l'amiodarone) provoquent également une stéatose. La phospholipidose peut être prédite à partir de modèles *in vivo* et *in vitro* (Donato et al., 2009) (Moya et al., 2010) (Antherieu et al., 2011).

- **La fibrose/cirrhose** : la fibrose puis la cirrhose du foie correspondent à un processus multi-étapes, partant d'un effet hépatotoxique primaire et aboutissant à une situation d'insuffisance des fonctions hépatiques en raison de dommages des hépatocytes. Il s'agit de lésions chroniques caractérisées par un état inflammatoire et le remplacement des hépatocytes morts par des fibres de collagène synthétisées par des myofibroblastes (cellules étoilées activées), en raison d'une perte de capacité de régénération du foie. Cette situation est associée à des changements biochimiques et physiologiques importants. La fibrose va s'étendre et devenir une cirrhose (apparition de septa fibreux), ce qui va fortement amplifier les altérations fonctionnelles du foie (Fausto et al., 2006). En plus d'être une condition très morbide et éventuellement mortelle, la cirrhose fournit également le support le plus approprié pour le développement d'un cancer hépatocellulaire (CHC) (Kew and Popper, 1984). En fait, la plupart des cas de CHC (>80%) se développent sur foie cirrhotique, indépendamment de l'étiologie.

Des nodules de régénération sont observés dans des foies cirrhotiques mais la régénération ne semble pas suivre le même schéma que dans le tissu hépatique normal. Un déséquilibre dans la séquence des voies moléculaires des dommages et de régénération est considéré comme importante pour le développement d'une cirrhose et donc d'une oncogenèse ultérieure (Michalopoulos and DeFrances, 1997).

I.3. Les modèles hépatiques d'études précliniques *in vivo* et *in vitro* des médicaments

Compte-tenu de la fréquence des effets adverses induits par les médicaments et du coût que représente leur développement il est essentiel de disposer d'approches expérimentales permettant d'une part de prédire le plus tôt possible la toxicité d'un médicament en développement et d'autre part d'identifier les mécanismes impliqués dans la toxicité, y compris lorsque les médicaments sont sur le marché. Des modèles *in vivo* et *in vitro* sont couramment utilisés.

I.3.1. Les modèles *in vivo*

Les modèles animaux sont utiles et nécessaires au développement préclinique des médicaments (Friese et al., 2006). En effet, certains tests sur animaux sont obligatoires. Différentes espèces sont utilisées car des différences inter-espèces sont habituellement observées. Des modèles de rongeurs KO et humanisés (souris notamment) permettent d'acquérir des informations particulières. Néanmoins, l'extrapolation des résultats à l'homme est toujours délicate dans ma mesure où des différences importantes peuvent exister dans la cinétique et les voies de biotransformation ainsi que dans le potentiel toxique des molécules. Ainsi, il n'existe aucun modèle animal capable de reproduire une toxicité hépatique associée à une réaction immune.

I.3.2. Les modèles *in vitro*

Plusieurs modèles peuvent être utilisés, par exemple le foie isolé perfusé, les coupes de foie, les fractions subcellulaires (mitochondries isolées, microsomes (Strittmatter and Velick, 1956)), les cellules non hépatiques exprimant un CYP, un transporteur,… Cependant ces modèles ont une durée courte et sont souvent d'obtention difficile et d'utilisation très limitée. Aussi, il est largement fait appel aux cultures de cellules hépatiques qui peuvent avoir une durée de vie longue et être d'origine humaine. Cependant, les hépatocytes primaires perdent rapidement une fraction importante de leurs fonctions lorsqu'ils sont ensemencés. De plus, les hépatocytes humains sont de qualité inégale, difficiles à obtenir et montrent des différences fonctionnelles d'un donneur à l'autre. Toutefois, diverses modifications des conditions de culture permettent d'améliorer la survie et un meilleur maintien des fonctions spécifiques (co-culture avec un autre type cellulaire, culture sur support matriciel ou mieux en sandwich ou encore en 3-D, sous forme de sphéroïdes notamment) (Guguen-Guillouzo and Guillouzo, 2010) (Swift et al., 2010). Les lignées de cellules hépatiques humaines représentent une alternative aux hépatocytes humains. Plusieurs lignées dérivées d'hépatome ont été obtenues, notamment les lignées HepG2 (Knowles et al., 1980) et Hep3B. Cependant elles ont un inconvénient majeur, surtout la lignée HepG2, qui est la très faible activité des enzymes de biotransformation, notamment les cytochromes P450 (Wilkening et al., 2003).

Cependant, une lignée plus récente, la lignée HepaRG, établie à partir d'un cholangio-carcinome humain provenant d'un patient souffrant d'une hépatite C, a révélé des propriétés d'hépatocytes matures. Durant la phase de prolifération, la population cellulaire de cette lignée apparaît assez homogène avec un phénotype de progéniteurs hépatiques. Lorsqu'elle atteint la confluence, sa

morphologie change progressivement. A ce stade, deux types cellulaires différents apparaissent. L'ajout de diméthylsulfoxyde (DMSO) renforce cette différenciation en cellules épithéliales granuleuses ressemblant à des hépatocytes adultes en culture primaire et d'autres cellules de type épithélial plus claires et aplaties. Après 2 semaines de confluence, environ 50-55% des cellules présentes dans la culture sont morphologiquement comparables à des hépatocytes humains primaires (Figure 6).

Les cellules HepaRG différenciées expriment des ARNm spécifiques du foie tels que ceux de l'albumine, l'aldolase B, de CYPs (1A1, 1A2, 2B6, 2C9, 2D6, 2E1 et 3A4), des enzymes de phase 2 (UGT1A1, GSTA4, GSTA1/A2, GSTM1) et des récepteurs nucléaires (Constitutive androstane receptor (CAR), Aryl hydrocarbon receptor (AhR), Pregnane X receptor (PXR)). Les taux de transcrits de ces différents marqueurs et les niveaux d'activité de la plupart des CYPs sont souvent comparables à ceux trouvés dans des cultures primaires d'hépatocytes humains (Aninat et al., 2006). En plus, ces cellules expriment la majorité des transporteurs d'efflux et d'influx des acides biliaires, des anions et des cations organiques et des médicaments , à savoir OCT1 (organic cation transporter 1), OATP (organic anion transporting polypeptide) -B, OATP-C, NTCP (Na+-taurocholate cotransporting polypeptide), MRP2 (multidrug resistance-associated protein), MRP3, BSEP (bile salt export pump) et MDR1 (multidrug resistance protein 1) (Le Vee et al., 2006) (Bachour-El Azzi et al., 2015). La présence des transporteurs hépatobiliaires et des enzymes de métabolisme des xénobiotiques rend cette lignée pertinente pour l'étude des effets des médicaments sur le flux biliaire.

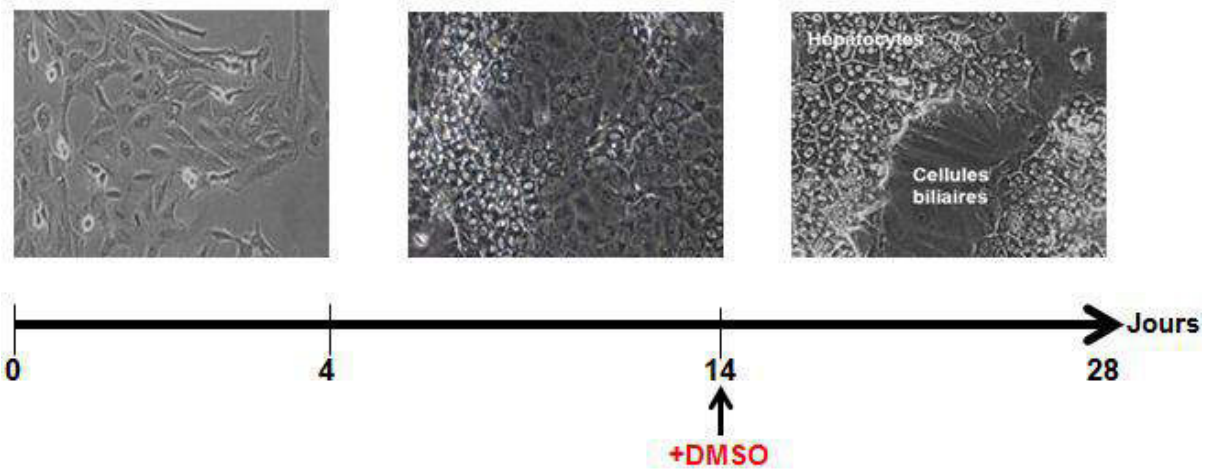

Figure 6: Différentes étapes de différenciation des cellules HepaRG en culture. « +DMSO » signifie ajout de diméthylsulfoxide. Ces cellules passent de l'état de progéniteur (à gauche) à un état bien différencié (à droite).

II. Classification des médicaments selon leur mode de toxicité

Selon leur mode de toxicité les médicaments peuvent être classés en deux grandes catégories : les médicaments à effet intrinsèque et les médicaments à mode d'action idiosyncratique.

II.1. Médicaments à effet intrinsèque

Les toxicologues se réfèrent souvent au foie comme « organe cible » des dommages induits par un médicament (Lehman-McKeeman, 2008). Le foie est en effet une cible pour de nombreux agents xénobiotiques intrinsèquement toxiques, y compris de nombreux médicaments. Ce type de toxicité est lié à la dose qui au-delà d'un seuil induit une toxicité de plus en plus importante avec l'accroissement de celle-ci.

Les lésions hépatiques induites par le médicament sont la principale cause de décès par insuffisance hépatique aiguë aux Etats-Unis et la raison la plus fréquente pour le retrait des médicaments du marché (Bleibel et al., 2007). L'acétaminophène (APAP) cible le foie, et le surdosage de ce médicament est responsable d'environ la moitié des cas d'insuffisance hépatique aiguë aux États-Unis (Bleibel et al., 2007) (Gunawan and Kaplowitz, 2007). Il provoque une hépatotoxicité liée à la dose chez les humains et les animaux et, en raison de l'importance clinique de sa toxicité, il est devenu le plus étudié des agents responsables d'une hépatotoxicité intrinsèque. Comme pour beaucoup d'autres agents hépatotoxiques, son activation métabolique est l'événement déclencheur. Elle conduit à la liaison covalente du métabolite réactif à des constituants cellulaires et le déclenchement de mécanismes secondaires pouvant aboutir à une nécrose hépatocellulaire dont la survenue peut dépendre de la dose mais aussi des conditions de traitement ainsi que de facteurs environnementaux et génétiques, en particulier l'activation de plusieurs types cellulaires non parenchymateux (cellules de Küpffer, cellules tueuses naturelles T, cellules endothéliales, etc.) et de voies de signalisation intracellulaire, la perturbation des mitochondries, la production de cytokines et d'espèces réactives de l'oxygène et de l'azote, l'hémostase, l'interférence avec la réparation de réplication d'ADN (Figure 7) (Ganey et al., 2004; Ganey et al., 2007; Gunawan and Kaplowitz, 2007).

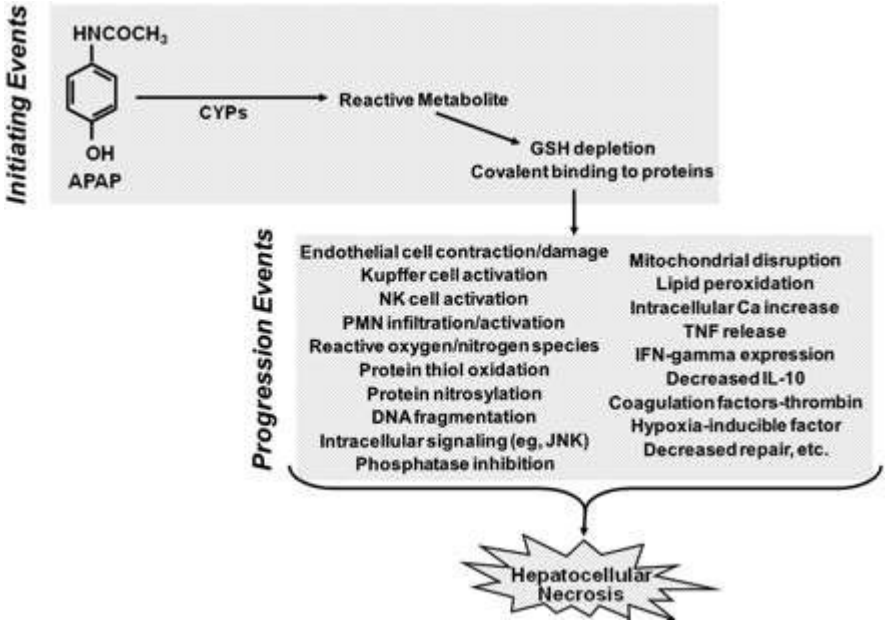

Figure 7: Initiation et progression de l'hépatotoxicité de l'APAP (Roth and Ganey, 2010). Les flèches désignent des réactions d'hydroxylation, de conjugaison et d'autres. L'APAP est métabolisé par des CYP450 pour donner des métabolites réactifs qui peuvent induire une déplétion de GSH aboutissant parsuite à une nécrose hépatocellulaire.

II.2. Médicaments à effet idiosyncratique

Les réactions médicamenteuses idiosyncrasiques (IDR) sont les effets indésirables imprévisibles qui ne se produisent pas chez la plupart des patients, mais quand elles se produisent, elles peuvent être mortelles. Elles sont souvent considérées comme indépendantes de la dose, mais ce n'est pas tout-à-fait exact ; en effet elles sont souvent associées à la prise de doses quotidiennes élevées. Des exemples de IDR sont l'insuffisance hépatique induite par la troglitazone, souvent mortelles ou ayant nécessité la transplantation de foie, l'agranulocytose induite par la clozapine (un type essentiel de globule blanc disparaît soudainement ce qui rend le patient vulnérable à l'infection) et la nécrolyse épidermique toxique induite par des sulfamides (lésion très sévère de la peau ressentie comme une brûlure thermique).

Ce type de réaction indésirable à un médicament est responsable d'un nombre important de décès et sa nature imprévisible le rend pratiquement impossible à prévenir. L'IDR n'est pas prédite par l'expérimentation animale et l'ampleur du problème peut généralement être évaluée seulement après le traitement de nombreux patients. Elle peut conduire au retrait du médicament ou à restreindre son emploi.

La toxicité idiosyncrasique a été différemment définie, et le terme a souvent été mal utilisé, ajoutant aux difficultés de mieux comprendre les effets indésirables et leurs mécanismes sous-jacents. Une des principales raisons de cette confusion est que les pharmacologues, les immunologistes, les hépatologues cliniciens et les toxicologues, tous ont leurs propres définitions de l'idiosyncrasie. L'idiosyncrasie concerne les caractéristiques propres à un individu, ce qui implique que dans ce cas celles-ci soient distinctes de celles de la grande majorité des individus. Parmi les causes qui déterminent la sensibilité de certains sous-ensembles de patients à un médicament, il y a en particulier les facteurs génétiques (Goldstein, 1974) ainsi que des déterminants acquis et induits par l'environnement, y compris les maladies sous-jacentes, l'état nutritionnel, la polymédication, le stress cellulaire, ou des infections (Boelsterli, 2003b) (Buchweitz et al., 2002). Toutefois, une distinction stricte dans la toxicité des médicaments entre intrinsèque (prévisible) et idiosyncratique (non prévisible) n'est pas toujours simple à établir pour les raisons suivantes: (1) les réactions idiosyncratiques peuvent être qualitativement semblables à celles observées chez tous les individus, mais peuvent prendre la forme d'une extrême sensibilité à de faibles doses. Ainsi, dans certains cas, le même médicament peut causer une hépatotoxicité idiosyncratique chez les humains tout en produisant des lésions hépatiques dans des modèles animaux à des doses très élevées (Amacher, 1998; Eaton, 1996); (2) les réactions idiosyncratiques sont des réponses biologiques (Uetrecht, 1999); et (3) les réactions idiosyncratiques (de l'avis des toxicologues) ne signifient pas nécessairement une implication de réactions immunoallergiques. Cependant avec certains médicaments on peut observer une toxicité classique limitée et réversible (augmentation de transaminases,…) chez un grand nombre de patients et une toxicité idiosyncratique associée à une réaction immune dans de très rares cas (par exemple avec l'halotane). En conséquence, les réactions idiosyncratiques peuvent être considérées comme des réponses toxiques déterminées par des facteurs individuels de sensibilité qui augmentent la pénétrance (proportion de personnes touchées) et l'expressivité (consistance ou gravité de la pathologie) de la toxicité intrinsèque d'un médicament ou de ses métabolites (Boelsterli, 2003c).

Dans le tableau suivant une liste de médicaments à effet idiosyncratiques :

Médicament	**Utilisation thérapeutique**
Diclofénac	Antiinflammatoire
Trovafloxacine	Antibiotique
Chlorpromazine	Antipsychotique
Troglitazone	Antidiabétique
Ximélagatran	anticoagulant
Tacrine	Anesthésiant
Isoniazide	Antibiotique
Flucloxacilline	Antibiotique
Bosentan	Traitement de l'hypertension artérielle
Amoxicilline/clavulanate	Antibiotique

Tableau 2: Quelques médicaments responsables d'une hépatotoxicité de type idiosyncratique.

L'hépatotoxicité idiosyncratique n'est le plus souvent pas liée à l'action pharmacologique d'un médicament. Par exemple, la trovafloxacine a causé une hépatotoxicité grave chez des patients, alors que la lévofloxacine, un antibiotique de la même classe des fluoroquinolones, n'a aucun effet toxique. D'autre part, les médicaments anti-inflammatoires non stéroïdiens (AINS) qui sont des inhibiteurs non spécifiques de cyclooxygénases 1 et 2 (par exemple, le diclofénac, le sulindac) semblent tous avoir la capacité de causer des lésions hépatiques, de sorte que le potentiel de causer une hépatotoxicité idiosyncratique semble s'appliquer à l'ensemble de cette classe de médicaments.

La liste des médicaments qui causent une hépatotoxicité idiosyncratique est longue et continue de croître en partie parce qu'il n'existe pas de tests précliniques efficaces pour identifier des médicaments candidats ayant le potentiel de provoquer une telle hépatotoxicité (Kaplowitz, 2005). Bien que plusieurs hypothèses aient émergé au fil des ans pour les expliquer, de telles réactions restent mal comprises. Différents facteurs peuvent être impliqués dans les réactions médicamenteuses idiosyncratiques. Certains de ces facteurs sont énumérés dans le

Tableau **3**.

Age
Sexe
Métabolisme
Réaction Immunologique
Absorption/distribution
Maladie coexistante
Inflammation
Co-exposition à deux ou plusieurs xénobiotiques
Statut nutritionnel
Dose quotidienne

Tableau 3: Quelques déterminants de la sensibilité individuelle aux agents hépatotoxiques.

III. Inflammation et toxicité hépatique des médicaments

III.1. Le système immunitaire : structure et fonction

Le système immunitaire est le système de défense contre les organismes étrangers attaquant le corps humain en discriminant les cellules du soi et les cellules du non soi via la reconnaissance par le système HLA du corps étranger ou de molécules spécifiques à la surface des intrus. Ce système est composé de différents acteurs cellulaires (Figure 8) dont les missions dépendent du type de défense (immunité innée ou adaptative). Ces cellules dérivent toutes de la moelle osseuse mais leur lieu de maturation dépend de leur type : par exemple les lymphocytes B se différencient dans la moelle osseuse tandis que les lymphocytes T après formation dans la moelle se différencient dans le thymus. En fait, les progéniteurs lymphoïdes sont à l'origine des lymphocytes et des cellules NK tandis que les progéniteurs myéloides sont les précurseurs des macrophages, des granulocytes, des cellules dendritiques et des mastocytes (Charles A Janeway, 2001).

- Les lymphocytes B : ils sont synthétisés dans la moelle osseuse puis migrent vers le thymus pour se différencier en plasmocytes qui possèdent des vésicules de Golgi capables de sécréter des anticorps spécifiques afin de neutraliser les antigènes.

- Les lymphocytes T : ce sont les cellules responsables de la reconnaissance spécifique des antigènes. Il existe deux types : les CD4+ et les CD8+. Les CD4+ appelés aussi les Th ou « T helper » puisqu'ils activent les autres lymphocytes via la sécrétion des cytokines. Les CD8+ sont des lymphocytes à activité cytolytique ; ils peuvent détruire des cellules infectées par un virus ou par d'autres agents pathogènes, cette lyse cellulaire se fait via la sécrétion des perforines créant un pore au niveau de la cellule cible et les granzymes aboutissant à la mort cellulaire.

-Les macrophages: ils dérivent des monocytes, et leur rôle principal est un rôle de phagocytose. Ces cellules se trouvent dans plusieurs organes sous différents noms. Par exemple, dans le foie ces cellules sont les cellules de Küpffer.

- les cellules dendritiques : leur nom provient de leur structure composée des dendrites nécessaires à leur fonction principale qui est la présentation des antigènes aux autres cellules du système immunitaire ; on les appelle les chefs d'orchestre de ce système. Elles ont deux rôles principaux : le déclenchement de la réponse immunitaire adaptative via l'activation des

lymphocytes B et des lymphocytes T et le maintien de la tolérance du système immunitaire au soi.

Il faut noter que lors d'une maladie une interconnection existe entre les différents types cellulaires du système immunitaire mais finalement l'activation de ces cellules est dépendant du type d'infection, que celle-ci soit virale, bactérienne ou secondaire suite à l'exposition à un xénobiotique comme les médicaments.

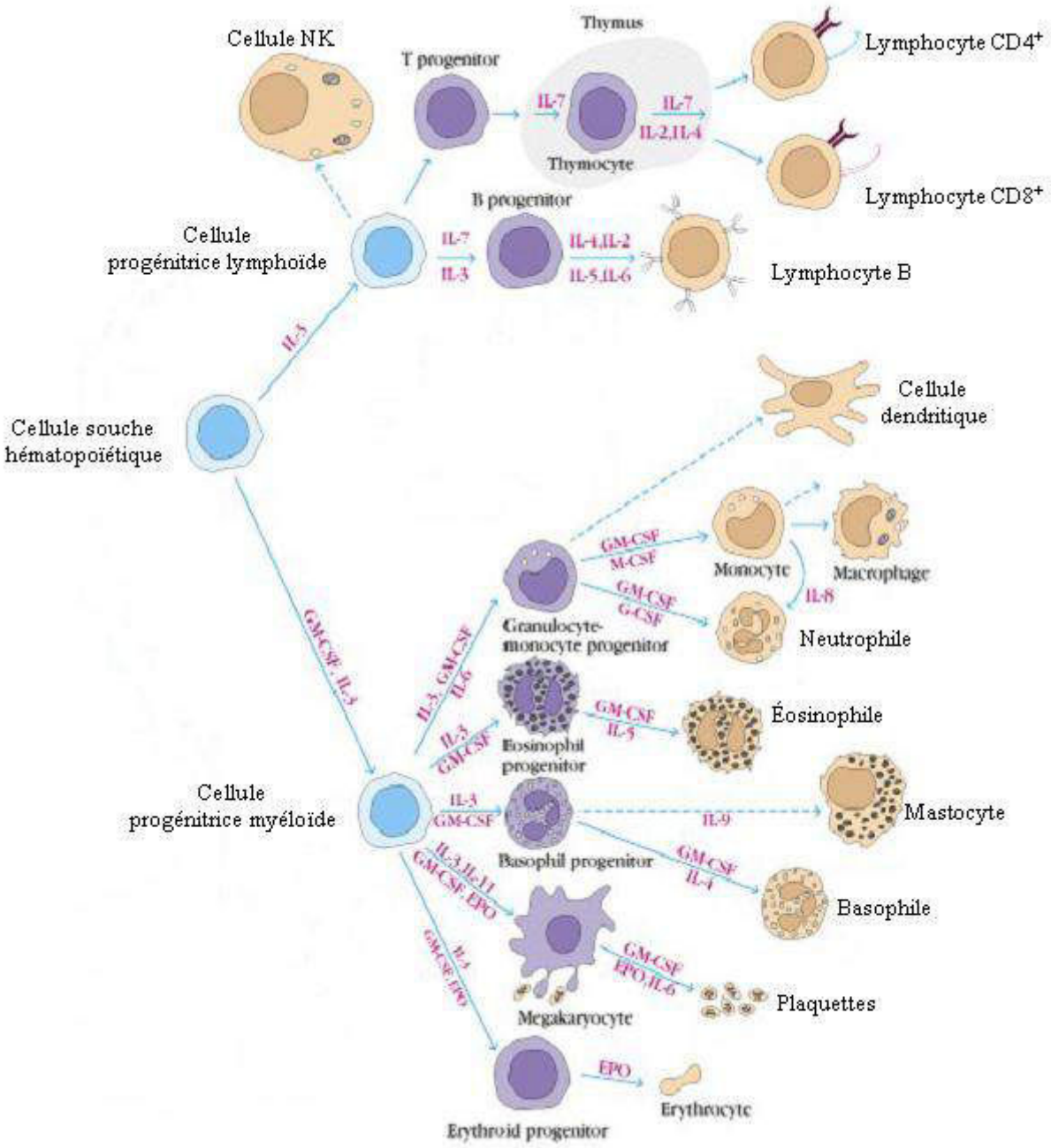

Figure 8: Hématopoïèse du système immunitaire (Goldsby R.A., 2000). Les flèches désignent la formation de différentes cellules immunitaires à partir des progéniteurs ainsi que leur maturation. Une cellule souche hématopoïétique donne naissance à un progéniteur lymphoïde ou myéloïde selon la cytokine sécrétée dans l'environnement entourant ces cellules. Ces progéniteurs donnent à leur tour les différentes cellules du système immunitaire (lymphocytes, basophiles…) en fonction des cytokines sécrétées dans le milieu péricellulaire.

III.2. Impact de l'inflammation sur le mécanisme de toxicité des médicaments

Dans ce contexte, de nombreux médicaments peuvent causer des lésions hépatiques via des réactions qui peuvent être prévisibles (doses dépendantes ou intrinsèques) ou non prévisibles non dose dépendantes (idiosyncratiques). Les médicaments sont une cause importante des différentes maladies du foie (les virus en sont sans doute la cause principale) et ils sont classés selon leur utilisation clinique (effets) et leur mode de toxicité. Dans ce contexte, l'inflammation peut jouer un rôle aggravant de la toxicité induite par ces molécules.

III.2.1. Le stress inflammatoire est un déterminant de la sensibilité des hépatotoxiques intrinsèques

Il est bien connu que la sensibilité des individus aux effets toxiques des médicaments et autres produits chimiques varient beaucoup. Par exemple, de grandes variations dans la susceptibilité à l'hépatotoxicité de l'APAP existent chez les humains et les animaux. Certaines personnes qui consomment l'APAP à des doses quotidiennes (4 g/jour) dans la fourchette thérapeutique, peuvent répondre par une augmentation des marqueurs de lésions hépatiques (transaminases), alors que la plupart des gens sont beaucoup moins sensibles (Watkins et al., 2006).

Un facteur déterminant dans la sensibilité semble être le stress inflammatoire. La réponse inflammatoire commence souvent par l'exposition à des micro-organismes ou leurs produits. Parmi ceux-ci, le lipopolysaccharide (LPS) de bactéries Gram négatif a reçu le plus d'attention. Les produits microbiens activent une variété de cellules en se liant à des récepteurs de type Toll ; ceci entraine une activation de voies de signalisation intracellulaires aboutissant à la production et / ou la libération de nombreux médiateurs de l'inflammation. Ces médiateurs comprennent plusieurs facteurs de transcription, des lipides bioactifs, tels que les prostanoïdes et leucotriènes, diverses cytokines et des enzymes, et des espèces réactives de l'oxygène et de l'azote (Figure 9). Grâce à l'action de ces facteurs, d'autres cellules sont activées et l'homéostasie tissulaire est altérée. La réaction se termine habituellement par l'élimination des microbes pathogènes à partir de tissus et est donc généralement bénéfique. Toutefois, si elle est trop prononcée, elle peut léser les organes de l'hôte. En effet, l'inflammation peut être considérée comme un facteur limitant qui doit être étroitement contrôlé pour éviter des dommages aux tissus.

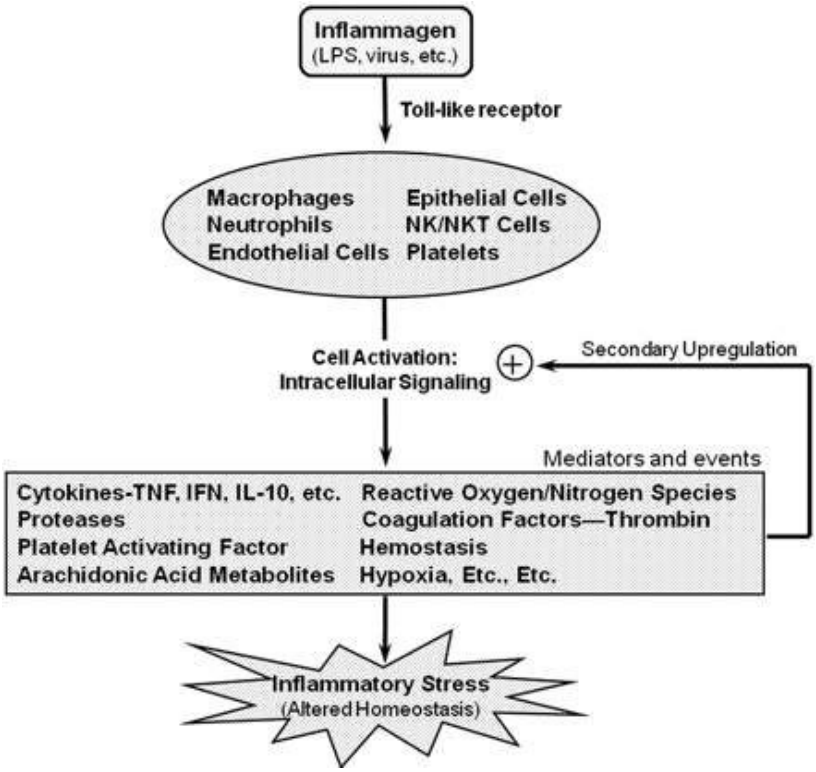

Figure 9: Réponse inflammatoire suite à une exposition au LPS (Roth and Ganey, 2010). Une atteinte par un agent inflammatoire peut activer les cellules du système immunitaire qui à leur tour peuvent déclencher un stress inflammatoire altérant l'homéostasie cellulaire. Le symbole « + » désigne une induction.

Il est facile de comprendre que l'homéostasie tissulaire modifiée par un stress inflammatoire pourrait être sensible à une contrainte secondaire imposée par une exposition à un xénobiotique. Par exemple, une comparaison entre les facteurs et les événements impliqués à la fois dans la progression de l'hépatotoxicité de l'APAP (Figure 7) et dans la réponse inflammatoire (Figure 9) révèle des points communs et par conséquent le potentiel d'interaction qui pourrait modifier la lésion. En effet, une interaction peut exister entre la consommation de l'APAP et les virus des hépatites (c'est-à-dire les agents inflammatoires qui ciblent le foie) et augmenter le risque de lésions hépatiques graves (Yaghi et al., 2006) (Moling et al., 2006) (Kc, 2007) (Nguyen et al., 2008). De même, il a été rapporté récemment que l'infection de souris avec un virus a induit une inflammation hépatique et rendu hépatotoxiques des doses non toxiques d'APAP (Maddox et al., 2010).

Un autre facteur de susceptibilité dans l'insuffisance hépatique induite par l'APAP chez l'homme est la consommation d'alcool. La capacité de l'alcool à réduire le taux de glutathion mitochondrial

et à accroître la bioactivation de l'APAP est largement admise pour expliquer l'interaction APAP-alcool dans les mécanismes de l'hépatotoxicité de ce médicament (Slattery et al., 1996) (Tanaka et al., 2000) (Zhao and Slattery, 2002); Cependant, l'éthanol augmente également l'exposition systémique au LPS, sans doute en augmentant la perméabilité intestinale à cet agent inflammatoire (Bode and Bode, 2003) (Bode and Bode, 2005) (Purohit et al., 2008). Il est à noter que les souris traitées avec une dose de LPS peu inflammatoire sont devenues plus sensibles à une lésion hépatique induite par l'APAP; l'exposition simultanée au LPS et à l'APAP rend des doses normalement non toxiques de l'APAP très toxiques (Maddox et al., 2010). Ainsi, la capacité de l'éthanol à faciliter la translocation intestinale du LPS dans le foie est susceptible de jouer un rôle dans l'hépatotoxicité de l'APAP.

Les études ont révélé que le LPS interagit avec de nombreux agents intrinsèquement hépatotoxiques. Ceux-ci comprennent le tétrachlorure de carbone, la monocrotaline, la cocaïne, l'aflatoxine B1, et d'autres (Ganey et al., 2004). Les résultats soutiennent l'idée que le stress inflammatoire peut sensibiliser le foie à une variété d'hépatotoxiques intrinsèques.

III.2.2. Hépatotoxicité idiosyncratique et stress inflammatoire

Comme suggéré plus haut, l'inflammation peut être considérée comme un facteur qui peut interagir avec des médicaments ou d'autres agents pour produire des lésions du foie. L'inflammation est associée à de nombreuses maladies, y compris l'arthrite, l'hépatite virale, les infections bactériennes, les maladies parodontales, l'asthme, et bien d'autres. En outre, l'augmentation de la translocation de LPS et d'autres agents inflammatoires de l'intestin dans la circulation peut être associée à la consommation d'alcool, au régime alimentaire et à d'autres facteurs (Ganey et al., 2004). L'interaction d'un médicament avec un facteur inflammatoire pourrait expliquer l'apparition imprévisible des réactions idiosyncratiques indésirables d'origine médicamenteuse (IADRs) et le manque apparent de relation à la dose.

Cette hypothèse d'interaction médicament-inflammation a été présentée comme un stress inflammatoire qui améliore la toxicité d'un médicament. Cependant, il est tout aussi plausible qu'un médicament puisse améliorer la sensibilité du foie à un agent inflammatoire potentiellement hépatotoxique comme le LPS. Cela pourrait se produire, par exemple, si le médicament a amélioré la sensibilité à une lésion des hépatocytes à la suite de l'exposition au LPS. Alternativement ou en plus, le médicament pourrait faciliter l'exposition à un agent

inflammatoire lorsque les concentrations hépatotoxiques sont atteintes. Un médicament peut accroître l'exposition au LPS, par exemple, en lésant l'intestin permettant ainsi une meilleure translocation de LPS dans la circulation, ce qui augmente l'exposition au LPS dans la gamme de doses hépatotoxiques.

Par exemple, l'utilisation de la trovafloxacine a été limitée parce qu'elle a été associée à une hépatotoxicité idiosyncratique sévère chez des patients. Le co-traitement des rats ou les souris avec des doses non toxiques de trovafloxacine et de LPS a entraîné une hépatotoxicité se développant rapidement (Waring et al., 2006) (Shaw et al., 2007). En revanche, la lévofloxacine, qui n'a pas des effets hépatotoxiques comme la trovafloxacine (De Sarro and De Sarro, 2001), n'a pas causé même en synergie avec le LPS un dommage au foie chez les animaux. De même, la chlorpromazine et la ranitidine ont été associées à de nombreux cas d'hépatotoxicité chez les humains, et ces deux médicaments associés à des doses non toxiques de LPS, entraînent des lésions hépatiques (Buchweitz et al., 2002) (Luyendyk et al., 2003) (Deng et al., 2009).

Comme indiqué plus haut, le diclofénac et le sulindac sont des exemples d'AINS qui causent une hépatotoxicité idiosyncratique (Lewis et al., 2002) (Boelsterli, 2003a) (O'Connor et al., 2003). Chez le rat, le LPS convertit une dose non toxique de diclofénac en une dose toxique (Deng et al., 2006). Récemment, il a été montré que le sulindac agit de manière similaire avec le LPS (Zou et al., 2009). Ces résultats sont d'un intérêt particulier car les inhibiteurs de cyclooxygénase causent des lésions intestinales chez les humains et les rongeurs (Seitz and Boelsterli, 1998) (Atchison et al., 2000) (O'Connor et al., 2003), pouvant augmenter l'entrée de LPS ou de bactéries intestinales dans la circulation. En effet, de fortes doses de diclofénac sont hépatotoxiques par elles-mêmes chez les rongeurs, et la lésion hépatique est associée à une accumulation de bactéries dans le foie ; celles-ci peuvent être éliminées par une stérilisation pharmacologique du tractus intestinal (Deng et al., 2006). Ceci suggère que le LPS ou la translocation des bactéries contribuent à l'hépatotoxicité de diclofénac. En revanche, l'interaction entre le LPS et une dose plus faible, non-toxique du diclofénac n'a pas été diminuée par stérilisation intestinale; ce qui suggère que le médicament ne peut pas agir uniquement par exposition à des doses croissantes de LPS et qu'il peut également accroître la sensibilité au stress inflammatoire hépatocellulaire induite par le LPS (Deng et al., 2006).

Du point de vue histopathologique, les lésions chez les animaux co-traités avec LPS/médicament (tous les médicaments IADR associés mentionnés ci-dessus) aboutissent à une nécrose hépatocellulaire principalement dans la zone médiane intralobulaire accompagnée d'une infiltration des neutrophiles. Les facteurs qui déclenchent ces lésions sont inconnus. Toutefois, les cytokines, les neutrophiles, et un système hémostatique activé semblent être généralement impliqués dans la progression de la lésion. Ceci pourrait suggérer que les médicaments agissent en augmentant la sensibilité du foie au LPS, parce que l'aspect des lésions et les facteurs de progression connus sont semblables à ceux qui caractérisent une lésion hépatique après exposition à de fortes doses de LPS hépatotoxiques. Toutefois, certaines différences qualitatives en réponse au médicament/LPS ou LPS seul existent selon les modèles expérimentaux. Il est intéressant de noter qu'au moins certains des facteurs impliqués dans les interactions médicaments idiosyncratiques/LPS sont les mêmes que celles qui participent aux interactions médicaments intrinsèques /LPS (Ganey et al., 2004).

Pour la chlorpromazine et la ranitidine, plus de la moitié des études publiées mentionnent des signes précoces chez les patients, tels que fièvre, vomissements, diarrhée, etc., qui sont compatibles avec les marqueurs inflammatoires de prédisposition.

Les bactéries tuées par des antibiotiques peuvent libérer des composants cellulaires inflammatoires tels que le LPS. Les patients traités avec des AINS ont généralement des conditions inflammatoires telles que l'arthrite. Des polymorphismes conduisant à une altération de la production des protéines anti-inflammatoires telles que l'interleukine 10 et l'interleukine 4, ont été rapportés chez des patients ayant montré une réaction hépatotoxique au diclofénac (Aithal et al., 2004).

III.3. Réaction immunitaire et lésions hépatiques

Des inflammations récurrentes au niveau du foie peuvent être la cause de l'aggravation de la toxicité hépatique ou bien le résultat de cette toxicité.

Dans le premier cas, que ce soit la maladie, surtout l'atteinte par une bactérie (par exemple le pneumocoque responsable de 30% des cas de pneumonie) ou un virus (par exemple le virus responsable de l'hépatite B) le système immunitaire va réagir pour éliminer l'agent pathogène via l'activation de différentes types des cellules immunitaires (LB, LT, macrophages, cellules

dendritiques, cellules NK…). Cette activation est l'une des causes de sécrétion des cytokines pro-inflammatoires (TNF-α, IL-6, IL-1β…) qui sont des inhibiteurs du métabolisme hépatique des xénobiotiques (Abdel-Razzak et al., 1993) et des modulateurs d'autres éléments intervenant dans l'ADME (absorption, distribution, métabolisme et excrétion), et donc des co-facteurs aggravant la toxicité des médicaments dans le foie. C'est le cas par exemple de la co-administration du LPS et de l'isoniazide à des rats, qui a été associée à une augmentation des marqueurs de toxicité hépatique aux niveaux sérique et histopathologique ainsi qu'une diminution du taux de FXR associée à une diminution de BSEP et MRP2 en parallèle à une augmentation du taux de TNF-α (Su et al., 2014).

Dans le deuxième cas, le traitement d'un patient par un médicament peut être lui-même un activateur de ce système ; par exemple, la formation d'un adduit aux protéines par un médicament ou bien la lésion hépatocytaire causée par une molécule stimulant l'immunité contre le soi causant des dégâts au niveau du foie. Le diclofénac est un bon exemple de médicaments formant des adduits aux protéines après biotransformation (Hargus et al., 1994).

Dans les deux cas, l'inflammation peut être donc l'une des causes interagissant avec les mécanismes de toxicité des médicaments dans le foie. Ces interactions peuvent être accompagnées des différents types de maladies hépatiques comme : la cholestase, la stéatose et la mort cellulaire que ce soit de l'apoptose ou de la nécrose.

III.3.1. Inflammation et cholestase

La cholestase ou la cholestase associée au sepsis induite par l'inflammation , est l'un des problèmes majeurs chez les patients présentant une infection extra-hépatique. En réponse à la sécrétion des endotoxines microbiennes, une inhibition de l'expression des gènes codant des transporteurs des acides biliaires est observée. Cette inhibition est l'une des causes les plus importantes de diminution de flux des acides biliaires impliquant une cholestase sévère (Kosters and Karpen, 2010).

III.3.1.1. Le rôle de l'inflammation dans la cholestase

Des dérégulations au niveau moléculaire sont observées dans les cellules impliquées dans le flux biliaire en réponse à une lésion et à des facteurs de stress. La formation de bile est rapidement réduite lors d'une infection et d'une inflammation (Moshage, 1997) (Baumann and Gauldie, 1994).

La cholestase induite par une inflammation est souvent causée par le lipopolysaccharide (LPS) ou l'endotoxine libérée par des bactéries Gram-négatives, bien que les infections microbiennes Gram-positives et d'autres peuvent également être impliquées. Le LPS circulant est principalement éliminé par le foie. Les cellules résidentes mononucléaires (principalement des cellules de Küpffer) produisent des niveaux élevés de substances pro-inflammatoires (cytokines). Ces cytokines produites localement activent les récepteurs membranaires des hépatocytes et des cholangiocytes qui transduisent des signaux intracellulaires conduisant à une altération de l'expression et de la fonction des transporteurs (Mulder et al., 2009) (Geier et al., 2006) (Trauner et al., 1999a). Dans les hépatocytes, la régulation négative de systèmes de transport hépatique impliqués dans l'absorption et l'excrétion des acides biliaires ainsi que la régulation négative de la phase I et de phase II de détoxification entraînent une réduction de la production de bile, et l'accumulation d'acides biliaires et de toxines dans le foie et le sérum (Wagner et al., 2009) (Trauner et al., 2005).

Les cytokines pro-inflammatoires induites par le LPS sont impliquées dans la phase hépatique aiguë comme le facteur de nécrose tumorale alpha (TNF-α), l'interleukine-1 bêta (IL-1β) et l'interleukine-6 (IL-6) (Gabay and Kushner, 1999) (Baumann and Gauldie, 1994). Celles-ci et d'autres produits sécrétés sont libérés suite à l'activation des cellules de Küpffer, des cellules endothéliales sinusoïdales ainsi que les hépatocytes et les cholangiocytes suite à l'exposition au LPS. Le sepsis induit également la libération d'autres petites molécules telles que l'oxyde nitrique (NO), dont la production est causée par l'augmentation de l'activité des oxydes nitriques synthases eNOS et iNOS dans les cellules de Küpffer et les cellules endothéliales. NO a un double effet sur le foie: de faibles niveaux sont hépatoprotecteurs (ils vasodilatent, maintiennent le débit cardiaque, empêchent l'apoptose, et stimulent la circulation de la bile), alors que des niveaux élevés sont préjudiciables (ils réagissent avec le superoxyde pour produire des radicaux libres et promouvoir des lésions, une hypotension sévère, un collapsus vasculaire et une cholestase). Les prostaglandines sont également induites par LPS dans les cellules de Küpffer; elles ont un rôle de protection par la régulation négative des cytokines pro-inflammatoires.

Bien que les cellules de Küpffer jouent un rôle majeur dans la réaction inflammatoire hépatique au LPS (Nakamura et al., 1999) (Sturm et al., 2005), d'autres types de cellules contribuent à cet effet. Les hépatocytes peuvent produire des cytokines (Luster et al., 1994; Ohlinger et al., 1993)

et répondent à la production de protéines de phase aiguë. Les cholangiocytes produisent la cytokine IL-8 et les chimiokines MCP1 (Fava et al., 2005; Morland et al., 1997) et le LPS induit la sécrétion de TNF-α et de l'IL-12 (Fava et al., 2005) (Harada et al., 2003) (Chen et al., 2008). Dans l'ensemble, les réponses des cellules mononucléaires résidentes au LPS et d'autres produits microbiens, ainsi que la capacité de la cellule cible à reconnaître ces produits et les protéines sécrétées, déterminent le degré de modification de la fonction des transporteurs et, finalement, le degré et la durée de la cholestase.

III.3.1.2. La signalisation intracellulaire

Les effets du LPS sur l'expression des gènes hépatiques sont médiés par plusieurs voies de signalisation intracellulaire. Dans le sang le LPS est lié à la protéine de liaison du LPS, qui forme un complexe avec CD14 et MD2 pour se lier au Toll-Like Receptor 4 (TLR4), exprimé sur plusieurs types de cellules dans le foie (Seki and Brenner, 2008). De nombreuses voies intracellulaires en aval sont activées, y compris les voies MAPK kinase et NFκB, pour réguler l'expression des gènes des transporteurs, leur activité et leur localisation.

Le principal effet du LPS sur les cellules de Küpffer est d'activer la production de cytokines, par l'intermédiaire de l'activation de NFκB et d'AP-1 dans le noyau des cellules de Küpffer. Après leur libération, TNF-α, IL-1β, IL-6 se lient à leurs récepteurs respectifs sur les hépatocytes.

Dans les hépatocytes, les signaux inflammatoires (LPS directement ou indirectement par l'intermédiaire des cytokines effectrices) réduisent les niveaux d'expression de gènes et de protéines de transporteurs hépatocellulaires. Des études chez les rongeurs ont montré que le LPS et plusieurs cytokines réduisent l'expression des transporteurs principaux d'acides biliaires Ntcp (Slc10a1) et Bsep (ABCB11), situés sur les membranes basolatérale et canaliculaire respectivement (Geier et al., 2005; Ghose et al., 2004) (Green et al., 1996). La réduction de la fonction et de la liaison des récepteurs nucléaires qui régulent ces gènes semble jouer un rôle majeur dans cette réduction de l'expression génique (Mulder et al., 2009; Zollner et al., 2006). Cela est particulièrement vrai pour la classe II des récepteurs nucléaires (qui hétérodimérisent avec RXRα) ainsi que pour HNF1 et HNF4α. La plupart des autres transporteurs impliqués dans la formation de la bile, comme mentionné ci-dessus, sont réduits dans des conditions inflammatoires, et sont régis par ces facteurs de transcription. Des différences spécifiques dans la

régulation de ces transporteurs existent et la plupart des données sont tirées des études sur Ntcp, Bsep et Mrp2 (ABCC2) chez les rongeurs.

Chez ces derniers, le traitement par LPS conduit à une réduction importante à la fois de l'ARNm et de la protéine de Ntcp (Ghose et al., 2004) (Geier et al., 2003; Green et al., 1996; Kim et al., 2000; Kosters et al., 2009; Trauner et al., 1998b), résultant d'une diminution de la liaison des facteurs de transcription nucléaire HNF1 et RXR :RAR sur le promoteur du gène Ntcp et HNF1 du rat (Denson et al., 2000; Karpen et al., 1996; Trauner et al., 1998a) mais pas RXR: RAR sur ce promoteur chez la souris (Geier et al., 2005). Il existe des sites de liaison potentielle de FXR/RXR sur le promoteur du gène Ntcp chez les souris (Thomas et al., 2010). La régulation de Ntcp par HNF1 est influencée par HNF4α, qui est en amont de HNF1 (Miura and Tanaka, 1993) et des signaux inflammatoires réduisent les taux de la protéine HNF4α dans le foie de rat (Wang et al., 2001) et les cellules HepG2 (Li et al., 2006), mais pas dans le foie de souris (Kosters et al., 2009), par l'intermédiaire d'un mécanisme-dépendant de JNK (Li et al., 2006).

Des injections intra-péritonéales des cytokines TNF-α, IL-1β ou l'IL-6 donnent des effets similaires sur l'expression de Ntcp (Geier et al., 2005; Green et al., 1996; Kosters et al., 2009; Siewert et al., 2004), alors que des études avec des anticorps contre IL-1β ont suggéré que l'IL-1β peut être un régulateur majeur *in vivo* de l'expression de Ntcp au cours de l'inflammation (Geier et al., 2003). De même, un traitement *in vitro* avec le TNF-α et l'IL-1β diminue l'activité du promoteur de Ntcp dans les cellules HepG2 (Denson et al., 2000). Outre Ntcp, une réduction de l'expression de HNF1, PXR et CAR pendant l'inflammation (Wang et al., 2001) (Li and Klaassen, 2004) inhibe un deuxième groupe de transporteurs basolatéraux impliqués dans l'absorption des acides biliaires, les transporteurs d'anions organiques Oatp1, 2 et 4 (Oatp1a1, 1a4, 1b2) (Cherrington et al., 2004; Geier et al., 2003; Li and Klaassen, 2004). L'expression réduite de NTCP humaine et OATP2 (OATP1B1) a également été observée dans les biopsies de foies de patients atteints de cholestase induite par l'inflammation (Zollner et al., 2001) mais le mécanisme exact de la régulation transcriptionnelle de NTCP n'a pas encore été identifié.

En plus des effets sinusoïdaux de l'inflammation (faible expression et fonction des gènes Ntcp et Oatp), des inhibitions sont également observées dans l'expression de Bsep et Mrp2, deux transporteurs canaliculaires principaux responsables de flux d'acides biliaires (Geier et al., 2005; Trauner, 1997; Trauner et al., 1998a). Les réductions rapides et importantes de l'expression de ces

gènes de transporteurs aboutissent à une cholestase. Une régulation post-traductionnelle existe également (Kubitz et al., 1999), mais l'effet durable majeur semble être la réduction de la transcription de ces facteurs déterminants de la sécrétion de la bile. La réduction coordonnée de l'expression de ces transporteurs semble être liée à des quantités nucléaires réduites de facteurs de transcription, dont la plupart sont des membres de la superfamille des récepteurs nucléaires: HNF4α, FXR, RAR, PXR, RCA, et RXRα (Zollner et al., 2006) (Denson et al., 2000) (Ananthanarayanan et al., 2001) (Gerloff et al., 2002; Karpen, 2002; Kast et al., 2002; Plass et al., 2002). Les cascades de signalisation inflammatoires ciblent ces facteurs de transcription, soit par des modifications covalentes (par exemple de phosphorylation), soit par addition de nouveaux facteurs dans le complexe de transcription (par exemple, phospho-c-jun, IRF3) (Ghose et al., 2004; Kosters et al., 2009) (Beigneux et al., 2000; Hisaeda et al., 2004; Zimmerman et al., 2006).

Parmi les multiples voies intracellulaires de signalisation activées par le LPS et l'IL-1β, dans les hépatocytes c'est la voie JNK médiée par la phosphorylation (soit JNK1 ou JNK2) qui est responsable de la médiation des modifications post-traductionnelles de RXRα qui conduit à la réduction de RXRα nucléaire. Puisque RXRα est un partenaire d'hétérodimérisation nécessaire pour FXR, RAR, PXR, CAR et d'autres récepteurs nucléaires, sa fonction réduite explique la suppression rapide et coordonnée de l'expression du gène du transporteur hépatique (c'est le cas de BSEP, NTCP et MRP2) au cours de la cholestase induite par le LPS (Ghose et al., 2004; Kosters et al., 2009; Li et al., 2002; Zimmerman et al., 2006).

En plus de réduire les niveaux de protéines RXRα et leur liaison, LPS, TNFα ou IL-1β diminue de façon significative les niveaux d'ARNm de partenaires de RXRα (FXR, CAR, PXR) et peut également conduire à leur modification post-traductionnelle (Beigneux et al., 2002; Fang et al., 2004; Frankenberg et al., 2008; Kim et al., 2003; Teng and Piquette-Miller, 2005). Comme pour Ntcp, IL-1β semble être le principal régulateur de l'expression de Mrp2 au cours de l'inflammation médiée par LPS car le prétraitement par un anticorps anti-IL-1β conduit à la préservation de l'expression de Mrp2 (Geier et al., 2003).

Au cours de l'accumulation intracellulaire des acides biliaires d'autres transporteurs basolatéraux ou sinusoïdaux, tels que MRP3, MRP4 et Ostα / β, sont mobilisés pour exporter l'excédent accumulé des acides biliaires (Wagner et al., 2010) (Zollner et al., 2006). Mais les changements induits par l'inflammation peuvent freiner cette augmentation , ce qui pourrait atténuer la réponse

adaptative et conduire à l'aggravation de la rétention des acides biliaires. Par contre, chez certaines espèces comme le rat, l'expression de MRP3 est induite après traitement par LPS (Donner et al., 2004) et dans les cellules HepG2 et Huh7 après le traitement par de cytokine (Lee and Piquette-Miller, 2003). Une étude récente chez le rat suggère que l'expression de MRP4 n'est pas modifiée par le traitement LPS (Brcakova et al., 2009), tandis que les données pour Ostα / β sont limitées dans l'inflammation. Tous ces transporteurs participent à l'exportation sinusoïdale des acides biliaires, et si leur expression est altérée par l'inflammation, ils pourraient ne plus être en mesure de répondre adéquatement à la charge d'acides biliaires, ce qui peut donc aggraver l'atteinte hépatique liée aux acides biliaires accumulés.

Des découvertes récentes montrent que NFκB interagit avec les récepteurs nucléaires, en particulier FXR et PXR, ce qui ajoute une complexité à la régulation des transporteurs dans des conditions inflammatoires (Wang et al., 2008; Zhou et al., 2006). Les résultats de ces études suggèrent une interaction réciproque entre FXR et NFκB lorsqu'ils sont activés par une inflammation ou un ligand, respectivement: l'activation de NFκB par LPS antagonise l'activité de FXR et suggère un rôle anti-inflammatoire pour FXR, où l'activation de FXR inhibe NFκB. En effet, l'expression des cytokines induite par le LPS est nettement accrue chez les souris n'exprimant pas FXR.

Les réponses inflammatoires cholestatiques du foie ne sont pas limitées à des hépatocytes, mais des réactions inflammatoires des voies biliaires se produisent également. IL-1β induit la dégradation par le protéasome d'Asbt dans les cholangiocytes (Xia et al., 2004) via sa phosphorylation par JNK.

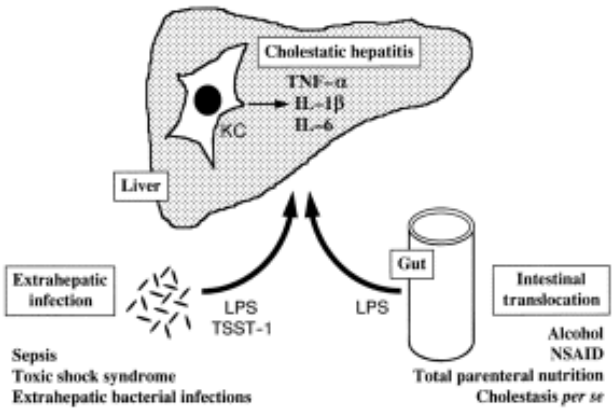

Figure 10: Médiateurs inflammatoires induisant la cholestase (Trauner et al., 1999a). Une infection extrahépatique par une bactérie peut aboutir à la sécrétion d'endotoxines comme le LPS, qui induit des cellules de küpffer ce qui crée un stress inflammatoire aggravant la cholestase hépatique. Les flèches désignent un transport d'un tissu à un autre.

III.3.1.3. Chlorpromazine : un exemple de la relation entre inflammation et cholestase

La chlorpromazine (CPZ) est le premier médicament psychotique typique. Malgré son réel bénéfice, il est aussi connu par ses effets hépatotoxiques dont la cholestase (Hollister, 1957) (Regal et al., 1987), la nécrose hépatocellulaire et la phospholipidose, chez certains patients (Velayudham and Farrell, 2003). Divers troubles hépatiques induits par CPZ ont également été décrits expérimentalement *in vivo* et *in vitro*, mais ils ont été principalement limités à des lésions hépatiques associées à la mort cellulaire, généralement amplifiées par un prétraitement avec des agents inflammatoires (Buchweitz et al., 2002; Gandhi et al., 2010; MacAllister et al., 2013). Aucune preuve d'une relation entre concentration de CPZ et altérations de canalicules biliaires n'a été apportée chez les rats traités avec LPS et CPZ (Buchweitz et al., 2002). Cependant, une étude récente sur les cellules HepaRG a montré que le co-traitement de ce modèle avec CPZ et des cytokines pro-inflammatoires (IL-6 et IL-1β) est associé à plus de toxicité, incluant des altérations des canalicules biliaires, par comparaison avec les cellules traitées par CPZ seule ou les cytokines seules, surtout après 5 jours de traitement. Outre la synergie prouvée entre la CPZ et les cytokines pro-inflammatoires dans l'aggravation de la toxicité dans les cellules HepaRG, cette étude a montré que l'inflammation peut augmenter l'effet cholestatique de la CPZ dans les hépatocytes via l'inhibition au moins au niveau de l'expression génique du NTCP et de BSEP impliquant donc une accumulation possible des acides biliaires et donc une augmentation de la toxicité. Une inhibition de l'activité de NTCP a été observée après 5 additions de CPZ, cette activité diminue de plus en plus après co-traitement avec les cytokines (Bachour-El Azzi et al., 2014). Toutefois une aggravation de la déformation des canalicules biliaires n'a pas été rapportée.

III.3.2. Inflammation et stéatose

Différentes études ont montré une relation entre l'inflammation et la stéatose hépatique. Un traitement des souris avec du TNF-α augmente le poids de leur foie, le niveau sérique des acides gras et le niveau des acides gras synthases ainsi que de l'élément régulateur de liaison du stérol à la protéine C. L'injection intrapéritonéale de LPS dans le but d'induire l'expression du TNF-α accélère l'accumulation des lipides dans le foie. Cet effet a été diminué après un prétraitement avec un anticorps anti-TNF-α qui réduit dans ce cas l'expression de l'élément régulateur de liaison du stérol à la protéine C (Endo et al., 2007). De même, la NAFLD (Non-alcoholic fatty

liver disease) ou la stéatose hépatique non alcoolique peuvent être améliorées lors de l'inflammation grâce à l'accumulation des cellules immunitaires comme les macrophages et les cellules NK T, ceci a été montré chez l'homme et confirmé chez les souris chez qui l'injection intrapéritonéale d'un anticorps anti-CXCL16 inhibe l'accumulation intrahépatique des cellules NK T, diminue l'infiltration hépatique des macrophages et diminue par conséquence le taux de TNF-α et du MCP-1 et donc l'accumulation des acides gras. En plus, chez les souris ayant une lésion hépatique une augmentation de l'expression de CXCL-16 a été observée (Wehr et al., 2014) montrant le rôle de ces chimiokines dans les maladies hépatiques. De même, chez les patients ayant une stéatose hépatique associée à l'alcool une augmentation des marqueurs hépatiques a été détectée dans les échantillons de sang ; parmi ces facteurs existent des chimiokines comme l'IL-8 et des marqueurs de l'inflammasome (IL-1β, IL-18, caspase-1, IL-6, CCL2 et CCL18) (Voican et al., 2015).

III.3.3. Inflammation et mort cellulaire

L'inflammation est l'un des facteurs les plus associés à la mort cellulaire qu'il s'agit de la nécrose ou de l'apoptose. C'est le cas par exemple de la consommation d'alcool qui entraine une stimulation du système immunitaire aboutissant à des lésions hépatiques (Voican et al., 2011). En fait, une fois consommé l'alcool est principalement métabolisé par le CYP2E1 et l'alcool déshydrogénase pour donner l'acétaldéhyde avec induction d'un stress oxydant inhibant l'hepcidine , ce qui entraine une accumulation de fer et donc une augmentation des radicaux libres stimulant la sécrétion des cytokines pro-inflammatoires (TNF-α, IL-1β, IL-6…). Le LPS peut agir en synergie avec cette stimulation immunitaire et ainsi aggraver l'effet inflammatoire (Figure 11).

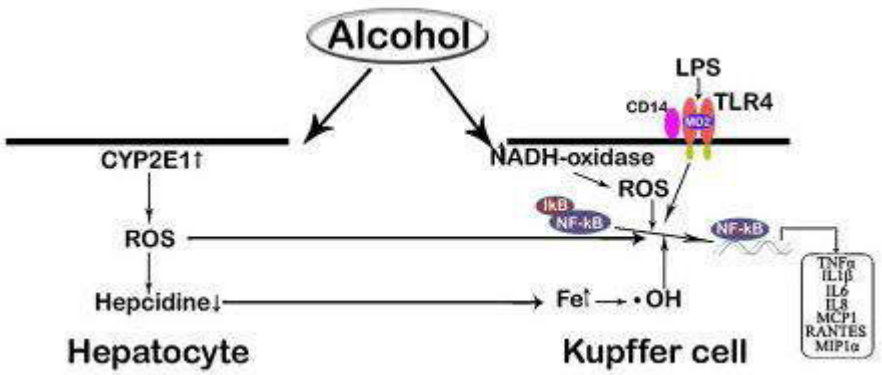

Figure 11: Effet du métabolisme de l'alcool sur les cellules de Küpffer (Voican et al., 2011) (modifiée). Les flèches désignent une induction. La biotransformation de l'alcool via le CYP2E1 peut aboutir à une induction de stress oxydant aggravée en présence de LPS et donc aboutissant à une hépatotoxicité.

La sécrétion des cytokines pro-inflammatoires par les cellules de Küpffer peut induire directement la génération de ROS (espèces réactives de l'oxygène) dans les hépatocytes, aboutissent directement à des lésions hépatiques qui se manifestent par une nécrose et/ou une apoptose. Les cellules de küpffer peuvent servir d'intermédiaires qui vont activer la différenciation des lymphocytes Th17 sécrétant à leur tour des chimiokines (CCL2 and CCL20) qui attireront les neutrophiles. Ceux-ci induisent des ROS et sécrètent des protéases provoquant des lésions hépatiques. Une autre activation des neutrophiles peut être faite directement par les cellules de Küpffer via une stimulation par le TNF-α et l'IL-1β (Figure 12). Dans ce cas, la lésion hépatique a pour cause principale l'alcoolisme associé à une activation du système immunitaire (Voican et al., 2011).

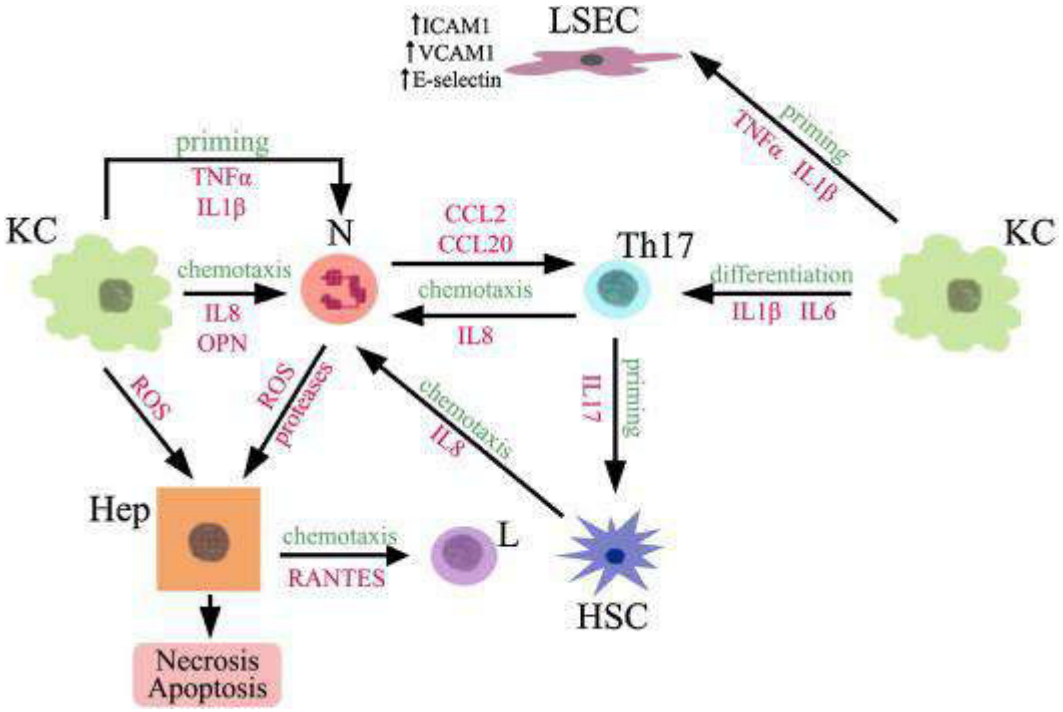

Figure 12: Effets de l'activation du système immunitaire sur les lésions hépatiques (Voican et al., 2011). L'activation des cellules de Küpffer aboutit à la sécrétion des cytokines inflammatoires et des chimiokines par ces cellules ce qui active d'autres cellules du système immunitaire (Th17, neutrophiles) et induit un stress inflammatoire conduisant à des lésions des cellules hépatiques.

Une réponse inflammatoire peut aussi être le résultat et non seulement la cause de la mort cellulaire (Rock and Kono, 2008). Cette activation diffère par sa rapidité et son mécanisme selon

que la cellule concernée est nécrotique ou apoptotique. La cellule nécrotique gonfle puis éclate en libérant le contenu cytoplasmique telles que des cytokines pro ou anti-inflammatoires activant les lymphocytes T au niveau du thymus et activant ainsi la réponse immunitaire adaptative; ce mécanisme rend la réponse immunitaire plus rapide dans le cas d'une nécrose que d'une apoptose. En effet, durant ce dernier processus la cellule n'éclate pas ; elle conserve son intégrité membranaire et dans ce cas l'activation de la réponse inflammatoire n'aura lieu qu'après la sécrétion des cytokines anti-inflammatoires comme l'IL-10 et le TGF-β qui vont stimuler l'activation des macrophages et donc la phagocytose de la cellule endommagée, source de ce qui est appelé signal de danger (Figure 12).

IV. Diclofenac, Trovafloxacine et Amiodarone

Parmi les nombreux médicaments pouvant induire des lésions hépatiques nous nous sommes particulièrement intéressés au diclofénac, à la trovafloxacine et à l'amiodarone. Leurs caractéristiques sont décrites ci-dessous.

IV.1. Diclofenac

IV.1.1. Structure chimique

Le diclofénac (sel de sodium, M.M. = 318,1 g/mol) est un composé lipophile et faiblement acide (Poct = 28,4; pKa = 3,9) (Sengupta, 1985), formé de deux cycles aromatiques (Sallmann, 1985). Il s'agit d'un dérivé de l'acide phénylacétique, avec un groupement acide carboxylique qui est le substrat pour la production de métabolites glucuronides réactifs. Il a une épine dorsale, la diphénylamine, dont l'amine secondaire contribue à son activité de découplage dans les mitochondries et également à la production d'un stress oxydant (Galati et al., 2002) (Figure 13).

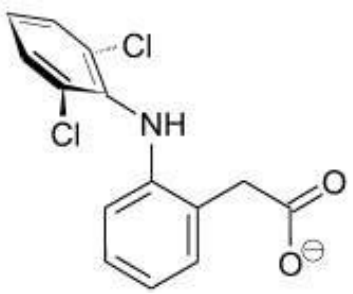

Figure 13: Structure chimique du diclofenac (https://pubchem.ncbi.nlm.nih.gov) (modifiée).

IV.1.2. Utilisation thérapeutique

Le diclofénac est un dérivé arylacétique ; il entre dans la classe des anti-inflammatoires non stéroïdiens (AINS) et est largement diffusé dans la pharmacopée mondiale sous diverses appellations. Au Canada, aux États-Unis, en Grèce et au Royaume-Uni, il est commercialisé sous le nom de Pennsaid®, un produit développé par la compagnie canadienne Nuvo Research. Au Canada, en France et aux États-Unis, il est aussi commercialisé sous le nom Voltaren® (ou Voltarène®) par Novartis (Altman et al., 2015). Il est couramment utilisé dans le traitement de diverses maladies en raison de ses propriétés antalgiques, antipyrétiques, anti-inflammatoires, inhibitrices des fonctions plaquettaires (Durrigl et al., 1975).

IV.1.3. Métabolisme hépatique

Le diclofénac est largement métabolisé dans le foie humain selon deux voies principales: tout d'abord, il subit une hydroxylation catalysée par CYP2C9, conduisant à la formation du principal métabolite hydroxylé (réactif), le 4'-hydroxydiclofénac (Stierlin and Faigle, 1979)(Figure 14). D'autres produits, quantitativement mineurs du métabolisme oxydatif comprennent le 5-hydroxydiclofénac, catalysé par CYP3A4 (k_m ~ 20 fois plus élevé que celui du CYP2C9) (Shen et al., 1999) (Tang et al., 1999a), et plusieurs autres métabolites mono-ou dihydroxylés ou méthoxylés (Blum et al., 1996) (Bort et al., 1999a). Le 4'-OH- et le 5-OH-diclofénac sont des protoxicants potentiels car ils peuvent eux-mêmes être oxydés en quinone-imines.

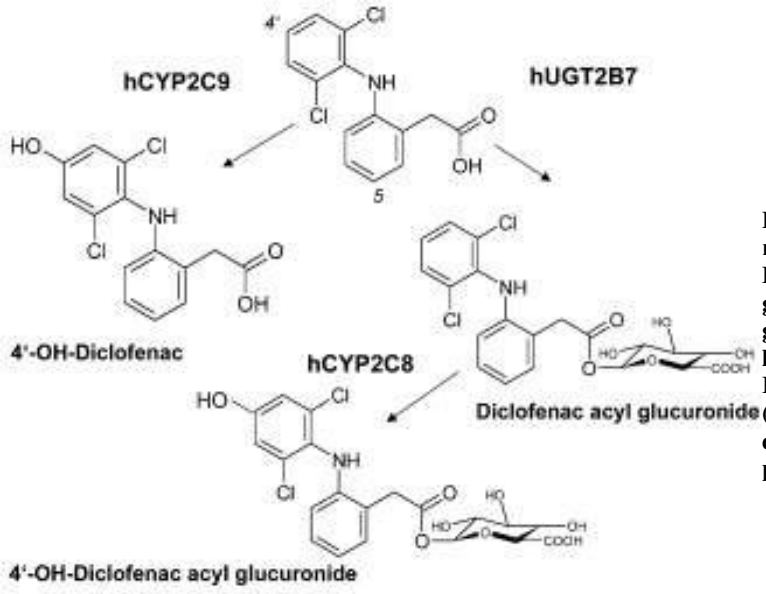

Figure 14: Les principales voies du métabolisme du diclofénac chez l'homme. Elles impliquent une hydroxylation et une glucuronidation. Une partie importante des glucuronides subit une hydroxylation de l'anneau secondaire (métabolisme de phase II suivi par un métabolisme de phase I) (Stierlin and Faigle, 1979). Les flèches désignent une réaction de phase I médiée par CYP.

La deuxième voie importante est la glucuronidation produisant le diclofénac 1-O-β-acylglucuronide (Stierlin and Faigle, 1979) (Kretz-Rommel and Boelsterli, 1993). Les isoformes impliquées dans la glucuronidation du diclofénac sont l'UGT2B7 chez l'homme et l'UGT2B1 chez le rat. Les deux isoformes présentent une faible K_m similaire et une V_{max} élevée (King et al., 2001). Ainsi les acylglucuronides sont eux-mêmes réactifs et sont impliqués dans la formation en aval des iso-glucuronides électrophiles.

D'autres données (Kumar et al., 2002) ont démontré que chez l'homme l'acyl glycuronide peut être hydroxylé par le CYP2C8 en 4'-hydroxydiclofénac acylglucuronide (Figure 14), majoritairement excrété par voie biliaire.

IV.1.4. Métabolites réactifs du diclofénac

IV.1.4.1. Quinone imine et oxydes d'arène

Les deux métabolites 4'-OH et 5-OH du diclofénac ont le potentiel d'être oxydés en une p-benzoquinone imine. Les quinone-imines sont des électrophiles bien connus qui peuvent, en raison de leur réactivité thiol, subir une liaison covalente avec des groupements sulfhydryle d'une protéine ou d'une molécule non protéique (Figure 15). Ils sont également impliqués dans le cycle rédox et dans la production d'un stress oxydant. En effet, dans les microsomes de rat, des adduits S-glutathionyl dérivés des 4'-OH et 5-OH diclofénac ont été détectés (Miyamoto et al., 1997) (Tang et al., 1999b). Ces produits peuvent être encore à leur tour dégradés et N-acétylés à la fois en 4'-OH- 3'-N-acétylcystéine (NAC) diclofénac et 5-OH-4-NAC diclofénac (Poon et al., 2001).

Dans l'urine humaine, seul le dérivé 5-OH-4-NAC a été identifié (Figure 15). Néanmoins, c'est une preuve claire que le foie humain peut activer un des principaux métabolites oxydés du diclofénac en un intermédiaire potentiellement thiol réactif.

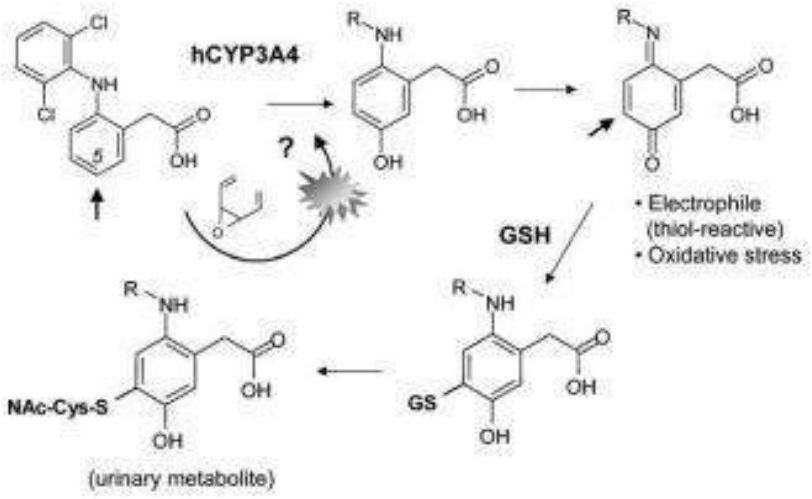

Figure 15: Métabolisme du 5-OH-diclofénac. Il conduit à la formation d'une p-benzoquinone imine potentiellement réactive , puis à une S-glutathionylation et une excrétion urinaire sous fome d'acide mercapturique chez l'homme. Le CYP3A4 peut également former un oxyde d'arène potentiellement réactif qui, en se liant, peut inactiver l'enzyme à des concentrations (1000µM) excessivement élevées *in vitro* (Poon et al., 2001) (modifiée). Les flèches désignent les différentes étapes aboutissant au métabolite urinaire (mercapturate)

Un tel complexe réactif protéine/métabolite peut aryler des cibles nucléophiles dans la cellule. L'un des principaux déterminants de la sélectivité de ces cibles est la réactivité intrinsèque de l'intermédiaire. Par exemple, dans le foie de rat un métabolite réactif de diclofénac formé *in vivo* se lie de manière covalente à Cyp2c11 comme une cible essentielle (Cyp2c11 est une forme

spécifique de Cyp du rat mâle, responsable de la 4'- et de 5-hydroxylation du diclofénac). La formation de cet adduit entraîne une diminution importante de l'activité de Cyp2c11 (Shen et al., 1997). Dans la mesure où le métabolite réactif n'a pas pu être piégé par GSH, il est probable qu'il s'agit d'un intermédiaire très réactif se liant au Cyp avant de pouvoir diffuser à distance et de réagir avec d'autres protéines. Comme l'addition du 4'- OH diclofénac ou du 5-OH diclofénac n'inactive pas le Cyp2c11 dans les microsomes (Masubuchi et al., 2001), il a été conclu qu'un oxyde d'arène, et non une quinone imine, est impliqué dans le mécanisme de l'inactivation de Cyp2c11.

Une inactivation similaire du CYP3A4 (mais pas du CYP2C9) a été démontrée dans des microsomes hépatiques humains (Masubuchi et al., 2002b). Là encore, la formation d'un oxyde d'arène, au lieu d'une p-benzoquinone imine, a été impliquée dans la liaison covalente. De telles études sont importantes car, pour d'autres médicaments, la liaison covalente et l'inactivation de certaines formes de CYP ont été impliquées dans l'apparition de l'hépatotoxicité idiosyncrasique à médiation immune. Alternativement, l'inhibition du CYP3A4, le principal CYP chez l'homme, pourrait conduire à des interactions médicamenteuses et une toxicité. Cependant, la Ki d'inhibition du CYP3A4 par le diclofénac est supérieure à 1 mM; par conséquent, la pertinence clinique de cette réactivité du CYP3A4 *in vivo* reste discutable (les concentrations plasmatiques thérapeutiques de diclofénac sont de l'ordre de 5-10µM) (Willis et al., 1979).

IV.1.4.2. Acyl glucuronides et iso-glucuronides

Le diclofénac 1-O-β-acyl glucuronide, comme les acyl glucuronides d'autres médicaments ayant un groupement acide carboxylique, est potentiellement très réactif en raison de sa liaison ester plutôt labile. Deux mécanismes majeurs de formation d'adduits covalents avec des résidus d'acides aminés sont possibles. Le premier mécanisme est une attaque nucléophile sur l'atome de carbone carboxylé par des groupes sulfhydryle, amino ou hydroxy (Faed, 1984). Le second mécanisme implique un réarrangement chimique spontané du glucuronide par la migration de l'aglycone le long des groupes hydroxy du cycle du sucre pour former les 2-O-β, 3-O-β et 4 -O-β glucuronides (= iso-acyl glucuronides) (Smith et al., 1986) (Spahn-Langguth and Benet, 1992) (Hayball, 1995) (Sallustio et al., 2000) (Boelsterli, 2002) (Bailey and Dickinson, 2003). Il a été déjà démontré que le diclofénac se lie aux protéines hépatocellulaires par deux mécanismes (Kretz-Rommel and Boelsterli, 1994a).

Des adduits aux protéines ont été trouvés dans des hépatocytes en culture exposés au diclofénac et chez le rat ou la souris *in vivo* (Kretz-Rommel and Boelsterli, 1993) (Gil et al., 1995; Hargus et al., 1994; Kretz-Rommel and Boelsterli, 1994b; Pumford et al., 1993; Wade et al., 1997). Un certain nombre de protéines modifiées de façon covalente ont été caractérisées par leur taille moléculaire, et certaines ont été identifiées par analyse de séquence. Chez les rongeurs, la grande majorité des adduits a été limitée à des domaines canaliculaires de la membrane plasmatique dans les hépatocytes (Hargus et al., 1994; Seitz and Boelsterli, 1998; Wade et al., 1997). Plus précisément, l'une des principales protéines cibles identifiées dans le foie de rat a été le dipeptidyl peptidase IV (DPP-IV) (Hargus et al., 1995). Cette sérine protéase est un ectoenzyme abondamment exprimé situé sur la membrane apicale des hépatocytes. Il est également une cible pour les acyl glucuronides des autres médicaments ayant un groupement d'acide carboxylique (Wang et al., 2002).

IV.1.4.3. Clairance des métabolites de diclofenac

Les premières études avaient estimé qu'environ 10-20 % de la dose totale de diclofénac administrée à l'homme est excrétée sous forme d'acyl glycuronide (Stierlin and Faigle, 1979). Mais les calculs ont montré un taux plus élevé équivalent à 75 % de la clairance totale du diclofénac (Kumar et al., 2002). Ces nouvelles données démontrent que l'acyl-glucuronidation est une voie principale de clairance du diclofénac chez l'homme, apportant des données cinétiques plus proches de celles mesurées chez le rat et le chien (70 et 98 % de la clairance totale respectivement).

Cependant, une fraction importante des glucuronides de diclofénac (M_r = 473) est éliminée par voie rénale chez l'homme, comparée à la voie biliaire chez les rongeurs, sans doute parce que l'homme a une limite de passage de molécules à travers la membrane plasmatique hépatobiliaire ayant un poids moléculaire plus élevé (~ 500 Da) que celle des rongeurs ou du chien (300-400 Da). Néanmoins, compte-tenu de la réactivité tissulaire importante des acylglucuronides et des iso-glucuronides, un rôle mécanistique possible de ces métabolites réactifs le long de la voie d'élimination hépatobiliaire devrait être envisagé.

Les glucuronides provenant du diclofénac ou de ses métabolites sont excrétés via la membrane plasmique canaliculaire dans la bile par l'intermédiaire de MRP2 (Seitz and Boelsterli,

1998)(Figure 16). En raison de l'existence d'un transport vectoriel ATP-dépendant, les concentrations de ces glucuronides dans les canalicules peuvent devenir très élevées.

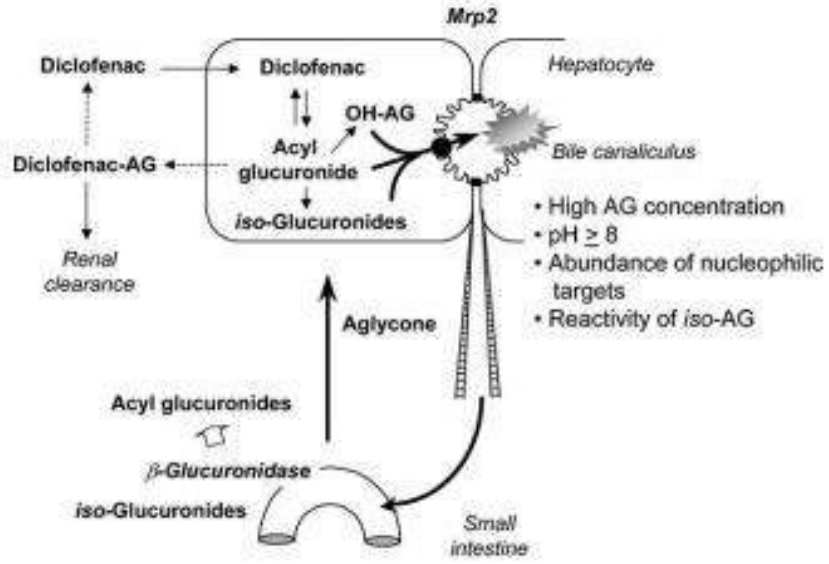

Figure 16: Clairance du diclofénac acylglucuronide (AG), de l'hydroxydiclofénac acylglucuronide, et des iso-glucuronides dans le foie. Tous ces glucuronides sont exportés dans le canalicule biliaire à travers la membrane canaliculaire par la pompe d'export de conjugués, Mrp2. Les intermédiaires glucuronidés réactifs peuvent se lier à des protéines cibles canaliculaires et à des protéines situées à distance. Dans l'intestin grêle, les acylglucuronides sont clivés par la β-glucuronidase (Boelsterli, 2003a). Les flèches désignent les différentes étapes d'absorption, de métabolisme et d'excretion.

Les acyl glucuronides peuvent être clivés dans l'intestin par la β-glucuronidase bactérienne, et ils peuvent, comme l'aglycone, subir plusieurs cycles de circulation entéro-hépatique, ce qui augmente le temps d'exposition hépatobiliaire à ce métabolite. En revanche, les iso-glucuronides, qui sont résistants à la dégradation de la β-glucuronidase, ne sont pas soumis à un cycle entéro-hépatique.

La liaison covalente n'est pas toujours un événement silencieux ; elle peut avoir des conséquences fonctionnelles. Par exemple, l'administration de diclofénac à des rats diminue l'activité d'un certain nombre de protéines de la membrane canaliculaire, comme la γGT, la Mg2 +-ATPase, ou la leucine aminopeptidase (Sallustio and Holbrook, 2001).

IV.1.5. L'induction de lésions hépatocellulaires

Les réponses toxiques au diclofénac sont habituellement retardées, et contrairement, par exemple à l'acétaminophène, l'atteinte hépatique aiguë secondaire à une forte exposition n'a pas été observée cliniquement. L'administration de doses orales uniques de diclofénac (jusqu'à 100-300 mg/kg) à des souris n'a pas entraîné de toxicité aiguë dans le foie alors que le rein était une cible (Hickey et al., 2001). Même l'exposition répétée (15 mg/kg/jour pendant 7 jours) chez le rat n'a pas augmenté l'activité de l'ALAT sérique (Sallustio and Holbrook, 2001). Mais dans une étude

plus récente chez la souris, 150 mg/kg de diclofénac a conduit à une augmentation de l'activité de l'ALAT sérique dès 1,5 h après administration, culminant à 3 h (> 6 fois plus) (Cantoni et al., 2003). Par conséquent, on peut penser que s'il est possible d'induire des lésions des cellules directement dans certains modèles expérimentaux, alors on pourrait avoir des indications sur des interactions entre le diclofénac et les cellules du foie.

Un certain nombre d'études sur des cultures d'hépatocytes de différentes espèces ont montré que des concentrations élevées (> 400 à 500 µM, en l'absence d'albumine ajoutée au milieu de culture) sont capables d'induire des lésions cellulaires aiguës (Kretz-Rommel and Boelsterli, 1993) (Jurima-Romet et al., 1994) (Bort et al., 1999b; Masubuchi et al., 1998; Ponsoda et al., 1995) (Masubuchi et al., 2000). Le mécanisme de cette toxicité cellulaire aiguë n'a pas été déterminé, et la pertinence de l'utilisation de ces concentrations élevées a été remise en question. Cependant, le choix de telles concentrations excessivement élevées d'un médicament n'a pas été fait pour mimer une situation thérapeutique mais plutôt pour définir un danger et, en utilisant des inhibiteurs spécifiques de voies biochimiques, pour obtenir des indices sur les mécanismes sous-jacents. Par exemple, la préexposition d'hépatocytes à 1 µM de sulfaphénazole (un inhibiteur spécifique de CYP2C), mais pas à d'autres inhibiteurs de cette sous-famille de CYP protège largement de la toxicité induite par diclofénac (Kretz-Rommel and Boelsterli, 1993). Ceci suggère que la toxicité aiguë pour les hépatocytes de rat peut être due à la formation d'un intermédiaire résultant de l'activité des CYP2C. En plus, l'inhibition du métabolisme oxydatif pourrait tout simplement conduire à une concentration plus élevée de la molécule mère de diclofénac disponible pour glucuroconjugaison.

IV.1.6. Le stress oxydant

Le stress oxydant induit par un médicament peut recruter principalement des voies de secours via l'activation des voies anti-oxydantes (catalase, superoxyde dismutase…) mais un stress prolongé peut provoquer des lésions mitochondriales, l'apoptose et/ou une nécrose.

Des preuves indirectes (avec des systèmes sans cellules) indiquent qu'un certain nombre d'AINS ayant des structures chimiques apparentées ne produisent pas un stress oxydant *in vitro,* bien que des concentrations élevées (100 µM à 1 mM) aient été utilisées (Galati et al., 2002). Le mécanisme sous-jacent reposerait sur la production des radicaux libres par la peroxydase, qui à leur tour peuvent oxyder GSH et NAD(P)H (Figure 17). Lors de la co-oxydation de GSH et de

NAD(P)H, de l'oxygène moléculaire peut être réduit et activé. En outre, les radicaux AINS peuvent subir un cycle rédox. Cependant, parmi un grand nombre d'AINS étudiés, le diclofénac a relativement une faible efficacité catalytique pro-oxydante. Il a été suggéré que la diphénylamine peut être oxydée en un radical cationique et/ou un radical nitroxyde.

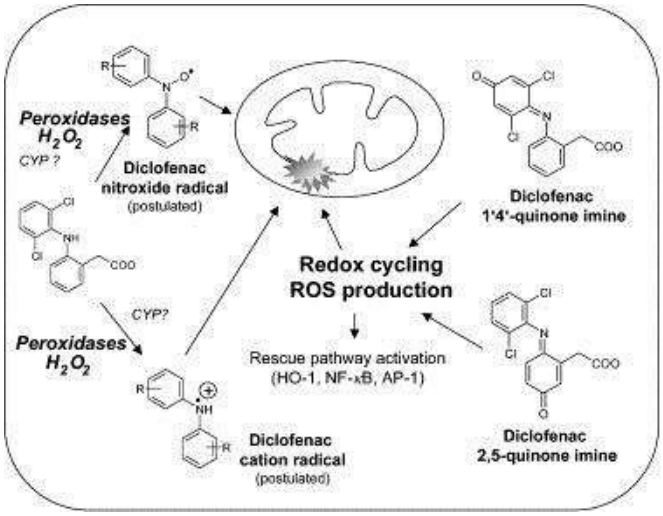

Figure 17: Stress oxydant et lésions mitochondriales induites par le diclofénac dans les hépatocytes. (Gauche) l'oxydation du diclofénac par la peroxydase conduit à un radical nitroxyde putatif (démontré pour la diphénylamine) ou un radical cationique. (Droite) L'imine 1'4'-diclofénac quinone (dérivée du 4'-OH-diclofénac) ou l'imine quinone 2,5-diclofénac (dérivée du 5-OH-diclofénac) peuvent potentiellement entraîner la génération d'un stress oxydant. HO-1, l'hème oxygénase-1 (Boelsterli, 2003a).

Le concept de la toxicité idiosyncrasique induite par les AINS dans le foie initiée par des radicaux libres et/ou le stress oxydant (provoquée par le métabolisme de la peroxydase) (Galati et al., 2002) apparaît intrigant; sa pertinence in *vivo* reste à démontrer. Il est possible que la formation de H_2O_2 endogène par des oxydases intracellulaires puisse initier un stress oxydant catalysé par la peroxydase (Siraki et al., 2002). D'autre part, à côté des réactions médiées par des CYP et des UGT d'autres voies métaboliques peuvent être impliquées comme les réactions dépendant de la voie peroxydasique.

D'autres études (Cantoni et al., 2003) ont fourni des preuves convaincantes en faveur d'un autre mécanisme contribuant au stress oxydant induit par le diclofénac. Chez les souris traitées avec des doses ≥ 100 mg/kg, l'hème-oxygénase hépatique-1 (HO-1) est induite au niveau transcriptionnel (HO-1 est un marqueur sensible et largement reconnu pour le stress oxydant). De plus, NF-kB et AP-1, deux facteurs de transcription rédox sensibles, sont facilement activés par le diclofénac. L'induction de HO-1 par le diclofénac dans des hépatocytes de rat en culture pouvant être largement réduite par des inhibiteurs des CYP2C et CYP3A (sulfaphénazole et kétoconazole, respectivement), on peut conclure que la production d'un stress oxydant accru lié à la bioactivation de diclofénac, est médiée par des CYP.

IV.1.7. Lésions mitochondriales

Un effet bien connu de fortes concentrations de diclofénac est un épuisement rapide de l'énergie cellulaire. Par exemple, l'exposition des hépatocytes de rat à 100 µM de diclofénac diminue la teneur en ATP cellulaire d'environ 30%, tandis que 500 µM de diclofénac a donné lieu à une perte presque complète de l'ATP (Masubuchi et al., 1998). La déplétion en ATP conduit à une diminution du potentiel transmembranaire mitochondrial (ΔΨm) (Masubuchi et al., 2002b; Moreno-Sanchez et al., 1999; Petrescu and Tarba, 1997). Le ΔΨm est maintenu par pompage en continu de protons à partir de la matrice à travers la membrane mitochondriale interne dans l'espace inter-membranaire. Parce que ces protons sont à leur tour utilisés par l'ATP synthase, une diminution de la ΔΨm conduit invariablement à un déséquilibre de la synthèse d'ATP.

Le diclofénac pourrait contribuer à cet effet par au moins trois mécanismes:

- des effets directs sur la membrane interne mitochondriale ;

- un découplage de la respiration à cause du mouvement de va et vient des protons

- une augmentation de la perméabilité de la membrane mitochondriale.

Les médicaments lipophiles à des concentrations extrêmement élevées peuvent en effet augmenter la perméabilité de la membrane aux protons par un effet direct sur la membrane en raison de la répartition du médicament dans la bicouche lipidique (Petrescu and Tarba, 1997). Bien qu'il n'y ait aucune preuve directe que cela se produit avec le diclofénac, il existe des preuves expérimentales pour les deux autres mécanismes.

Tout d'abord, le diclofénac, comme d'autres composés lipophiles et faiblement acides, possède la capacité protonophore c'est-à-dire qu'il peut faire une translocation de protons à travers la membrane mitochondriale interne. Parce que l'anion diclofénac, en raison de l'environnement acide dans l'espace inter-membranaire, devient protoné, la molécule non chargée qui en résulte, peut traverser la membrane interne et entrer dans la matrice. Dans l'environnement plus alcalin de la matrice, le diclofénac est déprotoné à nouveau et expulsé dans l'espace inter-membranaire (probablement par l'intermédiaire d'un transporteur d'anions), où un cycle du proton futile est déclenché, ce qui entraîne une perte du gradient de protons. Il est important de signaler qu'au cours de ce processus, le transport d'électrons le long de la chaîne de transport d'électrons pourrait être stimulé, et donc la consommation d'oxygène augmentée. Toutefois, en présence de

diclofénac, des protons entrent dans la matrice plutôt que de passer par l'ATP synthase, la respiration devient découplée de la phosphorylation oxydative. En effet, le diclofénac est un agent puissant de découplage, au moins *in vitro.* Par exemple, l'exposition des mitochondries de foie de rat à 25 µM de diclofénac entraîne une augmentation de plus du double de la respiration de base, alors que dans le même temps ADP stimulant la respiration est réduit de 40% (Masubuchi et al., 2000). Ceci est typique de composés qui induisent un découplage; en conséquence, la teneur en ATP cellulaire est effondrée.

Le deuxième mécanisme lié au découplage est l'ouverture des pores mitochondriaux (MP). Le MP est un méga canal formé d'un certain nombre de protéines et implique à la fois les membranes mitochondriales externe et interne. Normalement, le pore est fermé, mais il peut s'ouvrir suite à des augmentations de la concentration de Ca^{2+}, une augmentation du stress oxydant, ou une diminution préexistant du $\Delta\Psi m$ (Pessayre et al., 1999). L'ouverture du MP peut avoir un double effet: les protons peuvent rapidement entrer de nouveau dans la matrice et ainsi complètement supprimer le potentiel membranaire. En outre, les substances pro-apoptotiques telles que le cytochrome c, peuvent être libérées à partir de l'espace inter-membranaire et se retrouvent dans le cytosol (parce que la membrane mitochondriale externe se rompt souvent lors de l'ouverture du pore, en raison des effets osmotiques), où ils activent des pro-caspases. Si la grande majorité des mitochondries dans une cellule sont touchées (les hépatocytes abritent des centaines ou des milliers de mitochondries), la production d'énergie s'effondre totalement, et la cellule meurt par nécrose. Toutefois, si l'ouverture des pores se produit dans seulement une partie des mitochondries, l'ATP peut encore être produite, les caspases activées peuvent alors déclencher l'apoptose (processus qui requiert de l'ATP).

Dans ce concept, le diclofénac à des concentrations aussi faibles que 2 µM est capable d'induire l'ouverture des MP dans les mitochondries isolées (Masubuchi et al., 2002b; Uyemura et al., 1997). Cependant, la diminution de l'ATP, l'effondrement de $\Delta\Psi m$, le gonflement mitochondrial, et la libération mitochondriale du Ca^{2+} peuvent être tous bloqués par l'addition de faibles concentrations de cyclosporine A, qui est un inhibiteur spécifique de l'ouverture de MP, donnant ainsi des preuves solides que ce mécanisme est impliqué.

Les initiateurs moléculaires de l'ouverture de MP par le diclofénac sont encore mal définis. Mais un stress oxydant peut provoquer l'ouverture de ces pores (Costantini et al., 1996). En effet,

l'oxydation des groupes sulfhydryle des membranes mitochondriales par le diclofénac a été démontrée, la catalase et le dithiothréitol peuvent prévenir l'ouverture des pores (Masubuchi et al., 2002b). Une autre possibilité est que l'ouverture des pores est une conséquence directe de la protonophorisation du diclofénac et de l'activité de découplage (Kowaltowski et al., 1996).

IV.1.8. Diclofénac et apoptose

L'apoptose ou mort cellulaire programmée est un processus par lequel une cellule déclenche une auto-destruction en répondant à un signal. Selon son origine, la cellule répond par la voie extrinsèque (death receptor pathway) si l'origine de ce signal est externe ou intrinsèque (mitochondrial pathway) s'il est interne (Elmore, 2007). Ce processus est expliqué dans la Figure 18.

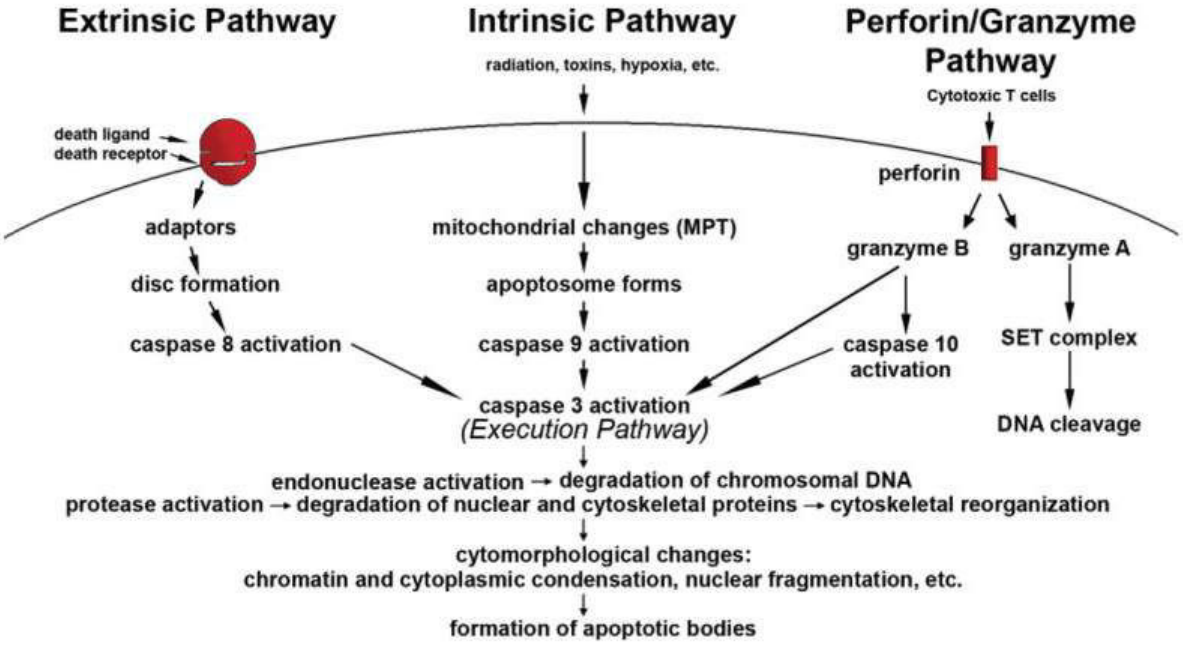

Figure 18: Différentes voies apoptotiques (Elmore, 2007). Ce mécanisme est médié principalement par la voie extrinsèque via le récepteur de mort et l'activation de la caspase 8 et par la voie intrinsèque via la mitochondrie et l'activation de la caspase 9. Ces deux voies aboutissent à l'activation de la caspase effectrice, la caspase 3, puis la formation des corps apoptotiques.

Des études récentes ont cherché à préciser le mécanisme apoptotique du diclofénac. Certaines ont montré que diclofénac est toxique via la voie mitochondriale. En effet, il est capable à des concentrations de 350 µM d'induire l'activité de caspase 9 avec une augmentation de l'expression de BclXL et la génération de ROS ainsi que d'induire l'activité de la caspase 8

indépendamment de la voie des récepteurs de mort. Par conséquent il peut activer à la fois des caspases promotrices et effectrice (caspase 3) (Gomez-Lechon et al., 2003).

Le diclofénac est administré dans le cas de maladies inflammatoires et il y a beaucoup d'hypothèses évoquant un effet possible sur l'activation des cellules immunitaires à cause d'une réaction d'immune. En effet, la molécule mère elle-même ou ses métabolites (acylglucuronides) peuvent former des liaisons covalentes avec des protéines du foie, ce qui peut activer le système immunitaire (Boelsterli, 2003a). Diverses études ont testé l'effet d'un co-traitement du diclofénac avec des cytokines pro-inflammatoires comme le TNF-α (Fredriksson et al., 2011; Fredriksson et al., 2014).

Ces études montrent que la voie extrinsèque peut être aussi une cible pour ce médicament puisqu'il a été déjà montré qu'un co-traitement du diclofénac avec du TNF-α augmente l'activité de la caspase 8 grâce à l'inhibition de la voie NF-kB qui normalement joue un rôle protecteur, cette inhibition induit en même temps l'activation de la voie mitochondriale et enfin l'activité de caspase 3, ce qui augmente l'effet apoptotique. La même étude montre que le diclofénac augmente l'activité des caspases 9 et 3 via l'ouverture des pores mitochondriaux induits par la phosphorylation de JNK, l'une des cibles de ce médicament à des concentrations proches de 500 µM (Fredriksson et al., 2011)(Figure 19).

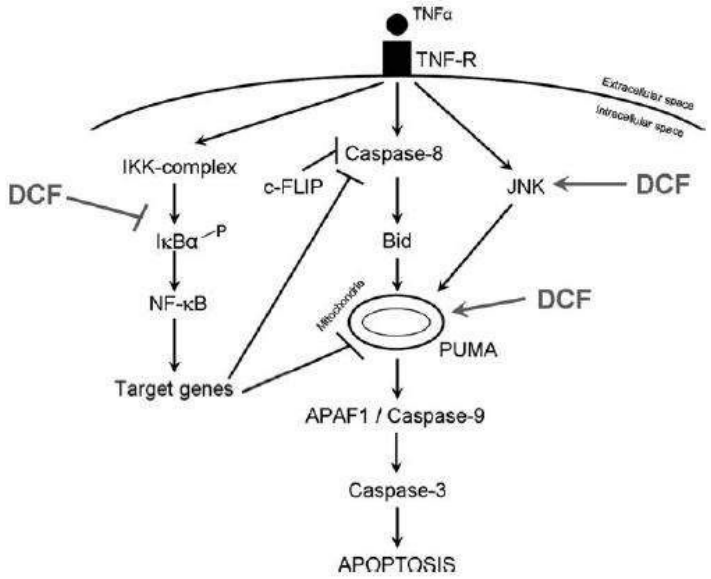

Figure 19: Schéma montrant le mécanisme de toxicité dans les cellules HepG2 après co-traitement de diclofenac avec du TNF-α (10 ng/ml) (Fredriksson et al., 2011). Les flèches indiquent une réaction d'induction.

Un autre facteur impliqué dans cette toxicité est le stress sous ses deux formes : stress du réticulum endoplasmique et stress oxydant. En effet, un traitement des cellules HepG2 par le diclofénac et TNF-α induit la génération d'un stress du réticulum endoplasmique manifesté par une augmentation de l'expression de certains gènes (CHOP, ATF4 et ATF6). En parallèle à ce mécanisme, le TNF-α induit l'activité de la caspase 8 qui va sensibiliser la voie mitochondriale associée à l'activation de la caspase 9 et donc la caspase 3. Le stress du réticulum active à son tour les mitochondries via Bim (Fredriksson et al., 2014) (Figure 20).

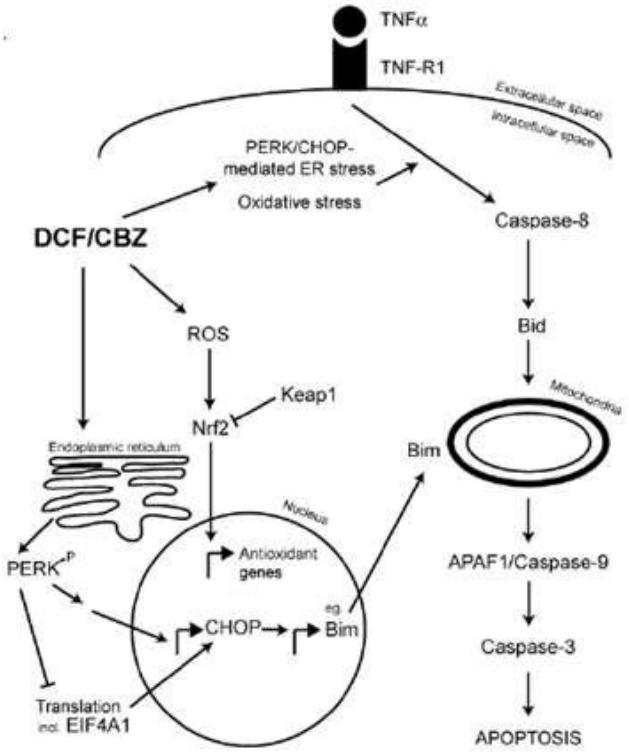

Figure 20: Schéma montrant un mécanisme de toxicité d'un co-traitement du diclofénac avec du TNF-α (10 ng/ml) dans les cellules HepG2 (Fredriksson et al., 2014). Les flèches désignent une réaction d'induction de l'apoptose.

IV.2. Trovafloxacine

IV.2.1. **Structure chimique**

La trovafloxacine (TVX) est un antibiotique de type fluoroquinolone de quatrième génération (commercialisé par Pfizer) et possédant trois atomes de fluor. Sa formule brute est $C_{20}H_{15}F_3N_4O_3$ (Figure 21), de masse moléculaire 416,35 g/mol et ayant une solubilité de 12.3 mg/l dans l'eau à 25ºC (http://www.drugbank.ca/drugs/DB00685).

TVX est un antibactérien très efficace à large spectre contre les bactéries gram négatives et surtout contre des pathogènes gram positifs par comparaison avec d'autres fluoroquinolones (Fischman et al., 1997). Les voies d'administration de TVX sont orale et intraveineuse. Il a une demi-vie longue; il peut provoquer de graves effets hépatiques (IDILI « Idiosyncratic Drug-Induced Liver Injury ») et de ce fait, a été retiré du marché en Europe.

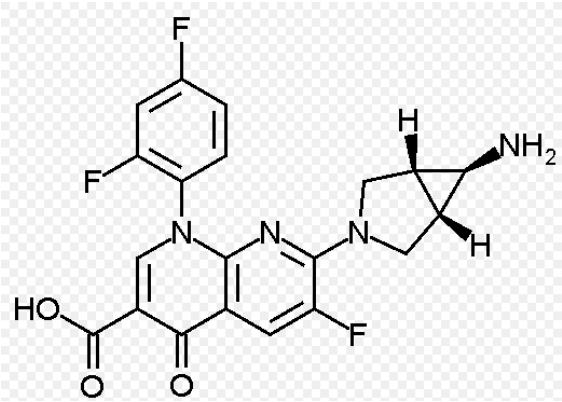

Figure 21: Structure chimique de la trovafloxacine (https://pubchem.ncbi.nlm.nih.gov/compound/Trovafloxacin#section=2D-Structure)

IV.2.2. **Métabolisme de la trovafloxacine**

La molécule mère de TVX est plus efficace que ses métabolites dans son activité bactéricide. La phase majeure du métabolisme de TVX est la phase II de conjugaison (glucuronidation, N-acétylation et N-sulfoconjuguaison) et donne plusieurs types de métabolites tels que des ester glucuronides et des N-sulfates. TVX est aussi métabolisé en acide hydroxycarboxylique par les enzymes de la phase I (CYP1A2) mais minoritairement (Vincent et al., 1998) (Dalvie et al., 1997).

Les premières études concernant le métabolisme de TVX n'ont pas révélé de métabolites réactifs intermédiaires mais d'autres, plus récentes, suggèrent qu'il peut être métabolisé en un aldéhyde α,β-insaturé.

Métabolites	**Sérum (%)**	**Fèces (%)**	**Urine (%)**
Ester glucuronide	21.7 ± 3.5	ND	12.8 ± 1.5
Trovafloxacine	51.6 ± 10.0	43.2 ± 6.3	5.9 ± 1.5
Sulfate	ND	3.9 ± 2.0	0.2 ± 0.1

Métabolites	Sérum (%)	Fèces (%)	Urine (%)
Diacide	ND	0.9 ± 0.5	0.2 ± 0.1
Acide hydroxycarboxylique	ND	NC	0.3 ± 0.1
Pyrroline	trace	trace	trace

Tableau 4: Pourcentages des différents métabolites de TVX dans le sérum, l'urine et les fécès chez des patients traités (Vincent et al., 1998). « ND » désigne « non déterminé » et % désigne « pourcentage ».

IV.2.3. Hépatotoxicité de la trovafloxacine chez l'homme

En 1999, un rapport médical a montré une hépatotoxicité causée par TVX chez des patients traités. Parmi les 2.5 millions de prescriptions 140 réactions hépatiques sévères ont été rapportées c'est-à-dire 1/18000 ; et parmi ces 140 cas 14 cas d'insuffisance hépatique, soit 1/178000 (Stahlmann, 2002). Cette hépatotoxicité a été trouvée à égalité chez des patients des 2 sexes âgés de 21 à 91 ans et indépendamment de la durée du traitement. Ce profil clinique montre que l'hépatotoxicité de TVX est de type idiosyncrasique.

Les études cliniques chez les patients ont montré des effets similaires de TVX se manifestant surtout par une nécrose hépatocellulaire centrolobulaire avec présence de cellules inflammatoires, comme les lymphocytes, les cellules plasmatiques et les éosinophiles, en grandes quantités (Chen et al., 2000; Lazarczyk et al., 2001; Lucena et al., 2000).

IV.2.4. Trovafloxacine et stress inflammatoire dans les modèles animaux

Des études des effets de TVX ont été réalisées chez différentes espèces animales. Par exemple, chez les rongeurs TVX seule n'a pas d'effet même à des doses atteignant 1g/kg. En revanche, chez les rats et les souris des concentrations non toxiques de TVX peuvent causer une atteinte hépatique aiguë après co-traitement avec du LPS qui peut induire un stress inflammatoire (Shaw et al., 2007; Waring et al., 2006). Cette hépatotoxicité se manifeste par une apoptose et une nécrose médiolobulaire chez la souris et centrolobulaire chez l'homme. Cette différence inter-espèce de localisation pourrait être due à une distribution intralobulaire différente des enzymes impliquées dans le métabolisme de TVX.

Le co-traitement TVX/LPS peut entrainer une activation des polynucléaires neutrophiles (PMN) et donc une sécrétion de protéases toxiques qui peuvent être la cause de cette hépatotoxicité (Shaw et al., 2009b). Cette hépatotoxicité est aussi associée à une activation de la thrombine (activateur de la coagulation) et de l'inhibiteur 1 de l'activation du plasminogène (PAI1). L'activation de PAI1 induit à son tour la sécrétion de chimiokines activant les PMN et donc des lésions hépatiques (Shaw et al., 2009a).

IV.2.5. **Mécanisme apoptotique de trovafloxacine**

Des études *in vivo* ont montré que TVX n'est pas hépatotoxique chez la souris mais le devient lorsqu'il est combiné avec du LPS (Shaw et al., 2007). Les examens histologiques montrent que le co-traitement TVX/LPS induit des dommages hépatiques caractérisés par l'apparition de nécrose et d'apoptose via la voie de TNF-α. L'inhibition du récepteur de TNF-α chez les souris traitées avec du LPS/TVX inhibe l'effet apoptotique de ce dernier montrant un rôle de la voie de TNF-α dans ce mécanisme (Figure 22) (Shaw et al., 2009a; Shaw et al., 2007). L'activation du récepteur du TNF-α induit à son tour l'activité de caspase et la voie de JNK (Ding and Yin, 2004) comme dans le cas des cellules HepG2 (Beggs et al., 2014).

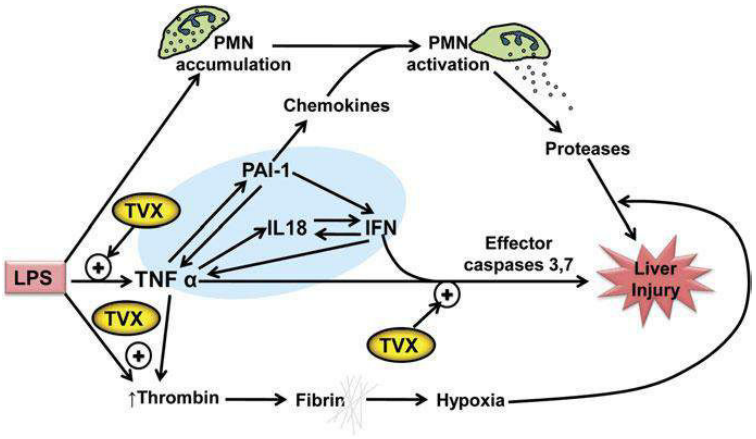

Figure 22: Différents mécanismes de toxicité de TVX +/- LPS (Shaw et al., 2007). Le symbole « + » désigne une induction et les points « une sécrétion ». LPS potentialise l'effet toxique de TVX via l'activation de neutrophiles sécrétant par la suite des protéases ainsi que par l'induction de la sécrétion de TNF-α activant la caspase 3 et aboutissant finalement à une lésion hépatique.

Des études récentes ont montré que TVX induit un effet apoptotique dans les cellules Jurkat grâce à un mécanisme dépendant de la pannexine 1 (PANX1), une protéine qui entre dans la famille des innexines responsables de la formation des jonctions communicantes intercellulaires. En effet TVX joue un rôle inhibiteur pour la pannexine, ce qui aboutit à la fragmentation des

cellules et la formation des corps apoptotiques. Ceci n'est pas été détecté avec une autre quinolone, la lévofloxacine (Poon et al., 2014).

Le traitement des cellules HepG2 avec TVX en présence de TNF-α montre une inhibition de MRP2. Ceci peut être responsable de l'effet hépatotoxique de ce médicament (Saab et al., 2013).

IV.3. Amiodarone

L'amiodarone est le médicament le plus connu pour ses effets anti-arythmiques parmi ses homologues de la classe III. Il est utilisé notamment pour le traitement des troubles du rythme cardiaque, surtout supraventriculaires. Sa structure chimique correspond au chlorhydrate de (2-butyl-3 -benzofuranyl)[4-[2-(diéthylamino)éthoxy]-3,5-diiodophényl]méthanone (Figure 23) (https://pubchem.ncbi.nlm.nih.gov).

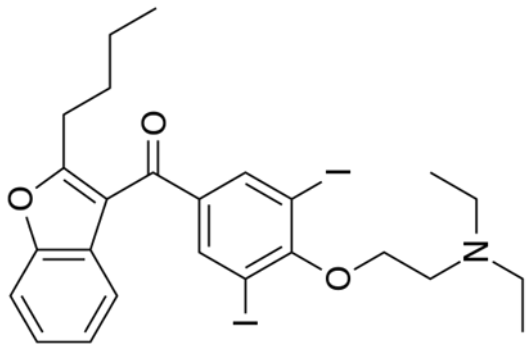

Figure 23: Structure chimique de l'amiodarone (https://pubchem.ncbi.nlm.nih.gov)

Son mécanisme d'action repose sur sa capacité à retarder la répolarisation du cycle cardiaque et à allonger la période réfractaire de manière homogène en diminuant l'amplitude du potentiel d'action sans modification du potentiel membranaire de repos et en augmentant la durée du potentiel d'action. En fait, la phase 2 est raccourcie par diminution de la conductance calcique et la phase 3 est très allongée par réduction de la conductance potassique, ce qui en fait son activité anti-arythmique de classe III. En plus, il a un effet dromotrope négatif ou activité de classe I basée sur le blocage des canaux sodiques aboutissant au ralentissement de la vitesse de

dépolarisation de la phase 0 du potentiel d'action et donc au ralentissement de la conduction (https://www.vidal.fr/substances/7069/amiodarone/).

Par son effet bradycardisant il peut ralentir aussi le rythme cardiaque au niveau du nœud sinusal et la conduction à plusieurs niveaux (nœuds auriculo-ventriculaire, sino-auriculaire et au niveau du His-Purkinje). Il faut noter finalement que l'amiodarone peut être utilisée comme antagoniste alpha et bêta-adrénergique non compétitif et comme anti-angoreux car il provoque une vasodilatation des artères coronaires (Wellens et al., 1984).

L'absorption de ce médicament est lente et variable (Meng et al., 2001) et il est connu par sa forte fixation aux protéines plasmatiques (95%), surtout à l'albumine (62%) et aux bêta-lipoprotéines (33%). Son importante liposolubilité permet son accumulation dans le tissus adipeux, y compris son métabolite déséthylamiodarone qui atteint parfois des concentrations plus élevées que celles de la molécule mère. La concentration de l'amiodarone devient maximale après 5 mois de traitement. Même après l'arrêt de la prise de ce médicament on peut détecter une grande quantité au niveau des tissus pendant une ou trois semaines. Le danger de médicament est lié à sa possibilité de traverser la barrière placentaire et de se retrouver dans certains cas en concentrations élevées dans le lait maternel (van Erven and Schalij, 2010).

Il est principalement pris par voie orale mais pour accélérer son efficacité il est parfois prescrit par injection intraveineuse, ce qui minimise son délai d'action à un quart d'heure. Normalement sa demi-vie est de l'ordre de 50 jours; elle est aussi dépendante de l'individu et peut se situer entre 20 et 100 jours. Cette durée est comparable pour son métabolite le désétylamiodarone ; celui-ci peut en effet persister pendant environ 60 jours (Siddoway, 2003).

Le CYP3A4 est l'enzyme majeure impliquée dans le métabolisme de ce médicament et de son principal métabolite la déséthylamiodarone qui atteint des concentrations plasmatiques proches de celles de la molécule mère et possède une efficacité thérapeutique comparable (Shayeganpour et al., 2006). La clairance ou l'élimination de l'amiodarone se fait normalement par les fécès et non par les reins et surtout sous forme de métabolites.

IV.3.1. Effets secondaires de l'amiodarone

Plusieurs effets secondaires ont été rapportés pour ce médicament. Ces effets se manifestent par un dysfonctionnement au niveau de la thyroïde, une fibrose pulmonaire, des symptômes oculaires

et cutanés, une neurotoxicité centrale et périphérique (Harris et al., 1983) (McGovern et al., 1983). Des anomalies hépatiques avec augmentation de transaminases, des hépatites aiguës, des maladies hépatiques chroniques chez 14 à 82% des patients traités ont été aussi décrites (Lewis et al., 1989) (Babatin et al., 2008; Ratz Bravo et al., 2005).

IV.3.2. Effets stéatosiques

Une étude sur des cellules HepaRG a montré que l'amiodarone peut provoquer une stéatose accompagnée d'une phospholipidose, en utilisant diverses approches : détection des lipides grâce à l'huile rouge (Figure 24), présence de gouttelettes lipidiques en microscopie optique et électronique (Figure 25) et augmentation du taux de triglycérides, après traitement pendant 14 jours (Antherieu et al., 2011). Ces mêmes effets ont été trouvés chez des personnes traitées par ce médicament où une hépatotoxicité fatale associée à l'apparition de corps de Mallory (corps trouvés dans le cytoplasme des cellules hépatiques), de stéatose, d'infiltrats inflammatoires intra-lobulaires, de fibrose et de phospholipidose a été observée surtout après exposition à des doses qui deviennent cumulatives avec le temps (Guigui et al., 1988; Richer and Robert, 1995).

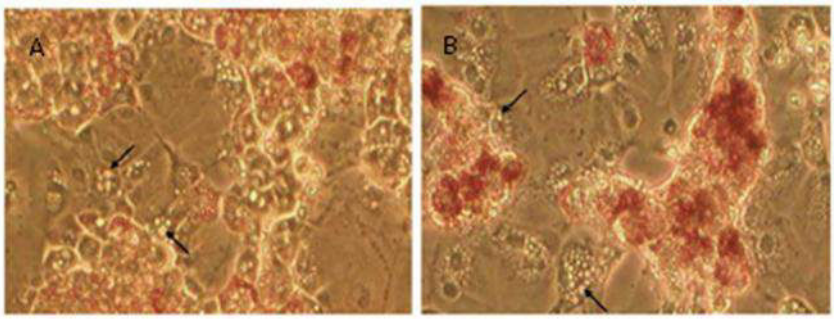

Figure 24: Accumulation de vésicules lipidiques détectées par le rouge neutre après traitement des cellules HepaRG avec l'amiodarone pendant 24 h (A) ou 14 jours (B) (Antherieu et al., 2011). Les flèches montrent les vésicules lipidiques.

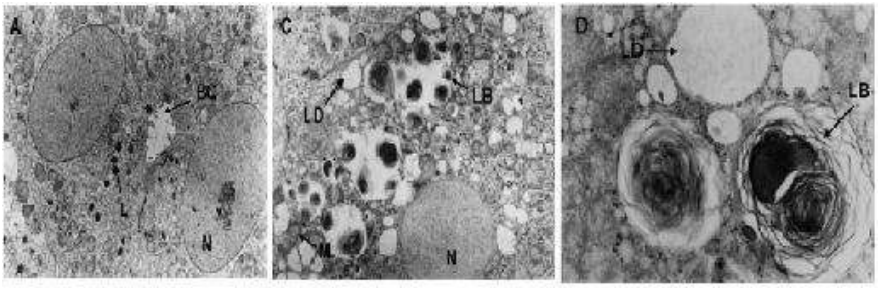

Figure 25: Corps lamellaires (phospholipidose) et gouttelettes lipidiques observés en microscopie électronique après traitement des cellules HepaRG par l'amiodarone (Antherieu et al., 2011). Les flèches montrent les corps lamellaires.

Des biomarqueurs stéatosiques (cholestérol, triglycérides) ont aussi été mis en évidence *in vivo* chez la souris après traitement par l'amiodarone pendant 1, 4 et 11 jours (Vitins et al., 2014). Cet

effet a été lié au « peroxisome proliferator activated-receptor » (PPAR) (Szalowska et al., 2014); les souris PPARα (-/-) présentant en effet une augmentation du taux des triglycérides après traitement par l'amiodarone et les souris PPARα (+/+) une protection contre cet effet (Ernst et al., 2010). Des études ont montré que l'un des mécanismes aboutissant à cette accumulation est l'inhibition de l'activité des protéines microsomales transférant les triglycérides (MTP) (Letteron et al., 2003). Cette stéatohépatite est associée à un dysfonctionnement mitochondrial représenté par une diminution de l'ATP en raison de l'inhibition de la respiration et d'une génération de ROS, conduisant à une augmentation de la peroxydation lipidique et finalement à la mort cellulaire (Berson et al., 1998) (Letteron et al., 1996). Il faut noter que cette hépatotoxicité a été associée à une altération de la β-oxydation mitochondriale (Figure 26) et de la transcription d'ADN mitochondrial et à une diminution de la réplication de cet ADN (Fromenty et al., 1990; Fromenty and Pessayre, 1995).

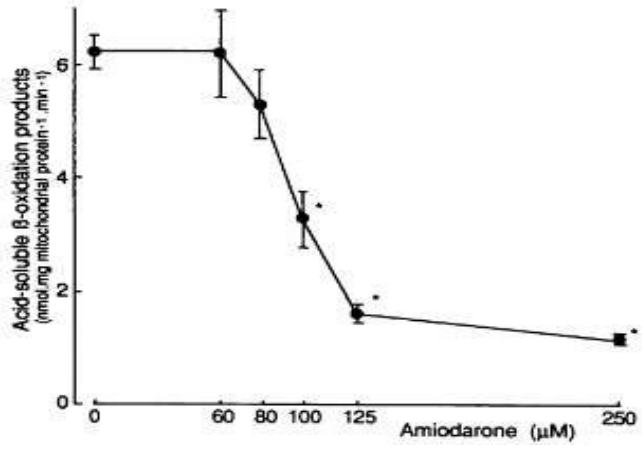

Figure 26: Effets de différentes concentrations d'amiodarone (μM) sur la formation de produits acide- soluble marqués au ^{14}C, provenant de la β-oxydation de l'acide palmitique (U-^{14}C) (Fromenty et al., 1990; Fromenty and Pessayre, 1995).

D'autres études ont montré que ce médicament peut causer une toxicité hépatique en absence de phospholipidose ou de stéatose (Cimic, 2013). Il peut aussi induire d'autres effets comme une cirrhose, pouvant être associée à une stéatose (Ishida et al., 2010; Puli et al., 2005) ou non (Bach et al., 1989). Les cliniciens conseillent de surveiller le niveau d'activité des enzymes hépatiques à cause de la diversité des symptômes observés chez certains patients (stéatose, altérations ressemblant à une hépatite alcoolique, hépatite cholestatique ou cirrhose micronodulaire) (Rumessen, 1986).

IV.3.3. Effet de l'inflammation sur la toxicité de l'amiodarone

Des études ont porté sur l'effet de LPS sur la toxicité de l'amiodarone et de son métabolite, le mono-N-deséthylamiodarone (DEA) (Talajic et al., 1987). Dans cette dernière étude chez la

souris, l'AMD a été administrée pendant 16 à 20 h avant le LPS ce qui a abouti à une augmentation de l'ALT, d'où l'importance du temps de traitement pour avoir un effet puisqu'aucun effet n'a été observé lorsqu'AMD a été ajoutée pendant 2-12h. En fait, le traitement par LPS n'a affecté le métabolisme de l'AMD ni dans le sérum ni dans les tissus indiquant que la toxicité de l'AMD n'est liée ni à la molécule mère ni à ses métabolites et que la toxicité liée à LPS n'est pas dépendant du métabolisme mais d'une autre cause sans doute associée, à savoir la présence de dommages de type cholestatique comme l'augmentation de ALP, de GGT et de la concentration totale des acides biliaires surtout en présence de LPS lorsqu'on a un synergisme LPS/AMD. Cette toxicité apparait liée à l'induction de la sécrétion de TNF-α par LPS puisque le co-traitement des souris avec des concentrations non toxiques de TNF-α induit une toxicité et que leur pré-traitement avec de l'étanercept pendant une heure avant leur injection avec du LPS et de l'AMD ou son métabolite DEA atténue cet effet (Lu et al., 2012). Notons que, même seule, AMD peut induire une inflammation et une toxicité pulmonaire chez des rats (Wilson et al., 1991).

V. *Saccharomyces cerevisiae* en toxicologie

Depuis plusieurs siècles, *S. cerevisiae* est utilisé dans la production d'aliments et de boissons alcoolisées. Depuis la naissance de la biologie cellulaire, ce microorganisme a servi de modèle pour les études structurales et fonctionnelles des cellules eucaryotes. À l'heure actuelle, cet organisme a de nombreuses applications dans l'industrie pharmaceutique et dans divers domaines de la toxicologie. La fermentation et le traitement technique disponibles pour la production à grande échelle de *S. cerevisiae* a rendu cet organisme approprié pour plusieurs utilisations biotechnologiques (Pereira et al., 2013).

V.1. Structure de *Saccharomyces cerevisiae*

La levure *Saccharomyces cerevisiae* est une cellule eucaryote, unicellulaire haploïde/diploïde, avec une paroi de glucanes/,mannanes/protéines- un espace périplasmique- une membrane en bicouche lipidique- un noyau avec un nucléole, des vacuoles, un appareil de sécrétion (RE, golgi, vésicules de sécrétion), des mitochondries. Elle se présente sous forme ovoïde arrondie, longue de 6 à 12 µM et large de 6 à 8 µM. Le schéma ci-dessous montre la structure cellulaire de *Saccharomyces cerevisiae* (Zinser and Daum, 1995) (Figure 27).

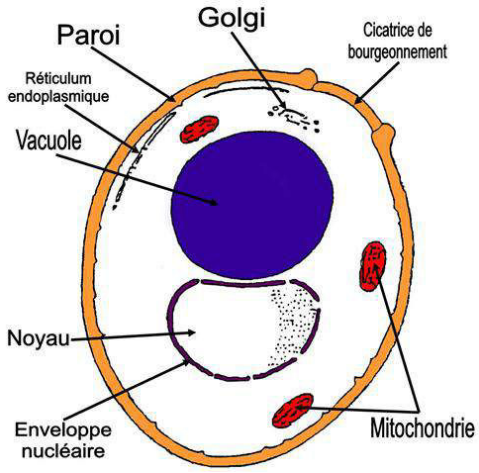

Figure 27: Schéma montrant la structure de la levure *S. cerevisiae* (Zinser and Daum, 1995) (modifiée).

V.1.1. Enveloppe cellulaire

L'enveloppe de *S. cerevisiae* est une capsule de protection, constituée de trois constituants principaux: la membrane plasmique, l'espace périplasmique, et la paroi cellulaire. Chez *S.*

cerevisiae, l'enveloppe cellulaire occupe 15% du volume total et joue un rôle majeur dans le contrôle des propriétés osmotiques et de la perméabilité de la cellule (Zinser and Daum, 1995).

La membrane plasmique est d'environ 7 nm d'épaisseur, avec des invaginations dans le cytosol. Comme d'autres membranes, c'est une bicouche lipidique avec des protéines insérées dans cette couche traversée par des protéines transmembranaires de diverses fonctions. La composition lipidique comprend essentiellement la phosphatidylcholine et la phosphatidyléthanolamine, avec des proportions mineures de phosphatidylinositol, phosphatidylsérine ou phosphatidyl-glycérol, ainsi que des stérols, principalement l'ergostérol et le zymostérol. Les protéines membranaires de levure comprennent les catégories suivantes: (i) protéines d'ancrage du cytosquelette; (ii) des enzymes pour la synthèse de la paroi cellulaire, (iii) des protéines de transduction de signaux transmembranaires; (iv) des protéines de transport de soluté (perméases, canaux, ATPases); (v) d'autres transporteurs, tels que les transporteurs ABC (ATP-binding cassette) qui sont des protéines impliquées dans le transport des xénobiotiques (Zinser and Daum, 1995).

La paroi d'une cellule de levure est une enveloppe remarquablement épaisse (100 à 200 nm), qui contient environ 15 à 25% de la masse sèche de la cellule. Les constituants structuraux majeurs de la paroi cellulaire sont des polysaccharides (80-90%); glucanes et mannanes principalement, avec un faible pourcentage de chitine. Les glucanes fournissent la force à la paroi cellulaire, formant un réseau microfibrillaire. La chitine est un polymère de N-acétylglucosamine représentant seulement 4.2% de la paroi cellulaire et principalement située dans les cicatrices du bourgeon (Zinser and Daum, 1995).

V.1.2. Cytosol et cytosquelette

Le cytoplasme de *S. cerevisiae* est un fluide colloïdale acide (pH 5,25), contenant principalement des ions et des composés organiques de poids moléculaires faibles ou intermédiaires, et des macromolécules solubles (par exemple les protéines enzymatiques et le glycogène). Les enzymes cytosoliques de la levure comprennent ceux: (i) de la voie glycolytique, (ii) du complexe de synthèse d'acide gras, et (iii) les enzymes de biosynthèse des protéines. Le cytosquelette assurant la stabilité interne de la cellule et fournissant l'organisation structurelle comprend les microtubules et les microfilaments. Ce sont des structures dynamiques qui remplissent leur fonction à travers l'ensemble réglementé et le démontage des sous-unités protéiques individuelles (Zinser and Daum, 1995).

V.1.3. Noyau

Le noyau de la levure est lobé rond de 1,5 μm de diamètre dont l'enveloppe présente des pores de 50 à 100 nm de diamètre. Les fuseaux de corps polaires sont situés à deux pôles opposés et ils sont reliés entre eux par les microtubules intranucléaires continus et les origines de microtubules discontinues. Sur la face extérieure, les fuseaux de corps polaires sont reliés aux microtubules cytosoliques. Ces éléments structurels jouent un rôle important au cours de la division cellulaire, la cytodiérèse et la formation des bourgeons. Contrairement à d'autres eucaryotes, la membrane nucléaire dans la levure ne se fragmente pas lors de la mitose (Riezman, 1993). *Saccharomyces cerevisiae* peut se multiplier sous deux formes : diploïde (2n) ou haploïde (1n). Le nombre des chromosomes au niveau du noyau de *Saccharomyces cerevisiae* est de 16 dans le cas « haploïde » et de 32 dans le cas « diploïde » (Engel et al., 2014).

V.1.4. Réticulum endoplasmique et appareil de Golgi

Le réticulum endoplasmique (RE) est le site de la biosynthèse et la modification des protéines qui sont destinées à être exportées. Dans la lumière du RE, où des protéines chaperonnes comme Hsp70 (Heat shock protein 70) et Bip/GRP78 (Immunoglobulin Heavy Chain-Binding Protein/ Glucose-Regulated Protein, 78-KD) accomplissent le repliement et la glycosylation des protéines. Du RE, les protéines sont dirigées vers l'appareil de Golgi par des vésicules, qui fusionnent sur le côté *cis* et sont exportés de l'appareil de Golgi vers le côté *trans*. Dans l'appareil de Golgi d'autres modifications des protéines de chaînes glucidiques secondaires peuvent avoir lieu, comme la mannosylation (Pelham et al., 1995).

V.1.5. Mitochondrie

Les mitochondries dans les levures comprennent: une membrane externe - contenant des enzymes impliquées dans le métabolisme des lipides ; une espace intermembranaire ; une membrane interne - contenant la NADH et la succinate déshydrogénases, les composants de la chaîne respiratoire et l'ATP synthase, et des différentes protéines de transport membranaire ; la matrice mitochondriale - contenant les enzymes de l'oxydation des acides gras, le cycle de l'acide citrique, l'ADN mitochondrial ainsi que la machinerie de transcription et de synthèse des protéines mitochondriales (Glick and Pon, 1995).

V.2. Cycle cellulaire de *Saccharomyces cerevisiae*

Le cycle de vie de *S. cerevisiae* peut se faire dans l'état haploïde et diploïde et comprend deux modes de reproduction, sexué (fusion de cellules haploïdes de sexe opposé puis sporulation par méiose) et asexué (mitose) (Figure 28) (Herskowitz, 1988).

Suite à un réarrangement génétique de leur ADN au locus MAT, certaines cellules haploïdes ont la capacité de changer de type sexuel. On dit alors que ces souches ont un cycle cellulaire homothallique. C'est-à-dire, un cycle cellulaire au cours duquel une colonie cellulaire haploïde issue d'une même spore peut donner naissance à des cellules diploïdes capables de méiose. À l'inverse, certaines souches de *S. cerevisiae* ont un cycle cellulaire hétérothallique. C'est-à-dire, que les cellules diploïdes sont seulement formées suite à la conjugaison entre deux cellules haploïdes de type sexuel opposé provenant de spores différentes (Herskowitz, 1988).

Selon les conditions environnementales externes, les cellules haploïdes et diploïdes débutant la phase G1 «pré-Start» doivent faire un choix. Si elles jugent que la quantité de nutriments est suffisante, elles poursuivent le cycle cellulaire mitotique (reproduction asexuée). Par contre, si elles jugent que la quantité de nutriments est insuffisante et qu'elles détectent la présence de phéromones sexuelles, les cellules haploïdes entrent alors en mode de conjugaison sexuelle (reproduction sexuée) tandis que les cellules diploïdes entrent en mode de sporulation (Herskowitz, 1988).

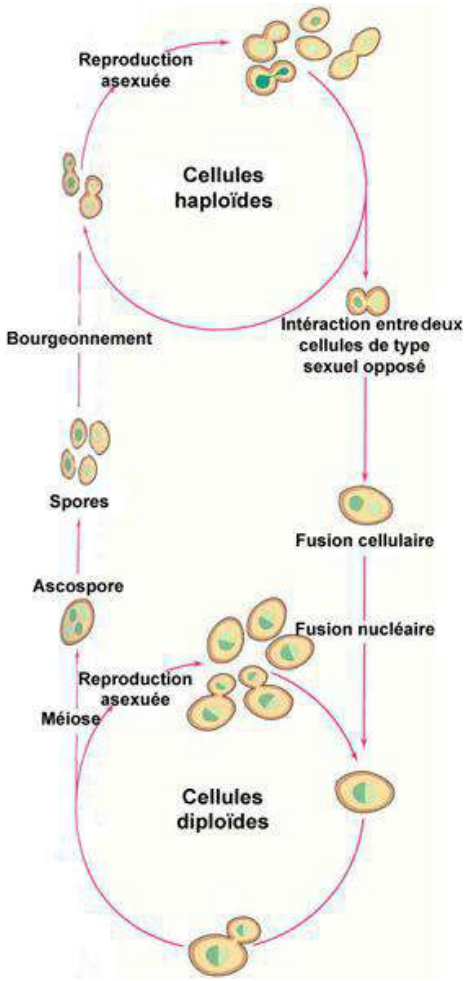

Figure 28: Représentation schématique du cycle cellulaire de *S. cerevisiae* (Hartwell, 1974). La cellule peut passer de l'état haploïde à l'état diploïde et inversement via deux types de reproduction sexuée et asexuée et via le phénomène de bourgeonnement.

V.3. Métabolisme de *Saccahromyces cerevisiae*

Pour assurer sa survie et sa reproduction la levure *Saccharomyces cerevisiae* utilise différentes voies métaboliques, la voie aérobie et la voie anaérobie. La voie aérobie où la respiration se base sur la transformation du glucose en dioxyde de carbone et ATP en utilisant l'oxygène du milieu d'une façon prioritaire mais elle peut être accompagnée d'une utilisation de l'éthanol avec une consommation de l'oxygène, c'est ce qu'on appelle la transition diauxique. La deuxième voie caractérisée par la fermentation alcoolique du glucose, c'est la voie anaérobie.

Les levures utilisent différentes sources de carbone qui se trouvent normalement dans le milieu de culture. Ces sources sont principalement des glucides comme le glucose, le maltose et le saccharose mais elles peuvent être des acides aminés mais minoritairement pour alimenter les voies de formation des métabolites (Fast, 1973).

V.3.1. Enzymes du métabolisme des xénobiotiques chez la levure (Phases I, II et III)

Saccharomyces cerevisiae possède un équipement enzymatique capable de métaboliser de xénobiotiques. Ces enzymes sont moins diversifiées par rapport à celle des cellules animales, mais on retrouve les enzymes de phases I, II et III.

-Les enzymes de phase I : les enzymes de cette phase I renferment surtout les cytochromes (Lindenmayer and Smith, 1964) couplés à un état intermédiaire de la transition de l'aérobie au métabolisme anaérobie, c'est ce qu'on appelle des conditions semi-anaérobies (Ishidate et al., 1969b) (Ishidate et al., 1969a) et qui peuvent être induites par des substrats carbonés (Lebeault et al., 1971). Notons que *S. cerevisiae* contient seulement trois cytochromes P450 endogènes, CYP51, CYP56 et CYP61, tous impliqués dans des activités d'entretien « House keeping activities » (Cresnar and Petric, 2011). Les CYP de levure se caractérisent par une spécificité élevée au substrat, comme la plupart des P450 des mammifères. La famille de CYP51 est ubiquitaire tandis que les enzymes CYP61 sont présents dans les champignons et les plantes et les enzymes de CYP56 ne se trouvent que dans les champignons. CYP56 est une N-formyle tyrosine oxydase qui catalyse la production de N, N- bisformyldityrosine, un composant nécessaire pour la maturation de paroi des spores (Briza et al., 1994). L'enzyme CYP61 est une Δ22 désaturase impliquée dans la biosynthèse de l'ergostérol de la membrane (Kelly et al., 1997a). En plus d'avoir une fonction de maintien, la CYP61 de *S. cerevisiae* également métabolise par exemple le benzo[a]pyrène en 3 hydroxybenzo [a] pyrène (Kelly et al., 1997b).

Les CYP de *S. cerevisiae* sont impliqués dans les derniers stades de la biosynthèse de l'ergostérol (Ohba et al., 1978) par la conversion de lanostérol en 4,4- diméthyle zymostérol dépendant de l'oxygène et de NADPH. En plus l'élimination par oxydation du groupe 14 α -méthyl de lanostérol est médié par un système reconstitué de CYP et CYP NADPH réductase qui peuvent détruire du Δ22- d' ergosta-5,7- diène-β-ol. En utilisant des souches mutantes n'ayant pas de 14 cx-déméthylase, la désaturation du Δ22- était encore possible. Cela indique que deux espèces distinctes de CYP peuvent être impliquées dans la biosynthèse d'ergostérol (Hata et al., 1983).

-Les enzymes de phase II : la phase II groupe différentes enzymes comme la gluthation transférase (GST), la flavine monooxygenase (FMO) et l'uridine diphosphate glycosyltransférase (UGT). Sept protéines possèdant l'activité de GST (Gtt1 et Gtt2; Gto1, Gto2 et Gto3; Grx1 et

Grx2) (Collinson and Grant, 2003) sont exprimées dans le *Saccharomyces cerevisiae*. L'expression de FMO « flavin-containing monooxygenase » a été aussi montrée dans le *Saccharomyces cerevisiae* surtout FMO 1B1 catalysant la méthimazole, la thiourée, la diméthylaniline et la cystéamine mais pas la chlorpromazine ou l'imipramine (Lawton and Philpot, 1993). Une autre enzyme de cette phase est aussi exprimée, c'est le cas d'UGT51 (YLR189C) (Warnecke et al., 1999) catalysant la synthèse de stérol de la membrane de ces cellules.

-Les enzymes de phase III renfermant principalement les transporteurs ABC (Figure 29). Ces derniers sont localisés principalement dans les mitochondries, les vacuoles, les membranes peroxisomales et plasmiques (Bauer et al., 1999). Ils jouent un rôle important dans la résistance aux antibiotiques, fongicides et herbicides (Rogers et al., 2001). Les principaux transporteurs qui se trouvent au niveau de ces cellules sont mentionnés dans le Tableau 5.

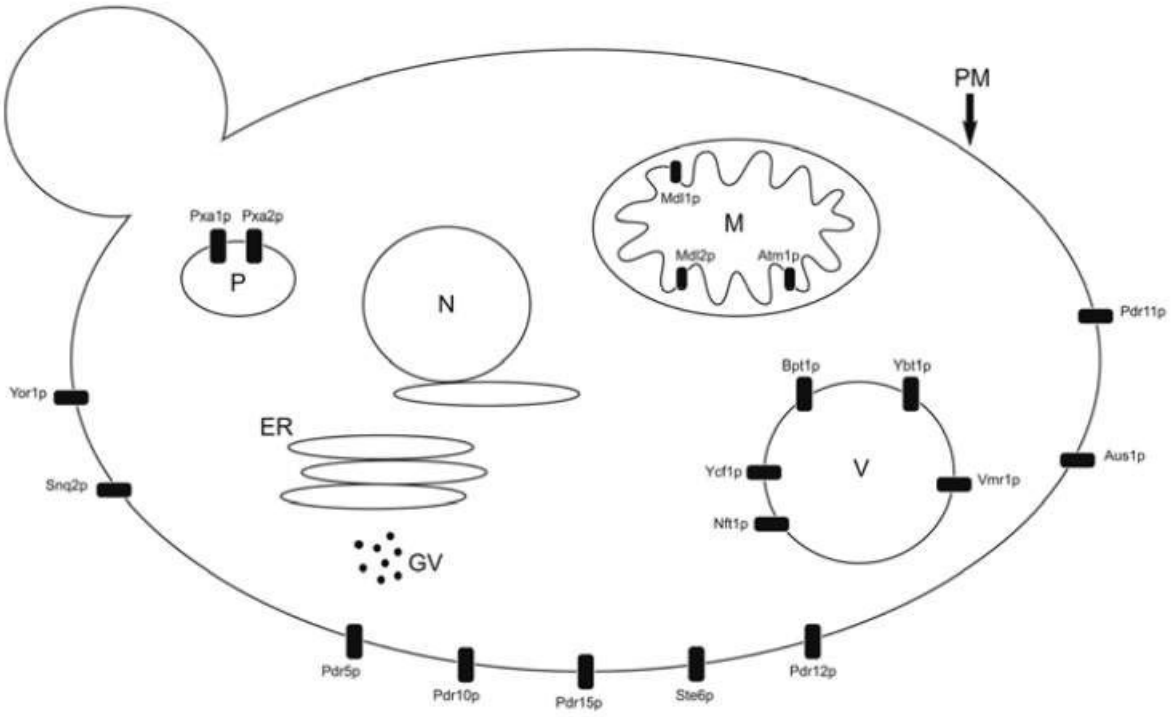

Figure 29: Localisation des transporteurs ABC dans la levure *Saccharomyces cerevisiae* (N-noyau ; V-vacuole ; M-mitochondries ; P-peroxisome ; PM-membrane plasmique) (Piecuch and Oblak, 2014)

Gène/protéine	Nom	Sous famille	fonction	localisation	références
STE6/Ste6p	STErile	MDR (ABCB)	Export du phéromone a	Membrane plasmique	(Kuchler et al., 1989)
MDL1/Mdl1p	MultiDrug resistance-Like	MDR (ABCB)	Transport des produits de dégradation des protéines	Membrane mitochondriale interne	(Chloupkova et al., 2003; Young et al., 2001)
MDL2/Mdl2p	MultiDrug resistance-Like	MDR (ABCB)	Inconnu	Membrane mitochondriale interne	(Chloupkova et al., 2003; Young et al., 2001)
ATM1/Atm1p	ABC Transporter, Mitochondrial	MDR (ABCB)	Tansport de soufre de fer	Membrane mitochondriale interne	(Chen and Cowan, 2006; Chloupkova et al., 2003)
YOR1/Yor1p	Yeast Oligomycin Resistance	MRP/CFTR (ABCC)	Pompe à efflux des médicaments	Membrane plasmique	(Cui et al., 1996)
YCF1/Ycf1p	Yeast Cadmium Factor	MRP/CFTR (ABCC)	Transport des métaux lourds	Membrane vacuolaire	(Gueldry et al., 2003)
YBT1/Ybt1p	Yeast Bile Transporter	MRP/CFTR (ABCC)	Transport des sels biliaires	Membrane vacuolaire	(Ortiz et al., 1997)
BPT1/Bpt1p	Bile Pigment Transporter	MRP/CFTR (ABCC)	Transport d'acide glucuronique, de bilirubine et de gluthatione	Membrane vacuolaire	(Klein et al., 2002; Petrovic et al., 2000)
VMR1/Vmr1p	Vacuolar Multidrug Resistance	MRP/CFTR (ABCC)	Pompe d'efflux des médicaments	Membrane vacuolaire	(Wawrzycka et al., 2010)
NFT1/Nft1p	New Full-length MRP-type Transporter	MRP/CFTR (ABCC)	Inconnu	Membrane vacuolaire	(Mason et al., 2003)
PXA1/Pxa1p	PeroXisomal ABC-transporter	ALDP (ABCD)	Transport des acides gras	Membrane peroxisomale	(Hettema et al., 1996; Swartzman et al., 1996)

Gène/protéine	Nom	Sous famille	fonction	localisation	références
PXA2/Pxa2p	PeroXisomal ABC-transporter	ALDP (ABCD)	Transport des acides gras	Membrane peroxisomale	(Hettema et al., 1996; Swartzman et al., 1996)
PDR5/Pdr5p	Pleiotropic Drug Resistance	PDR (ABCG)	Pompe d'efflux des médicaments, translocation des lipides	Membrane plasmique	(Hlavacek et al., 2009; Kihara and Igarashi, 2004; Mahe et al., 1996; Miyahara et al., 1996)
SNQ2/Snq2p	Sensitivity to 4-NitroQuinoline-N-oxide	PDR (ABCG)	Pompe d'efflux des médicaments	Membrane plasmique	(Servos et al., 1993)
PDR15/Pdr15p	Pleiotropic Drug Resistance	PDR (ABCG)	Détoxification de cellules pendant la réponse au stress	Membrane plasmique	(Wolfger et al., 2004)
PDR12/Pdr12p	Pleiotropic Drug Resistance	PDR (ABCG)	Transport des acides organiques faibles	Membrane plasmique	(Hatzixanthis et al., 2003)
PDR11/Pdr11p	Pleiotropic Drug Resistance	PDR (ABCG)	Transport de stérol	Membrane plasmique	(Marek et al., 2011)
AUS1/Aus1p	ABC protein involved in Uptake of Sterols	PDR (ABCG)	Transport de stérol	Membrane plasmique	(Marek et al., 2011)
PDR18/Pdr18p	Pleiotropic Drug Resistance	PDR (ABCG)	Incorporation de stérol de la membrane plasmique	Membrane plasmique	(Cabrito et al., 2011; Teixeira et al., 2012)

Tableau 5: les protéines ABC chez la levure *Saccharomyces cerevisiae.*

V.4. *Saccharomyces Cerevisiae* : un modèle de l'étude de toxicité des xénobiotiques

La levure *S. cerevisiae* représente un modèle eucaryote bien consolidé et largement utilisé. Un certain nombre de caractéristiques font de la levure un modèle idéal pour réaliser des études toxicologiques fonctionnelles. Ces avantages et inconvénients sont résumés dans la Figure 30.

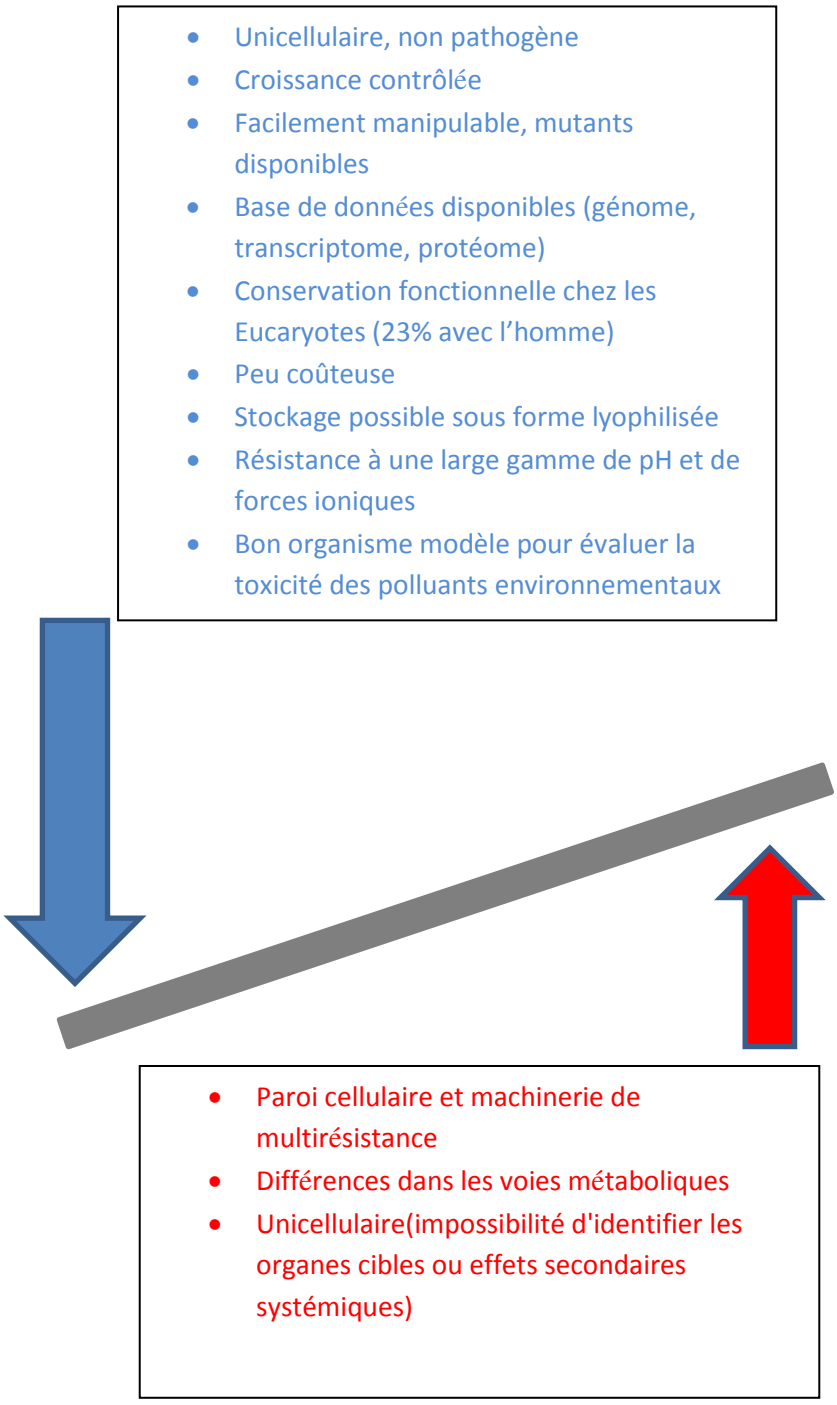

Figure 30: Avantages et inconvénients de *Saccharomyces cerevisiae* en toxicologie (modifiée) (Braconi et al., 2016; Cabral et al., 2003; Daniel et al., 2004; Gaytan et al., 2013; Gil et al., 2015; Papaefthimiou et al., 2004; Simoes et al., 2003).

V.4.1. *Saccharomyces cerevisiae* est un modèle d'étude de toxicité

Vue qu'il est facilement manipulable, peu coûteux, la grande homologie de son génome avec celui de l'être humain, sa facilité de stockage, sa croissance contrôlée et la disponibilité des bases de données au niveau génomique, transcriptomique et protéique, le *Saccharomyces cerevisiae* est utilisé jusqu'à aujourd'hui comme un bon modèle en toxicologie pour l'étude de mécanismes de toxicité de différentes catégories des xénobiotiques que ce soit des médicaments (DCF, CPZ, AMD…) ou des facteurs environnementaux (métaux lourds…).

V.4.1.1. Effet du diclofenac sur *Saccharomyces Cerevisiae*

L'effet du DCF sur différentes souches de *Saccharomyces cerevisiae* a été étudié afin de comprendre le mécanisme impliqué dans la toxicité induite par ce médicament. Le traitement de la souche BY4741 par DCF a induit l'expression de PDR5 et une mutation au niveau de ce gène a augmenté la toxicité induite par ce médicament dans le *Saccharomyces cerevisiae* (van Leeuwen et al., 2011b). Ce mécanisme de toxicité est médié par la voie de protéine kinase C (PKc) et il est aggravé en absence de zinc dans la souche Zap1p (zinc-responsive activator protein) (van Leeuwen et al., 2011b).

Le DCF inhibe la croissance de *Saccharomyces cerevisiae*, induit la mort cellulaire et la génération d'un stress oxydant. Cet effet a été accompagné par une diminution de la consommation d'oxygène donc un arrêt de respiration. Ainsi ceci a été confirmé en utilisant des souches mutées au niveau de deux gènes important dans la chaine respiratoire Rip1p et Cox9p dont l'inhibition a provoqué une aggravation de la toxicité induite par DCF (van Leeuwen et al., 2011a).

L'effet des métabolites du DCF a été étudié chez *Saccharomyces cerevisiae*. Dans ce contexte, les souches exprimant le cytochrome P450 BM3 M11 ont montré une croissance plus lente après traitement par DCF en comparaison avec la souche sauvage. Ainsi dans ces souches une génération de ROS a été induite et est en relation avec la toxicité du DCF et de ses métabolites. Mais le traitement de *Saccharomyces cerevisiae* par ces métabolites le 4' et le 5-hydroxydiclofénac n'a pas montré un effet sur la croissance des levures ni sur la génération de ROS, ce qui indique que le mécanisme de toxicité du DCF dans ces cellules n'est pas médié par son métabolisme (van Leeuwen et al., 2011c).

V.4.1.2. Effet de chlorpromazine sur *Saccharomyces cerevisiae*

Le traitement de ce microorganisme avec la chlorimipramine ou la chlorpromazine inhibe sa croissance avec une inhibition de l'entrée de pyruvate dans le cycle de Krebs et un arrêt de la respiration (Hughes and Wilkie, 1970). Cette inhibition diminue la prolifération cellulaire par une inhibition de l'entrée de calcium qui est nécessaire pour l'entrée dans la phase S de la mitose (Saavedra-Molina et al., 1983). En plus ce médicament a induit la phosphorylation du facteur initiateur de la translation (eIf2alpha) qui réduit la synthèse générale des protéines et stimule la production de Gcn4p, un facteur de transcription activé dans le cas de stress environnemental (infection virale, déficience en nutriments, accumulation des protéines dépliées dans le réticulum endoplasmique…) (De Filippi et al., 2007).

V.4.1.3. Effet de l'amiodarone sur *Saccharomyces cerevisiae*

Les mécanismes de toxicité de l'amiodarone ont été étudiés chez *Saccharomyces cerevisiae*. Ce médicament a été montré comme un inducteur d'apoptose via la génération de ROS dépendante de l'activation d'une protéine mitochondriale Ysp2 qui est un inducteur de l'acidification intracellulaire (Sokolov et al., 2006). Cette induction de la mort cellulaire programmée a été associée à une augmentation de la respiration mitochondriale et du potentiel membranaire ainsi qu'à une augmentation du Ca^{2+} cytoplasmique et un relargage du cytochrome c (Pozniakovsky et al., 2005).

En plus cette association entre la perturbation de l'homéostasie du calcium cytosolique et la toxicité induite par ce médicament a été montrée (Courchesne, 2002; Courchesne et al., 2009). Cet aspect paraît plus aggravé dans les souches hypersensibles à l'amiodarone surtout celles où il y a une mutation aux niveaux des transporteurs (pmr1 «Plasma Membrane ATPase Related », pdr5, et H+-ATPase vacuolaire) ou au niveau de la voie de synthèse d'ergosterol (erg3, erg6 et erg24) (Gupta et al., 2003).

De même l'AMD a causé des changements au niveau de la structure cellulaire de *Saccharomyces cerevisiae* comme l'augmentation de nombre des particules lipidiques interagissant avec les membranes des organites, apparition des mitochondries gonflées et le déplacement des chromatines à la péripherie du noyau. Ces changements ont été associés à la réponse spécifique à la phospholipidose et l'apoptose induite par ce médicament (Ozhovan et al., 2009).

L'effet toxique de l'amiodarone a été associé avec un autre facteur qui est l'inhibition des transporteurs au niveau de ces cellules surtout les transporteurs MDR où un traitement avec l'amiodarone a inhibé l'efflux du bromure d'éthidium un substrat spécifique de ces transporteurs (Knorre et al., 2009).

V.4.1.4. Effet de l'adriamycine sur *Saccharomyces cerevisiae*

L'adriamycine est un antibiotique anthracycline qui est largement utilisé dans le traitement de divers cancers. Cependant, l'efficacité de la chimiothérapie à base d'adriamycine est compromise par l'apparition d'effets indésirables et l'émergence de cellules cancéreuses résistantes à l'adriamycine. Dans une recherche de nouveaux mécanismes de résistance à l'adriamycine, des études ont cherché des gènes qui sont liés à la résistance d'adriamycine utilisant la levure *Saccharomyces cerevisiae* et identifiant plusieurs gènes de résistance à ce médicament (Akl1 « Ark family Kinase-Like protein », BSD2 « Bypass Sod1p Defects », SSL2 «Suppressor of Stem-Loop mutation » et Erg13 «Ergosterol biosynthesis» , etc.). Cette étude a montré le rôle de Akl1, un membre de la famille des kinases Ark / PRK, dans la résistance à l'adriamycine et que Akl1 pourrait réduire la toxicité de l'adriamycine par inhibition de l'étape d'internalisation dans l'endocytose via la phosphorylation de composant de complexe endocytique. En outre, les défauts du trafic vésiculaire de réticulum endoplasmique (ER) à vacuole réduit le degré de la résistance à l'adriamycine induit par la surexpression d'Akl1, ce qui suggère que l'inhibition de l'étape d'internalisation dans l'endocytose facilite le transport de la protéine à partir de ER à vacuole, et diminue la toxicité de l'adriamycine (Takahashi, 2013).

V.4.1.5. Effet du Cadmium sur *Saccharomyces cerevisiae*

Le cadmium, un métal lourd utilisé dans les instruments électriques, est un polluant environnemental dont les effets ont été étudiés dans le *Saccharomyces cerevisiae*. L'exposition de ces cellules à ce métal aboutit à une inhibition de la croissance et de la viabilité associées à une augmentation de malondialdéhyde et de glutathion et un accroissement de catalase et superoxyde dismutase (Muthukumar and Nachiappan, 2010). Ces dernières surtout le glutathion et la superoxyde dismutase 1 (Sod1) jouent un rôle protecteur pour les cellules contre ce métal mais la formation d'un complexe GSH-Cd altère ce rôle (Adamis et al., 2004a; Adamis et al., 2004b).

En plus des études ont montré que la toxicité induite par le *Saccharomyces cerevisiae* est une apoptose médiée par un stress oxydant et par une erreur de réparation de l'ADN (Banerjee and Flores-Rozas, 2005; Gomes et al., 2008). Ces mécanismes de stress altèrent la glutarédoxine 2 (GRX2) qui essaie d'activer la voie de secours qui est celle de glutathion (Gomes et al., 2008).

Cadre et buts du travail

Plusieurs facteurs de susceptibilité, autres que génétiques, sont considérés comme pouvant favoriser la survenue d'une toxicité hépatique d'origine médicamenteuse chez un petit nombre de patients traités.

Divers travaux expérimentaux *in vivo* chez l'animal et *in vitro* ont montré qu'un stress inflammatoire pouvait potentialiser l'hépatotoxicité induite par certains médicaments. Cependant, il est bien établi que des résultats obtenus chez l'animal ne sont généralement pas transposables à l'homme et qu'il n'existe pas de modèle animal pour prédire une toxicité idiosyncratique. D'autre part, les études *in vitro* ont souvent été réalisées sur des cellules HepG2 qui ont perdu l'essentiel de leur potentiel de biotransformation de phase 1 et de phase 2. Mais, il est bien connu que certains médicaments sont métabolisés en métabolites réactifs et les cytokines pro-inflammatoires peuvent fortement modifier la capacité de biotransformation des hépatocytes, en altérant notamment l'expression et l'activité de plusieurs cytochromes P450 majeurs.

Notre objectif a été, en utilisant les cellules humaines HepaRG, :

1. De déterminer si des cytokines pro-inflammatoires, en particulier le TNF-α, peuvent aggraver la cytotoxicité de médicaments connus pour induire une hépatotoxicité idiosyncratique chez l'homme, ajoutés séparément ou en mélange.

2. De rechercher si les effets des cytokines peuvent concerner uniquement la cytotoxicité ou également 2 autres types de lésions hépatiques, à savoir la cholestase et la stéatose.

3. D'évaluer la sensibilité des levures de type *Saccharomyces cerevisiae* vis-à-vis de ces mêmes molécules. Ce modèle de cellule eucaryote possède une faible capacité métabolique des xénobiotiques, mais possède des gènes liés à la toxicité similaires aux gènes humains (cycle cellulaire, cytosquelette, système endomembranaire,…)

Le diclofénac et la trovofloxacine qui induisent *in vivo* à la fois une hépatotoxicité et une cholestase et l'amiodarone qui induit une stéatose et à plus long terme une stéatohépatite ont été retenus pour ce travail.

Les différents résultats obtenus sont présentés en 4 chapitres :

I. Etude de la sensibilité différentielle des cellules HepaRG différenciées ou non à la toxicité du diclofénac en présence ou en absence de TNF-α

II. La N-acétylcystéine potentialise la toxicité du diclofénac chez *Saccharomyces cerevisiae*: implication possible des transporteurs ABC

III. TNF-α potentialise l'augmentation de l'effet hépatotoxique mais non l'effet cholestatique du co-traitement diclofenac/trovafloxacine dans les cellules HepaRG

IV. N-acétylcysteine empêche l'induction de la cytotoxicité et la stéatose hépatique par l'amiodarone ainsi que leur aggravation par le stress inflammatoire

Résultats

Chapitre I. Etude de la sensibilité différentielle des cellules HepaRG différenciées ou non à la toxicité du diclofénac en présence ou en absence de TNF-α

Résumé

Le rôle des métabolites réactifs et du stress inflammatoire a été largement évoqué dans l'hépatotoxicité idiosyncratique du diclofénac (DCF) mais les mécanismes sont encore mal compris. Nous avons cherché à évaluer l'influence du phénotype des cellules du foie sur l'hépatotoxicité du DCF combiné ou non avec du TNF-α en utilisant des cellules HepaRG différenciées et indifférenciées, et pour comparaison, les cellules HepG2. Nos résultats démontrent qu'après 24h de traitement les cellules HepaRG métaboliquement actives sont moins sensibles au DCF que leurs homologues non différenciés et non métaboliseurs comme en témoignant la génération d'un stress oxydant et d'un stress du réticulum endoplasmique moindres et une plus faible activité de la caspase 9. Les cellules HepaRG différenciées sont également moins sensibles que les cellules HepG2. Leur sensibilité inférieure au DCF semble liée à leur contenu élevé en glutathion transférases. De plus, l'apoptose induite par DCF est potentialisée par le TNF-α uniquement dans les cellules HepaRG différenciées et les cellules HepG2, qui expriment le récepteur de mort et est associée à l'activation de la caspase 8. Il faut noter que TNF-α n'aggrave pas l'effet cholestatique induit par DCF. Au total, nos résultats montrent que (i) la faible sensibilité des cellules HepaRG différenciées au DCF par comparaison avec leurs homologues non différenciés est liée à leur capacité de détoxification élevée, soutenant l'hypothèse évoquant une plus grande sensibilité des tissus non-hépatiques à ce médicament; (ii) la potentialisation de la cytotoxicité de DCF par le TNF-α est observée uniquement dans les cellules exprimant le récepteur de mort.

Ce travail a été publié sous le titre : 1.Differential sensitivity of metabolically competent and non-competent HepaRG cells to apoptosis induced by diclofenac combined or not with TNF-α (http://dx.doi.org/10.1016/j.toxlet.2016.06.008 (Toxicology Letters 258 (2016) 71–86)

Toxicology Letters 258 (2016) 71–86

Contents lists available at ScienceDirect

Toxicology Letters

journal homepage: www.elsevier.com/locate/toxlet

Differential sensitivity of metabolically competent and non-competent HepaRG cells to apoptosis induced by diclofenac combined or not with TNF-α☆

Houssein Al-Attrache[a,b,d], Ahmad Sharanek[a,b], Audrey Burban[a,b], Matthew Burbank[a,b], Thomas Gicquel[a,b,c], Ziad Abdel-Razzak[d], Christiane Guguen-Guillouzo[a,b], Isabelle Morel[a,b,c], André Guillouzo[a,b,*]

[a] Inserm U991, Faculty of Pharmacy, Rennes, France
[b] Rennes 1 University, Rennes, France
[c] Laboratory Emergency and Intensive Care, Hospital Pontchaillou, Rennes, France
[d] Laboratory of Applied Biotechnology: biomolecules, biotherapy and bioprocesses (LBA3B), AZM Center-Tripoli and EDST-PRASE-Beirut, Rafic Hariri Campus—Lebanese University, Lebanon

HIGHLIGHTS

- HepaRG hepatocytes are less sensitive to DCF than HepG2 cells and undifferentiated HepaRG cells.
- The lower sensitivity of HepaRG hepatocytes is related to their high detoxifying capacity.
- Inhibition of glutathione transferases results in increased DCF cytotoxicity.
- TNF-α potentiation of DCF cytotoxicity is not observed in undifferentiated HepaRG cells.
- DCF-induced cholestasis typified by bile canaliculi dilatation is not aggravated by TNF-α.

ARTICLE INFO

Article history:
Received 19 January 2016
Received in revised form 24 May 2016
Accepted 10 June 2016
Available online 14 June 2016

Keywords:
Drug metabolism
Differentiation status
Tumor necrosis factor α
Caspases
Reactive oxygen species
Endoplasmic reticulum stress
Cholestasis
Glutathione transferases

ABSTRACT

The role of reactive metabolites and inflammatory stress has been largely evoked in idiosyncratic hepatotoxicity of diclofenac (DCF); however mechanisms remain poorly understood. We aimed to evaluate the influence of liver cell phenotype on the hepatotoxicity of DCF combined or not with TNF-α using differentiated and undifferentiated HepaRG cells, and for comparison, HepG2 cells. Our results demonstrate that after a 24 h-treatment metabolizing HepaRG cells were less sensitive to DCF than their undifferentiated non-metabolizing counterparts as shown by lower oxidative and endoplasmic reticulum stress responses and lower activation of caspase 9. Differentiated HepaRG cells were also less sensitive than HepG2 cells. Their lower sensitivity to DCF was related to their high content in glutathione transferases. DCF-induced apoptotic effects were potentiated by TNF-α only in death receptor-expressing differentiated HepaRG and HepG2 cells and were associated with marked activation of caspase 8. TNF-α co-treatment did not aggravate DCF-induced cholestatic features. Altogether, our results demonstrate that (i) lower sensitivity to DCF of differentiated HepaRG cells compared to their non-metabolically active counterparts was related to their high detoxifying capacity, giving support to the higher

Abbreviations: ABT, 1-aminobenzotriazole; Ac-DEVD-AMC, *N*-acetyl-Asp-Glu-Val-Asp-7-amido-4-methylcoumarin; AC-IETD-AMC, Ac-Ile-Glu-Thr-Asp-7-amino-4-methylcoumarin; AC-LEHD-AMC, Ac-Leu-Glu-His-Asp-7-Amino-4-methylcoumarin; BSEP, bile salt export pump; CDF, 5 (and 6)-carboxy-2′,7′-dichlorofluorescein (CDF); CRP, C-reactive protein; CYP, cytochrome P450; DCF, diclofenac; DMSO, dimethyl sulfoxide; ER, endoplasmic reticulum; H2-DCFDA, 2′,7′-dichlorodihydrofluorescein; HO1, heme oxygenase 1; IL-8, interleukin-8; MnSOD, manganese superoxide dismutase; MRP2, multidrug associated protein 2; MTT, methylthiazoltetrazolium; NAC, *N*-acetyl cysteine; NTCP, Na^+-dependent taurocholate cotransporting polypeptide; PBS, phosphate buffered saline; ROS, reactive oxygen species; RT-qPCR, real-time quantitative polymerase chain reaction; TNF-α, tumor necrosis factor α.

☆ Presented in part at the 51st Congress of the European Societies of Toxicology (EUROTOX) Porto, Pl, September 2015 (Tox. Lett. 2015, 238:S304).

* Corresponding author at: Inserm UMR 991, Faculté des Sciences Pharmaceutiques et Biologiques, 35043 Rennes Cedex, France.
E-mail address: Andre.Guillouzo@univ-rennes1.fr (A. Guillouzo).

http://dx.doi.org/10.1016/j.toxlet.2016.06.008
0378-4274/

HepG2 cells
Primary human hepatocytes

sensitivity of nonhepatic tissues than liver to this drug; (ii) TNF-α-potentiation of DCF cytotoxicity occurred only in death receptor-expressing cells.

1. Introduction

Drug-induced idiosyncratic hepatotoxicity represents 13–17% of all cases of acute liver failure (Bjornsson and Olsson, 2006). Formation of reactive metabolites, generation of oxidative stress, inflammatory stress and immune response are recognized to be potential critical determinants (Uetrecht, 2006).

Diclofenac (DCF) is a non-steroidal anti-inflammatory drug widely used for the treatment of rheumatoid arthritis, osteoarthritis and acute injury pain. Its administration has been associated with adverse effects in various organs, especially the gastrointestinal tract and kidney. DCF has also caused rare cases of hepatocellular injury, cholestasis or mixed hepatocellular injury and cholestasis (Banks et al., 1995; Breen et al., 1986; Watanabe et al., 2007). DCF-induced liver toxicity has been related to the formation of reactive metabolites, i.e. quinone imines from 4'OH-DCF and 5'OH-DCF, and acyl glucuronides primarily catalyzed by UGT2B7 (Bort et al., 1999; Kretz-Rommel and Boelsterli, 1993; Wang et al., 2004). DCF-acyl glucuronides can bind selective proteins, including dipeptidyl peptidase IV, a canalicular membrane protein (Seitz and Boelsterli, 1998; Seitz et al., 1998). However, the role of these protein adducts in the pathogenesis of DCF-associated liver toxicity remains unclear (Aithal and Day, 2007; Banks et al., 1995).

DCF and its CYP-mediated metabolites 4'OH-DCF and 5'OH-DCF induce concentration-dependent apoptosis at equimolar concentrations, the greatest pro-apoptotic activity being produced by 5'OH-DCF in primary human hepatocytes (Bort et al., 1999). However, DCF does not appear to be more cytotoxic to human hepatocytes than to HepG2 cells which usually express low drug metabolizing enzyme activities (Fredriksson et al., 2011; Gomez-Lechon et al., 2003b). Moreover, DCF has been shown to be toxic to non-hepatic organs and cells at doses even lower than those required for liver toxicity (Ng et al., 2008). All these data make questionable the direct involvement of CYP-derived metabolites in DCF cytotoxicity *in vivo* and *in vitro*. DCF-induced apoptosis is strongly potentiated by TNF-α in HepG2 cells (Fredriksson et al., 2011; Maiuri et al., 2015) and lipopolysaccharide in rodent liver (Deng et al., 2006). The involvement of the intrinsic apoptotic pathway characterized by disruption of mitochondrial integrity has been demonstrated in various studies (Fredriksson et al., 2011; Gomez-Lechon et al., 2003a), and oxidative and endoplasmic reticulum (ER) stresses have been identified as independent cytotoxic responses to both DCF alone and the combination DCF/TNF-α (Fredriksson et al., 2014). The synergistic effect of DCF/TNF-α co-treatment appeared to occur mostly via activation of the extrinsic apoptotic pathway (Fredriksson et al., 2011).

In the present work, we further investigated mechanisms of DCF hepatotoxicity and cross-talk between hepatocyte apoptosis induced by DCF and TNF-α challenge using differentiated, metabolically competent and undifferentiated, non metabolically competent HepaRG cells and for comparison, HepG2 cells. At their undifferentiated stage HepaRG cells express markers of progenitors and do not exhibit detectable drug metabolizing enzyme activities; however, they can reach the capacity to express functions of mature hepatocytes, including activities of CYP2C9 and CYP3A4 which are the main CYPs involved in the formation of CYP-mediated metabolites of DCF (Aninat et al., 2006; Guillouzo and Guguen-Guillouzo, 2008), as well as detoxifying enzymes (Aninat et al., 2006; Gerets et al., 2012; Rogue et al., 2012). We show here that sensitivity of liver cells to DCF-induced apoptosis was related to their phenotype and that potentiation by TNF-α was observed only in differentiated HepaRG cells expressing liver-specific functions and in HepG2 cells.

2. Materials and methods

2.1. Chemicals and reagents

1-Aminobenzotriazole (ABT), diclofenac sodium salt (DCF), dithiothreitol (DTT), methylthiazoltetrazolium (MTT), *N*-acetyl-Asp-Glu-Val-Asp-7-amido-4-methylcoumarin (AC-DEVD-AMC), *N*-acetyl-cysteine (NAC), ethacrynic acid, 6β-hydroxy-testosterone and testosterone were purchased from Sigma Aldrich (St. Quentin Fallavier, France). 2′,7′-Dichlorodihydrofluorescein (H_2-DCFDA) was from Invitrogen Molecular Probe (Cergy-Pontoise, France). Ac-Ile-Glu-Thr-Asp-7-Amino-4-methylcoumarin (AC-IETD-AMC) and Ac-Leu-Glu-His-Asp-7-Amino-4-methylcoumarin (AC-LEHD-AMC) were supplied by Enzo Life Sciences (Lyon, France). TNF-α was provided by Promocell (Nuremberg, Germany). eIF2α (catalog 9722) and phospho-eIF2α (Ser51) (catalog 3597) were from Cell Signaling Technology (Danvers, MA, USA). CXCL8/IL-8 and Human C-reactive protein (CRP) DuoSet kits were from R&D (Abingdon, United Kingdom). N-benzyloxycarbonyl-Leu-Glu(OMe)-His-Asp (OMe)-fluoromethyl ketone (z-LEHD-fmk) was purchased from BD Biosciences (Le Pont de Claix, France) and etanercept was from Amgen (Thousand Oaks, CA, USA). Glutathione transferases (GST) A1/2 and M1/2 antibodies were gifts from Dr Caroline Aninat (Rennes).

2.2. Cell cultures and treatments

2.2.1. Cell cultures

HepaRG cells were seeded at a density of 2.6×10^4 cells/cm^2 in Williams' E medium supplemented with 10% Hyclone® fetal bovine serum (Thermo scientific, San Jose, USA), 100 U/mL penicillin, 100 μg/ml streptomycin, 5 μg/ml insulin, 2 mM glutamine, and 50 μM hydrocortisone hemisuccinate. After 2 weeks, these undifferentiated cells were shifted to the same medium supplemented with 1.7% dimethyl sulfoxide (DMSO) for further 2 weeks in order to obtain cells expressing liver-specific functions. At that time, cultures contained hepatocyte-like and progenitors/primitive biliary-like cells in nearly equal proportions (Cerec et al., 2007).

HepG2 cells were seeded at a density of 2.6×10^4 cells/cm^2 in minimum essential medium-α supplemented with 10% Hyclone® fetal bovine serum, non-essential amino acids, 100 U/ml penicillin and 100 μg/ml streptomycin, and were used at subconfluence.

Primary human hepatocytes were obtained from Biopredic International (St Grégoire, France). They were isolated by collagenase-perfusion of liver biopsies from adult donors (Guguen-Guillouzo et al., 1982). These cells were cultured at a density of $1.5.10^5$/cm^2 in a Williams' E medium containing 10% Hyclone® fetal bovine serum without hydrocortisone hemisuccinate for the first 24 h and in a medium deprived of serum and hydrocortisone thereafter. Cultures were used at day 4.

2.2.2. Treatments

All treatments were performed on cells maintained in a medium containing 2% Hyclone® fetal bovine serum and 0.2%

DMSO (used as a vehicle). Selection of TNF-α concentration (10 ng/ml) was based on previous studies (Bachour-El Azzi et al., 2014; Fredriksson et al., 2014) and preliminary experiments on determination of caspase 3 activity and CRP secretion levels. However, except otherwise indicated a co-treatment with DCF and cytokine meant a 24 h pre-treatment with the cytokine alone before treatment with DCF/cytokine combination.

2.3. MTT assay

Cytotoxicity was evaluated using the MTT colorimetric assay. Briefly, cells were seeded in 24-well plates and treated with either TNF-α or various concentrations of DCF (50, 100, 150, 200, 250, 350 or 500 μM) after pre-treatment or not with TNF-α. After medium removal, 500 μl of serum-free medium containing MTT (0.5 mg/ml) was added to each well and incubated for 2 h at 37 °C. The water-insoluble formazan was dissolved in 500 μl DMSO and absorbance was measured at 550 nm (Aninat et al., 2006).

2.4. Phase-contrast imaging analysis

Cells were treated with DCF, TNF-α and DCF ± TNF-α for different times (0, 4 and 24 h) and images were taken using a phase-contrast microscope (Inverted microscope Zeiss axiovert 200 M and Axiocam MRm).

2.5. ELISA assays

C-reactive protein (CRP) and interleukin-8 (IL-8) proteins were measured in cell supernatants using CRP and CXCL8/IL-8 DuoSet kits, according to manufacturer's instructions. Briefly, supernatants were collected after 24 h treatment and stored at −80 °C until analysis; 96-well microplates were coated with capture antibody and incubated overnight. Samples and standards were diluted appropriately and added for 2 h after a saturation step. Secondary antibody was added for 2 h after washing. Streptavidin-horseradish peroxidase and its substrate were used for the revelation step. Optical density was read at 450 nm with wavelength correction. All steps were performed at room temperature (Bachour-El Azzi et al., 2014).

2.6. Determination of ROS generation

ROS generation was determined by the H_2-DCFDA assay. After treatment with DCF ± TNF-α for 30 min, 2 h, 4 h, 8 h and 24 h, 10^6 cells were incubated for 2 h at 37 °C with 2 μM H_2-DCFDA and then washed with cold PBS, and scraped in potassium buffer (10 mM, pH 7.4)/methanol (v/v) complemented with Triton X-100 (0.1%). Fluorescence intensity of cell lysates was determined by spectrofluorimetry using excitation/emission wavelengths of 498/520 nm (Sharanek et al., 2014).

2.7. Determination of caspase 3, 8 and 9 activities

After treatment with DCF ± TNF-α, the cells were scraped in the culture medium, then centrifuged, washed with PBS, dried and stored at −80 °C. Cell lysates were re-suspended in 70 μl of 4-(2-hydroxyethyl)-ι-piperazine ethane sulfonic acid supplemented with anti-phosphatase and anti-protease. Then, 40 μg proteins of each sample was placed in an opaque plate in triplicate and supplemented with caspase buffer, 20 mM piperazine-1,4-bis-2-ethanesulfonic acid, pH 7.2, 100 mM NaCl, 10 mM dithiotreitol, 1 mM EDTA, 0.1% 3-[(3-cholamidopropyl)dimethylammonio]-1-propane sulfonic acid and 10% sucrose. Then 2 μl of DEVD-AMC, LEHD or IETD substrates for caspases 3, 9 and 8 respectively, was added. Fluorescence was measured at a wavelength between 380 and 420 nm for caspase 3 and between 405 and 465 nm for caspases 8 and 9 (Dumont et al., 2010; Maianski et al., 2004).

The influence of different inhibitors on caspase activities was also tested. The antioxidant N-acetyl cysteine (NAC) was added to cultures treated with DCF, TNF-α or their combination for 24 h at the concentration of 5 mM (Fredriksson et al., 2011; Sharanek et al., 2014; Son et al., 2013). Etanercept, a soluble p75 TNF-α receptor that prevents TNF-α to activate its membrane-bound receptor, thereby leading to inhibition of caspase 8 activation via the extrinsic apoptotic pathway (Jouan-Lanhouet et al., 2012), and z-LEHD-fmk, a specific inhibitor of caspase 9 activation (Maccarrone et al., 2000), were added at the concentrations of 10 μg/ml and 20 μM respectively, one hour before treatment with DCF and/or TNF-α.

2.8. Western blotting analysis

HepaRG cells were incubated in a medium added or not with DCF ± TNF-α for 2 h after pre-treatment or not with the cytokine. P-eIF2α, eIF2α, GSTA1/2 and GSTM1/2 were analyzed according to methods previously described (Fredriksson et al., 2011; Zeng et al., 2014).

Briefly, after treatment, cells were washed with cold PBS and re-suspended in cell lysis buffer and a protease inhibitor cocktail. Aliquots containing an equivalent total protein content, as determined by the Bradford's procedure with bovine serum albumin as the standard, were subjected to sodium dodecyl sulfate/4-12% polyacrylamide gel electrophoresis, electrotransferred to immobilon-P membranes, and probed overnight with p-eIF2α, eIF2α or GST antibodies. After incubation with a rabbit secondary antibody, a chemiluminescence reagent, and Hyperfilm ECL, bands were quantified by densitometry with Fusion-Capt software (Marne-La vallée, France).

2.9. Measurement of CYP3A4 activity

After treatment with DCF ± TNF-α cells were washed with PBS and incubated at 37 °C with testosterone dissolved in Williams' E medium without phenol red. After 2 h, medium was collected and CYP3A4 activity was measured using a high performance liquid chromatography equipment (Agilent 1100 series high performance liquid chromatograph equipped with an autosampler and Agilent 1100 series fluorescence and UV detectors) with two solvents, acetic acid (0.1%) and acetonitrile, as previously (Aninat et al., 2006).

2.10. Diclofenac biokinetics

Cultures were incubated with 200 μM DCF ± TNF-α for 2, 4 and 24 h; then cell supernatants and lysates were diluted 100 times in the mobile phase and analyzed by Liquid Chromatography – High Resolution – Mass Spectrometer (LC-HR-MS) Q ExactiveTM (Thermo Scientific). An HESI-II ion source was used for the electrospray ionization of target compounds. The chromatographic separation of the analytes was performed with an Accela pump (Thermo Scientific) equipped with a Thermo Fisher C18 Accucore column (100 × 2.1 mm, 2.6 μM) using a gradient of 10 mM ammonium acetate buffer containing 0.1% (v/v) formic acid and of acetonitrile with 0.1% (v/v) formic acid. Retention times were respectively 1.6 min and 1.3 min for DCF and OH-DCF. Calibration curves were obtained by spiking mobile phase with standards at 0.01–10 μM. Data were acquired in negative Full Scan mode and quantification was performed by extracting the exact mass value of deprotonated DCF (294.0095 m/z) and OH-DCF (310.0042 m/z) using a 5 ppm mass window. 4'OH DCF and 5'OH DCF were not

separated chromatographically; consequently OH-metabolites represented the sum of both.

2.11. Real-Time quantitative polymerase chain reaction (RT-qPCR) analysis

Total RNA was extracted from 10^6 HepaRG or HepG2 cells with the SV total RNA isolation system (Promega, Charbonnieres-les-Bains, France). RNAs were reverse-transcribed into cDNA and RT-qPCR was performed using a SYBR Green mix. Primer sequences are listed in Supplementary Table 1.

2.12. Taurocholic acid efflux

To estimate bile salt export pump (BSEP) activity cells were first exposed to 43.3 nM [^{3}H]- taurocholic acid ([^{3}H]-TA) for 30 min; after washing cells were incubated with DCF ± TNFα in a standard buffer containing Ca^{2+} and Mg^{2+}. After 2 h incubation cells were washed and then scraped in 0.1 N NaOH. The remaining radiolabeled substrate was measured through scintillation counting to determine TA efflux (Antherieu et al., 2013).

2.13. Na^+-dependent taurocholate co-transporting polypeptide activity (NTCP)

NTCP activity was estimated by determination of sodium-dependent intracellular accumulation of [^{3}H]-TA substrate. Cells were treated with DCF ± TNF-α followed by incubation with 43.3 nM radiolabeled TA for 30 min. Then, they were washed with standard buffer and lysed with 0.1 N NaOH. Accumulation of radiolabeled substrate was determined through scintillation counting (Sharanek et al., 2015).

2.14. CDF efflux determination

After treatment with DCF ± TNF-α for 4 h cells were incubated with 3 μM of 5 (and 6)-carboxy-2,7-dichlorofluorescein diacetate (CDFDA) for 30 min at 37 °C. Upon hydrolysis by intracellular esterases, CDFDA was converted to fluorescent CDF (excitation/emission: 488/509 nm) and directed towards the biliary pole by membrane transporters, mainly by the multidrug resistance-associated protein 2 (MRP2). After washing with phenol red-free Williams' E medium imaging was performed using a Cellomics ArrayScan VTI HCS Reader (Thermo Scientific) (Bachour-El Azzi et al., 2015).

2.15. Statistical analysis

One-way ANOVA with Bonferroni's multiple comparison test (GraphPad Prism 5.00) was performed to compare data between DCF-, TNF-α-, DCF + TNF-α-treated cells and control cultures. Each value corresponded to the mean ± standard error of the mean (SEM) of three independent experiments. Data were considered significantly different when $p < 0.05$.

3. Results

3.1. Differential sensitivity of metabolically and non metabolically competent HepaRG cells to DCF

DCF cytotoxicity was first estimated using the MTT assay after a 24 h treatment. A decrease in cell viability was observed in a dose-dependent manner with drug concentrations starting at 350 μM (IC50 ≈ 780 μM) in differentiated HepaRG cells. Human hepatocytes obtained from three donors showed similar sensitivity to DCF toxicity (IC50 ≈ 800 μM) as differentiated HepaRG cells. Undifferentiated HepaRG (8 days after seeding) and subconfluent HepG2 cells were more sensitive (IC50s = 468 and 688 μM respectively) (Fig. 1A–D).

Apoptotic effects of DCF were also estimated by determination of caspase 3 activity. A 1.8-fold augmentation was observed in differentiated HepaRG cells treated with 200 μM DCF. Interestingly, undifferentiated HepaRG and subconfluent HepG2 cells were respectively 3- and 2-fold more sensitive to DCF than differentiated HepaRG cells exposed to 200 μM DCF (Fig. 1E and F).

Accordingly, cell examination under phase-contrast microscopy after a 24 h treatment evidenced some cell detachment in undifferentiated HepaRG and HepG2 cell cultures exposed to 200 μM DCF (Fig. 2).

To confirm the lower sensitivity of HepaRG hepatocytes compared to primitive biliary cells, cultures containing 80% HepaRG hepatocytes (instead of 50%) were prepared by cell seeding at high density (Pernelle et al., 2011). In such cultures sensitivity to DCF was further reduced, not exceeding 2.9-fold (versus 5.8-fold) with 350 μM (data not shown). Based on all these results, DCF was usually used at 200 μM for further investigations.

3.2. Diclofenac metabolizing capacity of HepaRG and HepG2 cells

Drug metabolism capacity of differentiated cells was first evaluated by determination of CYP3A4 activity and transcript levels. CYP3A4 is the main expressed CYP gene in mature hepatocytes and is involved in DCF metabolism (Shen et al., 1999; Tang et al., 1999). As expected, high levels of transcripts and activity were measured in differentiated HepaRG cells; they were not significantly modulated by 200 μM DCF (Fig. 3A and B).

Then, in order to determine whether DCF was metabolized by differentiated HepaRG cells, undifferentiated HepaRG cells and HepG2 cells, its biokinetics was estimated over a 24 h period. DCF and OH-metabolites were measured in both media and cell lysates after 2, 4 and 24 h. In differentiated HepaRG cells, the percentage of unchanged DCF recovered in medium and cell layers decreased with time and represented only 14% of the initial 200 μM DCF concentration after 24 h. In parallel, increasing production of OH-metabolites was evidenced (Fig. 3C–F). DCF and/or OH-metabolites did not accumulate intracellularly. Formation of OH-metabolites was completely prevented by co-addition of 300 μM 1-amino-benzotriazole (ABT), a non selective inhibitor for human P450s. By contrast, no obvious loss of DCF was evidenced in undifferentiated HepaRG cells (data not shown) and in HepG2 cells after 24h-exposure (Supplementary Fig. 1). All these data supported the conclusion that undifferentiated HepaRG and HepG2 cells had low DCF metabolism capacity if any.

3.3. Only differentiated HepaRG and HepG2 cells are responsive to TNF-α

First, differentiated HepaRG cells were exposed to 10 ng/ml TNF-α and their responsiveness was estimated by determination of CRP and IL-8 transcripts levels and protein secretion rate. CRP and IL-8 secretion levels were measured in the medium of untreated and DCF-treated cells in the absence or presence of TNF-α for 24 h using ELISA assays. Untreated cells secreted 26 ± 4 pg/ml CRP and 21 ± 5 pg/ml IL-8, and a 37 and 31% decrease in the release of CRP and IL-8 respectively was evidenced after treatment with 200 μM DCF alone, compared to untreated cells. TNF-α strongly increased secretion levels of these two inflammatory markers (12.6- and 41.7-fold for CRP and IL-8 respectively) while a co-treatment with DCF resulted in lower increases (6.1- and 23.3-fold for CRP and IL-8 respectively compared to untreated cells) (Supplementary Fig. 2A and B). All these results were confirmed by measuring mRNA levels by PCR analysis. Co-treatments with

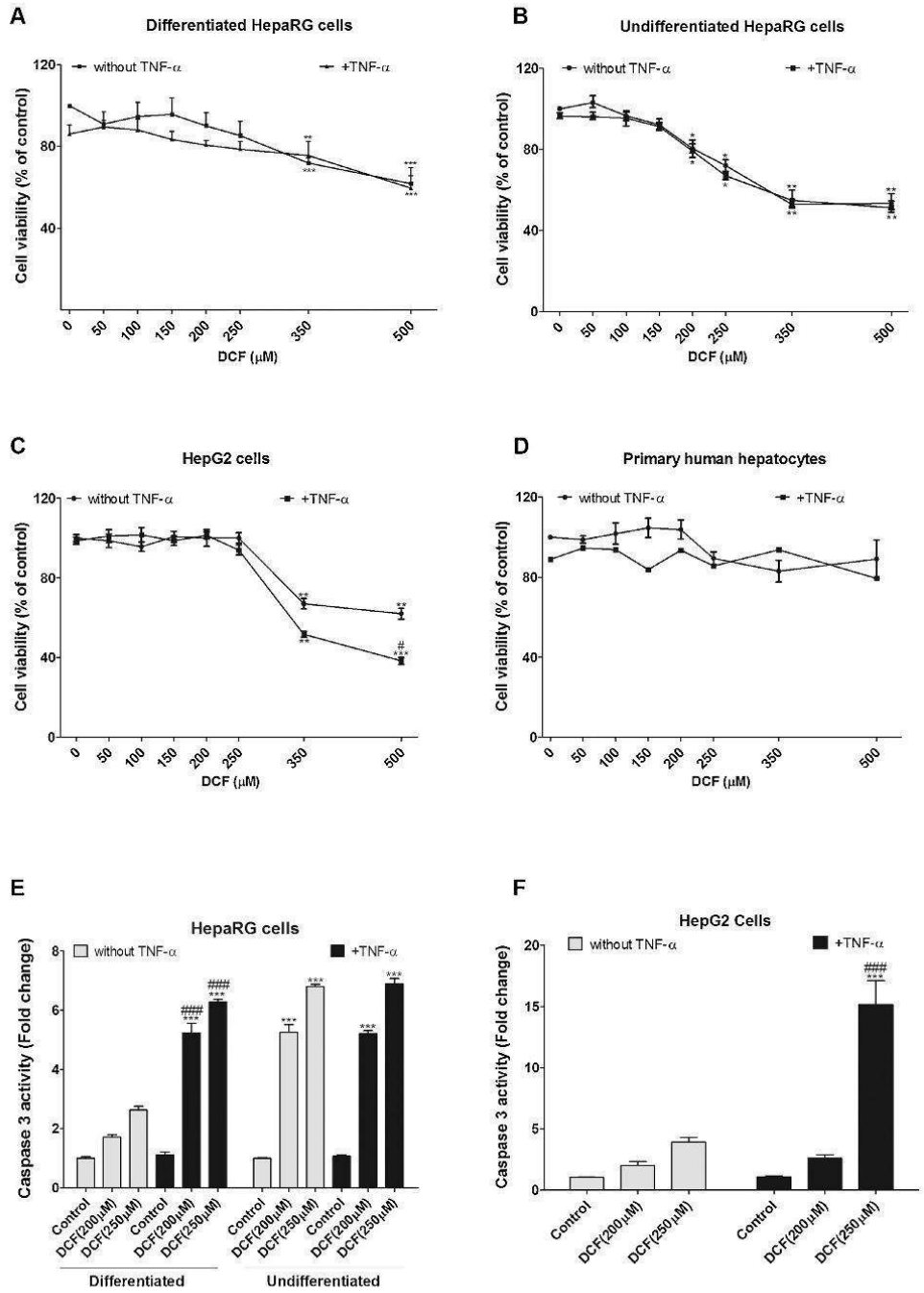

Fig. 1. Influence of TNF-α on DCF-induced toxicity in differentiated and undifferentiated HepaRG cells, HepG2 cells and primary human hepatocytes.
Cells were treated with diclofenac (DCF) ± TNF-α following pre-treatment or not with the cytokine. (A-D) MTT assay in the four cell models and (E) Caspase 3 activity in differentiated and undifferentiated HepaRG cells after treatment with DCF ± TNF-α. (F) Caspase 3 activity in HepG2 cells after the same treatments as in (E). All results are

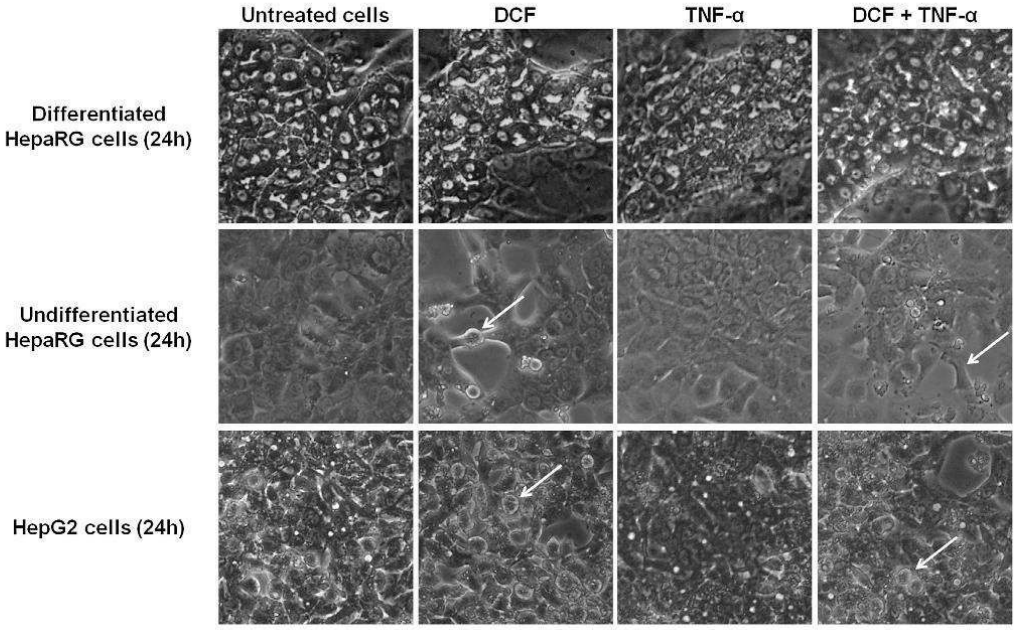

Fig. 2. Effects of DCF and TNF-α on morphology of differentiated HepaRG, undifferentiated HepaRG and HepG2 cells.
Phase-contrast microscopy examination of differentiated HepaRG, undifferentiated HepaRG and HepG2 cells after treatment with TNF-α for 24 h followed by 24 h co-treatment with 200 μM DCF ± TNF-α. White arrows demonstrate cell alterations characterized by cell detachment.

200 μM DCF also resulted in lower increase of both protein and transcripts levels (Supplementary Fig. 2C and D).

Then, the influence of TNF-α on DCF cytotoxicity was evaluated using the MTT and caspase 3 activity assays. When differentiated HepaRG cells were exposed to TNF-α for 24 h before co-exposure to the drug for further 24 h, cytotoxicity was not aggravated in differentiated HepaRG cells (Fig. 1A) and human hepatocytes (Fig. 1D) using the MTT assay. However, a significant increase in caspase 3 activity was observed with 200 μM DCF in combination with TNF-α (5.24-fold vs TNF-α alone) in differentiated cells after pre-treatment with the cytokine (Fig. 1E) while no change and only a slight increase were observed in undifferentiated HepaRG cells and HepG2 cells respectively (Fig. 1E and F). However, treatment with 250 μM DCF + TNF-α hugely activated caspase 3 (around 15-fold) in these latter (Fig. 1F).

Since pro-inflammatory cytokines are known to inhibit the major CYPs involved in drug metabolism (Abdel-Razzak et al., 1993), we then investigated whether a pre-treatment with TNF-α could modulate activity and expression of CYP3A4 in differentiated HepaRG cells treated with 200 μM DCF. Whereas CYP3A4 activity was not significantly modulated by DCF alone, it decreased to 44% with TNF-α and 34% with TNF-α + DCF (Fig. 3A). CYP3A4 transcript levels dropped by 54% and 85% of the control values with TNF-α alone and TNF-α + DCF, respectively (Fig. 3B). Of note, transcripts of CYP2C9, the other CYP involved in DCF metabolism (Shen et al., 1999), were similarly reduced by DCF, TNF-α and co-treatments (Data not shown).

DCF biokinetics and OH-metabolites formation were also measured in cultures of differentiated HepaRG cells co-treated with 200 μM DCF and TNF-α over a 24 h period. A limited decrease in DCF disappearance was observed with TNF-α + DCF (27%) compared to DCF alone (14%). Accordingly, a slight decrease in the formation of OH-metabolites was observed with TNF-α + DCF (22%) compared to DCF alone (28%). Noteworthy, ABT reduced DCF disappearance to 57% and completely inhibited OH-metabolites formation (Fig. 3C–G). As found with DCF alone no obvious loss of DCF and formation of OH-metabolites were evidenced in undifferentiated HepaRG (data not shown) and HepG2 cells after treatment with the combination DCF + TNF-α (Supplementary Fig. 1).

3.4. DCF-induced generation of oxidative stress

Treatment of differentiated HepaRG cells with DCF alone did not induce generation of detectable oxidative stress at concentrations up to 200 μM, even after 24 h as shown by measurement of reactive oxidative species (ROS) using the DCFDA assay. However, a first treatment with TNF-α followed by co-treatment with 200 μM DCF caused a slight generation of ROS within the first 8 h which reached 3.5-fold after 24 h (Fig. 4A). Transcript levels of the two oxidative stress-related genes HO-1 and MnSOD were also slightly

expressed relative to the levels found in corresponding untreated cells, arbitrarily set at a value of 1 or 100. $^{*}P < 0.05$, $^{**}P < 0.01$ and $^{***}P < 0.001$ compared with untreated cells, $^{\#}P < 0.05$ and $^{\#\#\#}P < 0.001$ compared with cells treated with TNF-α or DCF individually.

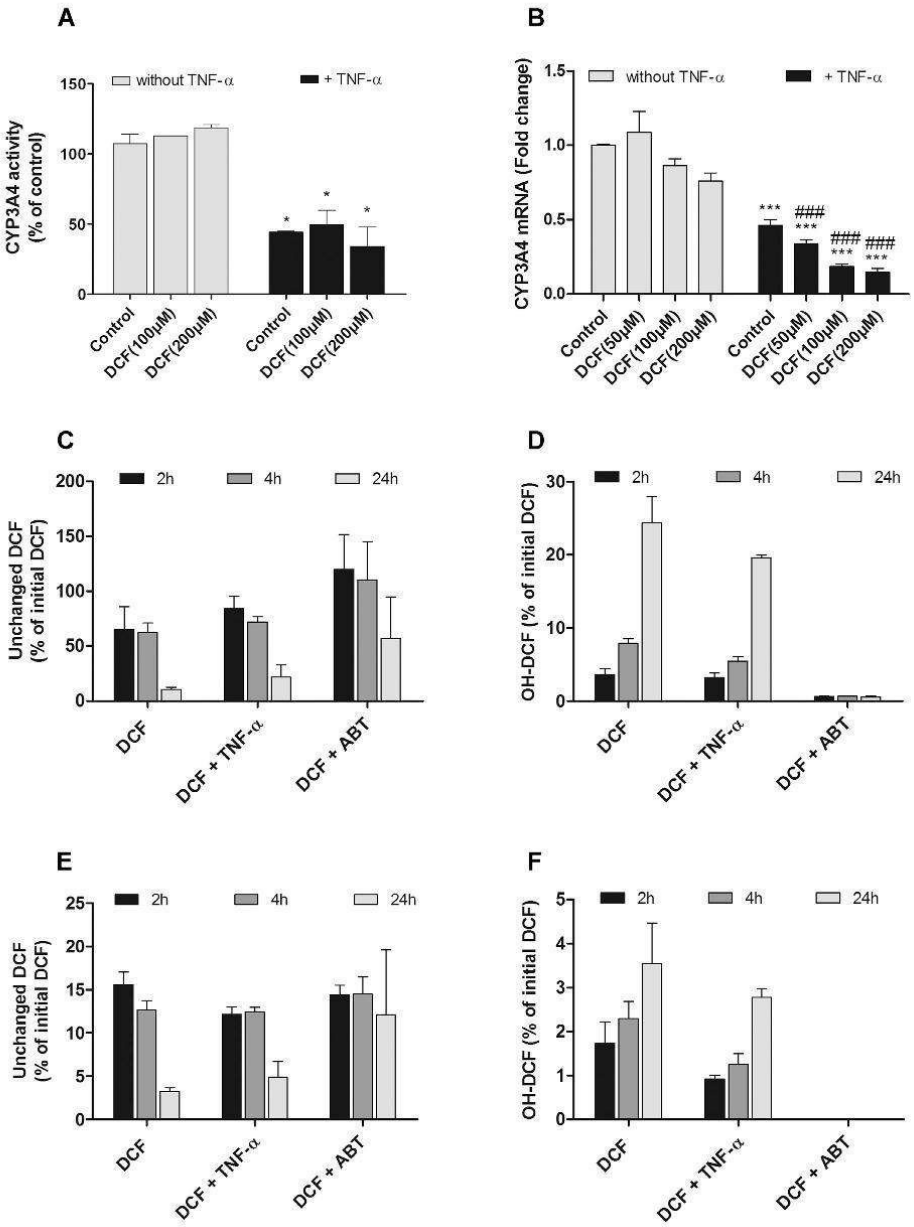

Fig. 3. Effects of DCF and TNF-α on CYP3A4 activity and transcript levels and analysis of DCF biokinetics.
Differentiated HepaRG cells were exposed to DCF ± TNF-α. (A) CYP3A4 activity determined by HPLC and (B) CYP mRNA levels measured by RT-PCR analysis. Unchanged DCF and OH-metabolites were measured by LC-HR-MS in both supernatants (C and D) and cell layers (E and F) after treatment with DCF alone or the combination DCF + TNF-α in differentiated HepaRG cells. Results in (A) and (B) are expressed relative to the levels found in control cells, arbitrarily set at a value of 100 or 1. Results in (C–F) are expressed relative to the levels found in unexposed media containing 200 μM DCF, arbitrarily set at a value of 100. $^{*}P < 0.05$ and $^{***}P < 0.001$ compared with untreated cells, $^{###}P < 0.001$ compared with cells treated with TNF-α and DCF individually.

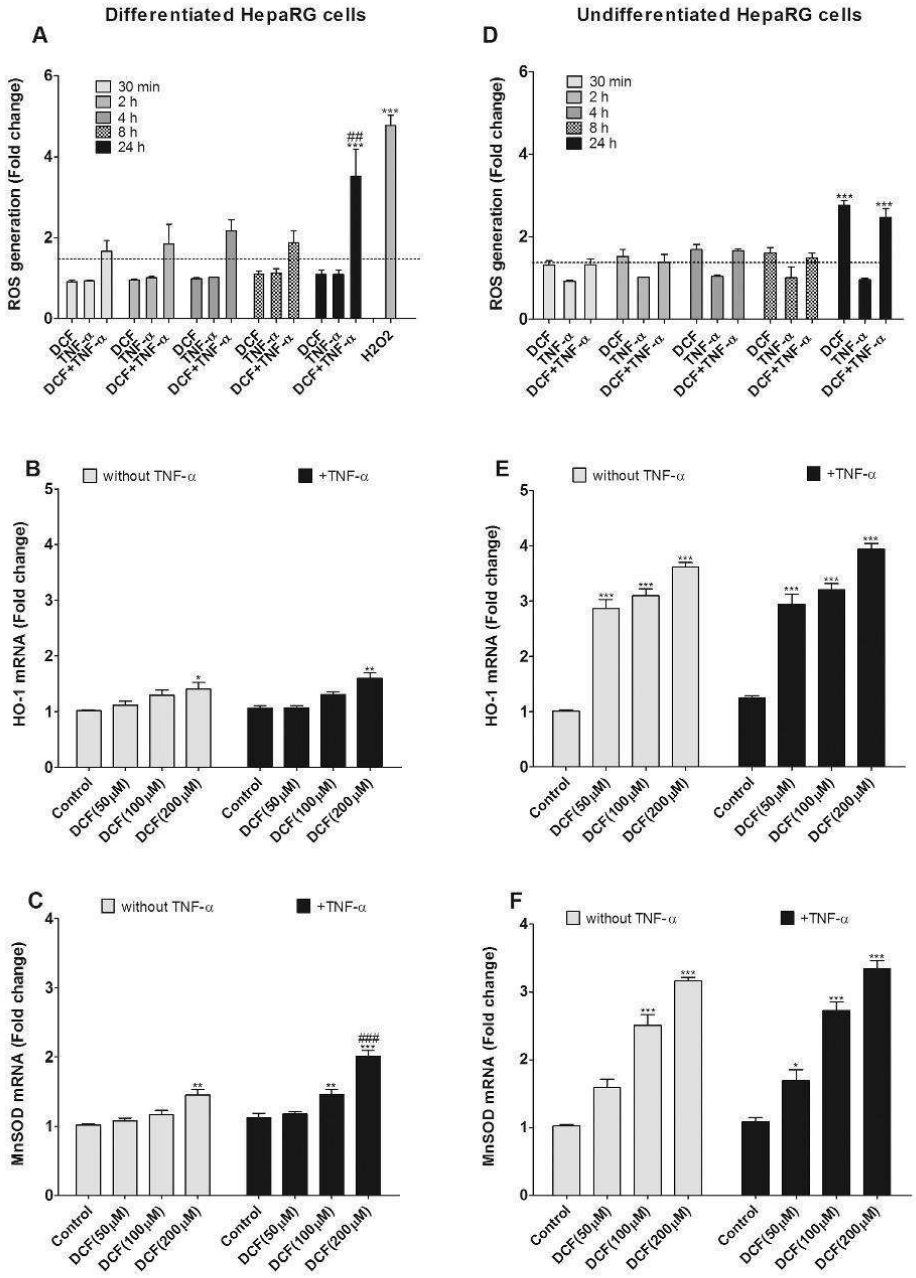

Fig. 4. Effects of DCF ± TNF-α on ROS generation and expression of HO-1 and MnSOD genes in differentiated and undifferentiated HepaRG cells.
Following exposure of cells to DCF ± TNF-α ROS generation was measured after 30 min, 2 h, 4 h, 8 h and 24 h, using the H_2DCFDA assay, and HO-1 and MnSOD transcripts levels were determined by RT-PCR analysis in (A–C) differentiated and (D–F) undifferentiated HepaRG cells. H_2O_2 (25 mM) was used as positive control after 2 h treatment. All results are expressed relative to the levels found in control cells, arbitrarily set at a value of 1. $^{*}P < 0.05$, $^{**}P < 0.01$ and $^{***}P < 0.001$ compared with untreated cells, $^{\#\#\#}P < 0.001$ compared with cells treated with TNF-α and DCF individually.

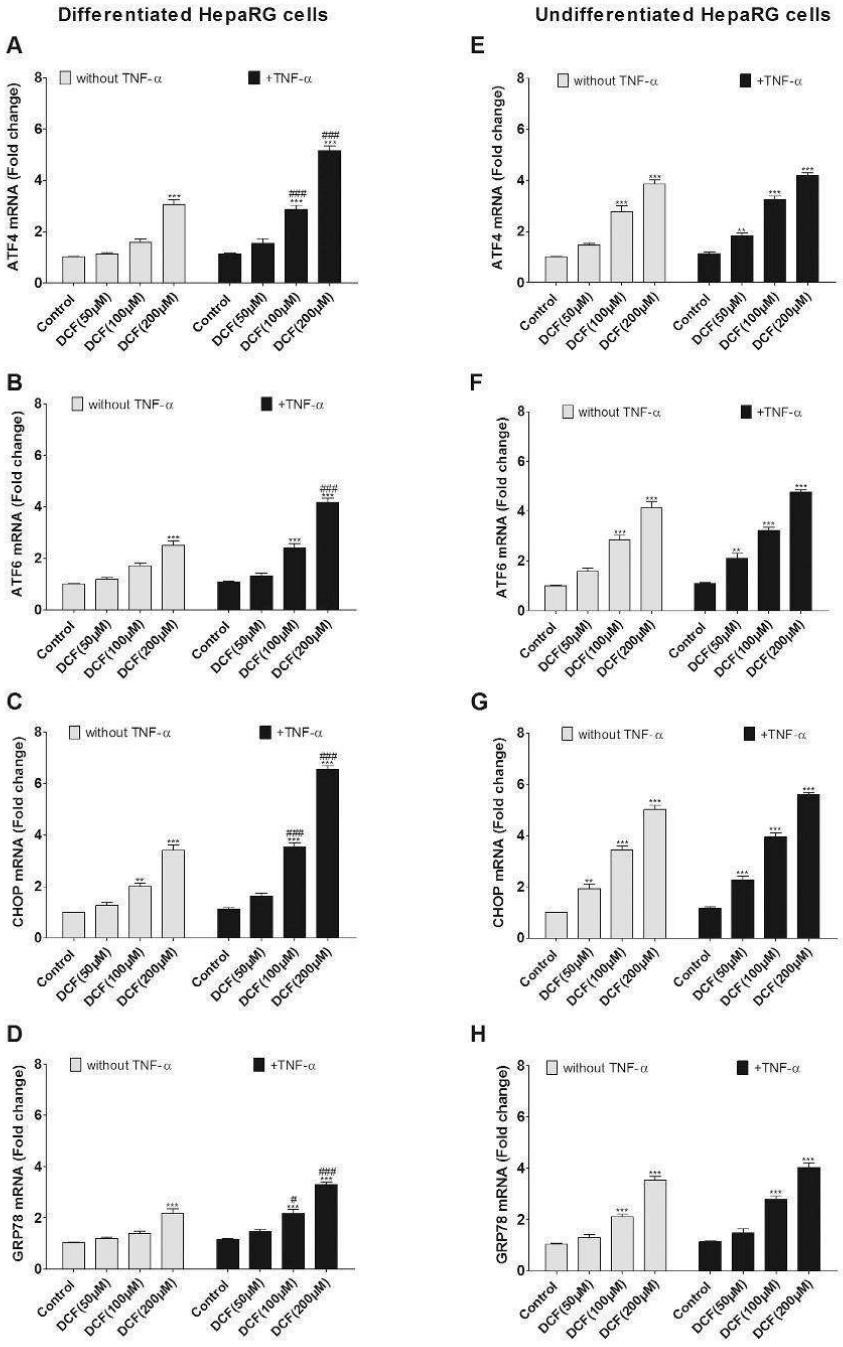

Fig. 5. Transcript levels of ER stress genes after treatment with DCF ± TNF-α.
ATF4, ATF6, CHOP and GRP78 gene expression was measured in differentiated (A–D) and undifferentiated HepaRG cells (E, F, G and H). All results are expressed relative to the corresponding levels found in control cells, arbitrarily set at a value of 1. $^{**}P < 0.01$ and $^{***}P < 0.001$ compared with untreated cells, $^{\#}P < 0.05$ and $^{\#\#\#}P < 0.001$ compared with cells treated with TNF-α and DCF individually.

augmented in differentiated HepaRG cells, i.e. 1.4- and 1.5-fold, after treatment with 200 μM DCF and 1.6- and 2-fold after co-treatment with DCF + TNF-α respectively after 24 h (Fig. 4B and C).

A slight production of ROS was detected in undifferentiated HepaRG cells during the first 8 h after treatment with 200 μM DCF (1.4-fold); this production reached 2.8-fold after 24 h (Fig. 4D). Noticeably, HO-1 and MnSOD gene expression was also augmented in undifferentiated HepaRG cells exposed to DCF alone (3.6- and 3.1-fold respectively) and slightly more after co-treatment with DCF + TNF-α, reaching 3.9- and 3.3-fold for HO-1 and MnSOD respectively (Fig. 4E and F).

In addition, ROS generation was measured in the presence of NAC, z-LEHD-fmk and etanercept. A high inhibition of ROS generation was observed in the presence of NAC in undifferentiated HepaRG cells treated with DCF alone, and in differentiated HepaRG cells treated with DCF + TNF-α, and in the presence of etanercept in co-treated differentiated HepaRG cells. z-LEHD-fmk exerted only a slight inhibition of ROS production (Supplementary Fig. 3A and B).

3.5. Enhancement of DCF-induced ER stress by TNF-α in differentiated cells

A specific activation of the ER stress route through the ATF4 transcriptional activity has also been reported in DCF-treated liver cells (Fredriksson et al., 2014). Our results showed that transcripts levels of ATF4, ATF6, CHOP and GRP78 were all overexpressed in differentiated HepaRG cells exposed to 200 μM DCF for 24 h. The increases were significant with 200 μM for the 4 genes and co-treatment with TNF-α led to a further significant increase. CHOP was more up-regulated than ATF4 and ATF6 (Fig. 5A–D).

These 4 genes were more responsive to DCF in undifferentiated HepaRG cells; they were already overexpressed with 50 μM and their increase reached values between 3.5-fold (ATF4, ATF6 and GRP78) and 5-fold (CHOP) with 200 μM. Co-treatment with TNF-α did not further enhance expression of these 4 genes (Fig. 5E–H). Phosphorylation of eIF2α, the upstream regulator of CHOP and ATF4 (Oslowski and Urano, 2011), was also analyzed by western blots after 2 h of treatment. While it had no obvious effect in differentiated HepaRG cells, the combination TNF-α + DCF increased p-eIF2 in undifferentiated HepaRG cells compared to DCF-treated cells (Fig. 6A and B).

3.6. Modulation of caspases 8, 9 and 3 activities by DCF and TNF-α

We further analyzed whether DCF ± TNF-α altered activity of the two initiator caspases 8 and 9. DCF alone increased nearly 2-fold more caspase 9 than caspase 8 (3.1- vs. 1.7-fold) in differentiated cells and more strongly both caspases in undifferentiated cells (5.4- and 2.4-fold caspases 9 and 8 respectively). As expected, compared to DCF alone co-treatment with TNF-α strongly enhanced caspase 8 in differentiated cells and only slightly in their undifferentiated counterparts. Caspase 9 was slightly enhanced if any in both differentiated and undifferentiated cells by co-treatment (Fig. 7A–D).

To confirm the involvement of caspases 3, 8 and 9 in DCF +/− TNF-α toxicity, cells were co-treated with different inhibitors, i.e. NAC, z-LEHD-fmk and etanercept. In DCF-treated differentiated HepaRG cells the slight increase of caspase 8 was nearly completely abolished by NAC and z-LEHD-fmk, and caspase 9 activation was also strongly reduced by these two inhibitors (i.e. 66.7 and 94.8% respectively) (Fig. 7C). Additional caspase 8 activation by DCF + TNF-α co-treatment was mostly abolished (85%) in the presence of etanercept. NAC and z-LEHD-fmk also strongly inhibited caspases 8 and 9 in DCF-treated undifferentiated HepaRG cells reaching 86 and 87.9% for the former and 65.3 and 95.9% for the latter respectively. As expected, addition of etanercept was without any effect (Fig. 7B and C). The effects of the different inhibitors in HepG2 cells treated with DCF or DCF + TNF-α were comparable to those observed in differentiated HepaRG cells treated in similar conditions (Supplementary Fig. 5). Activation of caspase 3 by DCF and DCF + TNF-α reflected changes in caspases 9 and/or 8 in the three cell models (Supplementary Fig. 4).

3.7. Sensitivity to DCF is inversely correlated to GST content

Several studies have demonstrated that GSTs play a key role in detoxifying processes (Board and Menon, 2013). We have analyzed GST A1/2 and M1/2 content in both differentiated and undifferentiated HepaRG cells, and in HepG2 cells. As shown in Fig. 8 both GSTs were less abundant in undifferentiated HepaRG cells (72.6 and 59.8% less for A1/2 and M1/2 respectively) and in HepG2 cells (35.6 and 17.51% less for A1/2 and M1/2 respectively) than in differentiated HepaRG cells (Fig. 8A–D).

Similarly, co-treatment of differentiated HepaRG cells with DCF + TNF-α caused a decrease in transcript levels of the two GST isoforms (35.5 and 37.2% for GST A1/2 and GST M1/2 respectively),

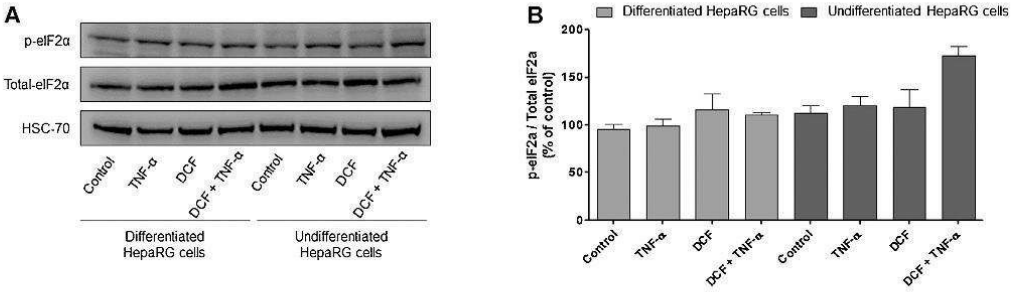

Fig. 6. Western blots analysis of p-elf2α in differentiated and undifferentiated HepaRG cells after exposure to DCF ± TNF-α.
Western blots (A) and quantification by densitometry (B) of p-elf2α content in differentiated and undifferentiated HepaRG cells after 2 h treatment. Results are expressed relative to the levels found in control cells, arbitrarily set at a value of 1.

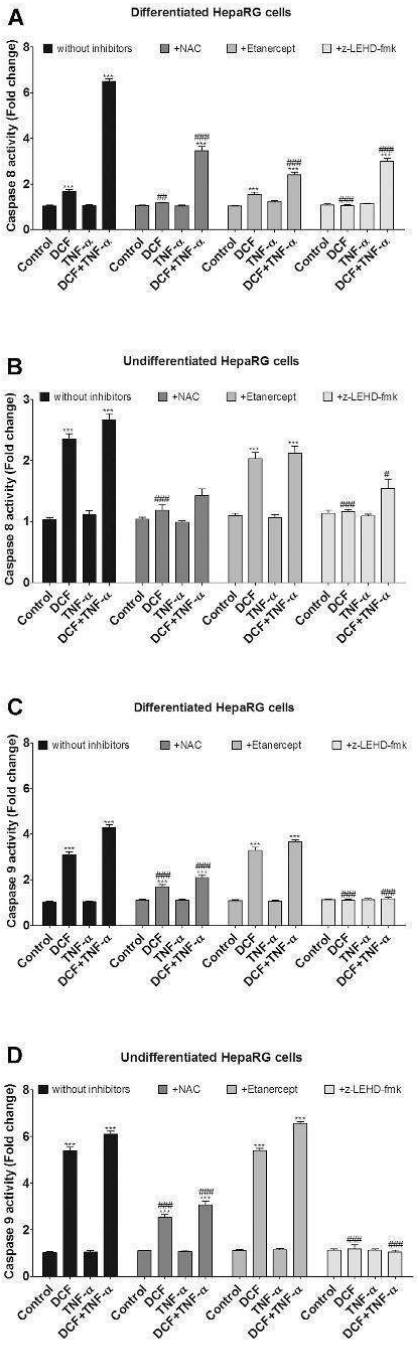

Fig. 7. Effects of inhibitors on caspases 8 and 9 activities in HepaRG cells exposed to DCF ± TNF-α.
NAC, etanercept and z-LEHD-fmk were added individually. A and C correspond to differentiated HepaRG cells and B and D to undifferentiated HepaRG cells. All results compared to treatment with DCF alone (Fig. 8E and F). Moreover, to confirm the protective role of GSTs against DCF cytotoxicity differentiated HepaRG cells were co-exposed to 10 μM ethacrynic acid, a GST inhibitor (Awasthi et al., 1993), for 24 h before determination of caspase 3 activity. As expected, DCF cytotoxicity was significantly enhanced (Fig. 9).

3.8. DCF-induced cholestatic features are not influenced by co-treatment with TNF-α

To determine whether DCF induced cholestatic effects in the presence or absence of TNF-α, differentiated HepaRG cells were regularly examined under phase-contrast microscopy following DCF ± TNF-α addition. Dilatation of many bile canaliculi was observed after 6 h with 50 μM DCF (data not shown). Dilatations appeared as early as 1 h treatment with 100 and 200 μM DCF (Fig. 10A). TNF-α alone had no effect and did not potentiate bile canaliculi deformations caused by DCF (Fig. 10A).

To look for whether DCF-induced bile canaliculi deformations were associated with alterations of bile acids transport, activities of NTCP and BSEP were measured using [^{3}H]-taurocholic acid as a substrate. NTCP activity was slightly reduced after 24 h treatment with 200 μM DCF whereas it was strongly inhibited by TNF-α alone (Fig. 10B). By contrast, a dose-dependent augmentation of BSEP activity was evidenced with DCF alone without any further significant change by co-treatment with TNF-α after 2 h (Supplementary Fig. 6). Both NTCP and BSEP transcripts were decreased by DCF and more extensively by co-treatment with TNF-α after 24 h. Noticeably, CDF accumulated in dilatated bile canaliculi of DCF-treated cells (Fig. 10A).

4. Discussion

Formation of reactive CYP-mediated 4'OH- and 5'OH-metabolites and/or acyl glucuronides from DCF has been associated with induction of intrinsic apoptosis resulting from ROS generation and alteration of the mitochondrial function both in rat and human hepatocytes (Gomez-Lechon et al., 2003a; Masubuchi et al., 2002) and in HepG2 cells (Fredriksson et al., 2014). In the current study, we demonstrated that DCF caused cytotoxicity in the absence of any biotransformation by comparing metabolically and non-metabolically competent HepaRG cells. Indeed, undifferentiated HepaRG cells as well as HepG2 cells which exhibited low CYP activity if any, and did not form OH-DCF metabolites were more sensitive to the drug than HepaRG hepatocytes. The capacity of differentiated HepaRG cells to actively metabolize DCF was verified by biokinetics analysis showing that drug disappearance was associated with formation of OH-metabolites.

Accordingly, primitive biliary cells were also found to be more sensitive than HepaRG hepatocytes to DCF in differentiated HepaRG cell cultures, further supporting that DCF could induce cytotoxicity in the absence of any metabolism. Moreover, sensitivity to DCF was found to be further reduced in differentiated HepaRG cell cultures when the percentage of HepaRG hepatocytes increased from 50 to 80%. The higher sensitivity of non-metabolically competent liver cells could be related to the capability of DCF to induce toxicity in several organs and non-hepatic cells. Indeed, DCF is also a powerful nephrotoxicant. DCF treatments have been associated with a number of cases of acute renal failure in humans (Rubio Garcia and Tellez Molina, 1992); they have also been shown to cause marked nephrotoxic effects in mouse in absence of evidence of any liver damage determined by serum alanine transaminase measurements, indicating that contribution of DCF metabolism and its consequences in the liver were not confounding factors towards culminating nephrotoxicity (Hickey et al., 2001). In agreement, the EC50 value of 250 μM

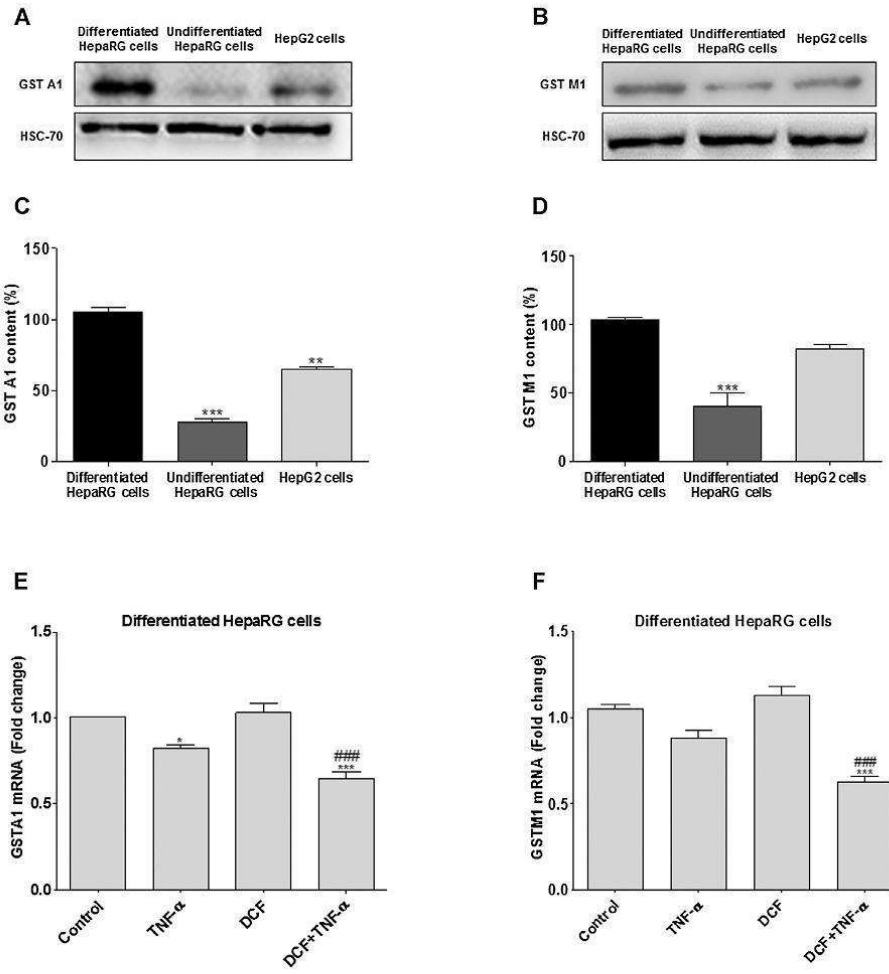

Fig. 8. Analysis of glutathione transferases (GSTs) in differentiated and undifferentiated HepaRG and HepG2 cells after exposure to DCF ± TNF-α. Western blots and their quantifications: (A and C) GSTA1/2 and (B and D) GSTM1/2 in differentiated and undifferentiated HepaRG cells and in HepG2 cells. HSC-70 was used as a loading control. (E and F) Measurement of GSTA1/2 and GSTM1/2 gene expression in differentiated HepaRG cells after treatment with DCF ± TNF-α. Results in (C and D) are expressed relative to the levels found in differentiated HepaRG cells, arbitrarily set at a value of 100. Results in (E and F) are expressed relative to the levels found in control cells, arbitrarily set at a value of 1. $^{*}P < 0.05$, $^{**}P < 0.01$ and $^{***}P < 0.001$ compared with untreated cells, $^{\#\#\#}P < 0.001$ compared with cells treated with TNF-α and DCF ± TNF-α individually without co-addition of inhibitors.

reported with DCF-treated kidney LLC-PK1 pig cells (Ng et al., 2008) was lower than the value obtained with differentiated HepaRG cells (780 μM, this study). Similarly, DCF-induced intestinal toxicity was recently found to be unrelated to its metabolism using precision-cut human intestinal slices (Niu et al., 2015). Noteworthy, while 70% of the patients receiving DCF therapy developed intestinal adverse effects (Zhu and Zhang, 2012) the risk of liver injury reached only 6 per 100,000 users with chronic DCF administration (de Abajo et al., 2004).

DCF induced an apoptotic response in both differentiated and undifferentiated HepaRG cell models at lower concentrations than necrosis, as shown by using caspase 3 activation and MTT assays, in agreement with previous studies using other liver cell models (Fredriksson et al., 2011; Gomez-Lechon et al., 2003b). The higher apoptotic response of non-metabolically competent liver cells to DCF was associated with generation of more reactive oxygen species, higher expression of the two oxidative stress-related genes HO1 and MnSOD and ER-stress-related genes, and higher activation of caspases 8, 9 and 3. Apoptosis can occur via two

are expressed relative to the levels found in control cells, arbitrarily set at a value of 1. $^{*}P < 0.05$, $^{**}P < 0.01$ and $^{***}P < 0.001$ compared with untreated cells, $^{\#\#}P < 0.01$ and $^{\#\#\#}P < 0.001$ compared with cells treated with TNF-α and DCF ± TNF-α individually without co-addition of inhibitors.

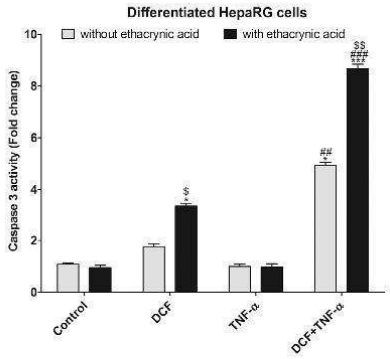

Fig. 9. Effects of ethacrynic acid on caspase 3 activity in differentiated HepaRG cells. Cells were treated with DCF ± TNF-α in the presence or absence of 10 μM ethacrynic acid for 24 h before determination of caspase 3 activity. All results are expressed relative to the levels found in control cells, arbitrarily set at a value of 1. $^{*}P < 0.05$ and $^{***}P < 0.001$ compared with untreated cells, $^{\#\#}P < 0.01$ and $^{\#\#\#}P < 0.001$ compared with cells treated with TNF-α and DCF individually. $^{\$}P < 0.05$ and $^{\$\$}P < 0.01$ compared with cells unexposed to ethacrynic acid.

pathways: the intrinsic resulting from mitochondrial dysfunction and the extrinsic resulting from activation of external death receptors. It has been proposed that DCF-induced apoptosis is mainly mediated by the mitochondrial pathway, which involved generation of ROS and ER stresses, induction of the mitochondrial pore transition and activation of JNK (Fredriksson et al., 2014; Gomez-Lechon et al., 2003a; Masubuchi et al., 2002). In support, it has been shown that DCF could act as an uncoupler of oxidative phosphorylation in mitochondria (LoGuidice et al., 2012; Somasundaram, 2001). Our results agree with these conclusions. Indeed, co-treatments of DCF with the antioxidant NAC or the caspase 9 inhibitor z-LEHD-fmk largely prevented caspases 9 and 3 activation, suggesting that oxidative and ER stresses mediating mitochondrial pore transition were crucial events in DCF-induced apoptosis in differentiated and undifferentiated HepaRG cells. Similarly, DCF activation of these different caspases in HepG2 cells was also strongly reduced with NAC and z-LEHD-fmk, further supporting the prominent involvement of the intrinsic pathway as previously reported (Masubuchi et al., 2002).

Pro-inflammatory cytokines are known to severely enhance liver injury induced by various xenobiotics including DCF (Ramm and Mally, 2013). We showed here that TNF-α potentiated DCF toxicity in differentiated HepaRG cells, mainly through activation of caspases 8 and 3. Similar results, although to a lower extent, were obtained with HepG2 cells while undifferentiated HepaRG cells were nearly unresponsive. The higher apoptotic response previously reported in HepG2 cells co-treated with DCF + TNF-α could likely be explained by the use of higher DCF concentrations (250–500 μM) (Fredriksson et al., 2011). Activation of caspase 8 in co-treated differentiated HepaRG cells and HepG2 cells was mostly inhibited by etanercept, supporting the involvement of the extrinsic apoptotic pathway in potentiation of DCF cytotoxicity by TNF-α. Of note, the two TNF-α receptors (R1 and R2) were well expressed in these cells while they were barely detectable in undifferentiated HepaRG cells, thus explaining the unresponsiveness of these latter to TNF-α when combined with DCF (Supplementary Table 2).

Differentiated HepaRG cells contain large amounts of detoxifying enzymes (Aninat et al., 2006; Gerets et al., 2012; Rogue et al., 2012), that could contribute to inactivation of DCF reactive metabolites and protection against apoptotic effects of the drug. DCF quinone imine metabolites have been shown to be reduced by NAD(P)H:quinone oxido-reductase1 and conjugated to GSH by GSTs (Dragovic et al., 2013; Vredenburg et al., 2014). Our data confirming that differentiated HepaRG cells contained higher levels of GST A1/2 and M1/2 than their undifferentiated counterparts and HepG2 cells and showing their higher sensitivity to DCF following GST inhibition by ethacrynic acid, brought further support to their lower sensitivity to apoptotic effects of DCF. Moreover, the higher sensitivity of differentiated HepaRG cells to apoptotic effects of DCF following pre-exposure to TNF-α, which is associated with inhibition of CYPs and GSTs, as well as the comparable sensitivity of primary human hepatocytes and differentiated HepaRG cells to DCF supported our conclusions. Noticeably, a lower sensitivity of differentiated HepaRG cells compared to HepG2 cells has previously been reported for several known hepatotoxic chemicals (Gerets et al., 2012). Accordingly, the differential sensitivity of differentiated HepaRG cells and HepG2 cells to DCF could be related to differences in both oxidative metabolism and detoxifying and antioxidant capacities. However, it cannot be excluded that GSTs were partly acting via their anti-apoptotic properties (Board and Menon, 2013; Gilot et al., 2002). Likelihood, its high content in GSTs and other detoxifying enzymes could also at least partly explain the lower sensitivity to DCF of the liver compared to other tissues.

Besides its capacity to induce hepatocellular injury DCF can also cause cholestasis in humans. As observed with several other cholestatic drugs (Sharanek et al., 2016), we found that DCF provoked early dilatation of bile canaliculi at lower concentrations than those causing cytotoxicity and these bile canaliculi deformations were associated with alterations of taurocholic acid clearance as well as of expression of influx and efflux bile acid transporters. Although TNF-α did not obviously alter these major DCF cholestatic effects when added prior to and/or simultaneously with the drug this did not exclude that the cytokine could modulate bile acids synthesis and/or secretion.

Altogether our results bring new insights in DCF-induced cytotoxicity and its potentiation by TNF-α. They demonstrate that DCF toxicity to human liver cells can occur in absence of biotransformation and through the intrinsic apoptotic pathway, and be related to the phenotype while its potentiation by TNF-α can be observed only in cells expressing death receptors and involves the extrinsic pathway. The lower sensitivity of human HepaRG hepatocytes to DCF-induced apoptosis can be explained by their high content in glutathione transferases and consequently by their ability to inactivate DCF reactive metabolites.

Conflicts of interest

The authors declare that there are no conflicts of interest.

Financial support

This work was supported by the European Community [Contract MIP-DILI-115336]. The MIP-DILI project has received support from the Innovative Medicines Initiative Joint Undertaking, resources of which are composed of financial contribution from the European Union's Seventh Framework Programme [FP7/20072013] and EFPIA companies' in kind contribution. http://www.imi.europa.eu/.

Houssein Al-Attrache was financially supported by the Association AZM-Lebanese University and the MIP-DILI project, Ahmad Sharanek by the Lebanese Association for Scientific Research (LASeR) and the MIP-DILI project, Audrey Burban by the MIP-DILI project and Matthew Burbank by a CIFRE contract with Servier.

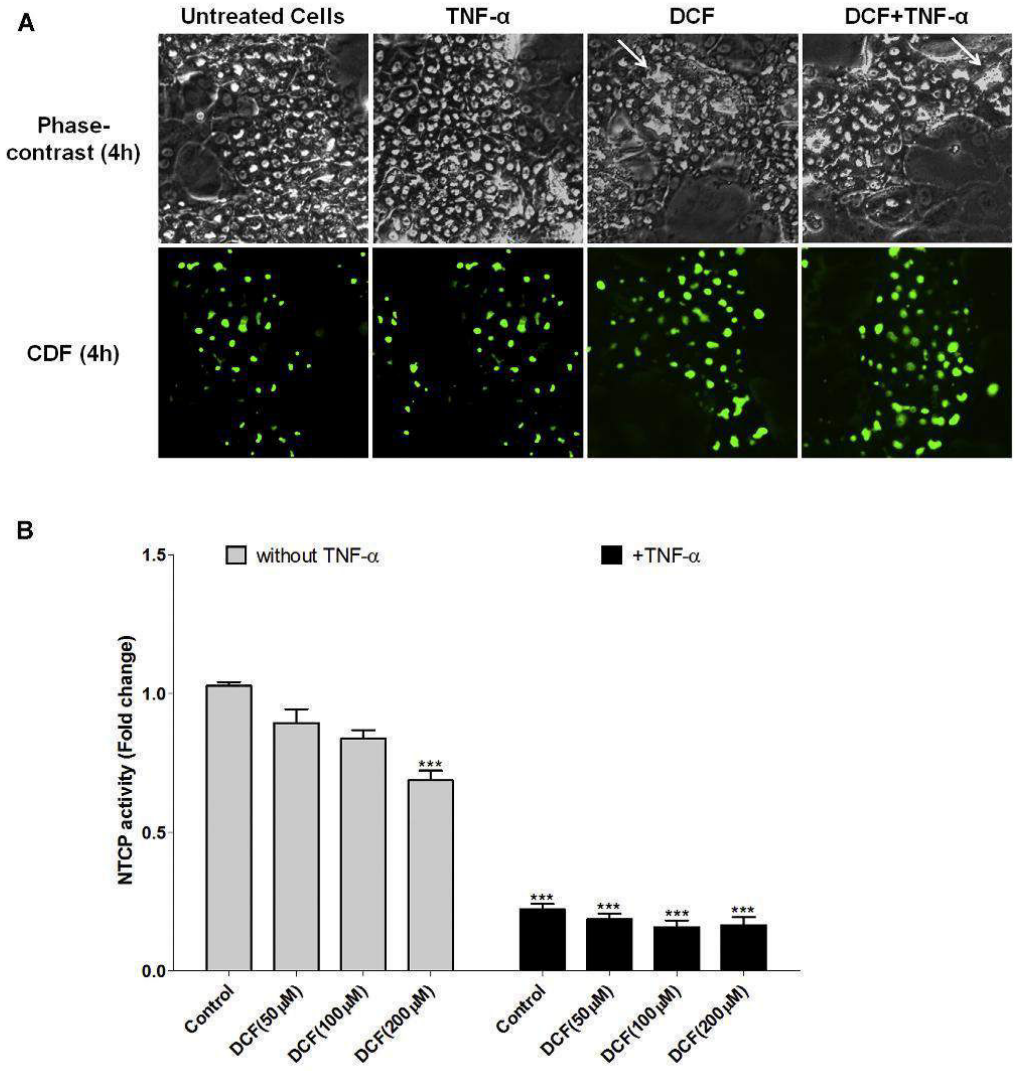

Fig. 10. Effects of DCF ± TNF-α on bile canaliculi morphology, DCF accumulation and NTCP activity in differentiated HepaRG cells.
(A) Phase-contrast microscopy images showing bile canaliculi and intracanicular accumulation of fluorescent CDF after 4 and 24 h of treatment (DCF at 200 μM). (B) NTCP activity after 24 h. White arrow shows dilatation of bile canaliculi. Results on NTCP activity are expressed relative to the levels found in control cells, arbitrarily set at a value of 1. ***$P < 0.001$ compared with untreated cells.

Transparency document

The http://dx.doi.org/10.1016/j.toxlet.2016.06.008 associated with this article can be found in the online version.

Appendix A. Supplementary data

Supplementary data associated with this article can be found, in the online version, at http://dx.doi.org/10.1016/j.toxlet.2016.06.008.

References

Abdel-Razzak, Z., Loyer, P., Fautrel, A., Gautier, J.C., Corcos, L., Turlin, B., Beaune, P., Guillouzo, A., 1993. Cytokines down-regulate expression of major cytochrome P-450 enzymes in adult human hepatocytes in primary culture. Mol. Pharmacol. 44, 707–715.

Aithal, G.P., Day, C.P., 2007. Nonsteroidal anti-inflammatory drug-induced hepatotoxicity. Clin. Liver Dis. 11, 563–575 vi–vii.

Aninat, C., Piton, A., Glaise, D., Le Charpentier, T., Langouët, S., Morel, F., Guguen-Guillouzo, C., Guillouzo, A., 2006. Expression of cytochromes P450, conjugating enzymes and nuclear receptors in human hepatoma HepaRG cells. Drug Metab. Dispos. 34, 75–83.

Antherieu, S., Bachour-El Azzi, P., Dumont, J., Abdel-Razzak, Z., Guguen-Guillouzo, C., Fromenty, B., Robin, M.A., Guillouzo, A., 2013. Oxidative stress plays a major role in chlorpromazine-induced cholestasis in human HepaRG cells. Hepatology 57, 1518–1529.

Awasthi, S., Srivastava, S.K., Ahmad, F., Ahmad, H., Ansari, G.A., 1993. Interactions of glutathione S-transferase-pi with ethacrynic acid and its glutathione conjugate. Biochim. Biophys. Acta 1164, 173–178.

Bachour-El Azzi, P., Sharanek, A., Abdel-Razzak, Z., Antherieu, S., Al-Attrache, H., Savary, C.C., Lepage, S., Morel, I., Labbe, G., Guguen-Guillouzo, C., Guillouzo, A., 2014. Impact of inflammation on chlorpromazine-induced cytotoxicity and cholestatic features in HepaRG cells. Drug Metab. Dispos. 42, 1556–1566.

Bachour-El Azzi, P., Sharanek, A., Burban, A., Li, R., Guevel, R.L., Abdel-Razzak, Z., Stieger, B., Guguen-Guillouzo, C., Guillouzo, A., 2015. Comparative localization and functional activity of the main hepatobiliary transporters in HepaRG cells and primary human hepatocytes. Toxicol. Sci. 145, 157–168.

Banks, A.T., Zimmerman, H.J., Ishak, K.G., Harter, J.G., 1995. Diclofenac-associated hepatotoxicity: analysis of 180 cases reported to the food and drug administration as adverse reactions. Hepatology 22, 820–827.

Bjornsson, E., Olsson, R., 2006. Suspected drug-induced liver fatalities reported to the WHO database. Dig. Liver Dis. 38, 33–38.

Board, P.G., Menon, D., 2013. Glutathione transferases, regulators of cellular metabolism and physiology. Biochim. Biophys. Acta 1830, 3267–3288.

Bort, R., Ponsoda, X., Jover, R., Gomez-Lechon, M.J., Castell, J.V., 1999. Diclofenac toxicity to hepatocytes: a role for drug metabolism in cell toxicity. J. Pharmacol. Exp. Ther. 288, 65–72.

Breen, E.G., McNicholl, J., Cosgrove, E., McCabe, J., Stevens, F.M., 1986. Fatal hepatitis associated with diclofenac. Gut 27, 1390–1393.

Cerec, V., Glaise, D., Garnier, D., Morosan, S., Turlin, B., Drenou, B., Gripon, P., Kremsdorf, D., Guguen-Guillouzo, C., Corlu, A., 2007. Transdifferentiation of hepatocyte-like cells from the human hepatoma HepaRG cell line through bipotent progenitor. Hepatology 45, 957–967.

de Abajo, F.J., Montero, D., Madurga, M., Garcia Rodriguez, L.A., 2004. Acute and clinically relevant drug-induced liver injury: a population based case-control study. Br. J. Clin. Pharmacol. 58, 71–80.

Deng, X., Stachlewitz, R.F., Liguori, M.J., Blomme, E.A., Waring, J.F., Luyendyk, J.P., Maddox, J.F., Ganey, P.E., Roth, R.A., 2006. Modest inflammation enhances diclofenac hepatotoxicity in rats: role of neutrophils and bacterial translocation. J. Pharmacol. Exp. Ther. 319, 1191–1199.

Dragovic, S., Boerma, J.S., Vermeulen, N.P., Commandeur, J.N., 2013. Effect of human glutathione S-transferases on glutathione-dependent inactivation of cytochrome P450-dependent reactive intermediates of diclofenac. Chem. Res. Toxicol. 26, 1632–1641.

Dumont, J., Josse, R., Lambert, C., Antherieu, S., Le Hegarat, L., Aninat, C., Robin, M.A., Guguen-Guillouzo, C., Guillouzo, A., 2010. Differential toxicity of heterocyclic aromatic amines and their mixture in metabolically competent HepaRG cells. Toxicol. Appl. Pharmacol. 245, 256–263.

Fredriksson, L., Herpers, B., Benedetti, G., Matadin, Q., Puigvert, J.C., de Bont, H., Dragovic, S., Vermeulen, N.P., Commandeur, J.N., Danen, E., de Graauw, M., van de Water, B., 2011. Diclofenac inhibits tumor necrosis factor-alpha-induced nuclear factor-kappaB activation causing synergistic hepatocyte apoptosis. Hepatology 53, 2027–2041.

Fredriksson, L., Wink, S., Herpers, B., Benedetti, G., Hadi, M., de Bont, H., Groothuis, G., Luijten, M., Danen, E., de Graauw, M., Meerman, J., van de Water, B., 2014. Drug-induced endoplasmic reticulum and oxidative stress responses independently sensitize toward TNFalpha-mediated hepatotoxicity. Toxicol. Sci. 140, 144–159.

Gerets, H.H., Tilmant, K., Gerin, B., Chanteux, H., Depelchin, B.O., Dhalluin, S., Atienzar, F.A., 2012. Characterization of primary human hepatocytes, HepG2 cells, and HepaRG cells at the mRNA level and CYP activity in response to inducers and their predictivity for the detection of human hepatotoxins. Cell Biol. Toxicol. 28, 69–87.

Gilot, D., Loyer, P., Corlu, A., Glaise, D., Lagadic-Gossmann, D., Atfi, A., Morel, F., Ichijo, H., Guguen-Guillouzo, C., 2002. Liver protection from apoptosis requires both blockage of initiator caspase activities and inhibition of ASK1/JNK pathway via glutathione S-transferase regulation. J. Biol. Chem. 277, 49220–49229.

Gomez-Lechon, M.J., Ponsoda, X., O'Connor, E., Donato, T., Castell, J.V., Jover, R., 2003a. Diclofenac induces apoptosis in hepatocytes by alteration of mitochondrial function and generation of ROS. Biochem. Pharmacol. 66, 2155–2167.

Gomez-Lechon, M.J., Ponsoda, X., O'Connor, E., Donato, T., Jover, R., Castell, J.V., 2003b. Diclofenac induces apoptosis in hepatocytes. Toxicol. In Vitro 17, 675–680.

Guguen-Guillouzo, C., Campion, J.P., Brissot, P., Glaise, D., Launois, B., Bourel, M., Guillouzo, A., 1982. High yield preparation of isolated human adult hepatocytes by enzymatic perfusion of the liver. Cell Biol. Int. Rep. 6, 625–628.

Guillouzo, A., Guguen-Guillouzo, C., 2008. Evolving concepts in liver tissue modeling and implications for in vitro toxicology. Expert Opin. Drug Metab. Toxicol. 4, 1279–1294.

Hickey, E.J., Raje, R.R., Reid, V.E., Gross, S.M., Ray, S.D., 2001. Diclofenac induced in vivo nephrotoxicity may involve oxidative stress-mediated massive genomic DNA fragmentation and apoptotic cell death. Free Radic. Biol. Med. 31, 139–152.

Jouan-Lanhouet, S., Arshad, M.I., Piquet-Pellorce, C., Martin-Chouly, C., Le Moigne-Muller, G., Van Herreweghe, F., Takahashi, N., Sergent, O., Lagadic-Gossmann, D., Vandenabeele, P., Samson, M., Dimanche-Boitrel, M.T., 2012. TRAIL induces necroptosis involving RIPK1/RIPK3-dependent PARP-1 activation. Cell Death Differ. 19, 2003–2014.

Kretz-Rommel, A., Boelsterli, U.A., 1993. Diclofenac covalent protein binding is dependent on acyl glucuronide formation and is inversely related to P450-mediated acute cell injury in cultured rat hepatocytes. Toxicol. Appl. Pharmacol. 120, 155–161.

LoGuidice, A., Wallace, B.D., Bendel, L., Redinbo, M.R., Boelsterli, U.A., 2012. Pharmacologic targeting of bacterial beta-glucuronidase alleviates nonsteroidal anti-inflammatory drug-induced enteropathy in mice. J. Pharmacol. Exp. Ther. 341, 447–454.

Maccarrone, M., Lorenzon, T., Bari, M., Melino, G., Finazzi-Agro, A., 2000. Anandamide induces apoptosis in human cells via vanilloid receptors: evidence for a protective role of cannabinoid receptors. J. Biol. Chem. 275, 31938–31945.

Maianski, N.A., Roos, D., Kuijpers, T.W., 2004. Bid truncation, bid/bax targeting to the mitochondria, and caspase activation associated with neutrophil apoptosis are inhibited by granulocyte colony-stimulating factor. J. Immunol. 172, 7024–7030.

Maiuri, A.R., Breier, A.B., Gora, L.F., Parkins, R.V., Ganey, P.E., Roth, R.A., 2015. Cytotoxic synergy between cytokines and NSAIDs associated with idiosyncratic hepatotoxicity is driven by mitogen-activated protein kinases. Toxicol. Sci. 146, 265–280.

Masubuchi, Y., Nakayama, S., Horie, T., 2002. Role of mitochondrial permeability transition in diclofenac-induced hepatocyte injury in rats. Hepatology 35, 544–551.

Ng, L.E., Halliwell, B., Wong, K.P., 2008. Nephrotoxic cell death by diclofenac and meloxicam. Biochem. Biophys. Res. Commun. 369, 873–877.

Niu, X., de Graaf, I.A., Langelaar-Makkinje, M., Horvatovich, P., Groothuis, G.M., 2015. Diclofenac toxicity in human intestine ex vivo is not related to the formation of intestinal metabolites. Arch. Toxicol. 89, 107–119.

Oslowski, C.M., Urano, F., 2011. Measuring ER stress and the unfolded protein response using mammalian tissue culture system. Methods Enzymol. 490, 71–92.

Pernelle, K., Le Guevel, R., Glaise, D., Stasio, C.G., Le Charpentier, T., Bouaita, B., Corlu, A., Guguen-Guillouzo, C., 2011. Automated detection of hepatotoxic compounds in human hepatocytes using HepaRG cells and image-based analysis of mitochondrial dysfunction with JC-1 dye. Toxicol. Appl. Pharmacol. 254, 256–266.

Ramm, S., Mally, A., 2013. Role of drug-independent stress factors in liver injury associated with diclofenac intake. Toxicology 312, 83–96.

Rogue, A., Lambert, C., Spire, C., Claude, N., Guillouzo, A., 2012. Interindividual variability in gene expression profiles in human hepatocytes and comparison with HepaRG cells. Drug Metab. Dispos. 40, 151–158.

Rubio Garcia, J.A., Tellez Molina, M.J., 1992. Acute renal failure and nephrotic syndrome associated with treatment with diclofenac. Rev. Clin. Esp. 191, 289–290.

Seitz, S., Boelsterli, U.A., 1998. Diclofenac acyl glucuronide, a major biliary metabolite, is directly involved in small intestinal injury in rats. Gastroenterology 115, 1476–1482.

Seitz, S., Kretz-Rommel, A., Oude Elferink, R.P., Boelsterli, U.A., 1998. Selective protein adduct formation of diclofenac glucuronide is critically dependent on the rat canalicular conjugate export pump (Mrp2). Chem. Res. Toxicol. 11, 513–519.

Sharanek, A., Azzi, P.B., Al-Attrache, H., Savary, C.C., Humbert, L., Rainteau, D., Guguen-Guillouzo, C., Guillouzo, A., 2014. Different dose-dependent mechanisms are involved in early cyclosporine a-induced cholestatic effects in hepaRG cells. Toxicol. Sci. 141, 244–253.

Sharanek, A., Burban, A., Humbert, L., Bachour-El Azzi, P., Felix-Gomes, N., Rainteau, D., Guillouzo, A., 2015. Cellular Accumulation and Toxic Effects of Bile Acids in Cyclosporine A-Treated HepaRG Hepatocytes. Toxicol. Sci. 147, 573–587.

Sharanek, A., Burban, A., Burbank, M., Le Guevel, R., Li, R., Guillouzo, A., Guguen-Guillouzo, C., 2016. Rho-kinase/myosin light chain kinase pathway plays a key role in the impairment of bile canaliculi dynamics induced by cholestatic drugs. Sci. Rep. 6, 24709.

Shen, S., Marchick, M.R., Davis, M.R., Doss, G.A., Pohl, L.R., 1999. Metabolic activation of diclofenac by human cytochrome P450 3A4: role of 5-hydroxydiclofenac. Chem. Res. Toxicol. 12, 214–222.

Somasundaram, S., 2001. Pathogenesis of diclofenac enteropathy. Gastroenterology 120, 1885; author reply 1886–1887.

Son, T.W., Yun, S.P., Yong, M.S., Seo, B.N., Ryu, J.M., Youn, H.Y., Oh, Y.M., Han, H.J., 2013. Netrin-1 protects hypoxia-induced mitochondrial apoptosis through HSP27 expression via DCC- and integrin alpha6beta4-dependent Akt, GSK-3beta, and HSF-1 in mesenchymal stem cells. Cell Death Dis. 4, e563.

Tang, W., Stearns, R.A., Wang, R.W., Chiu, S.H., Baillie, T.A., 1999. Roles of human hepatic cytochrome P450s 2C9 and 3A4 in the metabolic activation of diclofenac. Chem. Res. Toxicol. 12, 192–199.

Uetrecht, J., 2006. Evaluation of which reactive metabolite, if any, is responsible for a specific idiosyncratic reaction. Drug Metab. Rev. 38, 745–753.
Vredenburg, G., Elias, N.S., Venkataraman, H., Hendriks, D.F., Vermeulen, N.P., Commandeur, J.N., Vos, J.C., 2014. Human NAD(P)H:quinone oxidoreductase 1 (NQO1)-mediated inactivation of reactive quinoneimine metabolites of diclofenac and mefenamic acid. Chem. Res. Toxicol. 27, 576–586.
Wang, A.G., Xia, T., Yuan, J., Yu, R.A., Yang, K.D., Chen, X.M., Qu, W., Waalkes, M.P., 2004. Effects of phenobarbital on metabolism and toxicity of diclofenac sodium in rat hepatocytes in vitro. Food Chem. Toxicol. 42, 1647–1653.
Watanabe, N., Takashimizu, S., Kojima, S., Kagawa, T., Nishizaki, Y., Mine, T., Matsuzaki, S., 2007. Clinical and pathological features of a prolonged type of acute intrahepatic cholestasis. Hepatol Res. 37, 598–607.
Zeng, T., Zhang, C.L., Song, F.Y., Zhao, X.L., Xie, K.Q., 2014. CMZ reversed chronic ethanol-induced disturbance of PPAR-alpha possibly by suppressing oxidative stress and PGC-1alpha acetylation, and activating the MAPK and GSK3beta pathway. PLoS One 9, e98658.
Zhu, Y., Zhang, Q.Y., 2012. Role of intestinal cytochrome p450 enzymes in diclofenac-induced toxicity in the small intestine. J. Pharmacol. Exp. Ther. 343, 362–370.

Supplementary Fig. 1

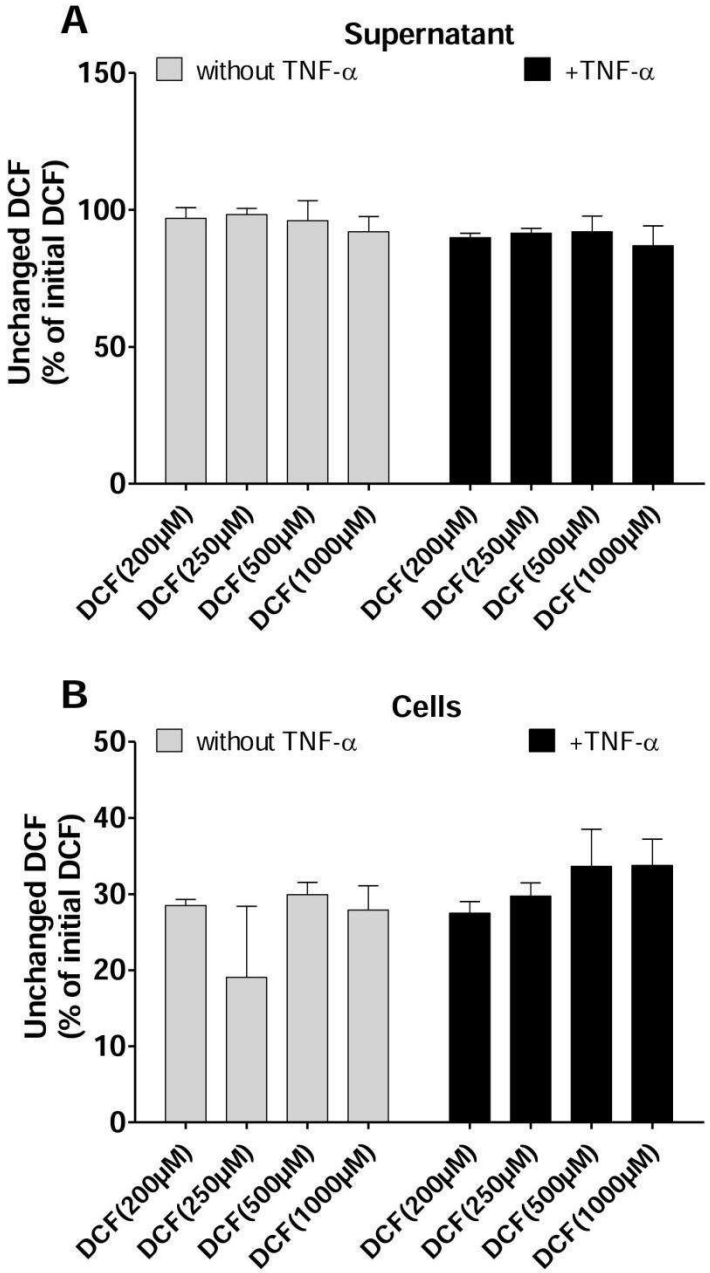

Supplementary Fig. 1. Concentrations of remaining DCF in HepG2 cell cultures after treatment with DCF±TNF-α.

Four concentrations of DCF were tested (200, 250, 500 and 1000µM). The cells were pre-treated or not with TNF-α and DCF concentrations were determined in (A) the supernatant and (B) cells after 24h incubation.

Supplementary Fig. 2

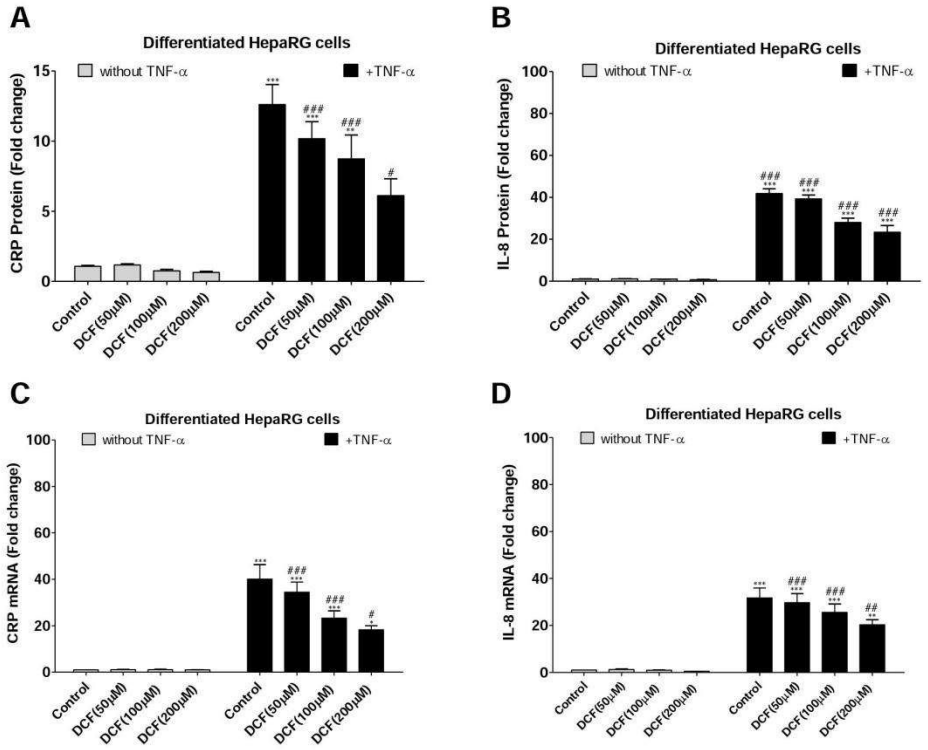

Supplementary Fig. 2. Measurements of protein and transcript levels of CRP and IL-8 after treatment with DCF and TNF-α.

CRP (A and C) and IL-8 (B and D) proteins and transcripts were quantified in differentiated HepaRG cells after treatment with DCF ± TNF-α. All results are expressed relative to the levels found in corresponding untreated cells, arbitrarily set at a value of 1. *P<0.01, **P<0.01 and ***P<0.001 compared with untreated cells, $^{\#}$P<0.05, $^{\#\#}$P<0.05 and $^{\#\#\#}$P<0.001 compared with cells treated with DCF individually.

Supplementary Fig. 3

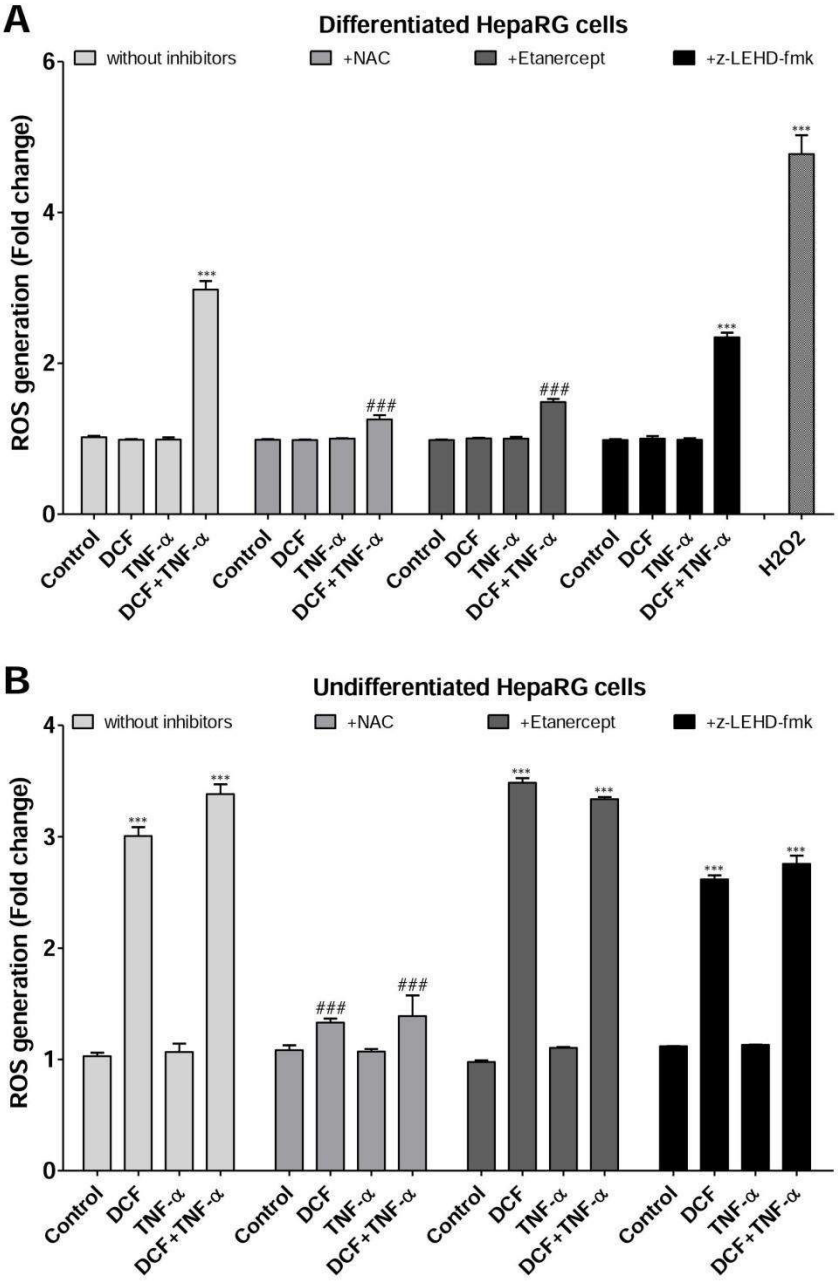

Supplementary Fig. 3. Effects of DCF±TNF-α on ROS generation in differentiated and undifferentiated HepaRG cells.

Cells were pretreated or not with TNF-α before co-treatment with DCF±TNF-α and co-addition of the inhibitors NAC, z-LEHD-fmk and etanercept separately. (A) differentiated and (B) undifferentiated HepaRG cells. All results are expressed relative to the levels found in control cells, arbitrarily set at a value of 1. $^{***}P<0.001$ compared with untreated cells, $^{\#\#\#}P<0.001$ compared with cells treated with DCF and DCF±TNF-α individually without inhibitor.

Supplementary Fig. 4

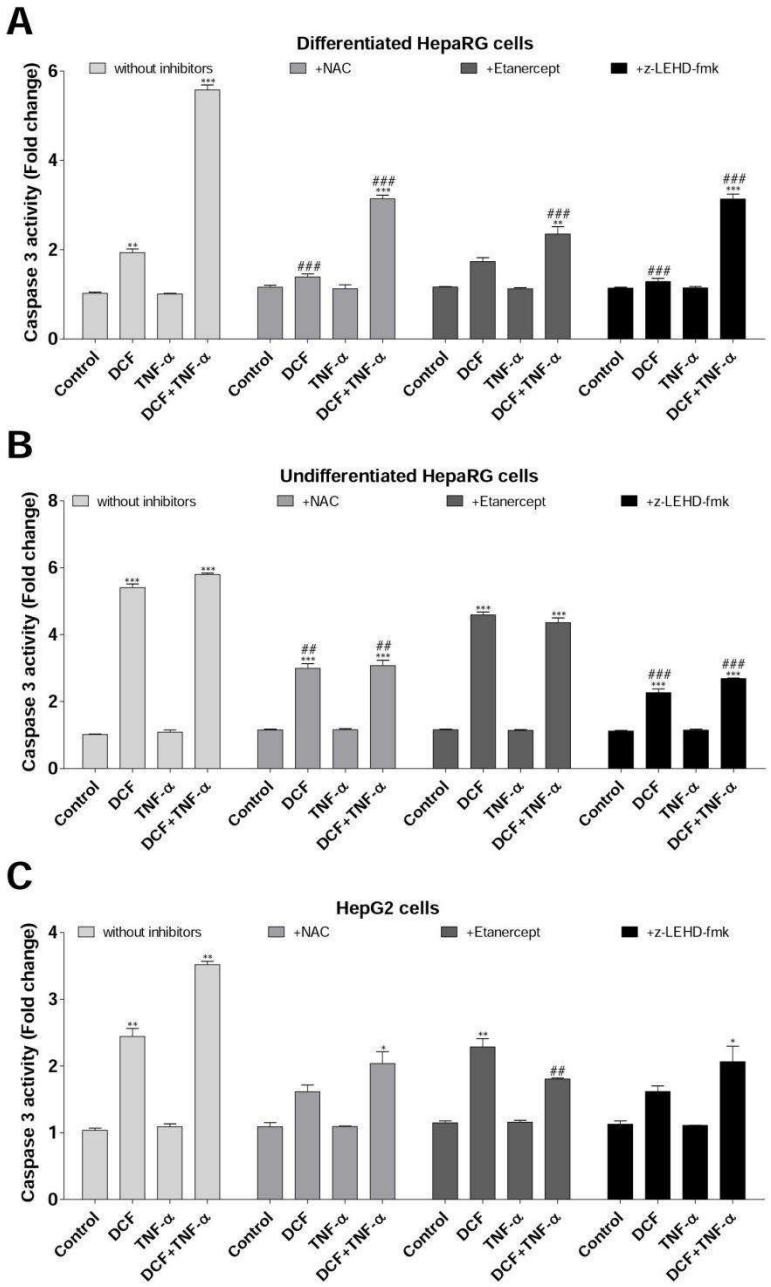

Supplementary Fig. 4. Effects of co-addition of NAC, etanercept and z-LEHD-fmk with DCF±TNF-α on caspase 3 activity in (A) differentiated (B) or undifferentiated HepaRG cells or in (C) HepG2 cells. Cells were pretreated on not with TNF-α prior to co-treatments and inhibitors were added separately. All results are expressed relative to the levels found in control cells, arbitrarily set at a value of 1. $*P<0.01$, $**P<0.01$ and $***P<0.001$ compared with untreated cells, $^{\#\#}P<0.01$ and $^{\#\#\#}P<0.001$ compared with cells treated with DCF or DCF±TNF-α without inhibitor.

Supplementary Fig. 5

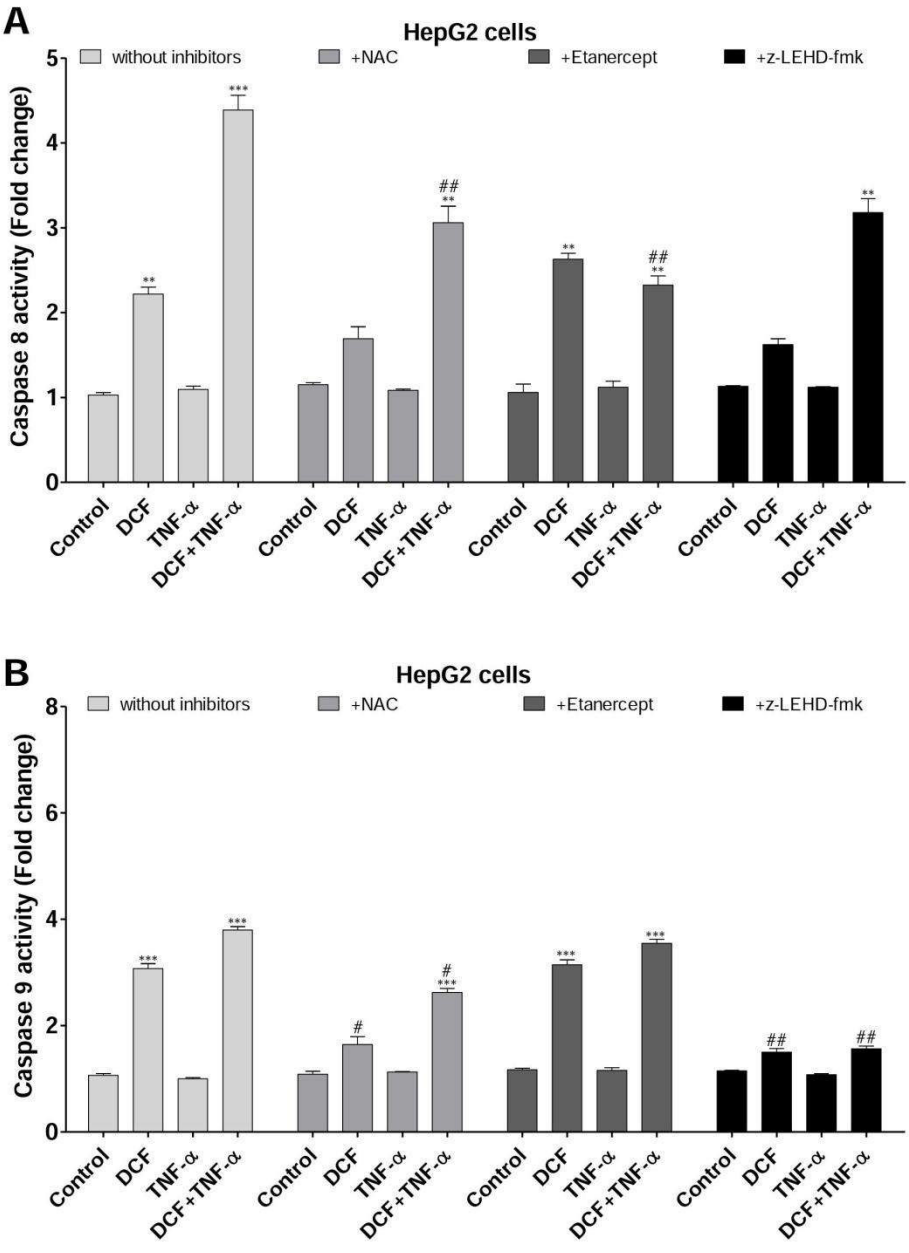

Supplementary Fig. 5. Caspase 8 and 9 activities in HepG2 cells

Caspase 8 (A) and caspase 9 (B) activities were measured in HepG2 cells after treatment with DCF±TNF-α (following pre-treatment or not with TNF-α) in the presence or not of the different inhibitors NAC, z-LEHD-fmk and etanercept. All results are expressed relative to the levels found in control cells, arbitrarily set at a value of 1. $^{**}P<0.01$ and $^{***}P<0.001$ compared with untreated cells, $^{\#}P<0.05$ and $^{\#\#}P<0.01$ compared with cells treated with DCF and DCF±TNF-α without inhibitor.

Supplementary Fig. 6

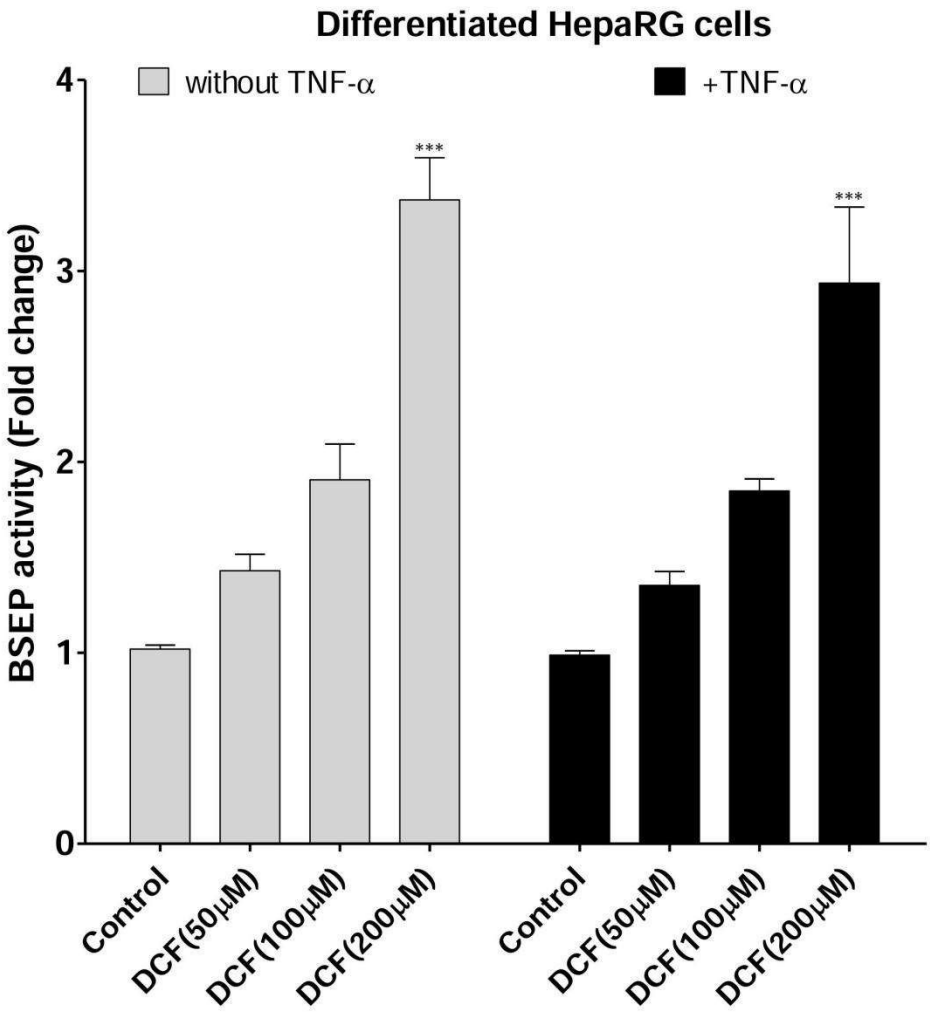

Supplementary Fig. 6. BSEP activity in differentiated HepaRG cells.
BSEP activity was measured after 2h of co-treatment with DCF±TNF-α. All results are expressed relative to the levels found in control cells, arbitrarily set at a value of 1. ****P*<0.001 compared with untreated cells.

Supplementary Table 1. List of primers

Gene	Name	Forward primer	Reverse primer
GAPDH	Glyceraldehyde-3-Phosphate dehydrogenase	TTCACCACCATGGAGAAGGC	GGCATGGACTGTGGTCATGA
CYP3A4	Cytochrome P450 3A4	CTTCATCCAATGGACTGCATAAAT	TCCCAAGTATAACACTCTACACAGACAA
CYP2C9	Cytochrome P450 2C9	GGACAGAGACGACAAGCACA	AATGGACATGAACAACCCTCA
CRP	C-Reactive Protein	GAACTTTCAGCCGAATACATCTTTT	CCTTCCTCGACATGTCTGTCT
IL-8	Interleukin 8	ATGACTTCCAAGCTGGCCGTGGCT	TCTCAGCCCTCTTCAAAAACTTCTC
HO-1	Heme oxygenase 1	ACTTTCAGAAGGGCCAGGT	TTGTTGCGCTCAATCTCCT
MnSOD	Manganese superoxide dismutase	GGGTTGGCTTGGTTTCAATA	CTGATTTGGACAAGCAGCAA
ATF4	Activating Transcription Factor 4	TGGCATGGTTTCCAGGTCATCT	CCAACAACAGCAAGGAGGATGC
ATF6	Activating Transcription Factor 6	CTGCACCCACTAAAGGCCAGA	GAGGGCAGAACTCCAGGTGCT
CHOP	C/Ebp-Homologous protein	ATGGCAGCTGAGTCATT	AGAAGCAGGGTCAAGAGTGGT
GRP78	Glucose Regulated Protein,78KD	GTTCTTGCCGTTCAAGGTGG	TGGTACAGTAACAACTGCATG
TNFR1	Tumor Necrosis Factor Receptor 1	ACCAAGTGCCACAAAGGAAC	CTGCAATTGAAGCACTGGAA
TNFR2	Tumor Necrosis Factor Receptor 2	TTCGCTCTTCCAGTTGGACT	CACCAGGGGAAGAATCTGAG
GSTA1/2	Glutathione S-Transferase A1/2	TGCAACAATTAAGTGCTTTACCTAAG TG	TTAACTAAGTGGGTGAATAGGAGTTGT ATT
GSTM1	Glutathione S-Transferase M1	ATGGTTGTCCAGGTCTGG	CGCCATCTTGTGCTACATT

Supplementary Table 2. RT-QPCR analysis of TNF receptors (R1 and R2) and GAPDH (Ct values) in differentiated and undifferentiated HepaRG cells and HepG2 cells

	Differentiated HepaRG cells (Ct)	**Undifferentiated HepaRG cells (Ct)**	**HepG2 cells (Ct)**
GAPDH	17.5±0.4	17.3±0.2	17.8±0.3
TNF-R1	18.8±0.7	27.5±0.6	18.5±0.3
TNF-R2	26.2±0.5	31.8±0.8	24.3±0.6

2.Résultats complémentaires : Influence de l'IL-6 et d'IL-1β sur les effets de diclofénac

Afin de mieux préciser les effets observés avec le TNF-α les cellules HepaRG différenciées ont également été traitées avec d'autres cytokines pro-inflammatoires, l'IL-6 (10ng/ml) et l'IL-1β (0.1ng/ml). Ces concentrations ont été utilisées dans plusieurs études précédentes.

Les résultats suivants ont été obtenus :

Effets inflammatoires : La réponse aux cytokines a été estimée par la détermination de l'expression des transcrits de CRP, d'IL-8 et de CYP3A4 ainsi que l'activité et/ou la sécrétion des protéines correspondantes.

Une forte augmentation de CRP et IL-8 a également été observée avec IL-1β (44.24 et 52.80 fois respectivement) et IL-6 (79.27 et 71.93 fois). Cette augmentation était réduite en présence de 200µM de DCF (30.3 et 15.02 fois pour CRP et 37.3 et 27.82 fois pour IL-8 avec IL-6 et IL-1β respectivement). Ces résultats ont été confirmés par analyse PCR : en effet, les niveaux des transcrits de CRP et d'IL-8 étaient fortement augmentés après traitement avec ces 2 cytokines (96 et 56 fois pour CRP, et 61 et 44 fois pour IL-8 avec IL-6 et IL-1β respectivement par comparaison avec les cellules non traitées). Cette augmentation était aussi légèrement diminuée dans les cas de co-traitement avec DCF, par exemple 49 et 21 fois pour CRP et 26 et 21 fois pour IL-8 avec IL-6 et IL-1β respectivement (Figure 31).

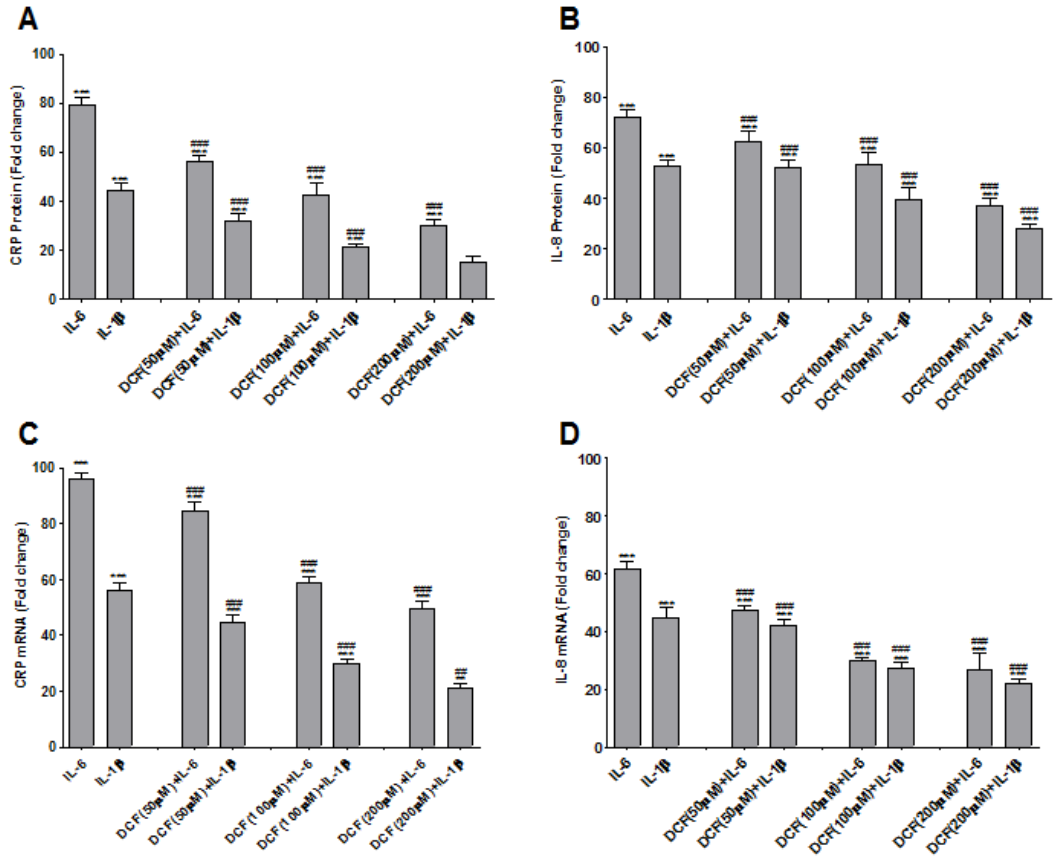

Figure 31: Effets d'IL-6 et d'IL-1β sur les niveaux des transcrits et des protéines de (A et C) CRP et (B et D) d'IL-8 dans les cellules HepaRG différenciées. Les cellules ont été prétraitées 24h avec des cytokines pro-inflammatoires (IL-6 et IL-1β) suivies par un traitement DCF ± cytokines pendant 24h supplémentaires. Tous les résultats ont été exprimés par rapport aux cellules contrôles non traitées arbitrairement fixés à 1. *P<0.05, **P<0.01 et ***P<0.001 comparées avec les cellules non traitées, $^{\#}$P<0.05, $^{\#\#}$P<0.01 et $^{\#\#\#}$P<0.001 comparées avec les cellules traitées avec les cytokines ou DCF séparément.

D'autre part, CYP3A4 étant connu pour être inhibé par des cytokines pro-inflammatoires (Abdel-Razzak et al., 1993) des co-traitements de cellules HepaRG différenciées avec DCF et ces cytokines ont été réalisés. L'activité de cette enzyme a beaucoup diminué, de 94 et 89% avec IL-6 et IL-1β respectivement. Il en était, de même, pour les niveaux de transcrits qui après co-traitement, ne représentaient plus que 6 et 7% respectivement avec IL-6 et IL-1β. De même, le niveau de transcrits de CYP2C9, l'autre CYP impliqué dans le métabolisme de DCF (Shen et al., 1999), était fortement diminué en présence de ces cytokines (Figure 32 et Tableau 6).

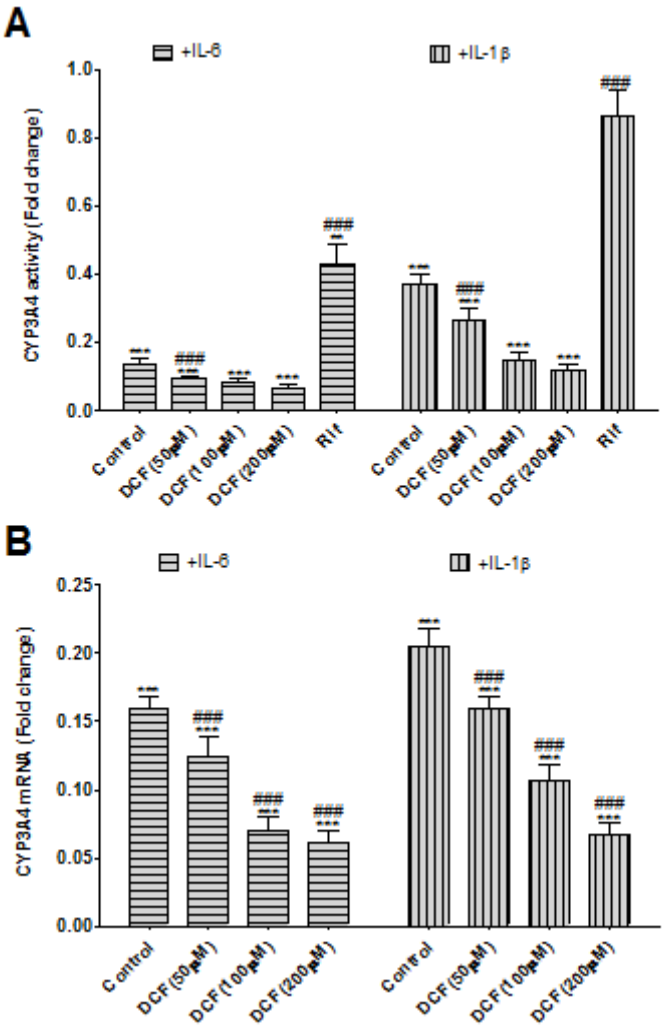

Figure 32: Effets d'IL6 et d'IL-1β sur CYP3A4. Les cellules HepaRG différenciées ont été pré-traitées avec IL-6 ou IL-1β pendant 24h suivi par un co-traitement DCF+IL-6 ou DCF+IL-1β pendant 24h puis (A) l'activité et (B) le niveau de transcrits de CYP3A4 ont été mesurés. Tous les résultats ont été calculés par rapport aux valeurs trouvées dans les cellules contrôles arbitrairement fixées à 1. *P<0.05, **P<0.01 et ***P<0.001 comparées avec les cellules non traitées, $^{\#}$P<0.05, $^{\#\#}$P<0.01 et $^{\#\#\#}$P<0.001 comparées avec les cellules traitées avec les cytokines ou DCF séparément.

Effets cytotoxiques : Ensuite, nous avons recherché si ces cytokines affectaient la toxicité de DCF avec le test MTT. Quand les cellules HepaRG différenciées ont été exposées à IL-6 et IL-1 pendant 24h suivies par un co-traitement avec DCF pendant de nouveau 24h une aggravation de

la cytotoxicité affectant la viabilité cellulaire à des concentrations de 250µM et plus avec IL-1β et IL-6 (IC50≈541 et 450µM avec IL-1β et IL-6 respectivement) ont été observées. La cytotoxicité la plus élevée a été observée avec IL-6 en présence de 500µM de DCF (64 vs 38% de perte cellulaire par rapport aux cellules traitées avec DCF seul). En mesurant l'activité de caspase 3, une augmentation significative de cette activité a été constatée avec des concentrations de DCF inférieures à 150µM en combinaison avec IL-6 (4.55 fois vs IL-6 seul) et 200µM avec IL-1β (6.49 fois vs IL-1β seul) dans les cellules HepaRG différenciées après prétraitement avec les cytokines qui étaient sans effet lorsqu'elles étaient ajoutées seules (Figure 33).

L'impact de ces cytokines sur les cellules HepaRG différenciées a été observé aussi au niveau des marqueurs de stress oxydant et du stress du réticulum endoplasmique. Les niveaux d'expression des gènes codant des protéines de ces 2 types de stress étaient plus élevés lorsque les cellules étaient co-traitées avec IL-6 et IL-1β augmentant de 5.8 et 6.8 fois pour HO-1 et MnSOD avec DCF + IL-6 et 3.4 et 3.8 fois avec DCF + IL-1β respectivement. De même, les transcrits d'ATF4, ATF6, CHOP et GRP78 étaient plus exprimés dans ces conditions (Tableau 6).

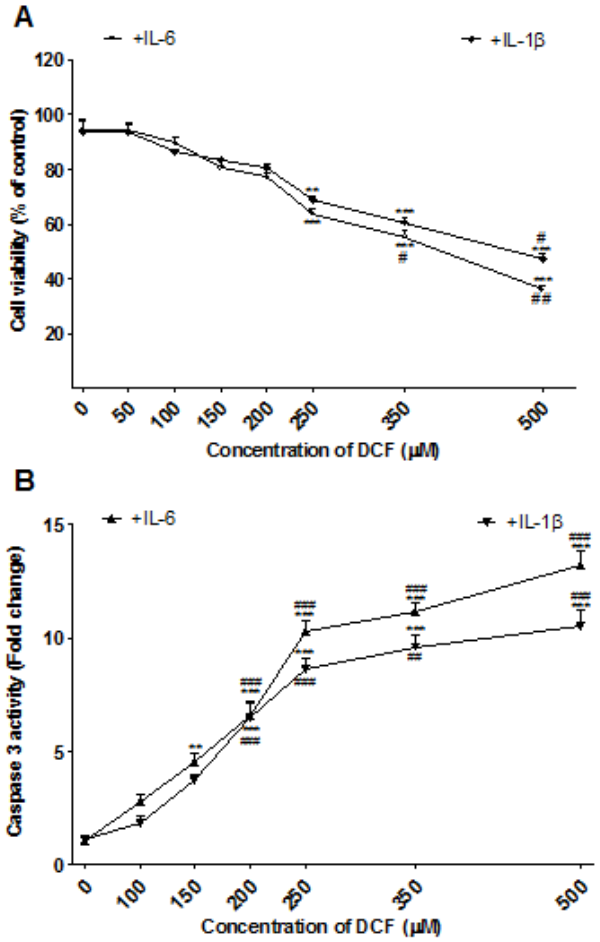

Figure 33: Effets d'IL-6 et d'IL-1β sur la toxicité de DCF dans les cellules HepaRG différenciées. (A) MTT et (B) activité de caspase 3 après traitement par DCF+ IL-6 ou DCF+IL-1β pour 24h précédé ou non par un pré-traitement avec ces cytokines (pendant 24h). Tous les résultats ont été calculés par rapport aux valeurs trouvées dans les cellules contrôles arbitrairement fixées à 1. *P<0.05, **P<0.01 et ***P<0.001 comparées avec les cellules non traitées, $^{\#}$P<0.05, $^{\#\#}$P<0.01 et $^{\#\#\#}$P<0.001 comparées avec les cellules traitées avec les cytokines ou DCF séparément.

	DCF 50µM	DCF100µM	DCF 200µM	TNF-α	TNF-α+DCF 50µM	TNF-α+DCF 100µM	TNF-α+DCF 200µM	IL-6	IL-6+DCF 50µM	IL-6+DCF 100µM	IL-6+DCF 200µM	IL-1β	IL-1β+DCF 50µM	IL-1β+DCF 100µM	IL-1β+DCF 200µM
CYP3A4	1.09±0.24	0.86±0.08	0.76±0.09	0.46±0.07***	0.34±0.05***c	0.18±0.02***c	0.15±0.04***c	0.16±0.01***	0.12±0.02***c	0.07±0.02***c	0.06±0.02***c	0.2±0.02***	0.16±0.02***c	0.11±0.02***c	0.06±0.01***c
CYP2C9	1.35±0.16**	0.89±0.24	0.72±0.13	0.74±0.07***	0.52±0.11***c	0.46±0.11***c	0.31±0.03***c	0.35±0.08***	0.25±0.03***c	0.21±0.02***c	0.15±0.03***c	0.53±0.04***	0.41±0.04***c	0.31±0.05***c	0.24±0.04***c
CRP	1.09±0.25	1.09±0.38	0.68±0.08	40.08±10.77***	34.43±7.56***c	23.27±5.57**b	18.28±2.9*a	96.08±3.8***	84.23±6***c	58.66±4.54***c	49.8±4.07***c	56.1±5.08***	44.77±4.37***c	30.03±2.95***c	21.17±2.29***c
IL-8	1.25±0.4	0.98±0.16	0.49±0.05	31.72±7.35***	29.73±6.73***c	25.62±6.03***c	20.32±3.64**b	61.68±4.63***	47.21±3.19***c	29.82±1.58***c	26.73±9.7***c	44.88±5.74***	41.9±4***c	27.36±3.24***c	21.76±3.31***c
HO-1	1.12±0.11	1.29±0.17	1.4±0.21*	1.060.08	1.07±0.08	1.31±0.09	1.6±0.16**	1.27±0.15	2.32±0.33***b	4.56±0.31***c	5.79±0.5***c	1.11±0.16	1.32±0.12	2.58±0.4***c	3.44±0.33***c
MnSOD	1.08±0.07	1.16±0.11	1.45±0.14**	1.12±0.11	1.18±0.05	1.46±0.12**	2±0.14***c	1.22±0.14	2.36±0.55***c	5.16±0.3***c	6.25±0.37***c	1.05±0.07	1.24±0.12	2.22±0.35***c	3.83±0.28***c
ATF4	1.14±0.09	1.59±0.20	3.06±0.32***	1.13±0.08	1.55±0.31	2.86±0.28***c	5.15±0.30***c	1.17±0.05	2.50±0.36***c	4.29±0.20***c	6.16±0.30***c	1.14±0.09	3.26±0.37***c	5.22±0.30***c	7.25±0.31***c
ATF6	1.19±0.15	1.72±0.19	2.51±0.29***	1.08±0.08	1.32±0.21	2.42±0.26***	4.19±0.25***c	1.14±0.04	1.97±0.29**a	3.79±0.26***c	5.45±0.30***c	1.19±0.04	1.92±0.26**	3.16±0.28***c	4.85±0.34***c
CHOP	1.27±0.20	2±0.24**	3.41±0.36***	1.12±0.09	1.63±0.20	3.54±0.29***c	6.55±0.25***c	1.09±0.10	3.45±0.30***c	5.30±0.29***c	7.96±0.40***c	1.02±0.09	2.51±0.36***c	3.97±0.27***c	7.04±0.45***c
GRP78	1.19±0.11	1.39±0.16	2.17±0.34***	1.16±0.06	1.47±0.16	2.17±0.29***a	3.29±0.21***c	1.26±0.33	1.53±0.30	2.81±0.22***c	4.45±0.26***c	1.19±0.06	1.20±0.14	2.21±0.23***b	3.04±0.16***b

Tableau 6: Effets de DCF et des cytokines sur l'expression des différents gènes (mésurée par RT-PCR) liés au métabolisme du médicament, à l'inflammation, au stress oxydant et au stress du réticulum endoplasmique dans les cellules HepaRG différenciées. Tous les résultats ont été exprimés relativement aux valeurs correspondant aux cellules non traitées. *P<0.05, **P<0.01 et ***P<0.001 comparées aux cellules non traitées, $^{\#}$P<0.05, $^{\#\#}$P<0.01 et $^{\#\#\#}$P<0.001 comparées aux cellules traitées avec les cytokines ou DCF séparement. a:#; b:##; c:###.

Effets cholestatiques : Les effets d'IL-6 et d'IL-1β ont aussi été analysés sur les paramètres cholestatiques. Ces cytokines ont aggravé l'effet de DCF sur l'expression des gènes codant les transporteurs d'acides biliaires, BSEP (efflux) et NTCP (entrée) (Tableau 6). Cependant, comme avec TNF-α aucune aggravation de la dilatation des canalicules biliaires induite par DCF n'a été observée par co-addition d'IL-6 ou IL-1β.

Conclusions : Ces études complémentaires montrent que des résultats comparables à ceux décrits pour le TNF-α peuvent être obtenus avec d'autres cytokines pro-inflammatoires. Cependant, d'autres études sont nécessaires pour préciser si IL-6 ou IL-1β peuvent également augmenter l'activité apoptotique du DCF. D'autre part des études dose-réponses seraient utiles pour mieux analyser l'influence de ces cytokines et donc la réponse des cellules hépatiques à DCF en présence d'un stress inflammatoire, en situation aiguë ou prolongée, c'est-à-dire après une ou plusieurs additions de DCF +/- IL-6 ou +/- IL-1β.

Chapitre II. La N-acétylcystéine potentialise la toxicité du diclofénac chez *Saccharomyces cerevisiae*: implication possible des transporteurs ABC

Résumé

Les réactions indésirables du diclofénac ont bien été décrites (Banks et al., 1995; Breen et al., 1986; Watanabe et al., 2007) et peuvent impliquer divers mécanismes d'action dans différents modèles expérimentaux. Nous avons démontré dans le « chapitre I » que la toxicité induite par DCF dans des lignées de cellules HepaRG diminue lorsque ces cellules expriment des enzymes du métabolisme et de détoxification du DCF (Al-Attrache et al., 2016). Chez la levure *Saccharomyces cerevisiae*, le métabolisme de DCF augmente sa toxicité (van Leeuwen et al., 2011c). Un autre médicament, la N-acétyl-cystéine, utilisé pour le traitement de diverses conditions médicales comme le traitement de la toxicité pulmonaire par l'oxygène, de l'intoxication par le paracétamol, de la cardiotoxicité par doxorubicine et de la toxicité par des métaux lourds (Rushworth and Megson, 2014; Samuni et al., 2013) et peut provoquer des réactions indésirables comme les symptômes gastro-intestinaux (Koppen et al., 2014). Les utilisations multiples de NAC sont dues à ses propriétés chimiques multiples. Elle est un antioxydant *in vitro* et *in vivo*, elle chélate des métaux lourds et échange le thiol-disulfure induisant une réduction de ponts di-sulfure dans les protéines cibles (Zafarullah et al., 2003). Ce dernier effet est responsable des effets mucolytiques de NAC. Cet effet potentiel de NAC pourrait s'élargir à d'autres cibles moléculaires potentielles ayant un pont di-sulfure, telles que des protéines impliquées dans la transduction des signaux (par exemple NFκB), les transporteurs ABC et beaucoup d'autres.

NAC et DCF agissent en synergie ou en antagonisme dans différents modèles puisqu'ils ont des mécanismes d'action multiples; par exemple, ils agissent en synergie comme anti-inflammatoire via l'inhibition de la cyclooxygénase (Parasassi et al., 2005) alors que NAC antagonise la toxicité hépatique induite par DCF (Al-Attrache et al., 2016). Notre étude visait à étudier l'interaction de ces deux molécules et l'implication possible des transporteurs ABC dans leur toxicodynamique *in vitro* dans la levure *Saccharomyces cerevisiae* de type sauvage ainsi que dans certaines souches mutantes (dans des gènes de transporteurs ABC). Nos résultats ont montré que le DCF inhibe la croissance cellulaire d'une manière dépendante de la dose et du temps et que les cellules commencent à s'adapter au DCF après 24 heures de traitement. Cette adaptation avait déjà été décrite chez la levure et implique des dizaines de gènes (van Leeuwen et al., 2011b).

Nous avons montré également que NAC potentialise l'inhibition de la croissance induite par DCF chez la levure si NAC est ajoutée avant ou parallèlement au DCF. Le pré-traitement avec NAC

augmente son effet de potentialisation et diminue la capacité d'adaptation des cellules au DCF. En outre, les souches mutantes en Pdr5, Yor1, Bpt1 ou Pdr15, étaient plus sensibles à DCF, alors que les souches mutantes dans Pdr5, Vmr1 ou Pdr12 étaient plus sensibles à l'interaction du NAC avec DCF. La souche mutante dans Yap1, un facteur de transcription médiant la réponse au stress oxydatif, a montré le même profil de croissance que la souche sauvage en présence de DCF + NAC. Par conséquent, le stress oxydatif ne semble pas être un facteur clé dans la toxicité du DCF dans notre modèle, et nous supposons que la potentialisation de cette toxicité par NAC est au moins due à sa capacité à perturber le pont disulfure dans diverses protéines qui aident les cellules de levure à surmonter la toxicité de DCF, entre autres des transporteurs ABC.

N-acetylcysteine potentiates diclofenac toxicity in *Saccharomyces cerevisiae*: possible involvement of ABC transporters.

Houssein Al-Attrache[1,2,3], Hala Chamieh[1], Monzer Hamzé[5], André Guillouzo[2,3], Isabelle Morel[2,3,4], Samir Taha[1] and Ziad Abdel-Razzak[1*]

[1]Laboratory of applied biotechnology: biomolecules, LBA3B - AZM Center –Tripoli, Lebanon
[2]Inserm U991, Faculty of Pharmacy, Rennes, France
[3]Rennes 1 University, Rennes, France
[4]Laboratory Emergency and Intensive Care, Hospital Pontchaillou, Rennes, France
[5]Laboratory of medical microbiology - AZM Center -Tripoli, Lebanon

*corresponding author: Pr. Ziad ABDEL-RAZZAK, ziad.abdelrazzak@ul.edu.lb; Lebanese University – Faculty of sciences I – Rafic Hariri Campus - Po. Box: 14-6573, Hadat - Beirut – Lebanon. Phone 00961 3 48 69 15

Abbreviations

Bpt1, Bile Pigment Transporter 1; DCF, Diclofenac; LC, L-Cysteine ; MPT, Mitochondrial Permeability Transition; NAC, N-acetylcysteine; OD, optical density; Pdr, Pleiotropic drug resistance; PKC, Protein Kinase C; ROS, Reactive Oxygen Species; Vmr1, Vacuolar Multidrug Resistance; Yap1, Yeast Activator Protein 1; YNB, Yeast Nitrogen Base; Yor1, Yeast Oligomycin Resistance; YPD, Yeast extract Peptone Dextrose; Zap1, Zinc-responsive Activator Protein.

Abstract

Diclofenac (DCF) adverse reactions are well documented and may involve diverse mechanisms of action in different experimental models. We recently demonstrated that DCF-induced toxicity in the HepaRG cell line decreases as the cells express DCF-metabolizing/detoxifying enzymes. In *Saccharomyces cerevisiae*, DCF metabolism promotes toxicity. Another drug, N-acetylcysteine (NAC) has been used for treatment of diverse medical conditions and may cause adverse drug reactions. NAC multiple use is due to its multi-sided chemical properties, antioxidant *in vitro* and *in vivo*, heavy metal chelation and thiol-disulfide exchange and disruption. This latter accounts for its mucolytic effects and widens its potential molecular targets such as signal transduction proteins (e.g. NFκB), ABC transporters and many others.

NAC and DCF were reported to act in synergism or antagonism in different models. Our study aimed to investigate the interaction of NAC with DCF and the possible involvement of ABC transporters in their toxicodynamics *in vitro* on *Saccharomyces cerevisiae* wild type and certain mutant strains. In the present study, DCF inhibited yeast cell growth in a dose- and time-dependent manner and the cells started adapting to DCF after 24 hours of treatment. NAC potentiated DCF-induced growth inhibition of yeast when it was added prior or parallel to DCF. Pre-treatment with NAC increased its potentiation effect and compromised cell ability to adapt to DCF. Post-treatment with NAC potentiated DCF toxicity without compromising adaptation. Moreover, mutant strains in Pdr5, Yor1, Bpt1 or Pdr15, were more sensitive to DCF, while mutant strains in Pdr5, Vmr1 or Pdr12 were more sensitive to the interaction of NAC with DCF. The mutant strain in Yap1, an oxidative stress-related transcription factor, elicited the same growth pattern as the wild type in presence of DCF ± NAC. Therefore, oxidative stress does not seem to be key actor in DCF toxicity in our model and we hypothesize that NAC potentiation effect is at least due to its ability to disrupt disulfide bridge in diverse proteins that help yeast cells overcoming DCF toxicity.

Keywords: Diclofenac, N-acetylcysteine, oxidative stress, di-sulfide bridge, ABC transporters, *Saccharomyces cerevisiae*.

Introduction

Administration of diclofenac (DCF), a non-steroidal anti-inflammatory drug, has been associated with adverse drug reactions in some patients (Banks et al., 1995; Breen et al., 1986; Watanabe et al., 2007). DCF adverse effects have been related to different factors including its metabolism into 4′-OH-DCF, 5-OH-DCF, and acyl glucuronides (Bort et al., 1999b; Kretz-Rommel and Boelsterli, 1993; Wang et al., 2004). We recently demonstrated that DCF-induced toxicity in hepatic HepaRG cell lines decreases as the cells differentiate and express DCF-metabolizing and detoxifying enzymes (Al-Attrache et al., 2016). The reverse was reported in *Saccharomyces cerevisiae* where heterologous expression of DCF-metabolizing cytochrome P450 potentiates DCF toxicity and reactive oxygen species (ROS) generation (van Leeuwen et al., 2011c). DCF-induced ROS generation originates in the mitochondrion and was shown to be respiratory chain-dependent in both mammalian and yeast cells (Masubuchi et al., 2002a; van Leeuwen et al., 2011a). Furthermore, in several cellular systems, including human hepatocytes, DCF induces ROS formation, causing opening of the mitochondrial permeability transition (MPT) pore, cytochrome c release, caspase activation and apoptosis (Gomez-Lechon et al., 2003; Inoue et al., 2004; Lim et al., 2006). The ROS-mediated DCF apoptotic effects are counteracted by N-acetylcysteine (NAC) (Inoue et al., 2004).

Moreover, in *Saccharomyces cerevisiae* DCF toxic effects and cells adaptation to this toxicant involved pleiotropic drug resistance (Pdr) 5 gene and some components of the protein kinase C (PKC) and MAPK signaling pathways. Indeed, adaption and tolerance of yeast cells to DCF has been associated with induction of PDR genes and Rlm1p-controlled genes; Rlm1p is a transcription factor in the PKC pathway. Moreover, increased DCF toxicity occurs after deletion of components of the cell wall stress-responsive PKC pathway or the Zinc (Zn)-responsive transcription factor Zap1p (Zn-responsive activator protein). In addition, Zn-chelator increases DCF toxicity (van Leeuwen et al., 2011b).

NAC has been used in clinical practice for mucolytic purpose in lung diseases that are associated with mucus hypersecretion, treatment of pulmonary oxygen toxicity, adult respiratory distress syndrome, acetaminophen intoxication, doxorubicin cardiotoxicity, ischemia-reperfusion cardiac injury, chemotherapy-induced toxicity, heavy metal toxicity and psychiatric disorders (Rushworth and Megson, 2014; Samuni et al., 2013). However, NAC causes adverse drug reactions such as pruritis, rash and gastrointestinal symptoms (Koppen et al., 2014).

This diversity of NAC pharmacological applications and adverse effects is due to the multi-sided chemical features of its cysteinyl thiol including nucleophilicity, ROS scavenging (antioxidant properties, *in vitro* and *in vivo*), heavy metal chelation and and its ability to undergo thiol-disulfide (di-S) exchange reactions with other thiol redox couples leading to di-S bridge disruption (Zafarullah et al., 2003) as in the case of mucous proteins. NAC is more efficient than other thiol-containing molecules (e.g. cysteine and glutathione) in terms of di-S bridge disruption due to its lower molecular weight (in comparison with glutathione) and might compete with

larger reducing molecules in sterically less accessible proteins cores. Moreover, NAC is a precursor of cysteine (by deacetylation) and increases glutathione levels.

Therefore NAC affects diverse molecular targets such as signal transduction proteins (e.g. NFkB, c-Src, STAT3, MAPK) through direct interaction with proteins and/or indirectly through ROS neutralization (Hou et al., 2015; Parasassi et al., 2010; Ramudo and Manso, 2010; Samuni et al., 2013). NAC affects cell division and differentiation causing change of expression of more than 900 genes including cytoskeleton- and cell cycle-related genes (Edlundh-Rose et al., 2005). NAC is also likely to affect expression and activity of many di-S bridge-containing protein types including ABC transporters as well as key transduction pathways in DCF-induced toxicity.

Given the diverse toxic and therapeutic effects and targets of these two commonly used drugs, NAC and DCF, and the common use of NAC as antioxidant in research, an important question arises about their interaction and the possible involvement of ABC transporters in their toxicodynamic in experimental model. In fact, previous clinical reports as well as reports from different experimental models showed diverging results in this respect. This is likely due to the multiple mechanisms of actions of both drugs. NAC and DCF act in synergy as anti-inflammatory drugs through cyclooxygenase inhibition (Parasassi et al., 2005), and inhibition of TNFα secretion (Mulhall et al., 2003). NAC was reported to reduce DCF-induced renal toxicity (Efrati et al., 2007) and ROS-mediated DCF-induced toxicity and apoptosis (Al-Attrache et al., 2016; Inoue et al., 2004). However, NAC has no effect on DCF-methyl phenyl pyridinium potentiated toxicity (Morioka et al., 2004).

In the present study we investigated the interaction of NAC and DCF on wild type and ABC-transporter mutant strains of *S. cerevisiae*. Our results showed that DCF inhibits cell growth in a dose and time-dependent manner and that NAC potentiates DCF-induced growth inhibition of yeast. Moreover, Mutant strains in some ABC transporters are more sensitive to DCF, and to the interaction of NAC with DCF.

Materials and methods

Chemicals and reagents

Diclofenac sodium salt, N-acetylcysteine and YPD broth and agarose were purchased from sigma Aldrich (St. Quentin Fallavier, France). L-cysteine (LC) was from BDH (England).

Cell culture, treatment and growth assessment

Saccharomyces cerevisiae BY4741 and the mutants strains illustrated in Table 2 were supplied by Euroscarf (Germany). Cells were seeded on YPD-agar (50 g/liter, 1.6 % agarose) for 48h at 30ºC. Colonies are diluted in YPD broth (50 g/l) to an OD (optical density) at 600 nm between 0.1 and 0.2 and treated with drugs, or grown for 48h and then diluted to obtain an OD between 0.1 and 0.2 and then treated with drugs for different periods of time. Culture shaking was performed only prior to growth assessment by OD measurement at 600 nm.

Statistical analysis

One-way ANOVA with Bonferroni's multiple comparison test (GraphPad Prism 5.00) was performed to compare data between DCF-, NAC-, DCF +NAC-treated cells and control cultures as well as data obtained with mutant with wild-type strains. Differences were considered significantly different when $p < 0.05$.

Results

Dose and time-dependent effect of diclofenac on growth of S. cerevisiae BY4147 strain

In order to assess DCF effect on growth of *Saccharomyces cerevisiae* BY4741 strain, different doses and treatment time points were used. Yeast growth was inhibited by DCF in a time and dose-dependent manner (Figure 1a and b) starting at the 3 hour-treatment time point and reaching a maximum after 9 hours. DCF effect appeared at the dose of 1000 µM and was more efficient at 2000 µM. This latter dose caused 22.6% and 55.8% inhibition at 3h and 6h treatment, respectively (Figure 1a). The inhibitory effect of DCF was partially abolished after 24 hour-treatment reflecting a previously described process of adaption of yeast cells to this drug (Figure 1b) (van Leeuwen et al., 2011b).

Interaction of N-acetylcysteinwith diclofenactoxic effect on S. cerevisiae BY4741

In order to assess interaction of NAC with DCF toxic effect, yeast cells (BY4741) were treated with DCF $\pm$ NAC, concomitantly or one after the other, and growth was assessed after the indicated time points (Table 1). Similarly to Figure 1b, DCF maximal inhibitory effect occurred after 9 hour-treatment (34.4% inhibition), and cells started to adapt at 24 hours where DCF-mediated inhibition decreased. NAC, which had no statistically significant inhibitory effect by itself, potentiated DCF toxicity in a significant manner regardless of whether drugs are added concomitantly or one after the other. A dose of 1 mM showed similar but mild potentiating

effects (data not shown). At 9h, NAC+DCF added together led to 64.7% growth inhibition while DCF alone caused only 34.4% inhibition. At 24h, adaptation of cells to DCF in the presence of NAC was decreased (19.1% versus 29.7% inhibition) but the difference was not statistically significant.

Moreover, when cells were pre-treated with NAC, more potentiation of DCF toxicity occurred (inhibition by 31.8%, 76.3%, 82.9% and 68% at 3, 6, 9 and 24h, respectively). Inhibition after concomitant addition of the two drugs was 10.7%, 39,6%, 64.7% and 29.7% at 3, 6, 9 and 24h, respectively (Table 1). Therefore, cells are more sensitive to DCF-induced toxicity when NAC is added prior to DCF than when they are added together. In addition, cells adaptation to DCF at 24 hours is seriously impaired by NAC pre-treatment. However, when yeast cells were pretreated with DCF, increase of DCF toxic effect by NAC was still evident, but NAC was no longer able to impair their adaptation to DCF. This result suggests the involvement of diverse cellular targets in NAC/DCF interaction.

Investigation ofdiclofenac, N-acetylcysteinand L-cysteineffects and interactions on growth of wild type and mutant strains of S. cerevisiae growth

We aimed here to assess the potential involvement of certain ABC transporters in terms of DCF toxicity and its potentiation by NAC. Moreover, other amino acids effects were investigated to check if the observed NAC/DCF interaction was relative to amino acids metabolic pathways, osmotic stress, or mediated by other mechanisms such as the antioxidant effect, di-S bridge disruption, signal transduction alteration, metal ion chelation. Wild type and mutant strains (illustrated in Table 2) in some ABC transporters and Yap1 were used.

DCF (1000 µM) was toxic for all used strains causing growth inhibition ranging from 21.2% to 64.9%. The strains Y02409, Y05933, Y01503, Y04242 which are mutant in the genes Pdr5, Yor1, Bpt1 and Pdr15 respectively, were more sensitive to DCF since growth inhibition percentage was significantly higher (inhibition by 45.7%, 63.3%, 63.9% and 64.9%, for the mutant strains respectively) in comparison with that of the wild type strain (34.4% inhibition) (Table 2). Therefore each one of these ABC transporters partially protects yeast cells against DCF. The other mutant strains showed no statistically significant change of sensitivity to DCF in comparison with the wild type strain. Regarding yeast cells adaptation to DCF, all of the investigated mutant strains were still able to adapt to the drug (data not shown) starting at 24 hours.

It is noteworthy emphasizing that the yeast strain mutant in Yap1 (Y00569), an AP-1 like transcription factor known to mediate oxidative stress response (Yano et al., 2009), had the same sensitivity to DCF as the wild-type one, thereby suggesting that oxidative stress is not a key factor in DCF-induced toxic effect in our experimental model and culture conditions.

In the presence of NAC, the strains mutants in Pdr5, Vmr1 and Pdr12 showed more potentiated DCF toxicity (inhibition range from 84.8 to 93.9%) in comparison with the BY4741 wild type

strain (inhibition by 64.7%). Therefore, these mutant strains are more sensitive to NAC/DCF interaction. Regarding interaction of DCF with the other amino acids, L-cysteine tended to potentiate DCF toxicity but the results did not reach statistical significance neither with the wild type nor with the mutant strains (Table 2), while L-lysine and L-isoleucine, individually, did not cause any DCF toxicity potentiation (data not shown).

Discussion

DCF induces adverse reactions in some patients (Boelsterli, 2003a). Involvement of oxidative stress enzymes and drug metabolizing enzymes in this toxicity was reported in *in vitro* hepatic and non-hepatic models (Al-Attrache et al., 2016; Fredriksson et al., 2011) (van Leeuwen et al., 2011c). DCF was reported to induce oxidative stress, apoptosis, cholestasis by diverse mechanisms (Al-Attrache et al., 2016; Fredriksson et al., 2011; Fredriksson et al., 2014; Maiuri et al., 2015) including deregulation of some ABC and SLC transporters (Al-Attrache et al., 2016), respiratory chain components and PKC signaling (van Leeuwen et al., 2011b).

Our study demonstrated that DCF inhibited yeast growth in a dose- and time-dependent and metabolism-independent manner. Our results are in accordance with previous studies (van Leeuwen et al., 2011c). Toxicity started with a DCF dose of 1000µM and was maximal after nine hours of treatment. Cells started to adapt to DCF and overcome its toxicity at 24 hours, this is also in agreement with previous reports which showed that adaptation to DCF was due to up-regulation of several tens of genes such as the Pdr genes and genes under the control of Rlm1p (MADS-box transcription factor), a transcription factor in the PKC pathway. In addition, many other genes are down-regulated (van Leeuwen et al., 2011b).

The efficient DCF dose in our study was 1000 µM, much higher than that reported in previous studies (van Leeuwen et al., 2011b) where DCF effects started at 50 µM and reached a maximum at 200 or 500 µM. Such high DCF concentration (>1000 µM) are not aberrant and was already used with another yeast, *Candida albicans* (Ghalehnoo et al., 2010). The great difference of *S. cerevisiae* response to DCF between our study and that of Leeuwen *et al.* is probably due to use of the minimal medium YNB (yeast nitrogen base, supplemented with amino acids and glucose) while the complete YPD broth is used in our case. Indeed, YNB pH is usually more acidic (about 5 (van Leeuwen et al., 2011a) than that of YPD (pH range 6.4 to 7). More acidic pH causes lower ratio of ionized/non ionized diclofenac thereby causing more efficient diffusion across the plasma membrane. In addition, YPD is a rich medium that contains many organic components that are likely to make complex with DCF thereby reducing its diffusion into cells.

NAC properties and its diverse mechanisms of action and clinical applications were summarized in the introduction of this article. Though previous studies in other cell models reported protective effect of NAC against DCF-induced toxicity (Al-Attrache et al., 2016; Efrati et al., 2007; Inoue et al., 2004), the present study clearly showed an original interaction between NAC and DCF since toxicity of the latter on yeast was potentiated in the presence of NAC, and cells adaptation to DCF was compromised, especially when NAC is added first and DCF second, with a 30 minute-delay. Potentiation of DCF toxic effect by NAC was in agreement with the result we obtained using the Yap1 mutant strain (Y00569, Table 2) which showed sensitivity to DCF similar to that of the wild-type strain BY4741. This result enabled us to hypothesize that NAC effect was not dependent on its antioxidant properties here. Other studies had reported antioxidant-independent NAC effects. For instance, NAC potentiates effect of $Cu_{(II)}$ H_2O_2 on the

mitochondrial diaphorase (Gutierrez-Correa and Stoppani, 1997), interferes with transport of As_2O_3 (Vernhet et al., 2003) and inhibits mitochondrial autophagy (Deffieu et al., 2009). In our experimental model, NAC had a protective effect against toxicity of chlorpromazine (unpublished data) probably through its antioxidant property.

However, and despite the lack of change of Yap1 mutant yeast (an oxidative stress-related transcription factor) sensitivity to DCF reported here, it is impossible to rule out involvement of the antioxidant properties of NAC in our context since ROS are known to trigger signaling pathways that could relief or alleviate toxicity (Hancock et al., 2001; Xu et al., 2002). Their early neutralization by NAC in the presence of DCF excess is likely to make the cells vulnerable to DCF toxic effects due to lack of protective signaling pathways activation.

In addition, NAC could potentiate DCF toxic effects through its ability to disrupt di-S bridges that occur in diverse proteins of signaling pathways, ABC efflux transporters, and house-keeping metabolic enzymes. Many ABC transporters such as Pdr5 and Yor1 (Egner et al., 1998; Pagant et al., 2008) have di-S bridge that are important to their stability and are potential targets that could be disrupted by NAC through its di-S bridge reducing effect. Our results demonstrated that mutant strains in these three ABC transporters made the cells more sensitive to DCF. This finding is supportive of the NAC-mediated di-S disruption hypothesis. The cells would become more vulnerable to DCF effect due to lack of drug efflux, especially because Pdr5 (ABC G, PgP homolog), Yor1 (ABC C, MRP member) and Pdr15 mediate efflux of a wide variety of toxicants (Piecuch and Oblak, 2014). It is also possible that NAC/DCF interaction we described in this work was due to competition of both drugs to some efflux transporters since both NAC and DCF are weak organic acids.

Di-S bridge disruption by NAC could occur for transcription factors that help the cell overcoming the toxic effects of DCF. It was reported that di-S bridge disruption occurs for signaling molecules such as NFkB (review by (Samuni et al., 2013)). Moreover, NAC could promote DCF toxicity by altering Zn-finger containing protein since NAC has metal ions chelator activity (Kelly, 1998). In fact, inactivation of the Zn-finger transcription factor Zap1 (by mutation or by Zn ion chelation) was reported to increase DCF toxicity in *S. cerevisiae* (van Leeuwen et al., 2011b). Many other Zn-finger containing proteins could be targets of NAC, such as Pdr1 and Pdr3 which are key transcription factors involved in the yeast pleiotropic drug resistance response. Their potential alteration by NAC would compromise cells response to chemical stress and aggravate toxicity. NAC could also disrupt key enzymes in the fermentation pathway, a preferred energetic mode in *S. cerevisiae*, thereby obligating cells to perform respiration-based metabolism, a situation known to make the cells more sensitive to DCF (van Leeuwen et al., 2011a). All the previous hypothetical mechanisms of NAC action are probable since pre-treatment of cells with NAC increases its ability to potentiate DCF toxic effects. A contribution of different mechanisms is likely since NAC pre-treatment impaired cells adaptation to DCF, a process involving nearly a hundred genes (van Leeuwen et al., 2011b).

Yeast cells are sensitive to the osmotic choc-induced stress (Chant, 1999). Treatment of our strains with two other amino acids in combination with DCF, L-lysine and L-isoleucine, at the same concentrations as NAC, showed no change in the DCF toxic response amplitude (data not shown). This helped us ruling out involvement of osmotic stress and amino acid metabolic alteration in the observed NAC interaction with DCF.

By deacetylation, NAC is a precursor of LC, which could mediate the observed effects. Nevertheless, treatment of yeast cells with LC did not increase DCF toxicity in a significant manner in our study. This result showed that NAC acted by itself to increase DCF toxicity, and this was in agreement with the fact that NAC has higher redox potential than cysteine and is more efficient in terms of di-S bridge disruption (Rushworth and Megson, 2014; Samuni et al., 2013).

In conclusion, we demonstrated here for the first time that NAC, but not LC, potentiated DCF toxicity in *S. cerevisiae* cells. Some ABC-transporter mutants were more sensitive to DCF toxic effects and NAC/DCF interaction. Diverse possible mechanisms could explain the observed NAC/DCF interaction including di-S bridge disruption and Zn-chelating effect of NAC on key proteins (transporters, signaling proteins or transcription factors,…). Oxidative stress did not seem to be involved in the interaction NAC/DCF. Further experiments will be performed to unravel the involved mechanism (s).

Acknowledgments and financial support

This work was supported by the Lebanese University Research funds. We are grateful to the AZM center assistants for their cooperation. Houssein Al-Attrache was financially supported by the Association AZM-Lebanese University and the MIP-DILI project.

Declaration of interest statement

The authors declare that there are no conflicts of interest.

References

Al-Attrache, H., Sharanek, A., Burban, A., Burbank, M., Gicquel, T., Abdel-Razzak, Z., Guguen-Guillouzo, C., Morel, I., Guillouzo, A., 2016. Differential sensitivity of metabolically competent and non-competent HepaRG cells to apoptosis induced by diclofenac combined or not with TNF-alpha. Toxicology letters 258, 71-86.

Banks, A.T., Zimmerman, H.J., Ishak, K.G., Harter, J.G., 1995. Diclofenac-associated hepatotoxicity: analysis of 180 cases reported to the Food and Drug Administration as adverse reactions. Hepatology 22, 820-827.

Boelsterli, U.A., 2003. Diclofenac-induced liver injury: a paradigm of idiosyncratic drug toxicity. Toxicology and applied pharmacology 192, 307-322.

Bort, R., Ponsoda, X., Jover, R., Gomez-Lechon, M.J., Castell, J.V., 1999. Diclofenac toxicity to hepatocytes: a role for drug metabolism in cell toxicity. The Journal of pharmacology and experimental therapeutics 288, 65-72.

Breen, E.G., McNicholl, J., Cosgrove, E., McCabe, J., Stevens, F.M., 1986. Fatal hepatitis associated with diclofenac. Gut 27, 1390-1393.

Chant, J., 1999. Cell polarity in yeast. Annual review of cell and developmental biology 15, 365-391.

Deffieu, M., Bhatia-Kissova, I., Salin, B., Galinier, A., Manon, S., Camougrand, N., 2009. Glutathione participates in the regulation of mitophagy in yeast. The Journal of biological chemistry 284, 14828-14837.

Edlundh-Rose, E., Kupershmidt, I., Gustafsson, A.C., Parasassi, T., Serafino, A., Bracci-Laudiero, L., Greco, G., Krasnowska, E.K., Romano, M.C., Lundeberg, T., Nilsson, P., Lundeberg, J., 2005. Gene expression analysis of human epidermal keratinocytes after N-acetyl L-cysteine treatment demonstrates cell cycle arrest and increased differentiation. Pathobiology : journal of immunopathology, molecular and cellular biology 72, 203-212.

Efrati, S., Berman, S., Siman-Tov, Y., Lotan, R., Averbukh, Z., Weissgarten, J., Golik, A., 2007. N-acetylcysteine attenuates NSAID-induced rat renal failure by restoring intrarenal prostaglandin synthesis. Nephrology, dialysis, transplantation : official publication of the European Dialysis and Transplant Association - European Renal Association 22, 1873-1881.

Egner, R., Rosenthal, F.E., Kralli, A., Sanglard, D., Kuchler, K., 1998. Genetic separation of FK506 susceptibility and drug transport in the yeast Pdr5 ATP-binding cassette multidrug resistance transporter. Molecular biology of the cell 9, 523-543.

Fredriksson, L., Herpers, B., Benedetti, G., Matadin, Q., Puigvert, J.C., de Bont, H., Dragovic, S., Vermeulen, N.P., Commandeur, J.N., Danen, E., de Graauw, M., van de Water, B., 2011. Diclofenac inhibits tumor necrosis factor-alpha-induced nuclear factor-kappaB activation causing synergistic hepatocyte apoptosis. Hepatology 53, 2027-2041.

Fredriksson, L., Wink, S., Herpers, B., Benedetti, G., Hadi, M., de Bont, H., Groothuis, G., Luijten, M., Danen, E., de Graauw, M., Meerman, J., van de Water, B., 2014. Drug-induced endoplasmic reticulum and oxidative stress responses independently sensitize toward TNFalpha-mediated hepatotoxicity. Toxicological sciences : an official journal of the Society of Toxicology 140, 144-159.

Ghalehnoo, Z.R., Rashki, A., Najimi, M., Dominguez, A., 2010. The role of diclofenac sodium in the dimorphic transition in Candida albicans. Microbial pathogenesis 48, 110-115.

Gomez-Lechon, M.J., Ponsoda, X., O'Connor, E., Donato, T., Castell, J.V., Jover, R., 2003. Diclofenac induces apoptosis in hepatocytes by alteration of mitochondrial function and generation of ROS. Biochemical pharmacology 66, 2155-2167.

Gutierrez-Correa, J., Stoppani, A.O., 1997. Inactivation of yeast glutathione reductase by Fenton systems: effect of metal chelators, catecholamines and thiol compounds. Free radical research 27, 543-555.

Hancock, J.T., Desikan, R., Neill, S.J., 2001. Role of reactive oxygen species in cell signalling pathways. Biochemical Society transactions 29, 345-350.

Hou, Y., Wang, L., Yi, D., Wu, G., 2015. N-acetylcysteine and intestinal health: a focus on its mechanism of action. Frontiers in bioscience 20, 872-891.

Inoue, A., Muranaka, S., Fujita, H., Kanno, T., Tamai, H., Utsumi, K., 2004. Molecular mechanism of diclofenac-induced apoptosis of promyelocytic leukemia: dependency on reactive oxygen species, Akt, Bid, cytochrome and caspase pathway. Free radical biology & medicine 37, 1290-1299.

Kelly, G.S., 1998. Clinical applications of N-acetylcysteine. Alternative medicine review : a journal of clinical therapeutic 3, 114-127.

Koppen, A., van Riel, A., de Vries, I., Meulenbelt, J., 2014. Recommendations for the paracetamol treatment nomogram and side effects of N-acetylcysteine. The Netherlands journal of medicine 72, 251-257.

Kretz-Rommel, A., Boelsterli, U.A., 1993. Diclofenac covalent protein binding is dependent on acyl glucuronide formation and is inversely related to P450-mediated acute cell injury in cultured rat hepatocytes. Toxicology and applied pharmacology 120, 155-161.

Lim, M.S., Lim, P.L., Gupta, R., Boelsterli, U.A., 2006. Critical role of free cytosolic calcium, but not uncoupling, in mitochondrial permeability transition and cell death induced by diclofenac oxidative metabolites in immortalized human hepatocytes. Toxicology and applied pharmacology 217, 322-331.

Maiuri, A.R., Breier, A.B., Gora, L.F., Parkins, R.V., Ganey, P.E., Roth, R.A., 2015. Cytotoxic Synergy Between Cytokines and NSAIDs Associated With Idiosyncratic Hepatotoxicity Is Driven by Mitogen-Activated Protein Kinases. Toxicological sciences : an official journal of the Society of Toxicology 146, 265-280.

Masubuchi, Y., Nakayama, S., Horie, T., 2002. Role of mitochondrial permeability transition in diclofenac-induced hepatocyte injury in rats. Hepatology 35, 544-551.

Morioka, N., Kumagai, K., Morita, K., Kitayama, S., Dohi, T., 2004. Nonsteroidal anti-inflammatory drugs potentiate 1-methyl-4-phenylpyridinium (MPP+)-induced cell death by promoting the intracellular accumulation of MPP+ in PC12 cells. The Journal of pharmacology and experimental therapeutics 310, 800-807.

Mulhall, K.J., Curtin, W.A., Given, H.F., 2003. Comparison of different anti-inflammatory agents in suppressing the monocyte response to orthopedic particles. Orthopedics 26, 1219-1223.

Pagant, S., Brovman, E.Y., Halliday, J.J., Miller, E.A., 2008. Mapping of interdomain interfaces required for the functional architecture of Yor1p, a eukaryotic ATP-binding cassette (ABC) transporter. The Journal of biological chemistry 283, 26444-26451.

Parasassi, T., Brunelli, R., Bracci-Laudiero, L., Greco, G., Gustafsson, A.C., Krasnowska, E.K., Lundeberg, J., Lundeberg, T., Pittaluga, E., Romano, M.C., Serafino, A., 2005. Differentiation of normal and cancer cells induced by sulfhydryl reduction: biochemical and molecular mechanisms. Cell death and differentiation 12, 1285-1296.

Parasassi, T., Brunelli, R., Costa, G., De Spirito, M., Krasnowska, E., Lundeberg, T., Pittaluga, E., Ursini, F., 2010. Thiol redox transitions in cell signaling: a lesson from N-acetylcysteine. TheScientificWorldJournal 10, 1192-1202.

Piecuch, A., Oblak, E., 2014. Yeast ABC proteins involved in multidrug resistance. Cellular & molecular biology letters 19, 1-22.

Ramudo, L., Manso, M.A., 2010. N-acetylcysteine in acute pancreatitis. World journal of gastrointestinal pharmacology and therapeutics 1, 21-26.

Rushworth, G.F., Megson, I.L., 2014. Existing and potential therapeutic uses for N-acetylcysteine: the need for conversion to intracellular glutathione for antioxidant benefits. Pharmacology & therapeutics 141, 150-159.

Samuni, Y., Goldstein, S., Dean, O.M., Berk, M., 2013. The chemistry and biological activities of N-acetylcysteine. Biochimica et biophysica acta 1830, 4117-4129.

van Leeuwen, J.S., Orij, R., Luttik, M.A., Smits, G.J., Vermeulen, N.P., Vos, J.C., 2011a. Subunits Rip1p and Cox9p of the respiratory chain contribute to diclofenac-induced mitochondrial dysfunction. Microbiology 157, 685-694.

van Leeuwen, J.S., Vermeulen, N.P., Vos, J.C., 2011b. Involvement of the pleiotropic drug resistance response, protein kinase C signaling, and altered zinc homeostasis in resistance of Saccharomyces cerevisiae to diclofenac. Applied and environmental microbiology 77, 5973-5980.

van Leeuwen, J.S., Vredenburg, G., Dragovic, S., Tjong, T.F., Vos, J.C., Vermeulen, N.P., 2011c. Metabolism related toxicity of diclofenac in yeast as model system. Toxicology letters 200, 162-168.

Vernhet, L., Allain, N., Le Vee, M., Morel, F., Guillouzo, A., Fardel, O., 2003. Blockage of multidrug resistance-associated proteins potentiates the inhibitory effects of arsenic trioxide on CYP1A1 induction

by polycyclic aromatic hydrocarbons. The Journal of pharmacology and experimental therapeutics 304, 145-155.

Wang, A.G., Xia, T., Yuan, J., Yu, R.A., Yang, K.D., Chen, X.M., Qu, W., Waalkes, M.P., 2004. Effects of phenobarbital on metabolism and toxicity of diclofenac sodium in rat hepatocytes in vitro. Food and chemical toxicology : an international journal published for the British Industrial Biological Research Association 42, 1647-1653.

Watanabe, N., Takashimizu, S., Kojima, S., Kagawa, T., Nishizaki, Y., Mine, T., Matsuzaki, S., 2007. Clinical and pathological features of a prolonged type of acute intrahepatic cholestasis. Hepatology research : the official journal of the Japan Society of Hepatology 37, 598-607.

Xu, Y.C., Wu, R.F., Gu, Y., Yang, Y.S., Yang, M.C., Nwariaku, F.E., Terada, L.S., 2002. Involvement of TRAF4 in oxidative activation of c-Jun N-terminal kinase. The Journal of biological chemistry 277, 28051-28057.

Yano, T., Takigami, E., Yurimoto, H., Sakai, Y., 2009. Yap1-regulated glutathione redox system curtails accumulation of formaldehyde and reactive oxygen species in methanol metabolism of Pichia pastoris. Eukaryotic cell 8, 540-549.

Zafarullah, M., Li, W.Q., Sylvester, J., Ahmad, M., 2003. Molecular mechanisms of N-acetylcysteine actions. Cellular and molecular life sciences : CMLS 60, 6-20.

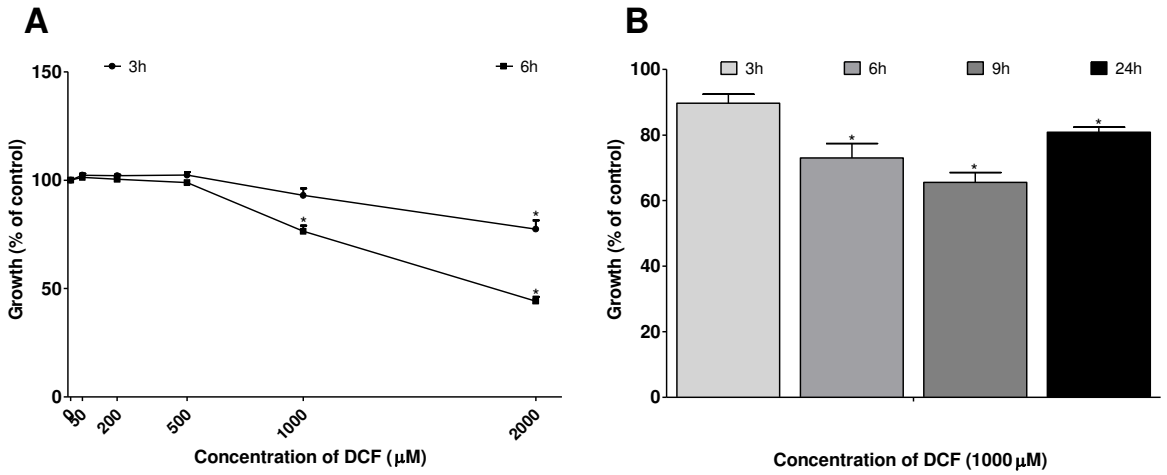

Figure 1: Dose- and time-dependent toxic response of DCF on BY4741 growth. Cells were treated with different DCF concentrations and growth was assessed by OD measurement at 3, 6, 9 and 24h. Results are expressed as OD% of the control untreated cells. They correspond to means±SD of at least three independent experiments. *Statistically significant difference ($p<0.05$) with respect to untreated cells. **(A)** Cells were treated with different concentrations of DCF for 3 and 6h after dilution of pre-culture for 48h **(B)** Cells from colonies are treated with DCF (1000µM) for 3, 6, 9 and 24 hours without pre-culture.

Conditions / Time (h)	DCF (1000 µM)	NAC (5 mM)	Co-treatment (NAC + DCF)	Pre-treatment with NAC, then NAC + DCF	Pre-treatment with DCF, then NAC + DCF
3	89.7±11.3	92.7±0.8	89.3±2.1	68.2±10.7$^{*, \#}$	70.4±12.0$^{*, \#}$
6	73.0±18.2*	94.6±1.3	60.4±6.9*	23.7±4.0$^{*, \#, @}$	32.0±5.3$^{*, \#, @}$
9	65.6±12.6*	101.2±8.9	35.3±8.1$^{*, \#}$	17.1±1.5$^{*, \#}$	28.4±12.7$^{*, \#}$
24	80.9±6.2*	89.7±4.1	70.3±3.0*	32.0±10.1$^{*, \#, @}$	83.1±3.3$^{\&}$

Table 1: Interaction of NAC (5 mM) with DCF (1000 µM) toxic effect on BY4741 growth as a function of time (3, 6, 9 and 24 h) and of the sequence in which the drugs are added to the cells. Yeast colonies are diluted in YPD to an OD between 0.1 and 0.2 and treated. Pretreatment corresponds to addition of a drug 30 minutes before the second one. The results are expressed as percentage of the control-untreated cells and represent the means± SD of at least three independent experiments. $^{*}P<0.05$ compared with untreated cells. $^{\#}P<0.05$ compared to cells treated with DCF. $^{@}P<0.05$ compared with co-treatment. $^{\&}P<0.05$ compared with NAC pre-treatment.

Strain name	Mutant gene	DCF	NAC	LC	NAC+DCF	LC+DCF
BY4741	Wild type	65.6+12.6*	101.2±8.9	90.5±11.4	35.3±8.1$^{*,\#}$	71.7±4.3
Y02409	Pdr5	54.3±5.8$^{*,\$}$	100.6±2.7	96.1±3.6	6.1±6.5$^{*,\#,\$}$	32.3±10.4*
Y05933	Yor1	36.7±8.3$^{*,\$}$	ND	ND	ND	ND
Y01503	Bpt1	36.1±4.6$^{*,\$}$	ND	ND	ND	ND
Y04242	Pdr15	35.1±4.2$^{*,\$}$	ND	ND	ND	ND
Y00569	Yap1	75.9±10.4*	100.5±13.6	ND	39.2±21.8$^{*,\#}$	ND
Y00928	Vmr1	76.5±3.1*	98.5±0.7	97.1±3.4	15.2±7.7$^{*,\#,\$}$	65.1±7.5*
Y02770	Pdr12	78.8±3.0*	98.9±1.5	95.0±1.5	17.7±10.8$^{*,\#,\$}$	65.4±5.2*

Table 2: Effect of DCF and NAC-DCF interaction on growth of ABC-transporter mutant strains. Wild type and mutant strains of *Saccharomyces cerevisiae* were pre-cultured and then diluted to an OD between 0.1 and 0.2 and treated with DCF (1000µM) ± NAC (5mM) or ± L-cysteine (LC, 5 mM) for 9h and growth was assessed by OD measurement. The results are expressed as percentage of the control-untreated cells and represent the means± SD of at least three independent experiments. *P<0.05 compared with untreated cells; $^{\#}$P<0.05 compared to cells treated with DCF; $^{\$}$P<0.05 compared with BY4741. For genes abbreviations refer to the abbreviation list. ND, not determined.

Chapitre III. TNF-α potentialise l'augmentation de l'effet hépatotoxique mais non l'effet cholestatique du co-traitement diclofenac/trovafloxacine dans les cellules HepaRG

Résumé

Deux ou plusieurs médicaments sont habituellement co-préscrits pour le traitement de nombreuses maladies. Ainsi, les antibiotiques et les anti-inflammatoires sont souvent associés pour traiter les patients souffrant d'une infection bactérienne. Ces deux classes de médicaments comprennent de nombreuses molécules hépatotoxiques idiosyncratiques. Ce travail visait à examiner si un co-traitement avec deux de ces médicaments, le diclofénac (DCF), qui possède des propriétés anti-inflammatoires, et la trovafloxacine (TVX), un antibiotique de la classe des fluoroquinolones, en absence ou en présence d'un stress inflammatoire concomitant induit par co-addition de cytokines pro-inflammatoires, aggravent les lésions hépatocytaires par rapport à l'addition de chaque médicament séparément, en utilisant les cellules humaines HepaRG différenciées. Nos résultats montrent que ces cellules, que ce soit après 24h ou 3 jours de traitement, étaient plus sensibles à un co-traitement avec DCF et TVX par rapport à l'ajout de chaque médicament séparément et que les effets cytotoxiques étaient aggravés par co-addition de TNF-α. Les effets cholestatiques des deux médicaments, caractérisés par une dilatation des canalicules biliaires et l'inhibition des transporteurs des acides biliaires, ont également été augmentés par le co-traitement sans aggravation en présence du TNF-α. Les effets cytotoxiques étaient associés à une production de ROS et l'induction des deux gènes associés, HO-1 et MnSOD ainsi que l'induction de gènes du stress enoplasmique. La potentialisation de la toxicité de DCF et TVX par TNF-α impliquait l'activation de la caspase 8 par la voie apoptotique extrinsèque. Contrairement à TVX, la lévofloxacine, une fluoroquinolone non-hépatotoxique, n'aggravait pas significativement la toxicité de DCF, même en présence de TNF-α.

En résumé, nos données montrent que les effets hépatotoxiques et cholestatiques du DCF et TVX étaient augmentés par un traitement combiné et que la co-addition de TNF-α potentialisait seulement la cytotoxicité. Ces données apportent de nouvelles informations sur les interactions médicamenteuses et l'influence d'un stress inflammatoire dans la survenue de l'hépatotoxicité induite par les médicaments.

TNF-α potentiates enhanced hepatotoxic but not cholestatic effects of diclofenac and trovafloxacin co-treatments in HepaRG cells

Abstract

Two or more drugs are usually co-prescribed for the treatment of many diseases. Thus, antibiotics and anti-inflammatory drugs are frequently associated to treat patients suffering from bacterial infection. These two drug classes include many idiosyncratic hepatotoxic molecules. This work aimed to investigate whether a co-treatment with the two idiosyncratic hepatotoxic drugs, diclofenac (DCF), that possesses anti-inflammatory properties, and the fluoroquinolone antibiotic trovafloxacin (TVX), in the absence or presence of a concomitant inflammatory stress induced by co-addition of pro-inflammatory cytokines, aggravated hepatocyte damage compared to separate addition of either drug, using differentiated human HepaRG cells. Our results showed that after either 24h or 3 days HepaRG cells were more sensitive to a co-treatment with DCF and TVX than to either drug added separately and that cytotoxic effects were aggravated by co-addition of TNF-α. Cholestatic effects of the two drugs, typified by dilation of bile canaliculi and inhibition of bile acids transporters, were also enhanced by a co-treatment without further aggravation by TNF-α. Cytotoxicity effects were associated with ROS generation and induction of the two related genes HO-1 and MnSOD. TNF-α potentiation of DCF and TVX toxicity involved activation of caspase 8 through the extrinsic apoptotic pathway. Contrary to TVX, levofloxacin, a non-hepatotoxic fluoroquinolone, did not significantly aggravate DCF toxicity, even in the presence of TNF-α.

Together, our data demonstrate that hepatotoxic and cholestatic effects of DCF and TVX were enhanced in a combined treatment and that co-addition of TNF-α potentiated only cytotoxicity. These data bring further insights in drug-drug interactions and the influence of an inflammatory stress in the occurrence of drug-induced hepatotoxicity.

Keywords: Drugs, cytotoxicity, cholestasis, hepatocytes, inflammatory stress, oxidative stress

Abbreviations: DCF, diclofenac; LVX, levofloxacin; TVX, trovafloxacin; ROS, reactive oxidative species; JNK, jun terminal N-kinase; BSEP, bile salt export pump; NTCP, Na++ -dependent taurocholate cotransporting polypeptide; MRP2, multidrug associated protein 2; DILI,

drug-induced liver injury; ER, endoplasmic reticulum; MTT, methylthiazoltetrazolium; H2-DCFDA, 2',7'-dichlorodihydrofluorescein; NAC, N-acetyl-cysteine; RT-qPCR, real-time quantitative polymerase chain reaction; TNF-α, tumor necrosis factor α; IL-6, interleukin-6; IL-1β, interleukin-1β; CYP450, cytochrome P450; HO1, heme oxygenase 1; MnSOD, manganese superoxide dismutase; CAR, constitutive androstane receptor; PXR, pregnane X receptor; MRP3, multidrug resistance-associated protein 3; Ac-DEVD-AMC, N-Acetyl-Asp-Glu-Val-Asp-7-amido-4-methylcoumarin; AC-LEHD-AMC, Ac-Leu-Glu-His-Asp-7-Amino-4-methylcoumarin; AC-IETD-AMC, Ac-Ile-Glu-Thr-Asp-7-Amino-4-methylcoumarin; CRP, C-reactive protein; IL-8, interleukin-8; PBS, phosphate buffered saline.

Introduction

Drug-induced liver injury (DILI) accounts for more than 50% of acute liver failure cases (Ostapowicz et al., 2002). Although many of these cases are attributable to acetaminophen overdose, 13-17% are due to idiosyncratic hepatotoxicity (Bjornsson and Olsson, 2006), for which formation of reactive metabolites, generation of oxidative stress, and inflammatory or immune response are recognized to be potential critical determinants (Uetrecht, 2006).

Two or more drugs are frequently prescribed together for the treatment of various diseases (Actis et al., 2014). For instance, antibiotics and anti-inflammatory drugs are frequently co-prescribed for the treatment of bacterial infection; it has been calculated that 40.2 and 12.7% of the patients take diclofenac (DCF) as an anti-inflammatory drug and quinolones as an antibiotic respectively (Tayem et al., 2013).

The non-steroidal anti-inflammatory drug DCF can cause rare cases of hepatocellular injury, cholestasis or mixed hepatocellular injury and cholestasis (Banks et al., 1995; Breen et al., 1986; Watanabe et al., 2007). Among the quinolone antibiotics the fluoroquinolone trovafloxacin (TVX) has been reported to have an incidence rate of adverse hepatic effects of 5.6/100000 prescriptions with 10% fatal cases, leading to its withdrawn from market (Qureshi et al., 2011); Like DCF, TVX can cause hepatocellular injury and cholestasis (Lazarczyk et al., 2001; Lucena et al., 2000), suggesting that co-administration of these two drugs could potentiate their individual hepatotoxicity.

Several studies have shown that an inflammatory stress aggravated hepatotoxicity induced by DCF and TVX, using *in vivo* animal models and liver cell cultures (Al-Attrache et al., 2016; Beggs et al., 2014; Deng et al., 2006; Shaw et al., 2007). However, most *in vitro* studies have been performed with the HepG2 cell line (Beggs et al., 2015; Fredriksson et al., 2011) which is known to exhibit very low phase 1 and phase 2 drug metabolizing enzyme activities (Westerink and Schoonen, 2007a, b), making questionable its use as representative of mature human hepatocytes. Recently, we demonstrated that metabolically competent HepaRG hepatocytes were less sensitive to DCF than their undifferentiated counterparts and HepG2 cells (Al-Attrache et al., 2016).

The aim of the present work was to determine whether a co-treatment with DCF and the fluoroquinolone antibiotic TVX led to an aggravation of their individual toxic effects in the presence or absence of TNF-α, using well differentiated human HepaRG cells as a cell model system. Another drug from the same family as TVX, levofloxacin (LVX), that is generally considered a safe antibiotic and non hepatotoxic was used as a control compound (Cosgrove et al., 2009). Our results showed that (i) in combination DCF-TVX aggravated their individual hepatotoxicity; (ii) in the presence of pro-inflammatory cytokines their toxicity was further enhanced; (iii) Except expression of some genes, their cholestatic effects were also potentiated by a co-treatment without any additional effect of the pro-inflammatory cytokines.

Materials and Methods

Chemicals and Reagents

Diclofenac sodium salt (DCF), trovafloxacin mesylate (TVX), levofloxacin (LVX), MTT (methylthiazoltetrazolium), DTT (dithiothreitol), AC-DEVD-AMC (N-Acetyl-Asp-Glu-Val-Asp-7-amido-4-Methylcoumarin), NAC (N-acetyl-cysteine), testosterone and 6β-hydroxytestosterone were purchased from Sigma Aldrich (St. Quentin Fallavier, France). H2-DCFDA (2',7'-dichlorodihydrofluorescein) from Invitrogen Molecular probe (Cergy-Pontoise, France) and AC-LEHD-AMC (Ac-Leu-Glu-His-Asp-7-Amino-4-methylcoumarin) and AC-IETD-AMC (Ac-Ile-Glu-Thr-Asp-7-Amino-4-methylcoumarin) from Enzo life sciences (Lyon, France). TNF-α, IL-6 and IL-1β were provided by Promocell (Nuremberg, Germany). SP600125 (ab120065) was obtained from Abcam, (Cambridge, UK). Phospho-SAPK/JNK

(Thr183/Tyr185) (Antibody #9251) and SAPK/JNK Antibody (Antibody #9252) from Cell signaling (Danvers, MA,United states). Human C-reactive protein (CRP) and CXCL8/IL-8 DuoSet kits were from R&D (Abingdon, United Kingdom). z-LEHD-fmk was purchased from BD Biosciences (Le Pont de Claix, France) and etanercept was from Amgen (Thousand Oaks, CA, USA).

Cell cultures and treatments

Cell cultures

HepaRG cells were seeded at a density of 2.6×10^4 cells/cm^2 in Williams'E medium supplemented with 10 % Hyclone® fetal bovine serum (HFBS) (Thermo Scientific, San Jose, USA), 100 U/mL penicillin, 100 mg/mL streptomycin, 5 µg/mL insulin, 2 mM glutamine, and 50 µM hydrocortisone hemisuccinate. After 2 weeks, they were shifted to the same medium supplemented with 1.7% dimethyl sulfoxide for further 2 weeks. At that time, cultures contained hepatocyte-like and progenitors/primitive biliary-like cells in about an equal proportion (Cerec et al., 2007).

Treatments

Tested concentrations of the three pro-inflammatory cytokines (10ng/ml TNF-α, 10ng/ml IL-6 and 0.1ng/ml IL-1β for 24h treatment and 4ng/ml TNF-α for 3days treatment) were selected from previous studies (Al-Attrache et al., 2016; Bachour-El Azzi et al., 2014; Beggs et al., 2014; Fredriksson et al., 2014) and preliminary experiments on determination of caspase 3 activity and CRP secretion levels. Treatments of HepaRG cells were performed using a medium containing 2% HFBS and 1% dimethyl sulfoxide and lasted either 24h (a single treatment) or 3 days (treatments at days 0, 1 and 2). When the cells were co-treated with both drugs and cytokines, they were first exposed to the cytokines for 24h.

MTT assay

Cytotoxicity was evaluated using the MTT colorimetric assay. Briefly, cells were seeded in 24-well plates and treated with various concentrations of DCF (50, 100, 200, 250, 350, 500µM) and/or TVX (5, 20, 50, 100, 250, 500µM) and/or LVX (5, 20, 50, 100, 200, 400, 1000µM) +/- cytokines at the pre-selected concentrations. After medium removal, 500µL of serum-free

medium containing MTT (0.5 mg/ml) was added to each well and incubated for 2 hours at 37°C. The water-insoluble formazan was dissolved in 500µl dimethyl sulfoxide and absorbance was measured at 550 nm (Aninat et al., 2006).

Determination of caspase 3, 8 and 9 activities

After treatment with DCF ± TVX ± TNF-α; DCF ± LVX ± TNF-α or TVX ± cytokines, the cells were scrapped in the culture medium, then centrifuged, washed with PBS, dried and stored at -80ºC. Cell lysates were re-suspended in 70µl of 4-(2-hydroxyethyl)-1-piperazine ethane sulfonic acid supplemented with anti-phosphatase and anti-protease. Then, 40 µg of protein of each sample was placed in an opaque plate in triplicate and supplemented with caspase buffer (20 mM piperazine-1,4-bis-2-ethanesulfonic acid, pH 7.2, 100 mM NaCl, 10mM dithiotreitol, 1mM EDTA, 0.1% 3- [(3-cholamidopropyl dimethylammonio)-1-propanesulfonic acid] and 10% sucrose. Then 2 µl of DEVD-AMC, LEHD or IETD substrates for caspases 3, 9 and 8 respectively, were added. Fluorescence was measured at a wavelength between 380 and 420 nm for caspase 3 and between 405 and 465 nm for caspases 8 and 9 (Dumont et al., 2010; Maianski et al., 2004).

Measurement of CYP3A4 activity

After treatment with DCF ± TVX ± TNF-α or DCF ± LVX ± TNF-α, cells were washed with PBS and incubated at 37ºC with testosterone dissolved in Williams' medium without phenol red. After 2h medium was collected and CYP3A4 activity was measured using a high performance liquid chromatography equipment (Agilent 1100 series high performance liquid chromatograph equipped with an autosampler and Agilent 1100 series fluorescence and UV detectors) with two solvents, acetic acid (0.1%) and acetonitrile as previously (Aninat et al., 2006).

Real-Time Quantitative Polymerase Chain Reaction (RT-qPCR) analysis

Total RNA was extracted from 10^6 HepaRG cells with the SV total RNA isolation system (Promega, Charbonnieres-les-Bains, France). RNAs were reverse-transcribed into cDNA and RT-qPCR was performed using a SYBR Green mix. Primer sequences are listed in Table 1.

Gene	Name	Forward primer	Reverse primer
GAPDH	Glycéraldéhyde-3-Phosphate déshydrogénase	TTCACCACCATGGAGAAGGC	GGCATGGACTGTGGTCATGA
CAR	constitutive androstane receptor	TGATCAGCTGCAAGAGGAGA	AGGCCTAGCAACTTCGCATA
PXR	pregnane X receptor	CCAGGACATACACCCCTTTG	CTACCTGTGATGCCGAACAA
FXR	farnesoid X receptor	AGGTAGCAGAGATGCCTGTAACAA	CACAGCTCATCCCCTTTGATC
CYP3A4	cytochrome P450 3A4	CTTCATCCAATGGACTGCATAAAT	TCCCAAGTATAACACTCTACACAGACAA
CYP2C9	cytochrome P450 2C9	GGACAGAGACGACAAGCACA	AATGGACATGAACAACCCTCA
CYP1A2	Cytochrome P450 1A2	TGGAGACCTTCCGACACTCCT	CGTTGTGTCCCTTGTTGTGC
CYP8B1	Cytochrome P450 8B1	TGGAGAAAGCTGGCAAAGTT	TGGTTCCCCTTTGACTTCAC
CYP7A1	Cytochrome P450 7A1	CTGTGGCAAACACTATTCCAACTA	TTGACCTGTTGACTGCAGCAA
CYP27A1	Cytochrome P450 27A1	GGCCCTAAGTAGGACATCCA	AGCTGCGCTTCTTCTTTCAG
SULT2A1	Sulfotransferase 2A1	CCAGTTATTCCCCAAGTCTTTCT	AAACATCTCTGGGATTTCTCATGAG
HO-1	heme oxygenase 1	ACTTTCAGAAGGGCCAGGT	TTGTTGCGCTCAATCTCCT
MnSOD	manganese superoxide dismutase	GGGTTGGCTTGGTTTCAATA	CTGATTTGGACAAGCAGCAA
ATF4	Activating Transcription Factor 4	TGGCATGGTTTCCAGGTCATCT	CCAACAACAGCAAGGAGGATGC
ATF6	Activating Transcription Factor 6	CTGCACCCACTAAAGGCCAGA	GAGGGCAGAACTCCAGGTGCT
CHOP	C/Ebp-Homologous protein	ATGGCAGCTGAGTCATT	AGAAGCAGGGTCAAGAGTGGT
GRP78	Glucose Regulated Protein,78KD	GTTCTTGCCGTTCAAGGTGG	TGGTACAGTAACAACTGCATG
CRP	C-Reactive Protein	GAACTTTCAGCCGAATACATCTTTT	CCTTCCTCGACATGTCTGTCT
IL-8	Interleukin8	ATGACTTCCAAGCTGGCCGTGGCT	TCTCAGCCCTCTTCAAAAACTTCTC
BSEP	bile salt export pump	TGATCCTGATCAAGGGAAGG	TGGTTCCTGGGAAACAATTC
NTCP	Na+-dependent taurocholic cotransporting polypeptide	GGGACATGAACCTCAGCATT	CGTTTGGATTTGAGGACGAT
MDR1	multidrug resistance protein 1	GCCAAAGCCAAAATATCAGC	TTCCAATGTGTTCGGCATTA

Gene	Name	Forward primer	Reverse primer
MDR3	multidrug resistance protein 3	GGCTTCAGCCGGCATTTTCA	GCAGCATCTGTGGCAAGTCT
MRP2	Multidrug resistance-associated protein 2	TGAGCAAGTTTGAAACGCACAT	AGCTCTTCTCCTGCCGTCTCT
MRP3	Multidrug resistance-associated protein 2	GTCCGCAGAATGGACTTGAT	TCACCACTTGGGGATCATTT
MRP4	multidrug resistance-associated protein 4	GCTCAGGTTGCCTATGTGCT	CGGTTACATTTCCTCCTCCA
OATP-B	organic anion-transporting polypeptide B	TGATTGGCTATGGGGCTATC	CATATCCTCAGGGCTGGTGT

Table 1: List of primers.

Determination of ROS generation

ROS generation was determined by the H_2-DCFDA assay. After treatment cells were incubated for 2 hours at 37°C with 2µM H_2-DCFDA and then washed with cold PBS, and scraped in potassium buffer (10 mM, pH 7.4) / methanol (v/v) complemented with Triton X-100 (0.1 %). Fluorescence intensity of cell lysates was determined by spectrofluorimetry using excitation/emission wavelengths of 498/520 nm (Sharanek et al., 2014).

Superoxide dismutase (SOD) activity

The activity of SOD was measured by using a kit assay (19160 SOD determination kit). After treatment cells were scrapped in the culture medium, centrifuged and washed with cold PBS and stored dried up at -80ºC. For activity measurement, the cells were re-suspended in PBS/Triton X-100 (1%) followed by sonication. Samples were distributed in 96 well plates and the substrate (WST) and dilution buffer were added. The absorbance was measured at 440nm.

ELISA assays

C-reactive protein (CRP) and interleukin-8 (IL-8) proteins were measured in cell supernatants using the CRP and CXCL8/IL-8 DuoSet kits, according to manufacturer's instructions. Briefly, supernatants were collected at appropriate time points and stored at -80°C until analysis; 96-well microplates were coated with capture antibody and incubated overnight. Samples and standards were diluted appropriately and added for 2 hours after a saturation step. Secondary antibody was added for 2 hours after washing. Streptavidin-horseradish peroxidase and its substrate were used

for the revelation step. Optical density was read at 450nm with wavelength correction. All steps were performed at room temperature (Bachour-El Azzi et al., 2014).

Western blotting

HepaRG cells were incubated in medium added or not with DCF ± TNF-α ± TVX ± LVX for 3 days. Then, protein level of CYP7A1, CYP27A1, CYP8B1, SULT2A1 and NTCP was evaluated as previously described (Sharanek et al., 2015). After treatment, cells were washed with cold PBS and re-suspended in cell lysis buffer and a protease inhibitor cocktail. Aliquots containing an equivalent total protein content, as determined by the Bradford's procedure with bovine serum albumin as the standard, were subjected to sodium dodecyl sulfate/12 % polyacrylamide gel electrophoresis, electrotransferred to immobilon-P membranes, and probed overnight with the primary antibodies already cited. After incubation with a rabbit secondary antibody, a chemiluminescence reagent, and Hyperfilm ECL, CYP7A1, CYP27A1, CYP8B1, SULT2A1, and NTCP bands were quantified by densitometry with Fusion-Capt software (Vilber Lourmat, Fusion FX7, France) and normalized compared to the HSC-70 protein.

Taurocholic acid efflux

To estimate bile salt export pump (BSEP) activity cells were first exposed to 43.4 nM [^{3}H]-TA for 30min, then washed with standard buffer and incubated with or without DCF ± TVX ± TNF-α; DCF ± LVX ± TNF-α or TVX ± TNF-α in a standard buffer containing Ca^{2+} and Mg^{2+}. After incubation for 2h cells were washed and then scrapped in 0.1N NaOH. The remaining radiolabeled substrate was measured through scintillation counting to determine TA efflux (Antherieu et al., 2013).

Na^+-dependent taurocholic cotransporting polypeptide activity (NTCP)

NTCP activity was estimated by determination of sodium-dependent intracellular accumulation of the radiolabeled [^{3}H]-TA substrate. Cells were treated with DCF ± TVX ± TNF-α or DCF ± LVX ± TNF-α or TVX ± TNF-α (pre-treated with TNF-α) followed by incubation with 43.3nM radiolabeled TA for 30min. Then, they were washed with PBS and lysed with 0.1N NaOH.

Accumulation of radiolabeled substrate was determined through scintillation counting (Antherieu et al., 2013).

Phase-contrast imaging

After cell treatment for different times (0, 2, 4, 6, 8 and 24h) images were taken using a phase-contrast microscope (Inverted microscope Zeiss axiovert 200M and Axiocam MRm).

CDF efflux determination

After treatment for 4h, 24h or 3days the cells were incubated with 3µM CDFDA, a substrate of the multidrug resistance-associated protein 2 (MRP2) for 20 min at 37ºC followed by washing with PBS and fluorescence was analyzed with an inverted microscope Zeiss (Bachour-El Azzi et al., 2014).

Statistical analysis

One-way ANOVA with Bonferroni's multiple comparison test (GraphPad Prism 5.00) was performed to compare data between DCF-, cytokine-, DCF/cytokine-treated cells, TVX-, TVX/cytokine-treated cells, LVX-, LVX/cytokine and control cultures. Each value corresponded to the mean ± standard deviation (SD) of at least three independent experiments. Data were considered significantly different when $p < 0.05$.

Results

Induction of inflammatory markers by the pro-inflammatory cytokines

Preliminary experiments were performed to verify the responsiveness of HepaRG cells to pro-inflammatory cytokines. Both transcript and secreted protein levels of CRP and IL-8 were

determined using RT-PCR and ELISA assays respectively after 24h- and 3day-exposure of the cells to the cytokines and/or tested drugs. As expected, a 24h-treatment with cytokines alone strongly enhanced secretion of both CRP and IL-8 in the culture medium, i.e. 13.07-, 79.23- and 43.42-fold for CRP and 41.81-, 72.86- and 57.73-fold for IL-8 after treatment with TNF-α, IL-6 and IL-1β respectively (Figure 1A and C). Transcripts levels showed similar profile changes; i.e.15.87-, 95.45- and 58.60-fold increase for CRP and 33.53-, 63.31- and 53.9-fold increase for IL-8 with TNF-α, IL-6 and IL-1β respectively after 24h (Figure 1B and D and Table 2). At 50μM TVX alone slightly diminished production of the two proteins; it also dose-dependently lowered increase of CRP and IL-8 mRNA and protein levels caused by either cytokines (Figure 1A, B, C and D)**.** LVX alone had no significant effect. The two inflammatory proteins were more lowered with DCF. In addition, when DCF was combined with TVX or LVX a limited further reduction in both transcript and secreted protein levels was found (Figure 1E and F).

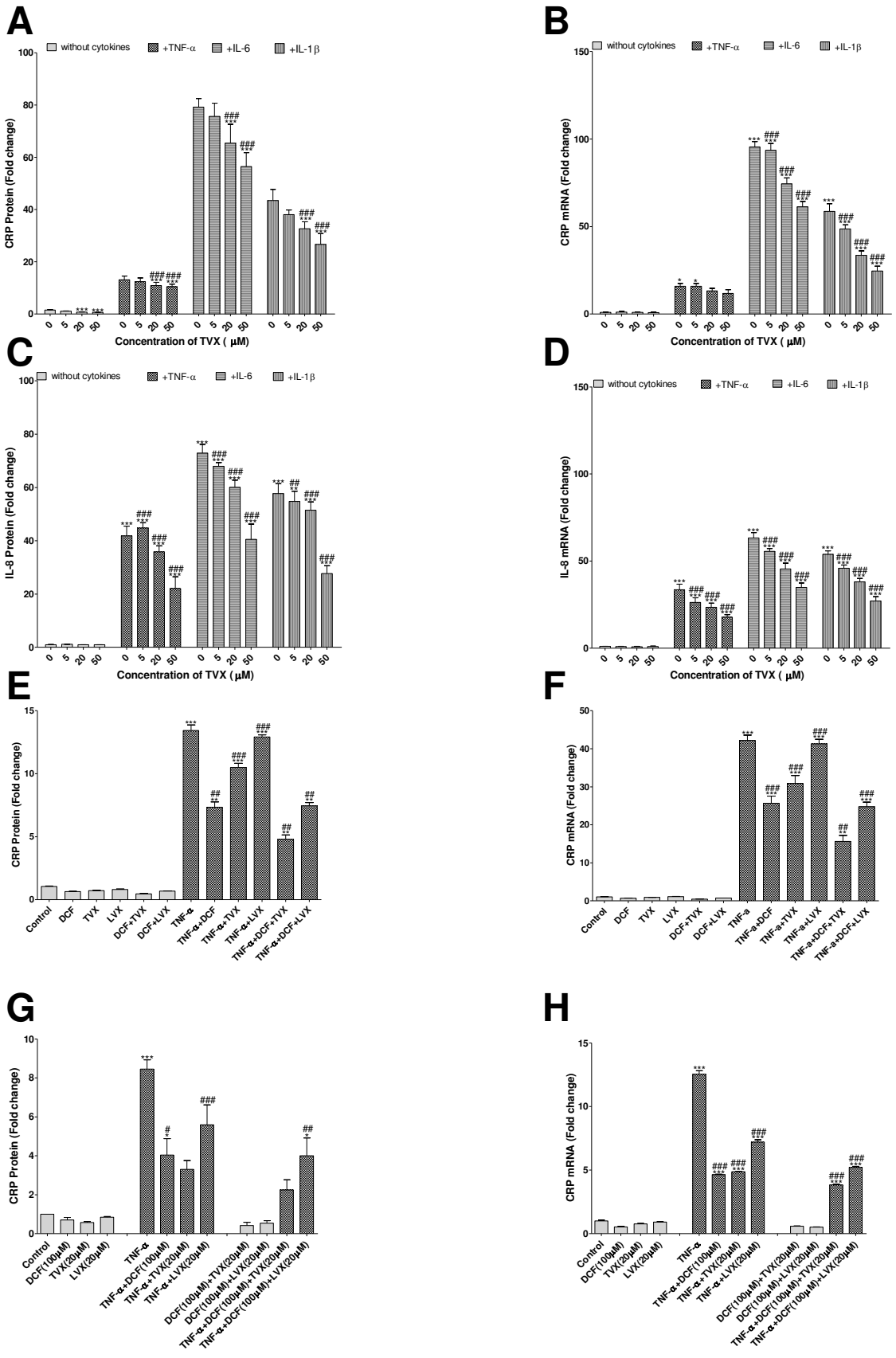
A
without cytokines
+TNF-α
+IL-6
+IL-1β
CRP Protein (Fold change)
Concentration of TVX (μM)
B
CRP mRNA (Fold change)
C
IL-8 Protein (Fold change)
D
IL-8 mRNA (Fold change)
E
CRP Protein (Fold change)
Control
DCF
TVX
LVX
DCF+TVX
DCF+LVX
TNF-α
TNF-α+DCF
TNF-α+TVX
TNF-α+LVX
TNF-α+DCF+TVX
TNF-α+DCF+LVX
F
CRP mRNA (Fold change)
G
CRP Protein (Fold change)
Control
DCF(100μM)
TVX(20μM)
LVX(20μM)
TNF-α
TNF-α+DCF(100μM)
TNF-α+TVX(20μM)
TNF-α+LVX(20μM)
DCF(100μM)+TVX(20μM)
DCF(100μM)+LVX(20μM)
TNF-α+DCF(100μM)+TVX(20μM)
TNF-α+DCF(100μM)+LVX(20μM)
H
CRP mRNA (Fold change)

Figure 1: Effects of DCF ± TVX ± cytokines on the inflammatory markers CRP and IL-8. Cells were treated with DCF, TVX, LVX, DCF-TVX or DCF-LVX with or without cytokines for (A, B, C, D, E and F) 24 h or (G and H) 3 days and protein and transcripts levels of CRP and IL-8 were measured. All results are expressed relative to the levels found in corresponding untreated cells, arbitrarily set at a value of 1. *P<0.05, **P<0.01 and ***P<0.001 compared with untreated cells, $^{\#}$P<0.05, $^{\#\#}$P<0.01 and $^{\#\#\#}$P<0.001 compared with cells treated with cytokine, DCF, TVX, LVX or the mix.

	TVX 5µM	TVX 20µM	TVX 50µM	TNF-α	TNF-α+TVX 5µM	TNF-α+TVX 20µM	TNF-α+TVX 50µM	IL-6	IL-6+TVX 5µM	IL-6+TVX 20µM	IL-6+TVX 50µM	IL-1β	IL-1β+TVX 5µM	IL-1β+TVX 20µM	IL-1β+TVX 50µM
Nuclear receptors															
FXR	1.12±0.24	0.96±0.09	0.71±0.03	0.53±0.06	0.61±0.13a	0.41±0.04*	0.38±0.08**	0.22±0.04***	0.15±0.04***c	0.11±0.03**a	0.08±0.03**	0.30±0.05**	0.25±0.03**c	0.16±0.05**a	0.11±0.03**a
PXR	1.03±0.09	0.71±0.16	0.64±0.11	0.38±0.07***	0.33±0.09**c	0.18±0.05**c	0.17±0.04***a	0.22±0.04***	0.18±0.03**c	0.09±0.03**c	0.07±0.02**c	0.29±0.04***	0.25±0.06**c	0.13±0.04**c	0.08±0.03**b
CAR	1.16±0.23	0.64±0.07	0.60±0.05*	0.45±0.06	0.23±0.03**b	0.20±0.12**	0.18±0.04***	0.26±0.05**	0.19±0.03**c	0.12±0.04**	0.07±0.02**	0.37±0.05*	0.20±0.04**b	0.14±0.04**	0.09±0.03**
Metabolizing enzymes (Phases I and II)															
CYP3A4	1.08±0.16	0.83±0.07	0.63±0.10	0.42±0.10	0.32±0.03	0.22±0.02	0.16±0.05*	0.22±0.03	0.16±0.04*a	0.11±0.03*	0.07±0.02**	0.32±0.03	0.25±0.04a	0.15±0.05*	0.11±0.04*
CYP2C9	1.13±0.09	0.89±0.04	0.68±0.07	0.73±0.11	0.82±0.06	0.68±0.04	0.48±0.07	0.49±0.06	0.62±0.03	0.35±0.04	0.20±0.06	0.60±0.07	0.77±0.05	0.51±0.06	0.32±0.04
CYP2B6	1.04±0.12	0.69±0.25	0.65±0.09	0.69±0.05	0.80±0.10	0.59±0.10	0.34±0.21	0.32±0.07*	0.22±0.07*b	0.14±0.04**	0.09±0.05**	0.35±0.11	0.38±0.05	0.26±0.06*	0.20±0.11*
CYP1A2	1.31±0.06	1.25±0.09	1.53±0.1*	0.81±0.07	1.02±0.04	0.83±0.02	0.76±0.01*	0.72±0.03*	0.84±0.05	0.67±0.02**	0.52±0.01***	0.69±0.04**	0.81±0.04	0.62±0.03**	0.49±0.06***
CYP8B1	1.12±0.08	0.9±0.1	0.73±0.02**	0.77±0.13*	0.98±0.06	0.75±0.01**	0.61±0.03***	0.81±0.05*	1.02±0.1	0.82±0.01*	0.65±0.03***	0.72±0.06*	0.88±0.02*	0.65±0.05**	0.54±0.03***
CYP7A1	1.34±0.2	1.04±0.08	0.69±0.08	0.83±0.07	0.91±0.09	0.7±0.1	0.52±0.05	0.75±0.06	0.89±0.12	0.67±0.03	0.41±0.02	0.79±0.09	0.95±0.1	0.83±0.18	0.57±0.12
CYP27A1	1.17±0.31	0.96±0.11	0.80±0.14	0.85±0.12	1.02±0.16	0.86±0.06	0.67±0.08	0.79±0.13	0.96±0.06	0.78±0.09	0.61±0.11	0.68±0.12	0.87±0.08	0.63±0.05	0.46±0.07
SULT2A1	1.23±0.18	1.36±0.15	1.12±0.31	0.75±0.15	1.22±0.13	0.68±0.09	0.46±0.04	0.86±0.10	1.12±0.23	1.04±0.31	0.78±0.09	0.73±0.07	1.11±0.13	0.59±0.03	0.38±0.01

	TVX 5µM	TVX 20µM	TVX 50µM	TNF-α	TNF-α+TVX 5µM	TNF-α+TVX 20µM	TNF-α+TVX 50µM	IL-6	IL-6+TVX 5µM	IL-6+TVX 20µM	IL-6+TVX 50µM	IL-1β	IL-1β+TVX 5µM	IL-1β+TVX 20µM	IL-1β+TVX 50µM
GSTA1/2	1.13±0.02	0.91±0.05	0.74±0.07	0.83±0.03	0.85±0.05	0.63±0.04	0.41±0.07	0.72±0.07	0.72±0.02	0.46±0.01	0.37±0.04	0.76±0.02	0.78±0.04	0.58±0.03	0.32±0.06
GSTM1/2	1.12±0.11	1.06±0.09	0.69±0.04	0.85±0.03	0.90±0.07	0.60±0.01	0.30±0.03	0.73±0.05	0.76±0.08	0.43±0.02	0.23±0.06	0.71±0.04	0.73±0.03	0.36±0.09	0.18±0.05
UGT1A1	1.13±0.09	1.61±0.08	0.80±0.02	0.75±0.05	0.73±0.08	0.83±0.06	0.42±0.01	0.51±0.1	0.57±0.06	0.61±0.04	0.26±0.03	0.43±0.08	0.48±0.07	0.52±0.05	0.37±0.02
UGT1A3	1.04±0.13	1.53±0.12	0.85±0.06	0.62±0.04	0.61±0.02	0.84±0.09	0.32±0.06	0.37±0.01	0.40±0.04	0.57±0.02	0.13±0.02	0.42±0.05	0.50±0.03	0.39±0.04	0.27±0.02
Bile acid transporters															
BSEP	1.30±0.09	0.85±0.07	0.50±0.34	0.74±0.06	0.77±0.21c	0.52±0.14***	0.26±0.09***c	0.45±0.12***	0.32±0.05***c	0.19±0.03***c	0.12±0.02***	0.61±0.06	0.38±0.05***c	0.27±0.03***c	0.18±0.06***
NTCP	1.12±0.08	0.80±0.17	0.70±0.09	0.68±0.07	0.95±0.12	0.25±0.07***c	0.20±0.08***c	0.46±0.07***	0.34±0.07***c	0.21±0.06***c	0.19±0.03***c	0.58±0.04**	0.45±0.06***c	0.31±0.08***c	0.27±0.04***b
OATP-B	1.28±0.12	0.92±0.08	0.65±0.07	0.76±0.12	0.89±0.07	0.68±0.09	0.51±0.03	0.73±0.1	0.92±0.14	0.78±0.03	0.42±0.09	0.7±0.16	0.95±0.1	0.63±0.01	0.31±0.02
MDR1	1.16±0.09	1.28±0.12	1.67±0.1	0.78±0.06	1.03±0.13	1.17±0.16	1.21±0.07	0.65±0.02	1.12±0.1	1.13±0.04	1.02±0.07	0.68±0.05	0.89±0.07	0.99±0.09	0.92±0.05
MDR3	1.33±0.1	1.05±0.09	0.72±0.06	0.82±0.02	0.96±0.11	0.69±0.02	0.55±0.1	0.69±0.08	1.05±0.09	0.76±0.01	0.42±0.06	0.73±0.09	1.12±0.11	0.7±0.03	0.48±0.09
MRP2	1.06±0.07	1.21±0.23	0.78±0.08	0.75±0.11	1.14±0.1	0.79±0.04	0.49±0.06	0.72±0.06	0.94±0.07	0.73±0.06	0.38±0.02	0.65±0.02	1.25±0.08	0.68±0.09	0.33±0.04
MRP3	1.23±0.14	0.88±0.06	0.69±0.12	0.69±0.04	0.99±0.15	0.65±0.06	0.37±0.09	0.61±0.12	1.11±0.23	0.61±0.08	0.32±0.06	0.71±0.02	0.96±0.09	0.69±0.02	0.41±0.07
MRP4	1.19±0.22	1.32±0.13	1.89±0.19	1.22±0.15	1.19±0.09	1.92±0.1	2.42±0.21	1.36±0.2	1.38±0.13	2.03±0.17	2.63±0.13	1.42±0.1	1.53±0.06	2.24±0.19	2.71±0.26

	TVX 5µM	TVX 20µM	TVX 50µM	TNF-α	TNF-α+TVX 5µM	TNF-α+TVX 20µM	TNF-α+TVX 50µM	IL-6	IL-6+TVX 5µM	IL-6+TVX 20µM	IL-6+TVX 50µM	IL-1β	IL-1β+TVX	TVX 5µM	TVX 20µM
Markers of oxidative stress															
HO-1	1.12±0.09	1.51±0.28	2.08±0.23	1.26±0.15	1.55±0.22	2.16±0.31*	3.22±0.40***a	1.87±0.29	3.09±0.43***c	4.57±0.43***c	6.16±0.73***c	1.41±0.29	2.23±0.32*	3.63±0.37***c	4.72±0.37***c
MnSOD	1.09±0.10	1.37±0.26	2.13±0.25**	1.51±0.29	1.96±0.35	3.03±0.16**	4.02±0.34**	2.44±0.29***	3.49±0.25**	4.56±0.36**	6.34±0.51**	1.73±0.18	2.61±0.46**	3.50±0.37**	4.47±0.23**
Nrf2	1.05±0.08	1.29±0.10	1.95±0.12	1.32±0.09	1.84±0.13	2.56±0.11	3.62±0.09	1.92±0.11	3.58±0.23	4.12±0.19	5.89±0.12	1.56±0.14	2.55±0.16	3.12±0.10	4.63±0.22
Markers of ER stress															
ATF4	1.23±0.12	1.12±0.16	1.83±0.06	1.29±0.10	1.15±0.08	1.56±0.11	3.03±0.18	1.05±0.14	1.16±0.04	2.87±0.11	4.12±0.16	1.28±0.10	1.12±0.13	3.01±0.21	4.52±0.19
ATF6	1.18±0.09	1.26±0.15	1.72±0.04	1.17±0.09	1.22±0.13	2.01±0.04	2.96±0.21	1.29±0.05	1.25±0.17	2.19±0.08	3.36±0.21	1.33±0.05	1.37±0.09	2.64±0.08	4.19±0.15
CHOP	1.35±0.05	1.34±0.09	2.25±0.08	1.23±0.12	1.13±0.07	2.51±0.14	3.62±0.17	1.16±0.09	1.29±0.12	3.72±0.22	5.69±0.25	1.12±0.02	1.20±0.15	2.86±0.14	5.97±0.26
GRP78	1.31±0.17	1.47±0.04	1.79±0.07	1.12±0.06	1.27±0.11	1.61±0.06	2.57±0.13	1.19±0.07	1.11±0.09	2.59±0.13	3.16±0.12	1.25±0.07	1.16±0.06	1.79±0.11	2.91±0.21
Markers of inflammation															
CRP	1.09±0.64	0.94±0.39	0.83±0.46	15.87±2.81*	15.84±2.71*a	13.24±2.42	11.77±3.70	95.45±5.36***	93.51±6.78***c	74.35±5.83***c	61.27±5.30***c	58.60±7.64***	48.57±4.07***c	33.56±4.22***c	24.63±4.69***c
IL-8	0.89±0.37	0.77±0.47	0.97±0.45	33.53±5.63***	26.34±4.46***c	23.46±4.11***c	17.83±2.46***c	63.31±5.20***	55.62±2.83***c	45.49±5.74***c	34.86±4.47***c	53.90±3.41***	45.87±3.23***c	38.06±3.43***c	27.07±4.33***c

Table 2: Effects of TVX ± cytokines (TNF-α, IL-6 and IL-1β) on expression of mRNAs measured by RT-PCR encoding genes related to oxidative stress, inflammation, hepatobiliary transporters, nuclear receptors, phase I and phase II metabolizing enzymes in HepaRG cells (24 h). All results are expressed relative to the levels found in corresponding untreated cells, arbitrarily set at a value of 1. *P<0.05, **P<0.01 and ***P<0.001 compared with untreated cells, #P<0.05, ##P<0.01 and ###P<0.001 compared with cells treated with cytokine or TVX individually. a:#; b:##; c:###.

A 3-day exposure of HepaRG cell cultures to 4ng/ml TNF-α led to a 8.45-fold increase in CRP release, that fell to around 73% in cultures exposed simultaneously to 100μM DCF or 20μM TVX and to around 33.85% in cultures exposed to LVX. Similar effects were evidenced by measuring CRP mRNA levels. When DCF was combined with TVX or LVX a further limited reduction in both transcript and secreted protein levels was observed (Figure 1G and H andTable 3).

	DCF 100µM	TVX 20µM	LVX 20µM	TNF-α	TNF-α+DCF 100µM	TNF-α+TVX 20µM	TNF-α+LVX 20µM	DCF 100 +TVX 20	DCF 100 +LVX 20	TNF-α+DCF100+TVX20	TNF-α+DCF100+LVX20
Nuclear receptors											
CAR	0.75±0.2	0.64±0.07	0.62±0.08	0.45±0.06	0.37±0.05	0.41±0.04	0.46±0.08	0.55±0.03	0.72±0.11	0.28±0.05	0.41±0.09
PXR	0.85±0.07	0.71±0.16	0.92±0.04	0.38±0.07	0.33±0.06	0.18±0.05	0.42±0.07	0.76±0.05	0.83±0.09	0.16±0.02	0.35±0.19
FXR	1.23±0.37	0.96±0.09	0.86±0.06	0.53±0.06	0.29±0.03	0.41±0.04	0.55±0.04	0.92±0.10	1.02±0.13	0.52±0.07	0.62±0.11
Metabolizing enzymes (Phases I and II)											
CYP3A4	0.86±0.08	0.83±0.07	0.56±0.09	0.42±0.10	0.38±0.02	0.22±0.02	0.48±0.05	0.73±0.07	1.06±0.10	0.51±0.09	0.62±0.12
CYP2C9	0.89±0.24	0.89±0.04	0.79±0.07	0.73±0.11	0.56±0.11	0.68±0.04	0.71±0.11	0.82±0.09	1.08±0.07	0.59±0.10	0.63±0.09
CYP1A2	0.92±0.13	1.25±0.09	0.82±0.13	0.81±0.07	0.75±0.16	0.83±0.02	0.85±0.04	1.12±0.04	0.68±0.02	0.69±0.03	0.72±0.06
CYP8B1	0.88±0.08	0.9±0.1	0.63±0.05	0.77±0.13	0.63±0.08	0.75±0.01	0.72±0.03	0.75±0.06	0.76±0.08	0.58±0.09	0.65±0.12
CYP7A1	1.10±0.13	1.04±0.08	1.08±0.07	0.83±0.07	0.86±0.10	0.7±0.1	1.21±0.12	0.92±0.17	1.03±0.05	1.85±0.18	1.56±0.19
CYP27A1	1.12±0.17	0.96±0.11	0.98±0.02	0.85±0.12	0.82±0.04	0.86±0.06	1.35±0.14	0.86±0.06	0.8±0.02	1.12±0.13	1.03±0.11
SULT2A1	1.08±0.14	1.36±0.15	0.93±0.06	0.75±0.15	0.79±0.02	0.68±0.09	0.69±0.05	0.94±0.12	0.86±0.09	0.68±0.06	0.57±0.08
GSTA1/2	0.96±0.12	0.91±0.05	1.23±0.08	0.83±0.03	0.78±0.05	0.63±0.04	0.85±0.11	0.84±0.06	1.13±0.12	0.62±0.11	0.72±0.02
GSTM1/2	1.13±0.09	1.06±0.09	1.12±0.11	0.85±0.03	0.82±0.06	0.60±0.01	0.86±0.06	0.82±0.09	1.07±0.06	0.58±0.07	0.81±0.07
UGT1A1	0.96±0.15	1.61±0.08	1.19±0.04	0.75±0.05	0.69±0.02	0.83±0.06	0.78±0.09	0.96±0.10	1.12±0.14	0.78±0.04	0.85±0.01
UGT1A3	1.12±0.11	1.53±0.12	1.08±0.10	0.62±0.04	0.58±0.04	0.84±0.09	0.83±0.11	0.92±0.11	1.22±0.13	0.79±0.06	0.88±0.12

	DCF 100µM	TVX 20µM	LVX 20µM	TNF-α	TNF-α+DCF 100µM	TNF-α+TVX 20µM	TNF-α+LVX 20µM	DCF 100 +TVX 20	DCF 100 +LVX 20	TNF-α+DCF100+TVX20	TNF-α+DCF100+LVX20
Bile acid transporters											
BSEP	0.75±0.1	0.85±0.07	0.79±0.12	0.74±0.06	0.47±0.17	0.52±0.14	0.62±0.07	0.55±0.03	0.51±0.03	0.38±0.06	0.42±0.09
NTCP	0.79±0.09	0.80±0.17	0.69±0.02	0.68±0.07	0.47±0.14	0.25±0.07	0.87±0.13	0.48±0.06	0.70±0.09	0.39±0.12	0.46±0.11
OATP-B	0.92±0.04	0.92±0.08	0.92±0.05	0.76±0.12	0.65±0.08	0.68±0.09	0.71±0.08	0.85±0.12	0.81±0.04	0.65±0.09	0.76±0.02
MDR1	1.12±0.08	1.28±0.12	1.06±0.08	0.78±0.06	0.68±0.02	1.17±0.16	0.72±0.05	1.23±0.09	1.11±0.13	1.56±0.20	1.32±0.04
MDR3	0.98±0.05	1.05±0.09	0.97±0.10	0.82±0.02	0.75±0.04	0.69±0.02	0.85±0.05	0.79±0.04	0.92±0.12	0.62±0.12	0.92±0.08
MRP2	1.27±0.07	1.21±0.23	1.03±0.11	0.75±0.11	0.85±0.02	0.79±0.04	0.82±0.14	1.09±0.13	1.12±0.10	1.12±0.07	1.03±0.13
MRP3	1.06±0.19	0.88±0.06	1.11±0.14	0.69±0.04	0.68±0.04	0.65±0.06	0.72±0.10	0.91±0.06	1.15±0.17	0.71±0.04	0.86±0.08
MRP4	0.93±0.09	1.32±0.13	1.24±0.12	1.22±0.15	1.28±0.10	1.92±0.1	1.33±0.11	1.03±0.12	1.03±0.04	1.81±0.13	1.42±0.03
Markers of oxidative stress											
HO-1	1.29±0.17	1.51±0.28	1.08±0.18	1.26±0.15	1.31±0.09	2.16±0.31	1.13±0.16	1.39±0.18	1.23±0.11	2.51±0.16	1.52±0.12
MnSOD	1.16±0.11	1.37±0.26	1.13±0.13	1.51±0.29	1.46±0.12	3.03±0.16	1.42±0.12	1.46±0.05	1.15±0.13	2.03±0.19	1.49±0.15
Nrf2	1.32±0.15	1.29±0.10	0.99±0.06	1.32±0.09	1.53±0.06	2.56±0.11	1.39±0.13	1.57±0.08	1.11±0.15	2.36±0.2	1.52±0.09
Markers of ER stress											
ATF4	1.59±0.20	1.12±0.16	1.09±0.12	1.29±0.10	2.86±0.28	1.56±0.11	1.32±0.13	1.83±0.14	1.61±0.11	2.48±0.17	1.68±0.09
ATF6	1.72±0.19	1.26±0.15	0.91±0.06	1.17±0.09	2.42±0.26	2.01±0.04	1.04±0.09	2.03±0.07	1.71±0.16	3.43±0.21	1.75±0.12

	DCF 100µM	TVX 20µM	LVX 20µM	TNF-α	TNF-α+DCF 100µM	TNF-α+TVX 20µM	TNF-α+LVX 20µM	DCF 100 +TVX 20	DCF 100 +LVX 20	TNF-α+DCF100+TVX20	TNF-α+DCF100+LVX20
CHOP	2±0.24	1.34±0.09	1.17±0.04	1.23±0.12	3.54±0.29	2.51±0.14	0.99±0.15	2.51±0.17	1.86±0.14	3.67±0.18	1.81±0.06
GRP78	1.39±0.16	1.47±0.04	1.13±0.01	1.12±0.06	2.17±0.29	1.61±0.06	1.11±0.11	1.69±0.06	1.45±0.07	2.44±0.15	1.53±0.18
Markers of inflammation											
CRP	1.09±0.38	0.94±0.39	1.16±0.14	15.87±2.81	23.27±5.57	13.24±2.42	14.13±0.68	0.81±0.02	0.68±0.09	2.71±0.16	12.31±0.23

Table 3: Effects of DCF ± TVX ± LVX ± TNF-α on expression of mRNAs measured by RT-PCR encoding genes related to oxidative stress, inflammation, hepatobiliary transporters, nuclear receptors, phase I and phase II metabolizing enzymes in HepaRG cells (24 h). *P<0.05, **P<0.01 and ***P<0.001 compared with untreated cells, #P<0.05, ##P<0.01 and ###P<0.001 compared with cells treated with cytokine, DCF, TVX, LVX or the mix. a:#; b:##; c:###.

	DCF 100µM	TVX 20µM	LVX 20µM	TNF-α	TNF-α+DCF 100µM	TNF-α+TVX 20µM	TNF-α+LVX 20µM	DCF 100 +TVX 20	DCF 100 +LVX 20	TNF-α+DCF100+TVX20	TNF-α+DCF100+LVX20
Nuclear receptors											
CAR	0.54±0.15**	0.25±0.03***	0.42±0.13***	0.70±0.02***	0.51±0.16***	0.36±0.12***	0.44±0.06***	0.25±0.09***	0.43±0.13***	0.25±0.08***	0.45±0.13***
PXR	0.74±0.12	0.77±0.08	0.79±0.09	0.71±0.12	0.69±0.14	0.58±0.03*	0.65±0.12	0.91±0.20	0.65±0.07	0.51±0.09**a	0.68±0.19
FXR	0.82±0.15	0.60±0.08	0.65±0.09	1.00+0.14	0.85±0.10	0.53±0.15*	0.90±0.20	0.86±0.20	0.82±0.06	0.69±0.04	1.03±0.23
Metabolizing enzymes (Phases I and II)											
CYP3A4	2.23±0.28***	0.66±0.09	0.26±0.11**	0.48±0.10	1.09±0.04c	0.56±0.12	0.25±0.07**	1.73±0.17**	2.11±0.25***	1.49±0.40	1.68±0.23*
CYP2C9	1.83±0.24***	0.64±0.08*	0.52±0.03***	0.64±0.04*	1.05±0.08c	0.40±0.03***	0.40±0.06***	1.22±0.11	0.96±0.06	0.61±0.06**c	0.69±0.13
CYP1A2	0.33±0.08***	1.36±0.16**	0.54±0.11***	0.73±0.02	0.31±0.02***	0.63±0.07**c	0.28±0.08***	1.02±0.05	0.39±0.05***	0.29±0.04***c	0.40±0.18***
CYP8B1	0.74±0.12	0.29±0.12***	0.45±0.15***	0.49±0.07***	0.42±0.08***	0.31±0.08***	0.34±0.05***	0.33±0.09***	0.46±0.06***	0.32±0.07***	0.44±0.20***
CYP7A1	1.28±0.62	0.80±0.09	0.92±0.14	2.43±0.35**	2.37±0.39**	3.43±0.48***c	2.91±0.38***c	1.01±0.38	0.84±0.09	2.54±0.29**b	2.27±0.57*b
CYP27A1	0.88±0.14	0.57±0.08	0.71±0.05	1.37±0.16	1.32±0.20	1.23±0.15b	1.55±0.34*c	0.56±0.07	0.64±0.06	1.43±0.18c	1.19±0.24a
SULT2A1	1.19±0.16	0.68±0.03**	0.80±0.05	0.83±0.05	0.83±0.10c	0.41±0.09***a	0.61±0.03***	0.54±0.05***	0.66±0.06***	0.40±0.04***	0.57±0.06***
GSTA1/2	1.12±0.11	0.79±0.05	1.16±0.13	0.82±0.07	0.65±0.03	0.61±0.07	0.85±0.09	0.58±0.01	1.02±0.10	0.41±0.08	0.79±0.05
GSTM1/2	1.03±0.10	0.72±0.04	1.06±0.09	0.79±0.05	0.60±0.01	0.58±0.04	0.82±0.03	0.52±0.05	0.98±0.03	0.39±0.04	0.83±0.03
UGT1A1	0.92±0.13	1.26±0.11	1.12±0.10	0.75±0.04	0.72±0.06	0.92±0.03	0.73±0.06	0.85±0.02	1.05±0.13	0.65±0.07	0.82±0.08
UGT1A3	0.98±0.08	1.32±0.12	1.25±0.14	0.77±0.02	0.69±0.08	0.84±0.07	0.79±0.04	0.88±0.07	1.10±0.15	0.71±0.02	0.89±0.04

	DCF 100µM	TVX 20µM	LVX 20µM	TNF-α	TNF-α+DCF 100µM	TNF-α+TVX 20µM	TNF-α+LVX 20µM	DCF 100 +TVX 20	DCF 100 +LVX 20	TNF-α+DCF100+TVX20	TNF-α+DCF100+LVX20
Bile acid Transporters											
BSEP	0.30±0.07***	0.27±0.08***	0.33±0.16***	0.34±0.08***	0.21±0.02***	0.21±0.02***	0.32±0.10***	0.15±0.00***	0.20±0.06***	0.16±0.02***	0.20±0.06***
NTCP	0.39±0.07***	0.28±0.06***	0.38±0.04***	0.51±0.12***	0.27±0.08***	0.39±0.08***	0.37±0.11***	0.28±0.03***	0.51±0.15***	0.35±0.09***	0.39±0.08***
OATP-B	0.73±0.09*	0.51±0.02***	0.64±0.08**	0.65±0.04**	0.62±0.05***	0.46±0.07***	0.49±0.03***	0.71±0.14*	0.70±0.06*	0.55±0.11***	0.73±0.14*
MDR1	1.16±0.12	0.76±0.07	0.90±0.14	0.79±0.08	1.61±0.30	0.93±0.12	0.70±0.09	1.53±0.15	1.41±0.24	1.86±0.47**	1.64±0.30
MDR3	0.88±0.18	0.44±0.04***	0.75±0.13	0.78±0.18	0.72±0.03	0.58±0.12**	0.68±0.09	0.58±0.07**	0.79±0.05	0.65±0.15	1.03±0.06
MRP2	1.59±0.29**	0.78±0.12	0.89±0.08	0.90±0.10	1.09±0.19a	0.64±0.09	0.88±0.22	1.18±0.19	1.37±0.07	1.18±0.06	1.20±0.11
MRP3	0.85±0.13	0.62±0.10	0.78±0.11	0.95±0.17	0.80±0.16	0.45±0.09**	0.83±0.17	0.71±0.14	0.83±0.14	0.74±0.08	0.90±0.17
MRP4	0.86±0.20	1.02±0.10	0.90±0.05	1.43±0.12	1.30±0.14	2.08±0.20***c	1.64±0.07**c	1.15±0.17	0.93±0.09	2.27±0.24***c	1.90±0.15***c
Markers of oxidative stress											
HO-1	1.36±0.37	1.81±0.11*	0.95±0.20	1.10±0.21	1.42±0.10	2.24±0.17***	1.02±0.26	1.88±0.23**	1.18±0.07	3.43±0.37***c	1.31±0.21
MnSOD	0.97±0.14	1.59±0.01**	0.73±0.09	1.34±0.10**	1.47±0.14*b	2.15±0.24***b	1.62±0.09***c	1.89±0.09***	1.01±0.19	3.23±0.14***c	2.06±0.16***c
Nrf2	1.09±0.11	1.92±0.13	0.86±0.07	1.12±0.06	1.52±0.03	1.96±0.10	1.43±0.05	2.02±0.11	1.22±0.08	3.56±0.16	1.63±0.10

	DCF 100µM	TVX 20µM	LVX 20µM	TNF-α	TNF-α+DCF 100µM	TNF-α+TVX 20µM	TNF-α+LVX 20µM	DCF 100 +TVX 20	DCF 100 +LVX 20	TNF-α+DCF100+TVX20	TNF-α+DCF100+LVX20
Markers Of ER stress											
ATF4	1.92±0.13	1.68±0.09	1.12±0.10	1.18±0.05	2.25±0.16	2.36±0.11	1.36±0.08	2.72±0.21	1.75±0.14	3.78±0.26	1.86±0.07
ATF6	1.84±0.09	1.52±0.04	0.96±0.08	1.25±0.10	2.46±0.12	1.88±0.04	1.15±0.02	2.91±0.15	1.82±0.09	4.12±0.23	1.97±0.19
CHOP	2.32±0.11	1.89±0.07	1.23±0.06	1.12±0.03	2.84±0.13	2.21±0.10	1.12±0.12	3.36±0.28	2.16±0.16	4.86±0.19	2.25±0.11
GRP78	1.73±0.15	1.76±0.08	1.09±0.03	1.19±0.05	1.92±0.07	2.01±0.12	1.24±0.14	2.87±0.17	1.62±0.05	3.59±0.21	1.69±0.10
Markers of inflammation											
CRP	0.53±0.05	0.75±0.07	0.90±0.06	12.55±0.45***	4.63±0.07***c	4.86±0.06***c	7.19±0.34***c	0.58±0.04	0.50±0.04	3.83±0.11c	5.22±0.12c

Table 4: Effects of DCF±TVX±LVX±TNF-α on Expression of mRNAs (by RT-PCR) Encoding Genes Related to Oxidative stress, Inflammation, Hepatobiliary Transporters, Nuclear Receptors, Phase I and Phase II Metabolizing Enzymes in HepaRG Cells (3 days). *P<0.05, **P<0.01 and ***P<0.001 compared with untreated cells, #P<0.05, ##P<0.01 and ###P<0.001 compared with cells treated with cytokine, DCF, TVX, LVX or the mix. a:#; b:##; c:###.

CYP3A4 activity and transcripts

The main TVX metabolites formed by the liver are glucuronides, and N-acetyl- and sulfo-conjugates (Dalvie et al., 1997; Fujiwara et al., 2015) while DCF is first oxidized mainly by CYP3A4 (Shen et al., 1999; Tang et al., 1999b) that together with some other CYPs is strongly repressed by pro-inflammatory cytokines (Abdel-Razzak et al., 1993). At 20 and 50μM TVX inhibited CYP3A4 activity by 28.89% and 47.9% respectively compared to untreated cells after 24h treatment; the inhibition reached 83.78, 93.71 and 88.85% by co-treatment of 20μMTVX with TNF-α, IL-6 or IL-1β respectively (Figure 2A). Comparable changes were observed at the corresponding transcript levels (Figure 2B and Table 2). No further significant change occurred with a co-treatment of TVX/DCF (Figure 2C and D).

After 3 days, DCF at 100μM increased CYP3A4 activity by around 1.7-fold; this activity remained close to the normal value by co-exposure with TNF-α. When added separately 20μMTVX or LVX only slightly decreased CYP3A4 activity and in combination with DCF did not significantly modulate its effect in presence or absence of TNF-α. Comparable inhibitory effects of TVX and TNF-α separately or in combination were observed at the transcripts levels. While 20μM LVX had a higher repressive effect on CYP3A4 mRNA levels in the presence or absence of TNF-α (Figure 2E and F).

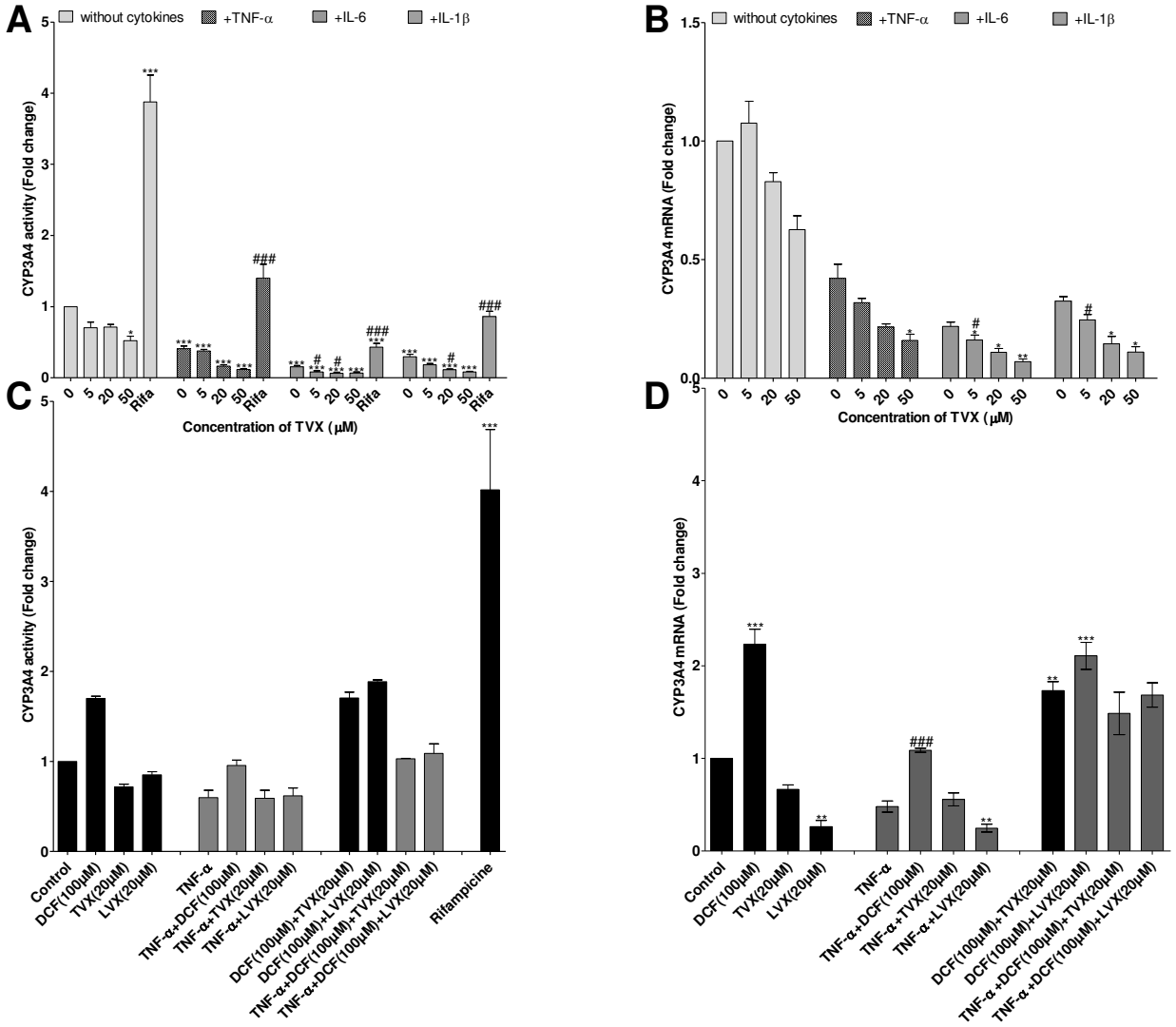

Figure 2: Measurement of gene level expression and activity of CYP3A4. Cells were treated with (A and B) TVX ± TNF-α for 24h or (C, D, E and F) with DCF, TVX, LVX, DCF-TVX or DCF-LVX with or without TNF-α for (C and D) 24 h or (E and F) 3 days and CYP3A4 activity and gene level expression were measured (A-C-E and B-D-F respectively). All results are expressed relative to the levels found in corresponding untreated cells, arbitrarily set at a value of 1. *P<0.05, **P<0.01 and ***P<0.001 compared with untreated cells, $^{\#}$P<0.05, $^{\#\#}$P<0.01 and $^{\#\#\#}$P<0.001 compared with cells treated with cytokine, DCF, TVX, LVX or the mix.

Modulation of other genes related to drug metabolism and transport

Several other genes encoding drug metabolism enzymes and transporters were analyzed by RT-qPCR after 24-hour and 3-day treatments; these genes included nuclear receptors (CAR, PXR, FXR), phase 1 (CYP2C9, CYP2B6, CYP1A2) and phase 2 (UGT1A1, UGT1A3, GSTA1/2 and GSTM1) enzymes, and influx and efflux transporters (NTCP, OATP-B, BSEP, MDR1, MDR3, MRP2, MRP3, and MRP4). After 24h treatment expression of several of these genes, including CYP2C9, CYP2B6, CAR and PXR, was inhibited, especially after co-treatment with cytokines. CYP1A2 and FXR were also repressed by co-treatment but to a

lower extent (Tables 2, 3 and 4). No significant changes were observed in genes encoding transporters after treatments with 20µMTVX while 50µMTVX and TNF-α caused a limited decrease of most of them. A strong inhibition of BSEP and NTCP was obtained with co-treatments while, when observed, inhibition of other transporters was much lower. Similar results were obtained with co-treatments with IL6 and IL1. After 3 days BSEP and NTCP were still strongly repressed by either DCF, TVX or LVX separately. Transcripts of several genes were decreased and to a more extent with the combination DCF/TVX and DCF/LVX and these effects were aggravated after 3 days by comparison with those observed at 24 h (Tables 2, 3 and 4).

Co-treatments with TVX ± cytokines and DCF ± TVX ± cytokines also repressed transcription of genes encoding detoxifying GSTA1/2 and GSTM1/2 enzymes. By contrast UGT1A1 and UGT1A3 were overexpressed with low concentrations and repressed with high concentrations of TVX and co-addition of TNF-α. Only a slight inhibition was observed when the cells were co-treated with 4ng/ml TNF-α (Tables 2, 3 and 4).

In general, the effects of DCF and TVX on the major of genes were aggravated when the two drugs was added together and were potentiated by co-treatment with TNF-α at 24 h and more after 3 days (Tables 2, 3 and 4).

Cytotoxicity of trovafloxacin is aggravated by co-treatment with diclofenac and cytokines

Differentiated HepaRG cells were treated with various concentrations of TVX for 24h or 3 days, then cytotoxicity was estimated using the MTT assay. A significant decrease in cell viability was observed in a dose-dependent manner with drug concentrations starting at 500µM (IC50≈827.73µM). However, when TVX was added together with either TNF-α, IL-1β or IL-6 cytotoxicity was aggravated (IC50≈ 250µM, 150µM, 100µM respectively); a decrease in cell viability was evidenced with 100µM TVX regardless of the cytokine. However, the extent of cytotoxicity was higher with IL-6 compared to the two other cytokines, especially with 100 µM TVX, reaching 50.98% cell loss. No cytotoxic effect was observed with the cytokines alone (Figure 3A). IC50 values were lowered when TVX was co-added with DCF, and to a higher extent in the presence of TNF-α (For example the combination of DCF 200µM with TVX 20µM and TNF-α 10ng/ml contributed to more than 50% of cell death) (Figure 3B).

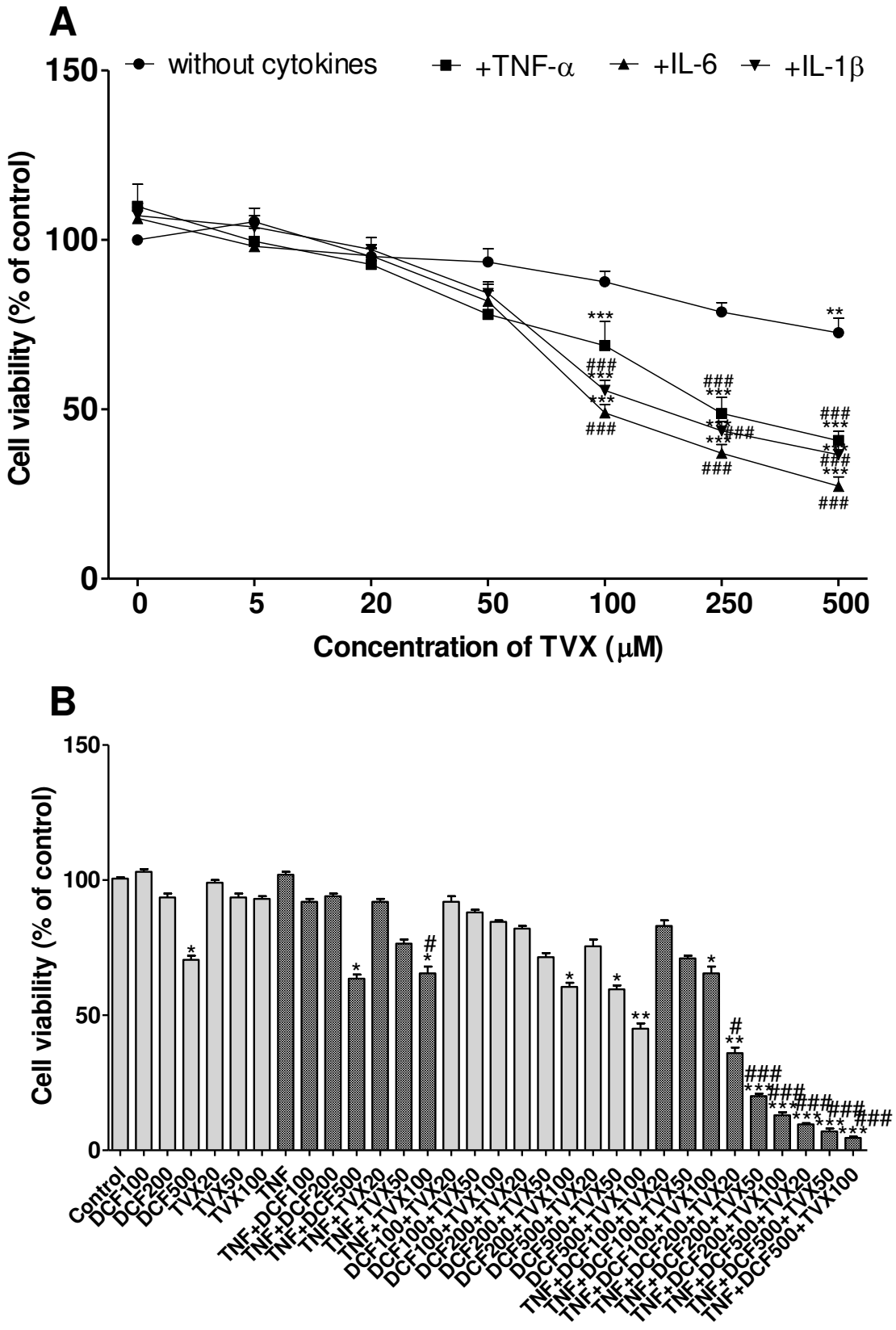

Figure 3: Cytotoxic effect s of TVX in HepaRG cells. Cells were treated with (A) various concentrations of TVX ± cytokines (TNF-α, IL-6 or IL-1β) or (B) with DCF or TVX separately or with the mix TVX/DCF +/- TNF-α for 24 h and cytotoxicity was measured with the MTT assay. All results are expressed relative to the levels found in

corresponding untreated cells, arbitrarily set at a value of 1. *P<0.05, **P<0.01 and ***P<0.001 compared with untreated cells, $^{\#}$P<0.05, $^{\#\#}$P<0.01 and $^{\#\#\#}$P<0.001 compared with cells treated with cytokines or TVX individually.

TVX cytotoxicity was augmented after 3 days of treatment and further aggravated in the presence of TNF-α. At 50 µM TVX caused 37.38 and 66.31% cell loss when added alone and with TNF-α respectively. By contrast, even at 1mM LVX did not cause any effect, whether added separately or with TNF-α (Figure 4A). Similar observations were done with DCF; at 200µM this drug caused 29.75 and 70.88% cell loss when added alone and with TNF-α respectively (Figure 4A). Co-treatments with DCF/TVX and DCF/LVX at various concentrations in the absence or presence of TNF-α were also investigated. The combination 200µM DCF/50µM TVX led to 40.33% cell loss and to 91.03% cell loss when combined to TNF-α (Figure 4B) whereas at 50µM LVX did not enhance DCF toxicity in both conditions (Figure 4C).

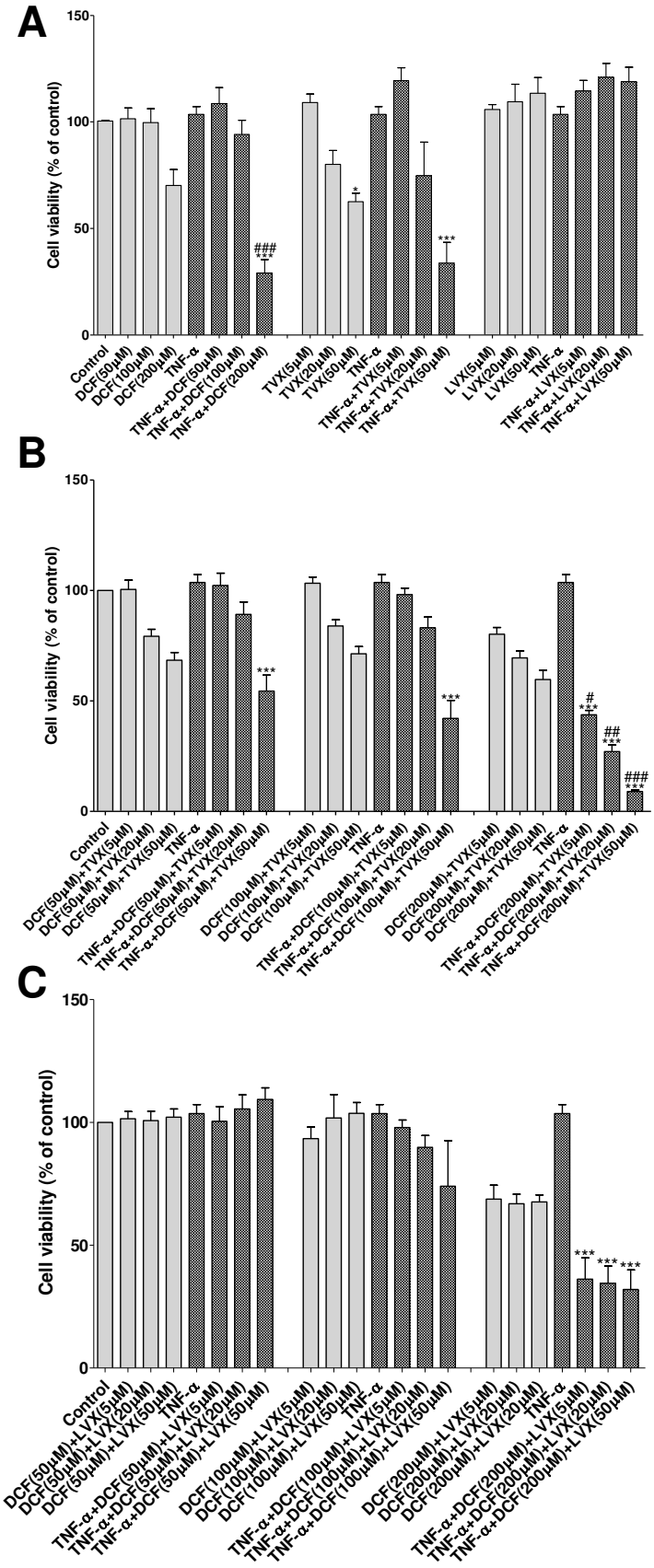

Figure 4: Effect s of repeated (3-day) treatments with combinations DCF-TVX or DCF-LVX with or without TNF-α, on cell viability in HepaRG cells. Cells were treated with different doses of DCF, TVX or LVX in the presence or not of TNF-α for 3 days and MTT toxicity was measured (A, B and C). All results are expressed relative to the levels found in corresponding untreated cells, arbitrarily set at a value of 1. *P<0.05, **P<0.01 and ***P<0.001 compared with untreated cells, $^{\#}$P<0.05, $^{\#\#}$P<0.01 and $^{\#\#\#}$P<0.001 compared with cells treated with cytokine, DCF, TVX, LVX or the mix.

Caspase-3 activity was measured at the two time-points. After 24h treatment a 4.26-fold increase was observed with 50µM TVX compared to untreated cells. In the presence of cytokines which were ineffective when added alone, an increase in caspase 3 activity was observed with lower TVX concentrations, i.e. 20µM with IL-6 (5.15-fold vs IL-6 alone) and 20µM with TNF-α (2.9-fold vs TNF-α alone) and IL-1β (3.54 fold vs IL-1β alone) (Figure 5A). Moreover, caspase 3 activity was slightly enhanced when TVX was co-administered with DCF in the absence and more extensively in the presence of TNF-α (2.03 and 4.09-fold changes respectively) (Figure 5A).

After 3 days, a slight increase in caspase 3 activity was observed after co-treatment of HepaRG cells with 100µM DCF and 20µM TVX (2.8 -fold change versus corresponding untreated cells); this increase was more pronounced by co-treatment with the combination DCF-TVX-TNF-α (4.97-fold) (Figure 5B).

Of note, as expected treatment of undifferentiated HepaRG cells with DCF augmented caspase 3 activity while but it was not the case with TVX , even at high concentrations (Figure 5D).

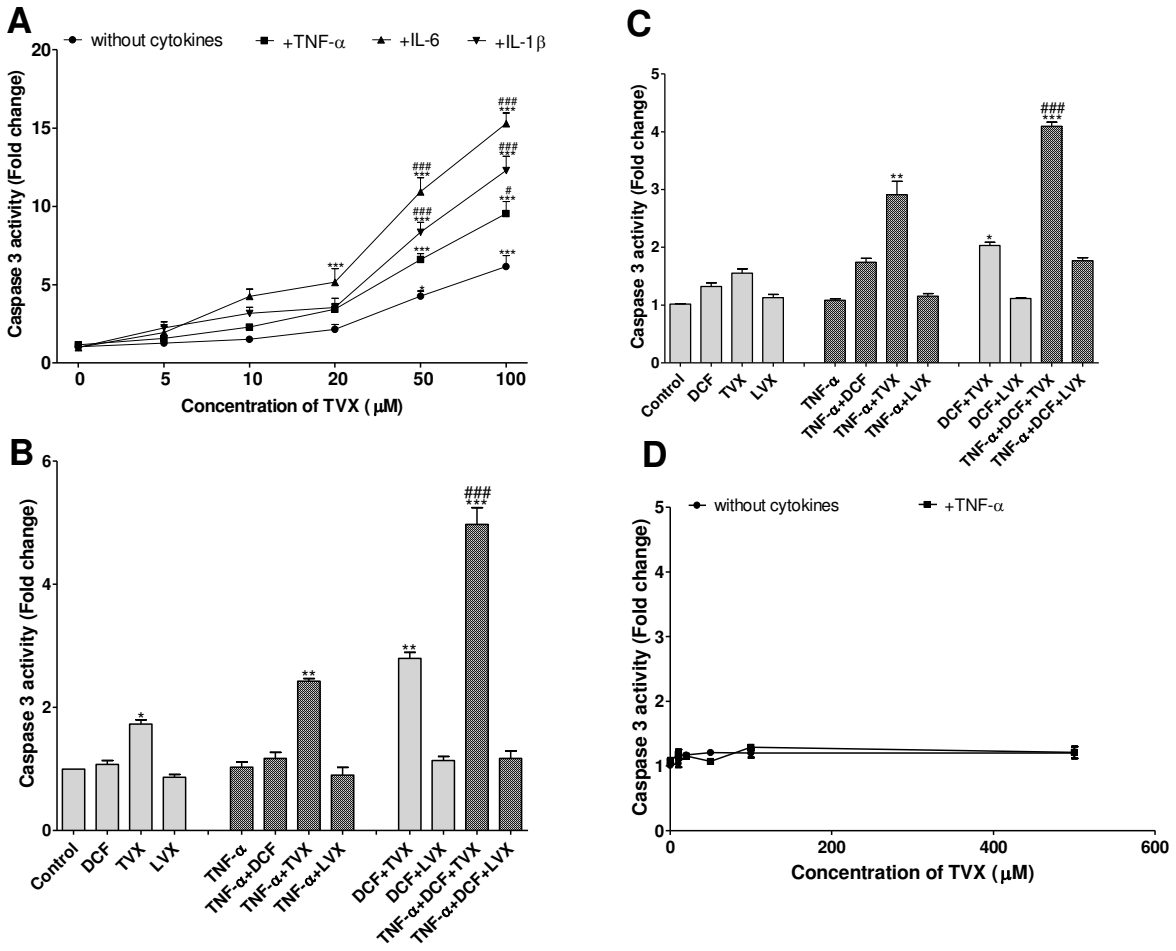

Figure 5: Measurement of caspase 3 activity. Differentiated HepaRG cells were treated with various concentrations of TVX ± cytokines (A), with DCF, TVX, LVX or the mix DCF/TVX or DCF/LVX ±TNF-α for 24h (B) or 3days (C) . For comparison undifferentiated HepaRG cells were also tested for 24h (D). All results are expressed relative to the levels found in corresponding untreated cells, arbitrarily set at a value of 1. *P<0.05, **P<0.01 and ***P<0.001 compared with untreated cells, $^{\#}$P<0.05, $^{\#\#}$P<0.01 and $^{\#\#\#}$P<0.001 compared with cells treated with cytokine, DCF, TVX, LVX or the mix.

Light microscopic examination showed that while DCF and TVX first altered primitive biliary cells and HepaRG hepatocytes respectively, co-treatment with DCF/TVX in the presence or absence of TNF-α affected both cell types simultaneously (Figure 6).

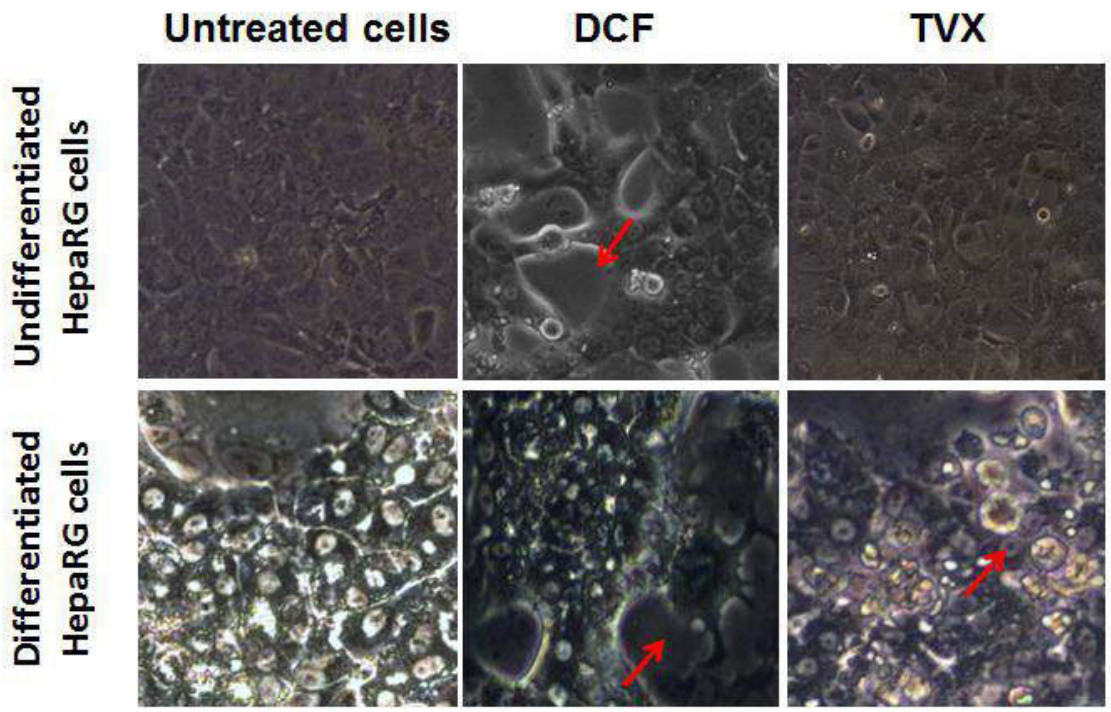

Figure 6: Effects of DCF and TVX on HepaRG cell morphology. Differentiated and undifferentiated HepaRG cells were treated with these drugs for 24 h and images were taken (Phase-contrast microscopy ; magnification 20x).

ROS generation induced by trovafloxacin is aggravated by co-treatment with diclofenac and cytokines

A 24h treatment with 20µM TVX caused a slight generation of ROS (1.61-fold) that was further moderately augmented by co-exposure to cytokines, especially IL-6 (2.3-fold). A higher response was obtained with 50µM TVX, representing 2.66-, 3.63- and 3.12-fold increase when co-added with TNF-α, IL-6 and IL-1β respectively (Figure 7A andFigure 8). Similar changes were observed in transcripts levels of the related gene HO-1, that were increased 2.08-fold with 50 µM TVX alone and 3.22-, 6.16- and 4.72-fold by co-addition of TNF-α, IL-6 and IL-1β respectively (Table 2). Transcripts levels of MnSOD, another ROS-related gene, raised to 2.13-fold after treatment with 50µM TVX alone and 4.02-, 6.34- and 4.47-fold after co-treatment with TNF-α, IL-6 and IL-1β respectively (Table 2). SOD activity was also augmented 2.15-fold with 50µM TVX and to a higher extent after co-treatment with TNF-α (3.22-fold) (Figure 7B). Co-treatment of TVX with DCF aggravated ROS generation mainly in the presence of TNF-α (4.58-fold) (Figure 7C). Similarly co-treatment of TVX with DCF also aggravated SOD activity after 24h (2.88-fold) (Figure 7D).

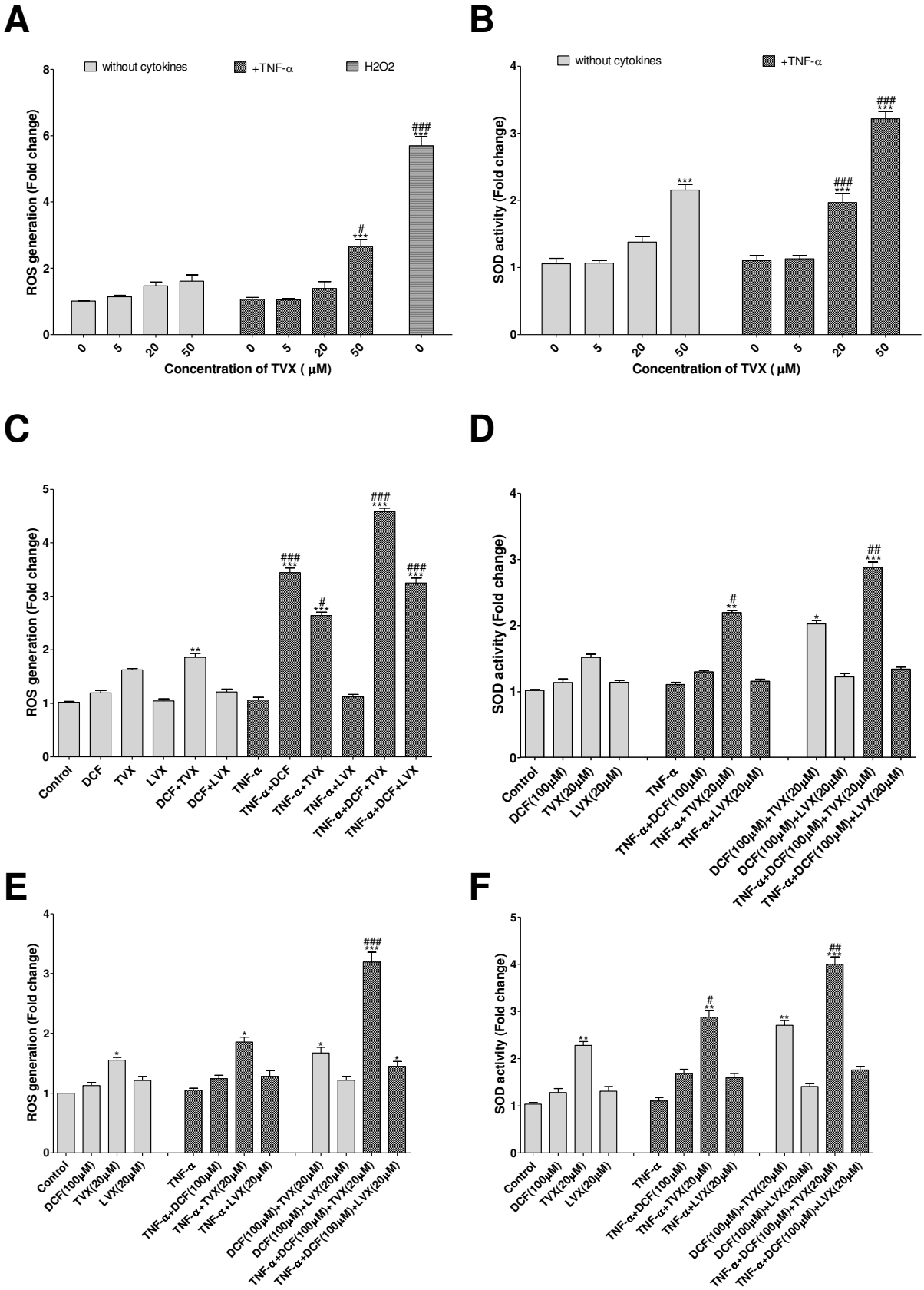
A
without cytokines
+TNF-α
H2O2
ROS generation (Fold change)
Concentration of TVX (μM)
B
without cytokines
+TNF-α
SOD activity (Fold change)
Concentration of TVX (μM)
C
ROS generation (Fold change)
Control
DCF
TVX
LVX
DCF+TVX
DCF+LVX
TNF-α
TNF-α+DCF
TNF-α+TVX
TNF-α+LVX
TNF-α+DCF+TVX
TNF-α+DCF+LVX
D
SOD activity (Fold change)
Control
DCF(100μM)
TVX(20μM)
LVX(20μM)
TNF-α
TNF-α+DCF(100μM)
TNF-α+TVX(20μM)
TNF-α+LVX(20μM)
DCF(100μM)+TVX(20μM)
DCF(100μM)+LVX(20μM)
TNF-α+DCF(100μM)+TVX(20μM)
TNF-α+DCF(100μM)+LVX(20μM)
E
ROS generation (Fold change)
Control
DCF(100μM)
TVX(20μM)
LVX(20μM)
TNF-α
TNF-α+DCF(100μM)
TNF-α+TVX(20μM)
TNF-α+LVX(20μM)
DCF(100μM)+TVX(20μM)
DCF(100μM)+LVX(20μM)
TNF-α+DCF(100μM)+TVX(20μM)
TNF-α+DCF(100μM)+LVX(20μM)
F
SOD activity (Fold change)
Control
DCF(100μM)
TVX(20μM)
LVX(20μM)
TNF-α
TNF-α+DCF(100μM)
TNF-α+TVX(20μM)
TNF-α+LVX(20μM)
DCF(100μM)+TVX(20μM)
DCF(100μM)+LVX(20μM)
TNF-α+DCF(100μM)+TVX(20μM)
TNF-α+DCF(100μM)+LVX(20μM)

Figure 7: Effects of TVX ± DCF ± TNF-α on ROS generation and SOD activity. Cells were treated with (A and B) TVX ± TNF-α and (C and D) the mix TVX±DCF±TNF-α for 24 h or (E and F) for 3 days and ROS generation (A, C and E) and (B, D and F) SOD activity were measured. All results are expressed relative to the levels found in corresponding untreated cells, arbitrarily set at a value of 1. *P<0.05, **P<0.01 and ***P<0.001 compared with untreated cells, $^{\#}$P<0.05, $^{\#\#}$P<0.01 and $^{\#\#\#}$P<0.001 compared with cells treated with cytokine or TVX individually.

After 3 days of treatment ROS generation was increased 1.55-fold with 20μM TVX and was further slightly augmented by co-addition of TNF-α (1.92-fold) and much more by the combination DCF/TVX/TNF-α (3.19-fold) (Figure 7E). These results were confirmed by measurement of HO-1 transcripts that showed 1.81-, 2.24- and 3.43-fold increase with TVX alone, TVX + TNF-α and TVX + DCF+ TNF-α respectively (Table 3). The highest increase was obtained with the combination TVX+ DCF+ IL-6 (data not shown). In parallel, SOD activity was similarly augmented with 20μM TVX (2.28-fold), TVX+TNF-α co-treatment (2.88-fold) and further more with 20μMTVX + 100μMDCF + TNF-α (4-fold) (Figure 3G). Similar results were observed with MnSOD transcripts that were augmented 1.59-, 2.15- and 3.23-fold with TVX, TVX/TNF-α and TVX/DCF/TNF-α, respectively (Table 3). An increase of Nrf2 gene expression was also found (Table 3).

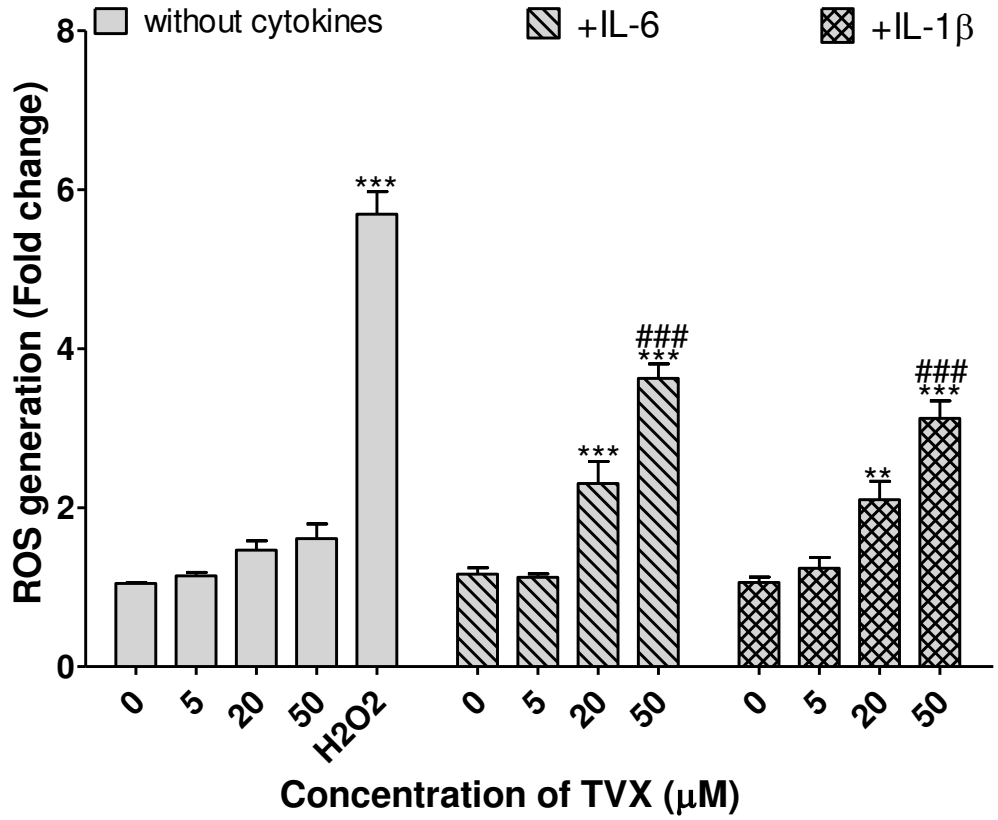

Figure 8: Measurement of ROS generation. Cells were treated with TVX ± DCF ± cytokines (IL-6 or IL-1β) for 24 h and ROS generation was measured using the H_2DCFDA assay. All results are expressed relative to the levels found in corresponding untreated cells, arbitrarily set at a value of 1. *P<0.05, **P<0.01 and ***P<0.001 compared with untreated cells, $^{\#}$P<0.05, $^{\#\#}$P<0.01 and $^{\#\#\#}$P<0.001 compared with cells treated with cytokine or TVX individually.

Endoplasmic reticulum stress

An activation of several ER stress genes has been previously evidenced in either HepG2 or HepaRG cells exposed to DCF (Al-Attrache et al., 2016; Fredriksson et al., 2014). Expression of several genes related to ER stress, ATF4, ATF6, CHOP and GRP78, were also measured by RT-qPCR in the present study. After 24h of treatment, the 4 genes were overexpressed with 50µM TVX and this overexpression was enhanced by co-exposure to the cytokines; the highest values being obtained with co-treatment of 50µM TVX with IL6 or IL1. The cytokines or LVX alone were ineffective (Table 3). After 3 days, a moderate increase in the expression of the 4 genes was observed with 100µM DCF and 20µM TVX, that was slightly higher by co-addition of TNF-α. However, co-treatment with DCF and TVX resulted in a marked overexpression of ER stress-related genes, that was further augmented by co-addition of TNF-α. LVX had no effect; it did not affect changes associated with DCF or DCF+ TNF-α co-treatments (Tables 3 and 4).

Involvement of intrinsic and extrinsic apoptotic pathways

A 24h treatment of HepaRG cells with 50µM TVX resulted in 3.53-fold activation of caspase 8 that reached 5.02-fold with a co-treatment with TNF-α. Caspase 8 activation by TVX was strongly inhibited by co-addition of the anti-oxidant NAC (65.93%), the JNK inhibitor SP600125 (53.19%) and the caspase 9 inhibitor z-LEHD-fmk (58.09%). Co-addition of the soluble p75 TNF receptor etanercept completely inhibited the fraction of caspase 8 activated by TNF-α (Figure 9A).

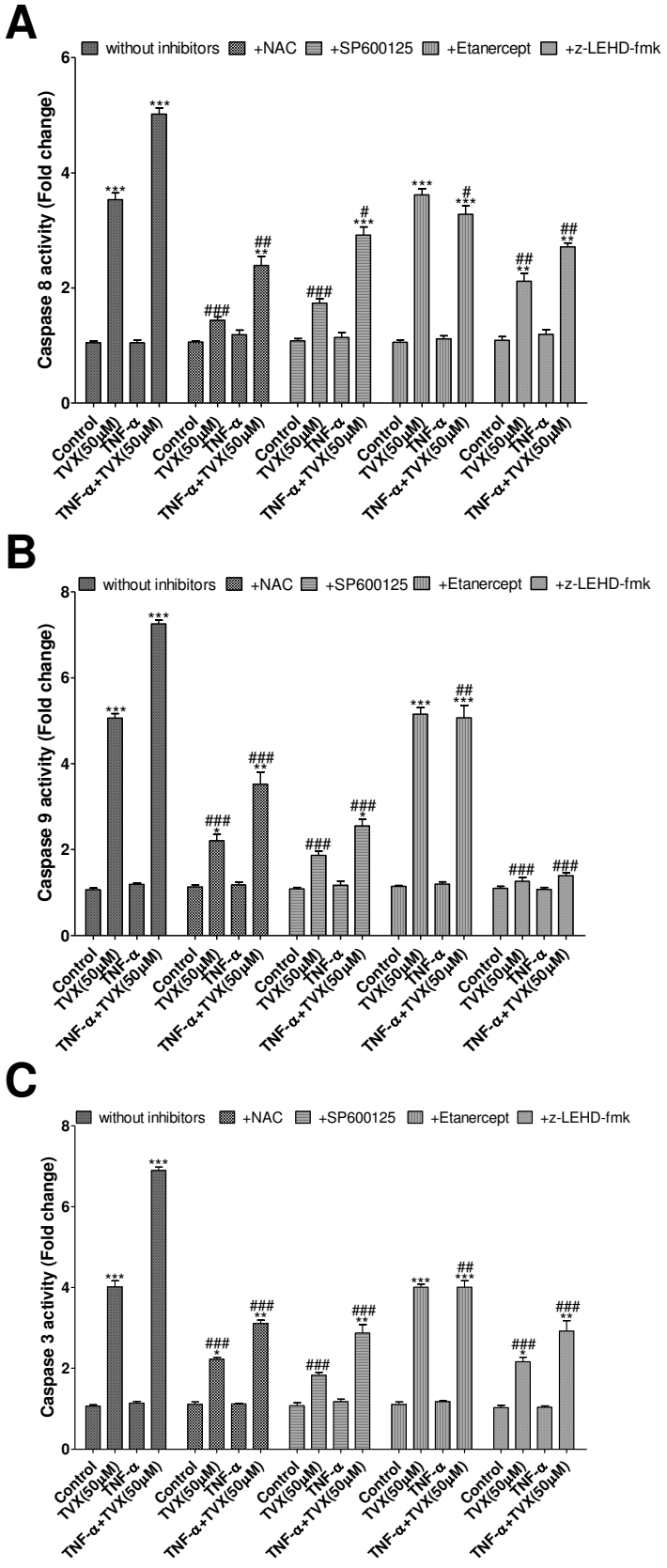

Figure 9: Measurement of activities of caspases 8, 9 and 3 after TVX ± TNF-α treatment. Cells were treated with TVX ± TNF-α in the presence or not of NAC, SP600125, Etanercept and z-LEHD-fmk and (A) caspases 8, (B) 9 and (C) 3 activities were measured. All results are expressed relative to the levels found in corresponding untreated cells, arbitrarily set at a value of 1. *P<0.05, **P<0.01 and ***P<0.001 compared with untreated cells, $^{\#}$P<0.05, $^{\#\#}$P<0.01 and $^{\#\#\#}$P<0.001 compared with cells treated with cytokine or TVX individually.

Caspase 9 activity was also increased 5.06- and 7.26-fold with TVX and TVX+TNF-α respectively. Its activation was inhibited with NAC, SP600125 and z-LEHD-fmk (70.20;

78.57 and 93.59% with TVX alone and 59.74; 75.24 and 90.23% with TVX + TNF-α respectively. As for caspase 8 only the fraction induced by TNF-α was inhibited by etanercept (Figure 9B). Similar changes in caspase 3 activity were observed when HepaRG cells were co-treated with TVX/TNF-α and the inhibitors (Figure 9C). This was also the case with the combination DCF/TVX/TNF-α (Figure 10A, B and C).

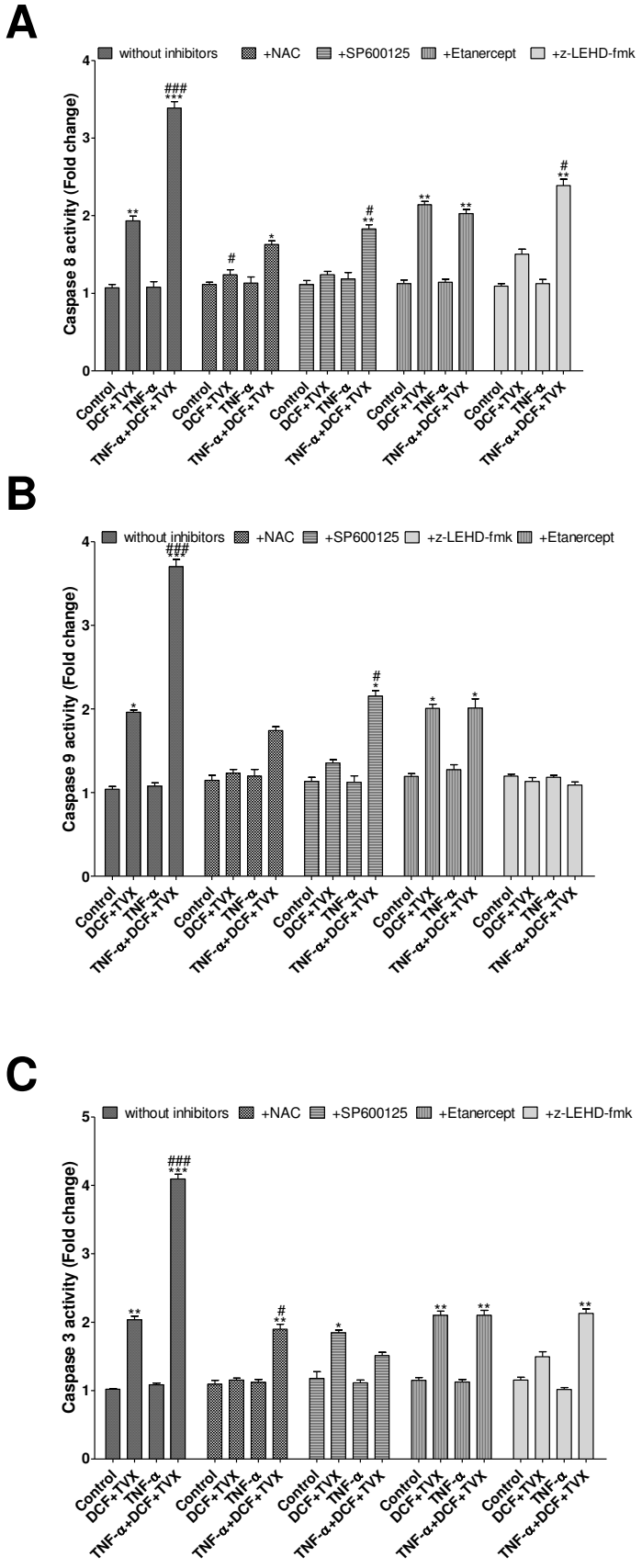

Figure 10: Effects of drug combinations on the caspases 8, 9 and 3. Cells were treated for 24h with TVX, DCF, LVX or the mix with or without TNF-α and in the presence or not of the inhibitors NAC, SP600125, Etanercept and z-LEHD-fmk followed by measure of the caspases (A) 8, (B) 9 and (C) 3. All results are expressed relative to the levels found in corresponding untreated cells, arbitrarily set at a value of 1. *P<0.05, **P<0.01 and ***P<0.001 compared with untreated cells, $^{\#}$P<0.05, $^{\#\#}$P<0.01 and $^{\#\#\#}$P<0.001 compared with cells treated with cytokine, DCF, TVX, LVX or the mix.

After 3 days caspase 8 activity was increased 2.51- and 4.89-fold with TVX/DCF and DCF/TVX/TNF-α respectively (Figure 11A and B). Similarly, the fraction induced by co-addition of TNF-α was inhibited by etanercept (Figure 11C and D) while the other fraction increased by TVX/DCF combination was inhibited by NAC, SP600125 and z-LEHD-fmk (Figure 11E and F).

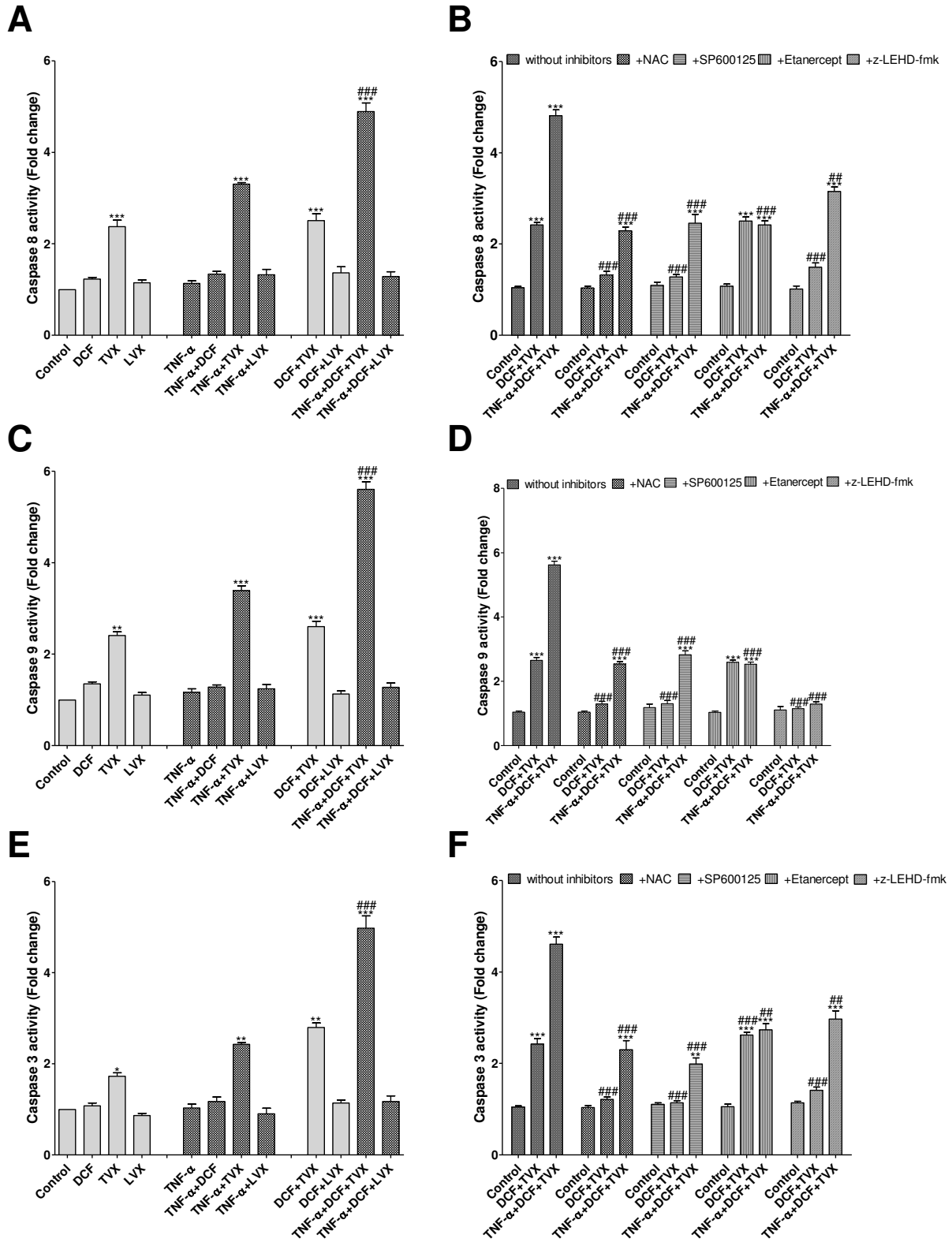

Figure 11: Effects of drugs separately of in combinations +/- TNF-α on the caspases 8, 9 and 3 activities. Cells were treated for 3 days with TVX, DCF, LVX or the mix with or without TNF-α and in the presence or not of the inhibitors NAC, SP600125, Etanercept and z-LEHD-fmk followed by measure of the caspases (A and B) 8, (C and D) 9 and (E and F) 3. All results are expressed relative to the levels found in corresponding untreated cells, arbitrarily set at a value of 1. *P<0.05, **P<0.01 and ***P<0.001 compared with untreated cells, $^{\#}$P<0.05, $^{\#\#}$P<0.01 and $^{\#\#\#}$P<0.001 compared with cells treated with cytokine, DCF, TVX, LVX or the mix.

IL-6 also aggravated activation of the three caspases when co-added with the combination 100μMDCF+20μMTVX and its effect was mostly abrogated by addition of NAC whil e etanercept was ineffective (Figures 12, 13 and 14).

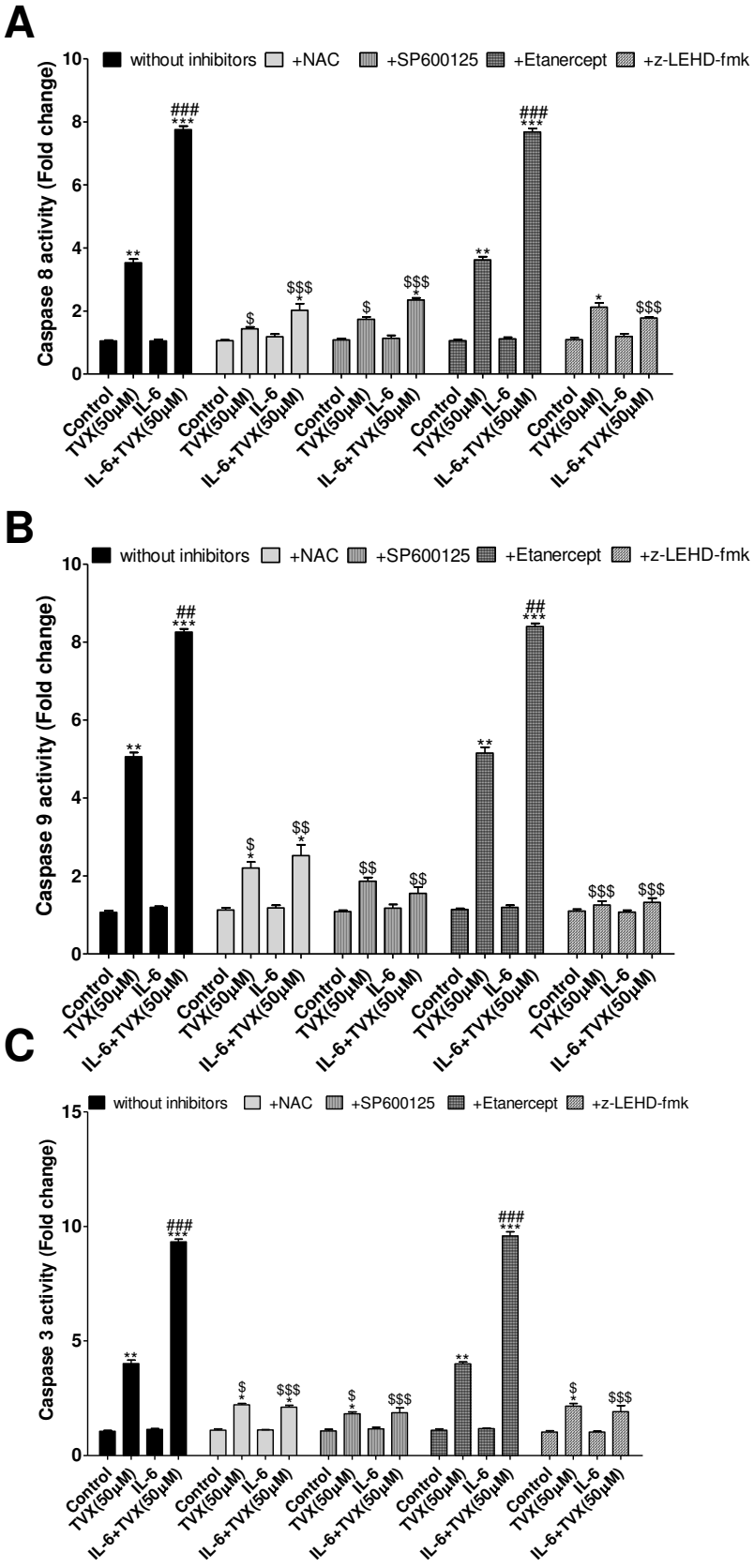

Figure 12: Effects of TVX ± IL-6 on the caspases 8, 9 and 3 activities (A, B and C) in the presence or not of the inhibitors (NAC, SP600125, Etanercept and z-LEHD-fmk). All results are expressed relative to the levels found in corresponding untreated cells, arbitrarily set at a value of 1. *P<0.05, **P<0.01 and ***P<0.001 compared with untreated cells, $^{\#}$P<0.05, $^{\#\#}$P<0.01 and $^{\#\#\#}$P<0.001 compared with cells treated with cytokine or TVX individually.

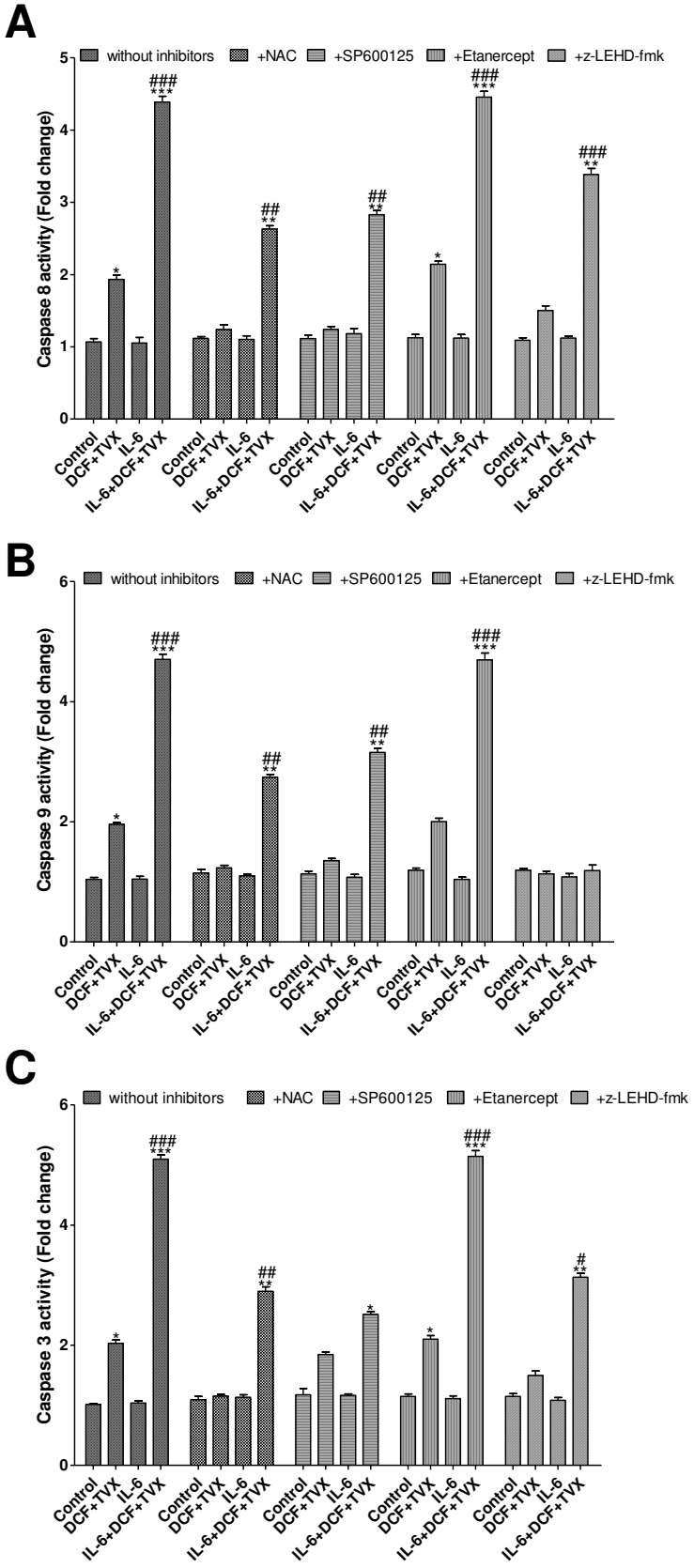

Figure 13: Effects of TVX ± DCF ± IL-6 on caspases 8, 9 and 3 activities (A, B and C) in the presence or not of the inhibitors (NAC, SP600125, Etanercept and z-LEHD-fmk) after 24h treatment. All results are expressed relative to the levels found in corresponding untreated cells, arbitrarily set at a value of 1. *P<0.05, **P<0.01 and ***P<0.001 compared with untreated cells, $^{\#}$P<0.05, $^{\#\#}$P<0.01 and $^{\#\#\#}$P<0.001 compared with cells treated with cytokine or TVX individually.

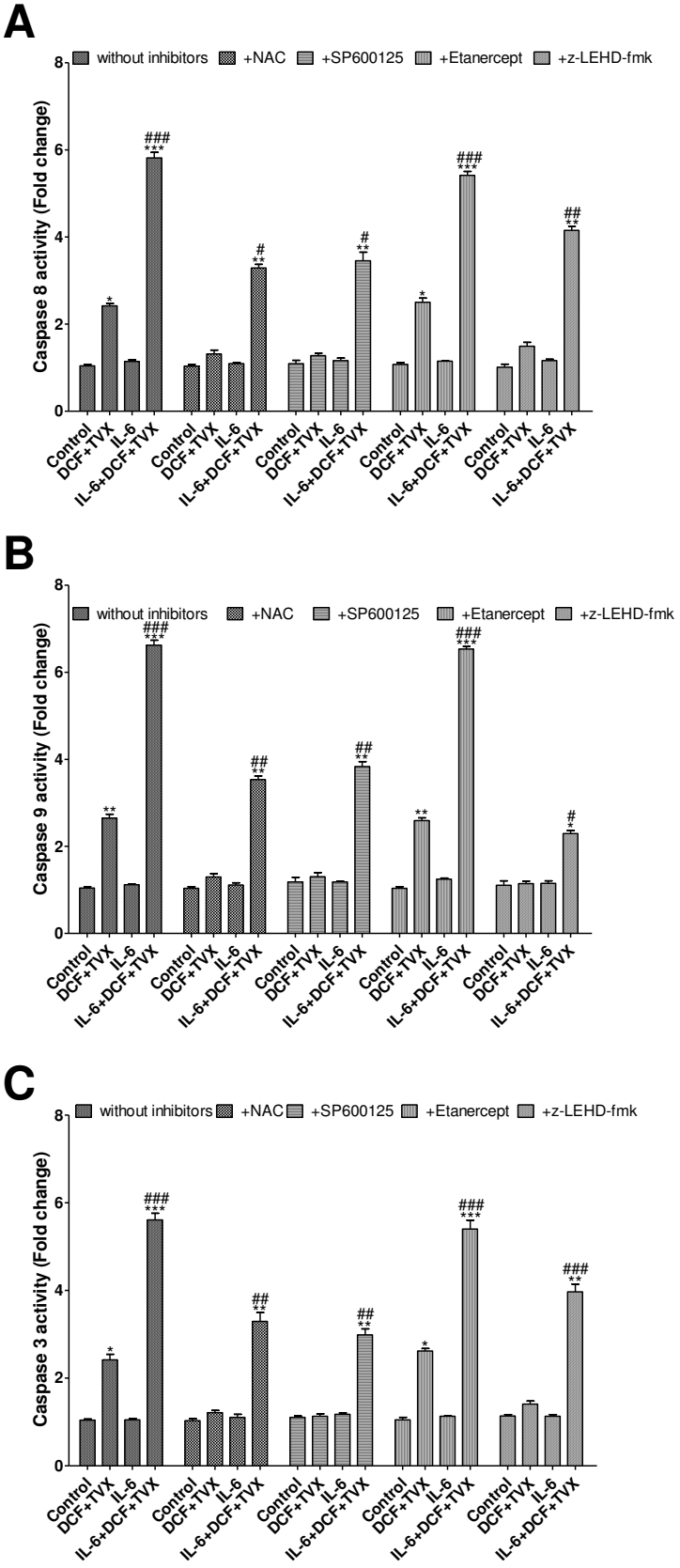

Figure 14: Effects of TVX ± DCF± IL-6 on caspases 8, 9 and 3 activities (A, B and C) in the presence or not of the inhibitors (NAC, SP600125, Etanercept and z-LEHD-fmk) after 3 days treatment. All results are expressed relative to the levels found in corresponding untreated cells, arbitrarily set at a value of 1. *P<0.05, **P<0.01 and ***P<0.001 compared with untreated cells, $^{\#}$P<0.05, $^{\#\#}$P<0.01 and $^{\#\#\#}$P<0.001 compared with cells treated with cytokine or TVX individually.

Effects of trovafloxacin and diclofenac on cholestatic features

Morphological changes. Alterations of bile canaliculi dynamics (BC) were observed as early as 30min after DCF addition at 100µM with a phase-contrast microscope, consisting in dilation of the canalicular lumen. This dilation was aggravated after 2h and became maximum after 6h. After 24h, only a slight dilation of some BC was still visible by comparison with untreated cells and was not further observed after 3 days. At 20µM TVX also caused BC dilation after 6h but to a lower extent compared to DCF and this dilatation was reversible after 24h. LVX was ineffective, at concentrations up to 1mM. Noteworthy, the combination DCF/TVX induced large dilatations of BC that were irreversible and more pronounced after 3 days of treatment. Limited dilations were also evidenced with DCF/LVX after 3 days (Figure 15).

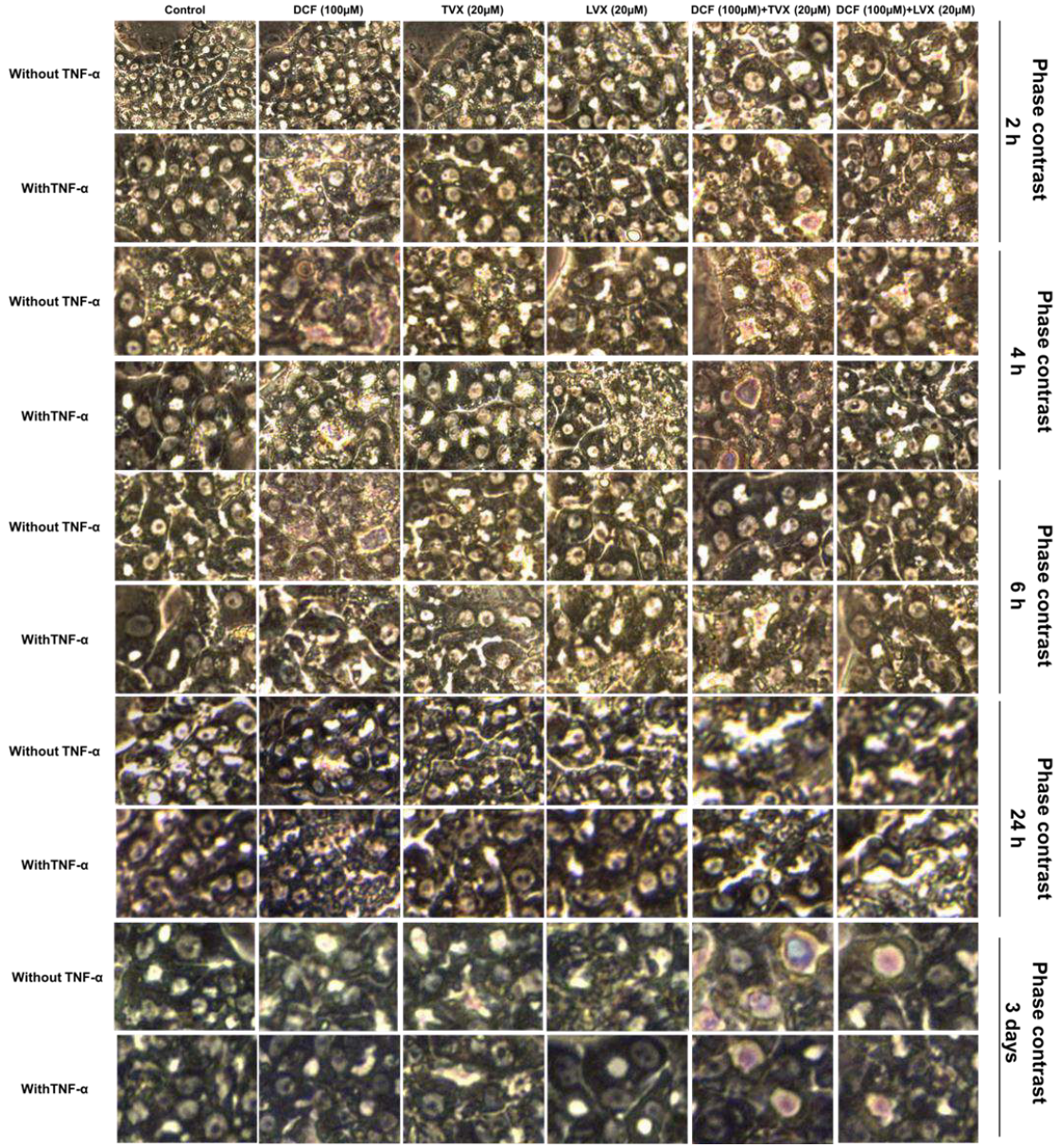

Figure 15: Effect s of DCF, TVX and LVX or combinations with or without TNF-α on the morphology of bile canaliculi. Cells were observed at different times (2, 4, 6 and 24 h and 3 days) and images were taken (Phase-contrast microscopy, magnification 20x).

Taurocholate acid efflux . [^{3}H]-TA efflux was decreased after 2h of treatment with TVX (50μM) but not with LVX (even at high concentrations) (Figure 16A). The combination 20μM TVX-100μM DCF or 50μM TVX-100μM DCF-did not aggravate inhibition of [^{3}H]-TA efflux observed with DCF alone (Figure 16B). After 24h and 3 days of treatment BSEP transcripts were decreased with DCF, TVX and LVX individually and to a higher extent with the combinations DCF+TVX and DCF+LVX (Tables 2, 3 and 4).

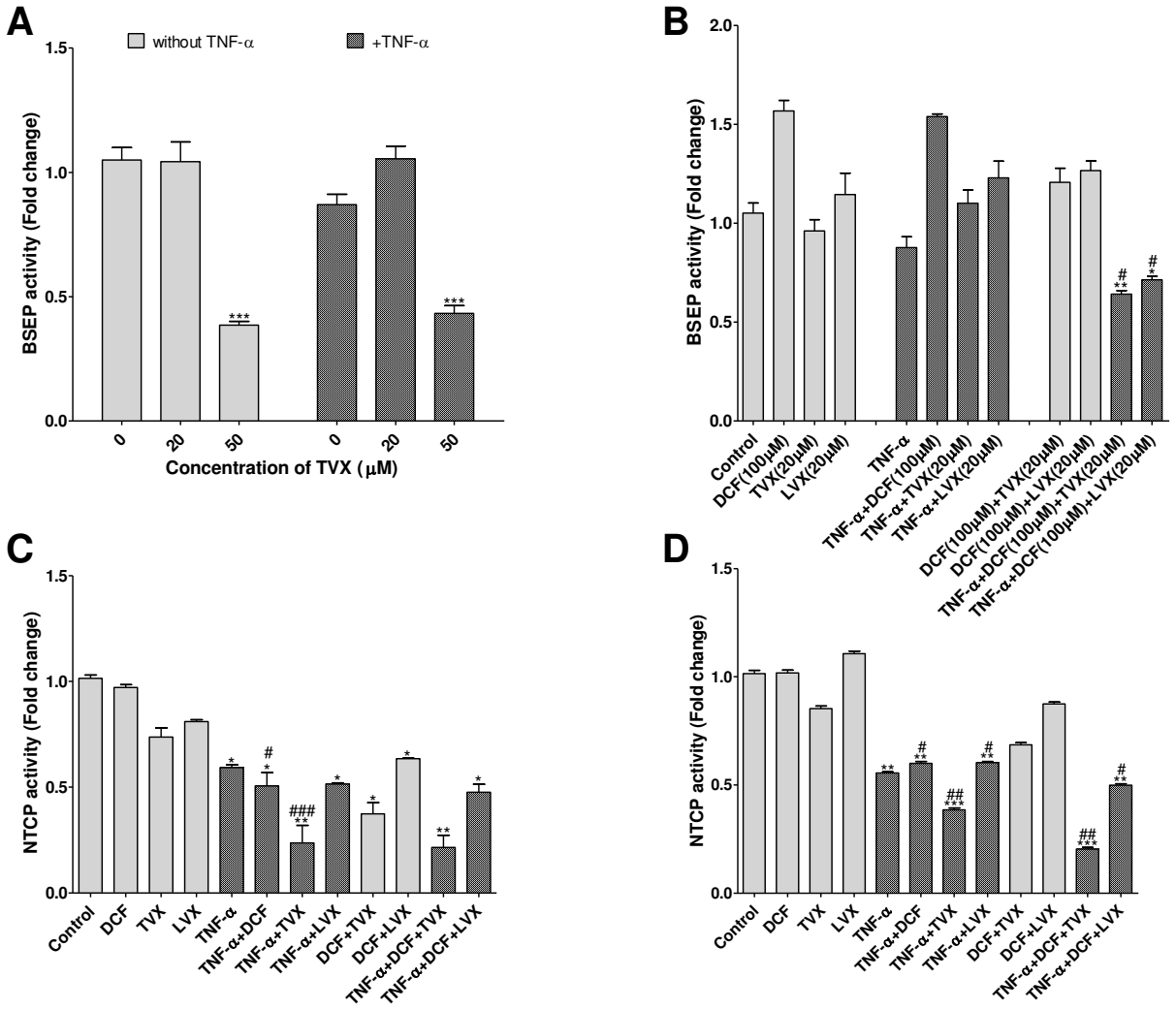

Figure 16: Measurement of BSEP and NTCP activities. Cells were treated with (A) TVX ± TNF-α or (B, C and D) the mix DCF±TVX±TNF-α and BSEP (A and B) and NTCP activities (C and D) were measured. All results are expressed relative to the levels found in corresponding untreated cells, arbitrarily set at a value of 1. *P<0.05, **P<0.01 and ***P<0.001 compared with untreated cells, $^{\#}$P<0.05, $^{\#\#}$P<0.01 and $^{\#\#\#}$P<0.001 compared with cells treated with cytokine, DCF, TVX, LVX or the mix.

Expression of transporters; NTCP was also inhibited at the transcript and activity levels (Figure 16C and D), even at a higher extent than BSEP by the combination DCF±TVX±TNF-α. Similarly, expression of OATP-B was strongly repressed, especially by co-treatment with DCF-TVX-TNF-α and DCF-LVX-TNF-α (Tables 3 and 4). In addition, MDR1 and MRP4 transcripts were increased with TNF-α+DCF+TVX while those of MDR3 and MRP3 were lowered (Tables 3 and 4). Noticeably, a diminution of MRP2 mRNAs was obtained with the combination TNF-TVX (Tables 2, 3 and 4). Of note, even alone cytokines alone exerted an inhibitory effect on several genes, including NTCP and BSEP.

Bile acids enzymes. Transcript and protein levels of several enzymes implicated in metabolism of biliary acids were also analyzed after 24h and 3 days, including CYP7A1,

CYP8B1, CYP27A1 and SULT2A1. After 24h, expression of the 3 CYPs was diminished with 50µM TVX and either cytokine and more extensively by the co-treatment of TVX with either cytokine. SULT2A1 was repressed by the 3 cytokines and the co-treatments (Tables 2, 3 and 4). A greater inhibition of transcript levels of these 4 genes was observed after co-treatment with DCF/TVX.

Of note, these inhibitions were confirmed at the protein levels by western blotting analysis (Figures 17 and 18). Any effect was observed with TNF-α alone except of these related to transcripts level.

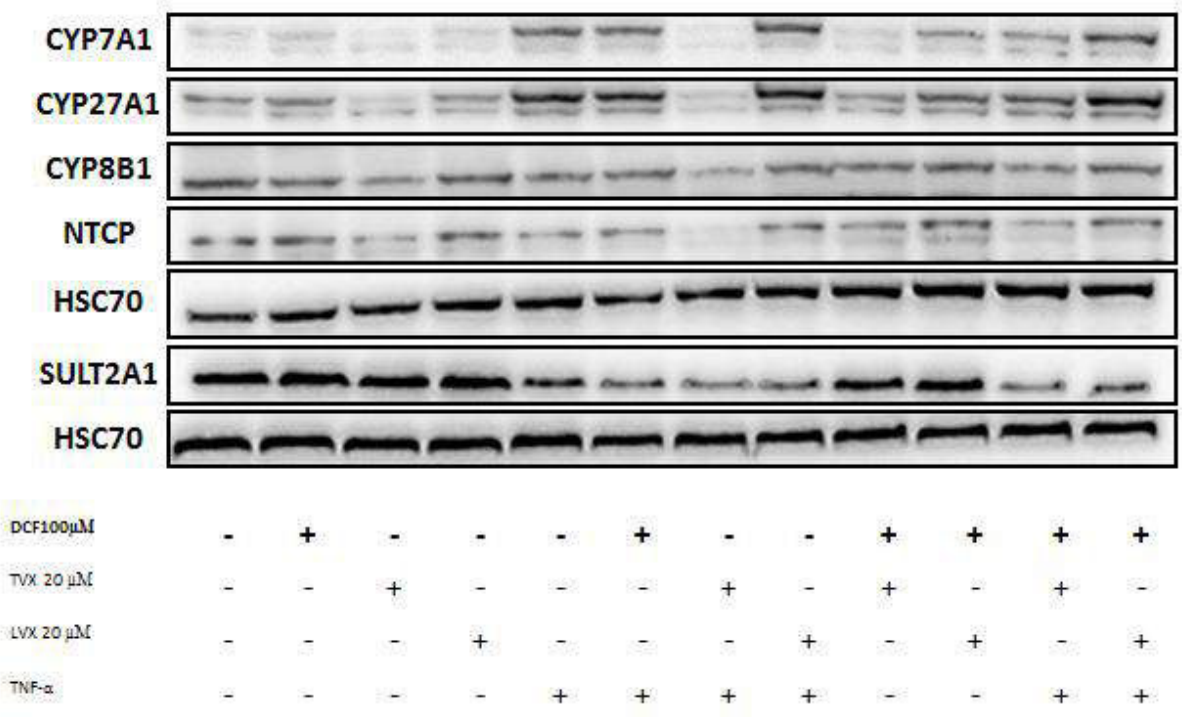

Figure 17: Effects of TVX ± DCF ± TNF-α on some genes involved in bile acid synthesis and transport. Cells were treated with the drugs separately or in combination, then protein contents of CYP7A1, 27A1, 8B1, SULT2A1 and NTCP were measured by western blotting.

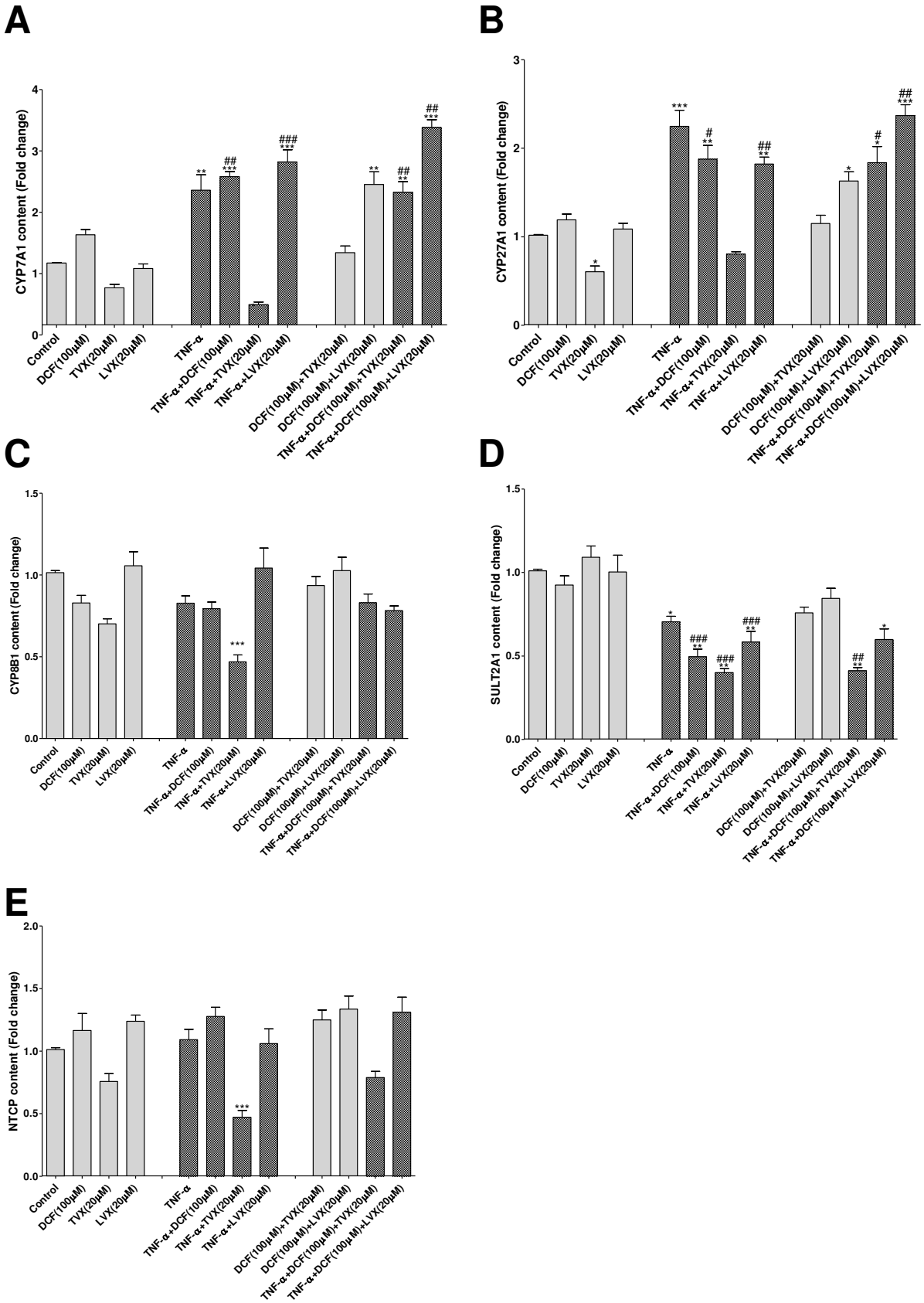
A
CYP7A1 content (Fold change)
B
CYP27A1 content (Fold change)
C
CYP8B1 content (Fold change)
D
SULT2A1 content (Fold change)
E
NTCP content (Fold change)
Control
DCF(100μM)
TVX(20μM)
LVX(20μM)
TNF-α
TNF-α+DCF(100μM)
TNF-α+TVX(20μM)
TNF-α+LVX(20μM)
DCF(100μM)+TVX(20μM)
DCF(100μM)+LVX(20μM)
TNF-α+DCF(100μM)+TVX(20μM)
TNF-α+DCF(100μM)+LVX(20μM)

Figure 18: Quantification of the western blots shown in Figure 17. (A) CYP7A1 (B) CYP27A1 (C) CYP8B1 and (D) NTCP. *P<0.05, **P<0.01 and ***P<0.001 compared with untreated cells, #P<0.05, ##P<0.01 and ###P<0.001 compared with cells treated with cytokine, DCF, TVX, LVX or the mix.

CDF efflux. Moreover, efflux of CDF, a substrate of multidrug resistance-associated protein 2 (MRP2), was measured and found to be induced after a 4h treatment with 100µM DCF and more greatly after 24h. It was more slightly augmented, with TVX after 24h. This increase of CDF efflux was enhanced by the combination DCF-TVX without any additional effect of TNF-α (Figure 19**).** The treatment for 3 days was enhanced very slightly this efflux (Figure 19).

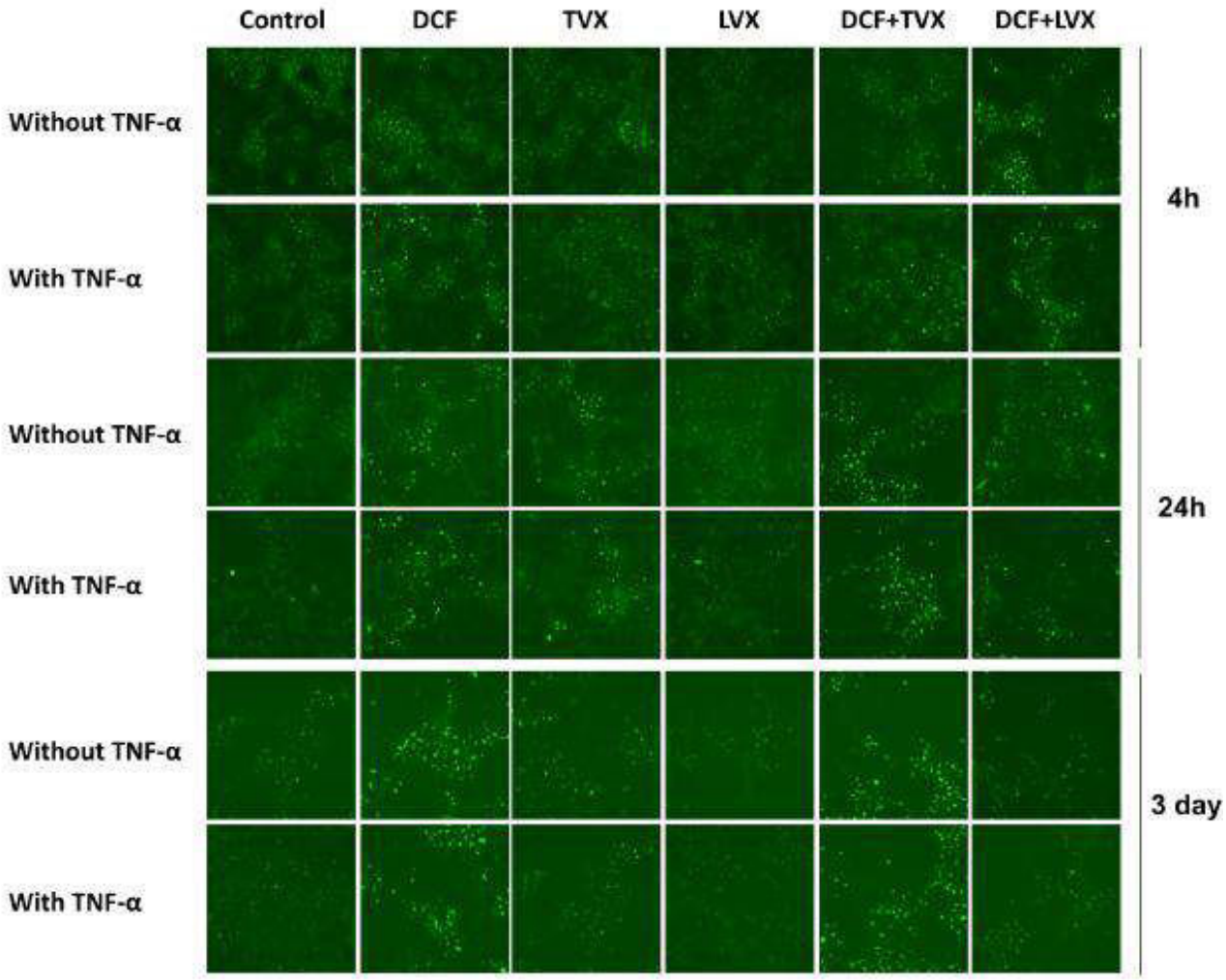

Figure 19: CDF efflux. Cells were treated with the DCF ± TVX ± TNF-α then images of florescent CDF efflux were taken after 4, 24 and 72h of treatment.

Discussion

Antibiotics and anti-inflammatory drugs are frequently co-prescribed to patients suffering from bacterial infection and many of them are recognized able to cause idiosyncratic hepatotoxicity (Actis et al., 2014; Tayem et al., 2013). In the current study we showed that concomitant treatment with the two idiosyncratic hepatotoxic drugs DCF, an anti-inflammatory drug and TVX, an antibiotic, enhanced cytotoxicity and cholestatic lesions compared to their separate addition and that co-addition of pro-inflammatory cytokines aggravated cytotoxicity in differentiated human HepaRG cells. Moreover, the damage was extended by repeated treatment.

TVX has been reported to cause hepatotoxicity in animals and *in vitro*, either in primary human hepatocytes or in HepG2 cells (Cosgrove et al., 2009; Liguori et al., 2008). Changes in a set of genes involved in mitochondrial damage and oxidative stress were identified in primary human hepatocytes treated with 400µM TVX for 24h (Liguori et al., 2008). In the current study we showed that 50 µM TVX caused generation of ROS, overexpression of related genes and enhanced activity of SOD and caspase 3 activation after a 24h treatment confirming that HepaRG hepatocytes were sensitive to TVX and supporting that toxicity involved induction of an oxidative stress and apoptosis. We also found that HepaRG hepatocytes were more sensitive than the surrounding, non metabolically active primitive biliary cells to TVX. Noticeably, a transcriptomic analysis showed that the profiles of deregulated genes by TVX were quite different in primary human hepatocytes and HepG2 cells (Liguori et al., 2008). In support, IL8 was found to be repressed 2-fold in the former and overexpressed 9.4-fold in the latter. A decreased expression of IL8 was also found in TVX-treated HepaRG cells further confirming that HepaRG hepatocytes are functionally close to primary human hepatocytes (Guillouzo et al., 2007) (Tables 2, 3 and 4).

When TVX was combined with DCF its cytotoxicity was increased. Noticeably, contrary to TVX, DCF first damaged primitive biliary cells, suggesting that it was more cytotoxic than its metabolites. Although DCF was metabolized to reactive metabolites it appeared that they are inactivated by the high capacity of detoxification of HepaRG hepatocytes (Al-Attrache et al., 2016). This drug-drug interaction resulted in increased ROS production and apoptosis activity supporting the view that both drugs caused mitochondrial damage. Accordingly, the antioxidant NAC and the JNK inhibitor, SP600125 strongly attenuated cytotoxicity of the two drugs whether added separately or combined. Although their Cmax are comparable, 7.4µM

and 5-10 µM for TVX and DCF (Willis et al., 1979) respectively, the former was cytotoxic at a lower concentration (20 vs 100µM respectively). Importantly, various activities and gene expression were differently deregulated when the two drugs were added simultaneously, as for example CYP3A4 activity and expression of various CYPs (Figure 2 ;Tables 2, 3 and 4).

Toxicity of both TVX and DCF has been reported to be aggravated by an inflammatory stress induced by LPS or TNF in animal models and liver cell cultures (Deng et al., 2006; Shaw et al., 2009b). Our data confirmed these observations and demonstrated that when the two drugs were combined their cytotoxicity was further aggravated by TNF. TNF has been shown to be a critical mediator for manifestation of TVX hepatotoxicity in LPS-treated mice (Shaw et al., 2007). LPS treatment of HepaRG cells also resulted in marked activation of TNF synthesis (See chapter 4). LPS and TNF induced many similarities in gene expression changes in TVX-treated rats (Liguori et al., 2010) If pro-inflammatory cytokines can induce similar changes as LPS in several cell signaling networks the endotoxin has however broader effects with more pathways impacted and more extensive perturbation of gene regulation. LPS acts partly by stimulating toll-like receptors resulting in the synthesis of various immune activators (Cosgrove et al., 2010).

Co-administration of TNF potentiated the toxicity of the two drugs as shown by increased caspases 8, 9 and 3 activation and ROS generation. Since co-addition of etanercept nearly completely abolished this additional effect it might be concluded that TNF mainly enhanced the extrinsic apoptotic pathway via activation of caspase 8.

Previous studies have shown that JNK activation contributes to cytotoxicity mediated by LPS and TNF when added with TVX (Beggs et al., 2014) or DCF (Fredriksson et al., 2011). Our data shows that co-addition of SP600125, an inhibitor of JNK activation, mostly eliminated cytotoxicity mediated by the cytokines of these two drugs alone or in combination in HepaRG cells, further supporting the major role of this signaling pathway in the hepatotoxicity of these two drugs in an inflammatory context (Maiuri et al., 2015).

If mitochondrial dysfunction and oxidative stress are two major mechanisms involved in drug-induced injuries ER stress is also becoming as an important mechanism; it can be a mitochondrial dependent or independent pathway of apoptosis (Scull and Tabas, 2011). We showed that several genes related to ER stress were overexpressed with TVX and DCF treatments and that their action was greatly increased by the combination of the two drugs and still much more with co-addition of TNF. Since up-regulation of these genes was greatly

alleviated by the antioxidant NAC, the JNK inhibitor SP600125 and the caspase 9 inhibitor z-LEHD-fmk, it might be concluded that oxidative and ER stresses mediating the mitochondrial pore transition were crucial events in apoptosis induced by these different treatments.

In vivo drug hepatotoxicity is usually aggravated after repeated administration. Interestingly, repeated co-treatment of HepaRG cells with TVX/DCF potentiated cytotoxicity that was further aggravated by co addition of TNF, suggesting a cumulating effect and consequently supporting the increasing sensitivity with repeated administration.

Both TVX and DCF are also idiosyncratic cholestatic drugs. Noteworthy, while they both transiently caused BC dilation, in combination they induced large irreversible dilations that were further increased after 3 days. This synergistic effect was associated with higher decrease of BSEP and MRP2 activities and transcripts of all tested transporters except MRP4. Co-addition of TNF did not modify BC dilation caused by the drugs either separately or in combination. However, decreased expression of transporters with pro-inflammatory cytokines agrees with previous studies (Bachour-El Azzi et al., 2014; Le Vee et al., 2009). The specific increase in MRP4 transcripts could be related to a compensatory mechanism of bile acids sinusoidal secretion following BSEP inhibition as previously described. Noteworthy, we got preliminary data supporting that like DCF and various other cholestatic drugs , TVX decreased phosphorylation of the myosin light chain 2 (MLC2) (not shown). To our knowledge, this is the first description of the increased severity of cholestatic features resulting from drug-drug interactions. The absence of potentiation by pro-inflammatory cytokines confirmed our previous observations with chlorpromazine and cyclosporine A (Bachour-El Azzi et al., 2014). Noticeably, down-regulation of CYP7A1, CYP8B1, CYP27A, 3 major CYPs involved in bile acids synthesis by DCF and TVX also supported previous reports (Makishima, 2006).

Together, our data demonstrate that hepatotoxic and cholestatic effects of DCF and TVX were enhanced in a combined treatment and increased after repeated treatment while co-addition of TNF-α potentiated only cytotoxicity. These data bring further insights in drug-drug interactions and the influence of an inflammatory stress in the occurrence of drug-induced hepatotoxicity.

.

References

Abdel-Razzak, Z., Loyer, P., Fautrel, A., Gautier, J.C., Corcos, L., Turlin, B., Beaune, P., Guillouzo, A., 1993. Cytokines down-regulate expression of major cytochrome P-450 enzymes in adult human hepatocytes in primary culture. Molecular pharmacology 44, 707-715.

Actis, G.C., Pellicano, R., Fadda, M., Rosina, F., 2014. Antibiotics and non-steroidal anti-inflammatory drugs in outpatient practice: indications and unwanted effects in a gastroenterological setting. Current drug safety 9, 133-137.

Al-Attrache, H., Sharanek, A., Burban, A., Burbank, M., Gicquel, T., Abdel-Razzak, Z., Guguen-Guillouzo, C., Morel, I., Guillouzo, A., 2016. Differential sensitivity of metabolically competent and non-competent HepaRG cells to apoptosis induced by diclofenac combined or not with TNF-alpha. Toxicology letters 258, 71-86.

Aninat, C., Piton, A., Glaise, D., Le Charpentier, T., Langouet, S., Morel, F., Guguen-Guillouzo, C., Guillouzo, A., 2006. Expression of cytochromes P450, conjugating enzymes and nuclear receptors in human hepatoma HepaRG cells. Drug metabolism and disposition: the biological fate of chemicals 34, 75-83.

Antherieu, S., Bachour-El Azzi, P., Dumont, J., Abdel-Razzak, Z., Guguen-Guillouzo, C., Fromenty, B., Robin, M.A., Guillouzo, A., 2013. Oxidative stress plays a major role in chlorpromazine-induced cholestasis in human HepaRG cells. Hepatology 57, 1518-1529.

Bachour-El Azzi, P., Sharanek, A., Abdel-Razzak, Z., Antherieu, S., Al-Attrache, H., Savary, C.C., Lepage, S., Morel, I., Labbe, G., Guguen-Guillouzo, C., Guillouzo, A., 2014. Impact of inflammation on chlorpromazine-induced cytotoxicity and cholestatic features in HepaRG cells. Drug metabolism and disposition: the biological fate of chemicals 42, 1556-1566.

Banks, A.T., Zimmerman, H.J., Ishak, K.G., Harter, J.G., 1995. Diclofenac-associated hepatotoxicity: analysis of 180 cases reported to the Food and Drug Administration as adverse reactions. Hepatology 22, 820-827.

Beggs, K.M., Fullerton, A.M., Miyakawa, K., Ganey, P.E., Roth, R.A., 2014. Molecular mechanisms of hepatocellular apoptosis induced by trovafloxacin-tumor necrosis factor-alpha interaction. Toxicological sciences : an official journal of the Society of Toxicology 137, 91-101.

Beggs, K.M., Maiuri, A.R., Fullerton, A.M., Poulsen, K.L., Breier, A.B., Ganey, P.E., Roth, R.A., 2015. Trovafloxacin-induced replication stress sensitizes HepG2 cells to tumor necrosis factor-alpha-induced cytotoxicity mediated by extracellular signal-regulated kinase and ataxia telangiectasia and Rad3-related. Toxicology 331, 35-46.

Bjornsson, E., Olsson, R., 2006. Suspected drug-induced liver fatalities reported to the WHO database. Digestive and liver disease : official journal of the Italian Society of Gastroenterology and the Italian Association for the Study of the Liver 38, 33-38.

Breen, E.G., McNicholl, J., Cosgrove, E., McCabe, J., Stevens, F.M., 1986. Fatal hepatitis associated with diclofenac. Gut 27, 1390-1393.

Cerec, V., Glaise, D., Garnier, D., Morosan, S., Turlin, B., Drenou, B., Gripon, P., Kremsdorf, D., Guguen-Guillouzo, C., Corlu, A., 2007. Transdifferentiation of hepatocyte-like cells from the human hepatoma HepaRG cell line through bipotent progenitor. Hepatology 45, 957-967.

Cosgrove, B.D., Alexopoulos, L.G., Hang, T.C., Hendriks, B.S., Sorger, P.K., Griffith, L.G., Lauffenburger, D.A., 2010. Cytokine-associated drug toxicity in human hepatocytes is associated with signaling network dysregulation. Molecular bioSystems 6, 1195-1206.

Cosgrove, B.D., King, B.M., Hasan, M.A., Alexopoulos, L.G., Farazi, P.A., Hendriks, B.S., Griffith, L.G., Sorger, P.K., Tidor, B., Xu, J.J., Lauffenburger, D.A., 2009. Synergistic drug-cytokine induction of hepatocellular death as an in vitro approach for the study of inflammation-associated idiosyncratic drug hepatotoxicity. Toxicology and applied pharmacology 237, 317-330.

Dalvie, D.K., Khosla, N., Vincent, J., 1997. Excretion and metabolism of trovafloxacin in humans. Drug metabolism and disposition: the biological fate of chemicals 25, 423-427.

Deng, X., Stachlewitz, R.F., Liguori, M.J., Blomme, E.A., Waring, J.F., Luyendyk, J.P., Maddox, J.F., Ganey, P.E., Roth, R.A., 2006. Modest inflammation enhances diclofenac hepatotoxicity in rats: role of neutrophils and bacterial translocation. The Journal of pharmacology and experimental therapeutics 319, 1191-1199.

Dumont, J., Josse, R., Lambert, C., Antherieu, S., Le Hegarat, L., Aninat, C., Robin, M.A., Guguen-Guillouzo, C., Guillouzo, A., 2010. Differential toxicity of heterocyclic aromatic amines and their mixture in metabolically competent HepaRG cells. Toxicology and applied pharmacology 245, 256-263.

Fredriksson, L., Herpers, B., Benedetti, G., Matadin, Q., Puigvert, J.C., de Bont, H., Dragovic, S., Vermeulen, N.P., Commandeur, J.N., Danen, E., de Graauw, M., van de Water, B., 2011. Diclofenac inhibits tumor necrosis factor-alpha-induced nuclear factor-kappaB activation causing synergistic hepatocyte apoptosis. Hepatology 53, 2027-2041.

Fredriksson, L., Wink, S., Herpers, B., Benedetti, G., Hadi, M., de Bont, H., Groothuis, G., Luijten, M., Danen, E., de Graauw, M., Meerman, J., van de Water, B., 2014. Drug-induced endoplasmic reticulum and oxidative stress responses independently sensitize toward TNFalpha-mediated hepatotoxicity. Toxicological sciences : an official journal of the Society of Toxicology 140, 144-159.

Fujiwara, R., Sumida, K., Kutsuno, Y., Sakamoto, M., Itoh, T., 2015. UDP-glucuronosyltransferase (UGT) 1A1 mainly contributes to the glucuronidation of trovafloxacin. Drug metabolism and pharmacokinetics 30, 82-88.

Guillouzo, A., Corlu, A., Aninat, C., Glaise, D., Morel, F., Guguen-Guillouzo, C., 2007. The human hepatoma HepaRG cells: a highly differentiated model for studies of liver metabolism and toxicity of xenobiotics. Chemico-biological interactions 168, 66-73.

Lazarczyk, D.A., Goldstein, N.S., Gordon, S.C., 2001. Trovafloxacin hepatotoxicity. Digestive diseases and sciences 46, 925-926.

Le Vee, M., Lecureur, V., Stieger, B., Fardel, O., 2009. Regulation of drug transporter expression in human hepatocytes exposed to the proinflammatory cytokines tumor necrosis factor-alpha or interleukin-6. Drug metabolism and disposition: the biological fate of chemicals 37, 685-693.

Liguori, M.J., Blomme, E.A., Waring, J.F., 2008. Trovafloxacin-induced gene expression changes in liver-derived in vitro systems: comparison of primary human hepatocytes to HepG2 cells. Drug metabolism and disposition: the biological fate of chemicals 36, 223-233.

Liguori, M.J., Ditewig, A.C., Maddox, J.F., Luyendyk, J.P., Lehman-McKeeman, L.D., Nelson, D.M., Bhaskaran, V.M., Waring, J.F., Ganey, P.E., Roth, R.A., Blomme, E.A., 2010. Comparison of TNFalpha to lipopolysaccharide as an inflammagen to characterize the idiosyncratic hepatotoxicity potential of drugs: Trovafloxacin as an example. International journal of molecular sciences 11, 4697-4714.

Lucena, M.I., Andrade, R.J., Rodrigo, L., Salmeron, J., Alvarez, A., Lopez-Garrido, M.J., Camargo, R., Alcantara, R., 2000. Trovafloxacin-induced acute hepatitis. Clinical infectious diseases : an official publication of the Infectious Diseases Society of America 30, 400-401.

Maianski, N.A., Roos, D., Kuijpers, T.W., 2004. Bid truncation, bid/bax targeting to the mitochondria, and caspase activation associated with neutrophil apoptosis are inhibited by granulocyte colony-stimulating factor. Journal of immunology 172, 7024-7030.

Maiuri, A.R., Breier, A.B., Gora, L.F., Parkins, R.V., Ganey, P.E., Roth, R.A., 2015. Cytotoxic Synergy Between Cytokines and NSAIDs Associated With Idiosyncratic Hepatotoxicity Is Driven by Mitogen-Activated Protein Kinases. Toxicological sciences : an official journal of the Society of Toxicology 146, 265-280.

Makishima, M., 2006. Nuclear receptors sense bile acid metabolism: A hormonal action of bile acids Functional and Structural Biology on the Lipo-network, 17-35.

Ostapowicz, G., Fontana, R.J., Schiodt, F.V., Larson, A., Davern, T.J., Han, S.H., McCashland, T.M., Shakil, A.O., Hay, J.E., Hynan, L., Crippin, J.S., Blei, A.T., Samuel, G., Reisch, J., Lee, W.M., Group, U.S.A.L.F.S., 2002. Results of a prospective study of acute liver failure at 17 tertiary care centers in the United States. Annals of internal medicine 137, 947-954.

Qureshi, Z.P., Seoane-Vazquez, E., Rodriguez-Monguio, R., Stevenson, K.B., Szeinbach, S.L., 2011. Market withdrawal of new molecular entities approved in the United States from 1980 to 2009. Pharmacoepidemiology and drug safety 20, 772-777.

Scull, C.M., Tabas, I., 2011. Mechanisms of ER stress-induced apoptosis in atherosclerosis. Arteriosclerosis, thrombosis, and vascular biology 31, 2792-2797.

Sharanek, A., Azzi, P.B., Al-Attrache, H., Savary, C.C., Humbert, L., Rainteau, D., Guguen-Guillouzo, C., Guillouzo, A., 2014. Different dose-dependent mechanisms are involved in early cyclosporine a-induced cholestatic effects in hepaRG cells. Toxicological sciences : an official journal of the Society of Toxicology 141, 244-253.

Sharanek, A., Burban, A., Humbert, L., Bachour-El Azzi, P., Felix-Gomes, N., Rainteau, D., Guillouzo, A., 2015. Cellular Accumulation and Toxic Effects of Bile Acids in Cyclosporine A-Treated HepaRG Hepatocytes. Toxicological sciences : an official journal of the Society of Toxicology 147, 573-587.

Shaw, P.J., Ganey, P.E., Roth, R.A., 2009. Trovafloxacin enhances the inflammatory response to a Gram-negative or a Gram-positive bacterial stimulus, resulting in neutrophil-dependent liver injury in mice. The Journal of pharmacology and experimental therapeutics 330, 72-78.

Shaw, P.J., Hopfensperger, M.J., Ganey, P.E., Roth, R.A., 2007. Lipopolysaccharide and trovafloxacin coexposure in mice causes idiosyncrasy-like liver injury dependent on tumor necrosis factor-alpha. Toxicological sciences : an official journal of the Society of Toxicology 100, 259-266.

Shen, S., Marchick, M.R., Davis, M.R., Doss, G.A., Pohl, L.R., 1999. Metabolic activation of diclofenac by human cytochrome P450 3A4: role of 5-hydroxydiclofenac. Chemical research in toxicology 12, 214-222.

Tang, W., Stearns, R.A., Wang, R.W., Chiu, S.H., Baillie, T.A., 1999. Roles of human hepatic cytochrome P450s 2C9 and 3A4 in the metabolic activation of diclofenac. Chemical research in toxicology 12, 192-199.

Tayem, Y.I., Qubaja, M.M., Shraim, R.K., Taha, O.B., Abu Shkheidem, I.A., Ibrahim, M.A., 2013. Non-steroidal anti-inflammatory drugs and antibiotics prescription trends at a central west bank hospital. Sultan Qaboos University medical journal 13, 567-573.

Uetrecht, J., 2006. Evaluation of which reactive metabolite, if any, is responsible for a specific idiosyncratic reaction. Drug metabolism reviews 38, 745-753.

Watanabe, N., Takashimizu, S., Kojima, S., Kagawa, T., Nishizaki, Y., Mine, T., Matsuzaki, S., 2007. Clinical and pathological features of a prolonged type of acute intrahepatic cholestasis. Hepatology research : the official journal of the Japan Society of Hepatology 37, 598-607.

Westerink, W.M., Schoonen, W.G., 2007a. Cytochrome P450 enzyme levels in HepG2 cells and cryopreserved primary human hepatocytes and their induction in HepG2 cells. Toxicology in vitro : an international journal published in association with BIBRA 21, 1581-1591.

Westerink, W.M., Schoonen, W.G., 2007b. Phase II enzyme levels in HepG2 cells and cryopreserved primary human hepatocytes and their induction in HepG2 cells. Toxicology in vitro : an international journal published in association with BIBRA 21, 1592-1602.

Willis, J.V., Kendall, M.J., Flinn, R.M., Thornhill, D.P., Welling, P.G., 1979. The pharmacokinetics of diclofenac sodium following intravenous and oral administration. European journal of clinical pharmacology 16, 405-410.

Chapitre IV. N-acétylcysteine empêche l'induction de la cytotoxicité et la stéatose hépatique par l'amiodarone ainsi que leur aggravation par le stress inflammatoire

Résumé

En plus d'une phospholipidose, l'amiodarone, un médicament cationique amphiphile, peut induire une stéatose chez un petit nombre de patients traités, pouvant conduire à une stéatohépatite suite à une administration chronique. Le but de ce travail était d'évaluer l'influence de co-traitements aigus et répétés de l'amiodarone avec le lipolysaccharide (LPS) sur l'induction de la cytotoxicité et de la stéatose, en utilisant des cellules HepaRG humaines. Nos résultats montrent qu'après 24 heures un traitement avec l'amiodarone seule provoquait une accumulation de triglycérides, une dérégulation de divers gènes, en particulier les gènes liés à la lipogenèse de novo et une diminution de l'oxydation des acides gras. En outre, après 3 traitements répétés sur une période de 7 jours, la formation de nombreuses gouttelettes lipidiques intracytoplasmiques a été mise en évidence. Le co-traitement de l'amiodarone avec le LPS aggravait ses effets cytotoxique et stéatotique après 7 jours, comme indiqué par une perte marquée de la viabilité cellulaire, une plus grande accumulation de triglycérides et de gouttelettes lipidiques, et la dérégulation de différents gènes, y compris les gènes liés à la lipogenèse. Ces perturbations étaient associées à la génération de ROS et la surexpression de gènes associés notamment nrf2 et étaient empêchés par la co-addition d'un antioxydant, la N-acétylcystéine. Les effets aggravants d'un co-traitement par LPS ont été empêchés par la co-addition de l'étanercept le récepteur p75 soluble du TNF-α. La plupart des effets de LPS ont été reproduites par le TNF-α, à des concentrations proches de celles de l'endotoxine lors du co-traitement avec l'amiodarone. En conclusion, nos données montrent clairement pour la première fois que la cytotoxicité et la stéatose induite par l'amiodarone peuvent être aggravées par un stress inflammatoire, mimant ainsi la stéatohépatite induite par le médicament, et que ces effets étaient liés à la production de ROS et empêchés par la co-addition de N-acétylcystéine.

N-acetyl cysteine prevents amiodarone-induced hepatic cytotoxicity and steatosis and their aggravation by an inflammatory stress

Abstract

In addition to phospholipidosis the cationic amphiphilic drug amiodarone can induce steatosis in a small number of treated patients, leading to steatohepatitis following chronic administration. The aim of this work was to evaluate the influence of acute and repeated co-treatments of amiodarone with lipolysaccharide (LPS) on the induction of cytotoxicity and steatosis, using human HepaRG cells. Our results show that after a 24h single treatment amiodarone caused accumulation of triglycerides, deregulation of various genes, especially genes related to *de novo* lipogenesis and decrease in fatty acid oxidation. In addition, after 3 repeated treatments over a 7-day period, formation of many intracytoplasmic lipid droplets was evidenced. Co-treatment with LPS aggravated amiodarone-induced cytotoxicity and steatosis after 7 days as shown by marked loss in cell viability, higher accumulation of triglycerides and lipid droplets, and higher deregulation of various genes including genes related to lipogenesis. These disturbances were associated with ROS generation and overproduction of related genes including nrf2 and were prevented by co-addition of the antioxidant N-acetyl cysteine. Enhanced effects resulting from LPS co-treatment were prevented by co-addition of the soluble p75 TNF receptor etanercept. Most LPS effects were reproduced with TNF-α at concentrations close to those of the endotoxin during co-treatment with amiodarone. Together, our data clearly showed for the first time that both cytotoxicity and steatosis induced by amiodarone could be aggravated by an inflammatory stress, thereby mimicking drug–induced steatohepatitis, and that these effects were related to ROS production and prevented by co-addition of N-acetyl cysteine.

Keywords: HepaRG cells, lipopolysaccaride, TNF-α, reactive oxygen species, steatosis, steatohepatitis

Abbreviations

Lipopolysaccharide, LPS; amiodarone, AMD; ROS, reactive oxygen species; MTT, methylthiazoltetrazolium; H_2-DCFDA, 2',7'-dichlorodihydrofluorescein; NAC, N-acetyl-cysteine; RT-qPCR, real-time quantitative polymerase chain reaction; CYP450, cytochrome P450; HO1, heme oxygenase 1; MnSOD, manganese superoxide dismutase; CRP, C-reactive protein.

Financial support

This work was supported by the European Community [Contract MIP-DILI-115336]. The MIP-DILI project has received support from the Innovative Medicines Initiative Joint Undertaking, resources of which are composed of financial contribution from the European Union's Seventh Framework Programme [FP7/20072013] and EFPIA companies' in kind contribution. http://www.imi.europa.eu/.
Houssein Al-Attrache, Eva Klimcakova and Ahmad Sharanek were financially supported by the MIP-DILI project.

Introduction

Hepatic steatosis is characterized by accumulation of triglycerides (TG) in hepatocytes. It represents a reversible state of metabolic dysfunction that can possibly progress to inflammatory steatohepatitis, irreversible liver damage, fibrosis, cirrhosis, and even hepatocellular carcinoma (Farrell and Larter, 2006; Reddy and Rao, 2006). The many steatogenic drugs include amiodarone (AMD), a class III antiarrhythmic drug used for both ventricular and atrial arrhythmias. AMD is associated with many adverse effects, such as thyroid dysfunction, corneal microdeposits, and pulmonary and hepatic toxicities (Vassallo and Trohman, 2007). It also causes idiosyncratic hepatotoxic reactions in 1–3% of treated patients (Heger et al., 1981; Mattar et al., 2009; Vassallo and Trohman, 2007). Lipid macrovesicles and microvesicles are the most common pathological features of hepatic lesions but steatohepatitis is also frequently associated with chronic administration (Keshavarzian et al., 2009).

AMD hepatotoxicity can be recapitulated in animal models; it appears to be dose-dependent and consistent with increased production of cholesterol and accumulation of triglycerides and intracellular lipid vesicles in hepatocytes. These disturbances have been associated with deregulation of several genes related to lipogenesis in mouse liver (Vitins et al., 2014). AMD can also cause *in vitro* excessive accumulation of triglycerides together with appearance of lipid vesicles and overexpression of several genes involved in lipogenesis as shown in human HepaRG hepatocytes (Antherieu et al., 2011).

Several mechanisms can account for potential liver injury following amiodarone use. The drug and its primary lipophilic metabolite mono-N-desethylamiodarone concentrated in mitochondria and inhibit electron transport and uncoupled oxidative phosphorylation (Waldhauser et al., 2006). In animal models as well as in human HepaRG hepatocytes amiodarone induces generation of ROS and impairs mitochondrial β-oxidation (Antherieu et al., 2011; Fromenty et al., 1990; Spaniol et al., 2001). Thus, hepatotoxicity associated with amiodarone can at least partly be explained by decreased mitochondrial β-oxidation of fatty acids and subsequent production of microvesicular steatosis and induction of apoptosis and necrosis (Fromenty et al., 1990; Kaufmann et al., 2005).

Various studies have shown that lipopolysaccharide (LPS) and pro-inflammatory cytokines, especially TNF-α, can induce and accelerate hepatic steatosis (Endo et al., 2007; Fukunishi et al., 2014) and aggravate AMD toxicity in mouse Hepa1c1c7 cells and rodent liver (Lu et al., 2012; Lu et al., 2013). LPS can also induce ROS and overexpression of oxidative stress-

related genes including nrf2. Activation of this transcriptional factor has been associated with increased hepatic steatosis (Endo et al., 2007; Fukunishi et al., 2014) but other studies have come to the opposite conclusions (Hayes and Dinkova-Kostova, 2014). ER stress is also recognized to play an important role in the development of steatosis (Kammoun et al., 2009; Pagliassotti, 2012).

To our knowledge, whether an inflammatory stress can aggravate *in vitro* AMD-induced toxicity and steatosis has not been reported. Here, we show that repeated co-treatment of human HepaRG hepatocytes with AMD and LPS led to enhanced cytotoxicity and steatosis, thereby mimicking a steatohepatitis context. These alterations were associated with increased ROS production, overexpression of genes related to lipogenesis and endoplasmic reticulum stress, decrease of fatty acid oxidation and production of TNF-α. All these effects were largely prevented by co-addition of the antioxidant NAC.

Materials and methods

Chemicals and reagents

Amiodarone (AMD), methylthiazoltetrazolium (MTT), N-Acetyl-Asp-Glu-Val-Asp-7-amido-4-Methylcoumarin (DEVD-AMC) and N-acetyl-cysteine (NAC) were purchased from Sigma Aldrich (St. Quentin Fallavier, France). 2',7'-Dichlorodihydrofluorescein (H2-DCFDA) was from Invitrogen Molecular Probe (Cergy-Pontoise, France). LPS was provided by Promocell (Nuremberg, Germany). CRP kit was from R&D (Abingdon, United Kingdom) and Triglyceride (TG) kits from CliniSciences Biovision (Nanterre, France). Etanercept was obtained from Amgen (Thousand Oaks, CA, USA) and [14C]-palmitic acid from Perkin Elmer (Boston, MA).

Cell cultures and treatments

HepaRG cell cultures

HepaRG cells were seeded at a density of 2.6×10^4 cells/cm^2 in Williams' E medium supplemented with 10 % Hyclone® fetal bovine serum (HFBS) (Thermo scientific, San Jose, USA), 100 U/mL penicillin, 100 µg/mL streptomycin, 5 µg/mL insulin, 2 mM glutamine, and 50 µM hydrocortisone hemisuccinate. After 2 weeks, these cells were shifted to the same medium supplemented with 1.7% dimethyl sulfoxide for further 2 weeks in order to obtain

mature hepatocytes. At that time, cultures contained hepatocyte-like and progenitors/primitive biliary-like cells at around equal proportions (Cerec et al., 2007).

Treatments

All treatments were performed on cells maintained in a medium containing 2% HFBS and 1% dimethyl sulfoxide (used as a vehicle) instead of 10 and 2% respectively, as previously (Antherieu et al., 2011), to reduce their protective activity, especially their antioxidant properties. The selection of non cytotoxic LPS concentrations (0.01µg/ml and 1µg/ml) was based on previous studies (Aninat et al., 2008; Sharifnia et al., 2014) and preliminary experiments on determination of caspase 3 activity and CRP secretion levels. Cells were treated with AMD or LPS separately, or with a combination of AMD and LPS following a pre-treatment with LPS for 24h. Similarly, when they were co-exposed to NAC this anti-oxidant was first added 24h before AMD and/or LPS. The cells were treated for either 24h (one addition) or 7 days (addition every 2-3 days).

MTT cytotoxicity assay

Cytotoxicity was evaluated using the MTT colorimetric assay. Briefly, cells were seeded in 24-well plates and treated with LPS or various concentrations of AMD (5, 20 or 50µM) after pre-treatment with LPS. After medium removal, 500µl of serum-free medium containing MTT (0.5 mg/ml) was added to each well and incubated for 2h at 37°C. The water-insoluble formazan was dissolved in 500µl dimethyl sulfoxide and absorbance was measured at 550nm (Aninat et al., 2006).

Determination of caspase 3 activity

After treatment with AMD ± LPS, the cells were scrapped in the culture medium, then centrifuged, washed with PBS, dried and stored at – 80°C. Cell lysates were re-suspended in 70µl of 4-(2-hydroxyethyl)-1-piperazine ethane sulfonic acid supplemented with anti-phosphatase and anti-protease. Then, 40 µg of protein of each sample was placed in an opaque plate in triplicate and supplemented with caspase buffer (20 mM piperazine-1,4-bis-2-ethanesulfonic acid, pH 7.2, 100 mM NaCl, 10mM dithiotreitol, 1mM EDTA, 0.1% 3-[(3-cholamidopropyl)dimethylammonio)-1-propanesulfonic acid] and 10% sucrose. Then 2 µl of DEVD-AMC was added. Fluorescence was measured at a wavelength between 380 and 420 nm (Dumont et al., 2010).

Phase-contrast imaging analysis

Cells were treated with AMD ± LPS for 24h or 7 days and images were taken using a phase-contrast microscope (Inverted microscope Zeiss axiovert 200M and Axiocam MRm).

ELISA assays

C-reactive protein (CRP) and TNF-α protein were measured in cell supernatants using CRP and TNF-α DuoSet kits, according to manufacturer's instructions. Briefly, supernatants were collected after 24h or 7 days treatments and stored at -80°C until analysis; 96-well microplates were coated with capture antibody and incubated overnight. Samples and standards were diluted appropriately and added for 2h after a saturation step. Secondary antibody was added for 2h after washing. Streptavidin-horseradish peroxidase and its substrate were used for the revelation step. Optical density was read at 450nm with wavelength correction. All steps were performed at room temperature (Bachour-El Azzi et al., 2014).

Real-Time Quantitative Polymerase Chain Reaction (RT-qPCR) analysis

Total RNA was extracted from 10^6 HepaRG cells with the SV total RNA isolation system (Promega, Charbonnieres-les-Bains, France). RNAs were reverse-transcribed into cDNA and RT-qPCR was performed using a SYBR Green mix. Primer sequences are listed in Table 1.

Gene	Name	Forward Primer	Reverse Primer
ACLY	ATP-citrate synthase	AAGGAGTTCTTTGCCCGTCT	GATTTTGCGGGGTTCGTC
ADFP	Adipose differentiation-related protein	CTCATGGGTAGAGTGGAAAAGGAGCATTGG	TTGGATGTTGGACAGGAGGGTGTGGCACGT
ALB	Albumin	TGCTTGAATGTGCTGATGACAGG	AAGGCAAGTCAGCAGGCATCTCATC
ALDB	Aldolase B	GCATCTGTCAGCAGAATGGA	TAGACAGCAGCCAGGACCTT
ASML3A	Acid sphingomyelinase-like phosphodiesterase 3a	CAGAACATCTCCAAAAGGGC	AATCCTCCTCCGGCGATAG
ATF4	Activating Transcription Factor 4	TGGCATGGTTTCCAGGTCATCT	CCAACAACAGCAAGGAGGATGC
ATF6	Activating Transcription Factor 6	CTGCACCCACTAAAGGCCAGA	GAGGGCAGAACTCCAGGTGCT
CAR	Constitutive androstane receptor	TGATCAGCTGCAAGAGGAGA	AGGCCTAGCAACTTCGCATA
Cas3	Caspase 3	CAAAGATCATACATGGAAGCG	TGAAAAGTTTGGGTTTTCCAG
CHOP	C/Ebp-Homologous protein	ATGGCAGCTGAGTCATT	AGAAGCAGGGTCAAGAGTGGT
CPT1A	Carnitine O-palmitoyltransferase 1	GCCTCGTATGTGAGGCAAAA	TCATCAAGAAATGTCGCACG
CRP	C-Reactive Protein	GAACTTTCAGCCGAATACATCTTTT	CCTTCCTCGACATGTCTGTCT
CYP2E1	Cytochrome P450 2E1	TTGAAGCCTCTCGTTGACCC	CGTGGTGGGATACAGCCAA
CYP3A4	Cytochrome P450 3A4	CTTCATCCAATGGACTGCATAAAT	TCCCAAGTATAACACTCTACACAGACAA
FASN	Fatty acid synthase	AACTCCTGCAAGTTCTCCGA	GCTCCAGCCTCGCTCTC
GDPD3	Glycerophosphodiester phosphodiesterase domain containing 3	GCTGAAGGCTGCTTCAAAAT	GTGGTTTCGAAATGGCTGAT
GRP78	Glucose Regulated Protein,78KD	GTTCTTGCCGTTCAAGGTGG	TGGTACAGTAACAACTGCATG
GSTA1/2	Glutathione S-Transferase A1/2	TGCAACAATTAAGTGCTTTACCTAAGTG	TTAACTAAGTGGGTGAATAGGAGTTGTATT
GSTM1	Glutathione S-Transferase M1	ATGGTTGTCCAGGTCTGG	CGCCATCTTGTGCTACATT
HO-1	Heme oxygenase 1	ACTTTCAGAAGGGCCAGGT	TTGTTGCGCTCAATCTCCT
LPIN1	Lipin-1	GATGTCAATGCACCCTGAGA	GTGTTTGCAATACAAAGGCG
LPL	Lipoprotein lipase	AATGAGGTGGCAAGTGTCCT	CTCCAGAGTCTGACCGCCT
LSS	Lanosterol synthase	TATTTCCACAAGCGTTTCCC	TGAAGCAAACTCCCCAGG
MnSOD	Manganese superoxide dismutase	GGGTTGGCTTGGTTTCAATA	CTGATTTGGACAAGCAGCAA
Nrf2	NF-E2-Related Factor 2		
PGC1α	Peroxisome proliferator-activated receptor gamma coactivator 1-alpha	CTGCTAGCAAGTTTGCCTCA	AGTGGTGCAGTGACCAATCA
PLIN4	Perilipin-4	CAGATGCAGGAAGCATCAAA	GCGACTAAAAGGCACTCTGG
PXR	Pregnane X receptor	CCAGGACATACACCCCTTTG	CTACCTGTGATGCCGAACAA
SCD1	Acyl-CoA desaturase	GACGATGAGCTCCTGCTGTT	CTCTGCTACACTTGGGAGCC

Gene	Name	Forward Primer	Reverse Primer
SLC27A4	Long-chain fatty acid transport protein 4	CCTCCTTCCGTAGCTCTGTC	GAAGGAACTGCCCCTGTATG
SOAT1	Sterol O-acyltransferase 1	ATTCCTCTGCCTCTGCTGTC	GCTGTCAAAGTCCAGGGAAA
SREBP1	Sterol regulatory element-binding protein 1	AGGGAAGTCACTGTCTTGGTTG	CTGCTGACCGACATCGAA
TBP	TATA Box Binding Protein	GAGAGTTCTGGGATTGTACCG	ATCCTCATGATTACCGCAGC
THRSP	Thyroid hormone-inducible hepatic protein	AGGCCTTTCTGCTCTCATCA	AAATGACGGGACAAGTTTGG
TNF-α	Tumor Necrosis Factor-α	TGGCCAATGGCATGGAT	TCCTGGTATGAAGTGGCAAAT

Table 1: List of primers.

Determination of ROS generation

ROS generation was determined by the H_2-DCFDA assay. After treatment with AMD ± LPS, cells were incubated for 2h at 37°C with 2µM H_2-DCFDA and then washed with cold PBS, and scraped in potassium buffer (10mM, pH 7.4) / methanol (v/v) complemented with Triton X-100 (0.1%). Fluorescence intensity of cell lysates was determined by spectrofluorimetry using excitation/emission wavelengths of 498/520 nm (Sharanek et al., 2014).

Red oil Staining

Lipid accumulation was determined by red oil staining which allows detection of TG. Red oil was dissolved in isopropanol (0.5:100) for stock solution. After treatments, cells were washed with phosphate buffered saline, incubated for 1 hour with red oil saturated solution (isopropanol : water, 3:2), washed in water, and observed under a phase-contrast microscope (Antherieu et al., 2011).

Triglycerides quantification

After treatment for 24 h or 7 days, samples were scrapped, collected in NP-40 buffer and stored at -80°C until analysis. For triglyceride quantification these samples were distributed in duplicate in 96 well plates after a 1:4 dilution in distilled water. The final volume was adjusted to 50µl with the triglyceride assay buffer and 2µl of lipase was added to each well followed by 50µl of the triglyceride reaction mix **[**triglyceride quantification colorimetric/fluorometric kit (BioVision; catalog#k622-100)]. Finally, absorbance was measured at 570nm after a 60 min incubation at room temperature.

Fatty acid oxidation

After treatment the culture medium was removed and replaced with a fresh medium containing 0.5 mM L-carnitine and 10% fat-free bovine serum albumin. [U- ^{14}C]-palmitic acid (final concentration, 1 mM; 0.05 µCi/ml) was added, and the reaction was carried out for 90 min at 37°C. After addition of perchloric acid (final concentration, 3%) and centrifugation at 4000g for 10 min, an aliquot of the supernatant was counted for [^{14}C]-labeled acid-soluble β-oxidation products (Antherieu et al., 2011).

Statistical analysis

One-way ANOVA with Bonferroni's multiple comparison test (GraphPad Prism 5.00) was performed to compare data between AMD, LPS (or pro-inflammatory cytokines), AMD + LPS (or pro-inflammatory cytokines)-treated cells and control cultures. Each value corresponded to the mean ± standard error of the mean (SEM) of at least three independent experiments. Data were considered significantly different when $p < 0.05$.

Results

Lipopolysaccharide aggravates amiodarone-induced cytotoxicity

Preliminary experiments were performed to confirm the responsiveness of HepaRG cells to the two concentrations of endotoxin by measurement of transcript and secreted protein levels of CRP. Transcript levels were strongly increased, i.e 196.53- and 282.15-fold after 24h and 279.23- and 561.14-fold after 7 days with 0.01 and 1µg/ml endotoxin treatment respectively (Tables 2 and 3). Similarly, secreted protein levels assayed by ELISA increased up to 188.66- and 273.15-fold after 24h and 252.14- and 534.38-fold after 7 days with 0.01 and 1µg/ml endotoxin respectively (Figure 1A and B). Co-treatment with AMD did not affect CRP transcript and protein levels at both time-points.

	AMD (10µM)	AMD (20µM)	LPS (0.01µg/m)	AMD (10µM)+ LPS (0.01µg/ml)	AMD (20µM)+ LPS (0.01µg/ml)	LPS (1µg/ml)	AMD (10µM)+ LPS (1µg/ml)	AMD (20µM)+ LPS (1µg/ml)
Fatty acid transport and very low-density lipoprotein synthesis								
SLC27A4	1.29±0.26	1.68±0.28*	1.18±0.26	1.20±0.18	1.86±0.19*	1.12±0.17	1.28±0.15	1.99±0.33*
Fatty acid oxidation and mitochondrial biogenesis								
CPT1A	0.99±0.22	1.24±0.16	1.23±0.25	0.92±0.35	1.00±0.24	0.88±0.12	0.88±0.10	**1.72±0.14***
PGC1α	1.43±0.26	2.69±0.26*	0.87±0.16	1.43±0.08	2.18±0.26*	1.04±0.23	0.96±0.15	2.38±0.17*
De novo lipogenesis								
ACLY	1.75±0.23	1.47±0.05	1.52±0.08	**2.22±0.52***	**2.63±0.31****	1.65±0.16	**2.18±0.25***	**2.22±0.59***
FASN	1.38±0.17	1.29±0.28	1.25±0.25	1.21±0.30	**1.89±0.10***	1.16±0.24	**1.96±0.16***	**2.52±0.67***
SCD1	2.31±0.63*	2.12±0.41*	0.90±0.18	2.36±0.47*	2.52±0.14*	0.69±0.24	2.04±0.15*	2.76±0.15*
SREBP1	1.71±0.39	2.11±0.37*	0.93±0.04	1.63±0.43	2.00±0.22*	0.81±0.14	1.51±0.23	1.74±0.08*
THRSP	1.81±0.52	2.46±0.54*	0.36±0.11*	0.94±0.28	**0.65±0.20**	0.12±0.03**	**0.39±0.03**	**0.52±0.11**
Cholesterol and glycero-lipid metabolism								
LPIN1	1.32±0.30	2.12±0.39*	0.92±0.24	1.35±0.16	1.64±0.22	0.80±0.12	1.19±0.18	1.48±0.22
LSS	1.51±0.36	2.39±0.27*	1.23±0.16	**2.21±0.35***	2.85±0.23*	1.16±0.19	**2.24±0.28***	**3.47±0.26****
SOAT1	1.06±0.11	1.68±0.22	1.13±0.07	1.48±0.19	1.86±0.09*	1.32±0.16	1.58±0.17	2.27±0.37*
Lipid hydrolysis and formation of droplets								
ADFP	1.22±0.17	1.72±0.34*	0.92±0.11	1.67±0.47	1.78±0.26*	0.84±0.02	**1.95±0.20***	**2.57±0.44****
LPL	1.39±0.25	1.96±0.08*	1.20±0.17	1.73±0.30	2.19±0.56*	1.34±0.20	**1.85±0.05***	**2.93±0.36****
PLIN4	1.10±0.09	2.26±0.13**	1.80±0.17*	1.48±0.48	2.46±0.55*	1.66±0.28	**2.48±0.45****	3.00±0.55**

	AMD (10µM)	AMD (20µM)	LPS (0.01µg/m)	AMD (10µM)+ LPS (0.01µg/ml)	AMD (20µM)+ LPS (0.01µg/ml)	LPS (1µg/ml)	AMD (10µM)+ LPS (1µg/ml)	AMD (20µM)+ LPS (1µg/ml)
Degradation of phospholipids								
ASML3A	1.06±0.24	1.19±0.31	0.87±0.12	1.03±0.27	0.96±0.20	0.63±0.14*	0.91±0.22	0.98±0.24
GDPD3	1.07±0.16	1.39±0.20	1.11±0.03	1.23±0.12	1.38±0.19	1.11±0.12	**1.77±0.09***	1.92±0.15*
Cytochromes P450 and other genes related to metabolism								
CAR	0.82±0.25	0.72±0.21	0.47±0.12***	**0.31±0.09*****	**0.37±0.10*****	0.24±0.12***	**0.32±0.19*****	**0.37±0.13*****
CYP2E1	0.76±0.27	0.27±0.10*	2.54±0.49*	**3.16±0.31*****	0.95±0.13	2.04±0.30	**1.85±0.11**	**1.11±0.21**
CYP3A4	1.22±0.49	1.85±0.18*	0.13±0.09*	**0.21±0.11***	**0.29±0.09***	0.07±0.03**	**0.09±0.04****	**0.19±0.06***
PXR	1.16±0.34	0.79±0.24	0.97±0.27	0.82±0.19*	0.93±0.26	0.78±0.16*	0.79±0.10*	0.88±0.16*
Liver-specific proteins								
ALB	0.93±0.15	0.84±0.11	0.76±0.21	0.88±0.10	0.78±0.07*	0.89±0.07	0.85±0.17	0.76±0.16*
ALDB	0.82±0.15	0.92±0.13	0.94±0.04	0.90±0.07	0.88±0.14	0.92±0.06	0.95±0.17	0.89±0.07
Markers of oxidative stress								
GSTA1/2	1.15±0.28	1.41±0.19	0.78±0.13	0.84±0.11	0.35±0.10	0.48±0.04	0.32±0.06	0.20±0.04
GSTM1	1.12±0.06	0.96±0.13	0.77±0.09**	**0.74±0.21***	**0.56±0.06*****	0.66±0.09**	0.81±0.18	**0.50±0.19*****
HO-1	1.02±0.13	1.09±0.23	1.16±0.25	1.14±0.62	**1.58±0.10***	1.28±0.36	1.47±0.08	**2.22±0.59****
MnSOD	1.03±0.05	1.62±0.22	3.67±0.25*	**5.50±0.68****	**5.51±0.86****	5.53±1.07**	**5.93±0.80****	**9.30±1.03*****
Nrf2	1.32±0.18	1.49±0.11	1.54±0.17	1.94±0.16*	**2.19±0.10****	1.75±0.11*	**2.33±0.14****	**2.76±0.19*****
Markers of endoplasmic reticulum stress								
ATF4	0.83±0.18	0.88±0.15	0.97±0.22	0.86±0.07	1.38±0.04	0.91±0.28	1.11±0.13	**2.17±0.14*****
ATF6	1.25±0.15	1.52±0.24	1.16±0.10	1.23±0.06	0.94±0.19	1.24±0.10	0.89±0.12	1.61±0.07*
CHOP	1.41±0.27	2.35±0.26*	1.42±0.12	1.53±0.14	2.55±0.11**	0.93±0.39	1.53±0.19	**3.13±0.16*****
GRP78	1.18±0.06	1.01±0.15	1.53±0.04	2.32±0.19*	2.59±0.22*	1.78±0.37	2.76±0.09**	**3.19±0.18*****
Markers of inflammation								
CRP	1.17±0.19	1.23±0.15	196.53±8.32***	**200.35±7.15****	**202.51±10.19*****	282.15±6.14***	**286.16±9.23*****	**281.59±8.13*****
TNF-α	1.18±0.07	0.81±0.12	93.2±3.75***	**96.22±5.03*****	**92.61±3.89*****	106.22±4.71***	**107.7±6.77*****	**110.50±5.39*****

	AMD (10µM)	AMD (20µM)	LPS (0.01µg/m)	AMD (10µM)+ LPS (0.01µg/ml)	AMD (20µM)+ LPS (0.01µg/ml)	LPS (1µg/ml)	AMD (10µM)+ LPS (1µg/ml)	AMD (20µM)+ LPS (1µg/ml)
Markers of toxicity								
Cas3	1.07±0.21	1.19±0.23	1.35±0.57	0.79±0.28	0.94±0.26	0.92±0.07	0.84±0.33	0.81±0.24
Others								
ACACA	1.50±0.14	1.81±0.13*	1.36±0.08	1.38±0.15	1.07±0.10	1.20±0.19	1.09±0.13	1.55±0.14
CD36(FA	1.61±0.10	1.89±0.16*	0.76±0.18	0.73±0.13	**0.45±0.14****	0.69±0.24	**0.64±0.13**	**0.52±0.14***
HSP70	1.54±0.15	1.09±0.06	0.99±0.16	1.14±0.16	1.04±0.11	0.97±0.08	**0.79±0.12***	**0.66±0.19****
PKLR	1.15±0.25	0.73±0.19*	0.39±0.11**	**0.48±0.14****	**0.39±0.05****	0.28±0.07***	**0.33±0.02****	**0.27±0.12*****
TRIB3	2.12±0.12**	2.89±0.13**	1.07±0.17	1.96±0.11*	2.93±0.08**	1.32±0.06	2.59±0.12**	3.35±0.28***

Table 2: Effects of DCF and LPS on expression of various genes (by RT-PCR) related to drug metabolism, oxidative stress, fatty acid synthase and toxicity after 24 h. All results are expressed relative to the levels found in control cells, arbitrarily set at a value of 1. *P<0.05, **P<0.01 and ***P<0.001 compared with untreated cells, "bold character" when P<0.05 compared with cells treated with LPS and AMD individually.

	AMD (10µM)	AMD (20µM)	LPS (0.01µg/ml)	AMD (10µM)+ LPS (0.01µg/ml)	AMD (20µM)+ LPS (0.01µg/ml)	LPS (1µg/ml)	AMD (10µM)+ LPS (1µg/ml)
Fatty acid transport and very low-density lipoprotein synthesis							
SLC27A4	1.03±0.23	1.64±0.13*	1.06±0.14	0.93±0.10	1.59±0.02*	1.03±0.17	1.45±0.15
Fatty acid oxidation and mitochondrial biogenesis							
CPT1A	0.68±0.15*	0.98±0.15	0.76±0.12*	1.02±0.39	0.80±0.22	0.62±0.16*	0.68±0.20
PGC1α	1.58±0.16	1.78±0.14*	0.73±0.16	1.38±0.29	1.79±0.15*	1.14±0.23	1.75±0.21*
De novo lipogenesis							
ACLY	1.10±0.19	1.20±0.19	1.22±0.27	1.40±0.22	0.99±0.16	1.09±0.21	1.39±0.14
FASN	1.11±0.33	1.19±0.26	1.19±0.32	1.55±0.17	1.59±0.21	1.15±0.15	**1.68±0.13***
SCD1	1.79±0.28	1.80±0.26	1.12±0.22	1.33±0.28	1.56±0.12	0.52±0.13	1.38±0.12
SREBP1	1.32±0.22	1.62±0.16	0.84±0.23	1.17±0.07	1.08±0.18	0.87±0.26	1.27±0.16
THRSP	1.83±0.30	2.26±0.39*	0.61±0.07*	1.30±0.37	1.35±0.18	**0.27±0.09****	**0.68±0.20**
Cholesterol and glycerol-lipid metabolism							
LPIN1	1.19±0.21	1.01±0.21	0.81±0.24	1.18±0.13	1.21±0.23	0.74±0.16	1.22±0.17
LSS	1.40±0.15	1.35±0.20	1.18±0.23	1.85±0.18	1.79±0.23	1.30±0.14	**2.43±0.37****
SOAT1	1.06±0.20	1.39±0.27	1.12±0.11	1.17±0.19	1.82±0.11*	1.20±0.16	1.70±0.07*
Lipid hydrolysis and formation of droplets							
ADFP	1.25±0.32	1.83±0.12*	1.10±0.31	1.45±0.04	1.98±0.18*	0.79±0.12	1.19±0.26
LPL	1.41±0.29	1.65±0.17	1.10±0.24	1.61±0.14	**2.01±0.38***	1.01±0.36	1.64±0.27
PLIN4	0.94±0.03	1.28±0.19	1.15±0.11	1.74±0.11*	**2.46±0.21****	1.27±0.17	1.87±0.17*
Degradation of phospholipids							
ASML3A	0.96±0.19	1.07±0.28	0.86±0.13	1.07±0.11	**1.98±0.18****	0.94±0.29	**1.93±0.16****
GDPD3	0.78±0.16	1.55±0.10	1.03±0.25	1.22±0.18	1.84±0.12*	1.27±0.29	**2.18±0.23****
Cytochromes P450 and other genes related to metabolism							
CAR	1.03±0.22	0.92±0.31	0.59±0.13*	**0.64±0.27***	**0.27±0.21*****	0.39±0.13**	**0.24±0.11*****
CYP2E1	0.55±0.19	0.32±0.03*	2.51±0.69**	**1.78±0.21**	0.88±0.22	1.98±0.29*	1.15±0.30
CYP3A4	1.74±0.14*	2.11±0.39***	0.32±0.05*	0.78±0.14	0.82±0.15	0.15±0.03**	**0.33±0.09***
PXR	0.99±0.14	1.42±1.14	1.01±0.13	0.99±0.10	0.56±0.13	0.83±0.18	0.45±0.05

	AMD (10µM)	AMD (20µM)	LPS (0.01µg/ml)	AMD (10µM)+ LPS (0.01µg/ml)	AMD (20µM)+ LPS (0.01µg/ml)	LPS (1µg/ml)	AMD (10µM)+ LPS (1µg/ml)
Liver-specific proteins							
ALB	0.82±0.19	0.93±0.10	0.94±0.10	0.89±0.12	0.78±0.09	0.76±0.11	0.69±0.12
ALDB	1.28±0.10	1.08±0.14	0.98±0.12	0.99±0.10	0.75±0.07*	0.88±0.17	0.76±0.06*
Markers of oxidative stress							
GSTA1/2	1.14±0.07	1.36±0.19	0.83±0.14	**0.64±0.02****	**0.61±0.13****	0.33±0.02***	**0.29±0.07*****
GSTM1	0.78±0.16	0.57±0.18*	0.63±0.09*	0.83±0.05	**0.41±0.04*****	0.61±0.10*	**0.54±0.07****
HO-1	1.46±0.10	1.34±0.13	1.02±0.07	1.74±0.28*	**1.97±0.14***	1.14±0.18	1.88±0.16*
MnSOD	1.01±0.26	1.20±0.16	2.95±0.19*	**2.49±0.28***	**3.18±0.67***	4.99±0.89*	**4.38±0.69***
Nrf2	0.66±0.07	0.69±0.14	1.23±0.10	**1.53±0.26**	**1.77±0.12***	1.00±0.18	**1.81±0.19***
Markers of endoplasmic reticulum stress							
ATF4	0.84±0.11	0.87±0.18	1.30±0.14	1.21±0.26	0.93±0.13	1.48±0.17	0.61±0.05
ATF6	1.10±0.12	1.32±0.11	1.43±0.24	1.23±0.18	1.21±0.15	1.58±0.26	1.27±0.10
CHOP	1.45±0.18	1.67±0.09*	1.09±0.27	1.72±0.13*	**2.37±0.15*****	1.41±0.29	1.88±0.05**
GRP78	1.06±0.24	1.24±0.14	1.35±0.15	1.44±0.10	1.09±0.17	1.71±0.30	**2.02±0.07*****
Markers of inflammation							
CRP	1.25±0.37	1.31±0.18	279.23±11.3***	**281.12±6.57*****	**285.09±9.31*****	561.14±8.96***	**563.42±3.78*****
TNF-α	0.89±0.15	1.17±0.44	126.13±5.82***	**129.00±4.77*****	**125.68±6.97*****	189.31±8.23***	**196.3±5.23*****
Markers of toxicity							
Cas3	1.31±0.16	1.32±0.21	1.13±0.28	1.33±0.25	**2.34±0.31***	1.41±0.12	**2.18±0.09***
Others							
ACACA	1.61±0.17	1.71±0.11*	1.24±0.09	1.27±0.06	1.02±0.10	0.88±0.14	1.21±0.15
CD36 (FAT)	1.00±0.18	1.27±0.09	0.87±0.11	0.99±0.18	**0.69±0.05***	0.50±0.07**	**0.59±0.03****
PKLR	0.82±0.14	0.87±0.13	0.83±0.14	1.04±0.05	0.45±0.18**	0.43±0.01**	0.51±0.11**
TRIB3	1.12±0.23	1.88±0.03**	1.54±0.07	**2.56±0.13****	**3.21±0.11*****	1.40±0.09	**2.97±0.12****
HSP70	0.81±0.07	1.12±0.11	0.86±0.14	1.18±0.09	0.71±0.12*	1.10±0.11	0.75±0.18*

Table 3: Effects of AMD and LPS on expression of various genes (by RT-PCR) related to drug metabolism, oxidative stress, fatty acid synthase and toxicity after 7 d. All results are expressed relative to the levels found in control cells, arbitrarily set at a value of 1. *P<0.05, **P<0.01 and ***P<0.001 compared with untreated cells, "bold character" when P<0.05 compared with cells treated with LPS and AMD individually.

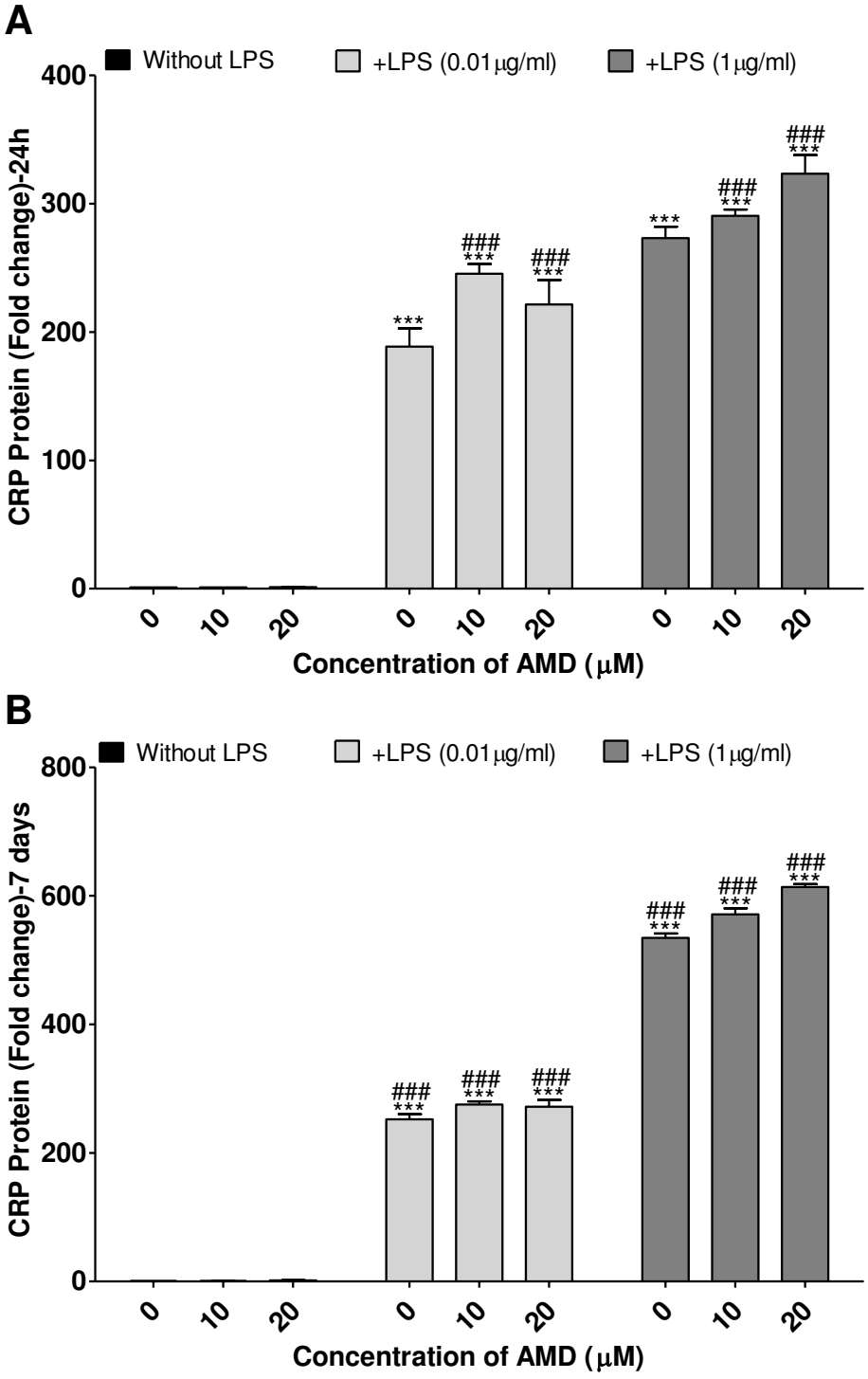

Figure 1 : Measurement of production of CRP.

Cells were pre-treated with LPS (0.01 or 1 μg/ml) for 24h followed by co-treatment with different concentrations of AMD (0, 10 and 20μM) or directly by AMD for 24 h or 7 days. Then CRP protein were measured. All results are expressed relative to the levels found in control cells, arbitrarily set at a value of 1. *P<0.05, **P<0.01 and ***P<0.001 compared with untreated cells, $^{\#}$P<0.05, $^{\#\#}$P<0.01 and $^{\#\#\#}$P<0.001 compared with cells treated with LPS and AMD individually.

Treatment of HepaRG cells with either varying AMD concentrations ranging from 0 to 50µM or LPS at 0.01 or 1µg/ml showed no significant decrease in cell viability after either 24h or 7 days using the MTT assay. However, co-treatment with 20µM AMD and 1µg/ml LPS caused a 55.34% loss in cell viability after 7 days (Figure 2A).

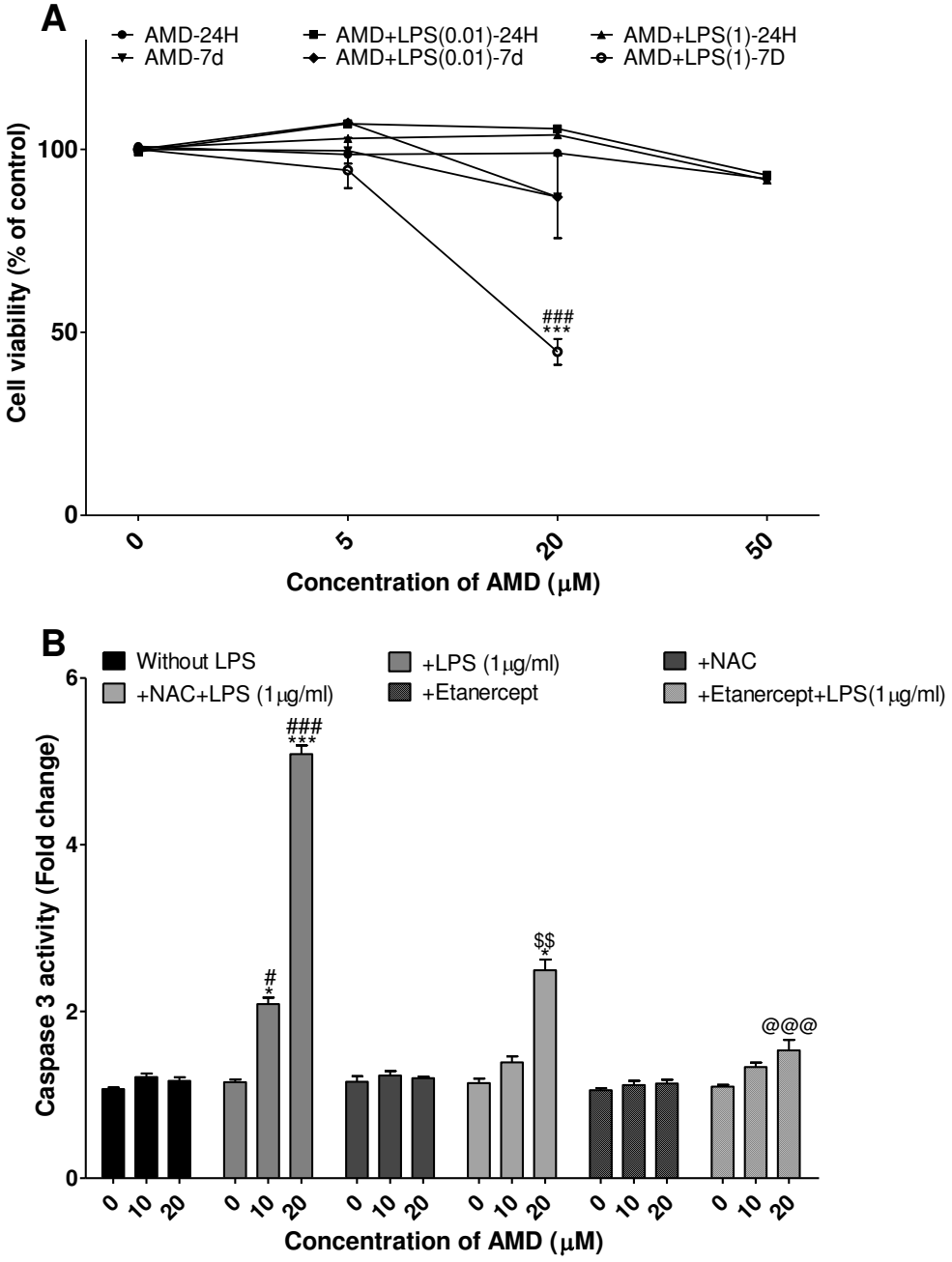

Figure 2 : Effects of LPS on AMD cytotoxicity. Cells were pre-treated with LPS (0.01 or 1 µg/ml) for 24h followed by co-treatment with different concentrations of AMD (0, 10 and 20µM) or directly with AMD, for 24h or 7 days in the absence or presence of NAC or etanercept. Then cytotoxicity was measured by (A) MTT or (B) caspase 3 activity. All results are

expressed relative to the levels found in control cells, arbitrarily set at a value of 1. *P<0.05, **P<0.01 and ***P<0.001 compared with untreated cells, #P<0.05, ##P<0.01 and ###P<0.001 compared with cells treated with LPS and AMD individually, $P<0.05, $$P<0.01 and $$$P<0.001 compared with cells treated with NAC, @P<0.05, @@P<0.01 and @@@P<0.001 compared with cells treated with etanercept.

Caspase 3 activity was also measured after 7 days and found to be slightly (2.09-fold) and strongly (5.09-fold) activated with 10 and 20 µM AMD in the presence of 1µg/ml LPS, respectively (Figure 2B). Accordingly, caspase 3 was found to be overexpressed 2.18- and 2.34-fold in cultures co-treated with 10µM AMD + 1µg/ml LPS and 20µM AMD + 0.01µg/ml LPS for 7 days respectively (Table 3). Co-addition of NAC largely inhibited caspase 3 activation (63.45%) while etanercept mostly suppressed the fraction of activation related to LPS co-treatment (Figure 2B).

ROS generation is increased by lipopolysaccharide and lipopolysaccharide/amiodarone treatments

Whatever its concentration AMD alone did not affect ROS generation after 24h while a co-treatment with 20µM AMD and 1µg/ml LPS led to a 2.48-fold increase (Figure 3A). After repeated treatments for 7 days ROS generation was augmented 1.83-fold with 20µM AMD alone and 2.77-fold with 20µM AMD/0.01µg/ml LPS (Figure 3B). Production of ROS was also enhanced with 10µM AMD in the presence of 0.01 and 1µg/ml LPS reaching 2.04- and 3.88-fold respectively (Figure 3B). This effect was strongly inhibited by co-addition of NAC (approximately 80%) (Figure 3C) and increased ROS production following co-exposure to LPS was completely blocked by etanercept (Figure 3C).

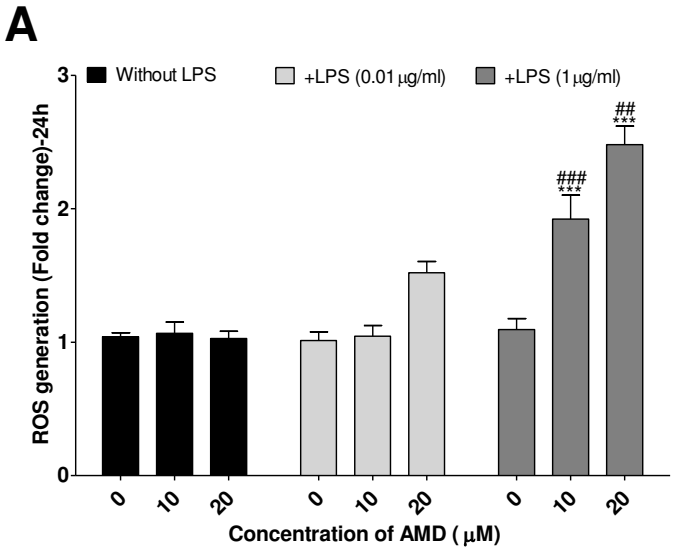

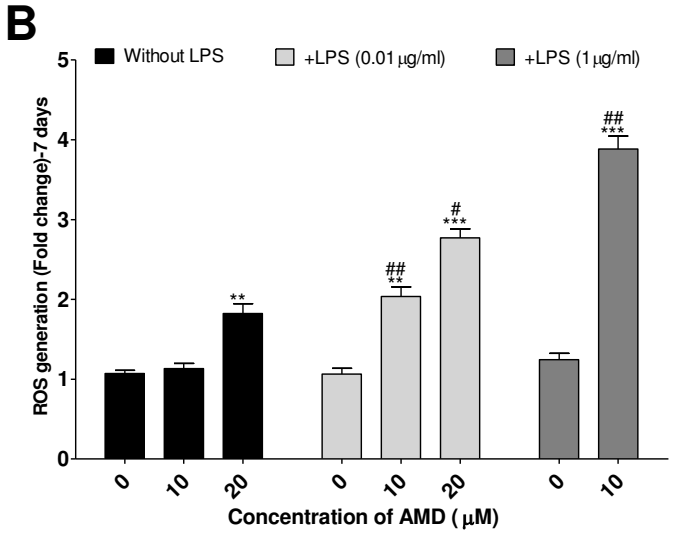

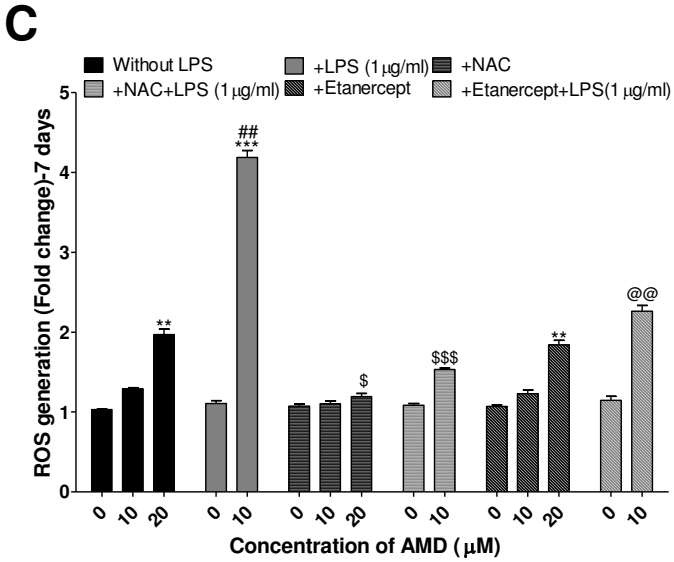

Figure 3 : Measurement of ROS generation.

Cells were pre-treated with LPS (0.01 or 1 μg/ml) for 24h followed by co-treatment with different concentrations of AMD (0, 10 and 20μM) or directly with AMD, for 24h (A) or 7 days in in the absence (B) or presence (C) of NAC or etanercept. ROS generation was measured by the H2-DCFDA assay. All results are expressed relative to the levels found in control cells, arbitrarily set at a value of 1. *P<0.05, **P<0.01 and ***P<0.001 compared with untreated cells, $^{\#}$P<0.05, $^{\#\#}$P<0.01 and $^{\#\#\#}$P<0.001 compared with cells treated with LPS and AMD individually, $^{\$}$P<0.05, $^{\$\$}$P<0.01 and $^{\$\$\$}$P<0.001 compared with cells treated with NAC, $^{@}$P<0.05, $^{@@}$P<0.01 and $^{@@@}$P<0.001 compared with cells treated with etanercept.

Increased ROS generation was associated with overexpression of HO-1, MnSOD and Nrf2 transcripts. Their levels were augmented by a co-treatment with 20µM AMD and 1µg/ml LPS for 24h (2.22-, 9.30- and 2.76-fold respectively) and with 10µM AMD/1µg/ml LPS after 7 days (1.88-, 4.38- and 1.81-fold respectively). In addition, several genes associated with an ER stress were also overexpressed depending on experimental conditions. CHOP and TRIB3 were overexpressed with AMD alone and more extensively with co-treatments with AMD and LPS after 24h. ATF4 and GRP78 transcripts were also increased with co-treatments, ATF4 with 20µM AMD/1µg/ml LPS only. After 7 days CHOP and TRIB3 were still overexpressed by AMD alone and more extensively by co-treatments with LPS (Tables 2 and 3). Co-addition of NAC strongly inhibited overexpression of HO-1, MnSOD and Nrf2 and only slightly if any that of genes related to ER stress (Figures 4 and 5).

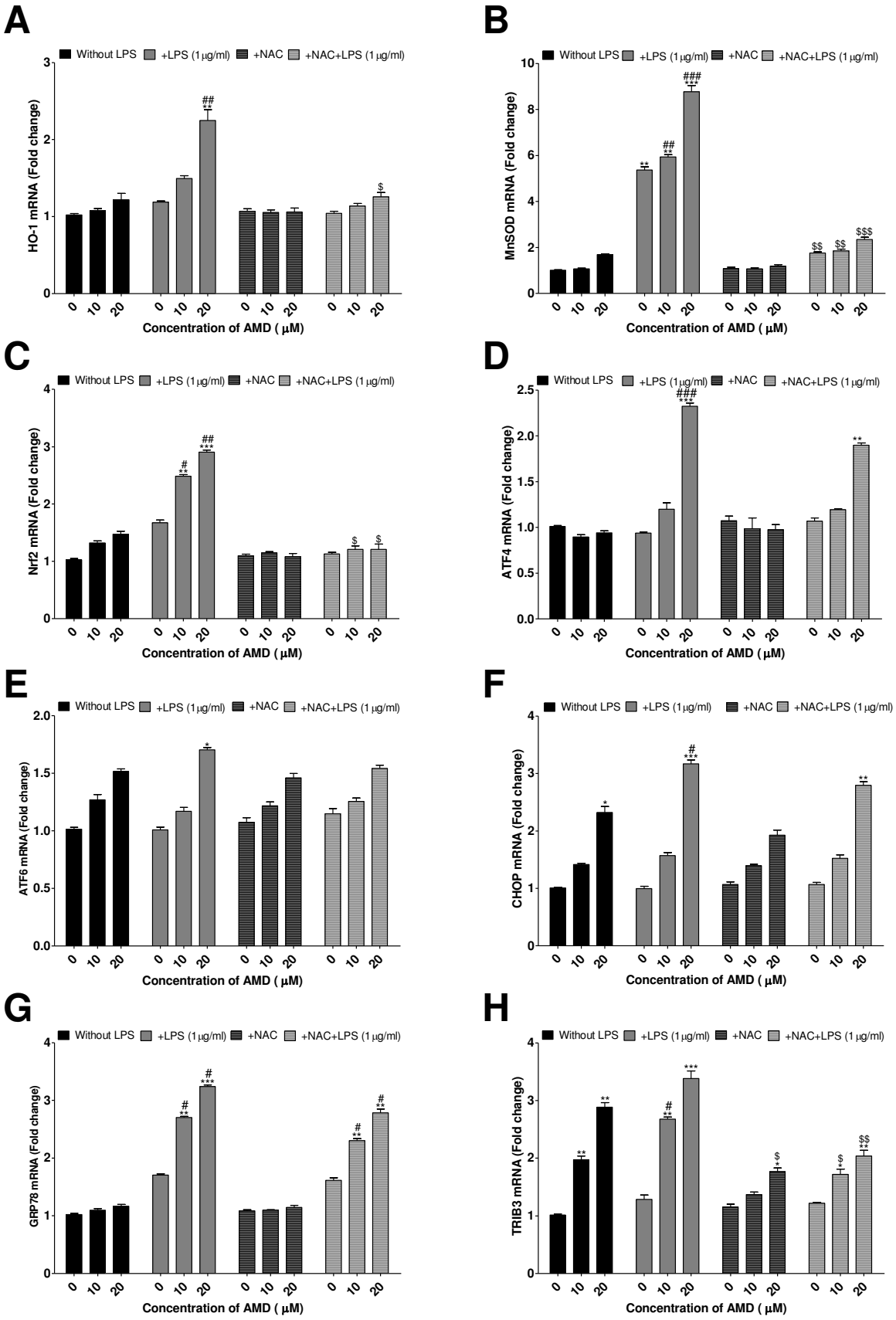
A
B
C
D
E
F
G
H
Without LPS
+LPS (1 μg/ml)
+NAC
+NAC+LPS (1 μg/ml)
HO-1 mRNA (Fold change)
MnSOD mRNA (Fold change)
Nrf2 mRNA (Fold change)
ATF4 mRNA (Fold change)
ATF6 mRNA (Fold change)
CHOP mRNA (Fold change)
GRP78 mRNA (Fold change)
TRIB3 mRNA (Fold change)
Concentration of AMD (μM)
0
10
20

Figure 4 : Effects of NAC on expression of ROS- and ER stress-related genes after 24h.

Cells were pre-treated with LPS (1 µg/ml) for 24h followed by co-treatment with different concentrations of AMD (0, 10 and 20µM) or directly with AMD for another 24h in the presence of NAC. Transcripts levels of some genes related to ROS (HO-1, MnSOD and Nrf2) or ER stress (ATF4, ATF6, CHOP, GRP78 and TRIB3) were measured. All results are expressed relative to the levels found in control cells, arbitrarily set at a value of 1. *P<0.05, **P<0.01 and ***P<0.001 compared with untreated cells, $^{\#}$P<0.05, $^{\#\#}$P<0.01 and $^{\#\#\#}$P<0.001 compared with cells treated with LPS and AMD individually, $^{\$}$P<0.05, $^{\$\$}$P<0.01 and $^{\$\$\$}$P<0.001 compared with cells treated with NAC.

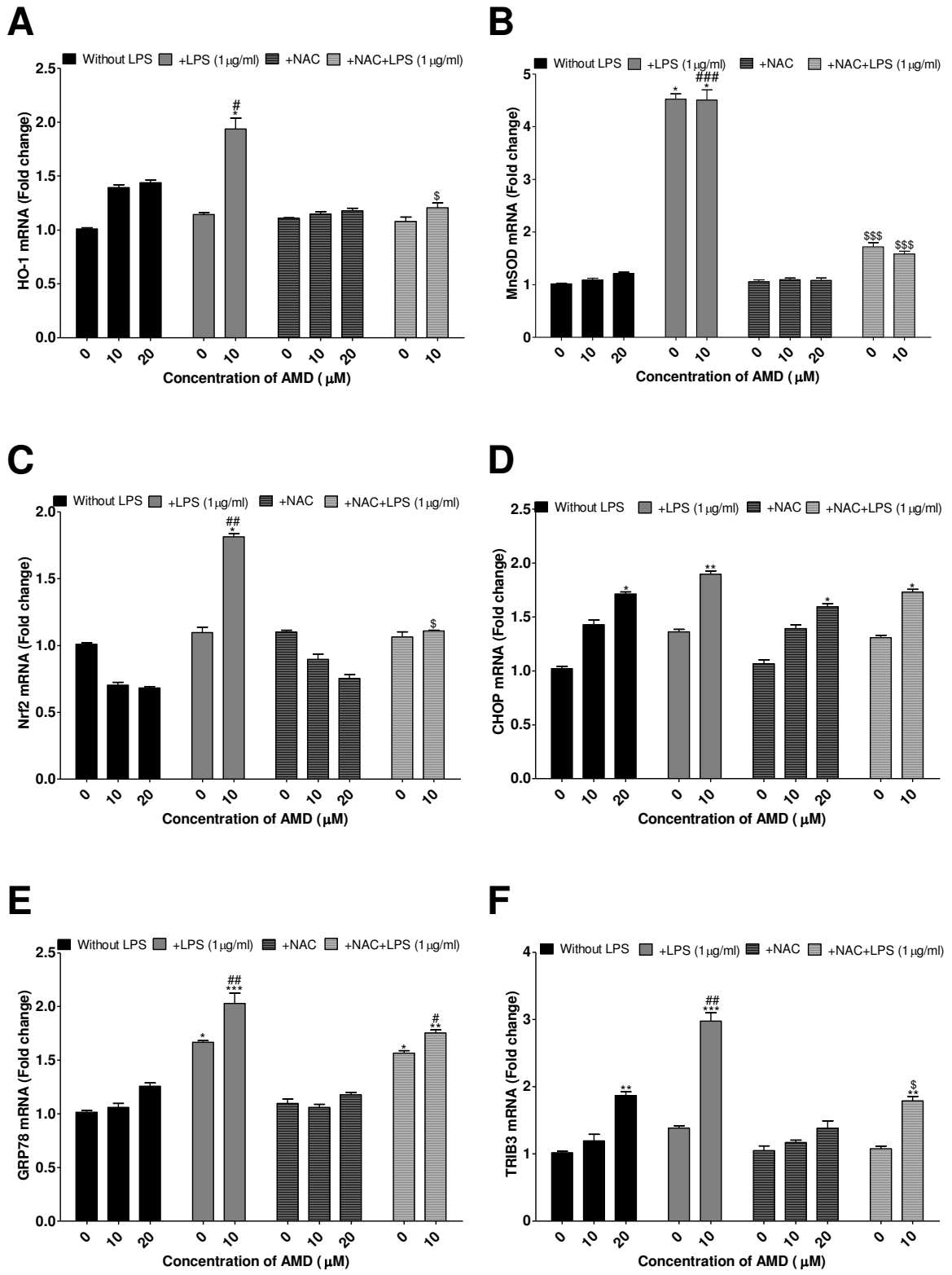

Figure 5 : Effects of NAC on expression of ROS- and ER stress-related genes after 7 days.

Cells were pre-treated with LPS (1 µg/ml) for 24h followed by co-treatment with different concentrations of AMD (0, 10 and 20µM) or directly with AMD for 7 days in the presence of NAC. Transcripts levels of some genes related to ROS (HO-1, MnSOD and Nrf2) or ER stress (CHOP, GRP78 and TRIB3) were measured. All results are expressed relative to the levels found in control cells, arbitrarily set at a value of 1. *P<0.05, **P<0.01 and ***P<0.001 compared with untreated cells, $^{\#}$P<0.05, $^{\#\#}$P<0.01 and $^{\#\#\#}$P<0.001 compared with cells treated with LPS and AMD individually, $^{\$}$P<0.05, $^{\$\$}$P<0.01 and $^{\$\$\$}$P<0.001 compared with cells treated with NAC.

Accumulation of lipid droplets

HepaRG cell cultures were stained by Oil-red O to detect intracytoplasmic lipid droplets following treatment with AMD +/- LPS after 24h and 7 days. AMD caused accumulation of Oil-red O-stained vesicles in HepaRG hepatocytes after 7 days (Figure 6). The number was markedly increased following co-treatment with LPS, especially at 1µg/ml. In addition, numerous small unstained vesicles were evidenced in both HepaRG cell types, after either 24h or 7 days, suggesting phospholipid accumulation in lamellar bodies as previously described (Antherieu et al., 2011) (Figure 6). Co-addition of NAC largely reduced accumulation of Oil-red-stained intracytoplasmic vesicles caused by AMD and AMD/LPS (Figure 7) while it had no obvious effect on the formation of unstained vesicles (phospholipidosis).

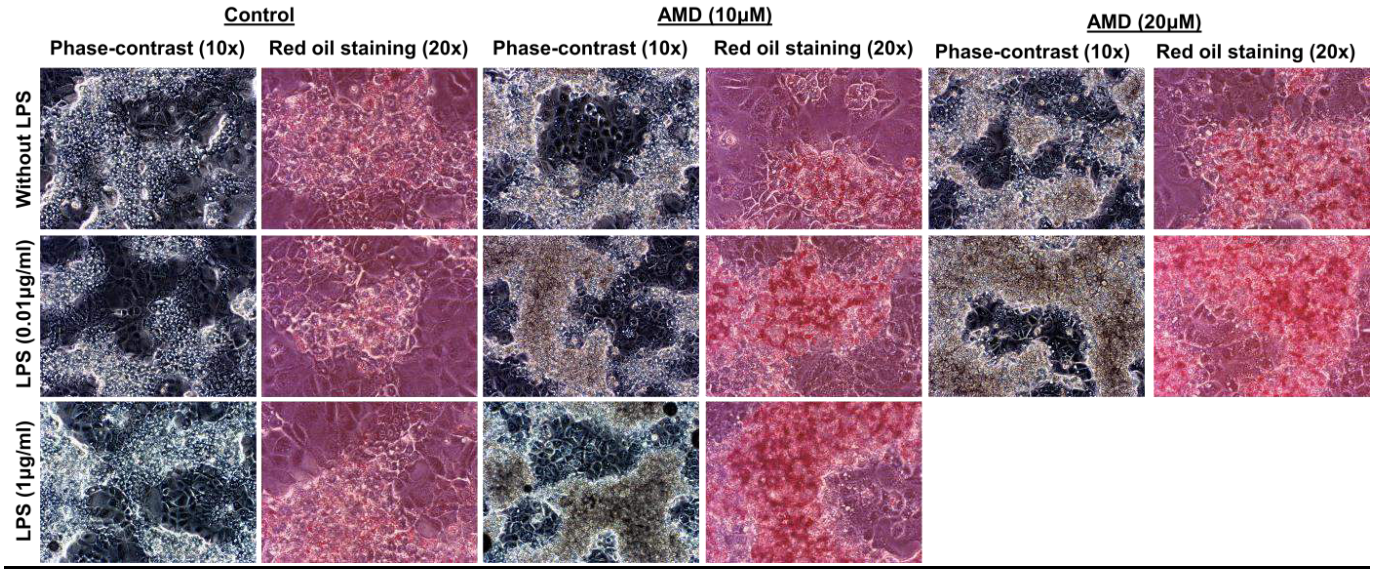

Figure 6 : Detection of the intracellular accumulation of lipid droplets.

Cells were pre-treated with LPS (0.01 or 1 µg/ml) for 24h followed by co-treatment with different concentrations of AMD (0, 10 and 20µM) or directly with AMD, for 7 days. Lipids were stained by Oil red oil. HepaRG cells were observed and photographed under a phase-contrast microscope (magnification 10 and 20X).

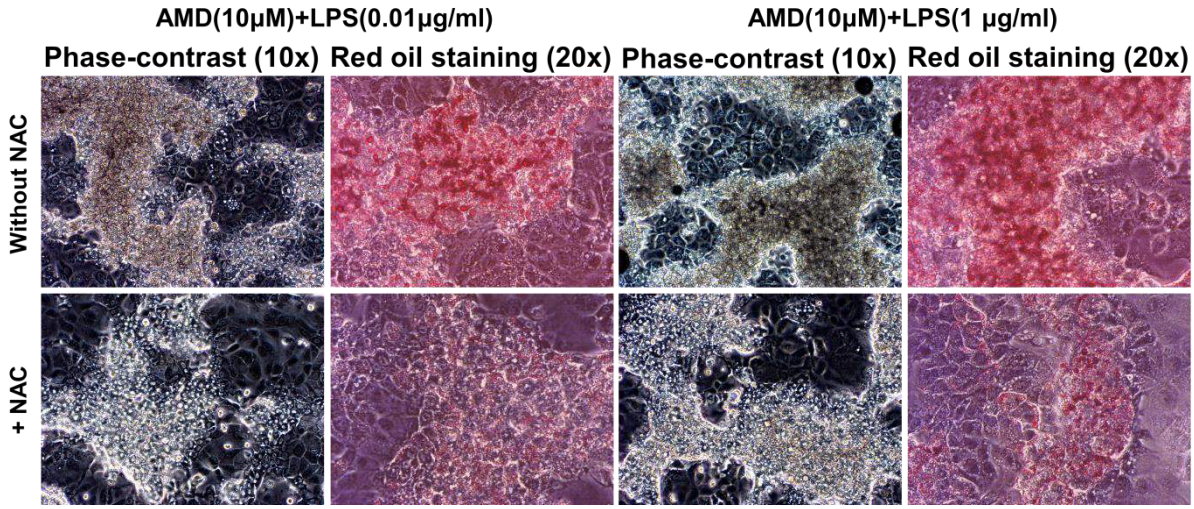

Figure 7 : Effects of NAC on the accumulation of lipid droplets.

Cells were pre-treated with LPS (0.01 or 1 µg/ml) for 24h followed by co-treatment with AMD (10µM) in the presence of the antioxidant NAC for 7 days. Lipids were stained by Oil red oil. HepaRG cells were observed and photographed under a phase-contrast microscope (magnification 10 and 20X).

Lipopolysaccharide aggravates accumulation of triglycerides in co-treated HepaRG hepatocytes

No significant changes in triglycerides content were observed with AMD alone or co-treatments after 24h (Figure 8A) while after 7 days at 20µM AMD caused a 2.31-fold increase (Figure 8B). This effect was markedly aggravated by co-treatments with LPS, representing 2.52- and 4.86–fold increase with 10µM AMD combined with 0.01 and 1µg/ml LPS respectively and 4.1-fold increase with 20µM AMD combined with 0.01µg/ml LPS (Figure 8B). Co-addition of NAC largely inhibited accumulation of triglycerides caused by AMD alone or in combination with LPS and the fraction of triglycerides resulting from co-exposure to LPS was completely alleviated by etanercept (Figure 8B).

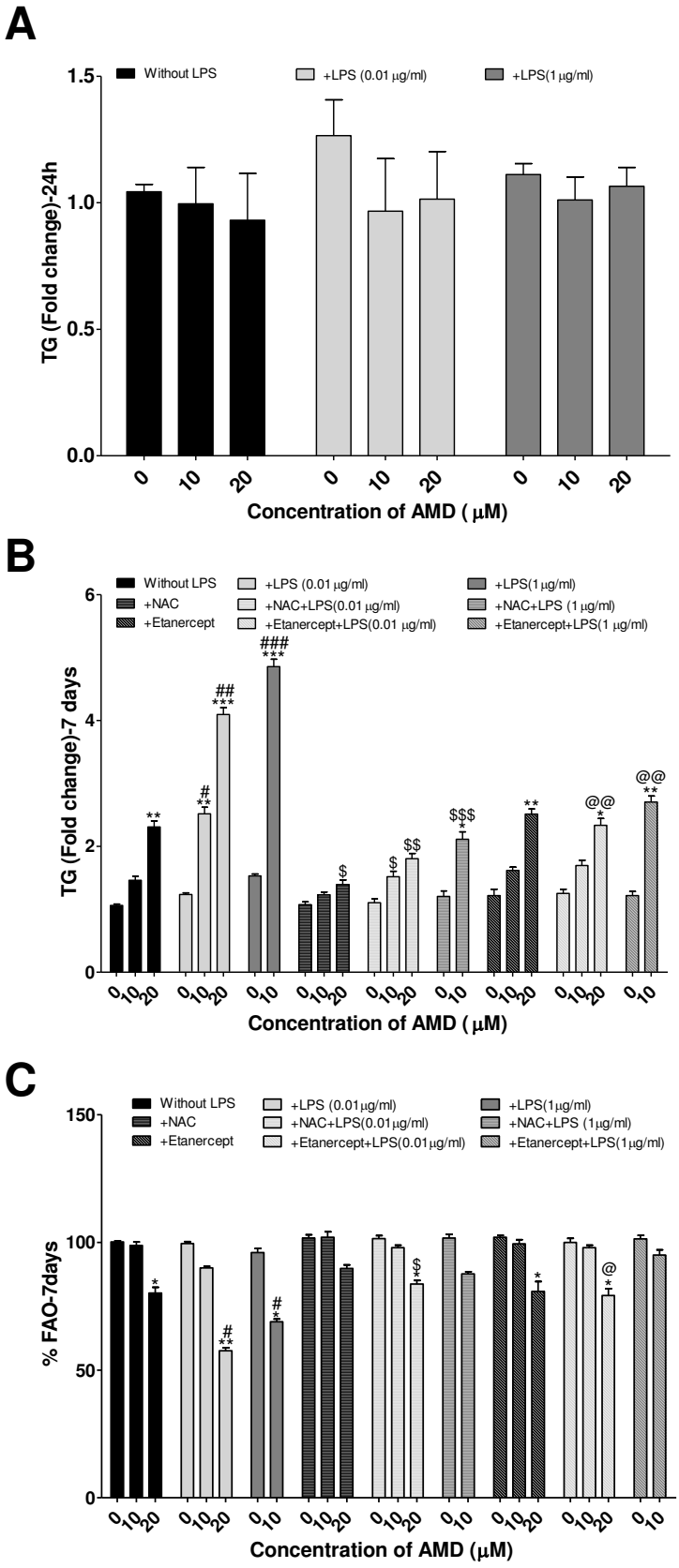

Figure 8 : Effects of AMD and LPS on triglycerides accumulation and fatty acid oxidation.

Cells were pre-treated with LPS (0.01 or 1 µg/ml) for 24h followed by co-treatment with different concentrations of AMD (0, 10 and 20µM) or directly with AMD, for 24 h (A) or 7 days (B and C) in the absence or presence of NAC or etanercept. Determination of (A and B) triglycerides content and (C) fatty acid oxidation activity. All results are expressed relative to the levels found in control cells, arbitrarily set at a value of 1. *P<0.05, **P<0.01 and ***P<0.001 compared with untreated cells, $^{\#}$P<0.05, $^{\#\#}$P<0.01 and $^{\#\#\#}$P<0.001 compared with cells treated with LPS and AMD individually, $^{\$}$P<0.05, $^{\$\$}$P<0.01 and $^{\$\$\$}$P<0.001 compared with cells treated with NAC, $^{@}$P<0.05, $^{@@}$P<0.01 and $^{@@@}$P<0.001 compared with cells treated with etanercept.

Inhibition of fatty acid oxidation

Impairment of mitochondrial FAO activity is considered as one of the major mechanisms of liver steatosis (Fromenty et al., 1990). FAO was evaluated by measuring [^{14}C]-labelled acid-soluble ß-oxidation products in HepaRG cells after 7 day-treatments with 10 and 20µM AMD alone or 10µM AMD combined with 0.01 or 1µg/ml LPS (Figure 8C). No change was observed after 24h while after 7 days FAO activity dropped by 19.94, 42.49 and 31.78% with 20µM amiodarone alone, 20µM amiodarone + 0.01µg/ml LPS and 10µM amiodarone + 1µg/ml LPS respectively (Figure 8C). Co-addition of NAC partly alleviated FAO decrease caused by AMD and AMD/LPS (Figure 8C). The increased effect related to co-addition of LPS was blocked by etanercept (Figure 8C).

Modulation of mRNA levels of genes related to lipid metabolism

To characterize gene expression changes associated with a treatment with AMD alone or combined with LPS a set of genes related to lipid metabolism, including ADFP, CD36, ACACA, CPT1A, LPL, THRSP, PGC-1α, SREBP1, SLC27A4, PLIN4, SOAT1, SCD1, FASN, SREBP1 and CYP3A4 or to phospholipidosis, such as LSS, LPIN1, ASML3A and GDPD3, was analysed by RT-PCR.

In cells treated with AMD alone for 24h a dose-dependent increase in CYP3A4, ADFP, LPL THRSP, PGC-1α, SREBP1, LPIN1, SLC27A4, PLIN4, LSS, SOAT1 and GDPD3 was evidenced. In addition SCD1, ACACA and CD36 were similarly increased with both AMD concentrations while CYP2E1 decreased dose-dependently. After 7 days, several of these genes were still increased by the drug, including CYP3A4, ADFP, THRSP, PGC-1α, SLC27A1 and ACACA while GSTM1 and CYP2E1 was diminished.

The major changes associated with a 24h co-treatment with AMD and LPS were an increase of FASN, ACLY, GDPD3, SOAT1 and CYP2E1 and a decrease of THRSP and CYP3A4 transcripts. After 7 days, FASN, ACLY, LSS, PLIN4, ASML3A and GDPD3 were overexpressed while both THRSP and CYP3A4 remained repressed (Tables 2 and 3).

At either 0.01 or 1µg/ml LPS did not significantly modulate expression of genes related to lipid metabolism whether after 24h or 7-day treatments.

Moreover, the influence of NAC co-addition was also tested after 24h and 7 days of treatment with AMD and AMD/LPS. When the genes were overexpressed a strong reduction was observed in both conditions in the presence of NAC (Figures 9 and 10).

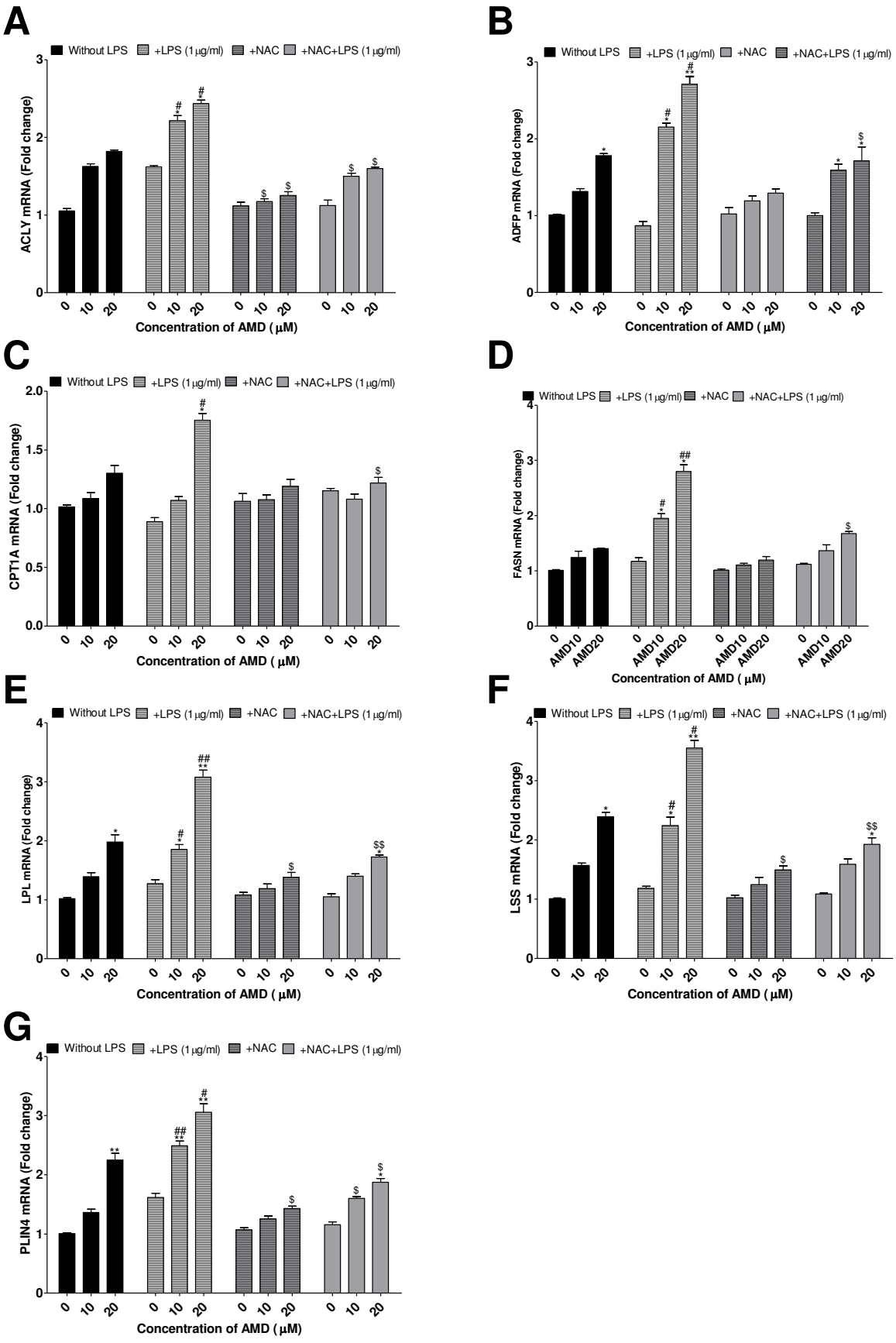
A
Without LPS
+LPS (1 μg/ml)
+NAC
+NAC+LPS (1 μg/ml)
ACLY mRNA (Fold change)
Concentration of AMD (μM)
B
ADFP mRNA (Fold change)
C
CPT1A mRNA (Fold change)
D
FASN mRNA (Fold change)
AMD10
AMD20
E
LPL mRNA (Fold change)
F
LSS mRNA (Fold change)
G
PLIN4 mRNA (Fold change)

Figure 9 : Effects of NAC on the expression of some genes related to steatosis and phospholipidosis after 24h.

Cells were pre-treated with LPS (1µg/ml) for 24h followed by co-treatment with different concentrations of AMD (0, 10 and 20µM) or directly with AMD for another 24h in the presence of NAC. Then expression of some genes related to steatosis and phospholipidosis was measured. All results are expressed relative to the levels found in control cells, arbitrarily set at a value of 1. *P<0.05, **P<0.01 and ***P<0.001 compared with untreated cells, $^{\#}$P<0.05, $^{\#\#}$P<0.01 and $^{\#\#\#}$P<0.001 compared with cells treated with LPS and AMD individually, $^{\$}$P<0.05, $^{\$\$}$P<0.01 and $^{\$\$\$}$P<0.001 compared with cells treated with NAC.

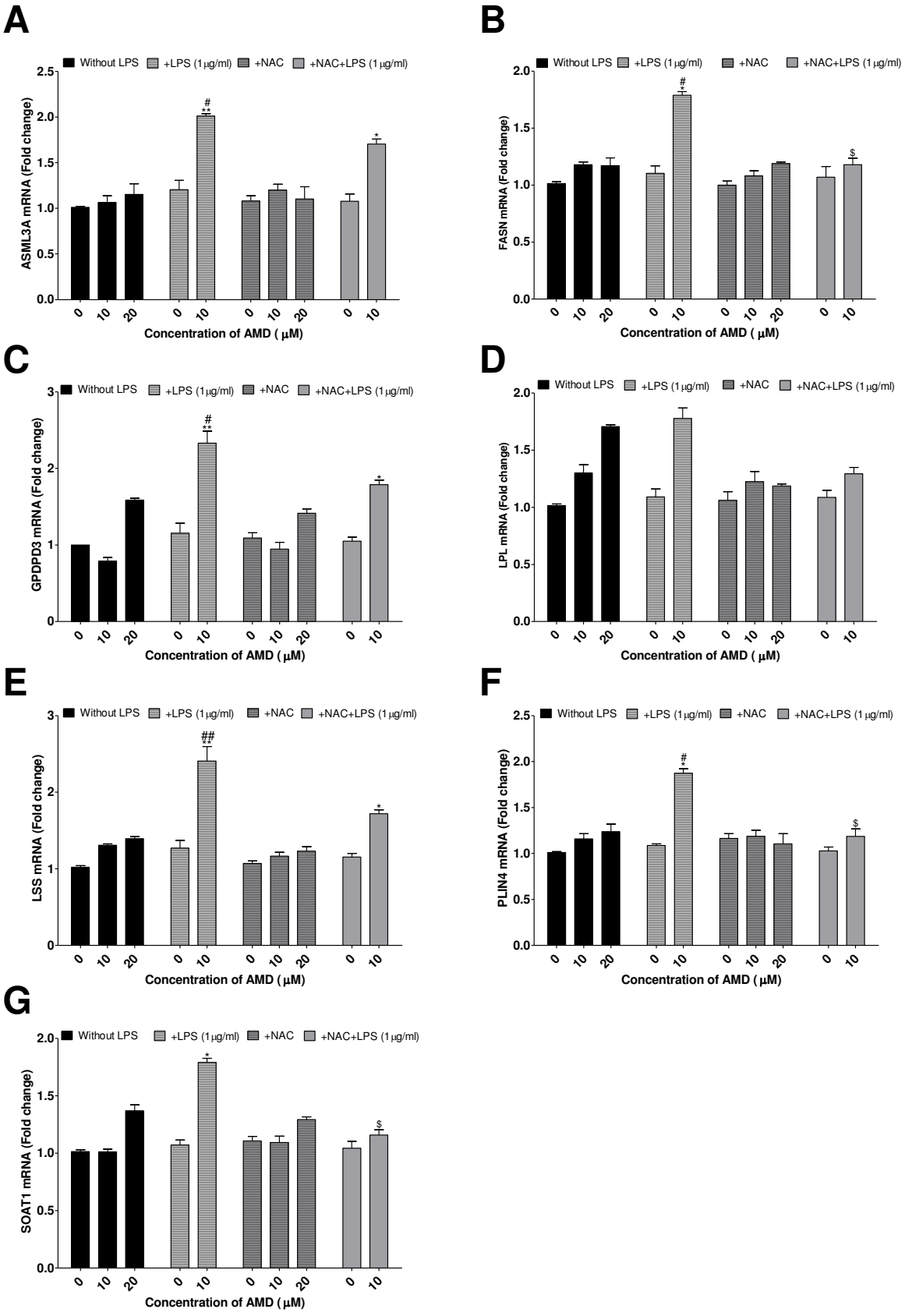
A
Without LPS
+LPS (1 μg/ml)
+NAC
+NAC+LPS (1 μg/ml)
ASML3A mRNA (Fold change)
Concentration of AMD (μM)
B
FASN mRNA (Fold change)
C
GPDPD3 mRNA (Fold change)
D
LPL mRNA (Fold change)
E
LSS mRNA (Fold change)
F
PLIN4 mRNA (Fold change)
G
SOAT1 mRNA (Fold change)

Figure 10 : Effects of NAC on the expression of some genes related to steatosis and phospholipidosis after 7 days.

Cells were pre-treated with LPS (1µg/ml) for 24h followed by co-treatment with different concentrations of AMD (0, 10 and 20µM) or directly with AMD for 7 days in the presence of NAC. Transcripts levels of some genes related to steatosis and phospholipidosis were measured. All results are expressed relative to the levels found in control cells, arbitrarily set at a value of 1. *P<0.05, **P<0.01 and ***P<0.001 compared with untreated cells, $^{\#}$P<0.05, $^{\#\#}$P<0.01 and $^{\#\#\#}$P<0.001 compared with cells treated with LPS and AMD individually, $^{\$}$P<0.05, $^{\$\$}$P<0.01 and $^{\$\$\$}$P<0.001 compared with cells treated with NAC.

Lipopolysaccharide effects are largely reproduced by neo-synthetized TNF-α

Previous works have shown that LPS effects are mainly mediated by stimulation of TNF-α neo-synthesis (Endo et al., 2007). TNF-α release in the medium of cultures exposed to LPS alone or LPS/AMD was estimated using an immunoassay. AMD alone had no effect on TNF-α production that did not exceed 0.012ng/ml after 7 days. Treatment with LPS resulted in a dose-dependent huge increase in TNF-α accumulation in the medium, reaching 1.61 and 2.82ng/ml with 0.01 and 1µg/ml LPS, respectively (Figure 11). Accordingly, TNF-α transcripts were also hugely increased (Tables 2 and 3).

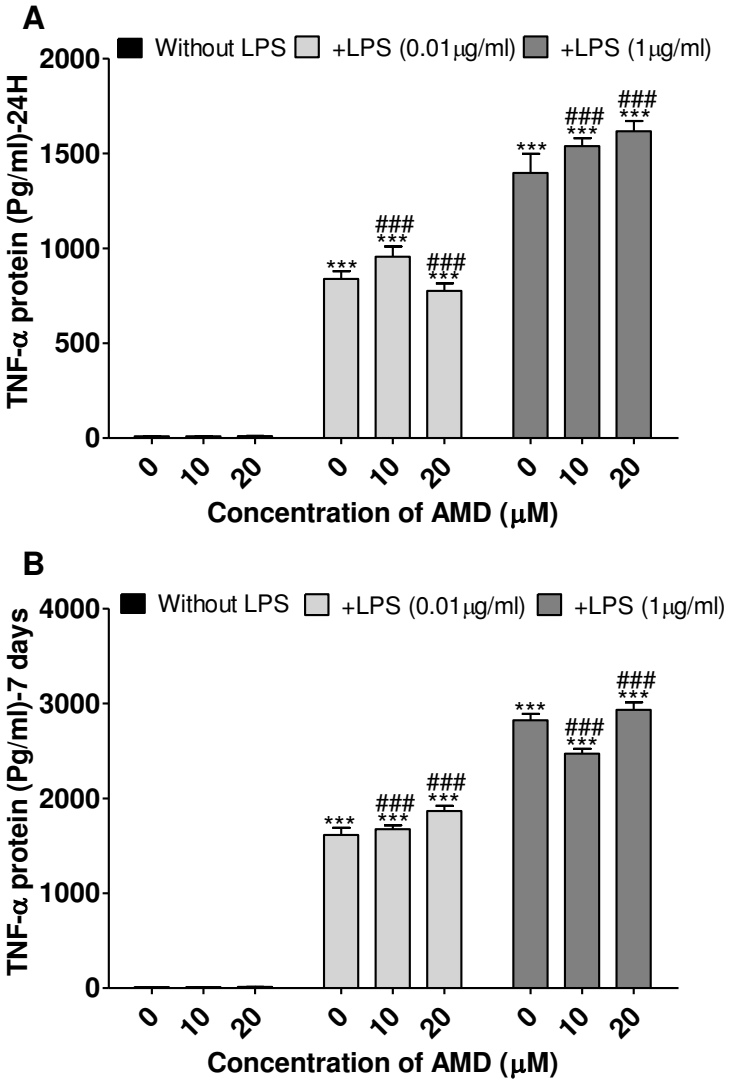

Figure 11 : Production of TNF-α by AMD and LPS-treated HepaRG cell cultures

Cells were pre-treated with LPS (0.01 or 1 µg/ml) for 24h followed by co-treatment with different concentrations of AMD (0, 10 and 20µM) or directly by AMD for 24 h or 7 days. Then TNF-α protein were measured. All results are expressed relative to the levels found in control cells, arbitrarily set at a value of 1. *P<0.05, **P<0.01 and ***P<0.001 compared with untreated cells, $^{\#}$P<0.05, $^{\#\#}$P<0.01 and $^{\#\#\#}$P<0.001 compared with cells treated with LPS and AMD individually.

To confirm that LPS effects were at least partly mediated by TNF-α, HepaRG cell cultures were exposed to 1, 3 and 5 ng/ml TNF-α in the presence or absence of AMD for 7 days and caspase 3 activity, ROS generation, fatty acid oxidation, intracellular triglycerides content (Figure 12A, B, C and D) and gene expression levels (Figures 13, 14, 15 and 16) were measured. At 5ng/ml TNF-α caused an increase in ROS generation, reduced fatty acid oxidation activity and enhanced accumulation of triglycerides. When added with AMD an aggravation of the effects was observed with a TNF-α concentration of 3ng/ml (Figure 12A, B, C and D).

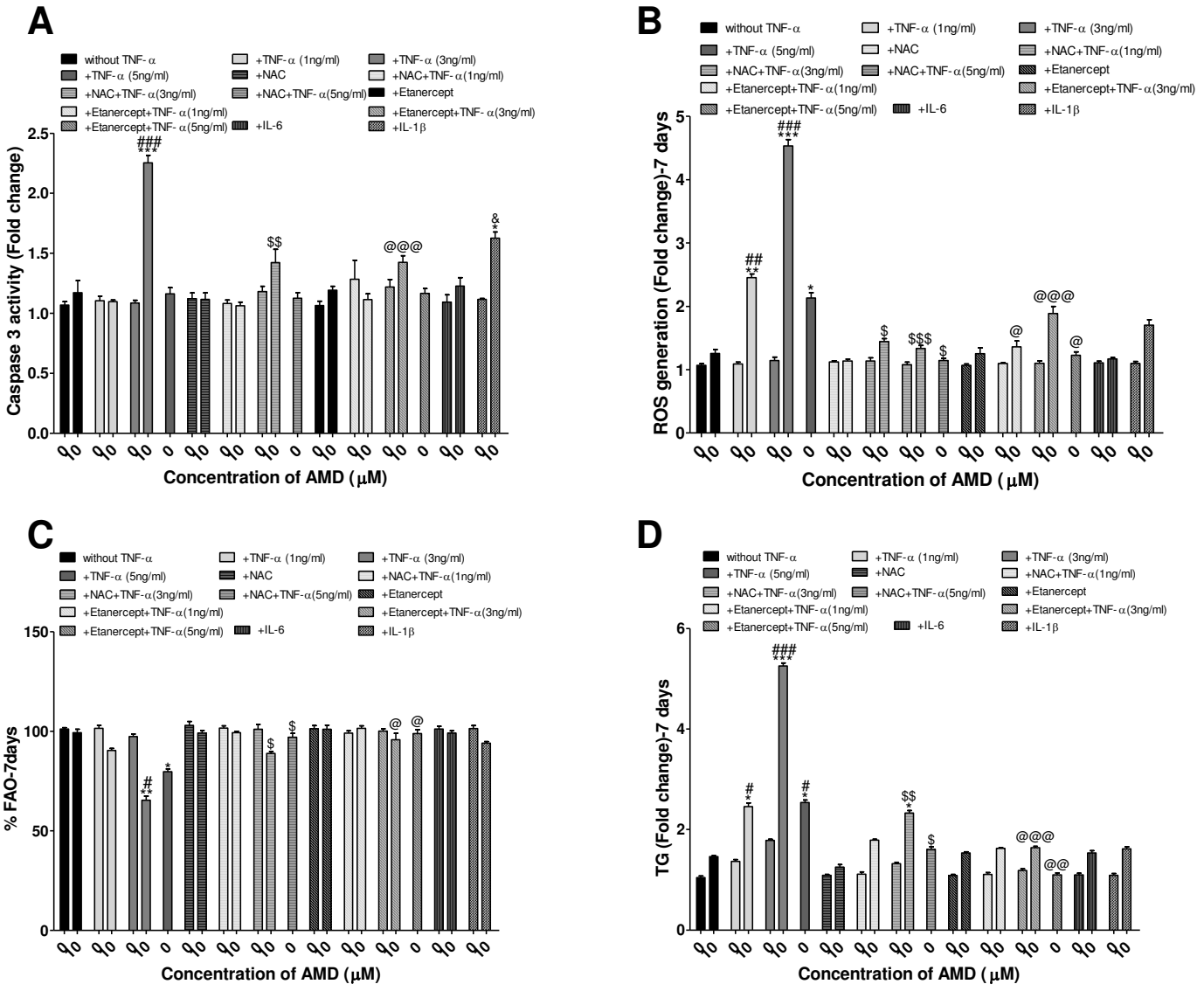

Figure 12 : Effects of AMD and TNF-α on different markers of cytotoxicity and steatosis

Cells were pre-treated with TNF-α (1; 3 and 5ng/ml) for 24h followed by co-treatment with different concentrations of AMD (10μM) or directly with AMD for 7 days in the presence of NAC or etanercept. (A) caspase 3 activity, (B) ROS generation, (C) fatty acid oxidation activity and (D) triglycerides content were measured. All results are expressed relative to the levels found in control cells, arbitrarily set at a value of 1. *P<0.05, **P<0.01 and ***P<0.001 compared with untreated cells, $^{\#}$P<0.05, $^{\#\#}$P<0.01 and $^{\#\#\#}$P<0.001 compared with cells treated with LPS and AMD individually, $^{\$}$P<0.05, $^{\$\$}$P<0.01 and $^{\$\$\$}$P<0.001 compared with cells treated with NAC.

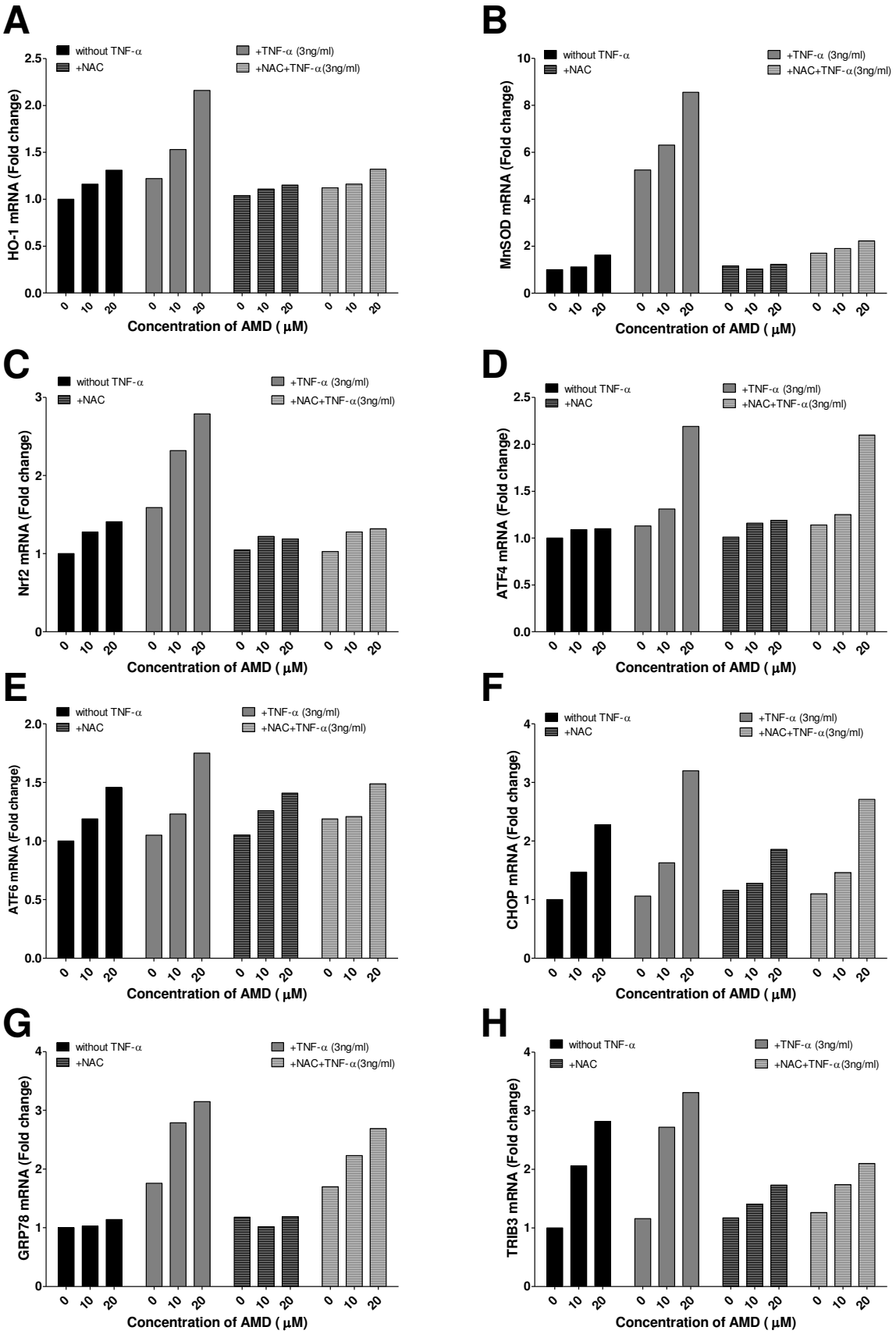
A
without TNF-α
+NAC
+TNF-α (3ng/ml)
+NAC+TNF-α(3ng/ml)
HO-1 mRNA (Fold change)
Concentration of AMD (μM)
B
MnSOD mRNA (Fold change)
C
Nrf2 mRNA (Fold change)
D
ATF4 mRNA (Fold change)
E
ATF6 mRNA (Fold change)
F
CHOP mRNA (Fold change)
G
GRP78 mRNA (Fold change)
H
TRIB3 mRNA (Fold change)

Figure 13 : Effect of NAC on the markers of ROS generation and ER stress after 24h.

Cells were pre-treated with TNF-α (3 ng/ml) for 24h followed by co-treatment with different concentrations of AMD (0, 10 and 20µM) or directly by AMD for another 24h in the presence of NAC. Then expression of some genes related to ROS (HO-1, MnSOD and Nrf2) or ER stress (ATF4, ATF6, CHOP, GRP78 and TRIB3) was measured. All results are expressed relative to the levels found in control cells, arbitrarily set at a value of 1.

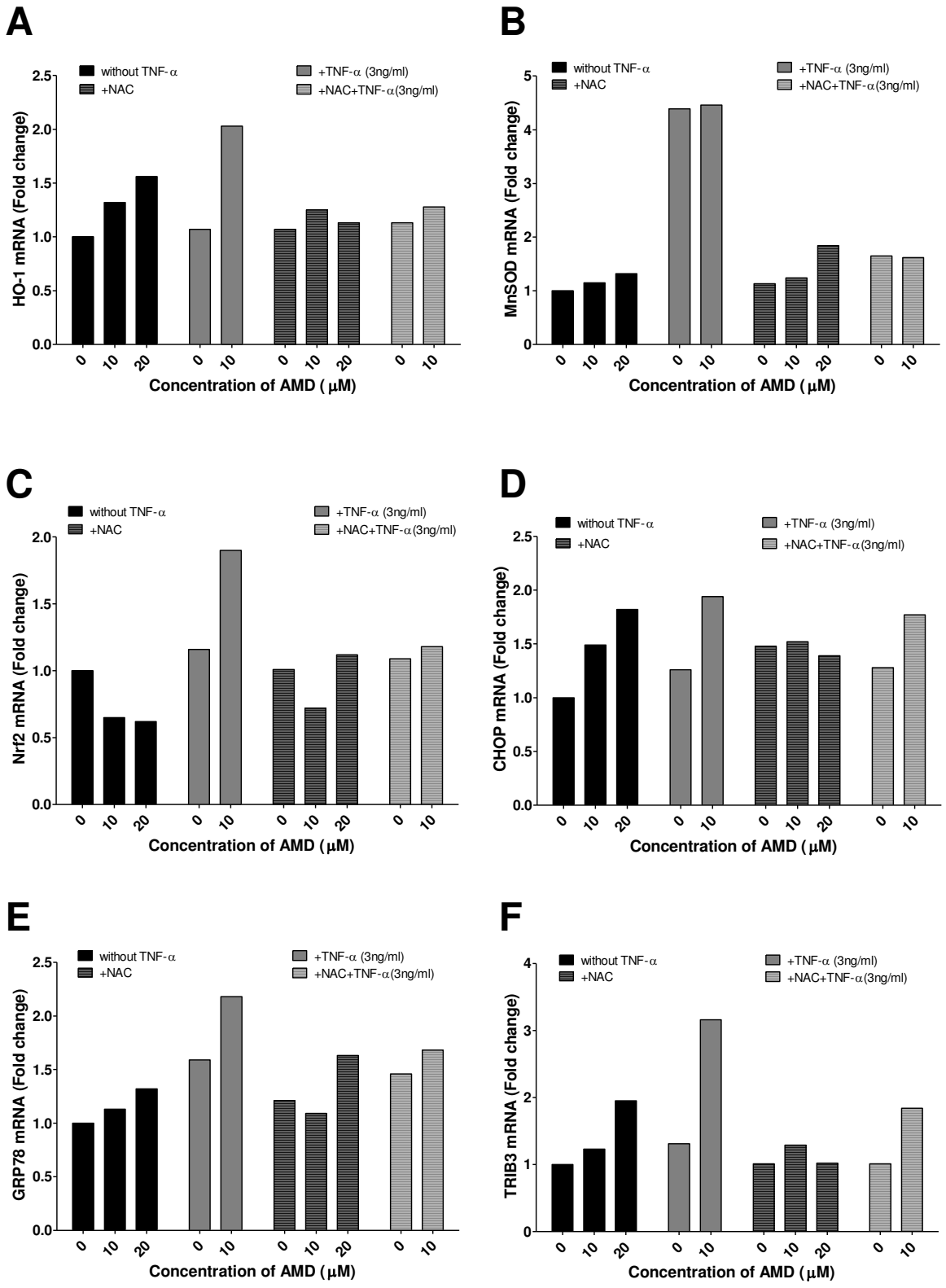

Figure 14 : Effect s of NAC on the markers of ROS generation and ER stress after 7 days.

Cells were pre-treated with TNF-α (3 ng/ml) for 24h followed by co-treatment with different concentrations of AMD (0, 10 and 20μM) or directly by AMD for 7 days in the presence of NAC. Then expression of some genes related to ROS (HO-1, MnSOD and Nrf2) or ER stress (CHOP, GRP78 and TRIB3) was measured. All results are expressed relative to the levels found in control cells, arbitrarily set at a value of 1.

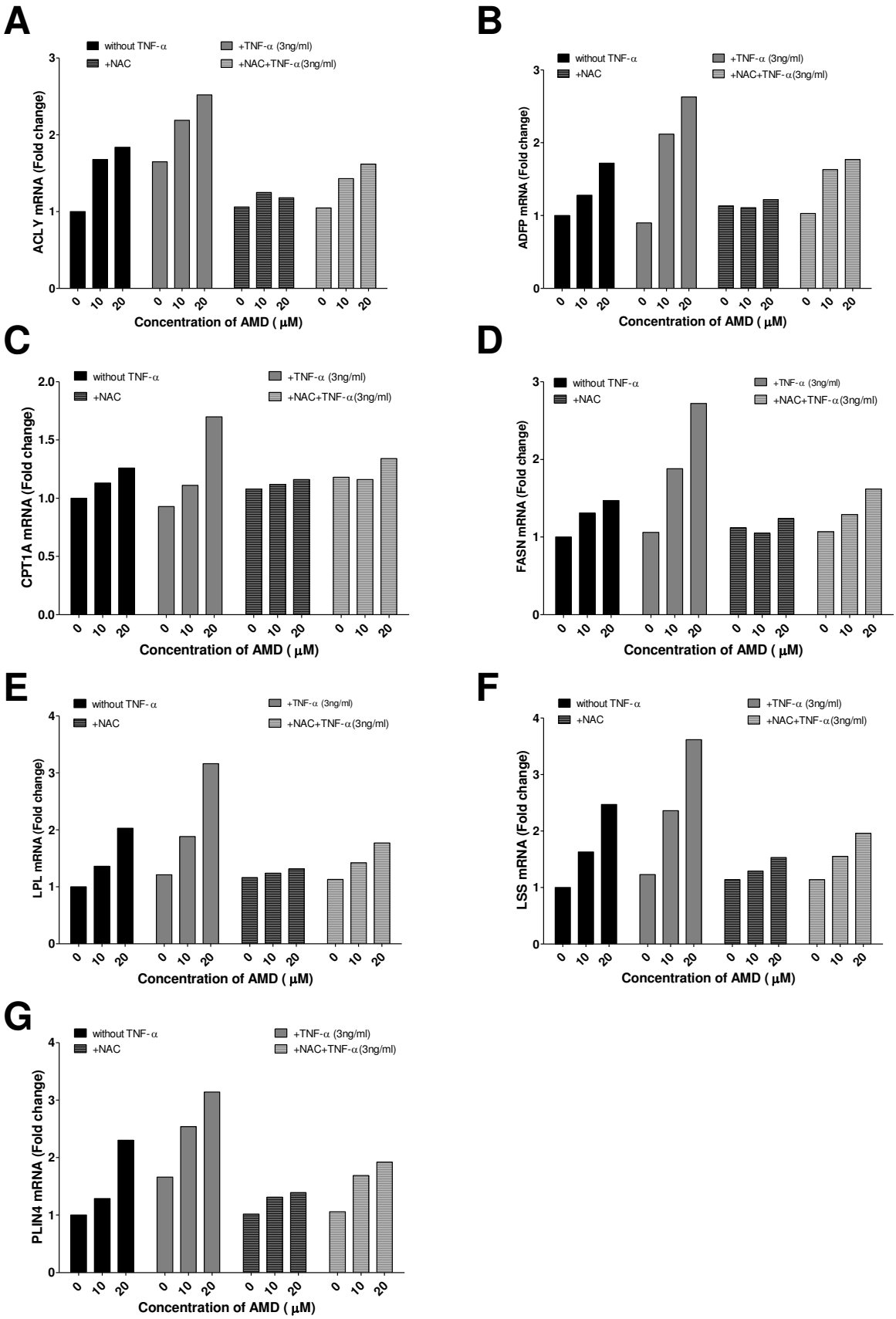
A
without TNF-α
+NAC
+TNF-α (3ng/ml)
+NAC+TNF-α(3ng/ml)
ACLY mRNA (Fold change)
Concentration of AMD (μM)
B
ADFP mRNA (Fold change)
C
CPT1A mRNA (Fold change)
D
FASN mRNA (Fold change)
E
LPL mRNA (Fold change)
F
LSS mRNA (Fold change)
G
PLIN4 mRNA (Fold change)

Figure 15 : Effects of NAC on the expression of some genes related to steatosis and phospholipidosis after 24h.

Cells were pre-treated with TNF-α (3 ng/ml) for 24h followed by co-treatment with different concentrations of AMD (0, 10 and 20µM) or directly by AMD for another 24h in the presence of NAC. Then expression of some genes related to steatosis and phospholipidosis was measured. All results are expressed relative to the levels found in control cells, arbitrarily set at a value of 1.

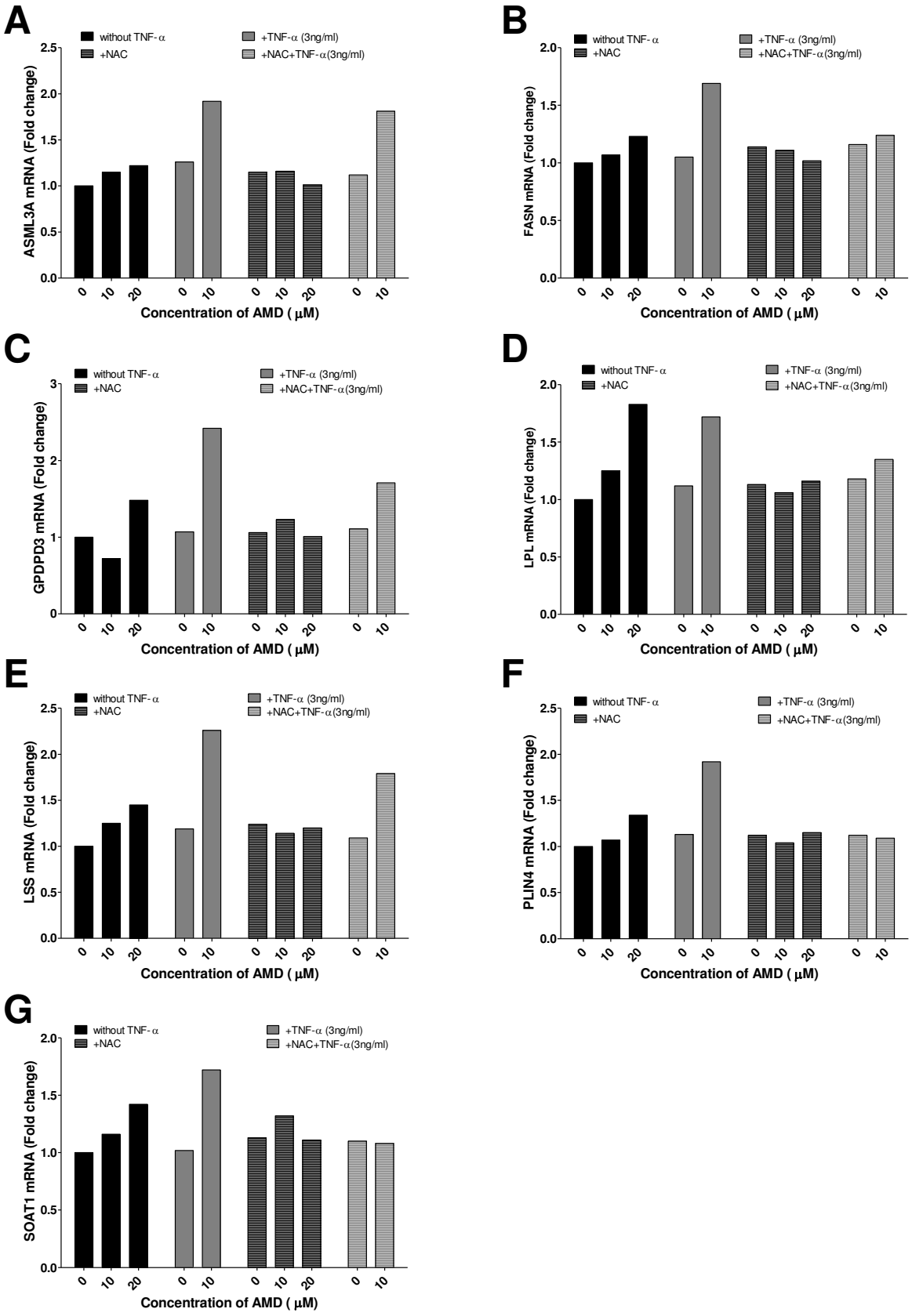
A
without TNF-α
+NAC
+TNF-α (3ng/ml)
+NAC+TNF-α(3ng/ml)
ASML3A mRNA (Fold change)
Concentration of AMD (μM)
B
FASN mRNA (Fold change)
C
GPDPD3 mRNA (Fold change)
D
LPL mRNA (Fold change)
E
LSS mRNA (Fold change)
F
PLIN4 mRNA (Fold change)
G
SOAT1 mRNA (Fold change)

Figure 16 : Effects of NAC on the expression of some genes related to steatosis and phospholipidosis after 7 days.

Cells were pre-treated with TNF-α (3 ng/ml) for 24h followed by co-treatment with different concentrations of AMD (0, 10 and 20µM) or directly by AMD for 7 days in the presence of NAC. Then expression of some genes related to steatosis and phospholipidosis was measured. All results are expressed relative to the levels found in control cells, arbitrarily set at a value of 1.

Co-exposure to etanercept resulted in nearly complete inhibition of ROS production and caspase 3 activation and most of the enhanced accumulation of triglycerides and decrease in FAO resulting from co-treatment with TNF-α in the presence of AMD (Figure 12A, B, C and D). NAC completely abolished AMD effects and most of those resulting from co-treatment with AMD/ TNF-α on genes related to lipid metabolism and oxidative stress but did not modulate expression of genes related to ER stress (Figures 13, 14, 15 and 16).

Moreover, when HepaRG cells were co-treated with AMD and IL-1β or IL6 instead of TNF-α, a modest activation of caspase 3 was observed with IL-1 β only (Figure 12A).

Discussion

In the current work, we show that AMD could aggravate *in vitro* cytotoxicity and steatosis under an inflammatory stress using human HepaRG cells and that co-addition of NAC exerted a protective effect against both AMD and AMD/LPS or AMD/TNF-α induced lesions

AMD has been shown to induce liver steatosis in experimental animals and in some patients (Vitins et al., 2014) as well as in HepaRG hepatocytes (Antherieu et al., 2011). In the present study, we confirmed that AMD could induce vesicular steatosis in HepaRG cells together with intracellular accumulation of triglycerides, overexpression of a variety of genes related to lipid metabolism and inhibition of FA oxidation. In addition, we showed that such alterations could occur within a 7-day period in a culture medium containing only 2% serum and 1% DMSO (instead of 10 and 2% respectively). Fold increases of overexpressed genes were usually higher after a single than a repeated treatment with AMD and none of the tested genes was deregulated in the opposite direction in the two studies.

AMD steatogenic effects have been shown to result from inhibition of beta-oxidation of fatty acids, likely via inhibition of CPT1 with, as a consequence, accumulation of free FA and triglycerides, leading to ROS production and mitochondrial permeability transition and apoptosis (Massart et al., 2013).

A treatment with LPS has also been shown to induce steatosis in rodents and its steatogenic effect has been attributed to its ability to enhance production of TNF-α and other pro-inflammatory cytokines (Endo et al., 2007; Fukunishi et al., 2014). In support, direct administration of TNF-α has been shown to increase steatosis in leptin-deficient mice (Xu et al., 2012). TNF-α effects are thought to result from activation of lipogenesis (Endo et al., 2007). However, no effect of LPS on both expression of genes related to lipid metabolism and intracellular triglycerides content was observed in HepaRG cells, probably because of the too low production of TNF-α. Indeed, this production did not exceed 3ng/ml over the 7-day repeated treatment and we showed that treatment with TNF-α caused intracellular accumulation of triglycerides only with a concentration of 5ng/ml.

Both cytotoxicity and steatosis of AMD were aggravated by co-exposure to LPS, as shown by increased ROS production, caspase 3 activation and intracellular accumulation of triglycerides and lipid droplets. To our knowledge such *in vitro* recapitulation of a drug–induced steatohepatitis has not been reported previously. Among the higher deregulated genes with the co-treatment than with AMD alone were ACLY and FASN, that play a key role in lipogenesis while by contrast, THRSP and CYP3A4 that are both genes regulated through activation of PXR and/or CAR , two transcriptomic factors known to be inhibited by pro-inflammatory cytokines, were repressed by the treatment. Compared to 24h data overexpression of some genes was still observed in 7-day co-treated cultures, in particular FASN and PLIN4 that is involved in the formation of lipid droplets, in agreement with increased accumulation of triglycerides. In addition, CYP2E1 was increased by the endotoxin as previously reported (Abdulla et al., 2006).

In agreement with previous studies showing that LPS potentiated AMD toxicity in mouse Hepa1c1c7 cells and rodent liver (Lu et al., 2012; Lu et al., 2013) we demonstrated here that LPS also enhanced cytotoxicity of AMD in HepaRG cells. Both AMD and LPS separately induced ROS generation and when combined they caused increased ROS production associated with higher expression of HO-1, MnSOD and Nrf2. Oxidative stress impaired mitochondrial function and induced the intrinsic mitochondrial apoptosis pathway. The potentiation of AMD toxicity by co-exposure to LPS was completely blocked by co-addition of etanercept, indicating that TNF-α effect was caused via the external apoptotic pathway as observed with co-treatments of other drugs with the cytokine (Al-Attrache et al., 2016; Fredriksson et al., 2011).

The transcriptional factor Nrf2 was strongly overexpressed by co-treatments. Nrf2 influences intrinsic resistance to oxidative stress and control adaptive responses to various environmental stressors. Its activation has been reported to increase steatosis in leptin-deficient mice (Xu et al., 2012). However conflicting data have been reported; thus, mitochondrial oxidation of FA was found to be depressed in the absence of Nrf2 (Ludtmann et al., 2014). In our study we observed both enhanced expression of Nrf2 and increased cytotoxicity and steatosis in cells co-treated with AMD and LPS.

In addition, to oxidative stress ER stress has been reported to play an important role in the development of steatosis and progression to steatohepatitis (Kammoun et al., 2009; Pagliassotti, 2012). We showed that several genes related to ER stress were overexpressed supporting an involvement of ER stress in steatosis and/or cytotoxicity effects induced by AMD ± LPS in HepaRG cells.

The ROS scavenger, NAC, remarkably relieved AMD, AMD/LPS and AMD/TNF-α oxidative stress, subsequently protecting HepaRG cells against apoptosis and steatosis. Although TNF-α was also reported to aggravate AMD toxicity in mouse Hepa1c1c7 cells, co-addition of NAC was found to only slightly attenuate cytotoxicity induced by the co-treatment (Lu et al., 2013). The higher sensitivity of HepaRG cells was probably related to their higher differentiation state**.**

A slight increase in AMD cytotoxicity was also observed in the presence of IL-6 or IL-1b as demonstrated by modest activation of caspase 3.

Noticeably, co-addition of vitamin E at 5µM, another antioxidant, also largely prevented caspase 3 activation and accumulation of triglycerides induced by AMD and AMD/LPS (data not shown).

AMD, like other cationic amphiphilic drugs, also induced phospholipidosis, identified as intracellular lamellar inclusion bodies formed by excessive accumulation of phospholipids. As previously reported (Antherieu et al., 2011) these lamellar bodies were observed in both hepatocyte-like and biliary-like HepaRG cells as early as the first 24h of treatment. AMD-induced phospholipidosis could be related to up-regulation of the fatty acid biosynthesis-related gene SCD causing enhanced synthesis of phospholipids and overexpression of lanosterol synthase (LSS), associated with cholesterol and glycerolipid metabolism (Sawada et al., 2005).

Another gene, LPIN1 that encodes the phosphatidate phosphatase-1 enzyme, was specifically overexpressed in HepaRG cells after both acute and repeat amiodarone exposure. This enzyme converts phosphatidate to diacylglycerol that can serve as substrate for the synthesis of triacylglycerol as well as phosphatidylethanolamine and phosphatidylcholine (Carman and Han, 2006). In addition, genes involved in phospholipid degradation (GDPD3 and ASML3A) were also up-regulated after 7 days. The major differences observed with co-treated cells were an overexpression of ASML3A, GDPD3 involved in degradation of phospholipids and LSS; they corresponded to a defence mechanism to reduce phospholipid accumulation and therefore could represent potential biomarkers of drug-induced phospholipidosis.

Together, the data described in the present work clearly showed that cytotoxicity and steatosis induced by AMD could be aggravated in an inflammatory stress, thereby mimicking a drug-induced steatohepatitis and that these effects were related to ROS generation and likely to ER stress generation and were prevented by NAC co-addition. Moreover, our results suggest that HepaRG cells represent a suitable *in vitro* model for the evaluation of the protective role of anti-oxidants and other molecules against drug-induced steatohepatitis.

Discussion et conclusions

Plus de 1000 molécules sont reconnues pour être potentiellement hépatotoxiques. L'importance d'un contexte inflammatoire associé à une réaction immune est largement évoquée pour expliquer les réactions idiosyncratiques observées chez un petit nombre de patients traités. Cette situation et le fait que les modèles animaux ne sont pas prédictifs de ce type de toxicité font que la prédiction d'une hépatotoxicité idiosyncratique au cours du développement préclinique et clinique de nouveaux médicaments reste un challenge majeur. Dans notre travail, nous avons montré que des cytokines pro-inflammatoires peuvent aggraver la cytotoxicité de médicaments connus pour induire une hépatotoxicité de type idiosyncratique, à savoir le diclofénac, la trovafloxacine et l'amiodarone, en utilisant comme modèle expérimental, les cellules hépatiques humaines différenciées HepaRG. Les résultats ont été principalement obtenus avec le TNF-α qui agit via l'activation des récepteurs de mort, ce qui conduit à une apoptose par la voie extrinsèque alors que les médicaments seuls induisent une apoptose par la voie intrinsèque. Des études plus approfondies sur le diclofénac ont montré que les cellules HepaRG indifférenciées (n'exprimant pas les enzymes majeurs de biotransformation) étaient plus sensibles que les cellules différenciées. Ceci s'explique par le fait que si des métabolites réactifs sont formés par l'activité de cytochromes P450 ils sont ensuite inactivés par les enzymes de conjugaison et en premier lieu, les glutathion transférases. Cette sensibilité plus grande des cellules indifférenciées est en accord avec des données *in vivo* montrant que le diclofénac est plus toxique pour l'intestin que pour le foie. Les cellules HepaRG sont également sensibles à l'IL-1 et l'IL-6 et une étude plus approfondie de ces 2 cytokines serait utile pour comparer plus précisément leurs effets cytotoxiques à ceux du TNF-α (Tableau 7).

La trovofloxacine, en revanche, était plus cytotoxique pour les cellules HepaRG différenciées que pour les cellules indifférenciées, suggérant un mécanisme de toxicité différent de celui du diclofénac. Cependant, comme ce dernier, la trovofloxacine était plus cytotoxique en présence de cytokines pro-inflammatoires. D'autre part, ajoutés en mélange les 2 médicaments avaient un effet additif qui était accru par des traitements répétés et la présence de cytokines.

Nous avons montré que le diclofénac et la trovofloxacine ont des effets cholestatiques *in vitro*, qui se traduisent notamment par une dilatation des canalicules biliaires. Des travaux récents du laboratoire suggèrent que des altérations des canalicules biliaires qui peuvent être des dilatations ou des constrictions, sont constamment induites par des molécules cholestatiques (Sharanek et al., 2016). Ces altérations n'étaient pas aggravées dans un contexte inflammatoire. Cette observation est importante et mérite d'être approfondie car elle permettrait de mieux estimer l'influence d'un stress inflammatoire. Il conviendrait notamment de s'assurer qu'il n'existe pas de différences d'effet entre les cytokines et qu'un traitement répété pendant plusieurs jours est toujours sans effet. Les cytokines sont, en effet, connues pour inhiber l'expression et l'activité de certains transporteurs d'acides biliaires mais les conséquences restent imprécises. On notera également qu'il n'a pas été démontré une accumulation intracellulaire d'acides biliaires en

présence de molécules cholestatiques, à l'exception d'acide lithocholique en présence de cyclosporine A, dans les cellules en culture (Sharanek et al., 2015). L'ajout d'acides biliaires exogènes, dans des concentrations comparables à celles présentes *in vivo*, permettra peut-être de répondre à cette question (Tableau 7).

Nous avons également abordé l'étude de l'influence d'un stress inflammatoire induit par le lipopolysaccharide bactérien sur le développement d'une stéatose d'origine médicamenteuse (amiodarone) et montré que cette endotoxine provoque une évolution vers un stade de stéato-hépatite qui peut cependant être évité par un traitement anti-oxydant, avec l'addition de N-acétyl-cystéine. Ces résultats originaux et intéressants méritent d'être confirmés et confortés par l'étude d'autres molécules stéatosiques et une analyse détaillée des effets des différentes cytokines pro-inflammatoires. Nos résultats suggèrent que le lipopolysaccharide agit principalement en induisant la production de diverses cytokines et en particulier le TNF-α (Tableau 7).

Le rôle des cellules immunes est constamment évoqué dans l'induction d'une hépatotoxicité idiosyncratique d'origine médicamenteuse. Nous avons réalisé plusieurs expériences de co-cultures associant des cellules HepaRG et des cellules immunes en ajoutant des monocytes humains qui se différenciaient en quelques jours en macrophages et cellules dendritiques. Cependant, nous avons été constamment confrontés à une perte importante de cellules monocytaires et à une perte d'activité des macrophages qui survivaient. Il nous est apparu que de telles co-cultures ne pouvaient être réalisées qu'en 3-D, avec ensemencement dans des gels pour éviter des pertes de cellules. Ce type de cultures 3-D fait actuellement l'objet de nombreuses recherches car il devrait permettre d'associer plusieurs types cellulaires et donc des hépatocytes avec des cellules étoilées, des cellules de Küpffer et des cellules endothéliales.

D'une autre part, nous avons étudié la toxicité du DCF dans le modèle de levure qui possède une très faible capacité de métabolisme des xénobiotiques. Nous avons reproduit l'effet toxique du DCF sur ces cellules et leur capacité à s'adapter au DCF et reprendre leur croissance. Nous avons aussi démontré, pour la première fois et différemment de ce que nous avons vu dans les cellules HepaRG (Al-Attrache et al., 2016) que la NAC aggrave la toxicité induite par DCF chez la levure *Saccharomyces cerevsiae* et que certaines souches mutées au niveau de certains transporteurs ABC (par exemple Pdr5) étaient plus sensibles aux effets toxiques de DCF et l'interaction NAC/DCF. A ce niveau, divers mécanismes possibles pourraient expliquer ce synergisme d'interaction observée entre NAC et DCF, y compris les perturbations de pont di-S et l'effet chélateur de Zinc (Kelly, 1998), par NAC, pour certaines protéines clés (transporteurs, protéines de signalisation ou des facteurs de transcription, ...). Par contre, le stress oxydant ne semble pas être impliqué dans l'interaction NAC/DCF dans le cas de *Saccharomyces cerevisiae*. Des études mécanistiques seront nécessaires pour élucider cette interaction originale (Tableau 7).

Les résultats opposés obtenus avec NAC dans les cellules HepaRG et les levures méritent d'être confortés par des études complémentaires, notamment par l'utilisation d'autres anti-oxydants,

d'autant que des effets divergents ont été rapportés avec NAC dans des conditions de traitements différentes.

Médicaments	**Sans co-traitement**	**Co-traitement avec LPS**	**Co-traitemen avec TNF-α**	**Co-traitement avec NAC**
Diclofénac	-Plus toxique dans les cellules HepaRG non différenciées -Induit une cholestase dans les cellules HepaRG différenciées -Sa toxicité est dépendante de la capacité de détoxification du modèle -Sa toxicité est aggravée dans les souches de *Saccharomyces cerevisiae* mutées dans certains transporteurs ABC	ND	-Aggrave la toxicité de DCF majoritairement via la voie extrinsèque dans les cellules HepaRG différenciées -Aggrave la génération de ROS et des marqueurs du RE -N'aggrave pas l'effet cholestatique de DCF sauf au niveau de certains gènes	-Diminue l'effet toxique de DCF et TNF-α dans les cellules HepaRG -Aggrave l'effet toxique de DCF dans le *Saccharomyces cerevisiae* et surtout dans les souches mutées dans certains transporteurs ABC
Trovafloxacine	-Plus toxiques dans les cellules HepaRG différenciées -Induit une cholestase dans	ND	-Aggrave la toxicité de DCF/TVX majoritaireemnt via la voie extrinsèque dans les cellules HepaRG	

	les cellules HepaRG différenciées -Co-traitement DCF/TVX aggrave la toxicité et l'effet cholestatique -Un traitement répété aggrave la toxicité		différenciées -Aggrave la génération de ROS et des marqueurs du RE -N'aggrave pas l'effet sur l'effet cholestatique de DCF/TVX sauf au niveau de certains gènes	
Amiodarone	-Induit une stéatose surtout à 7 jours après 3 additions	-Aggravation de la toxicité -Aggravation de ROS -Aggravation de la synthèse de triglycérides -Inhibition de la β-oxydation des acides gras -Induction de sécrétion de TNF-α	-Aggravation de la toxicité -Aggravation de ROS -Aggravation de la synthèse de triglycérides -Inhibition de la β-oxydation des acides gras -Mime l'effet de LPS	-Diminue l'effet toxique d'AMD/TNF-α ou AMD/ LPS dans les cellules HepaRG

Tableau 7: Tableau contenant les conclusions principales obtenues. « LPS » signifie « lipopolysaccharide », « TNF-α » signifie « facteur de nécrose tumorale α » et « NAC » « N-acétylcystéine ».

Au total, nos travaux ont démontré tout l'intérêt que représente le modèle des cellules humaines HepaRG en culture pour l'étude de molécules médicamenteuses quant à leurs effets cytotoxiques, cholestatiques et stéatosiques dans un contexte inflammatoire ou non et pour la prédiction des effets de nouvelles molécules en développement. Ils montrent aussi que l'effet de ces dernières seules ou en mélange dépend des caractéristiques du modèle cellulaire utilisé surtout au niveau du métabolisme et des transporteurs d'efflux et d'influx que ce soit au niveau

des cellules eucaryotes humaines (comme les cellules HepaRG et les cellules HepG2) ou non humaines (comme le *Saccharomyces cerevisiae*).

D'autres modèles que les cellules HepaRG et le hépatocytes humains en culture 2D pourraient être envisagés pour des études telles que celles que nous avons réalisées. Comme nous l'avons indiqué plus haut des cultures 3D (en sphéroïdes ou obtenues par bioprinting) devraient permettre d'avoir des co-cultures associant hepatocytes et cellules non parenchymateuses et des hepatocytes exprimant des fonctions à un niveau plus élevé qu'en culture 2D. Cependant, les cultures 2D nous semblent plus adaptées à des observations en microscopie optique (analyse de la dynamique des canalicules biliaires par exemple). Des cultures d'hépatocytes dérivées de cellules souches devraient pouvoir aussi être utilisées ; cependant, le niveau de différenciation reste encore insuffisant. Enfin nos études pourraient bénéficier de modèles in vivo, et en particulier d'animaux humanisés (transplantation d'hépatocytes humains ou de cellules HepaRG), ce qui permettrait d'analyser les réponses des cellules humaines dans un contexte d'organismes entiers.

Références

Abdel-Razzak, Z., Loyer, P., Fautrel, A., Gautier, J.C., Corcos, L., Turlin, B., Beaune, P., Guillouzo, A., 1993. Cytokines down-regulate expression of major cytochrome P-450 enzymes in adult human hepatocytes in primary culture. Molecular pharmacology 44, 707-715.

Abdulla, D., Goralski, K.B., Renton, K.W., 2006. The regulation of cytochrome P450 2E1 during LPS-induced inflammation in the rat. Toxicology and applied pharmacology 216, 1-10.

Actis, G.C., Pellicano, R., Fadda, M., Rosina, F., 2014. Antibiotics and non-steroidal anti-inflammatory drugs in outpatient practice: indications and unwanted effects in a gastroenterological setting. Current drug safety 9, 133-137.

Adamis, P.D., Gomes, D.S., Pereira, M.D., Freire de Mesquita, J., Pinto, M.L., Panek, A.D., Eleutherio, E.C., 2004a. The effect of superoxide dismutase deficiency on cadmium stress. Journal of biochemical and molecular toxicology 18, 12-17.

Adamis, P.D., Gomes, D.S., Pinto, M.L., Panek, A.D., Eleutherio, E.C., 2004b. The role of glutathione transferases in cadmium stress. Toxicology letters 154, 81-88.

Aithal, G.P., Ramsay, L., Daly, A.K., Sonchit, N., Leathart, J.B., Alexander, G., Kenna, J.G., Caldwell, J., Day, C.P., 2004. Hepatic adducts, circulating antibodies, and cytokine polymorphisms in patients with diclofenac hepatotoxicity. Hepatology 39, 1430-1440.

Al-Attrache, H., Sharanek, A., Burban, A., Burbank, M., Gicquel, T., Abdel-Razzak, Z., Guguen-Guillouzo, C., Morel, I., Guillouzo, A., 2016. Differential sensitivity of metabolically competent and non-competent HepaRG cells to apoptosis induced by diclofenac combined or not with TNF-alpha. Toxicology letters 258, 71-86.

Altman, R., Bosch, B., Brune, K., Patrignani, P., Young, C., 2015. Advances in NSAID development: evolution of diclofenac products using pharmaceutical technology. Drugs 75, 859-877.

Amacher, D.E., 1998. Serum transaminase elevations as indicators of hepatic injury following the administration of drugs. Regulatory toxicology and pharmacology : RTP 27, 119-130.

Ananthanarayanan, M., Balasubramanian, N., Makishima, M., Mangelsdorf, D.J., Suchy, F.J., 2001. Human bile salt export pump promoter is transactivated by the farnesoid X receptor/bile acid receptor. The Journal of biological chemistry 276, 28857-28865.

Aninat, C., Piton, A., Glaise, D., Le Charpentier, T., Langouet, S., Morel, F., Guguen-Guillouzo, C., Guillouzo, A., 2006. Expression of cytochromes P450, conjugating enzymes and nuclear receptors in human hepatoma HepaRG cells. Drug metabolism and disposition: the biological fate of chemicals 34, 75-83.

Antherieu, S., Bachour-El Azzi, P., Dumont, J., Abdel-Razzak, Z., Guguen-Guillouzo, C., Fromenty, B., Robin, M.A., Guillouzo, A., 2013. Oxidative stress plays a major role in chlorpromazine-induced cholestasis in human HepaRG cells. Hepatology 57, 1518-1529.

Antherieu, S., Rogue, A., Fromenty, B., Guillouzo, A., Robin, M.A., 2011. Induction of vesicular steatosis by amiodarone and tetracycline is associated with up-regulation of lipogenic genes in HepaRG cells. Hepatology 53, 1895-1905.

Atchison, C.R., West, A.B., Balakumaran, A., Hargus, S.J., Pohl, L.R., Daiker, D.H., Aronson, J.F., Hoffmann, W.E., Shipp, B.K., Treinen-Moslen, M., 2000. Drug enterocyte adducts: possible causal factor for diclofenac enteropathy in rats. Gastroenterology 119, 1537-1547.

Babatin, M., Lee, S.S., Pollak, P.T., 2008. Amiodarone hepatotoxicity. Current vascular pharmacology 6, 228-236.

Bach, N., Schultz, B.L., Cohen, L.B., Squire, A., Gordon, R., Thung, S.N., Schaffner, F., 1989. Amiodarone hepatotoxicity: progression from steatosis to cirrhosis. The Mount Sinai journal of medicine, New York 56, 293-296.

Bachour-El Azzi, P., Sharanek, A., Abdel-Razzak, Z., Antherieu, S., Al-Attrache, H., Savary, C.C., Lepage, S., Morel, I., Labbe, G., Guguen-Guillouzo, C., Guillouzo, A., 2014. Impact of inflammation on chlorpromazine-induced cytotoxicity and cholestatic features in HepaRG cells. Drug metabolism and disposition: the biological fate of chemicals 42, 1556-1566.

Bachour-El Azzi, P., Sharanek, A., Burban, A., Li, R., Guevel, R.L., Abdel-Razzak, Z., Stieger, B., Guguen-Guillouzo, C., Guillouzo, A., 2015. Comparative Localization and Functional Activity of the Main Hepatobiliary Transporters in HepaRG Cells and Primary Human Hepatocytes. Toxicological sciences : an official journal of the Society of Toxicology 145, 157-168.

Bailey, M.J., Dickinson, R.G., 2003. Acyl glucuronide reactivity in perspective: biological consequences. Chemico-biological interactions 145, 117-137.

Banerjee, S., Flores-Rozas, H., 2005. Cadmium inhibits mismatch repair by blocking the ATPase activity of the MSH2-MSH6 complex. Nucleic acids research 33, 1410-1419.

Banks, A.T., Zimmerman, H.J., Ishak, K.G., Harter, J.G., 1995. Diclofenac-associated hepatotoxicity: analysis of 180 cases reported to the Food and Drug Administration as adverse reactions. Hepatology 22, 820-827.

Bauer, B.E., Wolfger, H., Kuchler, K., 1999. Inventory and function of yeast ABC proteins: about sex, stress, pleiotropic drug and heavy metal resistance. Biochimica et biophysica acta 1461, 217-236.

Baumann, H., Gauldie, J., 1994. The acute phase response. Immunology today 15, 74-80.

Beggs, K.M., Fullerton, A.M., Miyakawa, K., Ganey, P.E., Roth, R.A., 2014. Molecular mechanisms of hepatocellular apoptosis induced by trovafloxacin-tumor necrosis factor-alpha interaction. Toxicological sciences : an official journal of the Society of Toxicology 137, 91-101.

Beggs, K.M., Maiuri, A.R., Fullerton, A.M., Poulsen, K.L., Breier, A.B., Ganey, P.E., Roth, R.A., 2015. Trovafloxacin-induced replication stress sensitizes HepG2 cells to tumor necrosis factor-alpha-induced cytotoxicity mediated by extracellular signal-regulated kinase and ataxia telangiectasia and Rad3-related. Toxicology 331, 35-46.

Beigneux, A.P., Moser, A.H., Shigenaga, J.K., Grunfeld, C., Feingold, K.R., 2000. The acute phase response is associated with retinoid X receptor repression in rodent liver. The Journal of biological chemistry 275, 16390-16399.

Beigneux, A.P., Moser, A.H., Shigenaga, J.K., Grunfeld, C., Feingold, K.R., 2002. Reduction in cytochrome P-450 enzyme expression is associated with repression of CAR (constitutive androstane receptor) and PXR (pregnane X receptor) in mouse liver during the acute phase response. Biochemical and biophysical research communications 293, 145-149.

Berson, A., De Beco, V., Letteron, P., Robin, M.A., Moreau, C., El Kahwaji, J., Verthier, N., Feldmann, G., Fromenty, B., Pessayre, D., 1998. Steatohepatitis-inducing drugs cause mitochondrial dysfunction and lipid peroxidation in rat hepatocytes. Gastroenterology 114, 764-774.

Bjornsson, E., Olsson, R., 2006. Suspected drug-induced liver fatalities reported to the WHO database. Digestive and liver disease : official journal of the Italian Society of Gastroenterology and the Italian Association for the Study of the Liver 38, 33-38.

Bleibel, W., Kim, S., D'Silva, K., Lemmer, E.R., 2007. Drug-induced liver injury: review article. Digestive diseases and sciences 52, 2463-2471.

Blouin, A., Bolender, R.P., Weibel, E.R., 1977. Distribution of organelles and membranes between hepatocytes and nonhepatocytes in the rat liver parenchyma. A stereological study. The Journal of cell biology 72, 441-455.

Blum, W., Faigle, J.W., Pfaar, U., Sallmann, A., 1996. Characterization of a novel diclofenac metabolite in human urine by capillary gas chromatography-negative chemical ionization mass spectrometry. Journal of chromatography B, Biomedical applications 685, 251-263.

Bode, C., Bode, J.C., 2003. Effect of alcohol consumption on the gut. Best practice & research Clinical gastroenterology 17, 575-592.

Bode, C., Bode, J.C., 2005. Activation of the innate immune system and alcoholic liver disease: effects of ethanol per se or enhanced intestinal translocation of bacterial toxins induced by ethanol? Alcoholism, clinical and experimental research 29, 166S-171S.

Boelsterli, U.A., 2002. Xenobiotic acyl glucuronides and acyl CoA thioesters as protein-reactive metabolites with the potential to cause idiosyncratic drug reactions. Current drug metabolism 3, 439-450.

Boelsterli, U.A., 2003a. Diclofenac-induced liver injury: a paradigm of idiosyncratic drug toxicity. Toxicology and applied pharmacology 192, 307-322.

Boelsterli, U.A., 2003b. Disease-related determinants of susceptibility to drug-induced idiosyncratic hepatotoxicity. Current opinion in drug discovery & development 6, 81-91.

Boelsterli, U.A., 2003c. Idiosyncratic drug hepatotoxicity revisited: new insights from mechanistic toxicology. Toxicology mechanisms and methods 13, 3-20.

Bort, R., Mace, K., Boobis, A., Gomez-Lechon, M.J., Pfeifer, A., Castell, J., 1999a. Hepatic metabolism of diclofenac: role of human CYP in the minor oxidative pathways. Biochemical pharmacology 58, 787-796.

Bort, R., Ponsoda, X., Jover, R., Gomez-Lechon, M.J., Castell, J.V., 1999b. Diclofenac toxicity to hepatocytes: a role for drug metabolism in cell toxicity. The Journal of pharmacology and experimental therapeutics 288, 65-72.

Braconi, D., Bernardini, G., Santucci, A., 2016. Saccharomyces cerevisiae as a model in ecotoxicological studies: A post-genomics perspective. Journal of proteomics 137, 19-34.

Brcakova, E., Fuksa, L., Cermanova, J., Kolouchova, G., Hroch, M., Hirsova, P., Martinkova, J., Staud, F., Micuda, S., 2009. Alteration of methotrexate biliary and renal elimination during extrahepatic and intrahepatic cholestasis in rats. Biological & pharmaceutical bulletin 32, 1978-1985.

Breen, E.G., McNicholl, J., Cosgrove, E., McCabe, J., Stevens, F.M., 1986. Fatal hepatitis associated with diclofenac. Gut 27, 1390-1393.

Briza, P., Eckerstorfer, M., Breitenbach, M., 1994. The sporulation-specific enzymes encoded by the DIT1 and DIT2 genes catalyze a two-step reaction leading to a soluble LL-dityrosine-containing precursor of the yeast spore wall. Proceedings of the National Academy of Sciences of the United States of America 91, 4524-4528.

Brooker, C., 2001. Le corps humain: Étude, structure et fonction. Foie et voies biliaires. Mosby.
Buchweitz, J.P., Ganey, P.E., Bursian, S.J., Roth, R.A., 2002. Underlying endotoxemia augments toxic responses to chlorpromazine: is there a relationship to drug idiosyncrasy? The Journal of pharmacology and experimental therapeutics 300, 460-467.

Cabral, M.G., Viegas, C.A., Teixeira, M.C., Sa-Correia, I., 2003. Toxicity of chlorinated phenoxyacetic acid herbicides in the experimental eukaryotic model Saccharomyces cerevisiae: role of pH and of growth phase and size of the yeast cell population. Chemosphere 51, 47-54.

Cabrito, T.R., Teixeira, M.C., Singh, A., Prasad, R., Sa-Correia, I., 2011. The yeast ABC transporter Pdr18 (ORF YNR070w) controls plasma membrane sterol composition, playing a role in multidrug resistance. The Biochemical journal 440, 195-202.

Cantoni, L., Valaperta, R., Ponsoda, X., Castell, J.V., Barelli, D., Rizzardini, M., Mangolini, A., Hauri, L., Villa, P., 2003. Induction of hepatic heme oxygenase-1 by diclofenac in rodents: role of oxidative stress and cytochrome P-450 activity. Journal of hepatology 38, 776-783.

Carman, G.M., Han, G.S., 2006. Roles of phosphatidate phosphatase enzymes in lipid metabolism. Trends in biochemical sciences 31, 694-699.

Cerec, V., Glaise, D., Garnier, D., Morosan, S., Turlin, B., Drenou, B., Gripon, P., Kremsdorf, D., Guguen-Guillouzo, C., Corlu, A., 2007. Transdifferentiation of hepatocyte-like cells from the human hepatoma HepaRG cell line through bipotent progenitor. Hepatology 45, 957-967.

Chant, J., 1999. Cell polarity in yeast. Annual review of cell and developmental biology 15, 365-391.

Charles A Janeway, J., Paul Travers, Mark Walport, and Mark J Shlomchik., 2001. Immunobiology, 5th edition: The Immune System in Health and Disease. Garland Science, New York.

Chen, C.A., Cowan, J.A., 2006. Characterization of Saccharomyces cerevisiae Atm1p: functional studies of an ABC7 type transporter. Biochimica et biophysica acta 1760, 1857-1865.

Chen, H.J., Bloch, K.J., Maclean, J.A., 2000. Acute eosinophilic hepatitis from trovafloxacin. The New England journal of medicine 342, 359-360.

Chen, X.M., O'Hara, S.P., LaRusso, N.F., 2008. The immunobiology of cholangiocytes. Immunology and cell biology 86, 497-505.

Cherrington, N.J., Slitt, A.L., Li, N., Klaassen, C.D., 2004. Lipopolysaccharide-mediated regulation of hepatic transporter mRNA levels in rats. Drug metabolism and disposition: the biological fate of chemicals 32, 734-741.

Chloupkova, M., LeBard, L.S., Koeller, D.M., 2003. MDL1 is a high copy suppressor of ATM1: evidence for a role in resistance to oxidative stress. Journal of molecular biology 331, 155-165.

Cimic, A.a.S., J., 2013. Amiodarone Hepatotoxicity with Absent Phospholipidosis and Steatosis: A Case Report and Review of Amiodarone Toxicity in Various Organs. Case reports in pathology, 4.

Collinson, E.J., Grant, C.M., 2003. Role of yeast glutaredoxins as glutathione S-transferases. The Journal of biological chemistry 278, 22492-22497.

Cosgrove, B.D., Alexopoulos, L.G., Hang, T.C., Hendriks, B.S., Sorger, P.K., Griffith, L.G., Lauffenburger, D.A., 2010. Cytokine-associated drug toxicity in human hepatocytes is associated with signaling network dysregulation. Molecular bioSystems 6, 1195-1206.

Cosgrove, B.D., King, B.M., Hasan, M.A., Alexopoulos, L.G., Farazi, P.A., Hendriks, B.S., Griffith, L.G., Sorger, P.K., Tidor, B., Xu, J.J., Lauffenburger, D.A., 2009. Synergistic drug-cytokine induction of hepatocellular death as an in vitro approach for the study of inflammation-associated idiosyncratic drug hepatotoxicity. Toxicology and applied pharmacology 237, 317-330.

Costantini, P., Chernyak, B.V., Petronilli, V., Bernardi, P., 1996. Modulation of the mitochondrial permeability transition pore by pyridine nucleotides and dithiol oxidation at two separate sites. The Journal of biological chemistry 271, 6746-6751.

Courchesne, W.E., 2002. Characterization of a novel, broad-based fungicidal activity for the antiarrhythmic drug amiodarone. The Journal of pharmacology and experimental therapeutics 300, 195-199.

Courchesne, W.E., Tunc, M., Liao, S., 2009. Amiodarone induces stress responses and calcium flux mediated by the cell wall in Saccharomyces cerevisiae. Canadian journal of microbiology 55, 288-303.
Cresnar, B., Petric, S., 2011. Cytochrome P450 enzymes in the fungal kingdom. Biochimica et biophysica acta 1814, 29-35.

Cui, Z., Hirata, D., Tsuchiya, E., Osada, H., Miyakawa, T., 1996. The multidrug resistance-associated protein (MRP) subfamily (Yrs1/Yor1) of Saccharomyces cerevisiae is important for the tolerance to a broad range of organic anions. The Journal of biological chemistry 271, 14712-14716.

Dalvie, D.K., Khosla, N., Vincent, J., 1997. Excretion and metabolism of trovafloxacin in humans. Drug metabolism and disposition: the biological fate of chemicals 25, 423-427.

Daniel, M., Sharpe, A., Driver, J., Knight, A.W., Keenan, P.O., Walmsley, R.M., Robinson, A., Zhang, T., Rawson, D., 2004. Results of a technology demonstration project to compare rapid aquatic toxicity screening tests in the analysis of industrial effluents. Journal of environmental monitoring : JEM 6, 855-865.

David Josephy, P., Peter Guengerich, F., Miners, J.O., 2005. "Phase I and Phase II" drug metabolism: terminology that we should phase out? Drug metabolism reviews 37, 575-580.

De Filippi, L., Fournier, M., Cameroni, E., Linder, P., De Virgilio, C., Foti, M., Deloche, O., 2007. Membrane stress is coupled to a rapid translational control of gene expression in chlorpromazine-treated cells. Current genetics 52, 171-185.

De Sarro, A., De Sarro, G., 2001. Adverse reactions to fluoroquinolones. an overview on mechanistic aspects. Current medicinal chemistry 8, 371-384.

Deffieu, M., Bhatia-Kissova, I., Salin, B., Galinier, A., Manon, S., Camougrand, N., 2009. Glutathione participates in the regulation of mitophagy in yeast. The Journal of biological chemistry 284, 14828-14837.

Degott, C., Feldmann, G., Larrey, D., Durand-Schneider, A.M., Grange, D., Machayekhi, J.P., Moreau, A., Potet, F., Benhamou, J.P., 1992. Drug-induced prolonged cholestasis in adults: a histological semiquantitative study demonstrating progressive ductopenia. Hepatology 15, 244-251.

Deng, X., Luyendyk, J.P., Ganey, P.E., Roth, R.A., 2009. Inflammatory stress and idiosyncratic hepatotoxicity: hints from animal models. Pharmacological reviews 61, 262-282.

Deng, X., Stachlewitz, R.F., Liguori, M.J., Blomme, E.A., Waring, J.F., Luyendyk, J.P., Maddox, J.F., Ganey, P.E., Roth, R.A., 2006. Modest inflammation enhances diclofenac hepatotoxicity in rats: role of neutrophils and bacterial translocation. The Journal of pharmacology and experimental therapeutics 319, 1191-1199.

Denson, L.A., Auld, K.L., Schiek, D.S., McClure, M.H., Mangelsdorf, D.J., Karpen, S.J., 2000. Interleukin-1beta suppresses retinoid transactivation of two hepatic transporter genes involved in bile formation. The Journal of biological chemistry 275, 8835-8843.

Desmet, V.J., 1997. Vanishing bile duct syndrome in drug-induced liver disease. Journal of hepatology 26 Suppl 1, 31-35.

Ding, W.X., Yin, X.M., 2004. Dissection of the multiple mechanisms of TNF-alpha-induced apoptosis in liver injury. Journal of cellular and molecular medicine 8, 445-454.

Donato, M.T., Martinez-Romero, A., Jimenez, N., Negro, A., Herrera, G., Castell, J.V., O'Connor, J.E., Gomez-Lechon, M.J., 2009. Cytometric analysis for drug-induced steatosis in HepG2 cells. Chemico-biological interactions 181, 417-423.

Donner, M.G., Warskulat, U., Saha, N., Haussinger, D., 2004. Enhanced expression of basolateral multidrug resistance protein isoforms Mrp3 and Mrp5 in rat liver by LPS. Biological chemistry 385, 331-339.

Dumont, J., Josse, R., Lambert, C., Antherieu, S., Le Hegarat, L., Aninat, C., Robin, M.A., Guguen-Guillouzo, C., Guillouzo, A., 2010. Differential toxicity of heterocyclic aromatic amines and their mixture in metabolically competent HepaRG cells. Toxicology and applied pharmacology 245, 256-263.

Durrigl, T., Vitaus, M., Pucar, I., Miko, M., 1975. Diclofenac sodium (Voltaren): results of a multi-centre comparative trial in adult-onset rheumatoid arthritis. The Journal of international medical research 3, 139-144.

Eaton, D.L., Klaassen, C.D.,, 1996. Principles of toxicology, in: Klaassen, C.D. (Ed.), Casarett and Doull's Toxicology: The Basic Science of Poisons. McGraw-Hill, fifth ed, New York.

Edlundh-Rose, E., Kupershmidt, I., Gustafsson, A.C., Parasassi, T., Serafino, A., Bracci-Laudiero, L., Greco, G., Krasnowska, E.K., Romano, M.C., Lundeberg, T., Nilsson, P., Lundeberg, J., 2005. Gene expression analysis of human epidermal keratinocytes after N-acetyl L-cysteine treatment demonstrates cell cycle arrest and increased differentiation. Pathobiology : journal of immunopathology, molecular and cellular biology 72, 203-212.

Efrati, S., Berman, S., Siman-Tov, Y., Lotan, R., Averbukh, Z., Weissgarten, J., Golik, A., 2007. N-acetylcysteine attenuates NSAID-induced rat renal failure by restoring intrarenal prostaglandin synthesis. Nephrology, dialysis, transplantation : official publication of the European Dialysis and Transplant Association - European Renal Association 22, 1873-1881.

Egner, R., Rosenthal, F.E., Kralli, A., Sanglard, D., Kuchler, K., 1998. Genetic separation of FK506 susceptibility and drug transport in the yeast Pdr5 ATP-binding cassette multidrug resistance transporter. Molecular biology of the cell 9, 523-543.

Elmore, S., 2007. Apoptosis: a review of programmed cell death. Toxicologic pathology 35, 495-516.
Endo, M., Masaki, T., Seike, M., Yoshimatsu, H., 2007. TNF-alpha induces hepatic steatosis in mice by enhancing gene expression of sterol regulatory element binding protein-1c (SREBP-1c). Experimental biology and medicine 232, 614-621.

Engel, S.R., Dietrich, F.S., Fisk, D.G., Binkley, G., Balakrishnan, R., Costanzo, M.C., Dwight, S.S., Hitz, B.C., Karra, K., Nash, R.S., Weng, S., Wong, E.D., Lloyd, P., Skrzypek, M.S., Miyasato, S.R., Simison, M., Cherry, J.M., 2014. The reference genome sequence of Saccharomyces cerevisiae: then and now. G3 4, 389-398.
Erlinger, S., 1997. Drug-induced cholestasis. Journal of hepatology 26 Suppl 1, 1-4.

Ernst, M.C., Sinal, C.J., Pollak, P.T., 2010. Influence of peroxisome proliferator-activated receptor-alpha (PPARalpha) activity on adverse effects associated with amiodarone exposure in mice. Pharmacological research 62, 408-415.

Evans, W.E., Relling, M.V., 1999. Pharmacogenomics: translating functional genomics into rational therapeutics. Science 286, 487-491.

Faed, E.M., 1984. Properties of acyl glucuronides: implications for studies of the pharmacokinetics and metabolism of acidic drugs. Drug metabolism reviews 15, 1213-1249.

Fang, C., Yoon, S., Tindberg, N., Jarvelainen, H.A., Lindros, K.O., Ingelman-Sundberg, M., 2004. Hepatic expression of multiple acute phase proteins and down-regulation of nuclear receptors after acute endotoxin exposure. Biochemical pharmacology 67, 1389-1397.

Farrell, G.C., Larter, C.Z., 2006. Nonalcoholic fatty liver disease: from steatosis to cirrhosis. Hepatology 43, S99-S112.

Fast, D., 1973. Sporulation synchrony of Saccharomyces cerevisiae grown in various carbon sources. Journal of bacteriology 116, 925-930.

Fausto, N., Campbell, J.S., Riehle, K.J., 2006. Liver regeneration. Hepatology 43, S45-53.

Fava, G., Glaser, S., Francis, H., Alpini, G., 2005. The immunophysiology of biliary epithelium. Seminars in liver disease 25, 251-264.

Fischman, A.J., Babich, J.W., Alpert, N.M., Vincent, J., Wilkinson, R.A., Callahan, R.J., Correia, J.A., Rubin, R.H., 1997. Pharmacokinetics of 18F-labeled trovafloxacin in normal and Escherichia coli-infected rats and rabbits studied with positron emission tomography. Clinical microbiology and infection : the official publication of the European Society of Clinical Microbiology and Infectious Diseases 3, 63-72.

Frankenberg, T., Miloh, T., Chen, F.Y., Ananthanarayanan, M., Sun, A.Q., Balasubramaniyan, N., Arias, I., Setchell, K.D., Suchy, F.J., Shneider, B.L., 2008. The membrane protein ATPase class I type 8B member 1 signals through protein kinase C zeta to activate the farnesoid X receptor. Hepatology 48, 1896-1905.

Fredriksson, L., Herpers, B., Benedetti, G., Matadin, Q., Puigvert, J.C., de Bont, H., Dragovic, S., Vermeulen, N.P., Commandeur, J.N., Danen, E., de Graauw, M., van de Water, B., 2011. Diclofenac inhibits tumor necrosis factor-alpha-induced nuclear factor-kappaB activation causing synergistic hepatocyte apoptosis. Hepatology 53, 2027-2041.

Fredriksson, L., Wink, S., Herpers, B., Benedetti, G., Hadi, M., de Bont, H., Groothuis, G., Luijten, M., Danen, E., de Graauw, M., Meerman, J., van de Water, B., 2014. Drug-induced endoplasmic reticulum and oxidative stress responses independently sensitize toward TNFalpha-mediated hepatotoxicity. Toxicological sciences : an official journal of the Society of Toxicology 140, 144-159.

Friese, M.A., Montalban, X., Willcox, N., Bell, J.I., Martin, R., Fugger, L., 2006. The value of animal models for drug development in multiple sclerosis. Brain : a journal of neurology 129, 1940-1952.

Fromenty, B., Fisch, C., Labbe, G., Degott, C., Deschamps, D., Berson, A., Letteron, P., Pessayre, D., 1990. Amiodarone inhibits the mitochondrial beta-oxidation of fatty acids and produces microvesicular steatosis of the liver in mice. The Journal of pharmacology and experimental therapeutics 255, 1371-1376.

Fromenty, B., Pessayre, D., 1995. Inhibition of mitochondrial beta-oxidation as a mechanism of hepatotoxicity. Pharmacology & therapeutics 67, 101-154.

Fujiwara, R., Sumida, K., Kutsuno, Y., Sakamoto, M., Itoh, T., 2015. UDP-glucuronosyltransferase (UGT) 1A1 mainly contributes to the glucuronidation of trovafloxacin. Drug metabolism and pharmacokinetics 30, 82-88.

Fukunishi, S., Sujishi, T., Takeshita, A., Ohama, H., Tsuchimoto, Y., Asai, A., Tsuda, Y., Higuchi, K., 2014. Lipopolysaccharides accelerate hepatic steatosis in the development of nonalcoholic fatty liver disease in Zucker rats. Journal of clinical biochemistry and nutrition 54, 39-44.

Gabay, C., Kushner, I., 1999. Acute-phase proteins and other systemic responses to inflammation. The New England journal of medicine 340, 448-454.

Galati, G., Tafazoli, S., Sabzevari, O., Chan, T.S., O'Brien, P.J., 2002. Idiosyncratic NSAID drug induced oxidative stress. Chemico-biological interactions 142, 25-41.

Gandhi, A., Guo, T., Ghose, R., 2010. Role of c-Jun N-terminal kinase (JNK) in regulating tumor necrosis factor-alpha (TNF-alpha) mediated increase of acetaminophen (APAP) and chlorpromazine (CPZ) toxicity in murine hepatocytes. The Journal of toxicological sciences 35, 163-173.

Ganey, P.E., Luyendyk, J.P., Maddox, J.F., Roth, R.A., 2004. Adverse hepatic drug reactions: inflammatory episodes as consequence and contributor. Chemico-biological interactions 150, 35-51.

Ganey, P.E., Luyendyk, J.P., Newport, S.W., Eagle, T.M., Maddox, J.F., Mackman, N., Roth, R.A., 2007. Role of the coagulation system in acetaminophen-induced hepatotoxicity in mice. Hepatology 46, 1177-1186.

Gaytan, B.D., Loguinov, A.V., Lantz, S.R., Lerot, J.M., Denslow, N.D., Vulpe, C.D., 2013. Functional profiling discovers the dieldrin organochlorinated pesticide affects leucine availability in yeast. Toxicological sciences : an official journal of the Society of Toxicology 132, 347-358.

Geier, A., Dietrich, C.G., Voigt, S., Ananthanarayanan, M., Lammert, F., Schmitz, A., Trauner, M., Wasmuth, H.E., Boraschi, D., Balasubramaniyan, N., Suchy, F.J., Matern, S., Gartung, C., 2005. Cytokine-dependent regulation of hepatic organic anion transporter gene transactivators in mouse liver. American journal of physiology Gastrointestinal and liver physiology 289, G831-841.

Geier, A., Dietrich, C.G., Voigt, S., Kim, S.K., Gerloff, T., Kullak-Ublick, G.A., Lorenzen, J., Matern, S., Gartung, C., 2003. Effects of proinflammatory cytokines on rat organic anion transporters during toxic liver injury and cholestasis. Hepatology 38, 345-354.

Geier, A., Fickert, P., Trauner, M., 2006. Mechanisms of disease: mechanisms and clinical implications of cholestasis in sepsis. Nature clinical practice Gastroenterology & hepatology 3, 574-585.

Gerloff, T., Geier, A., Roots, I., Meier, P.J., Gartung, C., 2002. Functional analysis of the rat bile salt export pump gene promoter. European journal of biochemistry / FEBS 269, 3495-3503.

Ghalehnoo, Z.R., Rashki, A., Najimi, M., Dominguez, A., 2010. The role of diclofenac sodium in the dimorphic transition in Candida albicans. Microbial pathogenesis 48, 110-115.

Ghose, R., Zimmerman, T.L., Thevananther, S., Karpen, S.J., 2004. Endotoxin leads to rapid subcellular re-localization of hepatic RXRalpha: A novel mechanism for reduced hepatic gene expression in inflammation. Nuclear receptor 2, 4.

Gil, F.N., Moreira-Santos, M., Chelinho, S., Pereira, C., Feliciano, J.R., Leitao, J.H., Sousa, J.P., Ribeiro, R., Viegas, C.A., 2015. Suitability of a Saccharomyces cerevisiae-based assay to assess the toxicity of pyrimethanil sprayed soils via surface runoff: comparison with standard aquatic and soil toxicity assays. The Science of the total environment 505, 161-171.

Gil, M.L., Ramirez, M.C., Terencio, M.C., Castell, J.V., 1995. Immunochemical detection of protein adducts in cultured human hepatocytes exposed to diclofenac. Biochimica et biophysica acta 1272, 140-146.

Glick, B.S., Pon, L.A., 1995. Isolation of highly purified mitochondria from Saccharomyces cerevisiae. Methods in enzymology 260, 213-223.

Goldsby R.A., K.T.J., and Osborne B.A.,, 2000. Immunologie, le cours de Janus Kuby. Dunod ed.

Goldstein, A., Aronow, L., Kalman, S.M.,, 1974. Principles of Drug Action. Wiley, New York.

Gomes, D.S., Pereira, M.D., Panek, A.D., Andrade, L.R., Eleutherio, E.C., 2008. Apoptosis as a mechanism for removal of mutated cells of Saccharomyces cerevisiae: the role of Grx2 under cadmium exposure. Biochimica et biophysica acta 1780, 160-166.

Gomez-Lechon, M.J., Ponsoda, X., O'Connor, E., Donato, T., Castell, J.V., Jover, R., 2003. Diclofenac induces apoptosis in hepatocytes by alteration of mitochondrial function and generation of ROS. Biochemical pharmacology 66, 2155-2167.

Green, R.M., Beier, D., Gollan, J.L., 1996. Regulation of hepatocyte bile salt transporters by endotoxin and inflammatory cytokines in rodents. Gastroenterology 111, 193-198.

Gueldry, O., Lazard, M., Delort, F., Dauplais, M., Grigoras, I., Blanquet, S., Plateau, P., 2003. Ycf1p-dependent Hg(II) detoxification in Saccharomyces cerevisiae. European journal of biochemistry / FEBS 270, 2486-2496.

Guengerich, F.P., 2006. Cytochrome P450s and other enzymes in drug metabolism and toxicity. The AAPS journal 8, E101-111.

Guguen-Guillouzo, C., Guillouzo, A., 2010. General review on in vitro hepatocyte models and their applications. Methods in molecular biology 640, 1-40.

Guigui, B., Perrot, S., Berry, J.P., Fleury-Feith, J., Martin, N., Metreau, J.M., Dhumeaux, D., Zafrani, E.S., 1988. Amiodarone-induced hepatic phospholipidosis: a morphological alteration independent of pseudoalcoholic liver disease. Hepatology 8, 1063-1068.

Guillouzo, A., Corlu, A., Aninat, C., Glaise, D., Morel, F., Guguen-Guillouzo, C., 2007. The human hepatoma HepaRG cells: a highly differentiated model for studies of liver metabolism and toxicity of xenobiotics. Chemico-biological interactions 168, 66-73.

Gunawan, B.K., Kaplowitz, N., 2007. Mechanisms of drug-induced liver disease. Clinics in liver disease 11, 459-475, v.

Gupta, S.S., Ton, V.K., Beaudry, V., Rulli, S., Cunningham, K., Rao, R., 2003. Antifungal activity of amiodarone is mediated by disruption of calcium homeostasis. The Journal of biological chemistry 278, 28831-28839.

Gutierrez-Correa, J., Stoppani, A.O., 1997. Inactivation of yeast glutathione reductase by Fenton systems: effect of metal chelators, catecholamines and thiol compounds. Free radical research 27, 543-555.

Halliwell, W.H., 1997. Cationic amphiphilic drug-induced phospholipidosis. Toxicologic pathology 25, 53-60.

Hancock, J.T., Desikan, R., Neill, S.J., 2001. Role of reactive oxygen species in cell signalling pathways. Biochemical Society transactions 29, 345-350.

Harada, K., Ohira, S., Isse, K., Ozaki, S., Zen, Y., Sato, Y., Nakanuma, Y., 2003. Lipopolysaccharide activates nuclear factor-kappaB through toll-like receptors and related molecules in cultured biliary epithelial cells. Laboratory investigation; a journal of technical methods and pathology 83, 1657-1667.

Hargus, S.J., Amouzedeh, H.R., Pumford, N.R., Myers, T.G., McCoy, S.C., Pohl, L.R., 1994. Metabolic activation and immunochemical localization of liver protein adducts of the nonsteroidal anti-inflammatory drug diclofenac. Chemical research in toxicology 7, 575-582.

Hargus, S.J., Martin, B.M., George, J.W., Pohl, L.R., 1995. Covalent modification of rat liver dipeptidyl peptidase IV (CD26) by the nonsteroidal anti-inflammatory drug diclofenac. Chemical research in toxicology 8, 993-996.

Harris, L., McKenna, W.J., Rowland, E., Holt, D.W., Storey, G.C., Krikler, D.M., 1983. Side effects of long-term amiodarone therapy. Circulation 67, 45-51.

Hartwell, L.H., 1974. Saccharomyces cerevisiae cell cycle. Bacteriological reviews 38, 164-198.

Hata, S., Nishino, T., Katsuki, H., Aoyama, Y., Yoshida, Y., 1983. Two species of cytochrome P-450 involved in ergosterol biosynthesis of yeast. Biochemical and biophysical research communications 116, 162-166.

Hatzixanthis, K., Mollapour, M., Seymour, I., Bauer, B.E., Krapf, G., Schuller, C., Kuchler, K., Piper, P.W., 2003. Moderately lipophilic carboxylate compounds are the selective inducers of the Saccharomyces cerevisiae Pdr12p ATP-binding cassette transporter. Yeast 20, 575-585.

Hayball, P.J., 1995. Formation and reactivity of acyl glucuronides: the influence of chirality. Chirality 7, 1-9.

Hayes, J.D., Dinkova-Kostova, A.T., 2014. The Nrf2 regulatory network provides an interface between redox and intermediary metabolism. Trends in biochemical sciences 39, 199-218.

Heger, J.J., Prystowsky, E.N., Jackman, W.M., Naccarelli, G.V., Warfel, K.A., Rinkenberger, R.L., Zipes, D.P., 1981. Clinical efficacy and electrophysiology during long-term therapy for recurrent ventricular tachycardia or ventricular fibrillation. The New England journal of medicine 305, 539-545.

Herskowitz, I., 1988. Life cycle of the budding yeast Saccharomyces cerevisiae. Microbiological reviews 52, 536-553.

Hettema, E.H., van Roermund, C.W., Distel, B., van den Berg, M., Vilela, C., Rodrigues-Pousada, C., Wanders, R.J., Tabak, H.F., 1996. The ABC transporter proteins Pat1 and Pat2 are required for import of long-chain fatty acids into peroxisomes of Saccharomyces cerevisiae. The EMBO journal 15, 3813-3822.

Hickey, E.J., Raje, R.R., Reid, V.E., Gross, S.M., Ray, S.D., 2001. Diclofenac induced in vivo nephrotoxicity may involve oxidative stress-mediated massive genomic DNA fragmentation and apoptotic cell death. Free radical biology & medicine 31, 139-152.

Hisaeda, K., Inokuchi, A., Nakamura, T., Iwamoto, Y., Kohno, K., Kuwano, M., Uchiumi, T., 2004. Interleukin-1beta represses MRP2 gene expression through inactivation of interferon regulatory factor 3 in HepG2 cells. Hepatology 39, 1574-1582.

Hlavacek, O., Kucerova, H., Harant, K., Palkova, Z., Vachova, L., 2009. Putative role for ABC multidrug exporters in yeast quorum sensing. FEBS letters 583, 1107-1113.

Hollister, L.E., 1957. Allergy to chlorpromazine manifested by jaundice. The American journal of medicine 23, 870-879.

Hou, Y., Wang, L., Yi, D., Wu, G., 2015. N-acetylcysteine and intestinal health: a focus on its mechanism of action. Frontiers in bioscience 20, 872-891.

Hughes, A.R., Wilkie, D., 1970. Preferential inhibition of respiration in Saccharomyces cerevisiae by chlorimipramine. Correlation with chlorpromazine. Biochemical pharmacology 19, 2555-2560.

Inoue, A., Muranaka, S., Fujita, H., Kanno, T., Tamai, H., Utsumi, K., 2004. Molecular mechanism of diclofenac-induced apoptosis of promyelocytic leukemia: dependency on reactive oxygen species, Akt, Bid, cytochrome and caspase pathway. Free radical biology & medicine 37, 1290-1299.

Ishida, S., Sugino, M., Hosokawa, T., Sato, T., Furutama, D., Fukuda, A., Kimura, F., Kuwabara, H., Shibayama, Y., Hanafusa, T., 2010. Amiodarone-induced liver cirrhosis and parkinsonism: a case report. Clinical neuropathology 29, 84-88.

Ishidate, K., Kawaguchi, K., Tagawa, K., 1969a. Change in P-450 content accompanying aerobic formation of mitochondria in yeast. Journal of biochemistry 65, 385-392.

Ishidate, K., Kawaguchi, K., Tagawa, K., Hagihara, B., 1969b. Hemoproteins in anaerobically grown yeast cells. Journal of biochemistry 65, 375-383.

Iyanagi, T., 2007. Molecular mechanism of phase I and phase II drug-metabolizing enzymes: implications for detoxification. International review of cytology 260, 35-112.

Jurima-Romet, M., Crawford, K., Huang, H.S., 1994. Comparative cytotoxicity of non-steroidal anti-inflammatory drugs in primary cultures of rat hepatocytes. Toxicology in vitro : an international journal published in association with BIBRA 8, 55-66.

Kammoun, H.L., Chabanon, H., Hainault, I., Luquet, S., Magnan, C., Koike, T., Ferre, P., Foufelle, F., 2009. GRP78 expression inhibits insulin and ER stress-induced SREBP-1c activation and reduces hepatic steatosis in mice. The Journal of clinical investigation 119, 1201-1215.

Kaplowitz, N., 2005. Idiosyncratic drug hepatotoxicity. Nature reviews Drug discovery 4, 489-499.

Karpen, S.J., 2002. Nuclear receptor regulation of hepatic function. Journal of hepatology 36, 832-850.

Karpen, S.J., Sun, A.Q., Kudish, B., Hagenbuch, B., Meier, P.J., Ananthanarayanan, M., Suchy, F.J., 1996. Multiple factors regulate the rat liver basolateral sodium-dependent bile acid cotransporter gene promoter. The Journal of biological chemistry 271, 15211-15221.

Kast, H.R., Goodwin, B., Tarr, P.T., Jones, S.A., Anisfeld, A.M., Stoltz, C.M., Tontonoz, P., Kliewer, S., Willson, T.M., Edwards, P.A., 2002. Regulation of multidrug resistance-associated protein 2 (ABCC2) by the nuclear receptors pregnane X receptor, farnesoid X-activated receptor, and constitutive androstane receptor. The Journal of biological chemistry 277, 2908-2915.

Kaufmann, P., Torok, M., Hanni, A., Roberts, P., Gasser, R., Krahenbuhl, S., 2005. Mechanisms of benzarone and benzbromarone-induced hepatic toxicity. Hepatology 41, 925-935.

Kc, S., 2007. Acute liver failure caused by hepatitis E virus and paracetamol. JNMA; journal of the Nepal Medical Association 46, 74-76.

Kelly, G.S., 1998. Clinical applications of N-acetylcysteine. Alternative medicine review : a journal of clinical therapeutic 3, 114-127.

Kelly, S.L., Lamb, D.C., Baldwin, B.C., Corran, A.J., Kelly, D.E., 1997a. Characterization of Saccharomyces cerevisiae CYP61, sterol delta22-desaturase, and inhibition by azole antifungal agents. The Journal of biological chemistry 272, 9986-9988.

Kelly, S.L., Lamb, D.C., Kelly, D.E., 1997b. Sterol 22-desaturase, cytochrome P45061, possesses activity in xenobiotic metabolism. FEBS letters 412, 233-235.

Keshavarzian, A., Farhadi, A., Forsyth, C.B., Rangan, J., Jakate, S., Shaikh, M., Banan, A., Fields, J.Z., 2009. Evidence that chronic alcohol exposure promotes intestinal oxidative stress, intestinal hyperpermeability and endotoxemia prior to development of alcoholic steatohepatitis in rats. Journal of hepatology 50, 538-547.

Kew, M.C., Popper, H., 1984. Relationship between hepatocellular carcinoma and cirrhosis. Seminars in liver disease 4, 136-146.

Kierszenbaum, A., 2002. Histologie et biologie cellulaire: Une introduction à l'anatomie pathologique. Glandes exocrines du tube digestif, foie et voies biliaires. Mosby.

Kihara, A., Igarashi, Y., 2004. Cross talk between sphingolipids and glycerophospholipids in the establishment of plasma membrane asymmetry. Molecular biology of the cell 15, 4949-4959.

Kim, M.S., Shigenaga, J., Moser, A., Feingold, K., Grunfeld, C., 2003. Repression of farnesoid X receptor during the acute phase response. The Journal of biological chemistry 278, 8988-8995.

Kim, P.K., Chen, J., Andrejko, K.M., Deutschman, C.S., 2000. Intraabdominal sepsis down-regulates transcription of sodium taurocholate cotransporter and multidrug resistance-associated protein in rats. Shock 14, 176-181.

King, C., Tang, W., Ngui, J., Tephly, T., Braun, M., 2001. Characterization of rat and human UDP-glucuronosyltransferases responsible for the in vitro glucuronidation of diclofenac. Toxicological sciences : an official journal of the Society of Toxicology 61, 49-53.

Klein, M., Mamnun, Y.M., Eggmann, T., Schuller, C., Wolfger, H., Martinoia, E., Kuchler, K., 2002. The ATP-binding cassette (ABC) transporter Bpt1p mediates vacuolar sequestration of glutathione conjugates in yeast. FEBS letters 520, 63-67.

Klingenberg, M., 1958. Pigments of rat liver microsomes. Archives of biochemistry and biophysics 75, 376-386.

Knorre, D.A., Krivonosova, T.N., Markova, O.V., Severin, F.F., 2009. Amiodarone inhibits multiple drug resistance in yeast Saccharomyces cerevisiae. Archives of microbiology 191, 675-679.

Knowles, B.B., Howe, C.C., Aden, D.P., 1980. Human hepatocellular carcinoma cell lines secrete the major plasma proteins and hepatitis B surface antigen. Science 209, 497-499.

Koppen, A., van Riel, A., de Vries, I., Meulenbelt, J., 2014. Recommendations for the paracetamol treatment nomogram and side effects of N-acetylcysteine. The Netherlands journal of medicine 72, 251-257.

Kosters, A., Karpen, S.J., 2010. The role of inflammation in cholestasis: clinical and basic aspects. Seminars in liver disease 30, 186-194.

Kosters, A., White, D.D., Sun, H., Thevananther, S., Karpen, S.J., 2009. Redundant roles for cJun-N-terminal kinase 1 and 2 in interleukin-1beta-mediated reduction and modification of murine hepatic nuclear retinoid X receptor alpha. Journal of hepatology 51, 898-908.

Kowaltowski, A.J., Castilho, R.F., Vercesi, A.E., 1996. Opening of the mitochondrial permeability transition pore by uncoupling or inorganic phosphate in the presence of Ca2+ is dependent on mitochondrial-generated reactive oxygen species. FEBS letters 378, 150-152.

Kretz-Rommel, A., Boelsterli, U.A., 1993. Diclofenac covalent protein binding is dependent on acyl glucuronide formation and is inversely related to P450-mediated acute cell injury in cultured rat hepatocytes. Toxicology and applied pharmacology 120, 155-161.

Kretz-Rommel, A., Boelsterli, U.A., 1994a. Mechanism of covalent adduct formation of diclofenac to rat hepatic microsomal proteins. Retention of the glucuronic acid moiety in the adduct. Drug metabolism and disposition: the biological fate of chemicals 22, 956-961.

Kretz-Rommel, A., Boelsterli, U.A., 1994b. Selective protein adducts to membrane proteins in cultured rat hepatocytes exposed to diclofenac: radiochemical and immunochemical analysis. Molecular pharmacology 45, 237-244.

Krishna, D.R., Klotz, U., 1994. Extrahepatic metabolism of drugs in humans. Clinical pharmacokinetics 26, 144-160.

Kubitz, R., Wettstein, M., Warskulat, U., Haussinger, D., 1999. Regulation of the multidrug resistance protein 2 in the rat liver by lipopolysaccharide and dexamethasone. Gastroenterology 116, 401-410.

Kuchler, K., Sterne, R.E., Thorner, J., 1989. Saccharomyces cerevisiae STE6 gene product: a novel pathway for protein export in eukaryotic cells. The EMBO journal 8, 3973-3984.

Kumar, S., Samuel, K., Subramanian, R., Braun, M.P., Stearns, R.A., Chiu, S.H., Evans, D.C., Baillie, T.A., 2002. Extrapolation of diclofenac clearance from in vitro microsomal metabolism data: role of acyl glucuronidation and sequential oxidative metabolism of the acyl glucuronide. The Journal of pharmacology and experimental therapeutics 303, 969-978.

Larrey, D., Erlinger, S., 1988. Drug-induced cholestasis. Bailliere's clinical gastroenterology 2, 423-452.

Lawton, M.P., Philpot, R.M., 1993. Functional characterization of flavin-containing monooxygenase 1B1 expressed in Saccharomyces cerevisiae and Escherichia coli and analysis of proposed FAD- and membrane-binding domains. The Journal of biological chemistry 268, 5728-5734.

Lazarczyk, D.A., Goldstein, N.S., Gordon, S.C., 2001. Trovafloxacin hepatotoxicity. Digestive diseases and sciences 46, 925-926.

Le Vee, M., Jigorel, E., Glaise, D., Gripon, P., Guguen-Guillouzo, C., Fardel, O., 2006. Functional expression of sinusoidal and canalicular hepatic drug transporters in the differentiated human hepatoma HepaRG cell line. European journal of pharmaceutical sciences : official journal of the European Federation for Pharmaceutical Sciences 28, 109-117.

Le Vee, M., Lecureur, V., Stieger, B., Fardel, O., 2009. Regulation of drug transporter expression in human hepatocytes exposed to the proinflammatory cytokines tumor necrosis factor-alpha or interleukin-6. Drug metabolism and disposition: the biological fate of chemicals 37, 685-693.

Lebeault, J.M., Lode, E.T., Coon, M.J., 1971. Fatty acid and hydrocarbon hydroxylation in yeast: role of cytochrome P-450 in Candida tropicalis. Biochemical and biophysical research communications 42, 413-419.

Lee, G., Piquette-Miller, M., 2003. Cytokines alter the expression and activity of the multidrug resistance transporters in human hepatoma cell lines; analysis using RT-PCR and cDNA microarrays. Journal of pharmaceutical sciences 92, 2152-2163.

Lee, W.M., 2003. Drug-induced hepatotoxicity. The New England journal of medicine 349, 474-485.

Lehman-McKeeman, 2008. Absorption, distribution, and excretion of toxicants, in Cassarett and Doull's Toxicology: The Basis Science of Poisons (Klaassen CD ed). McGraw-Hill Medical, New York.

Letteron, P., Fromenty, B., Terris, B., Degott, C., Pessayre, D., 1996. Acute and chronic hepatic steatosis lead to in vivo lipid peroxidation in mice. Journal of hepatology 24, 200-208.

Letteron, P., Sutton, A., Mansouri, A., Fromenty, B., Pessayre, D., 2003. Inhibition of microsomal triglyceride transfer protein: another mechanism for drug-induced steatosis in mice. Hepatology 38, 133-140.

Lewis, J.H., Ranard, R.C., Caruso, A., Jackson, L.K., Mullick, F., Ishak, K.G., Seeff, L.B., Zimmerman, H.J., 1989. Amiodarone hepatotoxicity: prevalence and clinicopathologic correlations among 104 patients. Hepatology 9, 679-685.

Lewis, S.C., Langman, M.J., Laporte, J.R., Matthews, J.N., Rawlins, M.D., Wiholm, B.E., 2002. Dose-response relationships between individual nonaspirin nonsteroidal anti-inflammatory drugs (NANSAIDs) and serious upper gastrointestinal bleeding: a meta-analysis based on individual patient data. British journal of clinical pharmacology 54, 320-326.

Li, D., Zimmerman, T.L., Thevananther, S., Lee, H.Y., Kurie, J.M., Karpen, S.J., 2002. Interleukin-1 beta-mediated suppression of RXR:RAR transactivation of the Ntcp promoter is JNK-dependent. The Journal of biological chemistry 277, 31416-31422.

Li, N., Klaassen, C.D., 2004. Role of liver-enriched transcription factors in the down-regulation of organic anion transporting polypeptide 4 (oatp4; oatplb2; slc21a10) by lipopolysaccharide. Molecular pharmacology 66, 694-701.

Li, T., Jahan, A., Chiang, J.Y., 2006. Bile acids and cytokines inhibit the human cholesterol 7 alpha-hydroxylase gene via the JNK/c-jun pathway in human liver cells. Hepatology 43, 1202-1210.

Liguori, M.J., Blomme, E.A., Waring, J.F., 2008. Trovafloxacin-induced gene expression changes in liver-derived in vitro systems: comparison of primary human hepatocytes to HepG2 cells. Drug metabolism and disposition: the biological fate of chemicals 36, 223-233.

Liguori, M.J., Ditewig, A.C., Maddox, J.F., Luyendyk, J.P., Lehman-McKeeman, L.D., Nelson, D.M., Bhaskaran, V.M., Waring, J.F., Ganey, P.E., Roth, R.A., Blomme, E.A., 2010. Comparison of TNFalpha to lipopolysaccharide as an inflammagen to characterize the idiosyncratic hepatotoxicity potential of drugs: Trovafloxacin as an example. International journal of molecular sciences 11, 4697-4714.

Lim, M.S., Lim, P.L., Gupta, R., Boelsterli, U.A., 2006. Critical role of free cytosolic calcium, but not uncoupling, in mitochondrial permeability transition and cell death induced by diclofenac oxidative metabolites in immortalized human hepatocytes. Toxicology and applied pharmacology 217, 322-331.

Lindenmayer, A., Smith, L., 1964. Cytochromes and Other Pigments of Baker's Yeast Grown Aerobically and Anaerobically. Biochimica et biophysica acta 93, 445-461.

Lu, J., Jones, A.D., Harkema, J.R., Roth, R.A., Ganey, P.E., 2012. Amiodarone exposure during modest inflammation induces idiosyncrasy-like liver injury in rats: role of tumor necrosis factor-alpha. Toxicological sciences : an official journal of the Society of Toxicology 125, 126-133.

Lu, J., Miyakawa, K., Roth, R.A., Ganey, P.E., 2013. Tumor necrosis factor-alpha potentiates the cytotoxicity of amiodarone in Hepa1c1c7 cells: roles of caspase activation and oxidative stress. Toxicological sciences : an official journal of the Society of Toxicology 131, 164-178.

Lucena, M.I., Andrade, R.J., Rodrigo, L., Salmeron, J., Alvarez, A., Lopez-Garrido, M.J., Camargo, R., Alcantara, R., 2000. Trovafloxacin-induced acute hepatitis. Clinical infectious diseases : an official publication of the Infectious Diseases Society of America 30, 400-401.

Ludtmann, M.H., Angelova, P.R., Zhang, Y., Abramov, A.Y., Dinkova-Kostova, A.T., 2014. Nrf2 affects the efficiency of mitochondrial fatty acid oxidation. The Biochemical journal 457, 415-424.

Luster, M.I., Germolec, D.R., Yoshida, T., Kayama, F., Thompson, M., 1994. Endotoxin-induced cytokine gene expression and excretion in the liver. Hepatology 19, 480-488.

Luyendyk, J.P., Maddox, J.F., Cosma, G.N., Ganey, P.E., Cockerell, G.L., Roth, R.A., 2003. Ranitidine treatment during a modest inflammatory response precipitates idiosyncrasy-like liver injury in rats. The Journal of pharmacology and experimental therapeutics 307, 9-16.

MacAllister, S.L., Young, C., Guzdek, A., Zhidkov, N., O'Brien, P.J., 2013. Molecular cytotoxic mechanisms of chlorpromazine in isolated rat hepatocytes. Canadian journal of physiology and pharmacology 91, 56-63.

Maddox, J.F., Amuzie, C.J., Li, M., Newport, S.W., Sparkenbaugh, E., Cuff, C.F., Pestka, J.J., Cantor, G.H., Roth, R.A., Ganey, P.E., 2010. Bacterial- and viral-induced inflammation increases sensitivity to acetaminophen hepatotoxicity. Journal of toxicology and environmental health Part A 73, 58-73.

Mahe, Y., Lemoine, Y., Kuchler, K., 1996. The ATP binding cassette transporters Pdr5 and Snq2 of Saccharomyces cerevisiae can mediate transport of steroids in vivo. The Journal of biological chemistry 271, 25167-25172.

Maianski, N.A., Roos, D., Kuijpers, T.W., 2004. Bid truncation, bid/bax targeting to the mitochondria, and caspase activation associated with neutrophil apoptosis are inhibited by granulocyte colony-stimulating factor. Journal of immunology 172, 7024-7030.

Maiuri, A.R., Breier, A.B., Gora, L.F., Parkins, R.V., Ganey, P.E., Roth, R.A., 2015. Cytotoxic Synergy Between Cytokines and NSAIDs Associated With Idiosyncratic Hepatotoxicity Is Driven by Mitogen-Activated Protein Kinases. Toxicological sciences : an official journal of the Society of Toxicology 146, 265-280.

Makishima, M., 2006. Nuclear receptors sense bile acid metabolism: A hormonal action of bile acids Functional and Structural Biology on the Lipo-network, 17-35.

Marek, M., Milles, S., Schreiber, G., Daleke, D.L., Dittmar, G., Herrmann, A., Muller, P., Pomorski, T.G., 2011. The yeast plasma membrane ATP binding cassette (ABC) transporter Aus1: purification,

characterization, and the effect of lipids on its activity. The Journal of biological chemistry 286, 21835-21843.

Mason, D.L., Mallampalli, M.P., Huyer, G., Michaelis, S., 2003. A region within a lumenal loop of Saccharomyces cerevisiae Ycf1p directs proteolytic processing and substrate specificity. Eukaryotic cell 2, 588-598.

Massart, J., Begriche, K., Buron, N., Porceddu, M., Borgne-Sanchez, A., Fromenty, B., 2013. Drug-Induced Inhibition of Mitochondrial Fatty Acid Oxidation and Steatosis. Current Pathobiology Reports 1, 147-157.

Masubuchi, Y., Nakayama, S., Horie, T., 2002a. Role of mitochondrial permeability transition in diclofenac-induced hepatocyte injury in rats. Hepatology 35, 544-551.

Masubuchi, Y., Ose, A., Horie, T., 2001. Mechanism-based inactivation of CYP2C11 by diclofenac. Drug metabolism and disposition: the biological fate of chemicals 29, 1190-1195.

Masubuchi, Y., Ose, A., Horie, T., 2002b. Diclofenac-induced inactivation of CYP3A4 and its stimulation by quinidine. Drug metabolism and disposition: the biological fate of chemicals 30, 1143-1148.

Masubuchi, Y., Saito, H., Horie, T., 1998. Structural requirements for the hepatotoxicity of nonsteroidal anti-inflammatory drugs in isolated rat hepatocytes. The Journal of pharmacology and experimental therapeutics 287, 208-213.

Masubuchi, Y., Yamada, S., Horie, T., 2000. Possible mechanism of hepatocyte injury induced by diphenylamine and its structurally related nonsteroidal anti-inflammatory drugs. The Journal of pharmacology and experimental therapeutics 292, 982-987.

Matouskova, P., Vokral, I., Lamka, J., Skalova, L., 2016. The Role of Xenobiotic-Metabolizing Enzymes in Anthelmintic Deactivation and Resistance in Helminths. Trends in parasitology 32, 481-491.

Mattar, W., Juliar, B., Gradus-Pizlo, I., Kwo, P.Y., 2009. Amiodarone hepatotoxicity in the context of the metabolic syndrome and right-sided heart failure. Journal of gastrointestinal and liver diseases : JGLD 18, 419-423.

McGovern, B., Garan, H., Kelly, E., Ruskin, J.N., 1983. Adverse reactions during treatment with amiodarone hydrochloride. British medical journal 287, 175-180.

Meng, X., Mojaverian, P., Doedee, M., Lin, E., Weinryb, I., Chiang, S.T., Kowey, P.R., 2001. Bioavailability of amiodarone tablets administered with and without food in healthy subjects. The American journal of cardiology 87, 432-435.

Michalopoulos, G.K., DeFrances, M.C., 1997. Liver regeneration. Science 276, 60-66.

Miura, N., Tanaka, K., 1993. Analysis of the rat hepatocyte nuclear factor (HNF) 1 gene promoter: synergistic activation by HNF4 and HNF1 proteins. Nucleic acids research 21, 3731-3736.

Miyahara, K., Mizunuma, M., Hirata, D., Tsuchiya, E., Miyakawa, T., 1996. The involvement of the Saccharomyces cerevisiae multidrug resistance transporters Pdr5p and Snq2p in cation resistance. FEBS letters 399, 317-320.

Miyamoto, G., Zahid, N., Uetrecht, J.P., 1997. Oxidation of diclofenac to reactive intermediates by neutrophils, myeloperoxidase, and hypochlorous acid. Chemical research in toxicology 10, 414-419.

Moling, O., Cairon, E., Rimenti, G., Rizza, F., Pristera, R., Mian, P., 2006. Severe hepatotoxicity after therapeutic doses of acetaminophen. Clinical therapeutics 28, 755-760.

Moore, K.a.D., A., 2001. Anatomie médicale: Aspects fondamentaux et applications cliniques. de boeck, pp. 1110.

Moreno-Sanchez, R., Bravo, C., Vasquez, C., Ayala, G., Silveira, L.H., Martinez-Lavin, M., 1999. Inhibition and uncoupling of oxidative phosphorylation by nonsteroidal anti-inflammatory drugs: study in mitochondria, submitochondrial particles, cells, and whole heart. Biochemical pharmacology 57, 743-752.

Morioka, N., Kumagai, K., Morita, K., Kitayama, S., Dohi, T., 2004. Nonsteroidal anti-inflammatory drugs potentiate 1-methyl-4-phenylpyridinium (MPP+)-induced cell death by promoting the intracellular accumulation of MPP+ in PC12 cells. The Journal of pharmacology and experimental therapeutics 310, 800-807.

Morland, C.M., Fear, J., McNab, G., Joplin, R., Adams, D.H., 1997. Promotion of leukocyte transendothelial cell migration by chemokines derived from human biliary epithelial cells in vitro. Proceedings of the Association of American Physicians 109, 372-382.

Moshage, H., 1997. Cytokines and the hepatic acute phase response. The Journal of pathology 181, 257-266.

Moya, M., Gomez-Lechon, M.J., Castell, J.V., Jover, R., 2010. Enhanced steatosis by nuclear receptor ligands: a study in cultured human hepatocytes and hepatoma cells with a characterized nuclear receptor expression profile. Chemico-biological interactions 184, 376-387.

Mulder, J., Karpen, S.J., Tietge, U.J., Kuipers, F., 2009. Nuclear receptors: mediators and modifiers of inflammation-induced cholestasis. Frontiers in bioscience 14, 2599-2630.

Mulhall, K.J., Curtin, W.A., Given, H.F., 2003. Comparison of different anti-inflammatory agents in suppressing the monocyte response to orthopedic particles. Orthopedics 26, 1219-1223.

Muthukumar, K., Nachiappan, V., 2010. Cadmium-induced oxidative stress in Saccharomyces cerevisiae. Indian journal of biochemistry & biophysics 47, 383-387.

Nakamura, J., Nishida, T., Hayashi, K., Kawada, N., Ueshima, S., Sugiyama, Y., Ito, T., Sobue, K., Matsuda, H., 1999. Kupffer cell-mediated down regulation of rat hepatic CMOAT/MRP2 gene expression. Biochemical and biophysical research communications 255, 143-149.

Nguyen, G.C., Sam, J., Thuluvath, P.J., 2008. Hepatitis C is a predictor of acute liver injury among hospitalizations for acetaminophen overdose in the United States: a nationwide analysis. Hepatology 48, 1336-1341.

O'Connor, N., Dargan, P.I., Jones, A.L., 2003. Hepatocellular damage from non-steroidal anti-inflammatory drugs. QJM : monthly journal of the Association of Physicians 96, 787-791.

Ohba, M., Sato, R., Yoshida, Y., Nishino, T., Katsuki, H., 1978. Involvement of cytochrome P-450 and a cyanide-sensitive enzyme in different steps of lanosterol demethylation by yeast microsomes. Biochemical and biophysical research communications 85, 21-27.

Ohlinger, W., Dinges, H.P., Zatloukal, K., Mair, S., Gollowitsch, F., Denk, H., 1993. Immunohistochemical detection of tumor necrosis factor-alpha, other cytokines and adhesion molecules in human livers with alcoholic hepatitis. Virchows Archiv A, Pathological anatomy and histopathology 423, 169-176.

Omura, T., Sato, R., 1962. A new cytochrome in liver microsomes. The Journal of biological chemistry 237, 1375-1376.

Omura, T., Sato, R., 1964. The Carbon Monoxide-Binding Pigment of Liver Microsomes. I. Evidence for Its Hemoprotein Nature. The Journal of biological chemistry 239, 2370-2378.

Ortiz, D.F., St Pierre, M.V., Abdulmessih, A., Arias, I.M., 1997. A yeast ATP-binding cassette-type protein mediating ATP-dependent bile acid transport. The Journal of biological chemistry 272, 15358-15365.

Ostapowicz, G., Fontana, R.J., Schiodt, F.V., Larson, A., Davern, T.J., Han, S.H., McCashland, T.M., Shakil, A.O., Hay, J.E., Hynan, L., Crippin, J.S., Blei, A.T., Samuel, G., Reisch, J., Lee, W.M., Group, U.S.A.L.F.S., 2002. Results of a prospective study of acute liver failure at 17 tertiary care centers in the United States. Annals of internal medicine 137, 947-954.

Ozhovan, S.M., Knorre, D.A., Severin, F.F., Bakeeva, L.E., 2009. [Yeast cell ultrastructure after amiodarone treatment]. Tsitologiia 51, 911-916.

Pagant, S., Brovman, E.Y., Halliday, J.J., Miller, E.A., 2008. Mapping of interdomain interfaces required for the functional architecture of Yor1p, a eukaryotic ATP-binding cassette (ABC) transporter. The Journal of biological chemistry 283, 26444-26451.

Pagliassotti, M.J., 2012. Endoplasmic reticulum stress in nonalcoholic fatty liver disease. Annual review of nutrition 32, 17-33.

Papaefthimiou, C., Cabral Mde, G., Mixailidou, C., Viegas, C.A., Sa-Correia, I., Theophilidis, G., 2004. Comparison of two screening bioassays, based on the frog sciatic nerve and yeast cells, for the assessment of herbicide toxicity. Environmental toxicology and chemistry / SETAC 23, 1211-1218.

Parasassi, T., Brunelli, R., Bracci-Laudiero, L., Greco, G., Gustafsson, A.C., Krasnowska, E.K., Lundeberg, J., Lundeberg, T., Pittaluga, E., Romano, M.C., Serafino, A., 2005. Differentiation of normal and cancer cells induced by sulfhydryl reduction: biochemical and molecular mechanisms. Cell death and differentiation 12, 1285-1296.

Parasassi, T., Brunelli, R., Costa, G., De Spirito, M., Krasnowska, E., Lundeberg, T., Pittaluga, E., Ursini, F., 2010. Thiol redox transitions in cell signaling: a lesson from N-acetylcysteine. TheScientificWorldJournal 10, 1192-1202.

Pelham, H.R., Banfield, D.K., Lewis, M.J., 1995. SNAREs involved in traffic through the Golgi complex. Cold Spring Harbor symposia on quantitative biology 60, 105-111.

Pereira, A.P., Mendes-Ferreira, A., Oliveira, J.M., Estevinho, L.M., Mendes-Faia, A., 2013. High-cell-density fermentation of Saccharomyces cerevisiae for the optimisation of mead production. Food microbiology 33, 114-123.

Pessayre, D., Haouzi, D., Fau, D., Robin, M.A., Mansouri, A., Berson, A., 1999. Withdrawal of life support, altruistic suicide, fratricidal killing and euthanasia by lymphocytes: different forms of drug-induced hepatic apoptosis. Journal of hepatology 31, 760-770.

Petrescu, I., Tarba, C., 1997. Uncoupling effects of diclofenac and aspirin in the perfused liver and isolated hepatic mitochondria of rat. Biochimica et biophysica acta 1318, 385-394.

Petrovic, S., Pascolo, L., Gallo, R., Cupelli, F., Ostrow, J.D., Goffeau, A., Tiribelli, C., Bruschi, C.V., 2000. The products of YCF1 and YLL015w (BPT1) cooperate for the ATP-dependent vacuolar transport of unconjugated bilirubin in Saccharomyces cerevisiae. Yeast 16, 561-571.

Piecuch, A., Oblak, E., 2014. Yeast ABC proteins involved in multidrug resistance. Cellular & molecular biology letters 19, 1-22.

Plass, J.R., Mol, O., Heegsma, J., Geuken, M., Faber, K.N., Jansen, P.L., Muller, M., 2002. Farnesoid X receptor and bile salts are involved in transcriptional regulation of the gene encoding the human bile salt export pump. Hepatology 35, 589-596.

Ponsoda, X., Bort, R., Jover, R., Gomez-Lechon, M.J., Castell, J.V., 1995. Molecular mechanism of diclofenac hepatotoxicity: Association of cell injury with oxidative metabolism and decrease in ATP levels. Toxicology in vitro : an international journal published in association with BIBRA 9, 439-444.

Poon, G.K., Chen, Q., Teffera, Y., Ngui, J.S., Griffin, P.R., Braun, M.P., Doss, G.A., Freeden, C., Stearns, R.A., Evans, D.C., Baillie, T.A., Tang, W., 2001. Bioactivation of diclofenac via benzoquinone imine intermediates-identification of urinary mercapturic acid derivatives in rats and humans. Drug metabolism and disposition: the biological fate of chemicals 29, 1608-1613.

Poon, I.K., Chiu, Y.H., Armstrong, A.J., Kinchen, J.M., Juncadella, I.J., Bayliss, D.A., Ravichandran, K.S., 2014. Unexpected link between an antibiotic, pannexin channels and apoptosis. Nature 507, 329-334.

Popper, H., Schaffner, F., 1970. Pathophysiology of cholestasis. Human pathology 1, 1-24.

Pozniakovsky, A.I., Knorre, D.A., Markova, O.V., Hyman, A.A., Skulachev, V.P., Severin, F.F., 2005. Role of mitochondria in the pheromone- and amiodarone-induced programmed death of yeast. The Journal of cell biology 168, 257-269.

Puli, S.R., Fraley, M.A., Puli, V., Kuperman, A.B., Alpert, M.A., 2005. Hepatic cirrhosis caused by low-dose oral amiodarone therapy. The American journal of the medical sciences 330, 257-261.

Pumford, N.R., Myers, T.G., Davila, J.C., Highet, R.J., Pohl, L.R., 1993. Immunochemical detection of liver protein adducts of the nonsteroidal antiinflammatory drug diclofenac. Chemical research in toxicology 6, 147-150.

Purohit, V., Bode, J.C., Bode, C., Brenner, D.A., Choudhry, M.A., Hamilton, F., Kang, Y.J., Keshavarzian, A., Rao, R., Sartor, R.B., Swanson, C., Turner, J.R., 2008. Alcohol, intestinal bacterial growth, intestinal permeability to endotoxin, and medical consequences: summary of a symposium. Alcohol 42, 349-361.

Qureshi, Z.P., Seoane-Vazquez, E., Rodriguez-Monguio, R., Stevenson, K.B., Szeinbach, S.L., 2011. Market withdrawal of new molecular entities approved in the United States from 1980 to 2009. Pharmacoepidemiology and drug safety 20, 772-777.

Ramadori G, R., P, 2010. Signaling Pathways in Liver Diseases. Springer.

Ramudo, L., Manso, M.A., 2010. N-acetylcysteine in acute pancreatitis. World journal of gastrointestinal pharmacology and therapeutics 1, 21-26.

Rappaport, A.M., Borowy, Z.J., Lougheed, W.M., Lotto, W.N., 1954. Subdivision of hexagonal liver lobules into a structural and functional unit; role in hepatic physiology and pathology. The Anatomical record 119, 11-33.

Ratz Bravo, A.E., Drewe, J., Schlienger, R.G., Krahenbuhl, S., Pargger, H., Ummenhofer, W., 2005. Hepatotoxicity during rapid intravenous loading with amiodarone: Description of three cases and review of the literature. Critical care medicine 33, 128-134; discussion 245-126.

Reddy, J.K., Rao, M.S., 2006. Lipid metabolism and liver inflammation. II. Fatty liver disease and fatty acid oxidation. American journal of physiology Gastrointestinal and liver physiology 290, G852-858.

Regal, R.E., Billi, J.E., Glazer, H.M., 1987. Phenothiazine-induced cholestatic jaundice. Clinical pharmacy 6, 787-794.

Richer, M., Robert, S., 1995. Fatal hepatotoxicity following oral administration of amiodarone. The Annals of pharmacotherapy 29, 582-586.

Riezman, H., 1993. Yeast endocytosis. Trends in cell biology 3, 273-277.

Rock, K.L., Kono, H., 2008. The inflammatory response to cell death. Annual review of pathology 3, 99-126.

Rogers, B., Decottignies, A., Kolaczkowski, M., Carvajal, E., Balzi, E., Goffeau, A., 2001. The pleitropic drug ABC transporters from Saccharomyces cerevisiae. Journal of molecular microbiology and biotechnology 3, 207-214.

Roth, R.A., Ganey, P.E., 2010. Intrinsic versus idiosyncratic drug-induced hepatotoxicity--two villains or one? The Journal of pharmacology and experimental therapeutics 332, 692-697.

Rumessen, J.J., 1986. Hepatotoxicity of amiodarone. Acta medica Scandinavica 219, 235-239.

Rushworth, G.F., Megson, I.L., 2014. Existing and potential therapeutic uses for N-acetylcysteine: the need for conversion to intracellular glutathione for antioxidant benefits. Pharmacology & therapeutics 141, 150-159.

Saab, L., Peluso, J., Muller, C.D., Ubeaud-Sequier, G., 2013. Implication of hepatic transporters (MDR1 and MRP2) in inflammation-associated idiosyncratic drug-induced hepatotoxicity investigated by microvolume cytometry. Cytometry Part A : the journal of the International Society for Analytical Cytology 83, 403-408.

Saavedra-Molina, A., Villalobos, R., Borbolla, M., 1983. Calcium uptake during the cell cycle of Saccharomyces cerevisiae. FEBS letters 160, 195-197.

Sallmann, A.R., 1985. The history of diclofenac. Seminars in arthritis and rheumatism 15, 57-60.

Sallustio, B.C., Holbrook, F.L., 2001. In vivo perturbation of rat hepatocyte canalicular membrane function by diclofenac. Drug metabolism and disposition: the biological fate of chemicals 29, 1535-1538.
Sallustio, B.C., Sabordo, L., Evans, A.M., Nation, R.L., 2000. Hepatic disposition of electrophilic acyl glucuronide conjugates. Current drug metabolism 1, 163-180.

Samuni, Y., Goldstein, S., Dean, O.M., Berk, M., 2013. The chemistry and biological activities of N-acetylcysteine. Biochimica et biophysica acta 1830, 4117-4129.

Sawada, H., Takami, K., Asahi, S., 2005. A toxicogenomic approach to drug-induced phospholipidosis: analysis of its induction mechanism and establishment of a novel in vitro screening system. Toxicological sciences : an official journal of the Society of Toxicology 83, 282-292.

Scull, C.M., Tabas, I., 2011. Mechanisms of ER stress-induced apoptosis in atherosclerosis. Arteriosclerosis, thrombosis, and vascular biology 31, 2792-2797.

Seitz, S., Boelsterli, U.A., 1998. Diclofenac acyl glucuronide, a major biliary metabolite, is directly involved in small intestinal injury in rats. Gastroenterology 115, 1476-1482.

Seki, E., Brenner, D.A., 2008. Toll-like receptors and adaptor molecules in liver disease: update. Hepatology 48, 322-335.

Sengupta, C., Afe`che, P., Meyer-Brunot, H.G., Rensing, U.,, 1985. Diclofenac sodium, in: Rainsford, K.D. (Ed.), Anti-Inflammatory and Anti-Rheumatic Drugs,. CRC Press, Boca Raton, FL,, 49–63.

Servos, J., Haase, E., Brendel, M., 1993. Gene SNQ2 of Saccharomyces cerevisiae, which confers resistance to 4-nitroquinoline-N-oxide and other chemicals, encodes a 169 kDa protein homologous to ATP-dependent permeases. Molecular & general genetics : MGG 236, 214-218.

Sharanek, A., Azzi, P.B., Al-Attrache, H., Savary, C.C., Humbert, L., Rainteau, D., Guguen-Guillouzo, C., Guillouzo, A., 2014. Different dose-dependent mechanisms are involved in early cyclosporine a-induced cholestatic effects in hepaRG cells. Toxicological sciences : an official journal of the Society of Toxicology 141, 244-253.

Sharanek, A., Burban, A., Burbank, M., Le Guevel, R., Li, R., Guillouzo, A., Guguen-Guillouzo, C., 2016. Rho-kinase/myosin light chain kinase pathway plays a key role in the impairment of bile canaliculi dynamics induced by cholestatic drugs. Scientific reports 6, 24709.

Sharanek, A., Burban, A., Humbert, L., Bachour-El Azzi, P., Felix-Gomes, N., Rainteau, D., Guillouzo, A., 2015. Cellular Accumulation and Toxic Effects of Bile Acids in Cyclosporine A-Treated HepaRG Hepatocytes. Toxicological sciences : an official journal of the Society of Toxicology 147, 573-587.

Shaw, P.J., Fullerton, A.M., Scott, M.A., Ganey, P.E., Roth, R.A., 2009a. The role of the hemostatic system in murine liver injury induced by coexposure to lipopolysaccharide and trovafloxacin, a drug with idiosyncratic liability. Toxicology and applied pharmacology 236, 293-300.

Shaw, P.J., Ganey, P.E., Roth, R.A., 2009b. Trovafloxacin enhances the inflammatory response to a Gram-negative or a Gram-positive bacterial stimulus, resulting in neutrophil-dependent liver injury in mice. The Journal of pharmacology and experimental therapeutics 330, 72-78.

Shaw, P.J., Hopfensperger, M.J., Ganey, P.E., Roth, R.A., 2007. Lipopolysaccharide and trovafloxacin coexposure in mice causes idiosyncrasy-like liver injury dependent on tumor necrosis factor-alpha. Toxicological sciences : an official journal of the Society of Toxicology 100, 259-266.

Shayeganpour, A., El-Kadi, A.O., Brocks, D.R., 2006. Determination of the enzyme(s) involved in the metabolism of amiodarone in liver and intestine of rat: the contribution of cytochrome P450 3A isoforms. Drug metabolism and disposition: the biological fate of chemicals 34, 43-50.

Shen, S., Hargus, S.J., Martin, B.M., Pohl, L.R., 1997. Cytochrome P4502C11 is a target of diclofenac covalent binding in rats. Chemical research in toxicology 10, 420-423.

Shen, S., Marchick, M.R., Davis, M.R., Doss, G.A., Pohl, L.R., 1999. Metabolic activation of diclofenac by human cytochrome P450 3A4: role of 5-hydroxydiclofenac. Chemical research in toxicology 12, 214-222.

Sherlock, S., 1998. Overview of chronic cholestatic conditions in adults: terminology and definitions. Clinics in liver disease 2, 217-233, vii.

Siddoway, L.A., 2003. Amiodarone: guidelines for use and monitoring. American family physician 68, 2189-2196.

Siewert, E., Dietrich, C.G., Lammert, F., Heinrich, P.C., Matern, S., Gartung, C., Geier, A., 2004. Interleukin-6 regulates hepatic transporters during acute-phase response. Biochemical and biophysical research communications 322, 232-238.

Simoes, T., Teixeira, M.C., Fernandes, A.R., Sa-Correia, I., 2003. Adaptation of Saccharomyces cerevisiae to the herbicide 2,4-dichlorophenoxyacetic acid, mediated by Msn2p- and Msn4p-regulated genes: important role of SPI1. Applied and environmental microbiology 69, 4019-4028.

Siraki, A.G., Pourahmad, J., Chan, T.S., Khan, S., O'Brien, P.J., 2002. Endogenous and endobiotic induced reactive oxygen species formation by isolated hepatocytes. Free radical biology & medicine 32, 2-10.

Slattery, J.T., Nelson, S.D., Thummel, K.E., 1996. The complex interaction between ethanol and acetaminophen. Clinical pharmacology and therapeutics 60, 241-246.

Smith, P.C., McDonagh, A.F., Benet, L.Z., 1986. Irreversible binding of zomepirac to plasma protein in vitro and in vivo. The Journal of clinical investigation 77, 934-939.

Sokolov, S., Knorre, D., Smirnova, E., Markova, O., Pozniakovsky, A., Skulachev, V., Severin, F., 2006. Ysp2 mediates death of yeast induced by amiodarone or intracellular acidification. Biochimica et biophysica acta 1757, 1366-1370.

Spahn-Langguth, H., Benet, L.Z., 1992. Acyl glucuronides revisited: is the glucuronidation process a toxification as well as a detoxification mechanism? Drug metabolism reviews 24, 5-47.

Spaniol, M., Bracher, R., Ha, H.R., Follath, F., Krahenbuhl, S., 2001. Toxicity of amiodarone and amiodarone analogues on isolated rat liver mitochondria. Journal of hepatology 35, 628-636.

Stahlmann, R., 2002. Clinical toxicological aspects of fluoroquinolones. Toxicology letters 127, 269-277.

Stierlin, H., Faigle, J.W., 1979. Biotransformation of diclofenac sodium (Voltaren) in animals and in man. II. Quantitative determination of the unchanged drug and principal phenolic metabolites, in urine and bile. Xenobiotica; the fate of foreign compounds in biological systems 9, 611-621.

Strittmatter, P., Velick, S.F., 1956. The isolation and properties of microsomal cytochrome. The Journal of biological chemistry 221, 253-264.

Sturm, E., Havinga, R., Baller, J.F., Wolters, H., van Rooijen, N., Kamps, J.A., Verkade, H.J., Karpen, S.J., Kuipers, F., 2005. Kupffer cell depletion with liposomal clodronate prevents suppression of Ntcp expression in endotoxin-treated rats. Journal of hepatology 42, 102-109.

Su, Y., Zhang, Y., Chen, M., Jiang, Z., Sun, L., Wang, T., Zhang, L., 2014. Lipopolysaccharide exposure augments isoniazide-induced liver injury. Journal of applied toxicology : JAT 34, 1436-1442.

Swartzman, E.E., Viswanathan, M.N., Thorner, J., 1996. The PAL1 gene product is a peroxisomal ATP-binding cassette transporter in the yeast Saccharomyces cerevisiae. The Journal of cell biology 132, 549-563.

Swift, B., Pfeifer, N.D., Brouwer, K.L., 2010. Sandwich-cultured hepatocytes: an in vitro model to evaluate hepatobiliary transporter-based drug interactions and hepatotoxicity. Drug metabolism reviews 42, 446-471.

Szalowska, E., van der Burg, B., Man, H.Y., Hendriksen, P.J., Peijnenburg, A.A., 2014. Model steatogenic compounds (amiodarone, valproic acid, and tetracycline) alter lipid metabolism by different mechanisms in mouse liver slices. PloS one 9, e86795.

Takahashi, T., 2013. [A screen for genes involved in adriamycin resistance in Saccharomyces cerevisiae]. Yakugaku zasshi : Journal of the Pharmaceutical Society of Japan 133, 393-396.

Talajic, M., DeRoode, M.R., Nattel, S., 1987. Comparative electrophysiologic effects of intravenous amiodarone and desethylamiodarone in dogs: evidence for clinically relevant activity of the metabolite. Circulation 75, 265-271.

Tanaka, E., Yamazaki, K., Misawa, S., 2000. Update: the clinical importance of acetaminophen hepatotoxicity in non-alcoholic and alcoholic subjects. Journal of clinical pharmacy and therapeutics 25, 325-332.

Tang, W., Stearns, R.A., Bandiera, S.M., Zhang, Y., Raab, C., Braun, M.P., Dean, D.C., Pang, J., Leung, K.H., Doss, G.A., Strauss, J.R., Kwei, G.Y., Rushmore, T.H., Chiu, S.H., Baillie, T.A., 1999a. Studies on cytochrome P-450-mediated bioactivation of diclofenac in rats and in human hepatocytes: identification of glutathione conjugated metabolites. Drug metabolism and disposition: the biological fate of chemicals 27, 365-372.

Tang, W., Stearns, R.A., Wang, R.W., Chiu, S.H., Baillie, T.A., 1999b. Roles of human hepatic cytochrome P450s 2C9 and 3A4 in the metabolic activation of diclofenac. Chemical research in toxicology 12, 192-199.

Tayem, Y.I., Qubaja, M.M., Shraim, R.K., Taha, O.B., Abu Shkheidem, I.A., Ibrahim, M.A., 2013. Non-steroidal anti-inflammatory drugs and antibiotics prescription trends at a central west bank hospital. Sultan Qaboos University medical journal 13, 567-573.

Teixeira, M.C., Godinho, C.P., Cabrito, T.R., Mira, N.P., Sa-Correia, I., 2012. Increased expression of the yeast multidrug resistance ABC transporter Pdr18 leads to increased ethanol tolerance and ethanol production in high gravity alcoholic fermentation. Microbial cell factories 11, 98.

Teng, S., Piquette-Miller, M., 2005. The involvement of the pregnane X receptor in hepatic gene regulation during inflammation in mice. The Journal of pharmacology and experimental therapeutics 312, 841-848.

Thomas, A.M., Hart, S.N., Kong, B., Fang, J., Zhong, X.B., Guo, G.L., 2010. Genome-wide tissue-specific farnesoid X receptor binding in mouse liver and intestine. Hepatology 51, 1410-1419.

Trauner, M., 1997. Molecular alterations of canalicular transport systems in experimental models of cholestasis: possible functional correlations. The Yale journal of biology and medicine 70, 365-378.

Trauner, M., Arrese, M., Lee, H., Boyer, J.L., Karpen, S.J., 1998a. Endotoxin downregulates rat hepatic ntcp gene expression via decreased activity of critical transcription factors. The Journal of clinical investigation 101, 2092-2100.

Trauner, M., Arrese, M., Soroka, C.J., Ananthanarayanan, M., Koeppel, T.A., Schlosser, S.F., Suchy, F.J., Keppler, D., Boyer, J.L., 1997. The rat canalicular conjugate export pump (Mrp2) is down-regulated in intrahepatic and obstructive cholestasis. Gastroenterology 113, 255-264.

Trauner, M., Fickert, P., Stauber, R.E., 1999a. Inflammation-induced cholestasis. Journal of gastroenterology and hepatology 14, 946-959.

Trauner, M., Meier, P.J., Boyer, J.L., 1998b. Molecular pathogenesis of cholestasis. The New England journal of medicine 339, 1217-1227.

Trauner, M., Meier, P.J., Boyer, J.L., 1999b. Molecular regulation of hepatocellular transport systems in cholestasis. Journal of hepatology 31, 165-178.

Trauner, M., Wagner, M., Fickert, P., Zollner, G., 2005. Molecular regulation of hepatobiliary transport systems: clinical implications for understanding and treating cholestasis. Journal of clinical gastroenterology 39, S111-124.

Uetrecht, J., 2006. Evaluation of which reactive metabolite, if any, is responsible for a specific idiosyncratic reaction. Drug metabolism reviews 38, 745-753.

Uetrecht, J.P., 1999. New concepts in immunology relevant to idiosyncratic drug reactions: the "danger hypothesis" and innate immune system. Chemical research in toxicology 12, 387-395.

Uyemura, S.A., Santos, A.C., Mingatto, F.E., Jordani, M.C., Curti, C., 1997. Diclofenac sodium and mefenamic acid: potent inducers of the membrane permeability transition in renal cortex mitochondria. Archives of biochemistry and biophysics 342, 231-235.

van Erven, L., Schalij, M.J., 2010. Amiodarone: an effective antiarrhythmic drug with unusual side effects. Heart 96, 1593-1600.

van Leeuwen, J.S., Orij, R., Luttik, M.A., Smits, G.J., Vermeulen, N.P., Vos, J.C., 2011a. Subunits Rip1p and Cox9p of the respiratory chain contribute to diclofenac-induced mitochondrial dysfunction. Microbiology 157, 685-694.

van Leeuwen, J.S., Vermeulen, N.P., Vos, J.C., 2011b. Involvement of the pleiotropic drug resistance response, protein kinase C signaling, and altered zinc homeostasis in resistance of Saccharomyces cerevisiae to diclofenac. Applied and environmental microbiology 77, 5973-5980.

van Leeuwen, J.S., Vredenburg, G., Dragovic, S., Tjong, T.F., Vos, J.C., Vermeulen, N.P., 2011c. Metabolism related toxicity of diclofenac in yeast as model system. Toxicology letters 200, 162-168.

Vassallo, P., Trohman, R.G., 2007. Prescribing amiodarone: an evidence-based review of clinical indications. Jama 298, 1312-1322.

Velayudham, L.S., Farrell, G.C., 2003. Drug-induced cholestasis. Expert opinion on drug safety 2, 287-304.

Vernhet, L., Allain, N., Le Vee, M., Morel, F., Guillouzo, A., Fardel, O., 2003. Blockage of multidrug resistance-associated proteins potentiates the inhibitory effects of arsenic trioxide on CYP1A1 induction by polycyclic aromatic hydrocarbons. The Journal of pharmacology and experimental therapeutics 304, 145-155.

Vincent, J., Teng, R., Dalvie, D.K., Friedman, H.L., 1998. Pharmacokinetics and metabolism of single oral doses of trovafloxacin. American journal of surgery 176, 8S-13S.

Vitins, A.P., Kienhuis, A.S., Speksnijder, E.N., Roodbergen, M., Luijten, M., van der Ven, L.T., 2014. Mechanisms of amiodarone and valproic acid induced liver steatosis in mouse in vivo act as a template for other hepatotoxicity models. Archives of toxicology 88, 1573-1588.

Voican, C.S., Njike-Nakseu, M., Boujedidi, H., Barri-Ova, N., Bouchet-Delbos, L., Agostini, H., Maitre, S., Prevot, S., Cassard-Doulcier, A.M., Naveau, S., Perlemuter, G., 2015. Alcohol withdrawal alleviates adipose tissue inflammation in patients with alcoholic liver disease. Liver international : official journal of the International Association for the Study of the Liver 35, 967-978.

Voican, C.S., Perlemuter, G., Naveau, S., 2011. Mechanisms of the inflammatory reaction implicated in alcoholic hepatitis: 2011 update. Clinics and research in hepatology and gastroenterology 35, 465-474.

Wade, L.T., Kenna, J.G., Caldwell, J., 1997. Immunochemical identification of mouse hepatic protein adducts derived from the nonsteroidal anti-inflammatory drugs diclofenac, sulindac, and ibuprofen. Chemical research in toxicology 10, 546-555.

Wagner, M., Zollner, G., Trauner, M., 2009. New molecular insights into the mechanisms of cholestasis. Journal of hepatology 51, 565-580.

Wagner, M., Zollner, G., Trauner, M., 2010. Nuclear receptor regulation of the adaptive response of bile acid transporters in cholestasis. Seminars in liver disease 30, 160-177.

Waldhauser, K.M., Torok, M., Ha, H.R., Thomet, U., Konrad, D., Brecht, K., Follath, F., Krahenbuhl, S., 2006. Hepatocellular toxicity and pharmacological effect of amiodarone and amiodarone derivatives. The Journal of pharmacology and experimental therapeutics 319, 1413-1423.

Wang, A.G., Xia, T., Yuan, J., Yu, R.A., Yang, K.D., Chen, X.M., Qu, W., Waalkes, M.P., 2004. Effects of phenobarbital on metabolism and toxicity of diclofenac sodium in rat hepatocytes in vitro. Food and chemical toxicology : an international journal published for the British Industrial Biological Research Association 42, 1647-1653.

Wang, B., Cai, S.R., Gao, C., Sladek, F.M., Ponder, K.P., 2001. Lipopolysaccharide results in a marked decrease in hepatocyte nuclear factor 4 alpha in rat liver. Hepatology 34, 979-989.

Wang, M., Gorrell, M.D., Abbott, C.A., Jaggi, R., Marguet, D., Dickinson, R.G., 2002. Hepatic covalent adduct formation with zomepirac in the CD26-deficient mouse. Journal of gastroenterology and hepatology 17, 66-71.

Wang, Y.D., Chen, W.D., Wang, M., Yu, D., Forman, B.M., Huang, W., 2008. Farnesoid X receptor antagonizes nuclear factor kappaB in hepatic inflammatory response. Hepatology 48, 1632-1643.

Waring, J.F., Liguori, M.J., Luyendyk, J.P., Maddox, J.F., Ganey, P.E., Stachlewitz, R.F., North, C., Blomme, E.A., Roth, R.A., 2006. Microarray analysis of lipopolysaccharide potentiation of trovafloxacin-induced liver injury in rats suggests a role for proinflammatory chemokines and neutrophils. The Journal of pharmacology and experimental therapeutics 316, 1080-1087.

Warnecke, D., Erdmann, R., Fahl, A., Hube, B., Muller, F., Zank, T., Zahringer, U., Heinz, E., 1999. Cloning and functional expression of UGT genes encoding sterol glucosyltransferases from Saccharomyces

cerevisiae, Candida albicans, Pichia pastoris, and Dictyostelium discoideum. The Journal of biological chemistry 274, 13048-13059.

Watanabe, N., Takashimizu, S., Kojima, S., Kagawa, T., Nishizaki, Y., Mine, T., Matsuzaki, S., 2007. Clinical and pathological features of a prolonged type of acute intrahepatic cholestasis. Hepatology research : the official journal of the Japan Society of Hepatology 37, 598-607.

Watanabe, N., Tsukada, N., Smith, C.R., Phillips, M.J., 1991. Motility of bile canaliculi in the living animal: implications for bile flow. The Journal of cell biology 113, 1069-1080.

Watanabe, S., Phillips, M.J., 1984. Ca2+ causes active contraction of bile canaliculi: direct evidence from microinjection studies. Proceedings of the National Academy of Sciences of the United States of America 81, 6164-6168.

Watkins, P.B., Kaplowitz, N., Slattery, J.T., Colonese, C.R., Colucci, S.V., Stewart, P.W., Harris, S.C., 2006. Aminotransferase elevations in healthy adults receiving 4 grams of acetaminophen daily: a randomized controlled trial. Jama 296, 87-93.

Wawrzycka, D., Sobczak, I., Bartosz, G., Bocer, T., Ulaszewski, S., Goffeau, A., 2010. Vmr 1p is a novel vacuolar multidrug resistance ABC transporter in Saccharomyces cerevisiae. FEMS yeast research 10, 828-838.

Wehr, A., Baeck, C., Ulmer, F., Gassler, N., Hittatiya, K., Luedde, T., Neumann, U.P., Trautwein, C., Tacke, F., 2014. Pharmacological inhibition of the chemokine CXCL16 diminishes liver macrophage infiltration and steatohepatitis in chronic hepatic injury. PloS one 9, e112327.

Wellens, H.J., Brugada, P., Abdollah, H., Dassen, W.R., 1984. A comparison of the electrophysiologic effects of intravenous and oral amiodarone in the same patient. Circulation 69, 120-124.

Westerink, W.M., Schoonen, W.G., 2007a. Cytochrome P450 enzyme levels in HepG2 cells and cryopreserved primary human hepatocytes and their induction in HepG2 cells. Toxicology in vitro : an international journal published in association with BIBRA 21, 1581-1591.

Westerink, W.M., Schoonen, W.G., 2007b. Phase II enzyme levels in HepG2 cells and cryopreserved primary human hepatocytes and their induction in HepG2 cells. Toxicology in vitro : an international journal published in association with BIBRA 21, 1592-1602.

Wheater PR, Y., B., and Heath, J.W, 2001. Histologie fonctionnelle. Le foie et le pancreas. Harcourt.
Wilkening, S., Stahl, F., Bader, A., 2003. Comparison of primary human hepatocytes and hepatoma cell line Hepg2 with regard to their biotransformation properties. Drug metabolism and disposition: the biological fate of chemicals 31, 1035-1042.

Willis, J.V., Kendall, M.J., Flinn, R.M., Thornhill, D.P., Welling, P.G., 1979. The pharmacokinetics of diclofenac sodium following intravenous and oral administration. European journal of clinical pharmacology 16, 405-410.

Wilson, B.D., Clarkson, C.E., Lippmann, M.L., 1991. Amiodarone-induced pulmonary inflammation. Correlation with drug dose and lung levels of drug, metabolite, and phospholipid. The American review of respiratory disease 143, 1110-1114.

Wolfger, H., Mamnun, Y.M., Kuchler, K., 2004. The yeast Pdr15p ATP-binding cassette (ABC) protein is a general stress response factor implicated in cellular detoxification. The Journal of biological chemistry 279, 11593-11599.

Xia, X., Roundtree, M., Merikhi, A., Lu, X., Shentu, S., Lesage, G., 2004. Degradation of the apical sodium-dependent bile acid transporter by the ubiquitin-proteasome pathway in cholangiocytes. The Journal of biological chemistry 279, 44931-44937.

Xu, J., Kulkarni, S.R., Donepudi, A.C., More, V.R., Slitt, A.L., 2012. Enhanced Nrf2 activity worsens insulin resistance, impairs lipid accumulation in adipose tissue, and increases hepatic steatosis in leptin-deficient mice. Diabetes 61, 3208-3218.

Xu, J.J., Diaz, D., O'Brien, P.J., 2004. Applications of cytotoxicity assays and pre-lethal mechanistic assays for assessment of human hepatotoxicity potential. Chemico-biological interactions 150, 115-128.

Xu, Y.C., Wu, R.F., Gu, Y., Yang, Y.S., Yang, M.C., Nwariaku, F.E., Terada, L.S., 2002. Involvement of TRAF4 in oxidative activation of c-Jun N-terminal kinase. The Journal of biological chemistry 277, 28051-28057.

Yaghi, C., Honein, K., Boujaoude, J., Slim, R., Moucari, R., Sayegh, R., 2006. Influence of acetaminophen at therapeutic doses on surrogate markers of severity of acute viral hepatitis. Gastroenterologie clinique et biologique 30, 763-768.

Yano, T., Takigami, E., Yurimoto, H., Sakai, Y., 2009. Yap1-regulated glutathione redox system curtails accumulation of formaldehyde and reactive oxygen species in methanol metabolism of Pichia pastoris. Eukaryotic cell 8, 540-549.

Young, L., Leonhard, K., Tatsuta, T., Trowsdale, J., Langer, T., 2001. Role of the ABC transporter Mdl1 in peptide export from mitochondria. Science 291, 2135-2138.

Zafarullah, M., Li, W.Q., Sylvester, J., Ahmad, M., 2003. Molecular mechanisms of N-acetylcysteine actions. Cellular and molecular life sciences : CMLS 60, 6-20.

Zhao, P., Slattery, J.T., 2002. Effects of ethanol dose and ethanol withdrawal on rat liver mitochondrial glutathione: implication of potentiated acetaminophen toxicity in alcoholics. Drug metabolism and disposition: the biological fate of chemicals 30, 1413-1417.

Zhou, C., Tabb, M.M., Nelson, E.L., Grun, F., Verma, S., Sadatrafiei, A., Lin, M., Mallick, S., Forman, B.M., Thummel, K.E., Blumberg, B., 2006. Mutual repression between steroid and xenobiotic receptor and NF-kappaB signaling pathways links xenobiotic metabolism and inflammation. The Journal of clinical investigation 116, 2280-2289.

Zimmerman, T.L., Thevananther, S., Ghose, R., Burns, A.R., Karpen, S.J., 2006. Nuclear export of retinoid X receptor alpha in response to interleukin-1beta-mediated cell signaling: roles for JNK and SER260. The Journal of biological chemistry 281, 15434-15440.

Zinser, E., Daum, G., 1995. Isolation and biochemical characterization of organelles from the yeast, Saccharomyces cerevisiae. Yeast 11, 493-536.

Zollner, G., Fickert, P., Zenz, R., Fuchsbichler, A., Stumptner, C., Kenner, L., Ferenci, P., Stauber, R.E., Krejs, G.J., Denk, H., Zatloukal, K., Trauner, M., 2001. Hepatobiliary transporter expression in percutaneous liver biopsies of patients with cholestatic liver diseases. Hepatology 33, 633-646.

Zollner, G., Marschall, H.U., Wagner, M., Trauner, M., 2006. Role of nuclear receptors in the adaptive response to bile acids and cholestasis: pathogenetic and therapeutic considerations. Molecular pharmaceutics 3, 231-251.

Zou, W., Devi, S.S., Sparkenbaugh, E., Younis, H.S., Roth, R.A., Ganey, P.E., 2009. Hepatotoxic interaction of sulindac with lipopolysaccharide: role of the hemostatic system. Toxicological sciences : an official journal of the Society of Toxicology 108, 184-193.

Annexe

1521-009X/42/9/1556–1566$25.00
Drug Metabolism and Disposition
http://dx.doi.org/10.1124/dmd.114.058123
Drug Metab Dispos 42:1556–1566, September 2014

Impact of Inflammation on Chlorpromazine-Induced Cytotoxicity and Cholestatic Features in HepaRG Cells[S]

Pamela Bachour-El Azzi, Ahmad Sharanek, Ziad Abdel-Razzak, Sebastien Antherieu,[1] Houssein Al-Attrache, Camille C. Savary, Sylvie Lepage, Isabelle Morel, Gilles Labbe, Christiane Guguen-Guillouzo, and André Guillouzo

Inserm UMR991, Foie, Métabolismes et Cancer, Rennes, France (P.B-E.A., A.S., S.A., H.A-A., C.C.S., I.M., C.G-G., A.G.); Université de Rennes 1, Rennes, France (P.B-E.A., A.S., S.A., H.A-A., C.C.S., I.M., C.G-G., A.G.); EDST-PRASE and EDST-AZM-Center-LBA3B, Université Libanaise, Lebanon (P.B-E.A., H.A-A., Z.A-R.); Laboratoire d'Urgence et de Réanimation, Hôpital Pontchaillou, Rennes, France (S.L., I.M.); Sanofi R&D, Alfortville, France (G.L.)

Received March 14, 2014; accepted July 7, 2014

ABSTRACT

Several factors are thought to be implicated in the occurrence of idiosyncratic adverse drug reactions. The present work aimed to question as to whether inflammation is a determinant factor in hepatic lesions induced by chlorpromazine (CPZ) using the human HepaRG cell line. An inflammation state was induced by a 24-hour exposure to proinflammatory cytokines interleukin-6 (IL-6) and IL-1β; then the cells were simultaneously treated with CPZ and/or cytokine for 24 hours or daily for 5 days. The inflammatory response was assessed by induction of C-reactive protein and IL-8 transcripts and proteins as well as inhibition of CPZ metabolism and down-regulation of cytochrome 3A4 (CYP3A4) and CYP1A2 transcripts, two major cytochrome P450 (P450) enzymes involved in its metabolism. Most effects of cotreatments with cytokines and CPZ were amplified or only observed after five daily treatments; they mainly included increased cytotoxicity and overexpression of oxidative stress-related genes, decreased Na^+-taurocholate cotransporting polypeptide mRNA levels and activity, a key transporter involved in bile acids uptake, and deregulation of several other transporters. However, CPZ-induced inhibition of taurocholic acid efflux and pericanalicular F-actin distribution were not affected. In addition, a time-dependent induction of phospholipidosis was noticed in CPZ-treated cells, without obvious influence of the inflammatory stress. In summary, our results show that an inflammatory state induced by proinflammatory cytokines increased cytotoxicity and enhanced some cholestatic features induced by the idiosyncratic drug CPZ in HepaRG cells. These changes, together with inhibition of P450 activities, could have important consequences if extrapolated to the in vivo situation.

Introduction

Drug-induced liver injury (DILI) is a major cause of attrition during both early and late stages of the drug development and marketing process (Meng, 2010). DILI is usually classified as dose dependent, which is typically reproducible, or unpredictable (idiosyncratic), occurring only in certain susceptible patients and being not overtly dose dependent (Greer et al., 2010). The mechanisms underlying idiosyncratic DILI (iDILI) remain largely unknown. Several factors are thought to be implicated, including genetic polymorphisms of drug metabolism-related or HLA genes, liver pathologies of various origins including viral infection, and/or environmental inflammatory stress. Among these factors, inflammation caused by agents such as bacterial lipopolysaccharide (LPS) and proinflammatory cytokines, has been shown to exacerbate toxicity of many hepatotoxic chemicals (Roth et al., 1997; Barton et al., 2000; Yee et al., 2000) and to induce hepatotoxicity of various drugs associated with idiosyncratic reactions,

This work was supported by the International Research Servier Group, the French-Lebanon Cèdre program 11 S F47/L2 (2011-2012), and the European Community (Contracts Predict-IV-202222 and MIP-DILI-115336). The MIP-DILI project received support from the Innovative Medicines Initiative Joint Undertaking, with resources composed of financial contributions from the European Union's Seventh Framework Programme (FP7/20072013) and EFPIA companies' in kind contribution; and the researchers were supported by grants from the Lebanese University and Lebanese National Council for Scientific Research (1015/347), the Philippe Jabre association (941/10), and the Doctorate School vie-agro-santé Rennes (to P.B-E.A.); and the Lebanese Association for Scientific Research (to A.S.).

P.B-E.A. and A.S. contributed equally to this work.

[1]Current affiliation: Université de Lille 2, EA4483, Lille, France.

dx.doi.org/10.1124/dmd.114.058123.

[S]This article has supplemental material available at dmd.aspetjournals.org.

ABBREVIATIONS: BCRP, breast cancer resistance protein; BSEP, bile salt export pump; CAR, constitutive androstane receptor; CDFDA, 5(6)-carboxy-2′,7′-dichlorofluorescein diacetate; CPZ, chlorpromazine; CRP, C-reactive protein; DILI, drug-induced liver injury; DMSO, dimethyl sulfoxide; FXR, farnesoid X receptor; H2-DCFDA, 2′,7′-dichlorodihydrofluorescein; HO1, heme oxygenase 1; HPLC-MS/MS, high-pressure liquid chromatography with tandem mass spectrometry; iDILI idiosyncratic drug-induced liver injury, ; IL, interleukin; LPS, lipopolysaccharide; MDR1, multidrug resistance protein 1; MnSOD, manganese superoxide dismutase; MRP, multidrug resistance-associated protein; MTT, methylthiazoletetrazolium; Nor-1 CPZ, *N*-desmethyl-CPZ; Nrf2, NF-E2-related factor; NTCP, Na^+-dependent taurocholate cotransporting polypeptide; OATP, organic anion-transporting polypeptide; OCT-1, organic cation transporter 1; 3-OH CPZ, 3-hydroxyl CPZ; 7-OH CPZ, 7-hydroxyl CPZ; P450, cytochrome P450; PBS, phosphate-buffered saline; PXR, pregnane X receptor; ROS, reactive oxygen species; RT-qPCR, real-time quantitative polymerase chain reaction; SO CPZ, sulfoxy-CPZ; TA, taurocholic acid.

such as trovafloxacin (Waring et al., 2006; Shaw et al., 2007) and chlorpromazine (CPZ) (Buchweitz et al., 2002).

The antipsychotic agent CPZ is known to cause hepatotoxicity, which includes cholestasis (Hollister, 1957; Regal et al., 1987), hepatocellular necrosis, and phospholipidosis, in some patients (Velayudham and Farrell, 2003). Various CPZ-induced liver disturbances have also been described in in vivo and in vitro animal models, but they were mainly limited to hepatic lesions related to cell death, which were usually amplified by pretreatment with inflammatory agents (Buchweitz et al., 2002; Gandhi et al., 2010; MacAllister et al., 2013). No evidence of changes in serum bile acid concentrations and alterations of bile canaliculi were observed in rats treated with LPS and CPZ (Buchweitz et al., 2002). Obviously, whether cholestatic effects of CPZ are aggravated by concomitant exposure to proinflammatory cytokines remains unclear.

LPS and proinflammatory cytokines have been reported to alter various liver functions, including drug metabolism and transport. In particular, they down-regulate activity of major cytochromes P450 (P450) involved in xenobiotic metabolism and also markedly impair phase-2 conjugating enzymes as well as basolateral and canalicular transporters of bile acids and organic anions (Abdel-Razzak et al., 1993; Aitken et al., 2006). Recently, our group reported that CPZ generated an early oxidative stress, altered mitochondrial membrane potential, and disorganized pericanalicular cytoskeletal F-actin distribution in human HepaRG cells. These effects were associated with inhibition of taurocholic acid (TA) efflux (Antherieu et al., 2013). These results led us to question as to whether the two major proinflammatory cytokines interleukin-6 (IL-6) and interleukin-1β (IL-1β) might enhance cytotoxic and cholestatic effects induced by CPZ in human hepatocytes. We showed that an inflammatory situation caused by both cytokines and resulting in a strong inhibition of cytochrome P450-mediated metabolism of CPZ decreased cell viability and aggravated some cholestatic markers in hepatocyte-like HepaRG cell cultures treated with this cholestatic drug.

Materials and Methods

Chemicals. CPZ, methylthiazoletetrazolium (MTT), and 5(6)-carboxy-2′, 7′-dichlorofluorescein diacetate (CDFDA) were purchased from Sigma (St. Quentin Fallavier, France). Human recombinant IL-6 and IL-1β were from Promokine, (Heidelberg, Germany). Human C-reactive protein (CRP) and CXCL8/IL-8 DuoSet kits were from R&D (Abingdon, United Kingdom). [^{3}H]Taurocholic acid ([^{3}H]TA) was from Perkin Elmer (Boston, MA). The 2′,7′-dichlorodihydrofluorescein (H2-DCFDA) was from Life Technologies-Molecular Probes (Saint Aubin, France). Phalloidin fluoprobe SR101 (200 U/ml) was purchased from Interchim (Montluçon France). Hoechst dye was from Promega (Madison, WI). CPZ metabolites [*N*-desmethyl-CPZ (Nor-1 CPZ), sulfoxy-CPZ (SO CPZ), 3-hydroxyl CPZ (3-OH CPZ), and 7-hydroxyl CPZ (7-OH CPZ)] were a gift from Sanofi (Alfortville, France).

Cell Culture. HepaRG cells were seeded at a density of 2.6×10^4 cells/cm^2 as previously described elsewhere (Gripon et al., 2002). After 2 weeks, the medium was supplemented with 2% dimethyl sulfoxide (DMSO) for 2 further weeks to obtain confluent differentiated HepaRG cell cultures. At that time, these cultures contained hepatocyte-like and progenitors/primitive biliary-like cells in around an equal proportion (Cerec et al., 2007) and were ready for experimental use. All treatments were done with a medium supplemented with 2% fetal bovine serum and 1% DMSO.

Cell Viability. Cytotoxicity was evaluated by the MTT colorimetric assay. Briefly, cells were seeded in 24-well plates and treated with various concentrations of cytokines and CPZ. After medium removal, 500 μl of serum-free medium containing MTT (0.5 mg/ml) was added to each well and incubated for 2 hours at 37°C. The water-insoluble formazan was dissolved in 500 μl of DMSO, and absorbance was measured at 550 nm.

Measurement of Reactive Oxygen Species. Reactive oxygen species (ROS) generation was determined by the H2-DCFDA assay. Cells were incubated for 2 hours at 37°C with 2 μM H2-DCFDA; then they were washed with cold phosphate-buffered saline (PBS), and scraped in phosphate buffer (10 mM, pH 7.4)/methanol (v/v) added with 0.1% Triton X-100. Fluorescence intensity of cell lysates was determined by spectrofluorometry using excitation/emission wavelengths of 498/520 nm.

CRP and IL-8 Protein Measurements. CRP and IL-8 proteins were measured in cell supernatants after 1 and 5 days of cotreatment with cytokines and CPZ using the CRP and CXCL8/IL-8 DuoSet kits, according to the manufacturer's instructions. Briefly, supernatants were collected at the appropriate time points and stored at −80°C until analysis; 96-well microplates were coated with capture antibody and incubated overnight. Samples and standards were diluted appropriately and added for 2 hours after a saturation step. Secondary antibody was added for 2 hours after washing. Streptavidin-horseradish peroxidase and its substrate were used for revelation. Optical density was read at 450 nm with wavelength correction. All steps were performed at room temperature.

Real-Time Quantitative Polymerase Chain Reaction analysis. Total RNA was extracted from 10^6 HepaRG cells with the SV total RNA isolation system (Promega). RNAs were reverse-transcribed into cDNA and real-time quantitative polymerase chain reaction (RT-qPCR) was performed using a SYBR Green mix. Primer sequences are listed in Supplemental Table 1.

F-Actin Distribution. After cell exposure to CPZ and/or cytokines, cells were washed twice with warm PBS, fixed with 4% paraformaldehyde for 20 minutes at 4°C, and permeabilized with 0.3% Triton in PBS for 20 minutes. F-actin and nuclei were labeled simultaneously using the phalloidin-fluoprobe diluted at 1/100 and 5 ng/ml Hoechst dye, respectively, for 20 minutes (Pernelle et al., 2011). Imaging was done using the Cellomics ArrayScan VTI HCS Reader (Thermo Scientific).

Na^+-Dependent Taurocholic Cotransporting Polypeptide Activity. Activity of the Na^+-Dependent Taurocholic Cotransporting Polypeptide (NTCP) transporter was estimated through determination of sodium-dependent intracellular accumulation of radiolabeled TA substrate, as previously described elsewhere (Antherieu et al., 2013). Briefly, treated cells were incubated with radiolabeled TA for 30 minutes. Cells were then washed twice with PBS and lysed with 0.1 N NaOH. Accumulation of radiolabeled substrates was determined through scintillation counting. Taurocholate accumulation values in the presence of sodium minus accumulation values in the absence of sodium represented NTCP activity.

TA Efflux Activity. Cells were first incubated with [^{3}H]TA, a substrate of bile salt export pump (BSEP), for 30 minutes, then washed with PBS and exposed to CPZ, cytokines, or both for 2 or 4 hours in a standard buffer containing Ca^{2+} and Mg^{2+} ions. At the end of the incubation time, cells were washed with PBS and incubated for 5 minutes with a Ca^{2+} and Mg^{2+}-free buffer to disrupt the canalicular tight junctions. Then, they were scraped in 0.1 N NaOH; the remaining radiolabeled substrate was measured through scintillation counting to determine TA efflux (Marion et al., 2012).

CDF Excretion. After 2 or 4 hours of exposure to CPZ and cytokines individually or simultaneously, cells were incubated with 3 μM CDFDA, which is hydrolyzed by intracellular esterases to CDF, a substrate of multidrug resistance-associated protein 2 (MRP2) (Zamek-Gliszczynski et al., 2003), for 20 minutes at 37°C and then washed with PBS. Imaging was done using inverted microscope Zeiss Axiovert 200M and AxioCam MRm (Carl Zeiss Microscopy GmbH, Jena, Germany).

Quantification of CPZ and Its Metabolites. After 1 and 5 days of treatment, incubation media were collected and stored at −20°C until analysis. Cells were washed twice with PBS and then lysed with 0.01N NaOH. An aliquot was used to determine protein concentration, and the remaining volume was stored at −20°C until analysis. Concentrations of CPZ and four of its metabolites (Nor-1 CPZ, SO CPZ, 3-OH CPZ, and 7-OH CPZ) were determined in both cell lysates and incubation media using a high-pressure liquid chromatography with tandem mass spectrometry (HPLC-MS/MS) system. HPLC separation was performed on a C18 column (Hypersil Gold, C18; particle size: 1.9 μm; 50 × 2.1 mm, i.d.; ThermoFisher Scientific). Mobile phase A consisted of 10 mM ammonium acetate with 0.1% formic acid. Mobile phase B was acetonitrile with also 0.1% formic acid. The gradient program was as follows: 0–2.50 minutes, 95% A; 2.51–3.70 minutes, 70% A; 3.71–5.50 minutes, 60% A; 5.51–6.60 minutes, 95% B; 6.61–8.00 minutes, 95% A. Under these conditions, retention times were, respectively, 3.16 minutes for SO CPZ, 3.57 minutes for 3-OH CPZ, 3.85 minutes for 7-OH CPZ, 4.60 minutes for Nor-1 CPZ, and 4.70 minutes for CPZ. The flow rate was kept

at 500 μl/min. The injected volume was 5 μl, and the temperature of column was maintained at 35°C. Detection parameters were set in MRM mode, with the following transitions: 304.9/72.0 (collision energy 18) for Nor-1 CPZ, 334.9/231.9 (collision energy 37) for SO CPZ, 334.9/86.0 (collision energy 20) for both 3-OH CPZ and 7-OH CPZ, 319.1/86.1 (collision energy 20) for CPZ, and 388.0/315.0 (collision energy 23) for flurazepam, as internal standard.

Statistical Analysis. One-way analysis of variance with Bonferroni's multiple comparison test (GraphPad Prism 5.00; GraphPad Software, San Diego, CA) was performed to compare data between the cells treated with CPZ, cytokine, cytokine plus CPZ and the control cultures. Each value corresponded to the mean ± standard deviation (S.D.) of at least three independent experiments. $P < 0.05$ was considered statistically significant.

Results

Dose- and Time-Dependent Effects of CPZ and Cytokines on HepaRG Cell Viability. First, the MTT assay was performed to estimate the cytotoxicity of CPZ, IL-6, and IL-1β in HepaRG cells after one and five daily additions. At 5 and 20 μM, CPZ elicited no toxicity regardless of treatment duration while at 50 μM it caused 90% cell death after three additions (data not shown). IL-6 did not alter cell viability at concentrations ranging from 0.01 (1 unit/ml) to 1 ng/ml regardless of the duration of treatment; at 10 ng/ml, it induced a 20% loss in cell viability after 5 daily treatments. IL-1β also caused 20%–30% decrease in cell viability at concentrations ranging from 0.1 (20 units/ml) to 1 ng/ml after 5 days of treatment (data not shown). Based on these results, nontoxic concentrations of 20 μM CPZ, 1 ng/ml IL-6, and 0.01 ng/ml IL-1β were selected for 1 and 5 day cotreatment, and 50 μM CPZ was used for short-term cotreatment.

To verify whether their viability was affected by cotreatments with cytokines, HepaRG cells were first incubated with IL-6 or IL-1β for 24 hours before simultaneous CPZ addition for 1 or 5 days. Compared with untreated cells, a significant although modest decrease of cell viability was observed after five additions of CPZ with either cytokine (12% and 20% with IL-6 + CPZ and IL-1β + CPZ, respectively) (Fig. 1).

Effects of Cytokines and CPZ on Inflammation Markers. Generation of an in vitro inflammatory response with the selected cytokine concentrations was validated by measurement of CRP and IL-8 mRNA and secreted protein levels after one and five additions of either IL-1β or IL-6. Both cytokines caused a statistically significant increase of CRP mRNA (8- to 95-fold) and protein (12- to 48-fold) levels at both time points compared with corresponding untreated cells (Fig. 2, A and C), thereby demonstrating an inflammatory response of HepaRG cells. At 20 μM, CPZ did not cause any significant change in CRP expression, excluding any inflammatory effect of this neuroleptic drug at least up to this concentration. However, combination of CPZ and IL-6 or IL-1β enhanced increase of CRP mRNAs (53-fold with IL-6 versus 80-fold with IL-6 + CPZ and 8-fold with IL-1β versus 12-fold with IL-1β + CPZ after 5 daily additions) (Fig. 2A). Although cytokine-mediated induction of CRP protein was also enhanced by CPZ after five simultaneous additions (41-fold by IL-6 versus 48-fold by IL-6 + CPZ and 12-fold by IL-1β versus 14-fold by IL-1β + CPZ), these variations were not statistically significant (Fig. 2C).

Regardless of treatment duration, IL-8 mRNA and protein levels were not affected by IL-6 or 20 μM CPZ individually nor by their combination. By contrast, IL-8 mRNAs were increased by IL-1β alone or associated with CPZ after one addition; this induction was lower after five additions (Fig. 2B). Similarly, IL-8 protein was also augmented (5- and 4-fold after one and five additions, respectively) (Fig. 2D). Secreted IL-1β and IL-6 proteins were undetectable in either untreated or 20 μM CPZ-treated HepaRG cells even after five additions (data not shown).

Additional experiments were performed with 50 μM CPZ, a concentration previously shown to induce early characteristic cholestatic features. At 50 μM, CPZ increased IL-8 at both mRNA (3.15-fold) and protein (6.6-fold) levels after 24 hours; induction of IL-8 protein was observed as early as 2 hours. Moreover, IL-1β and IL-6 transcripts were induced by 50 μM CPZ (6.6- and 2.3-fold after 24 hours) and secreted IL-6 protein became detectable after 4 hours exposure to 50 μM CPZ (Supplemental Fig. 1).

Inhibition of CPZ Metabolism by Proinflammatory Cytokines. At the selected concentrations and regardless of the duration of treatment, both IL-6 and IL-1β strongly repressed mRNA expression of CYP1A2 (a drop by 67% and 58%, respectively) and CYP3A4 (a drop by 90% and 75%, respectively), the two major P450 enzymes involved in CPZ oxidative metabolism, in HepaRG cells. Whereas CYP1A2 and CYP3A4 transcripts were induced 4- to 6-fold in 20 μM CPZ-treated HepaRG cells compared with untreated cells, their induction was abolished in the presence of cytokines (Fig. 3A). Of

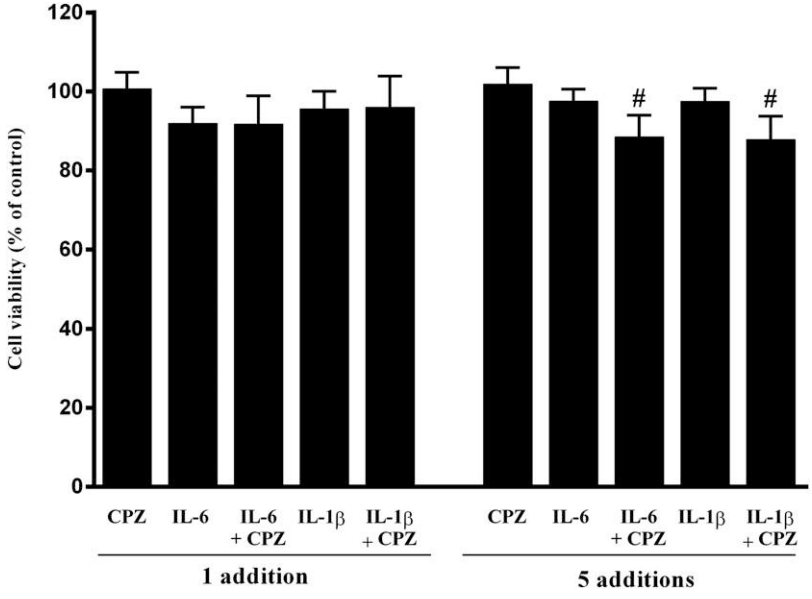

Fig. 1. Cytotoxic effects of CPZ and/or proinflammatory cytokines in HepaRG cells. Cells were pretreated with IL-6 (1 ng/ml) or IL-1β (0.01 ng/ml) for 24 hours, then 20 μM CPZ were added daily simultaneously with cytokines for 1 or 5 days (one and five additions, respectively). Cytotoxicity was measured by the MTT colorimetric assay. Each point is the mean ± S.D. of three independent experiments. $^{\#}P < 0.05$ compared with untreated cells.

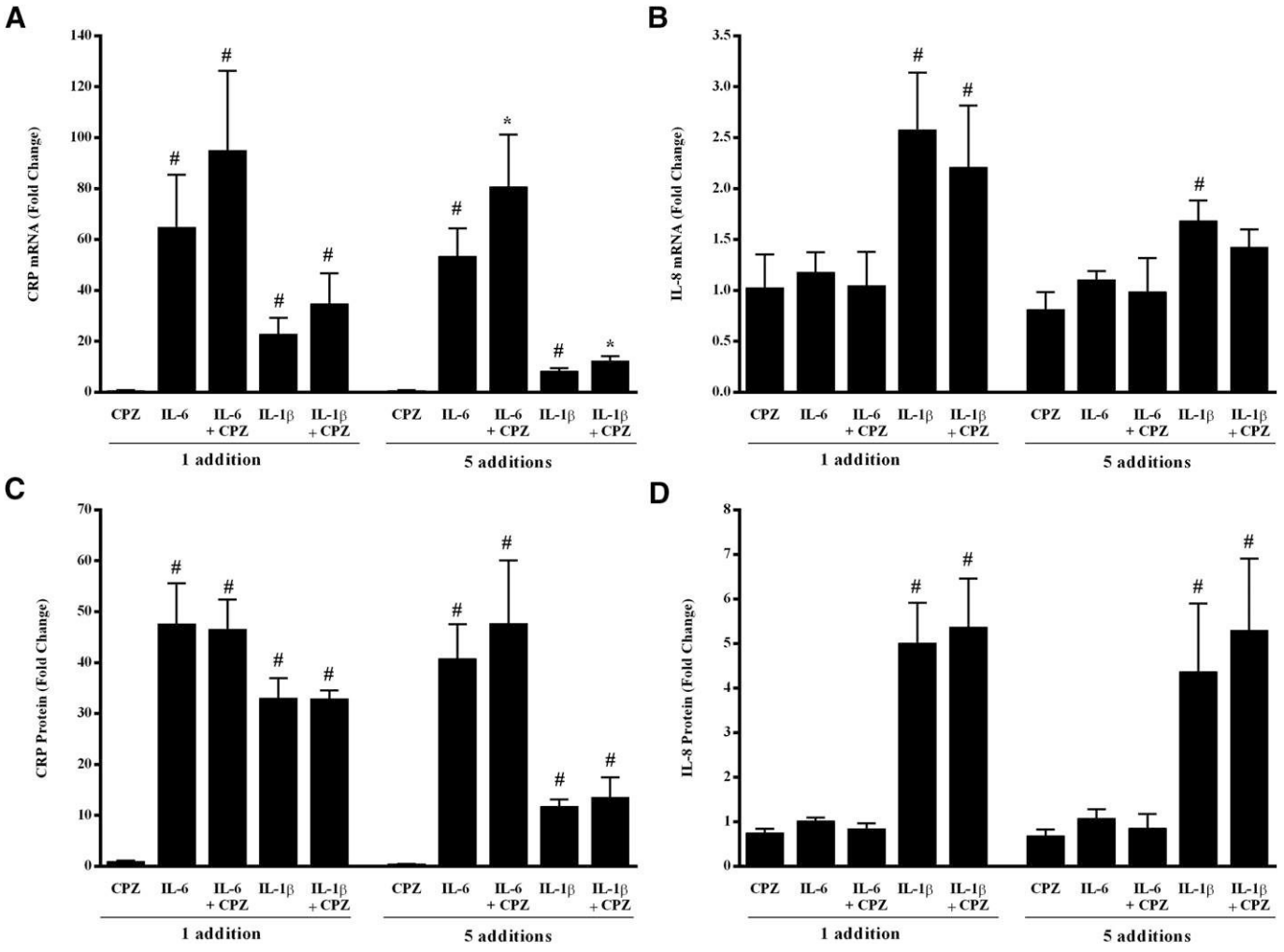

Fig. 2. Effects of CPZ and proinflammatory cytokines on inflammatory stress markers. Cells were pretreated with IL-6 (1 ng/ml) or IL-1β (0.01 ng/ml) for 24 hours, then 20 μM CPZ was added daily simultaneously with cytokines for 1 or 5 days (one and five additions, respectively). (A) CRP and (B) IL-8 mRNA levels were assessed by RT-qPCR. (C) CRP and (D) IL-8 proteins were measured by ELISA in culture media. Data represent the mean ± S.D. of three independent experiments. All results are expressed relative to the levels found in control cells, arbitrarily set at a value of 1. $^{\#}P < 0.05$ compared with untreated cells, $^{*}P < 0.05$ compared with cells treated with cytokine and CPZ individually.

note, cytokine-induced inhibition of both cytochromes was attenuated or even completely abolished with IL-1β after five additions in CPZ cotreated cells.

Moreover, four CPZ metabolites, Nor-1 CPZ, SO CPZ, 7-OH CPZ, and 3-OH CPZ, were quantified by HPLC-MS/MS in culture media and cell lysates after one and five drug additions. Detectable amounts of Nor-1 CPZ, SO-CPZ, and to a lesser extent 7-OH CPZ were found in both cell lysates (Fig. 3B) and incubation media (Fig. 3C) of untreated and cytokine-treated HepaRG cells, whereas 3-OH CPZ was barely detectable in all tested conditions, preventing its accurate quantification (data not shown). After 1 day of simultaneous treatment with cytokines, 7-OH CPZ and Nor-1 CPZ amounts were decreased by up to 42%, and CPZ content was statistically higher in cytokine-treated cells compared with the values obtained in cells treated with CPZ alone. After 5 days, all detectable metabolites were decreased in the presence of IL-6 and most of them with IL-1β (SO CPZ and Nor-1 CPZ). Accumulation of CPZ was nearly doubled in both cell lysates and supernatants of cytokine-treated cultures (Fig. 3, B and C).

Time-Dependent Effects of CPZ and Cytokines on Phospholipidosis Induction. Intracytoplasmic vesicles, corresponding to lamellar bodies, the hallmark of phospholipidosis, were detected in both hepatocyte-like and biliary-like cells after 3 days exposure to 20 μM CPZ, and their number increased during the following days. Cotreatment with cytokines did not seem to affect their accumulation (Fig. 4). This observation was confirmed by measurement of transcript levels of some genes related to phospholipidosis after one and five treatments. Indeed, adipose differentiation-related protein (ADFP) and perilipin-4 (PLIN4), two genes involved in the formation of lamellar vesicles, and Acyl-CoA desaturase (SCD1) and lipin-1 (LPIN1), both involved in lipid metabolism, were all up-regulated, especially after five daily treatments (Table 1). None of the cytokines prevented up-regulation of these genes by CPZ.

By contrast, THRSP, a lipogenic gene encoding the thyroid hormone responsive spot 14 protein, was down-regulated and its induction by CPZ completely abolished with both cytokines (Table 1).

Effects of CPZ and Cytokines on ROS Generation and Oxidative Stress Markers. We have previously reported that oxidative stress plays a major role as both primary causal and aggravating factor in intrahepatic cholestasis induced by 50 μM CPZ in HepaRG cells (Antherieu et al., 2013). To assess whether cotreatment of CPZ with inflammatory cytokines modulated ROS generation in HepaRG cells, H_2-DCFDA fluorescence intensity was measured after one and five

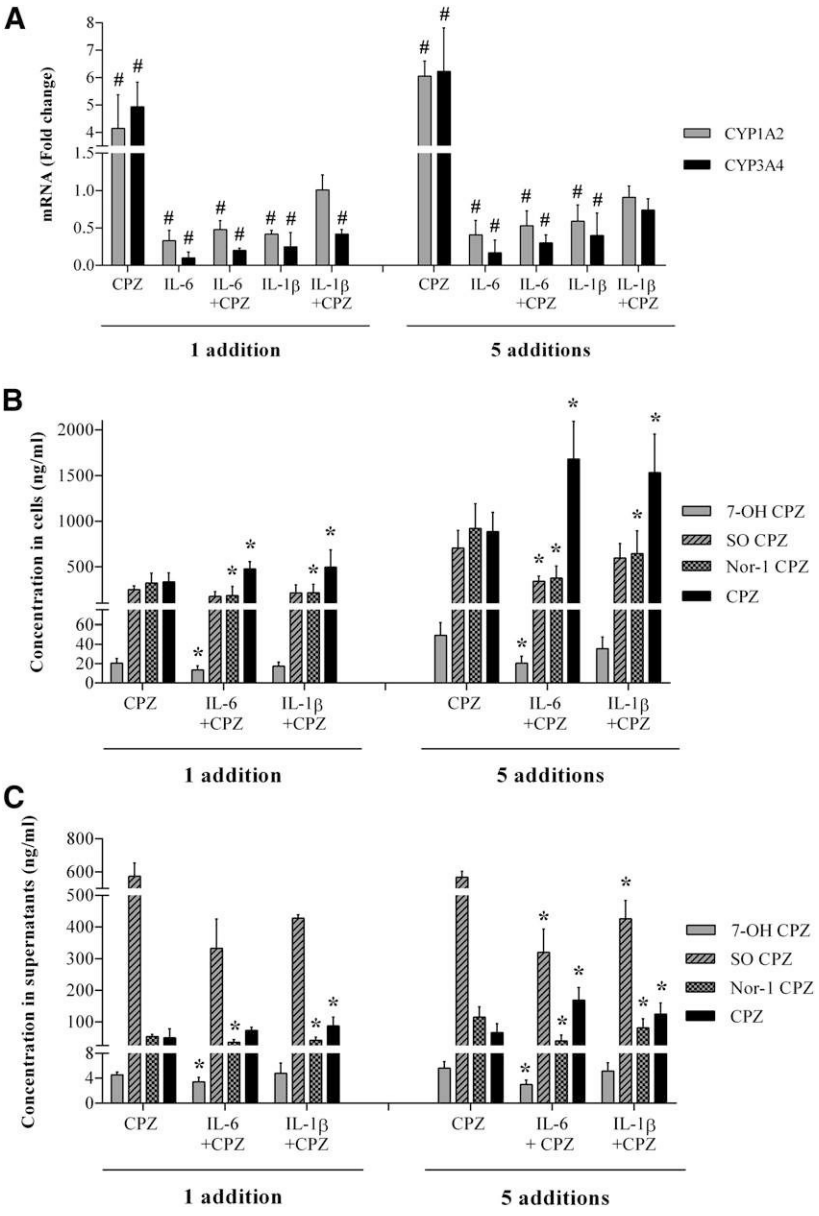

Fig. 3. Effects of proinflammatory cytokines and/or CPZ on CYP3A4 and CYP1A2 mRNA levels and CPZ metabolism in HepaRG cells. Cells were exposed to IL-6 (1 ng/ml) or IL-1β (0.01 ng/ml) for 24 hours before daily cotreatment with 20 μM CPZ for 1 or 5 days (one and five additions, respectively). (A) mRNA levels of CYP3A4 and CYP1A2 were estimated by RT-qPCR. Data represent the mean ± S.D. of three independent experiments. $^{\#}P < 0.05$ compared with untreated cells. (B and C) At each time point, cell lysates and incubation media were collected. Concentrations of CPZ and three metabolites (*N*-desmethyl CPZ (Nor-1 CPZ), sulfoxy-CPZ (SO CPZ), and 7-hydroxyl CPZ (7-OH CPZ)) were determined in cell lysates (B) and incubation media (C) by HPLC-MS/MS and were normalized relative to total protein content. $^{*}P < 0.05$ compared with cells treated with CPZ alone.

additions of CPZ and/or cytokines. A 1.8-fold increase in ROS formation was observed with 20 μM CPZ whereas none of the cytokines induced ROS nor altered their generation by CPZ at either time point (Fig. 5A). Because 50 μM CPZ was previously shown to cause an early oxidative stress in HepaRG cells, ROS generation was also assessed after 24-hour exposure to IL-6 or IL-1β followed by 2- or 4-hour cotreatment with 20 μM or 50 μM CPZ. No aggravation of CPZ-induced oxidative stress was observed with cytokine pretreatment (Fig. 5B).

Next, we measured mRNA levels of three oxidative stress-related genes, heme oxygenase 1 (HO1), manganese superoxide dismutase (MnSOD), and NF-E2-related factor (Nrf2). HO1 and MnSOD were induced by both IL-6 and IL-1β after one and five additions while CPZ caused a statistically significant increase of HO1 mRNA levels after five additions (2.4-fold) (Fig. 5, C and D). When HepaRG cells were coexposed to CPZ and either IL-6 or IL-1β, HO1 mRNA levels were statistically further augmented after five additions (2.7-fold with IL-6 versus 4.8-fold with IL-6 + CPZ and 1.6-fold with IL-1β versus 3.3-fold with IL-1β + CPZ) (Fig. 5C). MnSOD transcripts were also increased after five additions of cytokines and were further elevated by cotreatment with CPZ (1.7-fold with IL-6 versus 2.5-fold with IL-6 + CPZ and 2.2-fold induction with IL-1β versus 3-fold with IL-1β + CPZ) (Fig. 5D). Expression of NF-E2-related factor (Nrf2) was not affected by any of the treatment conditions (data not shown).

Effects of CPZ and Cytokines on Canalicular Efflux Membrane Transporters. Activity of two main apical efflux transporters, BSEP and MRP2, was estimated by using their prototypical substrates TA and CDF, respectively. To determine BSEP activity, no cytokine pretreatment was performed to avoid any inhibitory effect on NTCP activity, the main influx transporter of TA. CPZ at 20 μM and 50 μM induced a time-dependent intracellular accumulation of TA after 2 and 4 hours. Cytokines associated or not with CPZ were ineffective on TA efflux (Fig. 6A). To estimate MRP2 activity, HepaRG cells were exposed to IL-6 or IL-1β for 24 hours followed by 2- and 4-hour treatment with 20 μM or 50 μM CPZ, and canalicular excretion of CDF, characterized by accumulation of green fluorescence in bile canaliculi, was analyzed. CPZ inhibited canalicular excretion of CDF only at 50 μM while coexposure of cells to

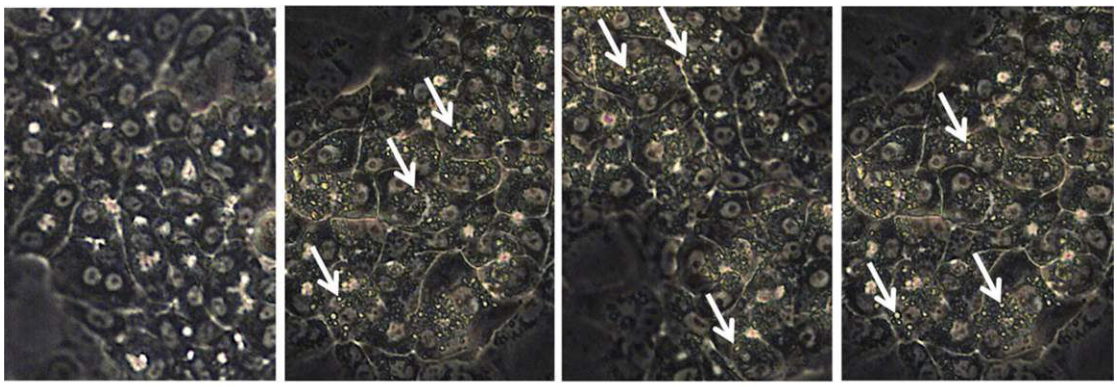

Fig. 4. Phase-contrast micrographs of HepaRG cells. Cells were either directly exposed to 20 μM CPZ or pretreated with IL-6 (1 ng/ml) or IL-1β (0.01 ng/ml) for 24 hours before adding daily 20 μM CPZ simultaneously with cytokines. After three CPZ additions, many intracytoplasmic vesicles are visible (arrow) in cells treated with CPZ alone or simultaneously with IL-6 or IL-1β. Control: untreated cells (magnification, 20×).

20 μM or 50 μM CPZ and cytokines did not result in additional effects on CDF excretion (Fig. 6B), even if cytokine concentrations were increased by 10-fold (data not shown).

Effects of CPZ and Cytokines on F-Actin Distribution. Phalloidin fluoprobe labeling was used to assess whether 20 μM CPZ and/or cytokines, affected the integrity of the pericanalicular F-actin microfilament network. Whatever the treatment, F-actin distribution was not disrupted even after 5 days (Fig. 7, A–C). Consequently, additional experiments were performed with 20 μM or 50 μM CPZ treatment of 2 or 4 hours. As expected from previous studies (Antherieu et al., 2013), at 50 μM, CPZ strongly altered distribution of cytoskeletal pericanalicular F-actin and bile canaliculi shape after 2 (data not shown) and 4 hours (Fig. 7D). These alterations were not aggravated by cytokine pretreatment (Fig. 7, E and F).

Effects of CPZ and Cytokines on NTCP Activity. To investigate whether CPZ and cytokines also affected NTCP-mediated uptake activity, HepaRG cells were exposed to CPZ and/or cytokines for 1 and 5 days and then incubated with [^{3}H]TA for 30 minutes. NTCP-dependent activity was assessed by measuring intracellular accumulation of radiolabeled TA; it was found to significantly drop by 51% or 61% and 36% or 42% in the presence of IL-6 and IL-1β after 1 or 5 days, respectively. CPZ was ineffective regardless of treatment duration. Combination of cytokines and CPZ led to a greater inhibition of NTCP activity, which was statistically significant after five additions (83% with IL-6 + CPZ and 78% with IL-1β + CPZ) (Fig. 8).

Effects of CPZ and Cytokines on Expression of Cholestasis-Related Genes. To further investigate interactions between proinflammatory cytokines and CPZ, the expression of the main genes involved in bile acids transport and synthesis was assessed by RT-qPCR (Table 2). Several transporters were modulated by cytokines alone; the major changes were represented by down-regulation of influx transporters, especially NTCP. The mRNA levels of the uptake transporter NTCP dropped by 80% and 60% in cells treated with IL-6 and IL-1β after either 1 or 5 days whereas 20 μM CPZ did not cause any significant change. However, combination of CPZ with either cytokine resulted in a statistically significant additional decrease of NTCP transcripts after five additions (75% with IL-6 versus 91% with IL-6 + CPZ and 58% with IL-1β versus 87% with IL-1β + CPZ). In addition, IL-6 down-regulated expression of other influx transporters, organic anion-transporting polypeptide (OATP)-B, and organic cation transporter 1 (OCT-1) after one addition and OATP-C at both treatment time points. IL-1β also down-regulated OCT-1 after the first addition. Increased expression of OATP-C by CPZ was observed after only one addition and was completely antagonized by both cytokines (Table 2).

Cytokines individually did not modulate expression of the canalicular transporter MDR3, which was down-regulated by CPZ. CPZ alone induced mRNA expression of breast cancer resistance protein (BCRP) and multidrug resistance protein (MDR1) after one addition; this increase was antagonized by both cytokines, which caused a 30–40% drop of BCRP at both time points and of MDR1 transcripts after one addition. Although neither CPZ nor IL-1β had a significant effect on BSEP transcripts, their combination caused a statistically significant decrease of BSEP mRNA expression after five additions. CPZ alone or with cytokines did not significantly change the relative mRNA levels of MRP2.

By contrast, CPZ associated or not with cytokines caused increased expression of the basolateral efflux gene MRP4 at both treatment time points. Noticeably, MRP3 expression was affected neither by CPZ nor by the cytokines individually, but their combinations caused a significant decrease after both one and five additions (CPZ + IL-6) and five additions (CPZ + IL-1β).

TABLE 1

Effects of CPZ and/or cytokines on expression of mRNAs encoding genes related to phospholipidosis in HepaRG cells

Cells were exposed to IL-6 (1 ng/ml) or IL-1 (0.01 ng/ml) and/or CPZ (20 μM) for 24 hours or daily for 5 days. mRNAs were analyzed by RT-qPCR. Results are expressed as fold of the value found in control cells arbitrarily set at 1. Data are mean ± S.D. of at least three independent experiments.

	One Addition					Five Daily Additions				
	CPZ	IL-6	IL-6 + CPZ	IL-1β	IL-1β + CPZ	CPZ	IL-6	IL-6 + CPZ	IL-1β	IL-1β + CPZ
ADFP	1.37 ± 0.21	0.87 ± 0.14	0.92 ± 0.33	1.07 ± 0.27	1.37 ± 0.27	2.08 ± 0.24[a]	1.18 ± 0.25	1.98 ± 0.15[a]	0.88 ± 0.09	2.36 ± 0.64[a]
PLIN4	1.13 ± 0.21	0.87 ± 0.27	0.74 ± 0.22	1.27 ± 0.31	1.02 ± 0.14	1.69 ± 0.29[a]	1.18 ± 0.19	2.01 ± 0.68[a]	1.02 ± 0.19	1.66 ± 0.14[a]
SCD1	1.97 ± 0.46[a]	0.75 ± 0.17	1.04 ± 0.56	1.01 ± 0.10	1.79 ± 0.47[a]	2.11 ± 0.26[a]	0.69 ± 0.21	1.21 ± 0.24	0.87 ± 0.11	1.50 ± 0.57
LPIN1	1.37 ± 0.08[a]	0.70 ± 0.12[a]	0.72 ± 0.04	1.01 ± 0.09	1.40 ± 0.29[a]	1.78 ± 0.43[a]	0.86 ± 0.18	1.43 ± 0.26	0.97 ± 0.11	1.41 ± 0.45
THRSP	1.93 ± 0.37[a]	0.18 ± 0.03[a]	0.51 ± 0.02[a]	0.52 ± 0.19	1.02 ± 0.22	2.25 ± 0.48[a]	0.18 ± 0.15[a]	0.32 ± 0.11[a]	0.65 ± 0.32	0.97 ± 0.28

[a] $P < 0.05$ compared with untreated cells.

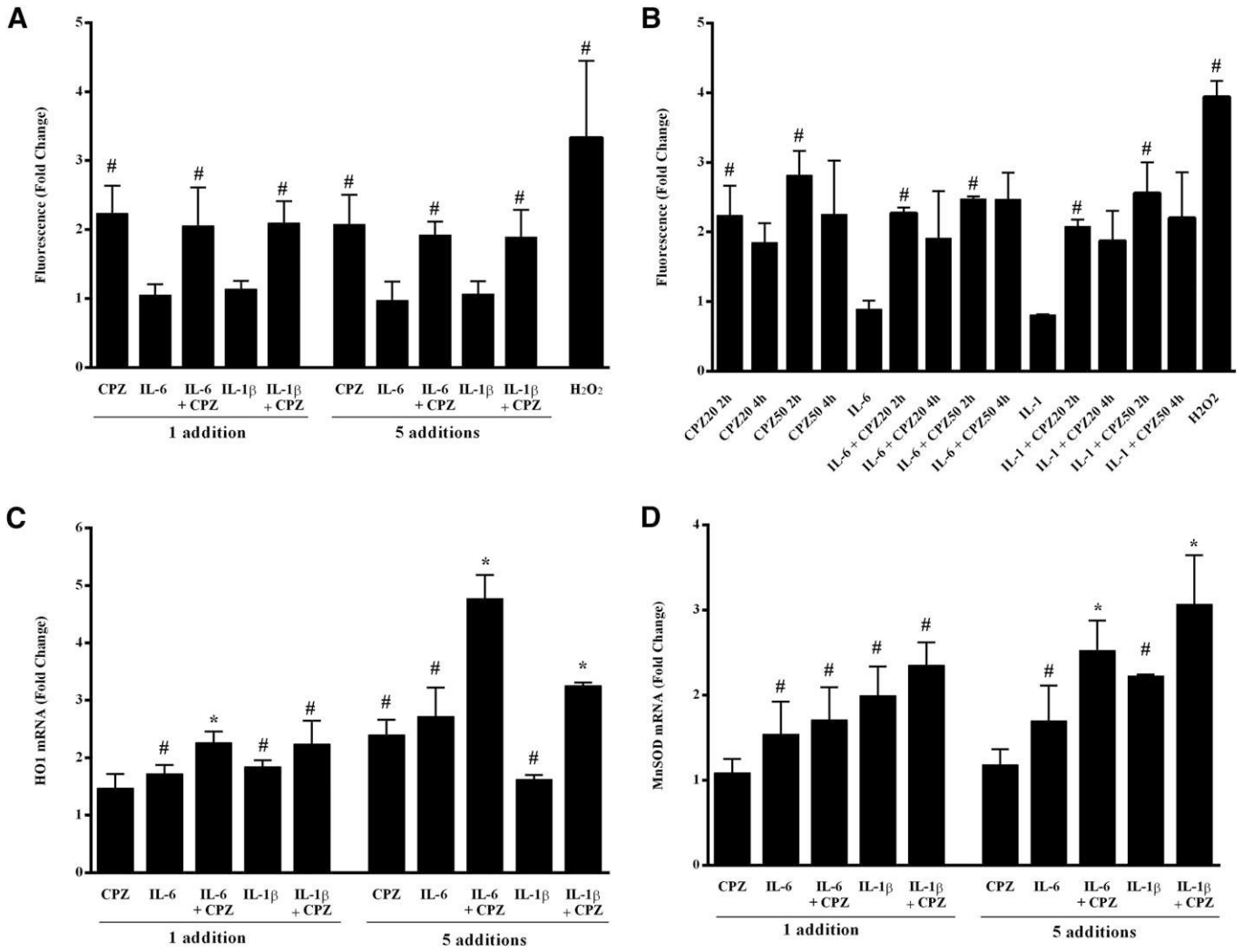

Fig. 5. Effects of CPZ and/or proinflammatory cytokines on ROS generation and expression of oxidative stress-related genes. Cells were pretreated with IL-6 (1 ng/ml) or IL-1β (0.01 ng/ml) for 24 hours before simultaneous addition of (A, C, D) 20 μM CPZ for 1 or 5 days (one and five additions, respectively) or (B) 50 μM CPZ for 2 or 4 hours. (A and B) ROS generation: hydrogen peroxides were quantified by the H2-DCFDA assay. A treatment with 25 mM H_2O_2 for 2 hours was used as a positive control. (C and D) HO1 and MnSOD relative mRNA levels were assessed by RT-qPCR. Data represent the mean ± S.D. of three independent experiments. All results are expressed relative to the levels found in control cells, arbitrarily set at a value of 1. $^{\#}P < 0.05$ compared with untreated cells. $^{*}P < 0.05$ compared with cells treated with cytokine and CPZ individually.

Expression of cytochrome P450 genes involved in bile acid synthesis was also analyzed. CYP8B1 mRNA levels were reduced by CPZ + IL-1β (44% drop compared with control) after five additions, whereas no change occurred in the presence of CPZ, IL-1β or IL-6 alone. By contrast, CYP7A1 was slightly overexpressed by cotreatment with CPZ and IL-1β after five additions while CYP27A1 was not affected by CPZ or cytokines, alone or in combination.

Transcripts of three major cholestasis-related nuclear receptors, the farsenoid X receptor (FXR), the pregnane X receptor (PXR) and the constitutive androstane receptor (CAR) were analyzed. Only IL-1β, alone or in combination with CPZ, slightly induced FXR expression after 5-day treatment. By contrast, PXR expression was down-regulated by both cytokines alone or in presence of CPZ after 1-day treatment and only by IL-6 and IL-6 + CPZ after 5 days. Expression of CAR was decreased by both cytokines and CPZ after 5 days. Combination of cytokines and CPZ did not exacerbate this repression.

Discussion

Inflammation is thought to play a role in the susceptibility to iDILI. Bacterial LPS and proinflammatory cytokines are frequently used to induce an inflammatory state in animals and in vitro cell models. In the present work, we used the metabolically competent HepaRG cell line to evaluate the influence of an inflammatory stress induced by the two proinflammatory cytokines, IL-6 and IL-1β, on the hepatotoxic and cholestatic effects of the idiosyncratic hepatotoxicant CPZ after either one or five daily treatments. Our data showed that in the presence of an inflammatory stress resulting in marked reduction of its metabolism, 20 μM CPZ was more cytotoxic, amplified inhibition of NTCP activity, and enhanced deregulation of expression of several other transporters. However, CPZ-induced TA efflux inhibition and bile canaliculi structures were not affected by cytokines cotreatment; most effects were amplified or observed only after five daily treatments.

HepaRG cells have been previously shown to exhibit an inflammatory response to bacterial LPS (Aninat et al., 2008). We showed in the current study that 1 ng/ml IL-6 and 0.01 ng/ml IL1-β strongly induced CRP mRNA and protein levels. IL-1β also induced mRNA and protein levels of IL-8, a proinflammatory CXC chemokine that plays an important role in liver inflammation, regeneration, and repair (Zimmermann et al., 2011). These data support the conclusion that, at these selected concentrations, both cytokines induced a chronic

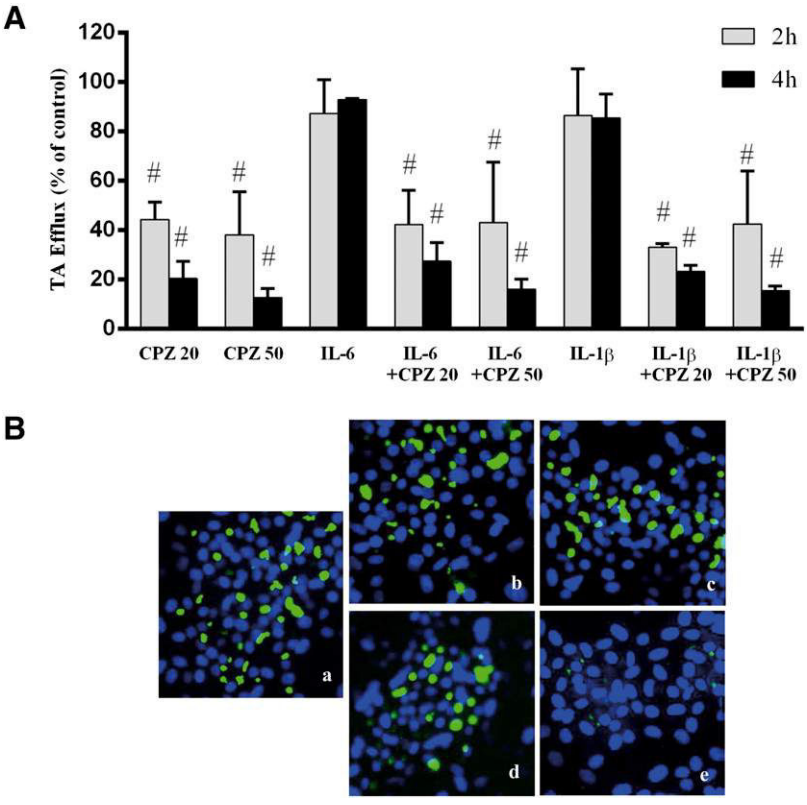

Fig. 6. [^{3}H]TA efflux and MRP2 activity in HepaRG cells treated with CPZ and proinflammatory cytokines. (A) Cells were exposed to [^{3}H]TA for 30 minutes to induce an intracellular accumulation of TA and then treated with IL-6 (1 ng/ml), IL-1β (0.01 ng/ml), and/or CPZ (20 or 50 μM) for 2 or 4 hours. TA efflux was determined at 2 and 4 hours in control and treated cells, by measuring intracellular TA accumulation. Efflux of TA was expressed relative to the levels found in control cells, arbitrarily set at a value of 100%. Data represent the mean ± S.D. of three independent experiments. $^{\#}P < 0.05$ compared with control cultures. (B) Cells were pretreated with IL-6 (1 ng/ml) or IL-1β (0.01 ng/ml) for 24 hours then CPZ (20 or 50 μM) was simultaneously added for 4 hours. MRP2 activity was estimated using CDF, a substrate of MRP2, and was characterized by accumulation of green fluorescence into bile canaliculi. Untreated cells (a); unchanged CDF canalicular excretion with 20 μM CPZ alone (b) or in combination with IL-6 (c) or IL-1β (d), and loss of canalicular CDF excretion with 50 μM CPZ (e).

inflammatory stress in HepaRG cells. Noticeably, at 20 μM CPZ had no effect on CRP expression after 5 days, but when associated with cytokine it enhanced CRP transcript levels as well as protein content although to a lower extent.

Pretreatment of HepaRG cells with either IL-1β or IL-6 followed by concomitant exposure to 20 μM CPZ resulted in a significant although modest enhanced cytotoxic response after five repeated additions compared with treatments with the cytokines or the drug individually. These results agree with previous observations in rodents (Buchweitz et al., 2002) and primary mouse hepatocytes (Gandhi et al., 2010). This increased cytotoxicity did not appear to be directly related to the strong inhibition of CPZ metabolism and the reduction in the formation of nontoxic metabolites in the presence of cytokines. Indeed, HepaRG cells and HepG2 cells that lack CYP3A4- and CYP1A2-mediated metabolic activity have been reported to be nearly equally sensitive to CPZ (Aninat et al., 2006; Gerets et al., 2012). Because expression of two oxidative stress-related genes HO1 and MnSOD were significantly induced in cotreated cells, especially after

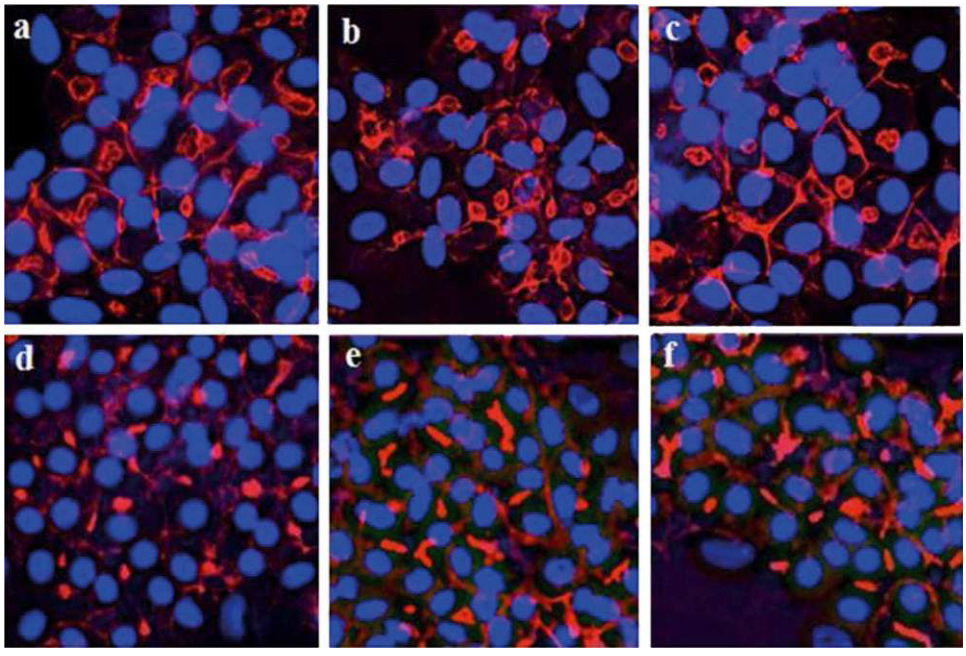

Fig. 7. Pericanalicular cytoskeletal F-actin distribution in CPZ- and cytokine-treated HepaRG cells. Cells were pretreated with IL-6 (1 ng/ml) or IL-1β (0.01 ng/ml) for 24 hours before simultaneous addition of 20 μM or 50 μM CPZ for 5 days (five additions) or 4 hours respectively, and then F-actin was localized by using the Phalloidin FluoProbe. Nuclei were stained in blue using Hoechst dye. Cells treated with 20 μM CPZ alone (A), or simultaneously with IL-6 (B) or IL-1β (C); 50 μM CPZ alone (D), or simultaneously with IL-6 (E) or IL-1β (F). Constricted bile canaliculi are observed only in 50 μM CPZ-treated cells in the absence or presence of cytokines.

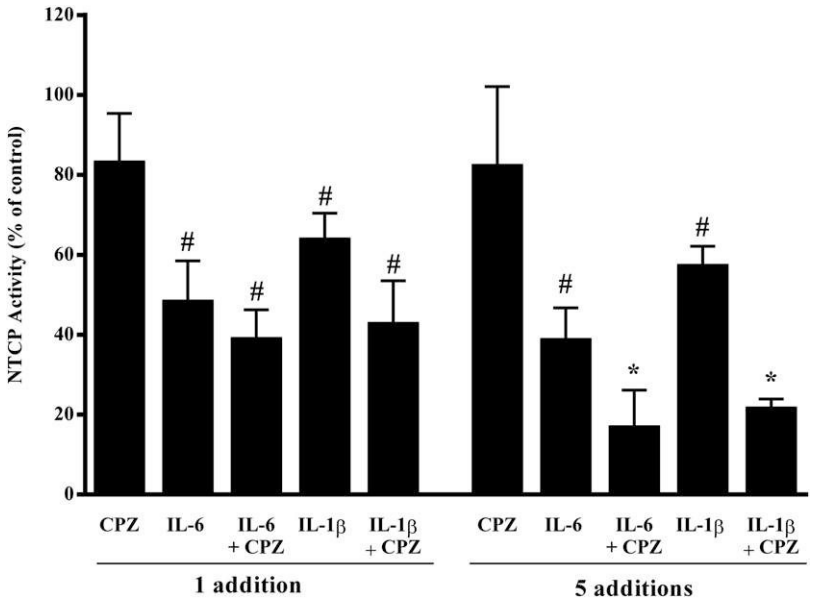

Fig. 8. NTCP activity in CPZ- and/or proinflammatory cytokine-treated HepaRG cells. Cells were pretreated with IL-6 (1 ng/ml) or IL-1β (0.01 ng/ml) for 24 hours, then 20-μM CPZ was added daily simultaneously with cytokines for 1 or 5 days (one and five additions, respectively). Cells were then incubated with [^{3}H]-TA for 30 minutes. NTCP activity was evaluated through measurement of intracellular accumulation of the radiolabeled substrate TA. Data represent the mean ± S.D. of three independent experiments. Uptake of [^{3}H]-TA was expressed relative to the levels found in untreated cells, arbitrarily set at a value of 100%. $^{\#}P < 0.05$ compared with untreated cells, $^{*}P < 0.05$ compared with cells treated with cytokine and CPZ individually.

5 days, increased cytotoxicity could be related to generation of an oxidative stress although an increase in ROS content could not be evidenced by the H2-DCFDA assay.

As expected, in agreement with previous reports (Abdel-Razzak et al., 1993), the two cytokines were also found to down-regulate CYP3A4 and CYP1A2, two major cytochrome P450 enzymes, together with CYP2D6 involved in CPZ oxidative metabolism (Wojcikowski et al., 2010). Accordingly, CPZ metabolism was highly repressed in cytokine-treated cells. Notably, a strong intracellular accumulation of CPZ was observed, especially after five daily treatments. As other cationic amphiphilic drugs, CPZ is able to induce phospholipidosis, which is characterized by lamellar bodies formed by excessive accumulation of phospholipids to which CPZ and its metabolites can possibly bind (Fujimura et al., 2007). Accordingly, an increasing accumulation of intracellular vesicles was observed in CPZ-treated cells starting after 2 days in the presence or absence of

TABLE 2

Effects of CPZ and/or cytokines on the relative mRNA levels of hepatobiliary transporters, bile acid synthesizing enzymes, and nuclear receptors in HepaRG cells

Cells were pretreated with IL-6 (1 ng/ml) or IL-1β (0.01 ng/ml) for 24 hours, then 20 μM CPZ was added with a continuous treatment with cytokines, for 1 or 5 days (one and five additions, respectively). Total RNAs were extracted, and mRNAs were analyzed by RT-qPCR. Results are expressed as fold of the value found in control cells arbitrarily set at 1. Data are mean ± S.D. of at least three independent experiments.

	One Addition					Five Daily Additions				
	CPZ	IL-6	IL-6 + CPZ	IL-1β	IL-1β + CPZ	CPZ	IL-6	IL-6 + CPZ	IL-1β	IL-1β + CPZ
Influx Transporters										
NTCP	0.92 ± 0.24	0.18 ± 0.06[a]	0.12 ± 0.05[a]	0.41 ± 0.08[a]	0.22 ± 0.07[a]	0.98 ± 0.14	0.25 ± 0.07[a]	0.10 ± 0.04[b]	0.42 ± 0.08[a]	0.14 ± 0.04[b]
OATP-B	1.34 ± 0.27	0.55 ± 0.10[a]	0.56 ± 0.05[a]	0.76 ± 0.13	0.73 ± 0.10	1.07 ± 0.27	0.62 ± 0.05	0.52 ± 0.16	0.79 ± 0.23	0.76 ± 0.20
OATP-C	1.57 ± 0.35[a]	0.46 ± 0.09[a]	0.65 ± 0.22	0.66 ± 0.19	0.76 ± 0.09	1.08 ± 0.33	0.54 ± 0.16[a]	0.49 ± 0.16[a]	0.77 ± 0.09	0.68 ± 0.14
OATP-8	1.37 ± 0.46	0.88 ± 0.19	1.05 ± 0.14	0.82 ± 0.12	0.86 ± 0.13	1.05 ± 0.18	0.74 ± 0.05	0.85 ± 0.13	0.86 ± 0.13	0.87 ± 0.35
OCT1	1.37 ± 0.29	0.49 ± 0.16[a]	0.52 ± 0.20[a]	0.61 ± 0.15[a]	0.65 ± 0.13[a]	1.36 ± 0.39	0.57 ± 0.21	0.48 ± 0.31	0.92 ± 0.08	0.83 ± 0.17
Efflux Transporters										
BSEP	1.21 ± 0.36	0.90 ± 0.15	0.96 ± 0.11	0.90 ± 0.17	0.81 ± 0.04	0.76 ± 0.23	1.11 ± 0.37	0.90 ± 0.48	0.77 ± 0.20	0.51 ± 0.27[a]
BCRP	1.43 ± 0.11[a]	0.60 ± 0.07[a]	0.68 ± 0.07[a]	0.67 ± 0.17[a]	0.72 ± 0.13[a]	1.05 ± 0.40	0.61 ± 0.06[a]	0.74 ± 0.13	0.70 ± 0.28	0.89 ± 0.22
MRP2	1.21 ± 0.39	0.72 ± 0.11	0.84 ± 0.08	0.74 ± 0.06	0.72 ± 0.26	1.38 ± 0.29	1.28 ± 0.45	1.28 ± 0.45	1.06 ± 0.22	1.01 ± 0.33
MDR1	1.40 ± 0.10[a]	0.65 ± 0.08[a]	0.85 ± 0.01	0.72 ± 0.11	0.83 ± 0.07	1.16 ± 0.14	0.82 ± 0.12	0.86 ± 0.07	0.93 ± 0.10	0.94 ± 0.10
MDR3	0.59 ± 0.21[a]	0.81 ± 0.18	0.59 ± 0.17[a]	0.98 ± 0.12	0.69 ± 0.15[a]	0.52 ± 0.20[a]	0.69 ± 0.29	0.46 ± 0.16[a]	1.16 ± 0.25	0.40 ± 0.13[a]
MRP3	1.00 ± 0.09	0.89 ± 0.07	0.64 ± 0.06[b]	0.84 ± 0.13	0.75 ± 0.12	0.73 ± 0.04	0.78 ± 0.12	0.52 ± 0.14[b]	0.84 ± 0.10	0.61 ± 0.23[a]
MRP4	1.41 ± 0.22[a]	1.25 ± 0.06	1.42 ± 0.10[a]	1.28 ± 0.11	1.51 ± 0.13[a]	2.02 ± 0.12[a]	1.42 ± 0.15[a]	2.19 ± 0.17[a]	1.37 ± 0.33	1.78 ± 0.25[a]
Bile acid Synthesis										
CYP7A1	1.21 ± 0.18	0.79 ± 0.13	0.95 ± 0.10	0.96 ± 0.12	1.10 ± 0.12	1.62 ± 0.30	0.83 ± 0.11	1.36 ± 0.24	0.98 ± 0.20	1.90 ± 0.24[a]
CYP27A1	1.16 ± 0.18	0.83 ± 0.03	0.92 ± 0.12	1.02 ± 0.14	1.10 ± 0.11	1.21 ± 0.08	0.75 ± 0.11	0.86 ± 0.13	1.01 ± 0.14	1.25 ± 0.34
CYP8B1	1.13 ± 0.24	0.68 ± 0.20	0.64 ± 0.23	0.94 ± 0.12	0.82 ± 0.04	1.07 ± 0.35	0.84 ± 0.17	0.78 ± 0.38	0.78 ± 0.15	0.56 ± 0.23[a]
Nuclear Receptors										
FXR	0.96 ± 0.14	1.07 ± 0.17	1.09 ± 0.10	1.12 ± 0.17	0.98 ± 0.10	1.02 ± 0.07	0.98 ± 0.04	1.03 ± 0.19	1.44 ± 0.24[a]	1.36 ± 0.16[a]
PXR	1.08 ± 0.21	0.52 ± 0.16[a]	0.43 ± 0.09[a]	0.55 ± 0.13[a]	0.69 ± 0.17[a]	1.19 ± 0.26	0.53 ± 0.08[a]	0.50 ± 0.03[a]	0.84 ± 0.25	0.95 ± 0.28
CAR	1.21 ± 0.35	0.59 ± 0.14	0.33 ± 0.18[a]	0.67 ± 0.17	0.53 ± 0.10[a]	0.43 ± 0.15[a]	0.36 ± 0.13[a]	0.39 ± 0.09[a]	0.58 ± 0.05[a]	0.48 ± 0.12[a]

[a] $P < 0.05$ compared with untreated cells.
[b] $P < 0.05$ compared with cells treated with cytokine and CPZ individually.

either cytokine. As previously reported (Antherieu et al., 2013), an accumulation of these vesicles is associated with an induction of genes involved in lipid metabolism and phospholipidosis (ADFP, PLIN4, SCD1, LPIN1, THRSP) in CPZ-treated cells. In agreement with morphologic observations, overexpression of ADFP, PLIN4, SCD1, LPIN1 was not prevented by cotreatment with either cytokine, suggesting that an inflammation stress does not affect induction of phospholipidosis by CPZ. It is noteworthy that expression of the PXR/CAR target gene THRSP was down-regulated by cytokines, especially IL-6, as a consequence of their ability to down-regulate these nuclear receptors (Breuker et al., 2010).

At 50 μM, CPZ was found to generate an early oxidative stress, which was associated with an inhibition of TA efflux, and shortly later, of its uptake, and alterations of bile canaliculi structures (Antherieu et al., 2013). Similarly, at 20 μM CPZ also induced an oxidative stress and inhibited TA efflux; however, it did not alter pericanalicular cytoskeletal F-actin distribution or bile canaliculi structures, even in the presence of either cytokine after five daily treatments. Nevertheless, many genes related to cholestasis were differentially deregulated by proinflammatory cytokines individually or combined with CPZ. In agreement with previous studies (Le Vee et al., 2008, 2009), we found that an IL-1β- and IL-6-induced inflammatory stress down-regulated mRNA and activity of NTCP, and altered the expression of several additional influx and efflux transporters in HepaRG cells. Interestingly, NTCP down-regulation was amplified by cotreatment with CPZ, suggesting that inhibition of sodium-dependent bile acids uptake was exacerbated by CPZ in proinflammatory cytokine-stimulated hepatocytes. Cytokines did not induce any change in MRP2 or BSEP transcripts or activity. Discrepant data have been reported in the effects of proinflammatory cytokines on the main canalicular transporters BSEP and MRP2. Thus, transcripts of these two transporters were not affected by LPS in human liver slices (Elferink et al., 2004); by contrast, they were repressed by IL-1β and IL-6 whereas BSEP protein, unlike MRP2, was induced in sandwich-cultured human hepatocytes (Diao et al., 2010). Such discrepancies are likely due to the use of different experimental models and conditions such as cytokine concentrations. It is noteworthy that our results agree with those obtained in liver biopsies of patients with inflammation-induced cholestasis where no change of MRP2 and slight reduction of BSEP mRNA were reported, while a strong down-regulation of NTCP mRNA and protein was observed (Zollner et al., 2001). Noticeably, mRNA expression of BSEP was down-regulated in IL-1 + CPZ–treated cells after 5 days of treatment although no effect was observed with each agent separately. Such data could explain the onset of cholestasis in patients treated chronically with CPZ.

In addition, SLC transporters, OATP-B, OATP-C and OCT-1, and ABC transporters, BCRP and MDR1, were down-regulated mainly by IL-6 after the first addition, which is in agreement with previous studies (Le Vee et al., 2008; Le Vee et al., 2009). By contrast, most deregulated genes by 20 μM CPZ were overexpressed (i.e., OATP-C, BCRP, MDR1, and MRP4), while only MDR3, which mediates biliary phospholipid excretion, was down-regulated by CPZ, whether in the presence or absence of cytokines. Cotreatment with cytokines and CPZ had an antagonist effect on the expression of genes induced by CPZ alone, including BCRP, MDR1, and OATP-C. By contrast, induction of MRP4 expression by CPZ was still increased, and to a higher level, after 5 days, even in the presence of cytokines. Overexpression of this basolateral transporter, together with down-regulation of NTCP, could be interpreted as a compensating mechanism aiming to reduce intrahepatic accumulation of toxic bile acids (Zollner et al., 2006; Wagner et al., 2009).

Changes in the expression of cytochromes P450 which are involved in the formation of bile acids could represent another means to modulate intracellular accumulation of bile acids (Zollner et al., 2006). Accordingly, differential deregulation of CYP7A1, CYP8B1, and CYP27A1 transcripts were observed depending on the treatment and its duration. As expected (Aitken et al., 2006), CAR and PXR were down-regulated by IL-6 and IL-1β in HepaRG cells. Noticeably, CAR was also down-regulated by CPZ after five daily treatments; this finding deserves further investigation.

An immune reaction has been evoked as an important determinant factor in CPZ-induced cholestasis but data, at least in animals, did not confirm an allergic hypersensitivity with CPZ (Mullock et al., 1983). An increased accumulation of neutrophils was observed in the liver of LPS + CPZ–treated rats but without evidence of cholestasis (Buchweitz et al., 2002). However, extrapolation of such data to the human situation is questionable. Coculturing HepaRG cells with immune cells, inflammatory cells, or nonparenchymal liver cells will be of interest in future investigations.

Taken together, our findings suggest that proinflammatory cytokines, which induced inflammatory stress and cholestatic features in HepaRG cells by themselves, in combination with CPZ increased cytotoxicity and aggravated some cholestatic features caused by this idiosyncratic drug. The decrease of NTCP activity, repression of P450 expression, and inhibition of CPZ metabolism could have major consequences if extrapolated to the in vivo situation. First, because NTCP is now recognized as required for the entry of hepatitis B and D viruses into hepatocytes (Yan et al., 2012; Ni et al., 2014), it might be postulated that proinflammatory cytokine-stimulated and cholestatic hepatocytes are less susceptible to viral infection. Second, inhibition of the major P450 enzymes involved in drug metabolism by proinflammatory cytokines led to postulate that CPZ-treated patients in an inflammation state would be more or less sensitive to other hepatotoxic drugs depending on whether these compounds are detoxified or activated by cytochrome P450-mediated metabolism. Finally, in the future, it would be of interest to evaluate in a similar inflammatory state other cholestatic drugs known to act by other mechanisms.

Acknowledgments

The authors thank R. Le Guevel from the ImPACcell platform (Biosit, Rennes) for imaging analyses and Dr. Eva Klimcakova for critical reading of the manuscript.

Authorship Contributions

Participated in research design: Bachour-El Azzi, Sharanek, Abdel-Razzak, Antherieu, Guguen-Guillouzo, Guillouzo.

Conducted experiments: Bachour-El Azzi, Sharanek, Al-Attrache.

Contributed new reagents or analytic tools: Morel, Lepage, Labbe.

Performed data analysis: Bachour-El Azzi, Abdel-Razzak, Savary.

Wrote or contributed to the writing of the manuscript: Bachour-El Azzi, Abdel-Razzak, Guillouzo.

References

Abdel-Razzak Z, Loyer P, Fautrel A, Gautier JC, Corcos L, Turlin B, Beaune P, and Guillouzo A (1993) Cytokines down-regulate expression of major cytochrome P-450 enzymes in adult human hepatocytes in primary culture. *Mol Pharmacol* **44**:707–715.

Aitken AE, Richardson TA, and Morgan ET (2006) Regulation of drug-metabolizing enzymes and transporters in inflammation. *Annu Rev Pharmacol Toxicol* **46**:123–149.

Aninat C, Piton A, Glaise D, Le Charpentier T, Langouët S, Morel F, Guguen-Guillouzo C, and Guillouzo A (2006) Expression of cytochromes P450, conjugating enzymes and nuclear receptors in human hepatoma HepaRG cells. *Drug Metab Dispos* **34**:75–83.

Aninat C, Seguin P, Descheemaeker PN, Morel F, Malledant Y, and Guillouzo A (2008) Catecholamines induce an inflammatory response in human hepatocytes. *Crit Care Med* **36**: 848–854.

Anthérieu S, Bachour-El Azzi P, Dumont J, Abdel-Razzak Z, Guguen-Guillouzo C, Fromenty B, Robin MA, and Guillouzo A (2013) Oxidative stress plays a major role in chlorpromazine-induced cholestasis in human HepaRG cells. *Hepatology* **57**:1518–1529.

Barton CC, Ganey PE, and Roth RA (2000) Lipopolysaccharide augments aflatoxin B(1)-induced liver injury through neutrophil-dependent and -independent mechanisms. *Toxicol Sci* **58**:208–215.

Breuker C, Moreau A, Lakhal L, Tamasi V, Parmentier Y, Meyer U, Maurel P, Lumbroso S, Vilarem MJ, and Pascussi JM (2010) Hepatic expression of thyroid hormone-responsive spot 14 protein is regulated by constitutive androstane receptor (NR1I3). *Endocrinology* **151**: 1653–1661.

Buchweitz JP, Ganey PE, Bursian SJ, and Roth RA (2002) Underlying endotoxemia augments toxic responses to chlorpromazine: is there a relationship to drug idiosyncrasy? *J Pharmacol Exp Ther* **300**:460–467.

Cerec V, Glaise D, Garnier D, Morosan S, Turlin B, Drenou B, Gripon P, Kremsdorf D, Guguen-Guillouzo C, and Corlu A (2007) Transdifferentiation of hepatocyte-like cells from the human hepatoma HepaRG cell line through bipotent progenitor. *Hepatology* **45**:957–967.

Diao L, Li N, Brayman TG, Hotz KJ, and Lai Y (2010) Regulation of MRP2/ABCC2 and BSEP/ABCB11 expression in sandwich cultured human and rat hepatocytes exposed to inflammatory cytokines TNF-alpha, IL-6, and IL-1beta. *J Biol Chem* **285**:31185–31192.

Elferink MG, Olinga P, Draaisma AL, Merema MT, Faber KN, Slooff MJ, Meijer DK, and Groothuis GM (2004) LPS-induced downregulation of MRP2 and BSEP in human liver is due to a posttranscriptional process. *Am J Physiol Gastrointest Liver Physiol* **287**: G1008–G1016.

Fujimura H, Dekura E, Kurabe M, Shimazu N, Koitabashi M, and Toriumi W (2007) Cell-based fluorescence assay for evaluation of new-drugs potential for phospholipidosis in an early stage of drug development. *Exp Toxicol Pathol* **58**:375–382.

Gandhi A, Guo T, and Ghose R (2010) Role of c-Jun N-terminal kinase (JNK) in regulating tumor necrosis factor-alpha (TNF-alpha) mediated increase of acetaminophen (APAP) and chlorpromazine (CPZ) toxicity in murine hepatocytes. *J Toxicol Sci* **35**:163–173.

Gerets HH, Tilmant K, Gerin B, Chanteux H, Depelchin BO, Dhalluin S, and Atienzar FA (2012) Characterization of primary human hepatocytes, HepG2 cells, and HepaRG cells at the mRNA level and CYP activity in response to inducers and their predictivity for the detection of human hepatotoxins. *Cell Biol Toxicol* **28**:69–87.

Greer ML, Barber J, Eakins J, and Kenna JG (2010) Cell based approaches for evaluation of drug-induced liver injury. *Toxicology* **268**:125–131.

Gripon P, Rumin S, Urban S, Le Seyec J, Glaise D, Cannie I, Guyomard C, Lucas J, Trepo C, and Guguen-Guillouzo C (2002) Infection of a human hepatoma cell line by hepatitis B virus. *Proc Natl Acad Sci USA* **99**:15655–15660.

Hollister LE (1957) Allergy to chlorpromazine manifested by jaundice. *Am J Med* **23**:870–879.

Le Vee M, Gripon P, Stieger B, and Fardel O (2008) Down-regulation of organic anion transporter expression in human hepatocytes exposed to the proinflammatory cytokine interleukin 1beta. *Drug Metab Dispos* **36**:217–222.

Le Vee M, Lecureur V, Stieger B, and Fardel O (2009) Regulation of drug transporter expression in human hepatocytes exposed to the proinflammatory cytokines tumor necrosis factor-alpha or interleukin-6. *Drug Metab Dispos* **37**:685–693.

MacAllister SL, Young C, Guzdek A, Zhidkov N, and O'Brien PJ (2013) Molecular cytotoxic mechanisms of chlorpromazine in isolated rat hepatocytes. *Can J Physiol Pharmacol* **91**:56–63.

Marion TL, Perry CH, St Claire RL, 3rd, and Brouwer KL (2012) Endogenous bile acid disposition in rat and human sandwich-cultured hepatocytes. *Toxicol Appl Pharmacol* **261**:1–9.

Meng Q (2010) Three-dimensional culture of hepatocytes for prediction of drug-induced hepatotoxicity. *Expert Opin Drug Metab Toxicol* **6**:733–746.

Mullock BM, Hall DE, Shaw LJ, and Hinton RH (1983) Immune responses to chlorpromazine in rats. Detection and relation to hepatotoxicity. *Biochem Pharmacol* **32**:2733–2738.

Ni Y, Lempp FA, Mehrle S, Nkongolo S, Kaufman C, Falth M, Stindt J, Koniger C, Nassal M, and Kubitz R, et al. (2014) Hepatitis B and D viruses exploit sodium taurocholate co-transporting polypeptide for species-specific entry into hepatocytes. *Gastroenterology* **146**:1070–1083.

Pernelle K, Le Guevel R, Glaise D, Stasio CG, Le Charpentier T, Bouaita B, Corlu A, and Guguen-Guillouzo C (2011) Automated detection of hepatotoxic compounds in human hepatocytes using HepaRG cells and image-based analysis of mitochondrial dysfunction with JC-1 dye. *Toxicol Appl Pharmacol* **254**:256–266.

Regal RE, Billi JE, and Glazer HM (1987) Phenothiazine-induced cholestatic jaundice. *Clin Pharm* **6**:787–794.

Roth RA, Harkema JR, Pestka JP, and Ganey PE (1997) Is exposure to bacterial endotoxin a determinant of susceptibility to intoxication from xenobiotic agents? *Toxicol Appl Pharmacol* **147**:300–311.

Shaw PJ, Hopfensperger MJ, Ganey PE, and Roth RA (2007) Lipopolysaccharide and trovafloxacin coexposure in mice causes idiosyncrasy-like liver injury dependent on tumor necrosis factor-alpha. *Toxicol Sci* **100**:259–266.

Velayudham LS and Farrell GC (2003) Drug-induced cholestasis. *Expert Opin Drug Saf* **2**: 287–304.

Wagner M, Zollner G, and Trauner M (2009) New molecular insights into the mechanisms of cholestasis. *J Hepatol* **51**:565–580.

Waring JF, Liguori MJ, Luyendyk JP, Maddox JF, Ganey PE, Stachlewitz RF, North C, Blomme EA, and Roth RA (2006) Microarray analysis of lipopolysaccharide potentiation of trovafloxacin-induced liver injury in rats suggests a role for proinflammatory chemokines and neutrophils. *J Pharmacol Exp Ther* **316**:1080–1087.

Wójcikowski J, Boksa J, and Daniel WA (2010) Main contribution of the cytochrome P450 isoenzyme 1A2 (CYP1A2) to N-demethylation and 5-sulfoxidation of the phenothiazine neuroleptic chlorpromazine in human liver—a comparison with other phenothiazines. *Biochem Pharmacol* **80**:1252–1259.

Yan H, Zhong G, Xu G, He W, Jing Z, Gao Z, Huang Y, Qi Y, Peng B, and Wang H, et al. (2012) Sodium taurocholate cotransporting polypeptide is a functional receptor for human hepatitis B and D virus. *eLife* **1**:e00049.

Yee SB, Kinser S, Hill DA, Barton CC, Hotchkiss JA, Harkema JR, Ganey PE, and Roth RA (2000) Synergistic hepatotoxicity from coexposure to bacterial endotoxin and the pyrrolizidine alkaloid monocrotaline. *Toxicol Appl Pharmacol* **166**:173–185.

Zamek-Gliszczynski MJ, Xiong H, Patel NJ, Turncliff RZ, Pollack GM, and Brouwer KL (2003) Pharmacokinetics of 5 (and 6)-carboxy-2′,7′-dichlorofluorescein and its diacetate promoiety in the liver. *J Pharmacol Exp Ther* **304**:801–809.

Zimmermann HW, Seidler S, Gassler N, Nattermann J, Luedde T, Trautwein C, and Tacke F (2011) Interleukin-8 is activated in patients with chronic liver diseases and associated with hepatic macrophage accumulation in human liver fibrosis. *PLoS ONE* **6**:e21381.

Zollner G, Fickert P, Zenz R, Fuchsbichler A, Stumptner C, Kenner L, Ferenci P, Stauber RE, Krejs GJ, and Denk H, et al. (2001) Hepatobiliary transporter expression in percutaneous liver biopsies of patients with cholestatic liver diseases. *Hepatology* **33**:633–646.

Zollner G, Marschall HU, Wagner M, and Trauner M (2006) Role of nuclear receptors in the adaptive response to bile acids and cholestasis: pathogenetic and therapeutic considerations. *Mol Pharm* **3**:231–251.

Address correspondence to: André Guillouzo, Inserm UMR 991, Faculté des Sciences Pharmaceutiques et Biologiques, 35043 Rennes Cedex, France. E-mail: andre.guillouzo@univ-rennes1.fr

OXFORD
SOT | Society of Toxicology
www.toxsci.oxfordjournals.org

TOXICOLOGICAL SCIENCES, 141(1), 2014, 244–253

doi: 10.1093/toxsci/kfu122
Advance Access Publication Date: June 27, 2014

Different Dose-Dependent Mechanisms Are Involved in Early Cyclosporine A-Induced Cholestatic Effects in HepaRG Cells

Ahmad Sharanek*,†, Pamela Bachour-El Azzi*,†, Houssein Al-Attrache*,†, Camille C. Savary*,†, Lydie Humbert‡, Dominique Rainteau‡, Christiane Guguen-Guillouzo*,†, and André Guillouzo*,†,[1]

*Inserm UMR991, Foie, Métabolisme et Cancer, Rennes, France, †Université de Rennes 1, Rennes, France and ‡ERL Inserm U1157/UMR7203, Faculté de Medecine Pierre et Marie Curie, Site Saint Antoine, Paris, France

[1]To whom correspondence should be addressed. Fax: +33223235385. E-mail: andre.guillouzo@univ-rennes1.fr.

ABSTRACT

Mechanisms involved in drug-induced cholestasis in humans remain poorly understood. Although cyclosporine A (CsA) and tacrolimus (FK506) share similar immunosuppressive properties, only CsA is known to cause dose-dependent cholestasis. Here, we have investigated the mechanisms implicated in early cholestatic effects of CsA using the differentiated human HepaRG cell line. Inhibition of efflux and uptake of taurocholate was evidenced as early as 15 min and 1 h respectively after addition of 10μM CsA; it peaked at around 2 h and was reversible. These early effects were associated with generation of oxidative stress and deregulation of cPKC pathway. At higher CsA concentrations (≥50μM) alterations of efflux and uptake activities were enhanced and became irreversible, pericanalicular F-actin microfilaments were disorganized and bile canaliculi were constricted. These changes were associated with induction of endoplasmic reticulum stress that preceded generation of oxidative stress. Concentration-dependent changes were observed on total bile acid disposition, which were characterized by an increase and a decrease in culture medium and cells, respectively, after a 24-h treatment with CsA. Accordingly, genes encoding hepatobiliary transporters and bile acid synthesis enzymes were differently deregulated depending on CsA concentration. By contrast, FK506 induced limited effects only at 25–50μM and did not alter bile canaliculi. Our data demonstrate involvement of different concentration-dependent mechanisms in CsA-induced cholestasis and point out a critical role of endoplasmic reticulum stress in the occurrence of the major cholestatic features.

Key words: oxidative stress; endoplasmic reticulum stress; cPKC signaling; hepatocytes; bile acids; transporters; tacrolimus

ABBREVIATIONS

CsA	cyclosporine A
FK506	tacrolimus
cPKC	classical protein kinase c
ADR	adverse drug reaction
DILI	drug-induced liver injury
BSEP	bile salt export pump
E17G	estradiol 17ß-D-glucuronide
MRP2	multidrug resistance-associated protein 2
MDR1	multidrug resistance 1
ER	endoplasmic reticulum
MTT	methylthiazoletetrazolium
DMSO	dimethyl sulfoxide
RNA	ribonucleic acid
RT-qPCR	real-time quantitative polymerase chain reaction
NTCP	Na^+-dependent taurocholate cotransporting polypeptide
TA	taurocholic acid
ROS	reactive oxygen species
H2-DCFDA	2',7'-dichlorodihydrofluorescein
NAC	N-acetyl-cysteine

Nrf2	NF-E2-related factor 2
HO1	heme oxygenase 1
MnSOD	manganese superoxide dismutase
ATF4	activating transcription factor 4
ATF6	activating transcription factor 6
GRP78	glucose regulated protein,78KD
CHOP	C/Ebp-homologous protein
PBA	4-phenyl butyric acid
CDF	5(6)-carboxy-2′,7′-dichlorofluorescein diacetate
BA	bile acids
H7	1-(5-isoquinolinylsulfonyl)-2-methyl-piperazine
CAR	constitutive androstane receptor
PXR	pregnane X receptor
FXR	farnesoid X receptor
BCRP	breast cancer resistance protein
MDR3	multidrug resistance 3
MRP3	multidrug resistance-associated protein 3
MRP4	multidrug resistance-associated protein 4
CYP7A1	cytochrome P450 7A1
CYP8B1	cytochrome P450 8B1
CYP27A1	cytochrome P450 27A1
CYP3A4	cytochrome P450 3A4

Adverse drug reactions (ADRs) are usually classified as either dose-dependent and reproducible (intrinsic) or unpredictable (idiosyncratic) occurring only in certain susceptible patients and being not overtly dose-dependent (Park *et al.*, 2005). Many different classes of marketed drugs and herbals have been reported to cause drug-induced liver injury (DILI) in humans, accounting for more than 50% of cases of acute liver failure in the United States (Lee, 2003). DILI encompasses a large spectrum of lesions, including apoptosis/necrosis, phospholipidosis, steatosis, and cholestasis.

Intra-hepatic cholestasis represents a frequent manifestation of DILI in humans (Lee, 2003). In many cases, it results from alterations of the hepatobiliary transporter system, in particular the bile salt export pump (BSEP), which is the most physiologically important canalicular bile transporter (Stieger *et al.*, 2007). Other disturbances, such as altered cell polarity, disruption of cell-to-cell junctions, and cytoskeleton disorganization, can also participate in cholestasis. The mechanisms by which drugs induce cholestasis are diverse and remain poorly understood (Anthérieu *et al.*, 2013). Intracellular signaling has emerged as a fundamental mechanism to explain the development of different models of cholestasis (Crocenzi *et al.*, 2004); thus, the Ca^{2+}-dependent PKC isoforms (cPKC) have been demonstrated to be involved in estradiol 17ß-D-glucuronide (E17G)- and tert-butylhydroperoxide-induced cholestasis (Barosso *et al.*, 2012; Pérez *et al.*, 2006). A role for oxidative stress as a primary causal agent and/or an aggravating factor has been evidenced in extrahepatic and intrahepatic cholestasis (Anthérieu *et al.*, 2013; Pérez *et al.*, 2006; Roma and Pozzi, 2008).

Cyclosporine A (CsA) is well recognized as a dose-dependent cholestatic inducing agent. It has been shown to alter bile secretion in *in vitro* (Princen *et al.*, 1991) and short-term *in vivo* studies (Mizuta *et al.*, 1999). CsA also acts as a competitive inhibitor of BSEP, MRP2, and MDR1 and caused disorganization of pericanalicular F-actin cytoskeleton (Román and Coleman, 1994). CsA disturbs the endoplasmic reticulum (ER)-Golgi transport by altering vesicle-mediated transport (Sarró *et al.*, 2012). By contrast, tacrolimus (FK506), another immunosuppressant that possesses similar immunosuppressive properties as CsA (Tocci *et al.*, 1989), has usually no effect even at supra-therapeutic concentrations in humans. The reasons why the liver is so differently sensitive to the two immunosuppressant agents remain unclear.

In the present study, we have investigated early effects of CsA and FK506 in the metabolically competent human HepaRG cells. In addition to phases I and II metabolizing enzymes (Aninat *et al.*, 2006), these cells exhibit functional sinusoidal and canalicular transporters and are now largely used for studying both acute and chronic effects of xenobiotics in human liver (Anthérieu *et al.*, 2012; Guguen-Guillouzo and Guillouzo, 2010). Our data show that unlike FK506, CsA induced early cholestatic effects, involving different dose-dependent mechanisms in HepaRG cells.

MATERIALS AND METHODS

Chemicals. Cyclosporine A (CsA), methylthiazoletetrazolium (MTT), N-acetyl-cysteine (NAC), 4-phenyl butyric acid (PBA), 1-(5-isoquinolinylsulfonyl)-2-methyl-piperazine (H7), and 5(6)-carboxy-2′,7′-dichlorofluorescein diacetate (CDF) were purchased from Sigma (St. Quentin Fallavier, France). Tacrolimus (FK506) was provided by Tocris Bioscience (Bristol, UK), 2',7'-dichlorodihydrofluorescein (H2- DCFDA) was obtained from Invitrogen Molecular Probe (Saint Aubin, France). [^{3}H]-Taurocholic acid ([^{3}H]-TA) was from Perkin Elmer (Boston, MA). The specific antibodies against phospho-p38 MAP kinase and p38 MAP kinase were purchased from Cell Signaling Technology (Beverly, MA). Go¨6976 and SB203580 were from Calbiochem (San Diego, CA). BAPTA/AM was obtained from Alexis Co. (Nottingham, UK). Phalloidin fluoprobe SR101 (200 U/ml) was purchased from Interchim (Montluçon France). Hoechst dye was from Promega (Madison, Wisconsin). Other chemicals were of reagent grade.

Cell cultures. HepaRG cells were seeded at a density of 2.6×10^4 cells/cm^2 in Williams E medium supplemented with 10% fetal bovine serum, 100 IU/ml penicillin, 100 mg/ml streptomycin, 5 mg/ml insulin, 2mM glutamine, and 50mM hydrocortisone hemisuccinate. After 2 weeks, HepaRG cells were shifted to the same medium supplemented with 2% dimethyl sulfoxide (DMSO) for further 2 weeks in order to obtain confluent differentiated cultures with maximum functional activities. At this time, these cultures contained hepatocyte-like and progenitors/primitive biliary-like cells (Cerec *et al.*, 2007).

Cell viability. Cytotoxicity was evaluated by the MTT colorimetric assay. Briefly, cells were seeded in 24-well plates and treated with various concentrations of CsA and FK506. After medium removal, 500 µl serum-free media containing MTT (0.5 mg/ml) were added to each well and incubated for 2 h at 37°C. The water-insoluble formazan was dissolved in 500 µl DMSO and absorbance was measured at 550 nm (Aninat *et al.*, 2006).

Measurement of reactive oxygen species. Reactive oxygen species (ROS) generation was determined by the H2-DCFDA assay. Cells were incubated for 2 h at 37°C with 2µM H2-DCFDA; then they were washed with cold phosphate buffered saline (PBS) and scraped in phosphate buffer (10mM, pH 7.4)/methanol (vol/vol) supplemented with Triton X-100 (0.1%). Fluorescence intensity of cell extracts was determined by spectrofluorimetry using excitation/emission wavelengths of 498/520 nm (Anthérieu *et al.*, 2013).

Real-time quantitative polymerase chain reaction analysis. Total RNA was extracted from 10^6 HepaRG cells with the SV total RNA isolation system (Promega). RNAs were reverse transcribed into cDNA

and real-time quantitative polymerase chain reaction (RT-qPCR) was performed using a SYBR Green mix. Primer sequences are listed in Supporting table 1.

Efflux of taurocholate acid. Cells were first exposed to 43.3nM [^{3}H]-TA for 30 min to induce intracellular accumulation of [^{3}H]-TA, then washed with PBS and incubated with or without CsA or FK506 at different time points (from 0 to 6 h) in a standard buffer with Ca^{2+} and Mg^{2+}. After the incubation time, cells were washed with PBS and incubated for 5 min with Ca^{2+}- and Mg^{2+}-free buffer in order to disrupt canalicular tight junctions. Then, they were scraped in 0.1 N NaOH and the remaining radiolabeled substrate was measured through scintillation counting to determinate TA efflux. To discriminate between basolateral and canalicular efflux, cells were incubated in parallel in either standard or Ca^{2+}- and Mg^{2+}-free buffer for 30 min after TA uptake before measuring the remaining radiolabeled TA. Canalicular efflux was calculated using this equation: Canalicular efflux = Radioactivity in efflux medium Ca^{2+}- and Mg^{2+}-free buffer - Radioactivity in efflux medium standard buffer (Marion *et al.*, 2012).

CDF excretion. After 2 h of exposure to CsA or FK506, cells were incubated with 3μM CDFDA, which is hydrolyzed by intracellular esterases to CDF, a substrate of multidrug resistance-associated protein 2 (MRP2) for 20 min at 37°C and then washed with PBS. Imaging was done using inverted microscope Zeiss Axiovert 200M and AxioCam MRm.

Na+-dependent taurocholic cotransporting polypeptide activity. Activity of the Na+-dependent taurocholic cotransporting polypeptide (NTCP) transporter was estimated through determination of sodium-dependent intracellular accumulation of the radiolabeled [^{3}H]-TA substrate. After treatment with either drug, cells were incubated with 43.3nM of radio-labeled TA for 30 min. Cells were then washed twice with PBS and lysed with 0.1 N NaOH. Accumulation of radiolabeled substrate was determined through scintillation counting. Taurocholate accumulation values in the presence of sodium minus accumulation values in the absence of sodium represented NTCP activity (Anthérieu *et al.*, 2013).

F-actin distribution. After cell exposure to CsA or FK506, cells were washed twice with warm PBS, fixed with 4% paraformaldehyde for 20 min at 4°C and permeabilized with 0.3% Triton in PBS for 30 min. F-actin and nuclei were labeled simultaneously using a phalloidin fluoprobe diluted at 1/100 and 5 ng/ml Hoechst dye, respectively, for 20 min. Imaging was done using the Cellomics ArrayScan VTI HCS Reader (Thermo Scientific) (Anthérieu *et al.*, 2013).

Time-lapse imaging. Phase-contrast images were taken each minute after exposure of HepaRG cells to both immunosuppressant agents, using time-lapse phase-contrast videomicroscopy (Zeiss Axiovert 200M and AxioCam MRm). The inverted microscope was equipped with a thermostatic chamber (temperature and CO_2) to maintain the cells under physiological conditions. Images were captured with a 20× objective and the mosaic tool of the microscope which enabled the automated acquisition of multi-image mosaics at the defined positions.

Measurement of endogenous bile acid content. After treatment of HepaRG cells with CsA for 4 and 24 h both cells and media were collected, lyophilized and stored at −80°C. Ten μl of water was added to 100 mg dried samples, homogenized using a Polytron homogenizer for 30 s, and clarified by centrifugation at 20,000 × g for 20 min. The supernatant was collected and extracted using a solid phase extraction cartridge (SPE). High pressure liquid chromatography coupled with tandem mass spectrometry (HPLC–MS/MS) was used to measure bile acid (BA) content in the samples. The chromatographic separation of BAs was carried out on a Zorbax eclipse XDB-C18 (Agilent Technology, Garches, France) fitted on an Agilent 1100 HPLC system (Massy, France). The column was thermostated at 35°C. The mobile phases consisted of (A) (ammonium acetate 15 mmol/l, pH 5.3) and (B) (methanol) at 65:35 (vol/vol). BAs were eluted by increasing B in A from 65 to 95 (vol/vol) for 30 min. Separation was achieved at a flow rate varying between 0.3 and 0.5 ml/min for 30 min. Mass spectra were obtained using an API 2000 Q-Trap (AB-Sciex, Concord, Ontario, Canada) equipped with a TurboIon electrospray interface set in the negative mode (needle voltage—4500 V) with nitrogen as the nebulizer set at 40 (arbitrary pressure unit given by the equipment provider). Curtain and heater pressures were set at 20 and 40, respectively (arbitrary units), and the ion source temperature was set at 400°C. Declustering and entrance potentials were set at −60 V and −10 V, respectively. The MS/MS detection was operated at unit/unit resolution. The acquisition dwell time for each transition monitored was 70 ms. Data were acquired by the Analyst software (version 1.4.2, AB-Sciex) in the Multiple Reaction Monitoring mode (Humbert *et al.*, 2012).

Western blot analysis of MAPK phosphorylation. Activation of p38-MAPK was assessed by evaluating its phosphorylation status in cell lysates by Western blotting. Briefly, HepaRG cells were incubated with medium alone or with CsA, FK506, and CsA plus inhibitors for 15 or 120 min, washed with cold phosphate-buffered saline, and finally resuspended in cell lysis buffer and a protease inhibitor cocktail. Aliquots containing an equivalent total protein content, as determined by the Bradford procedure with bovine serum albumin as the standard, were subjected to sodium dodecyl sulfate/12% polyacrylamide gel electrophoresis, electrotransferred to Immobilon-P membranes, and probed overnight with a rabbit antiphosphorylated p38 (Cell Signaling Technology, Beverly, MA). After using a mouse anti-rabbit IgG secondary antibody (1:5000, 1 h; ThermoFisher Scientific, Waltham, MA), a chemiluminescence reagent, and Hyperfilm ECL, phosphorylated and total MAPK bands were quantified by densitometry with Fusion-Capt software (Vilber Lourmat, Fusion FX7, France) (Boaglio *et al.*, 2012).

Statistical analysis. The student's *t*-test was applied to compare data between treated and corresponding control cultures. Data were considered as significantly different when $^*p < 0.05$, $^{**}p < 0.01$, and $^{***}p < 0.001$.

RESULTS

Cytotoxicity Effects of CsA and FK506

Cytotoxicity of both CsA and FK506 was evaluated in HepaRG cells using the MTT test. CsA did not cause any significant cytotoxicity after 24 h at concentrations up to 100μM. By contrast, FK506 was highly toxic at 100μM causing 94% cell death ($p < 0.001$; Fig. 1A). Based on these data, non-toxic concentrations from 0 to 50μM of both drugs were selected for further studies.

Induction of ROS and ER Stress by CsA

Because deregulation of the cellular redox status is a potent mechanism in DILI, generation of oxidative and ER stress was analyzed after exposure to the two immunosuppressant agents. Significant production of ROS was observed in HepaRG cells

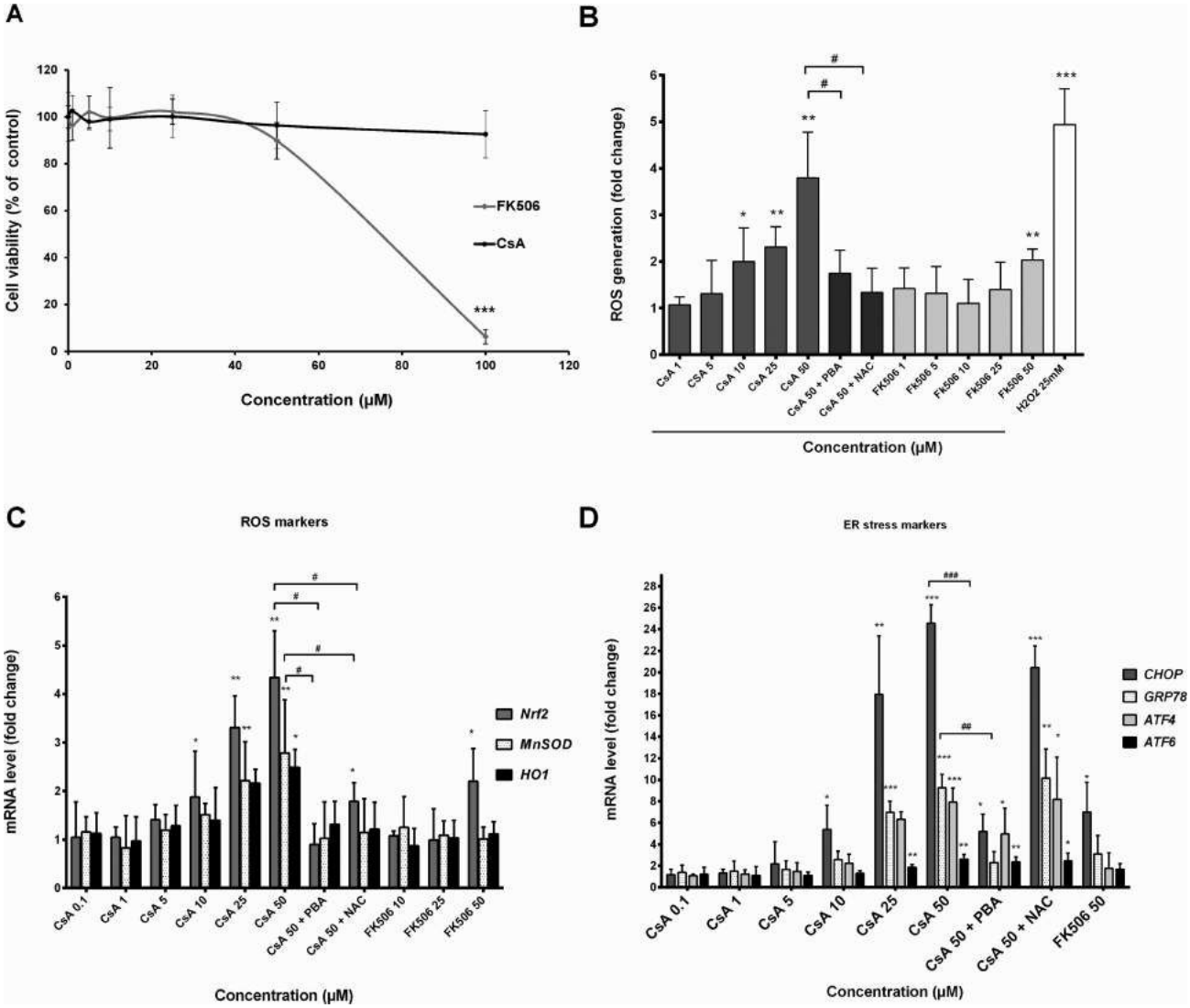

FIG. 1. Cytotoxicity and intracellular generation of ROS in CsA- and FK506-treated HepaRG cells. (A) Cells were incubated for different time points (0–24 h) with different concentrations of either CsA or FK506 (0–100μM). Cytotoxicity was measured by the MTT colorimetric assay. (B) Cells were treated with different concentrations of either CsA or FK506, or co-treated with 50μM CsA + 15mM NAC or 5mM PBA for 2 h. H_2O_2 at 25mM was used as a positive control. ROS generation was detected by the DCFDA specific substrate. (C and D) Cells were treated with CsA or FK506 or co-treated with 50μM CsA + (15mM NAC or 5mM PBA) for 6 h, then mRNA levels of ROS markers (*HO-1*, *MnSOD, and Nrf2*) and ER stress markers (*CHOP*, *GRP78*, *ATF4*, and *ATF6*) were estimated by RT-qPCR. Data represent the means ± SD of three independent experiments. All results are expressed relative to the levels found in untreated cells, arbitrarily set at 1 or 100% $^{*}p < 0.05$, $^{**}p < 0.01$, $^{***}p < 0.001$ compared with non-treated cells, $^{\#}p < 0.05$, $^{\#\#}p < 0.01$, $^{\#\#\#}p < 0.001$ compared with 50μM CsA.

starting at 10μM (twofold; $p < 0.05$) after 2 h (Fig. 1B). ROS formation occurred within the first 15 min after CsA addition (data not shown), peaked after 2 h (3.8-fold; $p < 0.01$) and was totally prevented by co-incubation with 15mM of the antioxidant NAC. Only a slight ROS production was obtained with 50μM FK506 after 2 h (Fig. 1B). Moreover, transcript levels of three ROS markers (*Nrf2*, *HO-1*, *and MnSOD*) were also measured and found to be significantly up-regulated as early as 6 h after CsA exposure (Fig. 1C). Overexpression of *Nrf2* was lower with FK506 and occurring only at 50μM.

Moreover, four ER stress-related genes (*ATF4*, *ATF6*, *GRP78*, and *CHOP*) were strongly up-regulated after 6 h treatment with 50μM CsA, whereas only a slight increase of *CHOP* transcripts was observed with 50μM FK506 (Fig. 1D). Co-treatment with PBA, an ER stress inhibitor, prevented induction of ER stress-related genes. Interestingly, co-treatment with PBA also reduced ROS generation and induction of ROS-related genes, suggesting a link between ER stress and ROS triggered by CsA. However, NAC reduced induction of ROS markers without affecting ER stress-related genes.

In addition, PBA failed to lower ROS induced by H_2O_2 and the cholestatic drug chlorpromazine where no ER stress was observed (Supplementary data 1), indicating that PBA was able to decrease ROS by reducing ER stress, as is the case with high CsA concentrations.

Effects of CsA and FK506 on Influx and Efflux Transporters

CDF and TA substrates were used to evaluate MRP2 and BSEP activity, respectively. To estimate BSEP activity, HepaRG cells were incubated with [^{3}H]-TA for 30 min and then treated for 2 h with either drug in standard buffer containing Ca^{2+}/Mg^{2+}.

A 5-min incubation with Ca^{2+}/Mg^{2+}-free buffer was used to disrupt Ca^{2+}/Mg^{2+}-dependent canalicular tight junctions and eventually evacuate bile canaliculi content; thus only intracellular accumulation of [^{3}H]-TA, which correlated to the effect on canalicular efflux, was measured. In treated cells, CsA inhibited [^{3}H]-TA canalicular efflux in a dose-dependent manner with a 33% ($p < 0.05$) significant inhibition starting at 5μM and reaching 90% ($p < 0.001$) at 50μM (Fig. 2A). On the other hand, 50μM FK506 decreased [^{3}H]-TA canalicular efflux to 58.2% ($p < 0.05$) without any inhibition observed at 10μM (Fig. 2A). To better characterize CsA effects on TA efflux, a time-dependent study was carried out between 0 and 6 h after treatment with 10 and 50μM. Efflux inhibition was evidenced as early as 15 min after CsA addition, whereas its maximum occurred after 2 h. At low CsA concentrations, inhibition was partially restored after 6 h. At higher CsA concentrations inhibition of TA efflux was totally maintained after 6 h (Fig. 2B).

To estimate MRP2 activity, HepaRG cells were exposed to both drugs for 2 h followed by incubation with CDF, an MRP2-specific substrate. CsA inhibited canalicular excretion of CDF at both 10 and 50μM concentrations; no effect was observed with FK506 even at 50μM (Fig. 2C).

The effect of the two immunosuppressant agents on Na^+-dependent BA uptake was estimated through measurement of intracellular accumulation of [^{3}H]-TA after a 30-min incubation. CsA-induced inhibition of NTCP activity started after 30 min with 50μM and 1 h with low doses (≤10μM); it reached a maximum after 2 h and started to be restored after 4 h exposure at low doses, whereas inhibition of [^{3}H]-TA uptake was maintained with 50μM (Fig. 2D). Only a slight inhibition of [^{3}H]-TA uptake was observed with 50μM FK506 after 24 h treatment. Both drugs had no significant effect on Na^+-independent [^{3}H]-TA uptake measured using Na^+-free buffer (data not shown). Further experiments were carried out on progenitors/primitive biliary-like cells after selective enzymatic detachment of hepatocyte-like cells (Cerec *et al.*, 2007) to determine the contribution of these cells in CsA effects. No [^{3}H]-TA uptake was detected (Supplementary data 2), indicating it was exclusively performed by hepatocyte-like cells.

Role of cPKC, ER, and Oxidative Stress in CsA-Induced Effects

It has been demonstrated that cPKC partly accounts for acute cholestasis caused by E17G (Barosso *et al.*, 2012) and that CsA can activate cPKC. We analyzed whether cPKC was involved in CsA-induced cholestatic effects. [^{3}H]-TA efflux was reduced to 21.9% of the control by treatment of HepaRG cells with 10μM CsA for 2 h and was partially restored by co-treatment with the PKC inhibitor H7, rising to 59.4% ($p < 0.05$) of the control (Fig. 3A). Because Ca^{2+} is required for activation of the classical PKCs, we investigated whether Ca^{2+}-mediated activation of these PKC isoenzymes was involved in CsA-induced deleterious effects. Both the intracellular Ca^{2+}-chelator BAPTA/AM and the specific inhibitor of Ca^{2+}-dependent PKCs, Go¨6976, prevented the decrease induced by CsA in [^{3}H]-TA efflux representing 47.4 and 48.7% ($p < 0.01$), respectively, compared with a 21.9% ($p < 0.001$) inhibition with 10μM CsA. When administered alone, none of these inhibitors had any effect on [^{3}H]-TA efflux (data not shown). At high CsA concentration (50μM), none of these inhibitors significantly modulated inhibition of [^{3}H]-TA efflux (Fig. 3A). However, this inhibition was totally restored by co-treatment with either PBA or NAC. Interestingly at low CsA concentrations, co-treatment with PBA has no counteraction effect, favoring a role of ER stress only at high CsA concentrations. By contrast, NAC was totally effective at low and high CsA concentrations indicating a role of ROS in CsA-induced cholestasis whatever the drug concentration (Fig. 3B).

The downstream effector of cPKC, p38, was previously shown to be involved in E17G-cPKC-dependent induced cholestasis (Boaglio *et al.*, 2012). Its specific inhibitor, SB203580, significantly reduced inhibition of [^{3}H]-TA by 10μM CsA to 47.5% ($p < 0.01$) instead of 21.9% ($p < 0.001$) (Fig. 3B). Accordingly, Western blotting analysis of phospho (p)-p38 showed that CsA increased the amount of p-p38 in a time-dependent manner with increment becoming apparent as soon as 5 min after CsA administration. Co-treatment with either the cPKC inhibitor Go¨6976 or NAC selectively prevented p-p38 increase, indicating that p38 activation was dependent on cPKC induction and ROS generation by CsA (Figs. 3C and 3D).

Effects of CsA on BA Disposition

In order to determine whether CsA altered disposition of endogenous BAs, total BA content was quantitated in both media and cells after 4 and 24 h exposure to 10 and 50μM CsA using HPLC–MS/MS. Although no changes were evidenced after 4 h, a concentration-dependent increase of BA content in the medium and decrease in cells was observed after 24 h of CsA treatment. The sum of total BAs content (media + cells) appeared to be nearly unchanged between 4 and 24 h (Fig. 4).

Induction of Cytoskeletal F-Actin Disruption and Bile Canaliculi Constriction by High CsA Concentrations

F-actin cytoskeleton is one of the primary targets of oxidative stress. To determine whether CsA and FK506 disrupted cytoskeletal F-actin distribution, HepaRG cells were exposed to both drugs at different time points and then cytoskeletal F-actin was visualized by phalloidin fluoprobe labeling. Untreated cells showed typical pericanalicular distribution of F-actin and large bile canaliculi with an open lumen (Fig. 5A). At 10μM CsA did not affect actin distribution in the pericanalicular area (Fig. 5B) whereas at 50μM it disrupted its distribution, lowered its labeling intensity, and caused constriction of bile canaliculi after 2-h exposure (Fig. 5D). These effects were confirmed by phase-contrast time-lapse imaging. Retraction and disappearance of bile canaliculi were observed in 50μM CsA-treated cells (Fig. 5G'). FK506 did not alter cytoskeletal F-actin distribution nor bile canaliculi structures (Figs. 5C and 5F').

Effects of CsA and FK506 on Expression of Genes Related to Cholestasis

Many genes involved in BA transport, synthesis, and metabolism are deregulated in cholestasis. A set of target genes was analyzed by RT-qPCR after 24-h treatment with various concentrations of CsA and FK506. These genes included nuclear receptors (*CAR*, *PXR*, *FXR*), efflux transporters (*BCRP*, *BSEP*, *MDR1*, *MDR3*, *MRP2*, *MRP3*, and *MRP4*), uptake transporter *NTCP*, BA metabolism enzymes (*CYP7A1*, *CYP8B1*, and *CYP27A1*), and *CYP3A4*, a BA detoxifying enzyme. At low concentrations up to 10μM CsA slightly induced *PXR*, *FXR*, *CAR*, *NTCP*, *MRP2*, *MRP3*, *MRP4*, *BCRP*, and *CYP3A4* expression whereas at doses >10μM it strongly inhibited most of the tested genes, i.e., *FXR*, *PXR*, *CAR*, *CYP3A4*, *BSEP*, *NTCP*, *MDR1*, *MDR3*, and *CYP8B1*. By contrast, at low concentrations, FK506 was found to induce only *MRP4* and *CYP3A4* whereas at high concentrations it inhibited expression of *PXR*, *CAR*, *BSEP*, *MDR3*, *NTCP*, *CYP27A1*, *CYP8B1*, and *CYP3A4* and induced basolateral transporters (*MRP3*, *MRP4*) as well as *MRP2* and *BCRP* to a similar extent as CsA at the same concentrations (Table 1). No transporter transcripts were detected in progenitors/primitive biliary-like cells when measurements

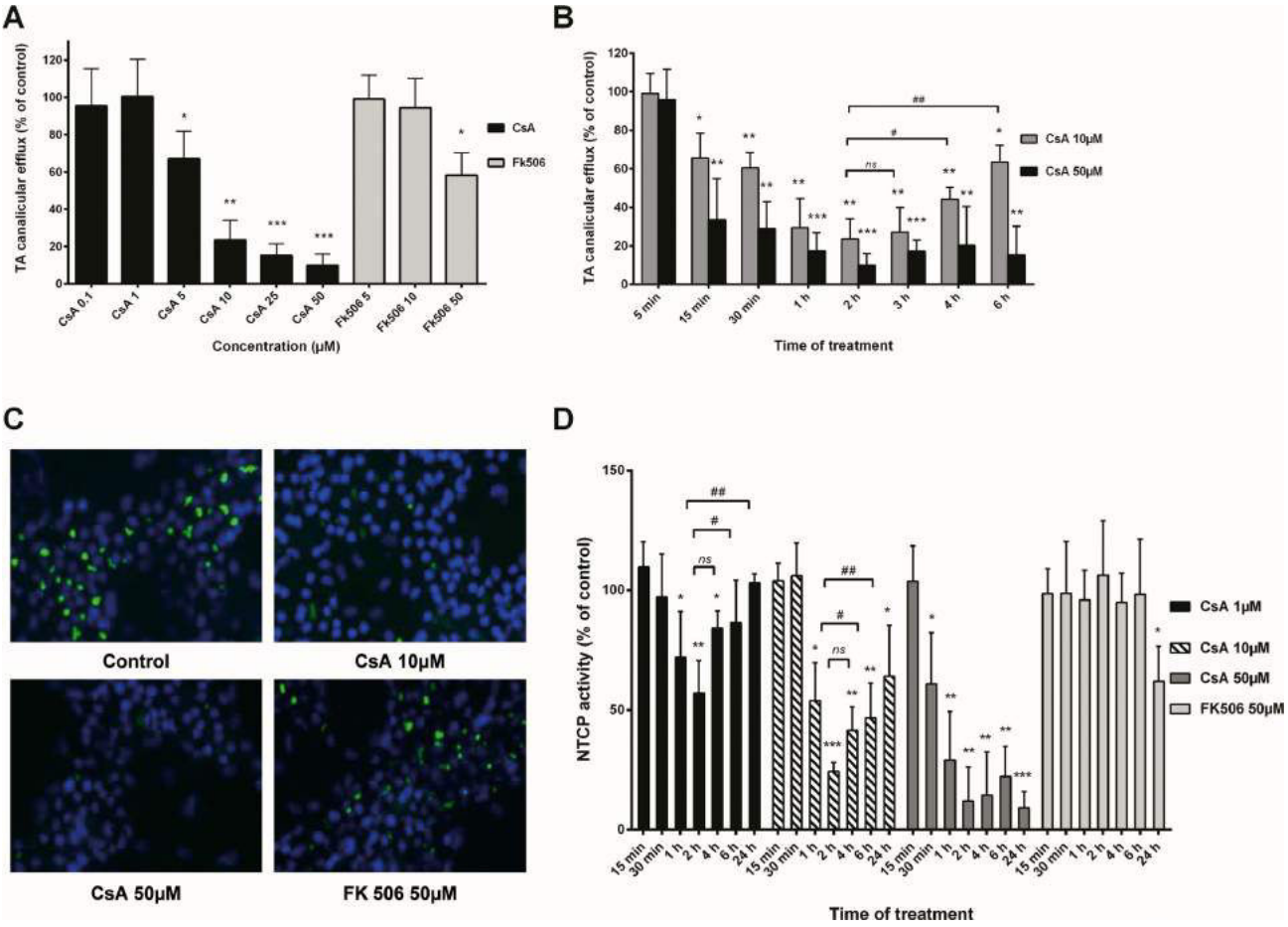

FIG. 2. Effects of CsA and FK506 on activity of efflux transporters. (A and B) Cells were exposed to [^{3}H]-TA in standard buffer for 30 min to induce intracellular accumulation of TA and then incubated with different concentrations of either CsA or FK506 for 2 h (A) or different time points (0–6 h) (B). Bile canaliculi were disrupted by additional 5-min incubation with Ca^{2+}- and Mg^{2+}-free buffer. TA efflux was determined by measuring intracellular TA accumulation. Efflux of TA was expressed relative to the level found in untreated cells, arbitrarily set at a value of 100%. (C) Cells were treated with either CsA or FK506 for 2 h. MRP2 activity was estimated using CDF, a specific substrate; nuclei were stained in blue using Hoechst dye. (D) HepaRG cells were treated with either CsA or FK506 at different concentrations for different time points (0–24 h) and then incubated with [^{3}H]-TA for 30 min. NTCP activity was evaluated by measurement of intracellular accumulation of [^{3}H]–TA. Data represent the means ± SD of three independent experiments. $^*p < 0.05$, $^{**}p < 0.01$, $^{***}p < 0.001$ compared with untreated cells, $^{\#}p < 0.05$, $^{\#\#}p < 0.01$ compared with CsA (same concentration) after 2 h.

were performed after selective detachment of hepatocyte-like cells (not shown).

DISCUSSION

Presently, there is no means for accurate prediction of cholestasis risks in humans; many cholestatic drugs do not induce hepatotoxicity in rats. Using the metabolically competent human HepaRG cells, we demonstrated that CsA induced dose- and time-dependent characteristic features of cholestasis typified by an early inhibition of efflux and uptake of BA and that FK506, another immunosuppressant agent which shares similar immunosuppressive properties and mechanism of action with CsA, was much less cholestatic, inducing some liver disturbances only at high concentrations.

CsA strongly inhibited canalicular efflux of [^{3}H]-TA in a dose-dependent manner in HepaRG hepatocytes, becoming significant at concentrations as low as 5µM after 15 min treatment. This inhibition was reversible at low doses and irreversible at concentrations of 25µM or higher. Recent works using sandwich-cultured primary hepatocytes have well demonstrated that CsA is a powerful inhibitor of BSEP (Pedersen *et al.*, 2013).

CsA also induced a concentration-dependent decrease in NTCP activity measured by Na^+-dependent TA uptake starting after 1 h at low doses (10µM) and even after 30 min at high doses, thereby indicating that inhibition of uptake occurred shortly after efflux inhibition. CsA has been previously shown to decrease uptake of BA in the liver (Murray *et al.*, 2011) but our observation represented the first direct demonstration that inhibition of TA uptake was reversible with low CsA concentrations.

Early effects on efflux and influx of BA by CsA were associated with generation of an oxidative stress and involved deregulation of the cPKC/p38 pathway. A role for oxidative stress as a primary causal agent in induction of drug-induced cholestasis has been reported (Anthérieu *et al.*, 2013; Pérez *et al.*, 2006). Several arguments support the involvement of an oxidative stress in CsA-induced cholestasis, especially ROS generation, and prevention of CsA-induced BSEP activity inhibition and decrease in phospho-p38 protein in the presence of NAC. Compelling evidence that ROS-mediated cholestasis can involve activation of intracellular signaling cascades via cPKC has been provided

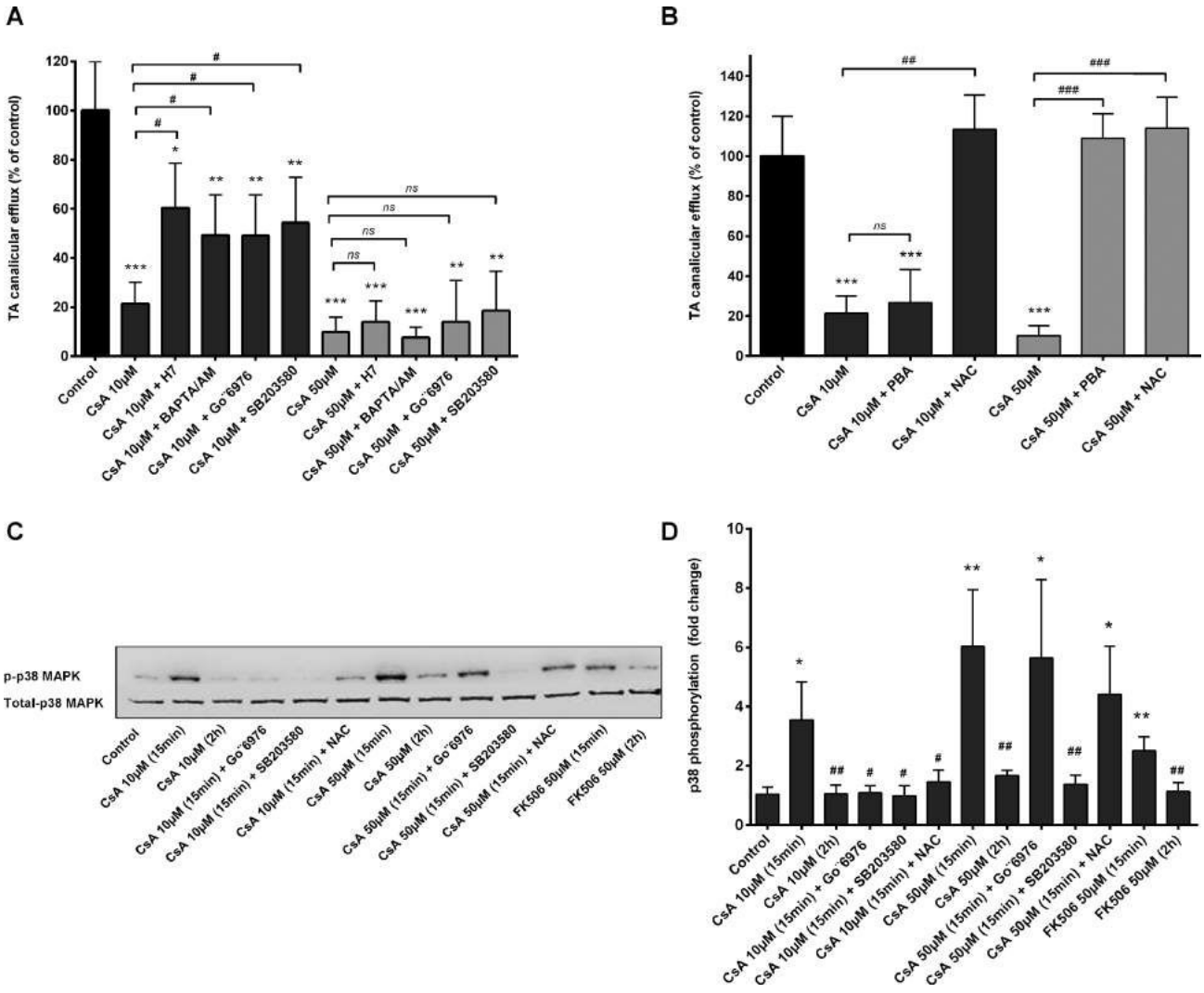

FIG. 3. Effect of Ca^{2+} chelation, cPKC, p38, ER stress, and ROS inhibition on CsA-induced effects. (A) HepaRG cells were exposed to [^{3}H]-TA for 30 min to induce intracellular accumulation of TA and then incubated for 2 h with CsA alone or with either (A) the PKC inhibitor H7 (25µM), cPKC inhibitor Go˜6976 (10µM), p38 inhibitor SB203580 (10µM), or intracellular Ca^{2+} chelator BAPTA/AM (20µM) or (B): 5mM PBA or 15mM NAC. (C) Representative Western blotting of p-p38 and total p38 forms obtained from whole cellular lysates of HepaRG cells incubated with CsA ± inhibitors. (D) Phosphorylation of p38-MAPK quantified as p-p38 to total-p38 ratio. The results are expressed as percentages of untreated cells and are shown as mean ± SD of three independent experiments. $^{*}p < 0.05$, $^{**}p < 0.01$, $^{***}p < 0.001$ compared with untreated cells, $^{\#}p < 0.05$, $^{\#\#}p < 0.01$, $^{\#\#\#}p < 0.001$ compared with CsA alone.

TABLE 1. Effects of CsA and FK506 on Expression of mRNAs Encoding Genes Related to Hepatobiliary Transporters, Nuclear Receptors, and Phase I Metabolizing Enzymes in HepaRG Cells After 24 h Exposure

	CSA 1µM	CSA 5µM	CsA 10µM	CsA 25µM	CsA 50µM	FK506 1µM	FK506 5µM	FK506 10µM	FK506 25µM	FK506 50µM
Nuclear receptors										
FXR	1.27±0.05*	1.18±0.09	1.05±0.18	0.88±0.05	0.69±0.09*	1.045±0.25	1.44±0.33	1.64±0.68	1.173±0.20	0.95±0.21
PXR	1.39±0.1	1.94±0.13***	1.14±0.14	0.44±0.07***	0.32±0.02***	1.07±0.08	1.15±0.09	0.83±0.02	0.94±0.04	0.58±0.12***
CAR	1.4±0.1*	1.25±0.55	1.01±0.30	0.4±0.03***	0.04±0.02***	1.03±0.44	1.44±0.40	0.81±0.21	0.76±0.18**	0.30±0.18**
BA transporters										
BSEP	1.09±0.09	1.01±0.15	0.79±0.17	0.61±0.11**	0.54±0.15**	1.17±0.03	0.76±0.22	0.77±0.14	0.72±0.11*	0.63±0.11**
BCRP	1.19±0.08	2.14±0.11***	2.51±0.50	2.76±0.09***	3.36±0.85*	0.92±0.15	0.95±0.13	0.95±0.13	1.02±0.12	1.74±0.42
MDR3	1.26±0.34	1.161±0.11	0.93±0.17	0.34±0.09***	0.23±0.05***	0.95±0.13	0.89±0.21	0.6±0.15	0.39±0.09**	0.47±0.18*
MRP2	0.9±0.24	1.06±0.21	1.3±0.18*	1.80±0.14***	1.8±0.15***	0.90±0.12	1.35±0.3	1.34±0.28	1.58±0.15*	2.04±0.41*
MRP3	1.02±0.11	1.4±0.18**	1.50±0.14***	1.57±0.07***	1.79±0.08***	1.18±0.13	1.371±0.41	1.41±0.43	1.6±0.23*	1.64±0.32*
MRP4	0.99±0.18	1.44±0.21	1.55±0.18*	2.8±0.09***	2.68±0.12***	1.34±0.17	1.68±0.03***	1.8±0.05***	1.8±0.09*	2.60±0.51*
NTCP	2.16±0.55*	2.64±0.54**	1.51±0.33	0.10±0.02***	0.05±0.01***	1.11±0.24	1.3±0.23	0.82±0.09	0.45±0.15***	0.23±0.08***
BA metabolizing enzymes										
CYP27A1	0.88±0.04	1.04±0.07	0.86±0.03	0.53±0.05***	0.41±0.08***	1.00±0.16	1.16±0.35	0.86±0.11	1.3±0.46	0.47±0.06***
CYP8B1	0.84±0.27	1.15±0.14	0.73±0.24	0.26±0.08	0.05±0.01	1.5±0.25	1.62±0.71	1.03±0.35	0.77±0.08**	0.32±0.1***
CYP7A1	1.08±0.03	1.11±0.07	1.11±0.05	0.92±0.01**	0.42±0.13**	1.06±0.29	1.42±0.37	0.87±0.08	1.4±0.11	0.9±0.12*
CYP3A4	1.62±0.05***	1.51±0.28*	1.33±0.57	0.23±0.05***	0.12±0.01***	1.3±0.23	1.8±0.21**	1.54±0.18*	0.93±0.13	0.34±0.08***

Note: Data represent the means ± SD of three independent experiments. All results are expressed relative to the levels found in untreated cells, arbitrarily set at a value of 1. $^{*}p < 0.05$, $^{**}p < 0.01$, $^{***}p < 0.001$ compared with non-treated cells.

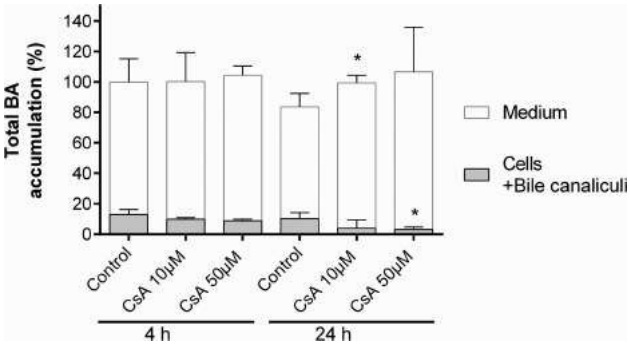

FIG. 4. Effects of CsA treatment on endogenous BAs content. Total BAs were measured in the medium and cells (intracellular + bile canaliculi content) from cultures treated with 10 or 50μM CsA for 4 and 24 h and in corresponding untreated HepaRG cells using LC-MS/MS as described in the Materials and Methods section. Data were normalized relative to the amount of proteins in each condition, and expressed in percentage relative to the total BA content (medium + cells) of untreated cells at 4 h which was arbitrary set at 100. Values represent the sum of means ± SD of duplicate measurements in three independent experiments, $^{*}p < 0.05$ compared with untreated cells. Total BA content (medium + cells) appeared to be nearly unchanged between 4 and 24 h.

(Pérez *et al.*, 2006), and its association with endocytic internalization of BA transporters, such as Mrp2 and Bsep, has been reported (Barosso *et al.*, 2012; Pérez *et al.*, 2006). The downstream effector p38-MAPK has been shown to be differently activated by cPKC isoforms in E17G-induced cholestasis (Boaglio *et al.*, 2012). If cPKC was recently reported to play a major role in CsA toxicity (Sarró *et al.*, 2012), to our knowledge our work is the first to link the sequential activation of cPKC-p38 as a mechanism of CsA-induced cholestasis.

Amplified and irreversible effects of high CsA concentrations on efflux and influx of TA were associated with ROS production and overexpression of ROS markers, *Nrf2, HO-1*, and *MnSOD*, disruption of cytoskeletal pericanalicular F-actin, and constriction of bile canaliculi structures. These effects appeared to be related primarily to induction of an ER stress. Indeed, four major ER stress markers, *ATF4*, *ATF6*, *GRP78*, and *CHOP*, were overexpressed and addition of NAC did not prevent their induction, contrary to PBA, a specific inhibitor of ER stress (Basseri *et al.*, 2009; Carlisle *et al.*, 2014). Obviously, these data support a hierarchical relationship between ER stress and ROS in CsA-induced effects. Contrary to CsA both H_2O_2 (this study) and chlorpromazine (Anthérieu *et al.*, 2013) were able to induce ROS without induction of an ER stress. Moreover, PBA failed to reduce ROS generation by these two molecules (Supplementary data 1), indicating that it cannot reduce ROS unless an ER stress is induced. These data suggest that ER stress might precede an oxidative stress in HepaRG cells treated with high CsA concentrations. This is supported by a recent study on renal proximal tubule cells, which identified ER stress as an early effector of CsA cytotoxicity, leading to ROS generation (Sarró *et al.*, 2012).

The mechanism of CsA-induced ER stress remains poorly studied. A recent proteomic analysis of CsA-treated HepG2 cells has evidenced deregulation of some proteins related to an ER stress without concluding whether it was a primary event in CsA action (Van Summeren *et al.*, 2011). ER stress has been linked to perturbation of cyclophilins A and B distribution in a CsA-treated human kidney cell line (Lamoureux *et al.*, 2011). The relevance between CsA-induced ER and oxidative stress could be related to deregulation of ER-mitochondria Ca^{2+}-signaling bridge. Indeed, ER stress often stimulates a cascade of cellular and molecular events that lead to changes in ER Ca^{2+} concentration resulting in activation of Ca^{2+}-dependent PKC and ROS production (Orrenius *et al.*, 2003). Several arguments support a role of Ca^{2+} in ER and oxidative stress-mediated effects during CsA-induced acute cholestasis, mostly the effectiveness of the Ca^{2+}-chelator BAPTA/AM in reducing CsA cholestatic effects at low concentrations. However, the lack of a Ca^{2+} chelation effect at high CsA concentrations could be explained by the severity and irreversibility of the effects induced by CsA at high doses.

Our data clearly showed that CsA induced ER stress and ROS in HepaRG cells at concentrations which were not cytotoxic whereas FK506 was highly toxic in the absence of ER stress and ROS formation. Accordingly, CsA, but not FK506, was recently reported to induce ER stress in endothelial cells (Bouvier *et al.*, 2009). There is currently no report showing induction of ER stress by FK506 *in vivo*.

Although no obvious change was found in the medium/cells ratio of BAs after a 4-h treatment with 10 or 50μM CsA a concentration-dependent increase in this ratio was observed after 24 h, indicating a cellular (intracellular + bile canaliculi) decrease and not, as it could be expected, an accumulation of BAs. This decrease was not related to a diminution in the content in total BA between 4 and 24 h. These data with CsA as well as those previously obtained with chlorpromazine (Anthérieu *et al.*, 2013) clearly showed that cholestatic features rapidly appeared in HepaRG cells after drug addition; inhibition of BSEP occurred within 1 h and only shortly preceded that of NTCP whereas bile canaliculi constriction was observed within 4 h, giving support to a rapid adaptation of the cells to cholestatic drug effects. The rapid inhibition of the uptake transporter NTCP, bile canaliculi constriction associated with BA discharge, and increased basolateral excretion likely explained the increased medium/cells ratio of BAs after 24 h of CsA treatment. Accordingly, troglitazone, another potent inhibitor of BSEP, failed to induce intracellular accumulation of BAs in human and rat sandwich-cultured hepatocytes, and this result was attributed to compensatory mechanisms which help to maintain BA homeostasis and low intracellular BA concentrations (Marion *et al.*, 2012).

Various cholestasis-related genes were also found to be differently deregulated depending on CsA concentration after a 24-h treatment. At low concentrations the major changes involved overexpression of *PXR, CAR, CYP3A4, NTCP,* and *BCRP*. Although CsA is recognized as a direct inhibitor of *CYP3A4* activity (Amundsen *et al.*, 2012), previous studies have reported induction of *CYP3A4* transcripts by CsA through activation of *PXR* in human primary hepatocytes (Wallace *et al.*, 2010). Because *BCRP* is known to be regulated by *Nrf2*, its overexpression could be related to early *Nrf2* activation by CsA (Singh *et al.*, 2010).

Conversely, overexpression of the basolateral *MRP3* and *MRP4* transporters, and down-regulation of *NTCP*, *CYP27A1*, and *CYP7A1*, the initiator of the BAs biosynthetic pathway, with high CsA concentrations could represent an adaptive defense response aimed at reducing BA accumulation and concomitant toxicity (Zollner and Trauner, 2008).

Compared with CsA, FK506 induced some cholestatic effects only at 50μM, a concentration close to its toxic concentration. Only, *NTCP*, *MRP3*, and *MRP4* were deregulated with 25μM FK506 and to a much lower extent than with 25μM CsA. Moreover, cytoskeletal pericanalicular F-actin and bile canaliculi were not altered. Because FK506 is used at 10- to 100-fold lower doses than CsA, the absence of hepatotoxic and cholestatic effects at concentrations up to 25μM fully agreed with its safety reported in clinics (Mihatsch *et al.*, 1998). Noteworthy, if similar *in vitro* observations as with CsA were recently reported with chlorpromazine

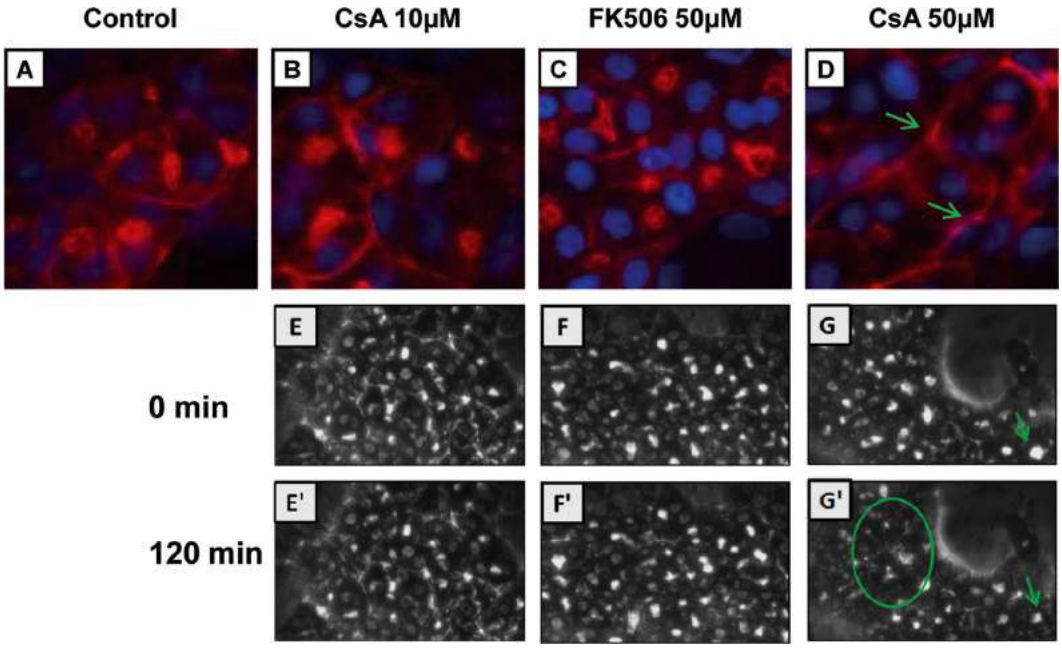

FIG. 5. Alteration of F-actin cytoskeletal distribution and bile canaliculi structures by CsA treatment. (A–D) Untreated cells (A), cells treated with 10μM CsA (B), 50μM FK506 (C), or 50μM CsA (D), after 2 h treatment; F-actin was localized using phalloidin fluroprobe. Nuclei were stained in blue (Hoechst). F-actin shows a predominant pericanalicular distribution around open bile canaliculi in untreated cells and a much less intense staining around constricted bile canaliculi in 50μM CsA-treated cells (arrow). Time-lapse imaging of HepaRG cells treated with 10μM CsA (E'), 50μM FK506 (F'), and 50μM CsA (G') after 120 min compared with corresponding cultures at 0 min (E, F, and G), respectively.

the effects of this idiosyncratic cholestatic drug were, however, observed only at 50μM, a concentration close to its maximum nontoxic concentration (Anthérieu *et al.*, 2013). Accordingly, considering the Cmax values measured in patients, i.e., 1.15, 0.1–0.2, and 0.05μM for CsA, chlorpromazine, and FK506, respectively, cholestatic concentrations are expected to be reached only in patients treated with CsA. These findings suggest that it might be possible to discriminate between dose-dependent and idiosyncratic cholestatic drugs using the HepaRG cell model.

In summary, we demonstrate that reversibility of CsA-induced cholestatic effects is concentration-dependent using HepaRG cells and that ER and oxidative stress are major causal events and involved Ca^{2+}-dependent signaling pathways.

SUPPLEMENTARY DATA

Supplementary data are available online at http://toxsci.oxfordjournals.org/.

FUNDING

European Community [Contracts Predict-IV-202222 and MIP-DILI-115336]. The MIP-DILI project has received support from the Innovative Medicines Initiative Joint Undertaking, resources of which are composed of financial contribution from the European Union's Seventh Framework Programme [FP7/20072013] and EFPIA companies' in kind contribution. http://www.imi.europa.eu/.

Ahmad Sharanek received financial support from the Lebanese Association for Scientific Research (LASeR), Pamela Bachour-El Azzi from Lebanese CNRS and Philippe Jabre Association, and Houssein Al-Attrache from the Association AZM-Lebanese University.

ACKNOWLEDGMENT

We thank Dr. Remy Le Guevel from the ImPACell platform (Biosit, Rennes) for imaging analyses and Dr. Eva Klimcakova for critical reading of the manuscript.

REFERENCES

Amundsen, R., Åsberg, A., Ohm, I. K. and Christensen, H. (2012). Cyclosporine A- and tacrolimus-mediated inhibition of CYP3A4 and CYP3A5 In Vitro. *Drug Metab. Dispos.* **40**, 655–661.

Aninat, C., Piton, A., Glaise, D., Le Charpentier, T., Langouët, S., Morel, F., Guguen-Guillouzo, C. and Guillouzo, A. (2006). Expression of cytochromes P450, conjugating enzymes and nuclear receptors in human hepatoma HepaRG cells. *Drug Metab. Dispos.* **34**, 75–83.

Anthérieu, S., Bachour-El Azzi, P., Dumont, J., Abdel-Razzak, Z., Guguen-Guillouzo, C., Fromenty, B., Robin, M-A. and Guillouzo, A. (2013). Oxidative stress plays a major role in chlorpromazine-induced cholestasis in human HepaRG cells. *Hepatology* **57**, 1518–1529.

Anthérieu, S., Chesné, C., Li, R., Guguen-Guillouzo, C. and Guillouzo, A. (2012). Optimization of the HepaRG cell model for drug metabolism and toxicity studies. *Toxicol. In Vitro* **26**, 1278–1285.

Barosso, I. R., Zucchetti, A. E., Boaglio, A. C., Larocca, M. C., Taborda, D. R., Luquita, M. G., Roma, M. G., Crocenzi, F. A. and Pozzi, E. J. S. (2012). Sequential activation of classic PKC and estrogen receptor α is involved in estradiol 17ß-D-glucuronide-induced cholestasis. *PloS One* **7**, e50711.

Basseri, S., Lhoták, S., Sharma, A. M. and Austin, R. C. (2009). The chemical chaperone 4-phenylbutyrate inhibits adipogenesis by modulating the unfolded protein response. *J. Lipid Res.* **50**,

2486–2501.
Boaglio, A. C., Zucchetti, A. E., Toledo, F. D., Barosso, I. R., Pozzi, E. J. S., Crocenzi, F. A. and Roma, M. G. (2012). ERK1/2 and p38 MAPKs are complementarily involved in estradiol 17ß-D-glucuronide-induced cholestasis: Crosstalk with cPKC and PI3K. *PloS One* **7**, e49255.
Bouvier, N., Flinois, J. P., Gilleron, J., Sauvage, F. L., Legendre, C., Beaune, P., Thervet, E., Anglicheau, D. and Pallet, N. (2009). Cyclosporine triggers endoplasmic reticulum stress in endothelial cells: A role for endothelial phenotypic changes and death. *Am. J. Physiol. Renal Physiol.* **296**, 160–169.
Carlisle, R. E., Brimble, E., Werner, K. E., Cruz, G. L., Ask, K., Ingram, A. J. and Dickhout, J. G. (2014). 4-Phenylbutyrate inhibits tunicamycin-induced acute kidney injury via CHOP/GADD153 repression. *PloS One* **9**, e84663.
Cerec, V., Glaise, D., Garnier, D., Morosan, S., Turlin, B., Drenou, B., Gripon, P., Kremsdorf, D., Guguen-Guillouzo, C. and Corlu, A. (2007). Transdifferentiation of hepatocyte-like cells from the human hepatoma HepaRG cell line through bipotent progenitor. *Hepatology* **45**, 957–967.
Crocenzi, F. A., Mottino, A. D. and Roma, M. G. (2004). Regulation of synthesis and trafficking of canalicular transporters and its alteration in acquired hepatocellular cholestasis. Experimental therapeutic strategies for its prevention. *Curr. Med. Chem.* **11**, 501–524.
Guguen-Guillouzo, C. and Guillouzo, A. (2010). General review on in vitro hepatocyte models and their applications. *Methods Mol. Biol.* **640**, 1–40.
Humbert, L., Maubert, M. A., Wolf, C., Duboc, H., Mahé, M., Farabos, D., Seksik, P., Mallet, J. M., Trugnan, G., Masliah, J. and Rainteau, D. (2012). Bile acid profiling in human biological samples: Comparison of extraction procedures and application to normal and cholestatic patients. *J. Chromatogr. B Analyt. Technol. Biomed. Life Sci.* **899**, 135–145.
Lamoureux, F., Mestre, E., Essig, M., Sauvage, F. L., Marquet, P. and Gastinel, L. N. (2011). Quantitative proteomic analysis of cyclosporine-induced toxicity in a human kidney cell line and comparison with tacrolimus. *J. Proteomics* **75**, 677–694.
Lee, W. M. (2003). Drug-induced hepatotoxicity. *N. Engl. J. Med.* **349**, 474–485.
Marion, T. L., Perry, C. H., St Claire, R. L. and Brouwer, K. L. (2012). Endogenous bile acid disposition in rat and human sandwich-cultured hepatocytes. *Toxicol. Appl. Pharmacol.* **261**, 1–9.
Mihatsch, M. J., Kyo, M., Morozumi, K., Yamaguchi, Y., Nickeleit, V. and Ryffel, B. (1998). The side-effects of ciclosporine-A and tacrolimus. *Clin. Nephrol.* **49**, 356–363.
Mizuta, K., Kobayashi, E., Uchida, H., Fujimura, A., Kawarasaki, H. and Hashizume, K. (1999). Influence of tacrolimus on bile acid and lipid composition in continuously drained bile using a rat model. Comparative study with cyclosporine. *Transpl. Int.* **12**, 316–322.
Murray, J. W., Thosani, A. J., Wang, P. and Wolkoff, A. W. (2011). Heterogeneous accumulation of fluorescent bile acids in primary rat hepatocytes does not correlate with their homogenous expression of ntcp. *Am. J. Physiol. Gastrointest. Liver Physiol.* **301**, 60–68.
Orrenius, S., Zhivotovsky, B. and Nicotera, P. (2003). Regulation of cell death: The calcium-apoptosis link. *Nat. Rev. Mol. Cell Biol.* **4**, 552–565.
Park, B. K., Kitteringham, N. R., Maggs, J. L., Pirmohamed, M. and Williams, D. P. (2005). The role of metabolic activation in drug-induced hepatotoxicity. *Annu. Rev. Pharmacol. Toxicol.* **45**, 177–202.
Pedersen, J. M., Matsson, P., Bergström, C. A., Hoogstraate, J., Norén, A., Lecluyse, E. L. and Artursson, P. (2013). Early identification of clinically relevant drug interactions with the human bile salt export pump (BSEP/ABCB11). *Toxicol. Sci.* **136**, 328–343.
Pérez, L. M., Milkiewicz, P., Elias, E., Coleman, R., Pozzi, E. J. S. and Roma, M. G. (2006). Oxidative stress induces internalization of the bile salt export pump, Bsep, and bile salt secretory failure in isolated rat hepatocyte couplets: A role for protein kinase C and prevention by protein kinase A. *Toxicol. Sci.* **91**, 150–158.
Princen, H. M., Meijer, P., Wolthers, B. G., Vonk, R. J. and Kuipers, F. (1991). Cyclosporin A blocks bile acid synthesis in cultured hepatocytes by specific inhibition of chenodeoxycholic acid synthesis. *Biochem. J.* **275**, 501–505.
Roma, M. G. and Pozzi, E. J. S. (2008). Oxidative stress: A radical way to stop making bile. *Ann. Hepatol.* **7**, 16–33.
Román, I. D. and Coleman, R. (1994). Disruption of canalicular function in isolated rat hepatocyte couplets caused by cyclosporin A. *Biochem. Pharmacol.* **48**, 2181–2188.
Sarró, E., Jacobs-Cachá, C., Itarte, E. and Meseguer, A. (2012). A pharmacologically-based array to identify targets of cyclosporine A-induced toxicity in cultured renal proximal tubule cells. *Toxicol. Appl. Pharmacol.* **258**, 275–287.
Singh, A., Wu, H., Zhang, P., Happel, C., Ma, J. and Biswal, S. (2010). Expression of ABCG2 (BCRP) is regulated by Nrf2 in cancer cells that confers side population and chemoresistance phenotype. *Mol. Cancer Ther.* **9**, 2365–2376.
Stieger, B., Meier, Y. and Meier, P. J. (2007). The bile salt export pump. *Pflugers Arch.* **453**, 611–620.
Tocci, M. J., Matkovich, D. A., Collier, K. A., Kwok, P., Dumont, F., Lin, S., Degudicibus, S., Siekierka, J. J., Chin, J. and Hutchinson, N. I. (1989). The immunosuppressant FK506 selectively inhibits expression of early T cell activation genes. *J. Immunol.* **143**, 718–726.
Van Summeren, A., Renes, J., Bouwman, F. G., Noben, J. P., van Delft, J. H., Kleinjans, J. C. and Mariman, E. C. (2011). Proteomics investigations of drug-induced hepatotoxicity in HepG2 cells. *Toxicol. Sci.* **120**, 109–122.
Wallace, K., Cowie, D. E., Konstantinou, D. K., Hill, S. J., Tjelle, T. E., Axon, A., Koruth, M., White, S. A., Carlsen, H., Mann, D. A., *et al.* (2010). The PXR is a drug target for chronic inflammatory liver disease. *J. Steroid Biochem. Mol. Biol.* **120**, 137–148.
Zollner, G. and Trauner, M. (2008). Mechanisms of cholestasis. *Clin. Liver Dis.* **12**, 1–26.